frontiers | Research Topics

Plant mineral microbe interactions

Edited by
Muhammad Zahid Mumtaz, Tereza Castellane, Brahim Bouizgarne, Elena Tamburini and Izzah Shahid

Published in
Frontiers in Microbiology



FRONTIERS EBOOK COPYRIGHT STATEMENT

The copyright in the text of individual articles in this ebook is the property of their respective authors or their respective institutions or funders. The copyright in graphics and images within each article may be subject to copyright of other parties. In both cases this is subject to a license granted to Frontiers.

The compilation of articles constituting this ebook is the property of Frontiers.

Each article within this ebook, and the ebook itself, are published under the most recent version of the Creative Commons CC-BY licence. The version current at the date of publication of this ebook is CC-BY 4.0. If the CC-BY licence is updated, the licence granted by Frontiers is automatically updated to the new version.

When exercising any right under the CC-BY licence, Frontiers must be attributed as the original publisher of the article or ebook, as applicable.

Authors have the responsibility of ensuring that any graphics or other materials which are the property of others may be included in the CC-BY licence, but this should be checked before relying on the CC-BY licence to reproduce those materials. Any copyright notices relating to those materials must be complied with.

Copyright and source acknowledgement notices may not be removed and must be displayed in any copy, derivative work or partial copy which includes the elements in question.

All copyright, and all rights therein, are protected by national and international copyright laws. The above represents a summary only. For further information please read Frontiers' Conditions for Website Use and Copyright Statement, and the applicable CC-BY licence.

ISSN 1664-8714
ISBN 978-2-8325-6968-9
DOI 10.3389/978-2-8325-6968-9

Generative AI statement
Any alternative text (Alt text) provided alongside figures in the articles in this ebook has been generated by Frontiers with the support of artificial intelligence and reasonable efforts have been made to ensure accuracy, including review by the authors wherever possible. If you identify any issues, please contact us.

About Frontiers

Frontiers is more than just an open access publisher of scholarly articles: it is a pioneering approach to the world of academia, radically improving the way scholarly research is managed. The grand vision of Frontiers is a world where all people have an equal opportunity to seek, share and generate knowledge. Frontiers provides immediate and permanent online open access to all its publications, but this alone is not enough to realize our grand goals.

Frontiers journal series

The Frontiers journal series is a multi-tier and interdisciplinary set of open-access, online journals, promising a paradigm shift from the current review, selection and dissemination processes in academic publishing. All Frontiers journals are driven by researchers for researchers; therefore, they constitute a service to the scholarly community. At the same time, the *Frontiers journal series* operates on a revolutionary invention, the tiered publishing system, initially addressing specific communities of scholars, and gradually climbing up to broader public understanding, thus serving the interests of the lay society, too.

Dedication to quality

Each Frontiers article is a landmark of the highest quality, thanks to genuinely collaborative interactions between authors and review editors, who include some of the world's best academicians. Research must be certified by peers before entering a stream of knowledge that may eventually reach the public - and shape society; therefore, Frontiers only applies the most rigorous and unbiased reviews. Frontiers revolutionizes research publishing by freely delivering the most outstanding research, evaluated with no bias from both the academic and social point of view. By applying the most advanced information technologies, Frontiers is catapulting scholarly publishing into a new generation.

What are Frontiers Research Topics?

Frontiers Research Topics are very popular trademarks of the *Frontiers journals series*: they are collections of at least ten articles, all centered on a particular subject. With their unique mix of varied contributions from Original Research to Review Articles, Frontiers Research Topics unify the most influential researchers, the latest key findings and historical advances in a hot research area.

Find out more on how to host your own Frontiers Research Topic or contribute to one as an author by contacting the Frontiers editorial office: frontiersin.org/about/contact

Plant mineral microbe interactions

Topic editors
Muhammad Zahid Mumtaz — Gansu Agricultural University, China
Tereza Castellane — São Paulo State University, Brazil
Brahim Bouizgarne — Ibn Zohr University, Morocco
Elena Tamburini — University of Cagliari, Italy
Izzah Shahid — Public University of Navarre, Spain

Citation
Mumtaz, M. Z., Castellane, T., Bouizgarne, B., Tamburini, E., Shahid, I., eds. (2025). *Plant mineral microbe interactions*. Lausanne: Frontiers Media SA.
doi: 10.3389/978-2-8325-6968-9

Table of contents

05 Editorial: Plant mineral microbe interactions
Muhammad Zahid Mumtaz, Tereza Cristina Luque Castellane, Izzah Shahid, Elena Tamburini and Brahim Bouizgarne

09 Investigating the impact of long-term bristlegrass coverage on rhizosphere microbiota, soil metabolites, and carbon–nitrogen dynamics for pear agronomic traits in orchards
Chunhui Shi, Xiaoqing Wang, Shuang Jiang, Jianfeng Xu and Jun Luo

26 Response of soil microbial community structure to temperature and nitrogen fertilizer in three different provenances of *Pennisetum alopecuroides*
Niandong Deng, Lili Nian, Shuolun Zhang, Yixuan Liang, Huiying Shang, Yang Li and Zhuxin Mao

44 Two new species and three new records of *Diachea* (Physarales) from China based on morphological and molecular evidence
Xuefei Li, Dan Dai, Yonglan Tuo, You Li, Jiajun Hu, Frederick Leo Sossah, Bo Zhang, Xiao Li and Yu Li

61 Enhancing carrot (*Daucus carota* var. sativa Hoffm.) plant productivity with combined rhizosphere microbial consortium
Liping Zhu, Peiqiang Zhang, Shunan Ma, Quan Yu, Haibing Wang, Yuexuan Liu, Song Yang and Yanling Chen

77 Mycorrhizal extraradical mycelium can reduce cadmium uptake by maize and cadmium leaching from contaminated soil: based on an in-growth core experiment
Yijie Yang, Yang Li, Xiaoyi Li, Jie Yan, Longhua Wu, Zhenwu Tang, Yongmei He and Fangdong Zhan

89 The process of nitrogen-adaptation root endophytic bacterial rather than phosphorus-adaptation fungal subcommunities construction unveiled the tomato yield improvement under long-term fertilization
Xiaoxia Li, Muhammad Awais, Shuang Wang, Zhu Zhang, Shuning Zhao, Yufeng Liu, Zhouping Sun, Hongdan Fu and Tianlai Li

106 Metagenomic insights into the development of microbial communities of straw and leaf composts
Anastasiia K. Kimeklis, Grigory V. Gladkov, Olga V. Orlova, Tatiana O. Lisina, Alexey M. Afonin, Tatiana S. Aksenova, Arina A. Kichko, Alla L. Lapidus, Evgeny V. Abakumov and Evgeny E. Andronov

118 Unraveling the microecological mechanisms of phosphate-solubilizing *Pseudomonas asiatica* JP233 through metagenomics: insights into the roles of rhizosphere microbiota and predatory bacteria
Yuhan Tang, Linlin Wang, Jing Fu, Fangyuan Zhou, Hailei Wei, Xiaoqing Wu, Susu Fan and Xinjian Zhang

130 Effects of tea plant endophytic phosphate-solubilizing bacteria on the growth and selenium uptake of maize seedlings in selenium-rich soil
Shuqing Zhang, Jinmei Guo, Jianfeng Li, Yousu Yang and Qiuyue Zhang

142 Research on soil bacterial community assembly and function under different straw returning practices in arid and semi-arid agricultural ecosystems over multiple years
Rui-Zhi Liu, Xiao-Ya Zhao, Biao Feng, Wen-Shan Zhao, Ming-Yu Li, Xiao-Fang Yu, Shu-Ping Hu, Rui-Ping Li, Ju-Lin Gao and Qinggeer Borjigin

155 Divergent responses of plant lignin and microbial necromass to the contribution of soil organic carbon under organic and chemical fertilization
Xingping Chang, Zhanjiang Pei, Xiaofei Wang, Hao Wang, Jie Mu, Yingjun Ma, Mingye Zhang, Keqiang Zhang and Lianzhu Du

169 Straw retention drives microbial community succession to improve soil C/N cycling: insights from a multi-year rice-based system
Shu Jia, Yue-Dong Li, Hang Qu, Bo Li, Ying-hua Juan, Yue-hua Xing, Yan Liu, Hong-jing Bao and Wen-tao Sun

182 Linkage of living microbial biomass, function, and necromass to soil organic carbon storage along a chronosequence of *Larix principis-rupprechtii* plantation in North China
Mengyun Yang, Xiaomeng He, Jingfei Liang, Qiang Liu, Lihua Fu, Xiaodong Cui, Shaohui Huang and Haoan Luan

199 Carbon components in organic amendments drive nitrogen metabolism in one-year-long anaerobic soil microcosms
Yiming Ma, Qiaoyu Wu, Xinhui Wang, Weikang Sui and Xiaojun Zhang

213 The impact of salt-tolerant plants on soil nutrients and microbial communities in soda saline-alkali lands of the Songnen plain
Junjie Song, Xueting Guan, Haojun Cui, Lin Liu, Yan Li, Yuhua Li and Shurong Ma

227 A review on microbe–mineral transformations and their impact on plant growth
Nikita Pradhan, Shikha Singh, Garima Saxena, Nischal Pradhan, Monika Koul, Amit C. Kharkwal and Riyaz Sayyed

frontiers | Frontiers in Microbiology

TYPE Editorial
PUBLISHED 25 September 2025
DOI 10.3389/fmicb.2025.1677458

Check for updates

OPEN ACCESS

EDITED AND REVIEWED BY
Jeanette M. Norton,
Utah State University, United States

*CORRESPONDENCE
Muhammad Zahid Mumtaz
✉ zahidses@gmail.com
Tereza Cristina Luque Castellane
✉ tereza.castellane@unesp.br

†These authors have contributed equally to this work

RECEIVED 31 July 2025
ACCEPTED 09 September 2025
PUBLISHED 25 September 2025

CITATION
Mumtaz MZ, Castellane TCL, Shahid I, Tamburini E and Bouizgarne B (2025) Editorial: Plant mineral microbe interactions. *Front. Microbiol.* 16:1677458. doi: 10.3389/fmicb.2025.1677458

COPYRIGHT
© 2025 Mumtaz, Castellane, Shahid, Tamburini and Bouizgarne. This is an open-access article distributed under the terms of the Creative Commons Attribution License (CC BY). The use, distribution or reproduction in other forums is permitted, provided the original author(s) and the copyright owner(s) are credited and that the original publication in this journal is cited, in accordance with accepted academic practice. No use, distribution or reproduction is permitted which does not comply with these terms.

Editorial: Plant mineral microbe interactions

Muhammad Zahid Mumtaz[1,2*†], Tereza Cristina Luque Castellane[3*†], Izzah Shahid[4], Elena Tamburini[5] and Brahim Bouizgarne[6]

[1]Institute of Molecular Biology and Biotechnology, The University of Lahore, Lahore, Pakistan, [2]College of Agronomy, Gansu Agricultural University, Lanzhou, China, [3]Plant Biochemistry and Microbiology Laboratory, Department of Agricultural and Environmental Biotechnology, School of Agricultural and Veterinary Sciences, São Paulo State University (UNESP), Jaboticabal/São Paulo, Brazil, [4]Institute of Multidisciplinary Research in Applied Biology, Public University of Navarra, Pamplona, Spain, [5]Department of Biomedical Sciences, University of Cagliari, Monserrato, Italy, [6]Laboratory of Plant Biotechnology (BiotecV), Faculty of Science, Ibn Zohr University, Agadir, Morocco

KEYWORDS

soil microbiome, biostimulants and sustainable agriculture, biogeochemical processes, biological nitrogen fixation (BNF), mineral solubilization, plant growth-promoting bacteria

Editorial on the Research Topic
Plant mineral microbe interactions

Plant-mineral-microbe interactions are the foundation of soil nutrient dynamics, but their underlying mechanisms and functional integration remain underexplored. Despite growing recognition of the beneficial microbes in the promotion of nutrient uptake through mineral weathering, nitrogen fixation, mineral solubilization, and promotion of plant health, the mechanistic pathways in shaping microbial community composition and functioning are still unclear. The lack of this mechanistic understanding limits our ability to harness these interactions to promote crop productivity under environmental harsh conditions (nutrient deficiency, drought, salinity or degraded soil conditions). Furthermore, conventional agricultural practices often overlook the synergistic relationships between mineral composition and microbial functionality, which limits the bio-based strategies to enhance soil health. Advancing knowledge in plant-mineral-microbe interactions is crucial for developing sustainable, microbe-assisted strategies to improve long-term soil health and agricultural sustainability. Soil health and nutrient cycling are fundamental for sustainable agriculture, directly affecting crop productivity, environmental quality, and ecosystem resilience. Soils, as the largest terrestrial biodiversity reservoir, regulate water quality, carbon sequestration, and greenhouse gas emissions. Therefore, maintaining soil health is essential to address global challenges such as food security, climate change mitigation, and ecosystem conservation. This Research Topic features 15 original research articles alongside a comprehensive review, contributed by over 124 researchers worldwide, demonstrating the expanding global interest in plant-mineral-microbe interactions.

Advancing knowledge in plant-mineral-microbe interactions is crucial for developing sustainable, microbe-assisted strategies to improve long-term soil health and agricultural sustainability. The studies published in this Research Topic cover diverse agroecosystems and management practices, focusing on how organic amendments influence nitrogen metabolism, microbial succession driven by straw retention, and the dynamics of soil organic carbon under different fertilization regimes.

Collectively, these works reveal how soil management shapes microbial communities that drive nutrient cycling and carbon stabilization, processes critical for sustainable crop production. Understanding these underlying mechanisms is essential for developing practices that improve yields while minimizing environmental impacts. Moreover, the research highlights adaptive shifts in microbial functional genes in response to organic inputs, influencing nutrient availability and greenhouse gas fluxes. Advances in soil microbiology and organic matter management demonstrate that integrating these approaches can optimize productivity and sustainability, balancing crop yield goals with ecological stewardship and supporting climate-smart agriculture.

In this context, the review by Pradhan et al. provides a comprehensive overview of the microbial mechanisms driving mineral dissolution, precipitation, and transformation, emphasizing their critical roles in regulating macro- and micronutrient availability in soils. By highlighting microbial activities such as phosphate solubilization, siderophore production, nitrogen fixation, and metal detoxification, this review underscores the vital contributions of microorganisms to soil fertility, sustainable agriculture, and environmental remediation.

Relationships between living microbial biomass, and necromass with soil organic carbon were reported in this topic. Chang et al. contributed critical insights into the effects of long-term organic fertilization on soil carbon dynamics. Over a decade, the application of cattle manure nearly tripled soil carbon stocks compared to conventional chemical fertilization. This increase was primarily attributed to the accumulation of plant-derived compounds and a microbial community shift favoring eutrophic decomposers. The study also reported a marked increase in microbial necromass, confirming the central role of the "microbial carbon pump" in stabilizing soil organic matter. These findings affirm that substrate availability and microbial community structure synergistically promote organic matter persistence, offering practical avenues to enhance soil carbon sequestration in agricultural landscapes. Complementing these findings, Yang et al. examined microbial biomass, necromass, and organic carbon stability in forest soils, highlighting microbial succession as a determinant of soil's capacity to function as a living carbon reservoir. This ecological perspective positions soil as a dynamic and interactive system, where microbial diversity and turnover maintain fertility and enhance carbon sequestration efficiency. The vital contribution of microbial necromass to long-term carbon stabilization informs management practices aiming to increase soil organic matter persistence.

Soil inputs that can drive microbial communities and enhance overall soil health are reflected in multiple interrelated aspects, such as the planting of beneficial species or the application of amendments, compost, and straw materials. Aiming to enhance soil fertility and restructure microbial communities in saline-alkali soils, Song et al., used salt-tolerant plants, and demonstrated their usefulness for improving soil health conditions (salinity, pH, nutrients, enzyme activities, and beneficial microbia diversity). In a comprehensive study by Ma et al., the distinct impacts of various organic amendments, compost, digestate, and straw, on microbial nitrogen cycling were elucidated in anaerobic fluvo-aquic soils. The application of organic matter significantly increased labile carbon fractions, which serve as energy sources for soil microorganisms, and modified the soil functional gene composition related to nitrogen metabolism. Compost-treated plots exhibited the highest abundance of nitrogen-related functional groups, reflecting enhanced microbial activity and nitrogen transformation potential. Although all amendments stimulated denitrification and transient emissions of N_2O and N_2 gases while compost significantly reduced N_2O emissions over the long term. They reported the enrichment of nitrogen mineralizing genes and a concurrent decline in genes involved in dissimilatory nitrate reduction to ammonium and assimilatory nitrate reduction pathways. This metabolic reorganization favors bioavailable nitrogen retention that plants can readily assimilate and promotes nitrogen use efficiency. Intriguingly, biological nitrogen fixation was specifically stimulated in straw-treated soils, underscoring the strategic importance of amendment selection to optimize nitrogen cycling. Key microbial taxa such as *Anaeromyxobacter* and *Lysobacter* emerged as critical players linking microbial community composition to functional soil outcomes to promote environmental sustainability and crop productivity, mitigation of greenhouse gas emissions.

The importance of straw application as a powerfull tool for soil health, acting by changes in microbial communities were exemplfied by four papers (Jia et al., Kimeklis et al., Liu et al., and Ma et al.). Jia et al., investigated the practical agronomic and ecological impacts of straw retention in croplands. Even short-term straw retention significantly increased soil organic carbon and available phosphorus, promoted fungal biomass, and enriched microbial taxa associated with cellulose degradation. Enzymatic activities essential for carbon and nitrogen cycling were elevated, and key genes involved in nitrogen fixation, nitrification, and carbon metabolism were enriched. Together, these changes boosted overall soil functional capacity. However, this practice increased the abundance of phytopathogenic fungi such as *Magnaporthe oryzae*, highlighting the necessity of integrated management approaches that balance agronomic benefits with phytosanitary control. This dual focus exemplifies the complexity of sustainable soil management, where improving soil quality must be harmonized with maintaining plant health.

Using functional metagenomics, Kimeklis et al. identified distinct enzymatic profiles in microbial communities involved in the degradation of straw compared to leaf litter. Their analysis revealed significant functional diversity, particularly enrichment of genes encoding enzymes involved in xylan and pectin degradation, indicating promising biotechnological applications for lignocellulosic residue valorization in agriculture and environmental management. Studies focusing on straw management, such as Liu et al., revealed that incorporation depth and cover crop type distinctly influence bacterial diversity, composition, and community assembly mechanisms. Deep straw incorporation and no-tillage cover enhanced microbial diversity and functional potential, directly contributing to soil resilience and health. Finally, Ma et al., showed that treatment by straw powder, promoted the proliferation of cellulolytic nitrogen-fixing bacteria, including *Clostridium,* and nitrogen-fixing archaea. These results illustrate how targeted agronomic interventions modulate ecological balances and microbial metabolism, supporting sustainable soil function.

Finally, works published in this topic highlighted the importance of bioinoculants which could be represented by (i) beneficial bacteria, either those living in the vicinity of the plant roots (plant growth-promoting bacteria; PGPRs) or those living inside roots (endophites) or and (ii) fungi (especially arbuscular mycorrhizal fungi AMF) in maintaining microbial communities networks (through multiple interactions) and contributing to soil and plant health. Zhu et al. identified promising plant growth-promoting bacteria in the carrot rhizosphere, addressing the limited knowledge on PGPR associated with this crop and highlighting their potential as bioinoculants to stimulate carrot growth. In turn, Li et al. showed that long-term fertilization regimes shape tomato root endophytic communities, with rare microbial taxa playing key roles in network stability and yield improvement. Together, these studies underscore the complementary roles of PGPR in crop-specific rhizospheres and the ecological importance of rare microbial groups in sustaining productivity, offering valuable insights for designing microbial-based strategies to advance sustainable agricultural intensification. Zhang et al. demonstrated that endophytic phosphorus-solubilizing bacteria from tea plants significantly enhanced maize growth and nutrient uptake, particularly phosphorus and selenium. The strain *Pseudomonas fungorum* PMS-05 notably doubled maize dry biomass and increased selenium content, underscoring the synergistic potential of microbial inoculants in optimizing plant nutrition. Such bioinoculants hold promise for tailored nutrient management, especially in soils with specific edaphic constraints. Tang et al. further showed that the efficacy of phosphorus-solubilizing bacterial inoculation depends on fertilization regimes and baseline soil phosphorus levels. Specifically, *Pseudomonas asiatica* JP233 performed optimally in phosphorus-rich soils, modulating the rhizosphere microbiota by enhancing metabolic pathways related to secondary metabolite biosynthesis and phosphorus cycling. Collectively, these findings highlight the need to contextualize bioinoculant application within soil nutrient status and microbial ecology frameworks to maximize agronomic benefits.

Complementing these investigations, the studies conducted by Li et al., Deng et al., and Shi et al. further expand our understanding of microbial biodiversity and its interactions with agricultural management. Li et al. described two new species of the genus *Diachea*, enriching taxonomic and ecological knowledge of slime molds in underexplored regions of China. They identified taxonomic keys and morphological comparisons to support future studies on their distribution and ecological roles. Deng et al. demonstrated how microbial communities associated with the rhizosphere of *Pennisetum alopecuroides* respond distinctly to nitrogen and temperature variations, highlighting the role of soil factors such as pH, potassium, and phosphorus in structuring these communities, revealing regional patterns of microbial cooperation and competition. Shi et al. showed the beneficial effects of organic ground cover on soil enzymatic activity, enrichment of plant growth-promoting rhizobacteria, metabolic shifts linked to sucrose synthesis, and significant increases in fruit yield and biochemical quality. Together, these studies underscore the importance of integrating taxonomy, microbial ecology, and soil management to build more resilient, productive, and sustainability-aligned agroecosystems. Finally, research on arbuscular mycorrhizal fungi (AMF), as illustrated by Yang et al., confirmed their crucial role in regulating heavy metal availability and toxicity in soils, thus protecting plants and mitigating environmental contaminant losses.

Collectively, published work in the current Research Topic reaffirms that sustainable soil management transcends mere input application. It requires embracing the complexity of microbial dynamics, strategically deploying organic amendments and bioinoculants, and integrating agronomic practices that honor the functional complexity of soil ecosystems. A detailed understanding of molecular and ecological mechanisms driving nutrient cycling and soil carbon stabilization opens innovative pathways toward reconciling agricultural productivity with environmental conservation. The agricultural disciplines, especially soil science and agricultural microbiology, are thus at the forefront of guiding the transformation toward more resilient, productive, and sustainable agroecosystems. Continued interdisciplinary research and knowledge transfer will be essential to realize these goals in the face of global challenges posed by climate change, resource limitations, and food security demands. The important insights and advances provided by the studies compiled in this Research Topic have directly contributed to the development and launch of its second volume. This new Research Topic will build upon the foundational knowledge generated here, further advancing our understanding of soil ecosystem processes and management strategies. By addressing emerging challenges and fostering innovative solutions, these ongoing efforts will support the creation of agroecosystems that are both highly productive and ecologically sustainable, capable of withstanding the pressures of a rapidly changing world.

Author contributions

MM: Conceptualization, Writing – review & editing. TCLC: Writing – original draft, Writing – review & editing. IS: Writing – review & editing. ET: Writing – review & editing. BB: Writing – review & editing.

Acknowledgments

We thank authors of the papers published in this Research Topic for their valuable contributions and the referees for their rigorous review.

Conflict of interest

The authors declare that the research was conducted in the absence of any commercial or financial relationships that could be construed as a potential conflict of interest.

The author(s) declared that they were an editorial board member of Frontiers, at the time of submission. This had no impact on the peer review process and the final decision.

Generative AI statement

The author(s) declare that no Gen AI was used in the creation of this manuscript.

Any alternative text (alt text) provided alongside figures in this article has been generated by Frontiers with the support of artificial intelligence and reasonable efforts have been made to ensure accuracy, including review by the authors wherever possible. If you identify any issues, please contact us.

Publisher's note

All claims expressed in this article are solely those of the authors and do not necessarily represent those of their affiliated organizations, or those of the publisher, the editors and the reviewers. Any product that may be evaluated in this article, or claim that may be made by its manufacturer, is not guaranteed or endorsed by the publisher.

frontiers | Frontiers in Microbiology

TYPE Original Research
PUBLISHED 05 September 2024
DOI 10.3389/fmicb.2024.1461254

Check for updates

OPEN ACCESS

EDITED BY
Muhammad Zahid Mumtaz,
Gansu Agricultural University, China

REVIEWED BY
Rubab Sarfraz,
Gyeongsang National University, Republic of Korea
Muhammad Rahil Afzal,
Jiangsu University, China

*CORRESPONDENCE
Jianfeng Xu
xjf@hebau.edu.cn
Jun Luo
zuowusuo@163.com

RECEIVED 08 July 2024
ACCEPTED 13 August 2024
PUBLISHED 05 September 2024

CITATION
Shi C, Wang X, Jiang S, Xu J and Luo J (2024) Investigating the impact of long-term bristlegrass coverage on rhizosphere microbiota, soil metabolites, and carbon–nitrogen dynamics for pear agronomic traits in orchards.
Front. Microbiol. 15:1461254.
doi: 10.3389/fmicb.2024.1461254

COPYRIGHT
© 2024 Shi, Wang, Jiang, Xu and Luo. This is an open-access article distributed under the terms of the Creative Commons Attribution License (CC BY). The use, distribution or reproduction in other forums is permitted, provided the original author(s) and the copyright owner(s) are credited and that the original publication in this journal is cited, in accordance with accepted academic practice. No use, distribution or reproduction is permitted which does not comply with these terms.

Investigating the impact of long-term bristlegrass coverage on rhizosphere microbiota, soil metabolites, and carbon–nitrogen dynamics for pear agronomic traits in orchards

Chunhui Shi[1,3], Xiaoqing Wang[1,3], Shuang Jiang[1,3], Jianfeng Xu[2]* and Jun Luo[1,3]*

[1]Forest & Fruit Tree Research Institute, Shanghai Academy of Agriculture Sciences, Shanghai, China, [2]College of Horticulture, Hebei Agricultural University, Baoding, Hebei, China, [3]Shanghai Key Laboratory of Facility Horticulture Technology, Shanghai Academy of Agriculture Sciences, Shanghai, China

Background: Grass coverage (GC) under no-tillage systems in orchards signifcantly infuences underground carbon (C) and nitrogen (N) sequestration, primarily through promoting mineral nutrient utilization by rhizospheric microorganisms. However, the comprehensive impact of GC on microbial communities and plant responses using soil metabolomics remains inadequately recognized.

Methods: We investigated two rhizosphere types established since 2002: bristlegrass (*Setaria viridis* (L.) P. Beauv.) coverage (SC) and clean cultivation (CC) to assess their efects on soil parameters, enzyme activities, and key pear agronomic traits, including yield (single fruit weight (SFW)) and qualities (soluble solids content (SSC), and total soluble sugar (TSS)). We combined microbiological analysis (16S rRNA sequencing) and non-targeted metabolomics (UPLC-MS/MS and GC–MS) to explore how microbial communities infuence fruit agronomic traits and soil nutrient dynamics in pear orchards under SC conditions.

Results: Our fndings indicate that SC signifcantly enhances soil organic carbon (SOC), soil organic nitrogen (SON), the C:N ratio, and available nitrogen (AN). Moreover, SC leads to pronounced increases in soil enzyme activities involved in the C cycle and storage, including soil sucrase, β-glucosidase, polyphenol oxidase and cellulase. Microbiome analysis revealed substantial diferences in microbial community composition and diversity indices between SC and CC rhizosphere soils within the 0–40cm depth. Metabolomic analysis demonstrated significant alterations in metabolite profiles across both the 0-20 cm and 20-40 cm layers under SC conditions. The identifed metabolites primarily involve sugar and amino acid-related metabolic pathways, refecting perturbations in C and N metabolism consistent with shifts in bacterial community structure. Several plant growth-promoting rhizobacteria (PGPRs) taxa (e.g., *Haliangium*, *Bacteroides*, *mle1-7*, *Subgroup_22*, *Ellin6067*, *MND1*, *Flavobacterium*, and *Cellvibrio*) were enriched under SC, associated with metabolites such as sucrose, N-acetyl-D-glucosamine, N-acetyl-L-glutamic acid, rhamnose, UDP-GlcNAc and D-maltose. These fndings suggest their roles in promoting C and N sequestration processes through sucrose synthesis and glycolytic pathways in the soil, which was signifcantly correlated with the formation of agronomic traits such as fruit yield, SFW SSC and TSS ($p<0.05$), and SC treatments signifcantly increased yields by 35.40–62.72% and sucrose content in TSS by 2.43–3.96 times than CC treatments.

Conclusion: This study provides valuable insights into the efects of SC on soil microbial communities and plant physiology, enhancing our understanding of their implications for sustainable orchard management.

KEYWORDS

grass coverage, carbon sequestration, mineral nutrient, rhizospheric microorganism, PGPRs, metabolomics, yield

1 Introduction

Grasslands are pivotal ecological systems globally. However, the persistent conversion of grasslands into arable land has resulted in significant degradation of terrestrial ecosystems (Baer et al., 2015; Song et al., 2022). Additionally, to satisfy the increasing fruit demand from expanding populations, orchard expansion has adversely impacted ecosystems worldwide (Bardgett et al., 2021). Clean cultivated (CC) orchards, characterized by clean tillage practices, substantially contribute to soil erosion and degradation (Mikha et al., 2018; Chen et al., 2021). Unfortunately, CC orchards remain prevalent across numerous regions, including North America, the Middle East, and other areas. The substantial global standing of China's pear industry has drawn researchers' attention to the issue of soil health within pear orchards. According to the Food and Agriculture Organization's 2021 statistics, Chinese pear orchards encompass an extensive area of 921,610 hectares, accounting for two-thirds of the planting area and 70% of the total global yield. Notably, CC pear orchards represent over 80% of orchard areas in China, significantly contributing to soil erosion and degradation in these environments (Xiang et al., 2023).

The conversion of grasslands to arable land often results in a reduction in soil organic carbon (SOC) stocks (Oberholzer et al., 2014; Li et al., 2016). Conversely, decreasing tillage intensity and implementing grass cover can mitigate the decline of soil organic matter (SOM) and soil biota, thereby maintaining soil structure and crop yield (Sleiderink et al., 2024). The depletion of SOC in orchards is more pronounced compared to that in cereal production, attributable to suboptimal management practices (Seitz et al., 2023). Long-term clean cultivation has been linked to a rapid loss of SOC (Xiang et al., 2023). Sugiura et al. (2017) demonstrated that even with the application of chemical fertilizers, CC orchards still experienced significant carbon loss compared to orchards with mulching grass. Furthermore, CC practices result in greater runoff losses of available nitrogen (AN) and available phosphorus (AP) compared to conditions where grass is allowed to grow and mulch naturally (Wang et al., 2016).

Grasslands play a crucial role in carbon sequestration, and the reintroduction of grasses has been widely adopted as an effective soil management practice in pear orchards across Europe, America, Japan, and other countries (Wang et al., 2017; Peters et al., 2019; Yang et al., 2022). Numerous studies have confirmed that grasses contribute to the restoration of soil health by enhancing nutrient cycling within the soil. This is particularly evident when perennial cover plants are grown between rows or in orchards without soil tillage (Qian et al., 2015). Converting CC orchards to grass-covered ones alters the abundance and composition of soil microbial communities in various orchards, including those for pears, apples, and jujubes (Li et al., 2022; Wang et al., 2020). Extensive research has examined changes in microbial biomass and diversity following the enhancement of soil carbon stocks with different grass species (Qian et al., 2015; Li et al., 2022; Xiang et al., 2023). However, the microbial mechanisms underlying soil organic mineralization and fruit tree response mechanisms remain unclear. It has been shown that restoring plant growth-promoting microorganisms (PGPMs) in orchards through the use of locally dominant natural grasses is vital for sustainable agriculture (Debasis et al., 2019). Several studies have demonstrated that grass coverage serves as a protective layer, accelerating soil nutrient cycling and facilitating SOC sequestration by enhancing microbial activity, ultimately improving plant and fruit growth (Fang et al., 2021; Gómez et al., 2022).

In recent years, 16S rRNA gene sequencing has been utilized to quickly and accurately identify the diversity of bacterial communities, including previously unknown bacterial species (Zakrzewski et al., 2012). This technique has been employed to analyze the carbon source utilization characteristics of microbial communities following intercropping, resulting in significant increases in microbial diversity indices and enhanced utilization of carboxylic acids, phenolic acids, amines, carbohydrates, amino acids, and other carbon substrates (Peng et al., 2017). Soil enzymes also play pivotal roles in the soil carbon cycle and serve as indicators of soil health. Soil microorganisms facilitate organic matter decomposition through the secretion of diverse enzymes, thereby influencing mineralization processes and impacting plant growth either positively or negatively (Fan et al., 2019). Soil cellulases (S-CL), hydrolytic enzymes responsible for breaking down simple substrates, and soil polyphenol oxidase (S-PPO), which decomposes recalcitrant substrates, are integral components of this cycle. Differences in soil enzyme activities between clean and sod cultivation modes were observed, with the highest invertase activity (including alkaline phosphatase, invertase, and catalase) in the 0–40 cm soil layer of orchards (Xiang et al., 2023). Researchers found that covering orchards with different grass seeds affected the proportion of soil fungi and bacteria (Wu et al., 2010; Wang et al., 2020). In a walnut orchard with grass cover, notable outcomes were observed compared to clean cultivation tillage. Soil samples under grass cover exhibited a significant enrichment of PGPRs, including notable genera such as Pseudomonas, Paraburkholderia, Burkholderia, Agrobacterium, and Flavobacterium (Wang et al., 2023). Specific PGPR genera were identified in apple orchard soils under varying long-term grass cover patterns. In addition, Clostridium, known for promoting soil nitrogen accumulation, was prevalent in the grass-covered model (Qian et al., 2015; Zhang et al., 2023).

Natural grass confers several adaptive advantages over artificial grasslands, enhancing soil physical properties in pear orchard cultivation layers and increasing microbial biomass C and N (Wang et al., 2016). However, the relationship between increased C and N and

the emergence of new bacterial species in cultivated soil warrants further investigation. Green bristlegrass (*Setaria viridis* (L.) P. Beauv.) coverage (SC) is widely distributed across temperate and subtropical regions in Asia, Europe, America, and Australia. It is one of the most advantageous grass varieties. Due to its strong adaptability and favorable growing season aligned with soil moisture conservation for orchard grasses, it is the preferred natural grass variety. During the dry season of pear growth, there was an increase in grass varieties and yield, with dry grass yielding 6,360 kg·ha^{-1}. This yield advantage compared to artificial turf also results in significant advantages in soil nutrient nitrogen, phosphorus, and potassium for regressing orchard areas (Liu et al., 2017). In addition, the average growth rate of SOC and total nitrogen (TN) in natural SC mode was higher than that in artificial grass growing mode in the orchard. SOC and TN had positive effect load and weight on yield and quality of fruit agronomic traits, especially soluble solid content (SSC) in fruit (Aghajani et al., 2008; Ku et al., 2018). Two genotypes of green bristlegrass (*Salvia*) accessions on poor soil were found to alter the abundance of the soil microbial community, particularly the group of deformable bacteria, compared to the bare soil, the rhizosphere soil of *Setaria italica* exhibited significantly higher values of organic carbon and total nitrogen, and the nitrogen-containing metabolites tyrosine-derived alkaloids, serotonin, and synephrine were also significantly increased in the rhizosphere (Peterson et al., 2021). Yet, studies on dominant PGPMs in natural grass and their correlations with pear fruit agronomic traits remain limited. Specifically, deeper exploration into the biological mechanisms of plant–microbe interactions, soil–microbe interactions, and their metabolic cycles is crucial. We speculate that intercropping pear trees with green grass and other crops may disrupt the rhizosphere microbial population and secretions of pear trees, thereby altering the enzyme activity released into the soil by microorganisms and further regulating C and N sources. Further experiments are needed to verify this hypothesis. We employed MiSeq sequencing of 16S rRNA genes alongside non-targeted metabolomics (ultra-performance liquid chromatography–tandem mass spectrometry (UPLC-MS/MS) and gas chromatography–mass spectrometry (GC–MS/MS)) to analyze the impact of SC versus CC in two soil layers (0–20 cm and 20–40 cm). Our study aimed to (1) evaluate the influence of natural green bristlegrass on carbon sequestration in degraded orchard soil; (2) investigate how rhizosphere soil microbial communities and secreted metabolites influence the C and N cycles and the biochar restoration mechanism in SC; and (3) explore the network between PGPMs and pear fruit development and quality through C and N cycles. Capturing beneficial PGPMs from SC and reintroducing them into pear orchards prove effective in sequestering biological C and N, offering a theoretical basis for developing specialized microbial fertilizers for pears as an alternative to excessive mineral fertilization.

2 Materials and methods

2.1 Site description

This study was conducted on the Chongming island of Shanghai, in the eastern region of China (31°51′15″N, 121°54′00″E), south of the Yangtze River, in an area suitable for the growth of sand pear (*Pyrus pyrifolia* (Burm. f.) Nakai) (Figure 1A). The orchard soil was originally saline-alkaline (pH = 7.70) and primarily sandy loam, which is ideal for tillage. The primary root system of the pear trees was concentrated at a depth of approximately 40 cm.

2.2 Experimental design and sampling

'Cuiguan' pear (*Pyrus pyrifolia* (Burm. f.)) trees, 20 years old and planted at a density of 1,005 plants/ha, were established in mid-February 2003. Two treatment groups were established: clean cultivated rhizosphere soil (CC) as a control and green bristlegrass (*Setaria viridis* (L.) P. Beauv.) coverage (SC) of rhizosphere soil for over 20 years. A random-arrangement design was adopted, with 20 trees per experimental group. Traditional management approaches were used for cultivation and pest control.

Rhizosphere soil samples were collected during the most active growth period of pear tree roots (October 12) using a soil sampler from two vertical soil layers (0–20 cm and 20–40 cm) within a 10 cm radius around each pear tree. Three replicates were selected for each sample using the 'S' shape sampling method (Zeng et al., 2021). After removing the rubble and soil impurities, the remaining soil was stored in sterile plastic containers. The collected soil samples were divided into two parts: One part was kept at −80°C for microbial community and non-target metabolomics analysis, while the other part was stored at −20°C for soil physicochemical parameter and enzyme activity evaluations (Figure 1B).

2.3 Soil physicochemical parameters and enzyme activity analysis

Electrical conductivity (EC values), potential of hydrogen (pH), and extractable medium/microelement contents (Ca, Mg, Cu, Fe, Mn, Zn, and B) were determined according to the protocol of Shi et al. (2023). The rhizosphere soil samples were analyzed for total carbon (TC), total organic carbon (SOC), total nitrogen (TN), total organic nitrogen (SON), and carbon-to-nitrogen ratio (C:N) using an automatic elemental analyzer (Primacs™ SNC-100; Skalar, China) (Dobosy et al., 2016). AN, AP, and available potassium (AK) in the pear root-zone soil under SC and CC treatments were determined according to the procedure outlined by Ma et al. (2021, 2022). Soil microbial biomass carbon (MBC) and soil microbial biomass nitrogen (MBN) were determined using the chloroform fumigation K_2SO_4 extraction method (Kumar et al., 2021). Soil sucrase (S-SC), β-glucosidase (S-β-GC), soil polyphenol oxidase (S-PPO), soil peroxidase (S-POD), and soil cellulase (S-CL) were determined using the visible spectrophotometric method, and kits were acquired from Shanghai Enzyme Linked Biotechnology Co., Ltd.

2.4 Agronomic contribution to pear fruit yield, quality, and nutritive value

The 'Cuiguan' pears reached maturity on 28 July from 2022 to 2023. For each treatment, a single plant was considered as an experimental unit for statistical evaluation, with three replicates for each treatment. Twenty fruits from each of the five pear trees were randomly selected from the upper, middle, and lower parts of the

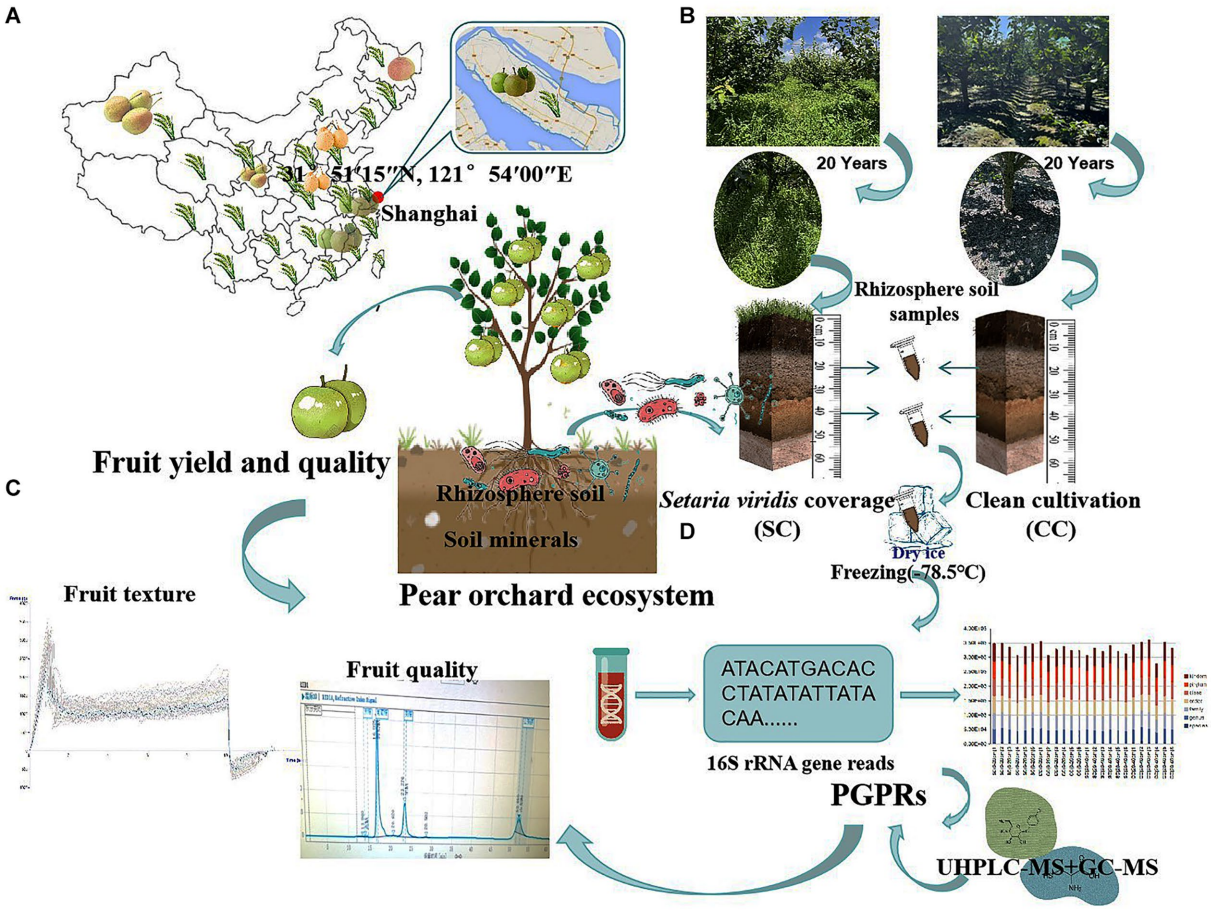


FIGURE 1
Sampling flow chart, evaluation of the agronomic traits contribution of pear, the soil nutrition, and the vertical distribution patterns of rhizosphere soil bacteria communities between SC mode and CC mode in different rhizosphere soil layers. **(A)** The geographic locations of the sampling site. **(B)** The schematic for collecting and preparing vertical rhizosphere soil samples in a pear orchards. **(C)** The schematic for measuring fruit yield and quality of aboveground pear trees in pear orchard. **(D)** The schematic for high-throughput sequencing and metabolite analysis of bacteria community in SC and CC rhizosphere soil at ASV level.

canopy. Single fruit weight (SFW) was weighed using an electronic balance (ME-T; Thermo Fisher, USA). Fruit number per plant (FNP) was determined using a counter. The lateral diameter (LD) and vertical diameter (VD) of the fruits were measured using an electronic caliper (505–732, Mitutoyo, Japan). During the harvest period, the middle portion of the soluble solids content (SSC) was measured using a handheld refractometer (Master-20a; ATAGO, Japan). To determine the total soluble sugar (TSS) content of pear fruits, a protocol previously described by Shi et al. (2023) was used with minor modifications. Fresh pear juice was extracted from the top, middle, and bottom of 20 randomly selected fruits from each treatment group using a juicer (Avance Collection HR1922/20; Philips, Netherlands). Subsequently, 2 mL of raw juice was diluted four times. Sucrose, glucose, fructose, and sorbitol contents were calculated using the external standard method, and the sum of these four sugars was considered as the TSS content. For further analysis, 1 mL of the supernatant was used for sugar and acid composition analyses by high-performance liquid chromatography (Waters e2695, USA). SS content was determined using a Ca-type sugar column (CARBOSep CHO-620; Transgenomic, USA) detected by a Water 2,414 Refractive Index Detector at 90°C, with a flow rate of 0.5 mL.min-1. The organic acid (OA) composition and content were determined using a C18 column (CNW Athena C18-WP; CNW, Germany) detected by Water 2,998 Photodiode Array Detector, with 0.2% metaphosphate as the mobile phase at a flow rate of 0.5 mL.min-1 and a temperature of 37°C. The sugar and acid standards used were of chromatographic purity provided by Sigma Corporation (USA). TSS and OA were mixed with different concentration gradients, and standard curves were drawn to measure their respective levels. The OA in the pears mainly consisted of tartaric acid, quinic acid, malic acid, and citric acid. Fruit texture was determined using a texture analyzer (TA-XT plus C; Stable Micro Systems, UK). Three test points were evenly spaced at the equatorial part of the fruit. A test probe P/5, cylindrical with a 5 mm diameter, was used with a test speed of 1 mm/s, test depth of 8 mm, and trigger value of 0.05 N (Figure 1C).

2.5 Soil DNA extraction and high-throughput sequencing of rhizosphere soil microbial communities

Pear tree rhizosphere soil samples from the SC and CC groups for two vertical soil layers (0–20 cm and 20–40 cm) were collected,

resulting in a total of four treatments. Each treatment consisted of six replicates per rhizosphere soil sample (Figures 1B,D). After collection, the samples were snap-frozen and stored at −80°C for further analysis. Bacterial DNA was isolated from the SC- and CC-treated rhizosphere soil samples using a MagPure Soil DNA LQ Kit (Magen, Guangdong, China) following the protocol described by Shi et al. (2023). Sextuplicate SC- and CC-treated rhizosphere soil samples of the hypervariable region V3–V4 of the bacterial 16S rRNA genes were amplified using universal primer pairs (343F: 5′-TACGGRAGGCAGCAG-3′; 798R: 5′-AGGGTATCTAATCCT-3′). Sequencing was performed on an Illumina NovaSeq6000 with two paired-end read cycles of 250 bases each (Illumina Inc., San Diego, CA, USA), following the protocol described by Shi et al. (2023).

Microbial diversity in the 24 pear tree rhizosphere soil samples was estimated using alpha diversity, which included the Chao1 and Shannon indices (Chao and Bunge, 2002; Hill et al., 2003). The UniFrac distance matrix generated using QIIME2 software (version 2018.2) was used for unweighted UniFrac principal coordinate analysis (PCoA) and phylogenetic tree construction. Sequencing and analysis of the 16S RNA gene amplicons were performed by OE Biotech Co., Ltd. (Shanghai, China). Based on the relative abundance of the soil samples, Spearman's correlation coefficient was calculated to determine the relationship between bacteria, physicochemical parameters, and metabolites in the sample group at the phylum and genus levels. By default, species with | Spearman Coef |> 0.8 and $p < 0.01$ were displayed on the map. If no matching results were found, a correlation network map was not provided.

2.6 UHPLC–MS and data analysis

Pear rhizosphere soil samples (500 mg) under the SC and CC treatments were analyzed using the ACQUITY UPLC I-Class system (Waters Corporation, Milford, USA) combined with a VION IMS QTOF mass spectrometer (Waters Corporation, Milford, USA). The metabolic spectra of the SC- and CC-treated soil samples were analyzed in the ESI positive ion and ESI negative ion modes. An ACQUITY UPLC HSS T3 column (100 mm × 2.1 mm, 1.8 μm) was employed in both positive and negative modes. Water containing 0.1% formic acid and acetonitrile containing 0.1% formic acid were used as mobile agents in Stage A and Stage B. The chromatographic gradient elution procedures were as follows: 0 min, 1% B; 1 min, 30% B; 2.5 min, 60% B; 6.5 min, 90% B; 8.5 min, 100% B; 10.7 min, 100% B; 10.8 min, 1% B; and 13 min, 1% B. The flow rate was 0.35 mL/min, and the column temperature was 45°C. Molecular masses of ion peaks were calculated for all extracts, and data analyses were conducted following the methods outlined by Hu et al. (2018).

2.7 GC–MS and data analysis

Rhizosphere soil samples (500 mg) under SC and CC treatments were analyzed using an Agilent 7,890 B gas chromatography system coupled with an Agilent 5,977 B MSD system (Agilent Technologies Inc., CA, USA). A DB-5MSfused-silica capillary column (30 m × 0.25 mm × 0.25 μm, Agilent J & W Scientific, Folsom, CA, USA) was utilized to separate the derivatives. Details of the GC–MS raw data, including chemical derivatization and gas chromatography–mass spectrometry (GC–MS) analyses, were carried out according to previous protocols (Kim et al., 2015).

2.8 Data preprocessing and statistical analysis

The matrix was imported into R to perform partial least squares discriminant analysis (PLS-DA) to observe the overall distribution among the soil samples and the stability of the entire analysis process. The metabolites were annotated using the Kyoto Encyclopedia of Genes and Genomes (KEGG) database[1] (Hill et al., 2003). Univariate analysis (*t*-test) was used to assess statistical significance (*p*-value). Metabolites that differed significantly between any two of the four treated groups were defined as those with a variable importance in the projection value >1.0, *p*-value <0.05, and fold change (FC) ≥ 1.5 or ≤ 0.667. Correlations between differential metabolites (DMs) were analyzed using the Pearson method in R.

3 Results

3.1 Impact of SC and CC on physicochemical rhizosphere soil parameters and enzyme activity

The physicochemical parameters of rhizosphere soil, encompassing EC, pH, TC, TN, SOC, SON, AN, and C:N ratio, were evaluated after a 20-year period in both SC and CC modes within pear orchards. The results demonstrated that SC treatment led to a significant increase in TC and TN levels, elevating from 12.70 g/kg to 17.65 g/kg and from 0.81 g/kg to 1.21 g/kg, respectively, in the 0–20 cm rhizosphere layer compared to CC treatment (Figure 2A) ($p < 0.001$). Moreover, SOC and SON content exhibited substantial increments under SC treatment, with a rise of 59.9 and 16.52% across both the 0–20 cm and 20–40 cm rhizosphere layers, while SON content specifically increased by 49.58% in the 0–20 cm rhizosphere layer. In addition, the C:N ratio in the SC group displayed an increasing trend in both the 0–20 cm and 20–40 cm layers, with a growth rate of 13.84% in the 20–40 cm soil layer ($p < 0.001$). Furthermore, AN content was significantly higher in SC groups compared to CC groups ($p < 0.05$), and SC treatment also resulted in increased AK content in the 0–20 cm rhizosphere layer (Supplementary Table S1).

The application of SC treatments led to a substantial decrease in soil EC, reducing from 669 μs/cm to 481 μs/cm in the 0–20 cm rhizosphere layer and from 666 μs/cm to 541 μs/cm in the 20–40 cm rhizosphere layer. Although SC treatment slightly lowered soil pH, this difference was not statistically significant (Figure 2B). In the 0–20 cm rhizosphere soil layer, the bioavailable fraction of AP experienced a significant long-term decrease under SC treatment. Medium elements such as calcium (Ca) and magnesium (Mg), as well as macroelements including iron (Fe), copper (Cu), manganese (Mn), zinc (Zn), and boron (B), showed significantly higher concentrations under SC treatment ($p < 0.05$) (Supplementary Table S1).

1 https://www.kegg.jp/

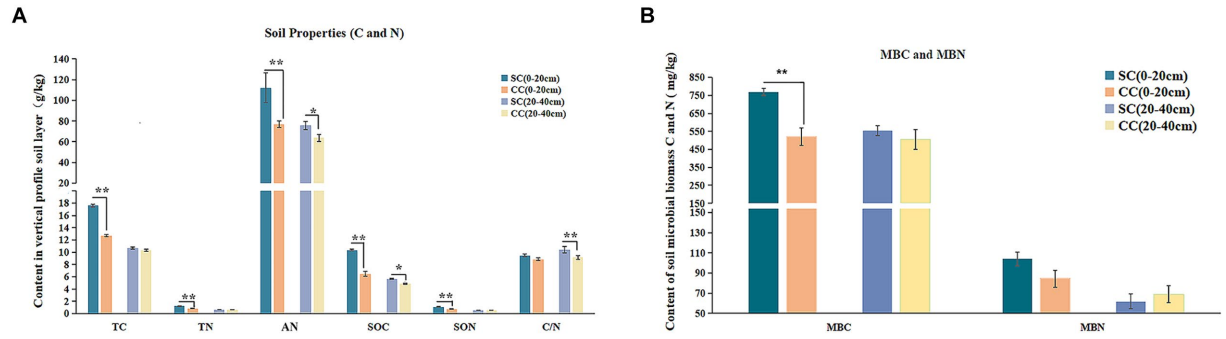


FIGURE 2
Physicochemical properties, enzyme activities, and microbial biomass between green bristlegrass coverage (SC) mode and clean cultivated mode (CC) in different rhizosphere soil layers in pear orchard. **(A)** The physicochemical properties of carbon and nitrogen. **(B)** The microbial biomass of carbon and nitrogen. Values are the means ($n = 3$) ± the standard deviation of the mean, * indicates statistical differences at $p < 0.05$ and ** indicates statistical extremely differences at $p < 0.01$.

TABLE 1 Soil enzyme activities between SC mode and CC mode in different rhizosphere soil layers in pear orchard.

Treatments	Vertical profile (cm)	SC (U/g)	β-GC (U/g)	CL (U/g)	S-PPO (U/g)	POD (U/g)
SC	0–20	119.67 ± 2.02 **	43.11 ± 2.53 *	3441.34 ± 152.40	73.44 ± 1.82 **	26.64 ± 0.68
CC		104.89 ± 7.24	37.10 ± 1.08	3308.23 ± 190.23	50.13 ± 3.06	27.64 ± 0.36
SC	20–40	129.08 ± 2.88 **	43.32 ± 0.82 *	4033.42 ± 131.59 **	73.01 ± 2.80 **	25.41 ± 0.40
CC		97.87 ± 0.90	36.58 ± 1.05	2482.27 ± 46.76	61.44 ± 3.12	30.40 ± 0.59**

S-SC, Soil sucrase; S-β-GC, soil-β-glucosidase; S-CL, soil cellulase; S-PPO, soil polyphenoloxidase; S-POD, soil peroxidase.
The table in the same column *indicates significant differences in independent sample t-test results between SC and CC treatments of 0–20 cm soil layer and 20–40 cm soil layer ($p < 0.05$), while **indicates extremely significant differences in independent sample t-test results between different treatments ($p < 0.01$).

The activities of five soil enzymes (S-SC, S-β-GC, S-PPO, S-POD, and S-CL) in SC and CC soil samples from pear orchards were measured. Notably, both S-β-GC and S-CL are critical enzymes for cellulose degradation. In the SC group, the activity of S-β-GC ranged from 43.11 U/g to 43.31 U/g in the 0–20 cm and 20–40 cm layers, representing increases of 16.20 and 18.41% compared to the CC group, respectively ($p < 0.001$). Similarly, S-CL activity showed increases of 4.02 and 62.49% in the same layers, respectively, compared to the CC group ($p < 0.001$) (Table 1). In addition, S-SC activity, responsible for sucrose breakdown into glucose and fructose, exhibited a similar rising trend as S-β-GC and S-CL activities ($p < 0.001$). Furthermore, SC treatment significantly enhanced S-PPO activity (increasing by 46.49 and 18.84%) during decomposition within the 0–40 cm rhizosphere of pear trees. However, S-POD activity in the SC group was notably decreased by 19.66% in the 20–40 cm rhizosphere layer compared to the CC group ($p < 0.001$). Pearson's correlation analysis revealed a significant negative correlation between S-β-GC activity and EC value ($r = 0.956$; $p < 0.05$) (Supplementary Figure S3).

3.2 Soil microbial biomass and soil microbial community response

In comparison with CC, SC significantly increased MBC and MBN by 47.78 and 23.33% in the 0–20 cm rhizosphere layer; however, no significant differences were observed in the 20–40 cm rhizosphere layer (Figure 2B). Pearson's correlation analysis revealed a significant positive correlation between MBC and SOC content, as well as between TC, TN, and SON contents ($R > 0.95$; $p < 0.05$) (Supplementary Figure S3).

Alpha diversity was assessed to analyze bacterial community complexity. Rarefaction curves for Chao and Shannon diversity per compartment reached a saturation plateau, indicating sufficient sequencing depth and reliable data across all samples (Supplementary Figures S1A,B). A total of 78,161–81,596 raw reads were obtained from 16S rRNA gene sequencing. After quality filtering and chimera elimination, the valid tags obtained ranged from 49,309 to 65,053, with 1,632–2,430 amplicon sequence variants (ASVs) per sample (Supplementary Table S2). The flower plot of ASV clustering analysis revealed that the SC (20–40 cm) group exhibited the highest number of ASVs (2,147), followed by the CC (0–20 cm) and SC (0–20 cm) groups, with the CC (20–40 cm) group showing the lowest (1,095 ASVs). The number of common and unique ASVs in different samples is shown in Figure 3A. Forty-three core ASVs were common among rhizosphere soils in both SC- and CC-treated groups. The Simpson index trended as SC (20–40 cm) > SC (0–20 cm) > CC (0–20 cm) > CC (20–40 cm), with Chao1, Shannon, and Simpson indices of SC in the 20–40 cm vertical rhizosphere soil layer significantly higher than those in the other three treatment groups (Figure 3B).

Differences within and between the CC- (control) and SC-treated groups across two vertical distributions were assessed using supervised discriminant analysis via PCoA based on Bray–Curtis distance. PC1 explained 12.76% of the variation, and PC2 explained 7.36%. Bacterial communities in SC-treated soils were distinctly separated from those in

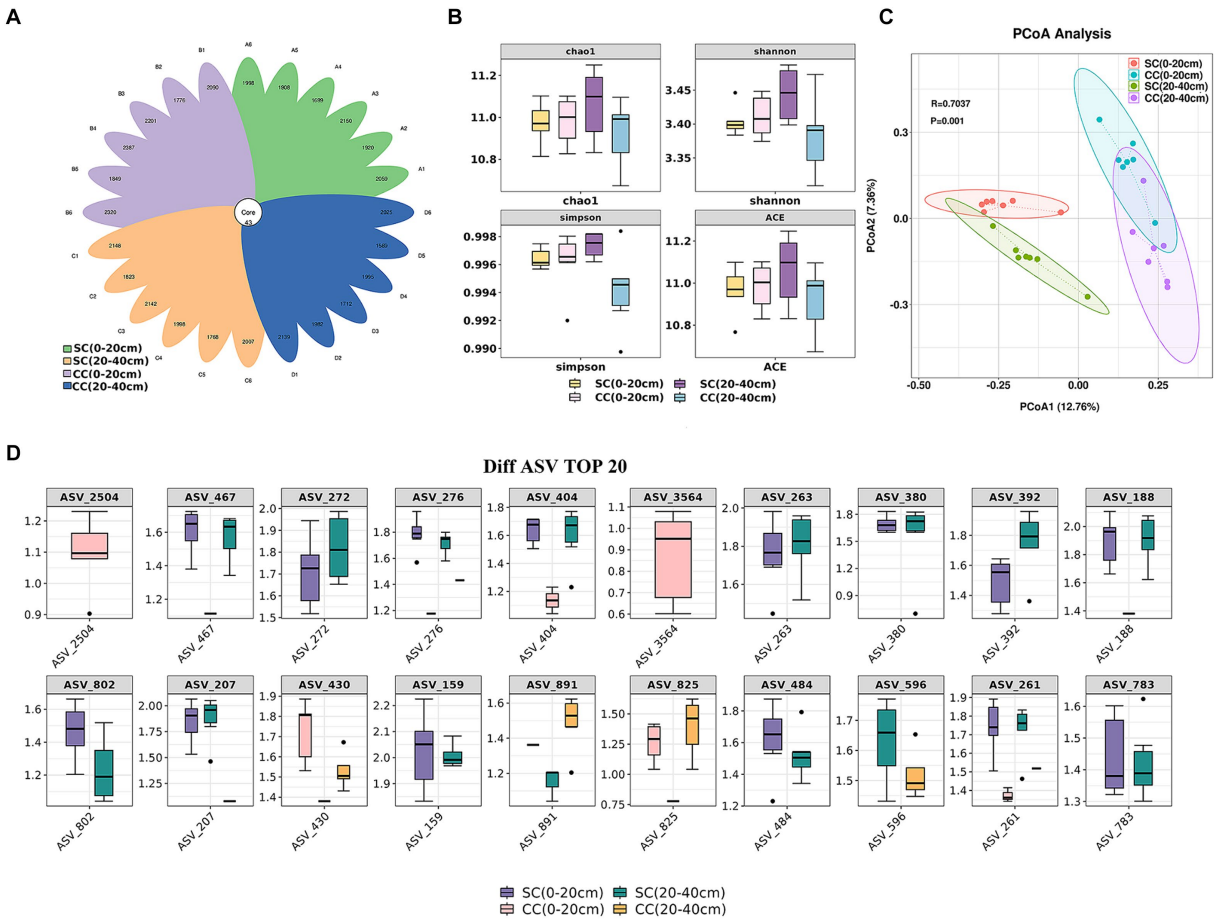


FIGURE 3
Vertical distribution of rhizosphere soil microbe diversity index between SC mode and CC in different rhizosphere soil layers in pear orchard. **(A)** The Venn diagram of difference AVS with each rhizosphere soil sample between SC mode and CC mode. **(B)** The boxplot of microbe diversity index at the AVS level. **(C)** Principal coordinate analysis (PCoA) diagram of SC and CC based on the Bray–Curtis distance matrix at the AVS level. **(D)** The box plot of the top 20 difference AVS with each rhizosphere soil sample at the AVS level.

CC in both the 0–20 cm and 20–40 cm soil layers (R^2 = 0.52, $p = 0.001$). The disparity in bacterial communities between treatments exceeded that between vertical layers (Figure 3C). The top 20 ASVs with differing abundances, identified via Kruskal–Wallis algorithm analysis (Figure 3D), indicated significant advantages in the CC-treated group for ASV_2504 and ASV_3546 (belonging to Burkholderiales and Candidatus Jorgensen bacteria, respectively) in the 0–20 cm rhizosphere; ASV_272, ASV_404, and ASV_188 (belonging to Gemmatimonadaceae) were more abundant in both the 0–20 cm and 20–40 cm vertical soil layers of the SC treatment group. ASV_276, ASV_263, and ASV_392 (belonging to Bacteroidia) also demonstrated a significant advantage in SC. Moreover, the relative abundances of ASV_159 and ASV_261 (belonging to CCD24) were significantly higher in SC than in CC.

3.3 Bacterial community composition and relationships with soil chemical properties at the phylum and genus levels

The relative abundance of bacterial communities exhibited similarity to that of dominant bacterial species; however, these dominant bacteria demonstrated distinct preferences in the SC- and CC-treated groups. The bacterial sequences were distributed across 35 phyla, 559 families, and 307 genera. At the phylum level, the dominant bacteria (relative abundance>2%) included Proteobacteria (37–43%), Bacteroidota (11–13%), Acidobacteriota (9–11%), Gemmatimonadota (6–7%), Firmicutes (3–5%), Actinobacteriota (3–5%), Myxococcota (3–4%), Nitrospirota (3–4%), RCP2-54 (2–3%), NB1-j (2–3%), and MBNT15 (2–3%) (Figure 4A). Pear orchards covered by SC exhibited a significant increase in Proteobacteria, Bacteroidetes, Gemmatimonadota, Firmicutes, Actinobacteria, and Fusobacteria and a decrease in Acidobacteriota, Nitrospirota, NB1-j, MBNT15, and Desulfobacterota compared to CC-treated orchards (Figure 4A). At the genus level, analysis of the top 50 genera revealed that SC treatment led to increased relative abundances of *MND1*, *Subgroup_22*, *Pseudomonas*, *mle1-7*, *Sphingomonas*, *BD2-11_terrestrial_group*, *Subgroup_5*, *CCD24*, *AKAU4049*, *Haliangium*, *Dongia*, *Ellin6067*, and *EPR3968-O8a-Bc78* in both rhizosphere layers (0–20 cm and 20–40 cm). Moreover, the relative abundances of *TRA3-20*, *NB1-j*, *bacteriap25*, *IS-44*, *Sva0485*, *Zixibacteria*, *Subgroup_13*, *MB-A2-108*, *Gaiella*, *Massilia*, *Subgroup_15*, and *Cellvibrio* differed in the CC group (Figure 4C).

Pearson's correlation analysis was conducted to define the correlation between chemical properties factors and the dominant phyla and genera

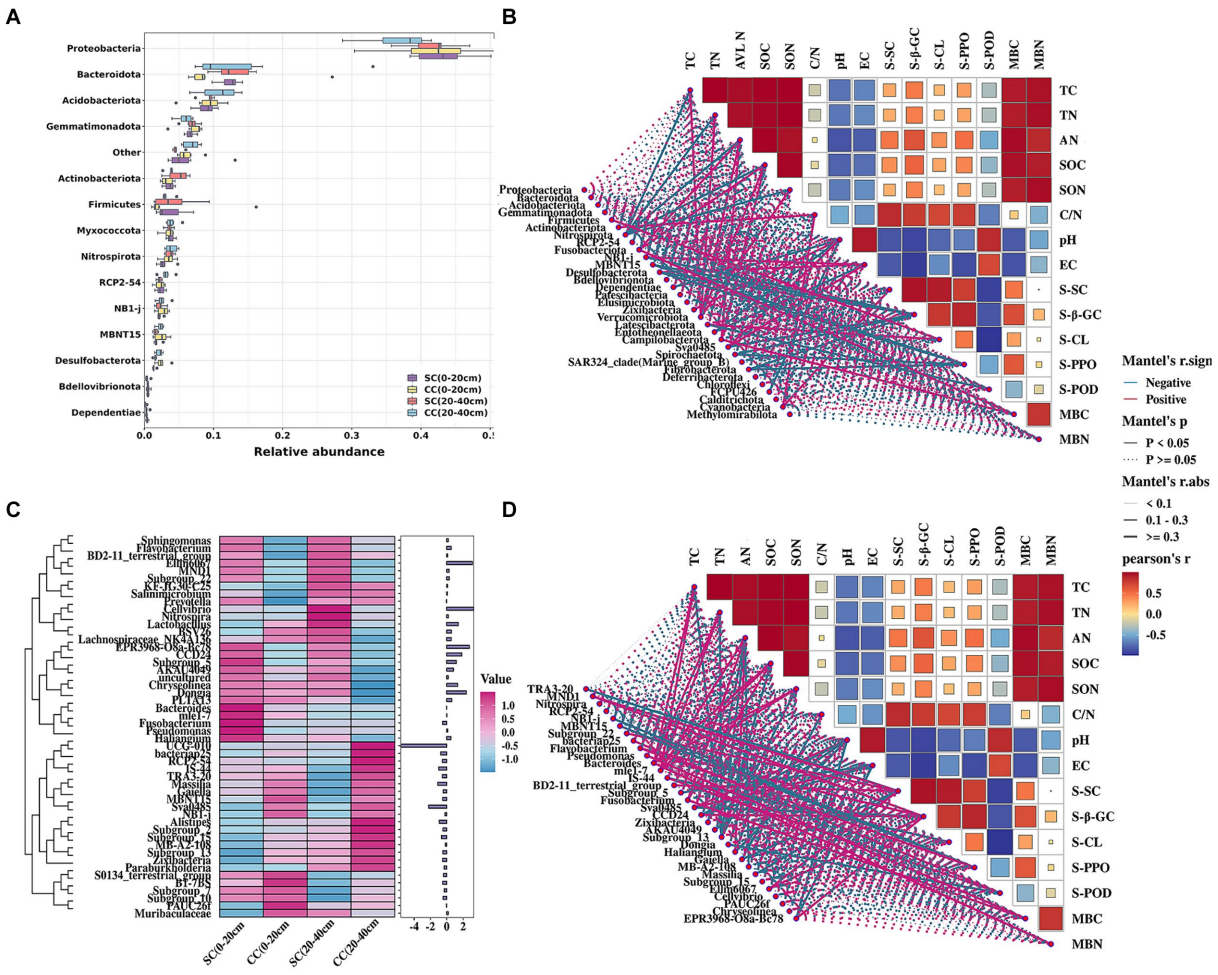


FIGURE 4
Relative abundance and the correlation between the soil bacterial community structure and physicochemical properties of pear rhizosphere soil between SC mode and CC mode in different rhizosphere soil layers in pear orchard. **(A)** The relative abundance of the top 15 dominant bacteria in phylum level. **(B)** The Spearman correlation heatmap of soil bacteria in phylum level and physicochemical properties. **(C)** The heatmap of relative expression of the top 50 dominant bacteria in genus levels. **(D)** The Spearman correlation heatmap of soil bacteria in genus level and physicochemical properties.

of the bacterial communities between SC and CC soils ($|R| > 0.80$ and $p < 0.05$). At the phylum level, Nitrospirota, Verrucomicrobiota, Chloroflexi, and Methylomirabilota were the key taxa highly related to soil properties, including TC, SOC, TN, SON, and AN. In addition, the activity of S-PPO was highly associated with Flavobacterium ($r = 0.967$), while S-SC was significantly positively associated with *MND1*, *Subgroup_22*, *BD2-11_terrestrial_group*, and *Ellin6067*. Soil salinization indicators, EC, and pH were significantly correlated with Sva0485 ($r = 0.982$) and Dependentiae ($r = 0.817$) (Figure 4B). Twenty-five genera were highly associated with soil physicochemical parameters (Figure 4D; Supplementary Table S3), soil enzyme activity, and microbial biomass.

We utilized linear discriminant analysis effect size (LEfSe) to identify biomarkers with significant differences between the treated groups (LDA > 2; $p < 0.05$) (Figure 5). This analysis revealed that the minimum number of discriminant clades was associated with soil organic carbon (SC) between the 0–20 cm (seven biomarkers) and 20–40 cm (six biomarkers) soil layers, while the maximum number was found in the SC (49) and conventional carbon (CC) groups (20) at the 20–40 cm soil depth (Figures 5A,B). The orders Veillonellales_Selenomonadales (LDA = 3.1446, $p = 0.022$) and Paenibacillaceae (LDA = 3.020, $p = 0.037$), belonging to Firmicutes, were significantly enriched in the SC (0–20 cm) group. In addition, several genera such as Candidatus_Accumulibacter (LDA = 3.525, $p = 0.022$), *Chryseolinea* (LDA = 3.018, $p = 0.004$), *AKAU4049* (LDA = 3.128, $p = 0.037$), *CCD24* (LDA = 3.492, $p = 0.004$), *Subgroup_5* (LDA = 3.244, $p = 0.010$), *Dongia* (LDA = 3.308, $p = 0.004$), *Ellin6067* (LDA = 3.348, $p = 0.004$), *Acidibacter* (LDA = 3.187, $p = 0.003$), *SWB02* (LDA = 3.024, $p = 0.010$), *Flavobacterium* (LDA = 3.013, $p = 0.004$), and *MND1* (LDA = 3.112, $p = 0.025$) were significantly enriched under the SC (20–40 cm) treatment. In the SC-treated group within the 0–20 cm soil layer, a significant increase in the abundance of 32 biomarkers was observed compared to the CC treatment. Notably, genera such as *Ellin6067*, *Acidibacter*, *Bacteroides*, *EPR3968_O8a_Bc78*, *CCD24*, and *MND1* belonging to the Proteobacteria phylum exhibited higher abundance in SC-treated soils (Figure 5D). Conversely, in the CC-treated group within the 20–40 cm soil layer, biomarkers from the Bacteroidota phylum, including MND1 and IS_44, as well as Sva0485, bacteriap25, and IS_44, were identified as highly abundant (Figure 5B). The KEGG pathway heatmap indicated a greater metabolic potential in

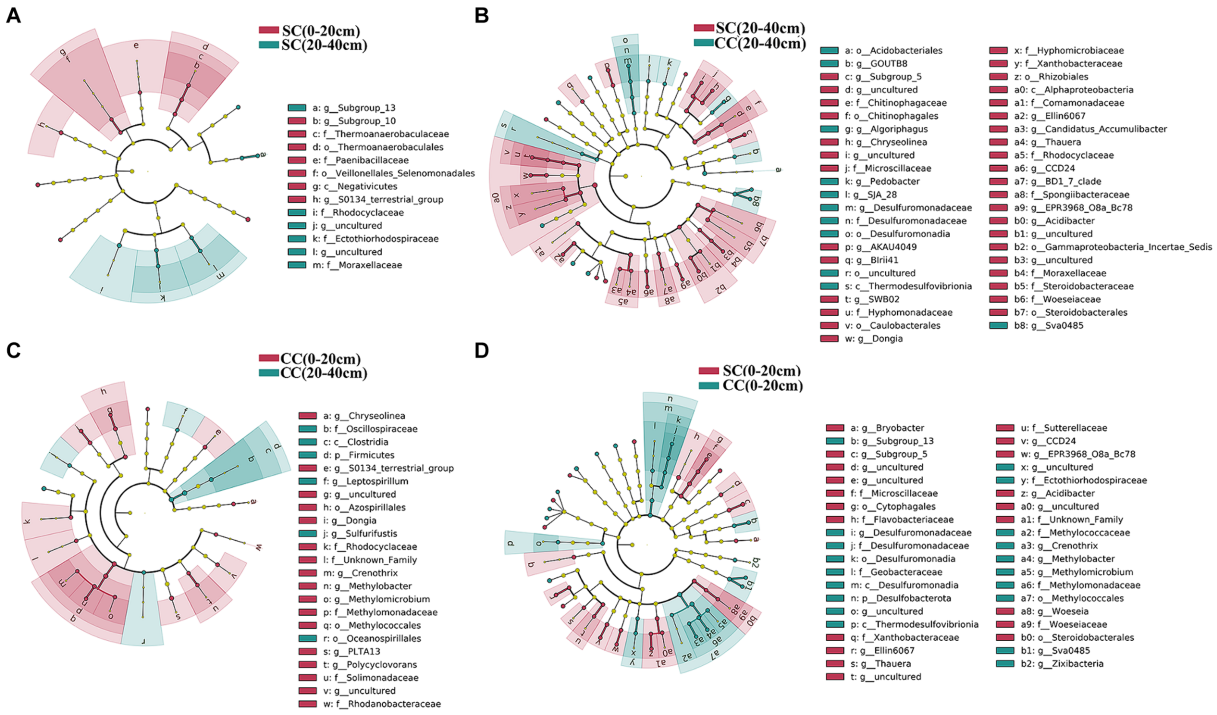


FIGURE 5
Cladogram plotted from LEfSe comparison analysis indicating the taxonomic representation of statistically and biologically consistent differences of identified biomarkers between SC and CC treatments in different rhizosphere soil layers. **(A)** SC (0–20 cm) vs. SC (20–40 cm); **(B)** SC (0–20 cm) vs. CC (0–20 cm); **(C)** CC (0–20 cm) vs. CC (20–40 cm); **(D)** SC (20–40 cm) vs. CC (20–40 cm). The colored shadows represent trends of the significantly different taxa. The red or blue shading depicts bacterial taxa that were significantly higher or lower in each proportioning of SC and CC treatment whereas species with no significant difference are uniformly colored black.

SC-treated soils compared to CC soils across both 0–20 cm and 20–40 cm soil layers. This enhanced potential encompassed cellular immunity, cell growth and death, xenobiotic biodegradation and metabolism, lipid metabolism, amino acid metabolism, carbohydrate metabolism, cofactor and vitamin metabolism, and energy metabolism (Figure 6A).

Redundancy analysis (RDA) was conducted to investigate the impact of soil physicochemical factors on bacterial communities. Eleven major environmental factors were found to significantly affect the distribution of rhizosphere bacterial communities in the SC and CC soil samples across both 0–20 cm and 20–40 cm soil layers ($p = 0.032$) (Figure 6B). The eigenvalues of the first two ranking axes of RDA explained 27.68 and 6.40% of bacterial community changes, respectively, which were positively correlated with the activity of S-PPO and the C:N ratio. This suggests that the observed change in microbial community structure may be attributed to the long-term application of SC treatment, leading to alterations in soil physicochemical factors. Furthermore, the C:N ratio and PPO activity emerged as the main factors affecting rhizosphere bacterial community structure ($F = 1.459$, $p = 0.032$), with Ellin6067 showing a positive correlation with S-PPO activity ($r = 0.60$, $p = 0.001$).

3.4 Response of soil metabolites to SC and CC in pear orchard rhizosphere

To investigate the impact of soil amendments on rhizosphere soil metabolites in pear orchards, we conducted a comprehensive metabolomic analysis using UHPLC–MS/MS and GC–MS/MS platforms. A total of 5,107 known metabolites were identified across two soil layers in both SC and CC treatment groups. Partial least squares discriminant analysis (PLS-DA) highlighted distinct metabolite profiles between SC and CC treatments across different soil layers. The model demonstrated robustness in discerning discriminant metabolites (DMs) from LC–MS and GC–MS data (R2Y = 0.97, Q2Y = 0.69 for LC–MS; R2Y = 0.90, Q2Y = 0.66 for GC–MS), indicating significant differences among treatment groups and soil depths (Figures 7E,F). Volcano plots identified 613 DMs (33 from GC; 580 from LC) and 645 DMs (29 from GC; 616 from LC) between SC and CC groups across soil metabolites (Figures 7A,B,D). Specifically, within the 0–20 cm soil layer, 612 DMs were observed in SC (0–20 cm) vs. CC (0–20 cm), predominantly consisting of fatty acyls (10.93%), glycerophosphoglycerols (7.18%), carboxylic acids and derivatives (6.53%), phenols and prenol lipids (5.71%), amino acids, peptides, and analogs (5.55%), as well as carbohydrates and carbohydrate conjugates (3.92%). In the 20–40 cm soil layer, 645 DMs were identified in SC (20–40 cm) vs. CC (20–40 cm), primarily including amino acids, peptides, and analogs (12.71%), fatty acyls (9.30%), carboxylic acids and derivatives (13.18%), carbohydrates and carbohydrate conjugates (5.89%), and phenols and prenol lipids (2.48%) (Supplementary Tables S5, S6).

KEGG pathway enrichment analysis revealed 50 DMs enriched in pathways related to sphingolipid metabolism, ABC transporters, glycerophospholipid metabolism, purine metabolism, phosphotransferase system, biosynthesis of secondary metabolites, fructose and mannose metabolism, and carbohydrate digestion and absorption (Figures 7G,H; Supplementary Table S7). Compared to CC treatment, SC treatment resulted in significant upregulation of several

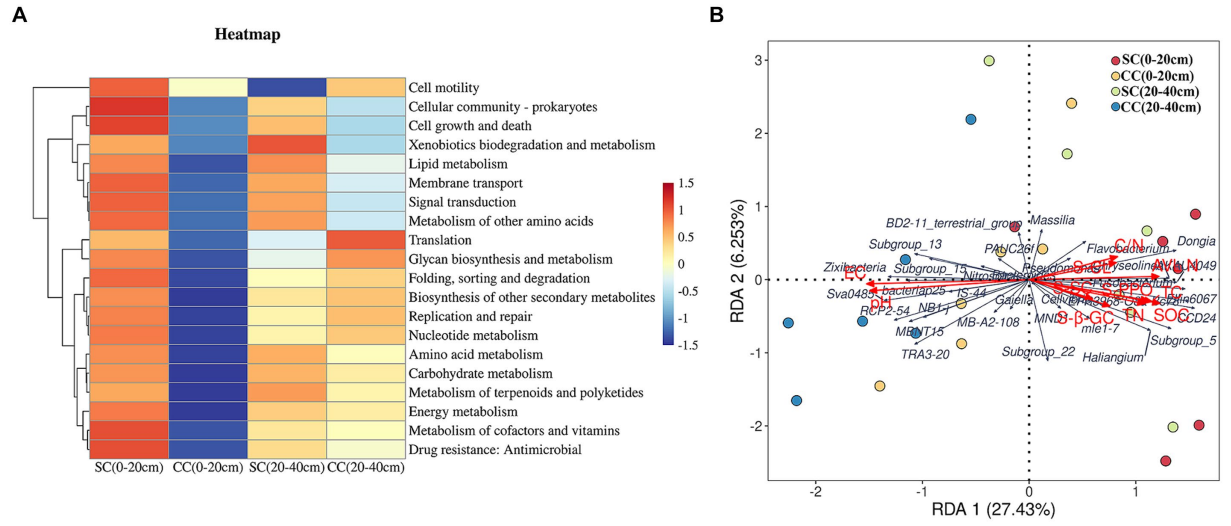


FIGURE 6
KEGG pathway heatmap of dominant soil bacteria and its relationship with soil properties and dominant soil in genus level between SC and CC treatments in different rhizosphere soil layers. **(A)** KEGG pathway heatmap of dominant soil bacterial in the genus level. **(B)** Redundancy analysis (RDA) of soil physicochemical properties with dominant soil bacterial in the genus level.

metabolites, including sucrose (1.48- and 2.52-fold), rhamnose (3.21- and 1.77-fold), N-acetyl-D-glucosamine (0.75- and 1.81-fold), D-(+)-raffinose (2.23- and 0.99-fold), stachyose (2.07- and 0.84-fold), D-mannitol (2.23- and 3.01-fold), D-maltose (4.28- and 2.29-fold), and beta-D-fructose 2,6-bisphosphate (3.42- and 0.53-fold), all belonging to carbohydrates and carbohydrate conjugates. In addition, OAs and derivatives such as pyrrolidonecarboxylic acid (4.59- and 27.70-fold), 2-keto-3-deoxy-D-gluconic acid (4.70- and 5.45-fold), and N-acetyl-L-glutamic acid (2.21- and 3.72-fold) were increased in SC-treated soils across both 0–20 cm and 20–40 cm soil layers. Conversely, organic nitrogen compounds including sphinganine, phytosphingosine, and diethanolamine were significantly downregulated in SC treatments ($p < 0.05$) (Supplementary Table S7).

3.5 Assessment of agronomic traits of pear trees (2022–2023): impacts of long-term SC and CC management

Based on the comprehensive evaluation of agronomic traits of pear trees conducted in 2022 and 2023, significant alterations were observed in both the rhizosphere environment and the agronomic characteristics of pear fruits following 20 years of natural grass management (Table 2; Supplementary Table S4). The study revealed that the yield in the SC group was markedly higher than in the CC group, attributable to increased SFW and a higher number of FNP, resulting in yield increments of 62.72 and 35.40%, respectively. Specifically, the average SFW in the SC treatment surpassed that in the CC treatment by 10.01 and 10.34%. In 2022, the significant difference ($p<0.05$) in fruit size between the SC and CC treatments was primarily reflected in the VD, with the SC treatment showing a significant increase of 5.06%, while the difference in LD was not statistically significant ($p \geq 0.05$). In 2023, the extremely significant difference ($p < 0.01$) in fruit size between the SC and CC treatments was reflected in the LD of fruit size, while there was no significant difference in VD between SC and CC groups ($p \geq 0.05$).

SSC is a critical indicator of fruit flavor quality and maturity. During the period from 2022 to 2023, the SSC in fruits from the SC treatment exhibited a substantial increase of 8.86 and 5.75% compared to the control (Table 2). SSC primarily comprises TSS and OAs. This study further analyzed specific sugars and acids based on SSC variations induced by SC treatment. The sum of sucrose, glucose, fructose, and sorbitol constituted the TSS content. The 'Cuiguan' pear fruits reached maturity, and the SC treatment significantly elevated TSS and sucrose content ($p < 0.001$). The sucrose content in SC-treated pear fruits was approximately 2.43–3.96 times higher than that in CC-treated fruits, with no significant differences observed for other sugars. The advantage in TSS content under SC treatment primarily stemmed from the increased sucrose content (Figure 8A). In 2022, the OA content of fruits in the SC group showed a significant increase of 11.12% compared to the CC group ($p < 0.001$), although this difference was not significant in 2023. Similar to TSS, malic acid was the primary organic acid contributing to the OA content difference (Figure 8B). The results of Pearson's correlation cluster analysis revealed a positive correlation between indicators such as fruit number per plant, vertical and lateral diameter, soil organic nitrogen (SON), soil organic carbon (SOC), available nitrogen in soil (AN), soil carbon content (C), microbial biomass carbon (MBC), and microbial biomass nitrogen (MBN) and a negative correlation with electrical conductivity (EC) and pH. Moreover, regarding fruit quality, TSS including sucrose and glucose, as well as titratable acidity in OA represented by quinic acid, exhibited a significant correlations with SON, SOC, AN, TC, MBC, MBN, and soluble polyphenol oxidase (S-PPO) in the SC-treated groups (Supplementary Figure S2) ($R > 0.9$; $p < 0.001$).

3.6 Interactions between metabolites and rhizosphere soil PGPMs contributing to agronomic traits in pear fruit

To further investigate PGPMs associated with pear fruit development and nutrient accumulation, we analyzed the

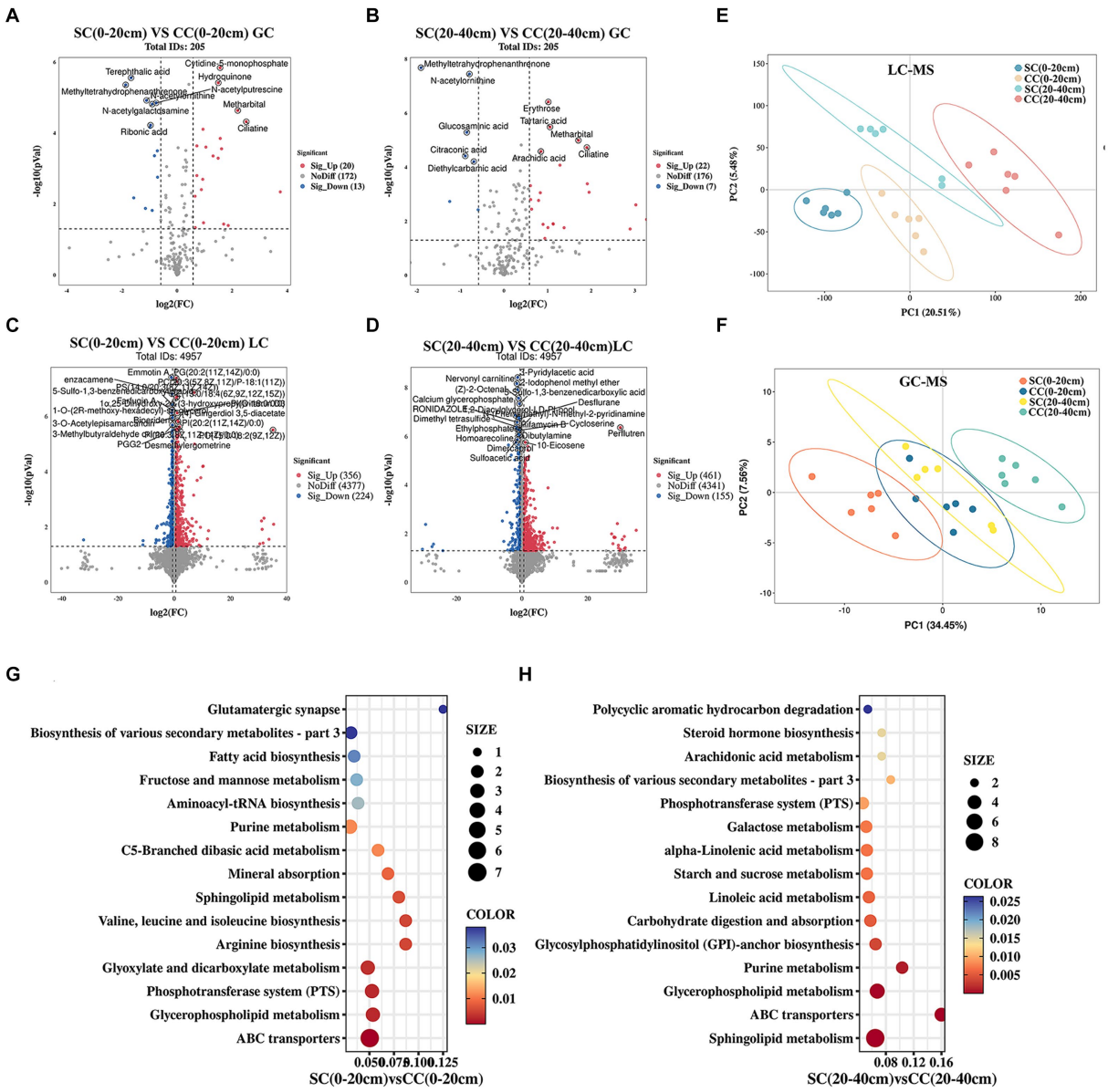


FIGURE 7
Metabolomic analysis of soil SC and CC treated in different rhizosphere soil layers. **(A,B)** The expression volcano map of DMs up- and downregulate between SC and CC in 0–20 cm and 20–40 cm soil layer by GC–MS. **(C,D)** The expression volcano map of DMs up- and downregulate between SC and CC in 0–20 cm and 20–40 cm soil layer by LC–MS. Green dots represent downregulated metabolites, red dots represent upregulated metabolites, and gray dots represent no-differential metabolites. **(E,F)** Principal coordinate analysis (PCoA) diagram of SC and CC based on the Bray–Curtis distance matrix based on the DMs by LC–MS and GC–MS. **(G,H)** Bubble diagram of the KEGG enrichment of DEMs from SC- and CC-treated groups in 0–20 cm and 20–40 cm soil layer.

TABLE 2 **Fruit qualities and yields between SC mode and CC mode in different rhizosphere soil layer in pear orchard (2022–2023).**

Treatment	Year	SFW (kg)	LD (mm)	VD (mm)	SSC (%)	FNP	Yield (kg)
SC	2023	423.00 ± 66.17 *	91.30 ± 7.28 **	94.00 ± 8.37	12.37 ± 0.59 *	122.10 ± 11.40 **	46247.00 ± 4316.54 **
CC		384.49 ± 30.20	79.92 ± 3.12	89.57 ± 2.58	11.70 ± 0.72	103.90 ± 9.10	34155.98 ± 2990.74
SC	2022	420.89 ± 6.70 *	95.13 ± 6.70	100.59 ± 6.55 *	12.61 ± 0.58 *	114.90 ± 10.65	41348.02 ± 3832.70 **
CC		381.42 ± 40.37	92.97 ± 3.91	95.75 ± 3.20	11.59 ± 0.57	105.60 ± 12.22	25410.84 ± 2941.02

SFW, Single fruit weight; LD, Lateral diameter; VD, Vertical diameter; SSC, Soluble solid content; FNP, Fruit number per plant.
The table in the same column *indicates significant differences in independent sample t-test results between SC and CC treatments of 0–20 cm soil layer and 20–40 cm soil layer ($p < 0.05$), while **indicates extremely significant differences in independent sample t-test results between different treatments ($p < 0.01$).

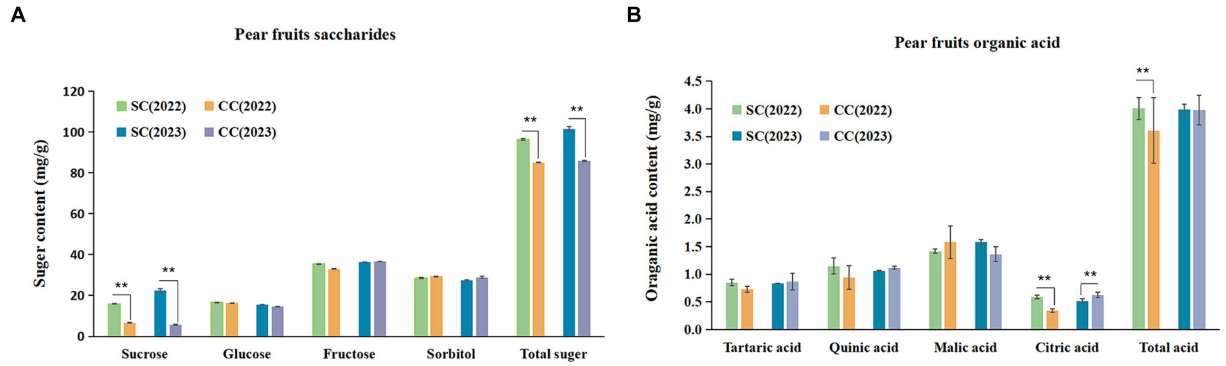


FIGURE 8
Soluble sugar (SS) composition and organic acid (OA) of pear fruits between SC and CC treatments in different rhizosphere soil layers. **(A)** The soluble sugar (SS) composition and organic acid (OA) of pear fruit. **(B)** The organic acid (OA) of pear fruits. Values are the means ($n = 3$) ± the standard deviation of the mean, * indicates statistical differences at $p < 0.05$, and ** indicates statistical extremely differences at $p < 0.01$.

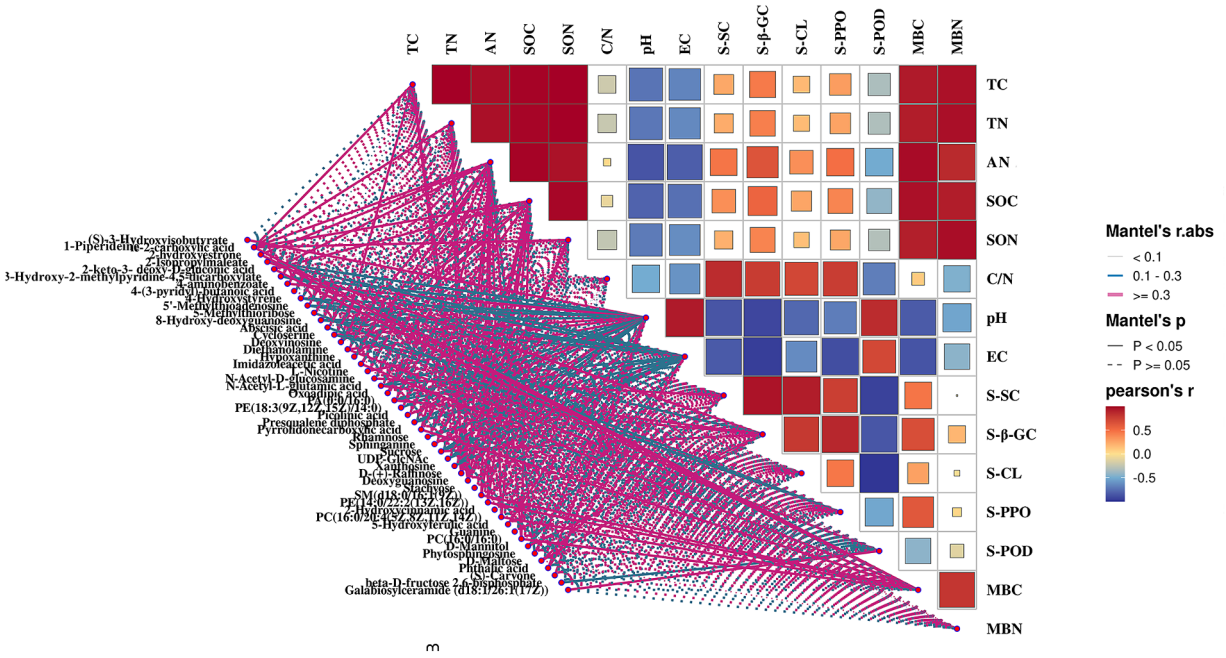


FIGURE 9
Spearman's correlation heatmap of soil bacteria in genus level and soil DMs.

correlation between carbon and nitrogen sources in SC and CC rhizosphere soils using Pearson's correlation. Soil microorganisms and their metabolites were primary sources of these elements. According to Pearson's correlation cluster analysis, fruit yield indicators, such as fruit number per plant, and vertical and lateral diameter, showed significant positive correlations with TC, TN, SON, SOC, AN, C:N, MBC, and MBN and negative correlations with EC and pH. In addition, in terms of quality, TTS (sucrose, glucose) and OA (quinic acid), which determine the intrinsic quality of fruit, were significantly correlated with TC, TN, SON, SOC, AN, C:N, MBC, MBN, and S-PPO and negatively correlated with EC and pH in SC-treated groups (Supplementary Figure S2) ($R > 0.9$; $p < 0.001$).

To optimize the presence of PGPMs for maximizing both pear yield and quality, we utilized the Mantel test ($p < 0.05$) to examine correlations between microorganisms and their metabolites (Figure 9). The results revealed significant correlations: diethanolamine ($r = 0.862$), N-acetyl-d-glucosamine ($r = 0.862$), D-maltose ($r = 0.849$), and galabiosylceramide (d18:1/26:1(17Z)) ($r = 0.618$) with the bacteria MND1, which also correlated with soil enzyme activities S-β-GC, S-CL, and S-POD. D-mannitol ($r = 0.876$) exhibited a significant correlation with the bacteria NB1-j, which further correlated with S-β-GC activity ($r = 0.977$). Galabiosylceramide (d18:1/26:1(17Z)) ($r = 0.811$), N-acetyl-d-glucosamine ($r = 0.801$), diethanolamine ($r = 0.680$), and D-maltose ($r = 0.520$) correlated with the bacteria IS-44 and significantly correlated with S-SC activity ($r = 0.742$). In

addition, metabolites such as 2-hydroxyestrone, 4-hydroxystyrene, imidazoleacetic acid, L-nicotine, presqualene diphosphate, sphinganine, SM (d18:0/16:1(9Z)), PE (14:0/22:2(13Z,16Z)), PC (16:0/20:4 (5Z,8Z,11Z,14Z)), PC (16:0/16:0), phytosphingosine, and phthalic acid showed significant correlations with Subgroup_5 and Sva0485, which in turn significantly correlated with MBC content ($r = 0.572$; $r = 0.583$). The bacteria from Subgroup_15 were found to positively correlate with deoxyinosine ($r = 0.977$), hypoxanthine ($r = 0.989$), oxoadipic acid ($r = 0.972$), D-(+)-raffinose ($r = 0.929$), deoxyguanosine ($r = 0.977$), and guanine ($r = 0.979$), as well as with TC ($r = 0.640$), TN ($r = 0.618$), SOC ($r = 0.761$), SON ($r = 0.592$), and AN ($r = 0.854$). Dongia bacteria showed positive correlations with S-CL ($r = 0.747$) and S-POD ($r = 0.872$) activities, diethanolamine ($r = 0.836$), N-acetyl-d-glucosamine ($r = 0.728$), D-maltose ($r = 0.712$), and galactosylceramide (d18:1/26:1(17Z)) ($r = 0.990$).

4 Discussion

4.1 Remediation effect of returning natural grass on soil carbon and nitrogen stocks and utilization in pear orchard

CC, where grass is removed through clean tillage, is the main reason for exacerbated soil degradation (Novikova et al., 2013). This study highlights that topsoil degradation in cleared orchards primarily manifests through chemical and biological processes. Over a 20-year period, CC-treated soil exhibited an EC value of 667 μs/cm, categorizing it under moderate saline-alkali conditions (400–800). Conversely, continuous SC treatment effectively mitigated soil salinization by reducing EC values and lowering alkaline soil pH. This suggests that SC application can alleviate the adverse effects of excessive chemical fertilizers in pear orchards. Significant reductions in rhizosphere and bulk soil pH were observed following ryegrass coverage (Wang et al., 2023; Zhou et al., 2023), likely attributed to OA secreted by grass roots (Matocha et al., 2018). In SC-treated groups, OA levels were notably higher compared to CC-treated soil. Further analysis of rhizosphere metabolites indicated substantial upregulation of OAs such as oxoadipic acid, N-acetyl-L-glutamic acid, 2-keto-3-deoxy-D-gluconic acid, and pyrrolidonecarboxylic acid post-SC treatment, suggesting their role in pH reduction. Zhalnina et al. (2018) demonstrated that plant rhizosphere bacteria preferentially utilize aromatic organic acids secreted by plants.

Numerous studies have illustrated that grass roots significantly influence SOC stocks. Water-soluble small molecules from SOC can be absorbed by roots, promoting their growth (Gregory et al.,2022; Gómez et al., 2022). Continuous grass coverage enhances TC and SOC content, contributing to orchard economic benefits (Liu et al., 2021). Despite a decrease in TC to 10.32 g/kg and SOC to 6.46 g/kg after over 20 years of pear fruit harvesting and pruning, SC-treated soil exhibited significant increases in TC, SOC, and C:N ratio by 38.9, 58.9, and 13.84%, respectively. This enhancement correlated significantly with TSS accumulation, fruit size, and yield, underscoring the positive impact of grass coverage on plant productivity. Grass mulching over 2 years improved soil nutrients and organic carbon, thereby enhancing total soluble fruit quality (Lienhard et al., 2013; Dong et al., 2021), a finding corroborated by Homma et al. (2012). While much research has focused on SOC's impact on soluble solids in fruits, investigations into soluble sugars and OA remain limited. In SC treatment group, the contents of sucrose and glucose in TSS and quinic acid in OA, which determine fruit quality, were significantly correlated with SON, SOC, and C: N ratio in soil. Moreover, fruit yield, linked to soil C, echoed findings from studies on organic carbon addition (Shi et al., 2023).

Research confirms that orchards emit significantly more carbon than other arable lands. Grass coverage enhances soil carbon storage and reduces carbon emissions (Zhao et al., 2022). Decomposing grass, as green manure, releases soil nutrients and undergoes mineralization into inorganic nitrogen by the soil microbiome (Daly et al., 2021). SC treatment increased soil TN and available nitrogen in soil AN, consistent with findings by Zhou et al. (2023) and Wang et al. (2023). Interestingly, different grass varieties have varied effects on AP values in orchards. Unlike CC, hairy vetch (*Vicia villosa* Roth.) coverage notably increased available phosphorus content, while ryegrass (*Lolium perenne* L.) had no significant effect. Green bristlegrass coverage, conversely, reduced available phosphorus levels. The experimental site exhibited high AP, exceeding the normal range (10–20 mg/g), as previously documented. High-phosphorus treatments enhance grass phosphorus absorption and accumulation, potentially mitigating AP accumulation in orchard soils (Kaneko et al., 2008). Therefore, SC emerges as a promising strategy to alleviate soil AP risks in the orchard.

4.2 Variations in the diversity and dynamics of rhizosphere soil communities

In comparing microbial diversity between SC and CC treatments across different soil layers, we observed that the highest species richness (ACE, Chao1) and microbial community diversity (Shannon diversity index, $p < 0.05$) occurred in SC-treated soil at the 20–40 cm layer. LEfSe analysis showed that the SC (49) and CC (20) groups in this layer had the highest number of discriminant clades, confirming greater bacterial community diversity in SC treatments. According to β-multivariate statistical analysis, the impact of grass growth on microbial diversity was significantly greater than the effect of vertical distribution within the same treatment. SC treatment increased bacterial population size and altered community composition, consistent with the results of Zhang et al. (2018). At the phylum level, Proteobacteria, Bacteroidetes, Acidobacteria, Gemmatimonadota, Firmicutes, Actinobacteria, Myxococcus, Nitrospirota, RCP2-54, NB1-j, and MBNT15 were dominant bacteria (relative abundance >2%) in pear orchards. SC-treated orchards showed significant increases in Proteobacteria, Bacteroidetes, Gemmatimonadota, Firmicutes, Actinobacteria, and Fusobacteria compared to CC-treated orchards. Firmicutes were highly correlated with soil nutrient content, as noted by Zhao et al. (2022) and Zhang et al. (2022).

The priming effect (PE) of grassland orchards returning ecosystems to exposed topsoil accelerates the process of soil SOC and SON input and decomposition into micromolecular monomers over a short period of time, with soil enzymes and microorganisms playing crucial roles (Guenet et al., 2010). On a large scale, SC treatment positively impacted MBC and MBN, particularly enhancing soil microbial diversity in pear orchards. The regulation of MBC and MBN was observed to be influenced by TC, TN, SOC, SON, and available nitrogen (AN) content ($R > 0.95$, $p < 0.05$). Gregory et al. (2022) and Xiang et al. (2023) reported that, compared with CC treatment, SC

generally increased soil MBC and bacterial abundance irrespective of orchard age. On a smaller scale, the analysis focused on the correlation between the dominant bacteria among the top 30 in soil microbial relative abundance and carbon and nitrogen utilization under SC treatment. Correlation analyses indicated significant positive associations between the relative abundances of Nitrospirota, Verrucomicrobiota, Chloroflexi, Actinobacteria, Cyanobacteria, and Methylomirabilota with the accumulation of TC, TN, SOC, SON, and the C:N ratio. Specifically, the phylum Nitrospirota (Nitrospirae) exhibited notable increases with SOC elevation under ryegrass coverage (Rodríguez-Loinaz et al., 2008). Bacteroides, mle1-7, and Fusobacterium showed positive correlations with SOC, SON, and AN, while MND1, Subgroup_22, BD2-11_terrestrial_group, Ellin6067, and Flavobacterium were associated with S-SC enzymes involved in soil carbon cycling. Prior research highlighted the significant relationship between MND1 and mle1-7 and increased organic carbon in soils (Shi et al., 2023). MND1 plays a critical role in soil carbon and nitrogen cycles, linked to enhanced recalcitrant SOC storage (Hu et al., 2018). Cellvibrio exhibited a significant association with the C:N ratio. Grass, acting as a carbon source, secretes cellulose that facilitates its decomposition into organic carbon sources, thereby enhancing soil carbon levels (Yu et al., 2019). The application of SC treatment resulted in an increased relative abundance of AKAU4049 within both rhizosphere layers (0–20 cm and 20–40 cm), accompanied by a decrease in soil pH. Conversely, a decline in the AKAU4049 genus of the Gemmatimonadota phylum following the introduction of ryegrass suggested optimal soil entropy and nutrient enrichment (Zhou et al., 2023). Variations in AKAU4049 levels may be attributed to differences in soil conditions and grass species utilized.

In the rhizosphere soil treated with SC, the activities of S-SC, S-CL, and S-β-GC enzymes showed significant increases compared to CC treatment. Particularly, S-CL activity exhibited positive correlations with the relative abundance of Firmicutes and Latescibacterota. In agricultural fields practicing multiple crop intercropping, S-CL levels were notably elevated, driven by Firmicutes, Latescibacteria, Gemmatimonadetes, and Acidobacteria, crucial for cellulose decomposition (Zhang et al., 2018). Moreover, S-SC enzyme activity demonstrated correlations with cyanobacteria. Research by Xu et al. (2023) conducted topsoil treatments with artificial cyanobacterial crusts, directly confirming their role in accelerating S-SC enzyme activity recovery.

4.3 Integrated analysis of microbial communities and metabolites reveals responses of soil microorganisms

The presence of active microbial communities in the rhizosphere significantly influences soil metabolites, thereby impacting the circulation and metabolism of exogenous nutrients (Cheng et al., 2022). This study examines the interplay between soil metabolites and bacterial communities. Treatment with SC (presumably a soil conditioner or similar) alters the synthesis of various compounds including carbohydrates, phenols, lipids, amino acids, peptides, fatty alcohols, carboxylic acids, and their derivatives. Sucrose, N-acetyl-D-glucosamine, and beta-D-fructose 2,6-bisphosphate are enzymatically catalyzed by NAGase to release nitrogen from the soil, enhancing carbon and nitrogen utilization (Omari et al., 2012). These compounds, synthesized via glycolysis, play crucial roles in plant growth and development (Cheng et al., 2022).

Of particular interest, SC promotes the sequestration of organic carbon in soil, leading to increased sucrose accumulation in aboveground pear fruits and rhizospheric secretion. This phenomenon suggests that Bacteroides mle1-7 and Fusobacterium accelerate organic carbon decomposition, thereby enhancing plant carbon absorption, utilization, and synthesis. D-(+)-raffinose, correlated significantly with SOC stock, is part of carbon allocation strategies and may signal stress responses (Li et al., 2020). Conversely, sphinganine, an organic nitrogen compound, is notably downregulated in SC-treated soils. Yang et al. (2021) identified a higher abundance of *Sphingomonas* genus in soil with ryegrass compared to soil without, with SC-treated rhizosphere soils showing significantly elevated Sphingomonas levels. The decrease in sphingosine levels could be attributed to sphingomonas utilizing sphingosine as a carbon and energy source, necessitating its decomposition. Abscisic acid (ABA), a key phytohormone regulating stress responses, is significantly downregulated in SC treatments, potentially promoting pear fruit growth. Studies by Li et al. (2019) suggest that ABA impacts rhizosphere microbial communities and plant physiology, influencing growth characteristics such as height in peanut plants. The relationship between soil bacterial communities and aboveground pear trees is progressively elucidated, highlighting their associations with soil properties and rhizosphere-secreted factors such as metabolites and plant hormones (Figure 10). This study underscores the importance of understanding soil microbial dynamics under prolonged grass cover, although it acknowledges the need for broader geographic observation data to strengthen findings. Future research endeavors should focus on expanding these datasets to enhance their comprehensiveness and robustness.

5 Conclusion

Long-term coverage of green bristlegrass in pear orchards has significant potential to enhance carbon and nitrogen storage, thereby improving overall soil nutrient levels, including TC, TN, SOC, SON, and C:N. This practice also promotes increased enzyme activity, such as that of S-SC, S-CL, and S-β-GC. The microbial community within these orchards, encompassing taxa such as Haliangium, Bacteroides, mle1-7, Subgroup_22, Ellin6067, MND1, and Cellvibrio, has exhibited enhanced diversity and functionality. These microorganisms, along with critical metabolites such as sucrose, N-acetyl-D-glucosamine, N-acetyl-L-glutamic acid, rhamnose, UDP-N-acetylglucosamine (UDP-GlcNAc), and D-maltose, play pivotal roles in carbon and nitrogen sequestration. They do so through various metabolic processes centered on carbon, including the synthesis, degradation, and transformation of sucrose and glycolysis during respiration (Figure 10). Furthermore, the coverage of bristlegrass contributes to the distribution of abscisic acid signal molecules in the pear rhizosphere soil. This distribution is primarily driven by the availability of carbon and nitrogen sources in the soil, which can be utilized by the pear fruit. The composition of crop species covered by natural grasses and different soil types also affects the structural distribution of rhizosphere microbial communities, soil metabolites, and enzyme activities, which in turn impact soil carbon sequestration capacity. In future, representative

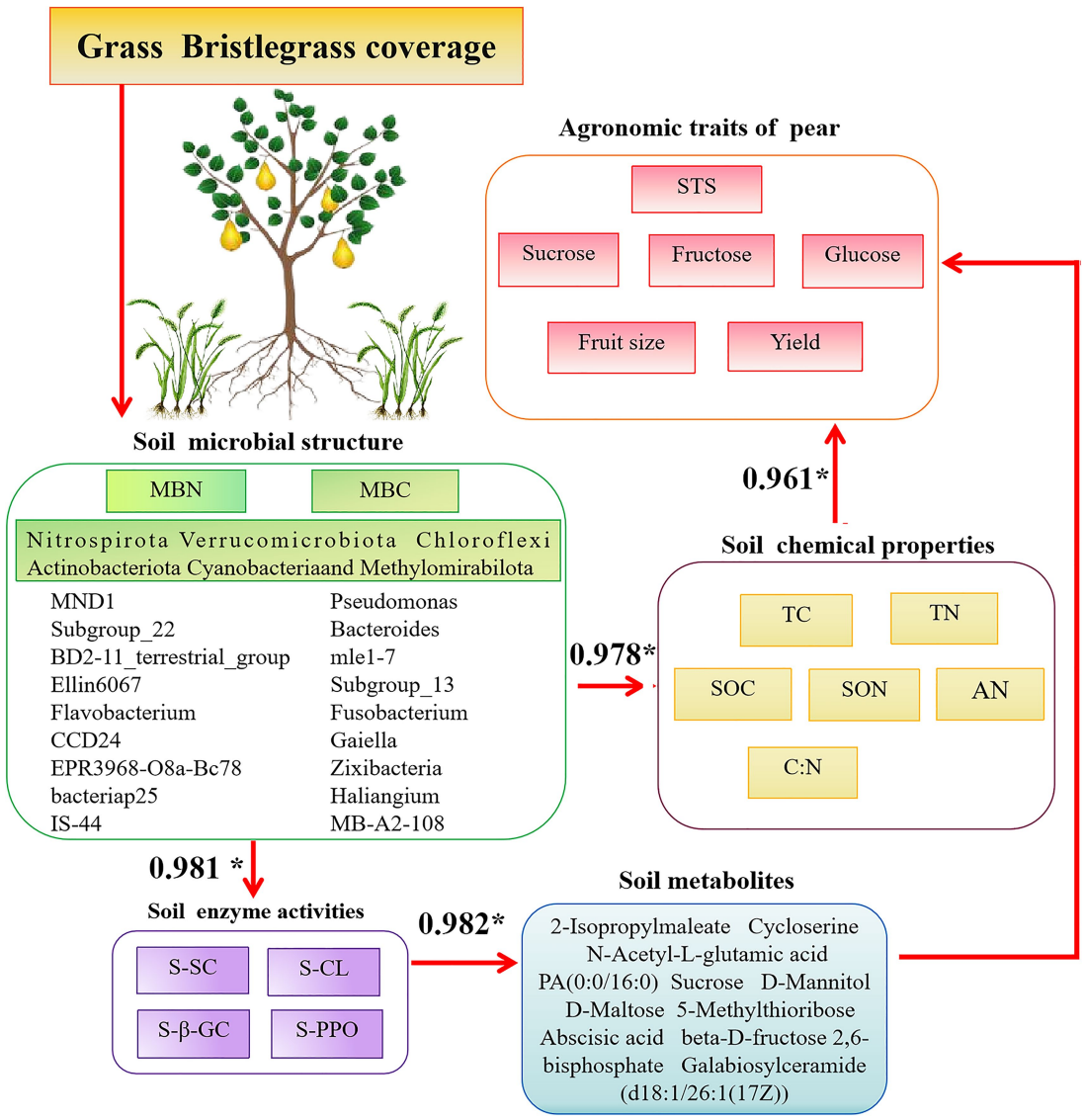


FIGURE 10
Conceptual diagram of associations among the aboveground part—fruit productivity (yield and quality) and the underground part—the soil physicochemical parameters, enzymes, and microbial community in pear. The values show the R-value by Pearson's correlation analysis. Up in red arrows indicate increasing and decreasing trends, and only the effects significant at $p < 0.05$ are presented.

areas with different soil types should be selected for sampling on a broader spatial–temporal scale to comprehensively capture the impact of natural grass cover on the soil microbial environment. This will help to more accurately assess its impact on biodiversity, water conservation, and the carbon and nitrogen cycle of the entire soil ecosystem, leading to more reliable conclusions. Furthermore, based on beneficial bacterial strains related to carbon fixation identified in this study, specific biological functions and mechanisms of action in increasing soil organic carbon were further explored.

Data availability statement

The original contributions presented in the study are publicly available. This data can be found here: https://www.ncbi.nlm.nih.gov/sra/?term=PRJNA1151655.

Author contributions

CS: Data curation, Formal analysis, Writing – original draft, Writing – review & editing. XW: Formal analysis, Methodology, Writing – review & editing. SJ: Software, Writing – review & editing. JX: Funding acquisition, Project administration, Writing – review & editing. JL: Funding acquisition, Writing – review & editing.

Funding

The author(s) declare that financial support was received for the research, authorship, and/or publication of this article. This study was supported by the Earmarked Fund for China Agriculture Research System (CARS-28-13) to JX and Shanghai Agriculture Applied Technology Development Program, China (Grant No. T2019 1-3) to JL.

Conflict of interest

The authors declare that the research was conducted in the absence of any commercial or financial relationships that could be construed as a potential conflict of interest.

Publisher's note

All claims expressed in this article are solely those of the authors and do not necessarily represent those of their affiliated organizations, or those of the publisher, the editors and the reviewers. Any product that may be evaluated in this article, or claim that may be made by its manufacturer, is not guaranteed or endorsed by the publisher.

Supplementary material

The Supplementary material for this article can be found online at: https://www.frontiersin.org/articles/10.3389/fmicb.2024.1461254/full#supplementary-material

References

Aghajani, M. A., Alizadeh, A., and Rahimian, H. (2008). First report of brown patch on bristle basket grass in Iran. *Plant Pathol.* 57:384. doi: 10.1111/j.1365-3059.2007.01741.x

Baer, S. G., Bach, E. M., Meyer, C. K., Du Preez, C. C., and Six, J. (2015). Belowground ecosystem recovery during grassland restoration: South African highveld compared to US tallgrass prairie. *Ecosystems* 18, 390–403. doi: 10.1007/s10021-014-9833-x

Bardgett, R. D., Bullock, J. M., Lavorel, S., Manning, P., Schaffner, U., Ostle, N., et al. (2021). Combatting global grassland degradation. *Nat. Rev. Earth Environ.* 2, 720–735. doi: 10.1038/s43017-021-00207-2

Chao, A., and Bunge, J. (2002). Estimating the number of species in a stochastic abundance model. *Biometrics* 58, 531–539. doi: 10.1111/j.0006-341X.2002.00531.x

Chen, D., Wang, Y., Zhang, X., Wei, X., Duan, X., and Muhammad, S. (2021). Understory mowing controls soil drying in a rainfed jujube agroforestry system in the loess plateau. *Agric. Water Manag.* 246:106703. doi: 10.1016/j.agwat.2020.106703

Cheng, H., Yuan, M., Tang, L., Shen, Y., Yu, Q., and Li, S. (2022). Integrated microbiology and metabolomics analysis reveal responses of soil microorganisms and metabolic functions to phosphorus fertilizer on semiarid farm. *Sci. Total Environ.* 817:152878. doi: 10.1016/j.scitotenv.2021.152878

Daly, A. B., Jilling, A., Bowles, T. M., Buchkowski, R. W., Frey, S. D., Kallenbach, C. M., et al. (2021). A holistic framework integrating plant-microbe-mineral regulation of soil bioavailable nitrogen. *Biogeochemistry* 154, 211–229. doi: 10.1007/s10533-021-00793-9

Debasis, M., Snežana, A., Panneerselvam, P., Manisha, C., Ansuman, S., and Vasić, T. (2019). Plant growth promoting microorganisms (PGPMs) helping in sustainable agriculture: current perspective. *Int. J. Agric. Vet. Sci.* 7, 50–74.

Dobosy, P., Sávoly, Z., Óvári, M., Mádl-Szőnyi, J., and Záray, G. (2016). Microchemical characterization of biogeochemical samples collected from the Buda thermal karst system, Hungary. *Microchem. J.* 124, 116–120. doi: 10.1016/j.microc.2015.08.004

Dong, Z., Xue, Z. Y., Chen, Q., Srivas, A. K., and Hu, C. X. (2021). Grass and plastic film mulching pattern improve soil organic carbon Pool, Physical Properties, Fertility and Fruit Quality of Ponkan Orchards. *Preprint*. doi: 10.21203/rs.3.rs-308925/v1

Fan, F., Yu, B., Wang, B., George, T. S., Yin, H., Xu, D., et al. (2019). Microbial mechanisms of the contrast residue decomposition and priming effect in soils with different organic and chemical fertilization histories. *Soil Biol. Biochem.* 135, 213–221. doi: 10.1016/j.soilbio.2019.05.001

Fang, L. F., Shi, X. J., Zhang, Y., Yang, Y. H., Zhang, X. L., Wang, X. Z., et al. (2021). The effects of ground cover management on fruit yield and quality: a meta-analysis. *Arch. Agron. Soil Sci.* 68, 1890–1902. doi: 10.1080/03650340.2021.1937607

Gómez, J. A., Reyna-Bowen, L., Rebollo, P. F., and Soriano, M. A. (2022). Comparison of soil organic carbon stocks evolution in two olive orchards with different planting Systems in Southern Spain. *Agriculture* 12:432. doi: 10.3390/agriculture12030432

Gregory, A. S., Joynes, A., Dixon, E. R., Beaumont, D. A., Murray, P. J., Humphreys, M. W., et al. (2022). High-yielding forage grass cultivars increase root biomass and soil organic carbon stocks compared with mixed-species permanent pasture in temperate soil. *Eur. J. Soil Sci.* 73:e13160. doi: 10.1111/ejss.13160

Guenet, B., Danger, M., Abbadie, L., and Lacroix, G. (2010). Priming effect: bridging the gap between terrestrial and aquatic ecology. *Ecology* 91, 2850–2861. doi: 10.1890/09-1968.1

Hill, T. C., Walsh, K. A., Harris, J. A., and Moffett, B. F. (2003). Using ecological diversity measures with bacterial communities. *FEMS Microbiol. Ecol.* 43, 1–11. doi: 10.1111/j.1574-6941.2003.tb01040.x

Homma, S. K., Tokeshi, H., Mendes, L. W., and Tsai, S. M. (2012). Long-term application of biomass and reduced use of chemicals alleviate soil compaction and improve soil quality. *Soil & Tillage Research* 120, 147–153. doi: 10.1016/j.still.2012.01.001

Hu, D., Chen, Y., Sun, C., Jin, T., Fan, G., Liao, Q., et al. (2018). Genome guided investigation of antibiotics producing actinomycetales strain isolated from a Macau mangrove ecosystem. *Sci. Rep.* 8:14271. doi: 10.1038/s41598-018-32076-z

Kaneko, M., Kurokawa, Y., Qing, H., Tanaka, H., Suzuki, S., and Kamata, T. (2008). Phosphorus accumulation in soil surface under Japanese lawngrass (*Zoysia japonica* Steud.) pasture. XXI International Grassland Congress & the VIII International Rangeland Congress.

Kim, Y. M., Nowack, S., Olsen, M. T., Becraft, E. D., Wood, J. M., Thiel, V., et al. (2015). Diel metabolomics analysis of a hot spring chlorophototrophic microbial mat leads to new hypotheses of community member metabolisms. *Front. Microbiol.* 6:132364. doi: 10.3389/fmicb.2015.00209

Ku, Y. L., Xu, G. Y., Zhao, H., Dong, T. W., and Cao, C. L. (2018). Effects of microbial fertilizer on soil improvement and fruit quality of kiwifruit in old orchard. *Chin. J. Appl. Ecol.* 29, 2532–2540. doi: 10.13287/j.1001-9332.201808.025

Kumar, B., Dhar, S., Paul, S., Paramesh, V., Dass, A., Upadhyay, P. K., et al. (2021). Microbial biomass carbon, activity of soil enzymes, nutrient availability, root growth, and total biomass production in wheat cultivars under variable irrigation and nutrient management. *Agronomy* 11:669. doi: 10.3390/agronomy11040669

Li, X., Chu, Y., Jia, Y., Yue, H., Han, Z., and Wang, Y. (2022). Changes to bacterial communities and soil metabolites in an apple orchard as a legacy effect of different intercropping plants and soil management practices. *Front. Microbiol.* 13:956840. doi: 10.3389/fmicb.2022.956840

Li, X., Jousset, A., de Boer, W., Carrión, V. J., Zhang, T., Wang, X., et al. (2019). Legacy of land use history determines reprogramming of plant physiology by soil microbiome. *ISME J.* 13, 738–751. doi: 10.1038/s41396-018-0300-0

Li, Q., Yu, P., Li, G. D., and Zhou, D. (2016). Grass-legume ratio can change soil carbon and nitrogen storage in a temperate steppe grassland. *Soil Tillage Res.* 157, 23–31. doi: 10.1016/j.still.2015.08.021

Li, T., Zhang, Y., Liu, Y., Li, X., Hao, G., and Han, Q. (2020). Raffinose synthase enhances drought tolerance through raffinose synthesis or galactinol hydrolysis in maize and Arabidopsis plants. *J. Biol. Chem.* 295, 8064–8077. doi: 10.1074/jbc.RA120.013948

Lienhard, P., Tivet, F., Chabanne, A., Dequiedt, S., Lelièvre, M., Sayphoummie, S., et al. (2013). No-till and cover crops shift soil microbial abundance and diversity in Laos tropical grasslands. *Agron. Sustain. Dev.* 33, 375–384. doi: 10.1007/s13593-012-0099-4

Liu, J. F., Li, H. F., Yu, X. M., and Miao, A. (2017). Advantageous natural grasses and their nutrition pattern in apple orchards in Taiyi mountainous area. *Shandong Agric. Sci.* 49, 120–124.

Liu, Y. P., Mao, Y. F., Hu, Y. L., Zhang, L. L., Yin, Y. J., Pang, H. L., et al. (2021). Effects of grass planting in apple orchard on soil microbial diversity, enzyme activities and carbon components. *J. Plant Nutr. Fertiliz.* 27, 1792–1805. doi: 10.11674/zwyf.2021140

Ma, X., Chao, L., Li, J., Ding, Z., Wang, S., Li, F., et al. (2021). The distribution and turnover of bacterial communities in the root zone of seven Stipa species across an arid and semi-arid steppe. *Front. Microbiol.* 12:782621. doi: 10.3389/fmicb.2021.782621

Ma, X., Li, J., Ding, F., Zheng, Y., Chao, L., Liu, H., et al. (2022). Changes of arbuscular mycorrhizal fungal community and Glomalin in the rhizosphere along the distribution gradient of zonal Stipa populations across the arid and semiarid steppe. *Microbiol. Spect.* 10:e0148922. doi: 10.1128/spectrum.01489-22

Matocha, C. J., Karathanasis, T. D., Murdock, L. W., Grove, J. H., Goodman, J., and Call, D. (2018). Influence of ryegrass on physico-chemical properties of a fragipan soil. *Geoderma* 317, 32–38. doi: 10.1016/j.geoderma.2017.12.004

Mikha, M. M., Obour, A. K., and Holman, J. D. (2018). Soil nutrients status after fifty years of tillage and nitrogen fertilization. *Commun. Soil Sci. Plant Anal.* 49, 1953–1975. doi: 10.1080/00103624.2018.1492599

Novikova, A. F., and Konyushkova, M. V. (2013). Anthropogenic transformation of soils in the northern Ergeni upland (studies at the first experimental plot of the Arshan'-Zelmen Research Station). *Eurasian Soil Sci.* 46, 241–253. doi: 10.1134/S106422931303006X

Oberholzer, H. R., Leifeld, J., and Mayer, J. (2014). Changes in soil carbon and crop yield over 60 years in the Zurich organic fertilization experiment, following land-use change from grassland to cropland. *J. Plant Nutr. Soil Sci.* 177, 696–704. doi: 10.1002/jpln.201300385

Omari, K. W., Dodot, L., and Kerton, F. M. (2012). A simple one-pot dehydration process to convert N-acetyl-D-glucosamine into a nitrogen-containing compound, 3acetamido-5-acetylfuran. *ChemSusChem* 5, 1767–1772. doi: 10.1002/cssc.201200113

Peng, S. I., Hui-Li, Y. U., Deng-Tao, G., Wei, S., Xian-Sheng, Q., Jin-Yong, C., et al. (2017). Effects of intercropping herbages on carbon source metabolism of soil microbial community in sandy vineyard. *Agricultural Research in the Arid Areas* 35, 247–254. doi: 10.7606/j.issn.1000-7601.2017.02.40

Peters, M. K., Hemp, A., Appelhans, T., Becker, J. N., Behler, C., Classen, A., et al. (2019). Climate–land-use interactions shape tropical mountain biodiversity and ecosystem functions. *Nature* 568, 88–92. doi: 10.1038/s41586-019-1048-z

Peterson, M. J., Handakumbura, P., Thompson, A. M., and Callister, S. J. (2021). Deciphering the microbial and molecular responses of geographically diverse setaria accessions grown in a nutrient-poor soil. *PloS one* 16:e0259937. doi: 10.1371/journal.pone.0259937

Qian, X., Gu, J., Pan, H. J., Zhang, K. Y., Sun, W., Wang, X. J., et al. (2015). Effects of living mulches on the soil nutrient contents, enzyme activities, and bacterial community diversities of apple orchard soils. *Eur. J. Soil Biol.* 70, 23–30. doi: 10.1016/j.ejsobi.2015.06.005

Rodríguez-Loinaz, G., Onaindia, M., Amezaga, I., Mijangos, I., and Garbisu, C. (2008). Relationship between vegetation diversity and soil functional diversity in native mixed-oak forests. *Soil Biol. Biochem.* 40, 49–60. doi: 10.1016/j.soilbio.2007.04.015

Seitz, V. A., Chaparro, J. M., Schipanski, M. E., Wrighton, K. C., and Prenni, J. E. (2023). Cover crop cultivar, species, and functional diversity is reflected in variable root exudation composition. *J. Agric. Food Chem.* 71, 11373–11385. doi: 10.1021/acs.jafc.3c02912

Shi, C. H., Wang, X. Q., Jiang, S., Zhang, L. Q., and Luo, J. (2023). Revealing the role of the rhizosphere microbiota in reproductive growth for fruit productivity when inorganic fertilizer is partially replaced by organic fertilizer in pear orchard fields. *Microb. Biotechnol.* 16, 1373–1392. doi: 10.1111/1751-7915.14253

Sleiderink, J., Deru, J. G. C., Weide, R. V. D., and Eekeren, N. V. (2024). Effects of reduced tillage and prolonged cover cropping in maize on soil quality and yield. *Soil Tillage Res.* 244:106196. doi: 10.1016/j.still.2024.106196

Song, S., Xiong, K., and Chi, Y. (2022). Grassland ecosystem service and its enlightenment on the revitalization of rural ecological animal husbandry in the rocky desertification area: a literature review. *Pol. J. Environ. Stud.* 31, 4499–4510. doi: 10.15244/pjoes/149742

Sugiura, H., Inoue, H., Kato, O., Tezuka, T., Furuya, S., and Furukawa, T. (2017). Changes in soil organic carbon after more than ten years of continuous organic matter application in orchards in Japan. *J. Agric. Meteorol.* 73, 68–72. doi: 10.2480/agrmet.D-16-00006

Wang, R., Cao, B., Sun, Q., and Song, L. (2020). Response of grass interplanting on bacterial and fungal communities in a jujube orchard in Ningxia, Northwest China. *Heliyon* 6:e03489. doi: 10.1016/j.heliyon.2020.e03489

Wang, J., Huang, J., Zhao, X., Wu, P., Horwath, W. R., Li, H., et al. (2016). Simulated study on effects of ground managements on soil water and available nutrients in jujube orchards. *Land Degrad. Dev.* 27, 35–42. doi: 10.1002/ldr.2334

Wang, C., Liang, Q., Liu, J., Zhou, R., Lang, X., Xu, S., et al. (2023). Impact of intercropping grass on the soil rhizosphere microbial community and soil ecosystem function in a walnut orchard. *Front. Microbiol.* 14:1137590. doi: 10.3389/fmicb.2023.1137590

Wang, Y., Weng, B., Ye, J., Wang, C., Liu, C., and Li, Y. (2017). Soil organic carbon sequestration potential in nectarine orchards under different reclamation systems. *Agric. Sci. Technol.* 18, 1192–1195. doi: 10.16175/j.cnki.1009-4229.2017.07.010

Wu, H., Kong, Y., Yao, Y., Bi, N., Qi, L., Fu, Z., et al. (2010). Effects of intercropping aromatic plants on soil microbial quantity and soil nutrients in pear orchard. *Scientia Agricultura Sinica* 43, 140–150. doi: 10.3864/j.issn.0578-1752.2010.01.017

Xiang, Y., Chang, S. X., Shen, Y., Chen, G., Liu, Y., Yao, B., et al. (2023). Grass cover increases soil microbial abundance and diversity and extracellular enzyme activities in orchards: a synthesis across China. *Appl. Soil Ecol.* 182:104720. doi: 10.1016/j.apsoil.2022.104720

Xu, W. W., Zhao, Y. Q., Wang, N., and Zhao, Y. (2023). Effects of artificial cyanobacterial crusts on enzyme activities and recovery rate of surface soil in sandy areas. *Acta Ecol. Sin.* 43, 2856–2864. doi: 10.5846/stxb202204201075

Yang, Y., Dou, Y., Wang, B., Wang, Y., Liang, C., An, S., et al. (2022). Increasing contribution of microbial residues to soil organic carbon in grassland restoration chronosequence. *Soil Biol. Biochem.* 170:108688. doi: 10.1016/j.soilbio.2022.108688

Yang, Y., Tong, Y. A., Liang, L. Y., Li, H. C., and Han, W. S. (2021). Dynamics of soil bacteria and fungi communities of dry land for 8 years with soil conservation management. *J. Environ. Manag.* 299:113544. doi: 10.1016/j.jenvman.2021.113544

Yu, X., Borjigin, Q., Julin, G., Zhigang, W., Shuping, H., Borjigin, N., et al. (2019). Exploration of the key microbes and composition stability of microbial consortium GF-20 with efficiently decomposes corn Stover at low temperatures. *J. Integr. Agric.* 18, 1893–1904. doi: 10.1016/s2095-3119(19)62609-2

Zakrzewski, M., Goesmann, A., Jaenicke, S., Jünemann, S., Eikmeyer, F., Szczepanowski, R., et al. (2012). Profiling of the metabolically active community from a production-scale biogas plant by means of high-throughput metatranscriptome sequencing. *J. Biotechnol.* 158, 248–258. doi: 10.1016/j.jbiotec.2012.01.020

Zeng, F., Zuo, Z., Mo, J., Chen, C., Yang, X., Wang, J., et al. (2021). Runoff losses in nitrogen and phosphorus from paddy and maize cropping systems: a field study in dongjiang basin, South China. *Front. Plant Sci.* 12:1675121. doi: 10.3389/fpls.2021.675121

Zhalnina, K., Louie, K. B., Hao, Z., Mansoori, N., Da Rocha, U. N., Shi, S., et al. (2018). Dynamic root exudate chemistry and microbial substrate preferences drive patterns in rhizosphere microbial community assembly. *Nat. Microbiol.* 3, 470–480. doi: 10.1038/s41564-018-0129-3

Zhang, Y., Bo, G., Shen, M., Shen, G., Yang, J., Dong, S., et al. (2022). Differences in microbial diversity and environmental factors in ploughing-treated tobacco soil. *Front. Microbiol.* 13:924137. doi: 10.3389/fmicb.2022.924137

Zhang, L., Huang, W., Xiao, W., Hu, D., Shao, J., and Yao, B. (2018). Comparison of soil enzyme activity and microbial community structure between rapeseed-rice and rice-rice plantings. *Int. J. Agric. Biol.* 20, 1801–1808. doi: 10.17957/IJAB/15.0692

Zhang, C., Zhao, X., Liang, A., Li, Y., Song, Q., Li, X., et al. (2023). Insight into the soil aggregate-mediated restoration mechanism of degraded black soil via biochar addition: emphasizing the driving role of core microbial communities and nutrient cycling. *Environ. Res.* 228:115895. doi: 10.1016/j.envres.2023.115895

Zhao, Z., Ma, Y., Feng, T., Kong, X., Wang, Z., Zheng, W., et al. (2022). Assembly processes of abundant and rare microbial communities in orchard soil under a cover crop at different periods. *Geoderma* 406:115543. doi: 10.1016/j.geoderma.2021.115543

Zhou, H., Zhang, M., Yang, J., Wang, J., Chen, Y., and Ye, X. (2023). Returning ryegrass to continuous cropping soil improves soil nutrients and soil microbiome, producing good-quality flue-cured tobacco. *Front. Microbiol.* 14:1257924. doi: 10.3389/fmicb.2023.1257924

frontiers | Frontiers in Microbiology

TYPE Original Research
PUBLISHED 23 October 2024
DOI 10.3389/fmicb.2024.1483150

Check for updates

OPEN ACCESS

EDITED BY
Muhammad Zahid Mumtaz,
Gansu Agricultural University, China

REVIEWED BY
Muhammad Saqlain Zaheer,
Khwaja Fareed University of Engineering and Information Technology (KFUEIT), Pakistan
Azhar Hussain,
Islamia University of Bahawalpur, Pakistan

*CORRESPONDENCE
Zhuxin Mao
✉ zhuxinmao@gmail.com

RECEIVED 19 August 2024
ACCEPTED 09 October 2024
PUBLISHED 23 October 2024

CITATION
Deng N, Nian L, Zhang S, Liang Y, Shang H, Li Y and Mao Z (2024) Response of soil microbial community structure to temperature and nitrogen fertilizer in three different provenances of *Pennisetum alopecuroides*.
Front. Microbiol. 15:1483150.
doi: 10.3389/fmicb.2024.1483150

COPYRIGHT
© 2024 Deng, Nian, Zhang, Liang, Shang, Li and Mao. This is an open-access article distributed under the terms of the Creative Commons Attribution License (CC BY). The use, distribution or reproduction in other forums is permitted, provided the original author(s) and the copyright owner(s) are credited and that the original publication in this journal is cited, in accordance with accepted academic practice. No use, distribution or reproduction is permitted which does not comply with these terms.

Response of soil microbial community structure to temperature and nitrogen fertilizer in three different provenances of *Pennisetum alopecuroides*

Niandong Deng[1], Lili Nian[2], Shuolun Zhang[1], Yixuan Liang[1], Huiying Shang[3], Yang Li[3] and Zhuxin Mao[3,4]*

[1]College of Geology and Environment, Xi'an University of Science and Technology, Xi'an, China, [2]Gansu Academy Agricultural Sciences, Lanzhou, China, [3]Xi'an Botanical Garden of Shaanxi Province, Institute of Botany of Shaanxi Province, Xi'an, China, [4]Shaanxi Engineering Research Centre for Conservation and Utilization of Botanical Resources, Xi'an, China

Soil microorganisms are key indicators of soil health, and it is crucial to investigate the structure and interactions of soil microbial communities among three different provenances of *Pennisetum alopecuroides* under varying nitrogen fertilizer and temperature levels in Northwest China. This study aims to provide theoretical support for the sustainable use of artificial grassland in this region. Employing a two-factor pot-control experiment with three nitrogen fertilizer treatments and three temperature treatments, a total of all treatments was utilized to examine the composition and abundance of soil microbial communities associated with *Pennisetum alopecuroides* using high-throughput sequencing, PCR technology, and molecular ecological network analysis. The results revealed that *Proteobacteria* was the dominant bacterial phylum while *Ascomycota* was the dominant fungal phylum in the soil samples from three provenances of *Pennisetum*. Specifically, *Proteobacteria* exhibited higher abundance in the N3T2 treatment compared to other treatments under N3T2 (25–30°C, 3 g/pot) treatment conditions in Shaanxi and Gansu provinces; similarly, *Proteobacteria* was more abundant in the N1T2 (25–30°C, 1 g/pot) treatment in Inner Mongolia under N1T2. Moreover, Ascomycota displayed higher abundance than other treatments in both Inner Mongolia and Gansu provinces. Additionally, *Pennisetum Ascomycota* demonstrated greater prevalence under (25–30°C, 3 g/pot) treatment compared to other treatments; furthermore, Shaanxi's *Pennisetum Ascomycota* exhibited increased prevalence under N3T1 (18–23°C, 3 g/pot) treatment compared to other treatments. The richness and diversity of soil microbial communities were significantly influenced by nitrogen fertilizer and temperature changes, leading to notable alterations in their structure. Molecular ecological network analyses revealed strong collaborative relationships among microbial species in Shaanxi *Pennisetum* and Inner Mongolia *Pennisetum* under high nitrogen and high temperature treatments, while competitive relationships were observed among microbial species in Gansu *Pennisetum* under similar conditions. Redundancy analysis indicated that soil pH, total potassium, and total phosphorus were the primary environmental factors influencing microorganisms. In summary, this study offers a theoretical foundation for assessing the sustainable utilization of *Pennisetum* artificial grasslands in Northwest China by investigating the shifts in soil microbial communities and the driving factors under varying nitrogen fertilizer and temperature levels.

KEYWORDS

Pennisetum, soil microbes, ecological networks, nitrogen addition, temperature

1 Introduction

Soil microbial communities have received considerable attention as valuable indicators of soil biodiversity and environmental quality (Bertola et al., 2021). Soil microorganisms exhibit a remarkable diversity and abundance of species, occupying a pivotal role within soil ecosystems (Yan et al., 2020; Yao and Zhou, 2022). Highly responsive to environmental changes, soil microbial communities undergo shifts in composition and diversity in response to changes in aboveground plant communities and soil environment, as well as alterations in the soil ecological environment (Liu et al., 2023; Shen et al., 2024; Wen et al., 2024). This connection facilitates the material cycling and energy flow between aboveground and underground ecosystems (Graham and Knelman, 2023). Among soil microorganisms, bacteria constitute the most abundant and versatile group versatile group, playing a pivotal role in soil formation, organic matter decomposition, and nutrient cycling (Zhan et al., 2024). Fungi not only play a crucial role in apoplastic decomposition and nutrient cycling, but also contribute significantly to soil formation and nutrient cycling (Xie et al., 2024). Moreover, fungi establish symbiotic relationships with higher plants, thereby providing essential nutrients for plant growth (Wang et al., 2022). The study revealed a significant increase in soil temperature due to warming (Seaton et al., 2022). Additionally, it was observed that warming significantly enhanced soil microbial biomass but resulted in a notable decrease in microbial diversity and alterations in community structure (Seaton et al., 2022). Conversely, no impact of warming on soil microbial community composition was detected (Zhang et al., 2020). Another aspect of the study demonstrated that warming induced elevated evaporation of soil water, leading to reduced soil moisture and subsequently diminished effectiveness of soil nutrients. Consequently, this reduction negatively affected soil microbial biomass and activity (Goncharov et al., 2023; Shao et al., 2023). Studies consistently indicate that nitrogen addition generally diminishes microbial diversity (Wang et al., 2018), with a decreasing trend observed as nitrogen input increases (Liu et al., 2020). Molecular ecological network analysis is a widely employed approach for characterizing soil microbial symbiosis patterns by elucidating network structural features and unveiling interactions among diverse soil microbial taxa (Layeghifard et al., 2017). Generally, increased connectivity and complexity of the network indicate active involvement of soil microbes in the ecosystem (Jiao et al., 2022). Moreover, the complexity of soil microbial networks is closely linked to their stability. Soil microorganisms maintain relative stability of the network to withstand environmental disturbances. Negative correlations, which signify competition, often enhance network stability through negative feedback mechanisms (Duchenne et al., 2022). Therefore, molecular ecological network analysis can effectively unveil interrelationships' complexity and stability among soil microbes while reflecting ecosystem intricacy and stability (Landi et al., 2018). It should be noted that soil microbial interactions are not static but exhibit significant spatial and temporal variability as well as sensitivity to environmental factors. Climate, altitude, and vegetation exert substantial influences on soil microbial interactions leading to variations in molecular ecological networks' complexity and stability (de Vries et al., 2018).

Northwest China is a representative ecologically fragile region characterized by severe soil erosion, low vegetation cover, and prominent soil degradation issues (Li et al., 2024; Yu et al., 2024; Zhang et al., 2023). *Pennisetum alopecuroides*, a perennial herbaceous plant belonging to the Gramineae family, derives its name from its inflorescence resembling a wolf's tail and has origins in western Australia and eastern Asia, including China (Kang et al., 2018; Wang et al., 2017). This species exhibits remarkable drought tolerance and adaptability while playing a crucial role in facilitating vegetation recovery, enhancing the ecological environment, and promoting local livestock development (Dang et al., 2017). However, suboptimal soils restrict the growth of *Pennisetums*, necessitating their adaptation to varying temperature zones due to significant altitudinal differences (Belesky and Malinowski, 2016). Consequently, this not only leads to abrupt declines in grass production and soil quality degradation but also exerts profound impacts on the structure and function of soil microbial communities. Thus, nitrogen fertilizers along with suitable temperature conditions are essential for sustaining its utilization (Yang et al., 2020). It has been suggested that moderate warming may enhance specific positive feedback mechanisms and promote network stability, whereas extreme temperatures could amplify negative correlations and result in network instability (Li et al., 2021). Addition of nitrogen fertilizer might improve network connectivity and stability; however, excessive nitrogen fertilizer application could intensify competitive relationships and disrupt network connectivity, leading to potential network instability (Widdig et al., 2020). The impact of temperature and N fertilizer addition on the stability of microbial communities in wolverine soils remains unclear. Therefore, investigating the dynamics of soil microbial community diversity patterns and network stability during temperature variations and N fertilizer addition in Northwest China will contribute to a comprehensive understanding of the formation and maintenance mechanisms underlying soil microbial community diversity patterns, as well as provide insights for guiding vegetation restoration efforts and biodiversity conservation.

Currently, numerous studies have been conducted in China on the characteristics of soil microbial communities of *Pennisetum* in Northwest China in response to temperature and nitrogen fertilizer addition. These studies primarily focus on soil microbial biomass, community composition and structure, exploring patterns of change with respect to temperature and nitrogen fertilizer, as well as their interrelationships with environmental factors. However, fewer studies have investigated co-occurrence patterns of soil microbial communities during temperature and nitrogen fertilizer addition for different seed sources of *Pennisetum* in Northwest China. Therefore, this study focuses on the composition and structural characteristics of soil microbial communities (fungi and bacteria) as well as changes in species co-occurrence patterns for three different seed sources of *Pennisetum* based on pot experiments. The aim is to provide a theoretical basis for sustainable use of artificial grasslands composed of *Pennisetum*.

2 Materials and methods

2.1 Test materials

The test materials were *Poaceae* plants *Pennisetum alopecuroides*, and the seeds of the three provenances of *Pennisetum* sourced from Shaanxi Province, Inner Mongolia Autonomous Region and Gansu Province, respectively, (Figure 1). All seeds were mature and collected in 2023. We list key properties and characteristics of soil to provide context for subsequent microbial community analyses. Basic soil properties: pH 8.09, organic matter 15.62 g/kg, total nitrogen 0.75 g/kg, total phosphorus 0.76 g/kg, and total potassium 18.77 g/kg.

2.2 Experimental design

The experiment was a factorial design, consisting of three nitrogen fertilizer treatments and three temperature treatments. An orthogonal experimental design was employed, resulting in a total of nine treatments with three replicates for each treatment and 27 pots per plant (Table 1). Seedlings were raised in May 2023 and emerged uniformly after 15 days. Nitrogen fertilizer treatment commenced at the beginning of August, followed by greenhouse temperature treatment (Plants are grown in a greenhouse environment with consistent temperature and light conditions) at the end of August. The pots used were made from commercially available pp. material, measuring 265 mm in caliber, with a ground diameter of 155 mm and a height of 175 mm. The soil was a mix of field soil and river sand (3:1 volume ratio), thoroughly mixed and uniformly potted with 2,500 g per pot. Nitrogen was commercially available urea. N1 was 0.5 g/pot of urea (1 kg/ha of pure nitrogen[2]), N2 was 1 g/pot of urea (2 kg/ha of pure nitrogen[2]), and N3 was 1.5 g/pot of urea (3 kg/ha of pure nitrogen[2]), fully dissolved in water and added in batches. During the experimental period, fertilization was applied only once.

2.3 Soil sample collection

The seedling nursery work was conducted in the greenhouse. Once the seedlings had emerged uniformly, those with similar growth patterns were selected for transplantation. Temperature control and fertilization experiments were carried out using pots. Nitrogen fertilizer treatment commenced in early August, followed by relocation to the greenhouse at the end of August for further temperature control and fertilization treatments. After a 30-day period of temperature control and fertilization treatments, both plants and soil samples were collected. The plants were manually divided into aboveground and underground (root system) parts. The process involved the following steps: First, the plants were removed from the greenhouse, and the surrounding soil was gently cleared to expose the

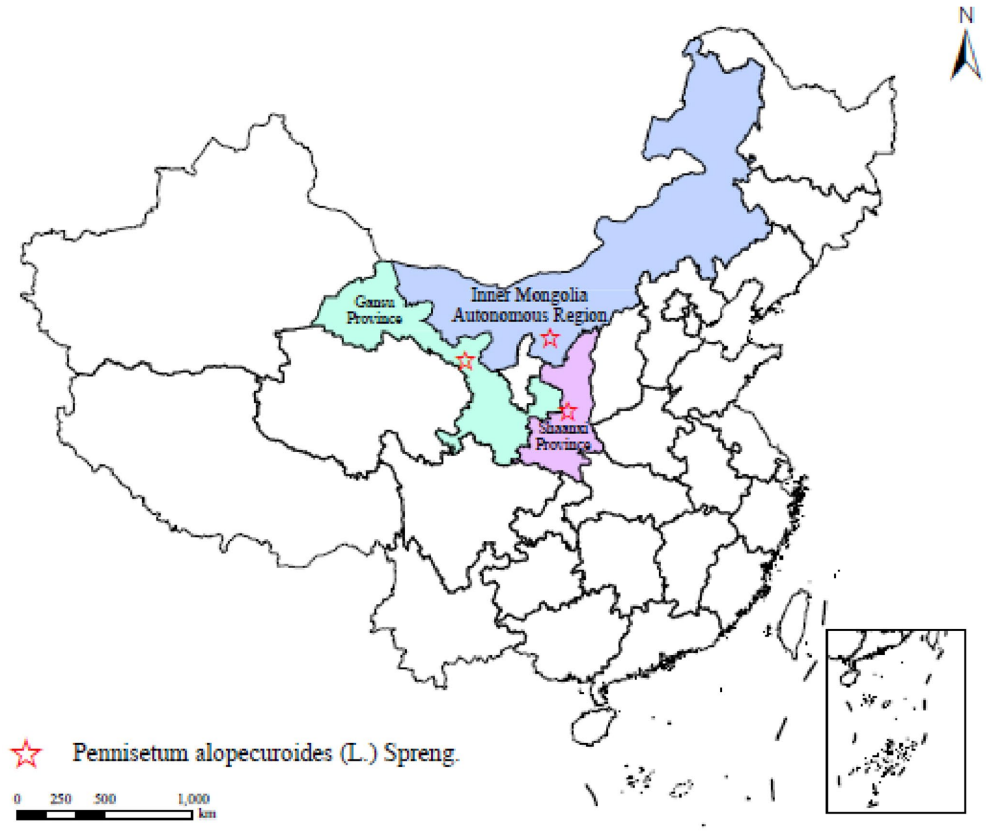


FIGURE 1
Distribution of experimental *Pennisetum alopecuroides* in China. This map shows the distribution of Pennisetum in China, marking three main planting areas: Gansu Province, Inner Mongolia Autonomous Region, and Shaanxi Province. Each area is marked with a different color on the map, with red stars indicating the distribution points of *Pennisetum* in the corresponding areas.

TABLE 1 Orthogonal experimental design.

Experiment No.	N1T1	N1T2	N1T3	N2T1	N2T2	N2T3	N3T1	N3T2	N3T3
Temperature (°C)	18–23	25–30	32–37	18–23	25–30	32–37	18–23	25–30	32–37
Urea (g/pot)	1	1	1	2	2	2	3	3	3

root system. The aboveground portion was then carefully separated from the root system using scissors. Both parts were subsequently washed separately to remove residual soil and impurities. Finally, the cleaned aboveground portion and root system were appropriately processed and frozen to preserve their physiological state for further analysis. Soil samples were divided into two parts: one part was filled into sterilized centrifuge tubes, placed in foam boxes equipped with ice packs, transported to the laboratory, and stored at −80°C for total soil DNA extraction; while the other part was brought back to the laboratory, placed in a cool and ventilated area to air dry naturally for subsequent determination of soil physicochemical properties.

2.4 Methods for determining soil physical and chemical indicators

Determination of Soil Organic Carbon Using the Potassium Dichromate External Heating Method (Nelson and Sommers, 1996) and total soil nitrogen using the semi-micro Kjeldahl method (Brookes et al., 1985). Total phosphorus was determined by the sodium hydroxide-molybdenum antimonide colourimetric method (Levine et al., 1954). Soil pH was determined by the water immersion potentiometric method (Guimaraes et al., 2020). The total soil potassium was determined by flame photometric method (Shen et al., 2019). Chlorophyll was determined by Seely's chlorophyll assay method (Jordan and Vilter, 1991). The procedure was as follows: Plant leaves were first cut into pieces and placed in a mortar. An appropriate amount of 95% ethanol and a small amount of calcium carbonate were then added to thoroughly grind the leaves, allowing for chlorophyll extraction. The mixture was subsequently filtered, and the filtrate was collected. Chlorophyll in the filtrate produced maximum absorption peaks at 649 nm and 665 nm. The absorbance values at these two wavelengths were measured using a spectrophotometer, and the chlorophyll content was calculated based on a standard curve.

2.5 High-throughput sequencing of soil microorganisms

Genomic DNA extraction from soil samples: The genomic DNA was extracted using the Power Soil® DNA kit, and the purity of the DNA was checked by running the gel through 1.0% agarose gel electrophoresis, and then stained with ethidium bromide and detected by a gel imaging system. PCR amplification: Bacterial 16S rRNA primers 515F (5′-GTGCCAGCMGCCGCGG-3′) and 907R (5'-CCGTCAATTCMTTTRAGTTT-3′) were used for amplification. 907R (5′-CCGTCAATTCMTTTRAGTTT-3′) (Yang et al., 2017) To carry out the V4-V5 region, fungal primers were used ITS1F (5′-CTTGGTCATTTAGAGGAAGTAA-3′) and ITS1R (5′-GCTGCGTTCTTCATCGATGC-3′) (Sinclair et al., 2015) PCR amplification of ITS region was carried out. PCR was performed using Trans Gen AP221-02: Trans StartFastpfu DNA Polymerase; PCR instrument: ABI Gene Amp® Model 9,700; PCR products of the same sample were mixed and detected by 2% agarose gel electrophoresis using AxyPrep DNA Gel The PCR products were cut and recovered using AxyPrep DNA Gel Recovery Kit (AXYGEN), eluted with Tris HCl and detected by 2% agarose electrophoresis. The PCR products were detected and quantified by applying Quanti Fluor™-ST Blue Fluorescence Quantification System (Promega) with reference to the first quantification step of electrophoresis (Mueller et al., 2014) Illumina Miseq PE300 sequencing was used.

2.6 Data processing

Soil physicochemical properties and microbial community composition data were processed using SPSS26.0 and Exce12010, with significance analysis performed using one-way ANOVA and multiple comparisons (LSD method, $p = 0.05$). Soil microbial genus Spearman correlation coefficients $R > 0.5$ and significant $p < 0.05$ species OUT were selected for constructing protozoa community correlation networks using the "igraph" package in R software, with network visualization analysis conducted using Gephi0.9.2 software. Redundancy analysis (RDA) of microbial communities and soil environmental factors was performed using CANOCO5.0, with graphical modifications using Al (Adobe Illustrator CS6) software.

3 Results and analyses

3.1 Soil physico-chemical factors

The physicochemical properties of the soil are presented in Figure 2. A study conducted on *Pennisetum* in Shaanxi revealed that changes in temperature and nitrogen fertilizer had no significant impact on soil total phosphorus, but significantly influenced pH, organic carbon, total nitrogen, and total potassium levels. The treatment N1T2 exhibited a significantly higher pH compared to other treatments ($p < 0.05$), while the N3T2 treatment showed a significantly lower pH than other treatments ($p < 0.05$). Organic matter content was significantly higher in the N2T3 treatment compared to other treatments ($p < 0.05$), whereas the N1T2 treatment displayed a significantly lower organic matter content than other treatments ($p < 0.05$). Total nitrogen levels were found to be significantly higher in the N3T2 treatment compared to other treatments ($p < 0.05$), with the N2T2 treatment exhibiting a significantly lower total nitrogen content than other treatments ($p < 0.05$). Additionally, the N1T1 treatment demonstrated a significantly higher total potassium level compared to other treatments, while the N1T3 treatment displayed a significantly lower total potassium level than other treatments ($p < 0.05$). Inner Mongolia *Pennisetum* study found that temperature and nitrogen changes had no significant effect on organic carbon, total

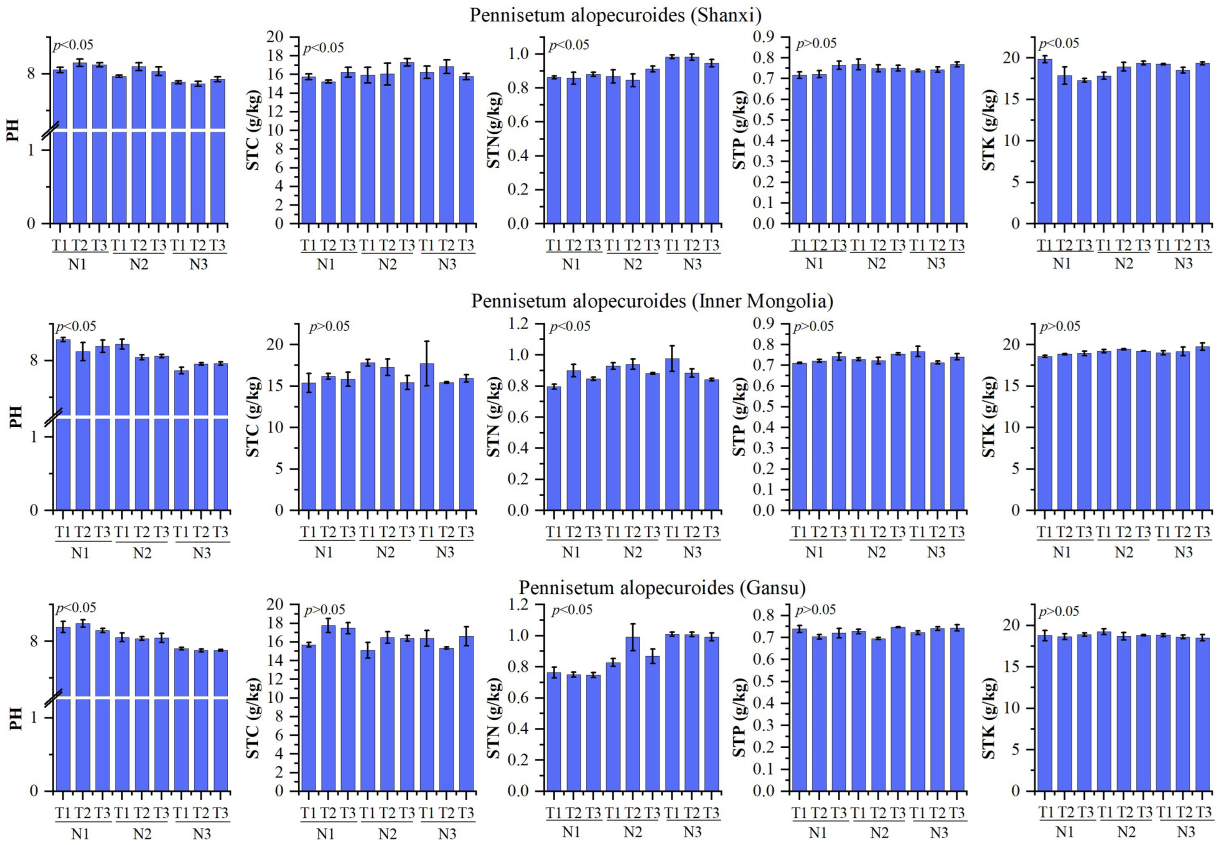


FIGURE 2
Physical and chemical properties of soil. N1-1 g/pot, N2-2 g/pot, N3-3 g/pot, T1-18/23°C, T2–25/30°C, T3: 32/37°C. $p < 0.05$: indicates that there is a significant difference between treatments, $p > 0.05$: indicates that there is no significant difference between treatments. The same below.

phosphorus, and total potassium but significantly affected pH and total nitrogen. The pH of the N1T1 treatment exhibited a significantly higher value compared to other treatments, while the N3T1 treatment showed a significantly lower value ($p < 0.05$). Additionally, the total nitrogen content in the N3T1 treatment was significantly higher than that in other treatments, whereas the N1T1 treatment displayed a significantly lower value ($p < 0.05$). Gansu *Pennisetum* research revealed that alterations in temperature and nitrogen fertilizer had no significant impact on organic carbon, total phosphorus, and total potassium levels; however, they did exert a significant influence on pH and total nitrogen content. Specifically, the pH of the N1T2 treatment was found to be significantly higher than that of other treatments ($p < 0.05$), while the N3T2 treatment exhibited a notably lower pH value compared to other treatments ($p < 0.05$). Furthermore, it was observed that the total nitrogen content in the N3T2 treatment was considerably higher than that in other treatments; conversely, the N1T3 treatment displayed a markedly lower level of total nitrogen when compared with other treatments ($p < 0.05$).

The nutrient composition of *Pennisetum* roots is presented in Figure 3. A study conducted on Shaanxi *Pennisetum* revealed that variations in temperature and nitrogen fertilizer did not have a significant impact on total nitrogen and organic carbon levels, but had a notable influence on biomass, total phosphorus, and total potassium concentrations. The biomass of the N2T1 treatment exhibited significantly higher values compared to other treatments ($p < 0.05$), while the N3T1 treatment showed significantly lower values ($p < 0.05$). Moreover, the N2T1 treatment displayed significantly higher levels of total phosphorus than other treatments, whereas the N1T3 treatment demonstrated significantly lower levels ($p < 0.05$). Additionally, the N1T1 treatment exhibited notably higher amounts of total potassium compared to other treatments, with the N2T3 treatment displaying significantly lower quantities ($p < 0.05$). The study conducted in Inner Mongolia on the Pennisetum species revealed that variations in temperature and nitrogen fertilizer did not exert a significant influence on biomass and organic carbon. However, they had a notable impact on the levels of nitrogen, phosphorus, and potassium. Specifically, the N3T2 treatment exhibited significantly higher total nitrogen content compared to other treatments ($p < 0.05$), while the N1T1 treatment showed significantly lower levels. Similarly, the N2T2 treatment displayed significantly higher total phosphorus content than other treatments ($p < 0.05$), whereas the N3T3 treatment demonstrated significantly lower levels. Moreover, the N1T2 treatment indicated a significant increase relative to other treatments ($p < 0.05$), while the N2T3 treatment exhibited a significant decrease ($p < 0.05$). Gansu *Pennisetum* study found that temperature and nitrogen changes significantly affected biomass, organic carbon, total nitrogen, total phosphorus, and total potassium. N2T1 treatment had significantly higher biomass than other treatments, while N3T2 treatment had significantly lower biomass than other treatments ($p < 0.05$). N1T2 treatment had significantly higher organic carbon than other

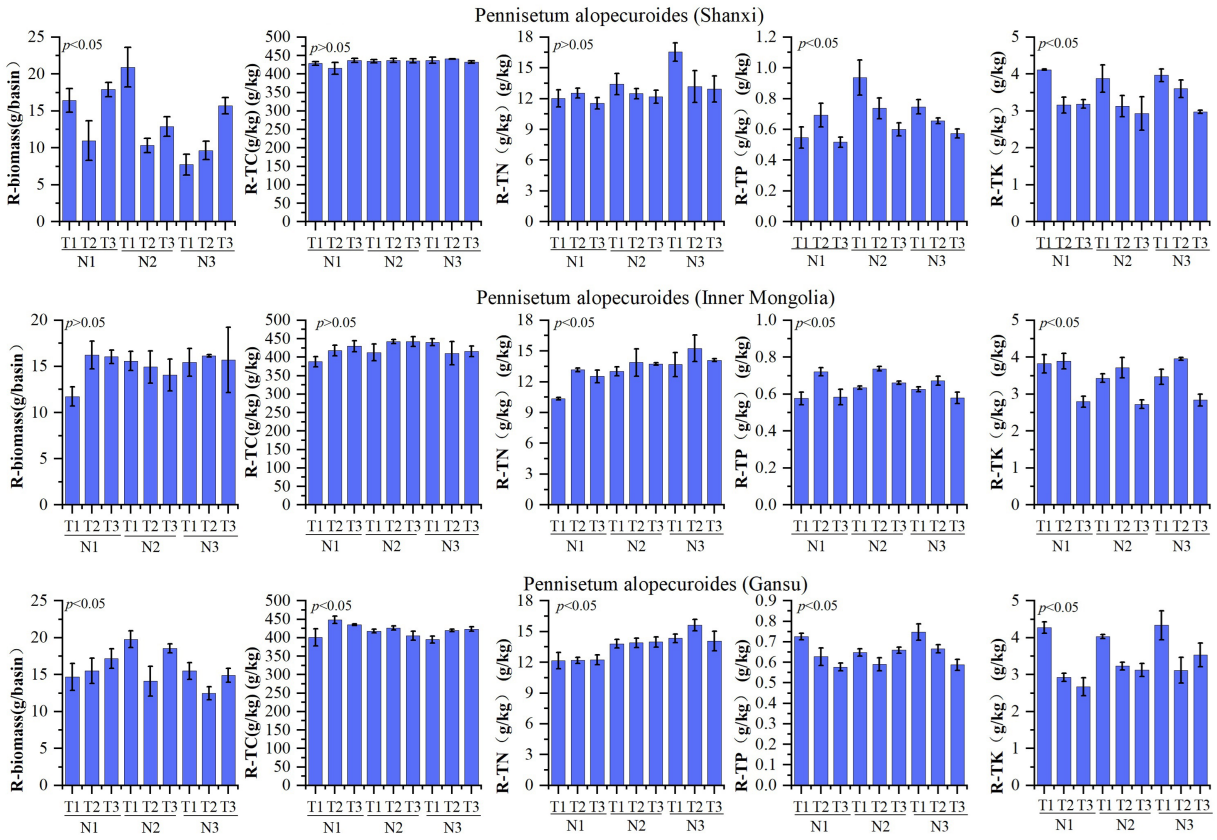


FIGURE 3
Plant root characteristics of different *Pennisetum alopecuroides* in the trail.

treatments, while N1T1 treatment had significantly lower organic carbon than other treatments ($p < 0.05$). N3T2 treatment had significantly higher total nitrogen than other treatments, while N1T2 treatment had significantly lower total nitrogen than other treatments ($p < 0.05$). N3T1 treatment had significantly higher total phosphorus than other treatments, while N1T3 treatment had significantly lower total phosphorus than other treatments ($p < 0.05$). N3T1 treatment had significantly higher total potassium than other treatments, while N1T3 treatment had significantly lower total potassium than other treatments ($p < 0.05$).

The leaf nutrient factors of *Pennisetum* are illustrated in Figure 4. A study conducted in Shaanxi revealed that variations in temperature and nitrogen fertilizer had no significant impact on organic carbon, total phosphorus, and total potassium levels. However, they did significantly influence chlorophyll content, biomass production, and total nitrogen concentration. Specifically, the N1T1 treatment exhibited significantly higher chlorophyll levels compared to other treatments, the N1T3 treatment resulted in significantly greater biomass production than other treatments, and the N3T2 treatment showed a significantly higher total nitrogen concentration ($p < 0.05$). Similarly, an investigation carried out in Inner Mongolia demonstrated that changes in temperature and nitrogen fertilizer had no notable effect on organic carbon or total phosphorus levels but did have a significant impact on chlorophyll content, biomass production, total nitrogen concentration as well as total potassium levels.The chlorophyll content in the N1T1 treatment exhibited a significant increase compared to other treatments, while the biomass in the N3T2 treatment showed a significantly higher value than other treatments. Moreover, the total nitrogen concentration was found to be significantly elevated in the N3T1 treatment relative to other treatments, and similarly, the total potassium level was notably higher in the N3T3 treatment ($p < 0.05$). The Gansu *Pennisetum* study revealed that variations in temperature and nitrogen fertilizer application did not exert a significant influence on organic carbon, total phosphorus, and total potassium levels. However, these factors had a pronounced impact on chlorophyll content, biomass production, and total nitrogen concentration. Specifically, the chlorophyll content of plants subjected to the N3T1 treatment displayed a significant increase compared to other treatments. Additionally, plants treated with N3T3 exhibited significantly higher biomass values than those under different conditions. Furthermore, an elevated level of total nitrogen was observed in plants treated with N3T2 when compared to other treatments ($p < 0.05$).

3.2 Structural composition of soil microbial communities

By employing high-throughput sequencing, we investigated the soil bacterial community of *Pennisetum* from three different seed sources (Figure 5). At the phylum taxonomic level, our results revealed that *Proteobacteria*, *Acidobacteriota*, *Actinomycetota*, *Candidatus*

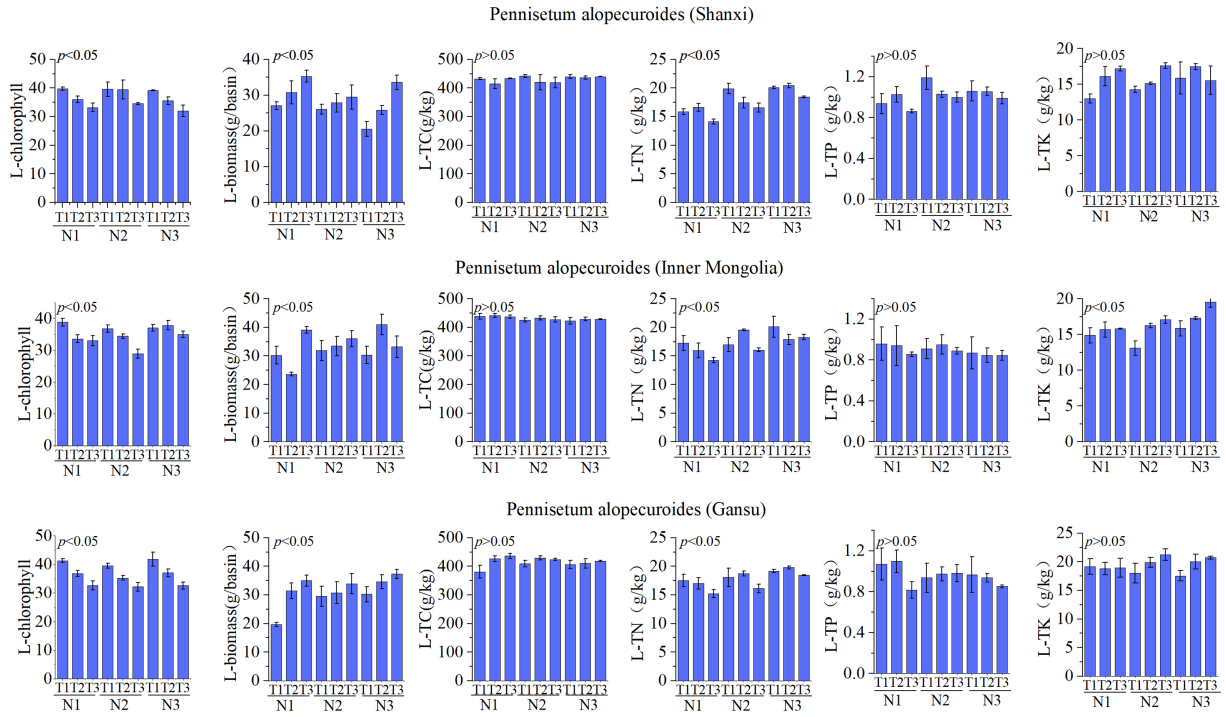


FIGURE 4
Physical and chemical properties of leaves.

Saccharibacteria, *Cyanobacteriota*, *Bacteroidota* and *Chlorobiota* were the predominant taxa in the *Pennisetum* soil bacterial community under varying temperatures and nitrogen fertilizer levels. Among these phyla, *Proteobacteria* exhibited the highest relative abundance at 49.63% in the N3T2 treatment and lowest at 37.16% in the N3T3 treatment; whereas *Acidobacteriota* showed its highest relative abundance at 23.22% in the N1T2 treatment and lowest at 9.13% in the N3T1 treatment. Furthermore, significant differences were observed in the abundance of *Acidobacteriota* and *Parcubacteria* among treatments ($p < 0.05$). In the study on *Pennisetum* in Inner Mongolia, the soil bacterial community associated with *Pennisetum* under varying temperatures and nitrogen fertilizer levels was found to be primarily composed of *Proteobacteria*, *Acidobacteriota*, *Actinomycetota*, *Candidatus Saccharibacteria*, *Cyanobacteriota*, *Bacteroidota*, *Gemmatimonadota* and *Chlorobiota* taxa. Among these phyla, *Proteobacteria* exhibited the highest relative abundance ranging from 51.09% (N1T2) to 22.84% (N3T3), while *Acidobacteriota* showed the highest relative abundance at 18.14% (N1T2) and lowest at 11.99%. In addition, *Gemmatimonadota*, *Cyanobacteriota*, *Planctomycetota*, *Bacillota* and *Thermomicrobiota* were significantly different among treatments ($p < 0.05$). For Gansu *Pennisetum*, it was found that the soil bacterial community of *Pennisetum* under different temperatures and nitrogen fertilizer levels mainly included *Proteobacteria*, *Cyanobacteriota*, *Acidobacteriota*, *Actinomycetota*, *CandidatusSaccharibacteria*, *Bacteroidota*, *Gemmatimonadota* and *Chlorobiota* taxa. The first three phyla were dominant, with total relative abundance of 63.82% (N1T1), 67.98% (N1T2), 68.89% (N1T3), 77.87% (N2T1), 76.99% (N2T2), 71.09% (N2T3), and 77.90% (N3T1) at different temperatures and nitrogen fertilization levels, respectively, 76.21% (N3T2), 64.05% (N3T3).The relative abundance of *Cyanobacteriota* was highest at 53.74% in the N2T2 treatment and lowest at 8.28% in the N3T3 treatment, whereas the relative abundance of *Proteobacteria* was highest at 49.94% in the N3T2 treatment and lowest at 16.87% in the N2T2 treatment. In addition, *Candidatus Saccharibacteria*, *Planctomycetota*, *Bacillota* and *Thermomicrobiota* were significantly different ($p < 0.05$) among treatments.

The results of principal component analysis (Figure 6) revealed distinct variations in soil bacterial communities among three different seed sources of *Pennisetum* under varying temperatures and nitrogen fertilizer levels. Additionally, the ANOSIM test demonstrated significant dissimilarities ($p < 0.05$) in soil microbial communities between *Pennisetum* samples from Inner Mongolia and Gansu at different temperature and nitrogen fertilizer conditions.

High-throughput sequencing of soil fungi from three different provenances of Pennisetum revealed (Figure 7) at the phylum level that Shaanxi *Pennisetum* soil fungal communities included *Ascomycota*, *Basidiomycota*, *Glomeromycota*, *Fungi_phy_Incertae_sedis*, *Mortierellomycota*, *Chytridiomycota*, *Mucoromycota*, and *Olpidiomycota*. *Ascomycota* was the dominant phylum, with relative abundances of 74.39% (N1T1), 57.35% (N1T2), 58.37% (N1T3), 86.51% (N2T1), 74.52% (N2T2), 54.02% (N2T3), 93.76% (N3T1), 72.57% (N3T2), and 86.88% (N3T3). In addition, *Olpidiomycota* and *lastocladiomycota* were significantly different among treatments ($p < 0.05$). For the Inner Mongolian Pennisetum study, *Ascomycota* and *Fungi_phy_Incertae_sedis* were found to be the dominant phylum in each treatment and the abundance was 89.63% (N1T1), 90.07% (N1T2), 91.43% (N1T3), 85.81% (N2T1), and 82.77% (N2T2), respectively, 89.42% (N2T3), 91.84% (N3T1), 88.23% (N3T2), 88.42% (N3T3). The relative abundance of Ascomycota was highest at 84.54% in the N3T2 treatment and lowest at 30.15% in the N3T3 treatment.

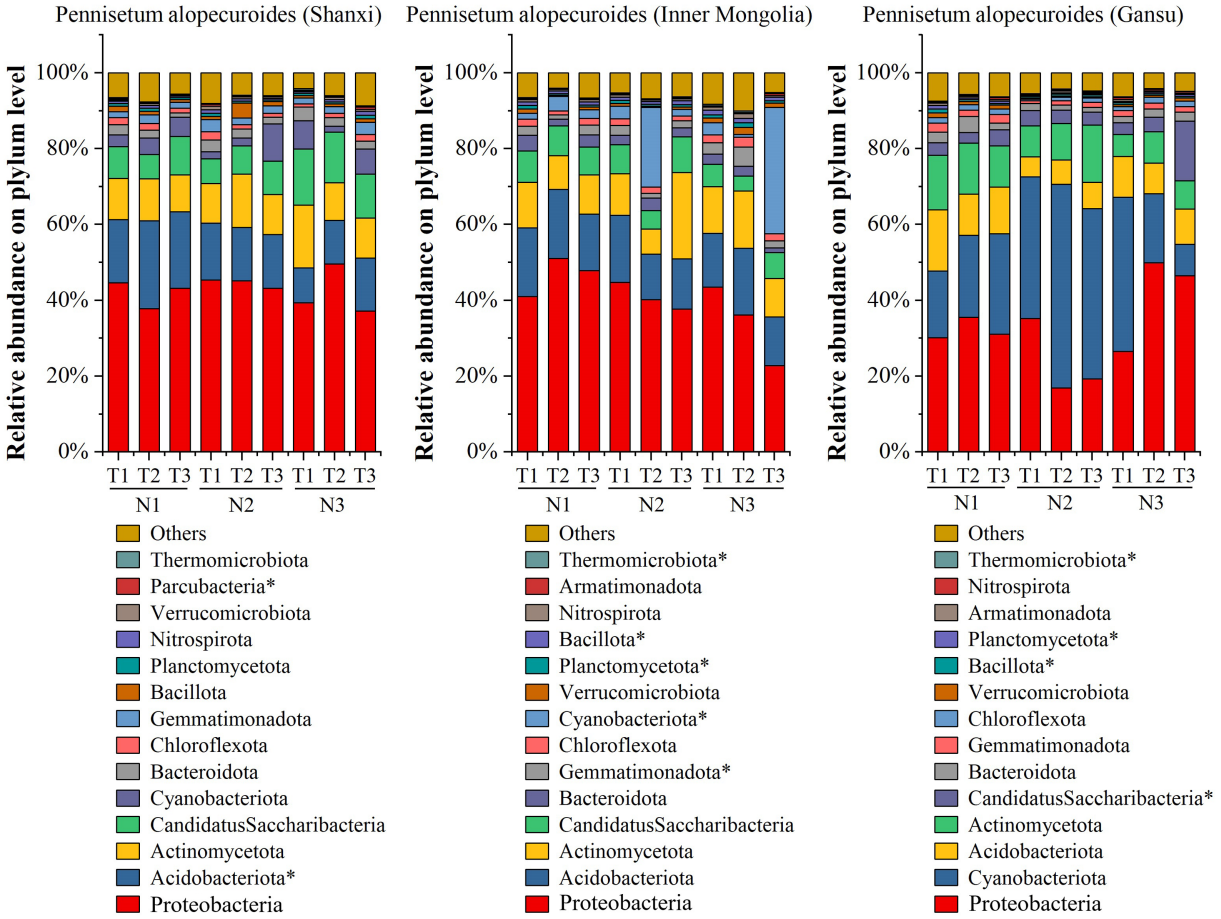


FIGURE 5
Soil bacterial community composition. * indicates significant differences between treatments ($p < 0.05$).

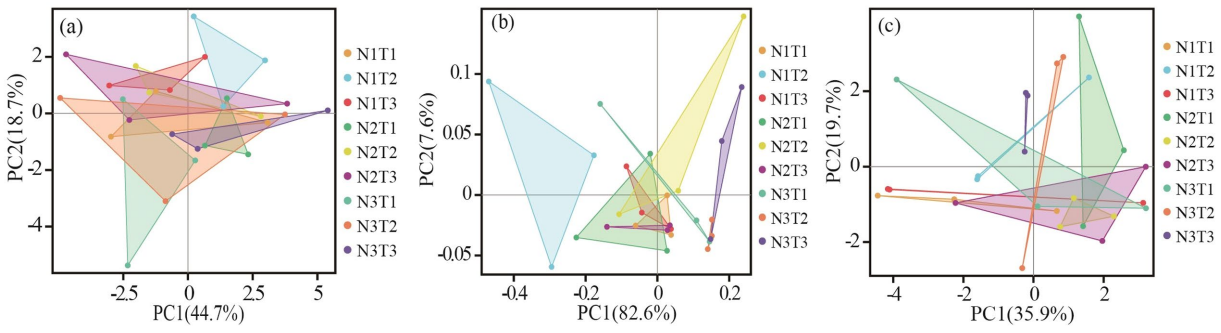


FIGURE 6
Principal component analysis (PCA) of soil bacteria. Panels **(a–c)** display the PCA for Pennisetum in Shaanxi, Inner Mongolia, and Gansu, respectively.

Additionally, there were significant differences in the abundance of *Ascomycota* and *Mucoromycota* among treatments ($p < 0.05$). For Gansu *Pennisetum*, both *Ascomycota* and Fungi_phy_Incertae_sedis were dominant phyla in each treatment, with abundances of 74.25% (N1T1), 78.73% (N1T2), 91.69% (N1T3), 90.46% (N2T1), and 92.85% (N2T2) respectively, as well as 79.42% (N2T3), 92.06% (N3T1),97.21% (N3T2), and 90.04% (N3T3).The relative abundance of *Ascomycota* was highest at 91.01% in the N3T2 treatment and lowest at 10.53% in the N2T1 treatment. Additionally, there were significant differences in the abundance of *Ascomycota*, *Glomeromycota*, and *Monoblepharomycota* among treatments ($p < 0.05$).

The results of principal component analysis (Figure 8) revealed distinct variations in soil fungal communities among three different seed sources of *Pennisetums* under varying temperatures and nitrogen fertilizer levels. Additionally, the ANOSIM test demonstrated significant differences ($p < 0.05$) in soil microbial communities among

10.3389/fmicb.2024.1483150

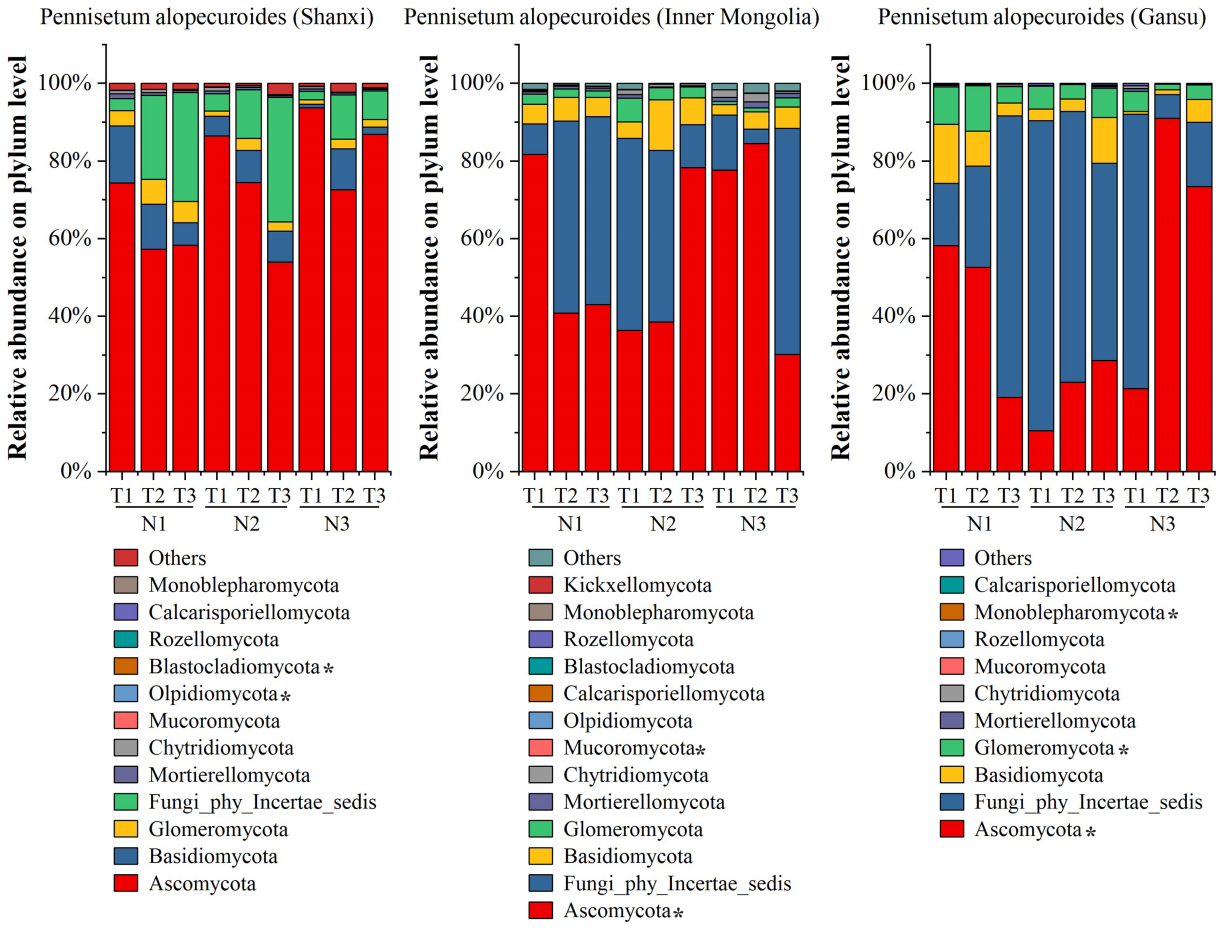


FIGURE 7
Soil fungal community composition.

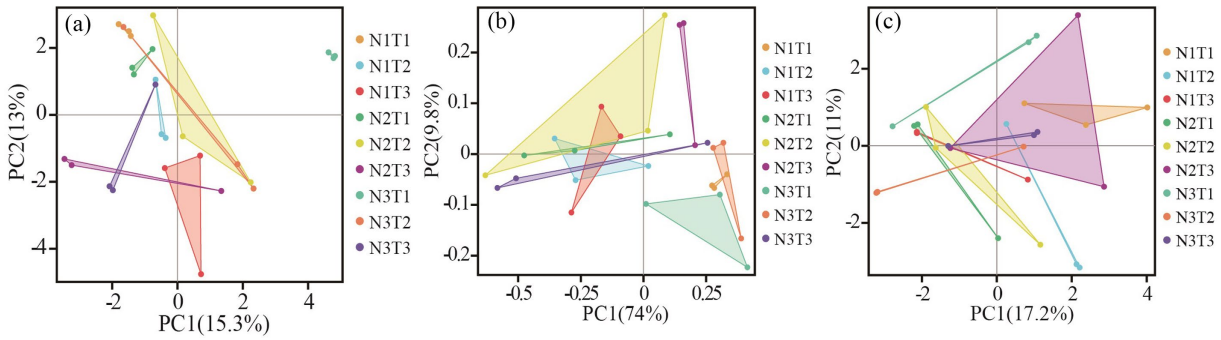


FIGURE 8
Principal component analysis (PCA) of soil fungi. Panels **(a–c)** display the PCA for Pennisetum in Shaanxi, Inner Mongolia, and Gansu, respectively.

the three seed sources of *Pennisetums* at different temperature and nitrogen fertilizer combinations.

3.3 Soil microbial diversity

Soil bacterial α-diversity (Figure 9) showed that Chao1 and Shannon indices for Shaanxi *Pennisetum* soil bacteria were higher in N2T1 treatment than other treatments. Inner Mongolia *Pennisetum* soil bacterial Chao1 and Shannon indices were higher in N3T2 treatment than other treatments and lower in N1T2 treatment. Gansu *Pennisetum* soil bacterial Chao1 and Shannon indices were higher in N1T1 treatment than other treatments and lower in N2T1 treatment.

Soil fungal α-diversity (Figure 10) showed that Chao1 index for Shaanxi *Pennisetum* soil fungi was higher in N3T1 treatment than other treatments, while Shannon index was higher in N3T3 treatment.

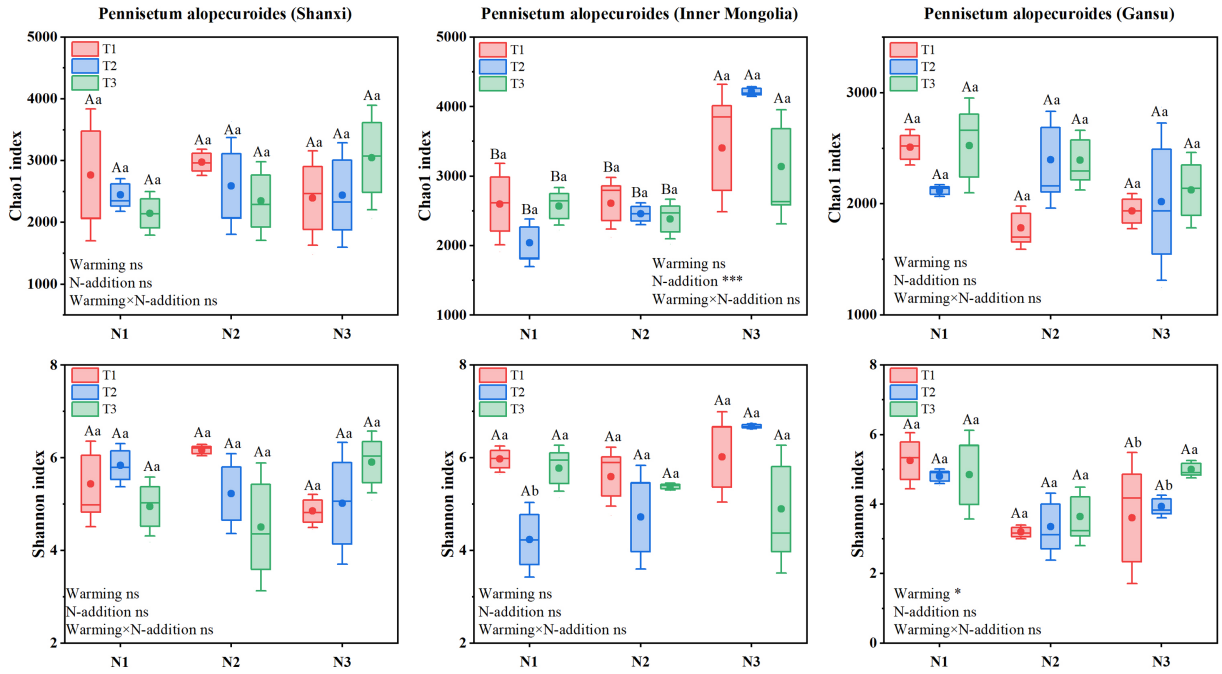


FIGURE 9
Soil bacterial community diversity index.

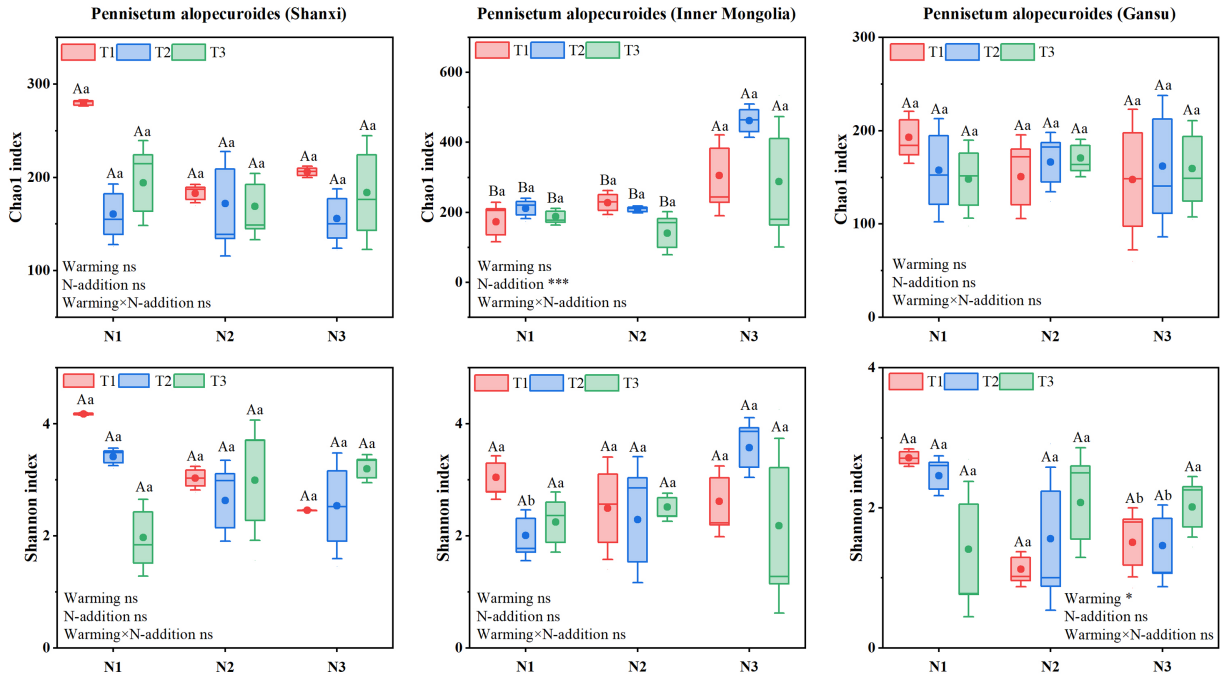


FIGURE 10
Soil fungal community diversity index.

Inner Mongolia *Pennisetum* soil fungal Chao1 and Shannon indices were higher in N3T2 treatment than other treatments. Gansu *Pennisetum* soil fungal Chao1 and Shannon indices were higher in N1T1 treatment than other treatments and lower in N2T1 treatment (see Figure 10).

3.4 Soil microbial community co-occurrence patterns

The microbial co-occurrence network characteristics of *Pennisetum* soil from three different seed sources exhibited significant

differences (Figure 11). Analysis of the microbial network characteristics in Shaanxi *Pennisetum* soil revealed that the N3T3 treatment displayed a higher number of edges (18955), nodes (995), average weighted degree, and graph density in the microbial co-occurrence network (Table 2). These findings indicate that the soil microbial co-occurrence network in this treatment is more complex with intricate interactions among different species, while also exhibiting a higher degree of modularity and distinct sub-structures. Moreover, the N1T1 treatment exhibited a lower proportion of positive correlation edges and a higher proportion of negative correlation edges compared to other treatments. Conversely, the N3T2 treatment displayed a higher proportion of positive correlation edges and a lower proportion of negative correlation edges in comparison to other treatments. These findings suggest that there exists a robust collaborative relationship among species within microbial communities subjected to high-concentration nitrogen additions and high-temperature treatments, while a strong competitive relationship is observed among species within microbial communities exposed to low-concentration nitrogen additions and low-temperature treatments. The relationship between microbial communities in the low-temperature and high-temperature treatments exhibited a robust association. Investigation and analysis of soil microbial networks in Inner Mongolia *Pennisetum* (Table 3) revealed that the N3T3 treatment displayed higher numbers of edges (19875), nodes (998), average weighted degree, and graph density within the microbial co-occurrence network, indicating increased complexity of species interactions. Conversely, the N1T2 treatment demonstrated higher modularity with evident substructure. Moreover, the N3T2 treatment exhibited a lower proportion of positive correlation edges and a higher proportion of negative correlation edges compared to the other treatments. Conversely, the N3T3 treatment showed a higher proportion of positive correlation edges and a lower proportion of negative correlation edges compared to the other treatments. These findings suggest that there exists a strong collaborative relationship among species within microbial communities under high nitrogen concentration and high temperature conditions, while a strong competitive relationship is observed between species in microbial communities subjected to high nitrogen concentration and low temperature conditions. The association between microbial communities under high nitrogen concentration and low temperature conditions was found to be significant. The research and analysis of soil microbial network characteristics in Gansu *Pennisetum* (Table 4) revealed that the N1T3 treatment exhibited a higher number of edges (30222), nodes (980), average weighted degree, and graph density in the microbial co-occurrence network. This indicates that the soil microbial co-occurrence network in this treatment displayed greater complexity and more intricate interactions among different species. Conversely, the N2T2 treatment demonstrated a higher degree of modularity with evident substructures. Furthermore, compared to other treatments, the N3T3 treatment had a lower proportion of positive correlation edges and a higher proportion of negative correlation edges, while the N3T1 treatment showed a higher proportion of positive correlation edges and a lower proportion of negative correlation edges. These findings suggest that there exists strong collaboration between species within high-concentration nitrogen additions and low-temperature treatments, whereas competitive relationships prevail among species within high-concentration nitrogen additions and high-temperature treatments. Notably, the negative correlation margins were lower than those observed in other treatments.

3.5 Relationship between soil microbial communities and physicochemical factors

The Mantel analysis (Figures 12a–c) revealed a significant positive correlation ($p < 0.05$) between Shaanxi *Pennisetum* L-chlorophyll and R-TK. Additionally, there was a significant positive correlation ($p < 0.05$) between L-biomass and soil pH, S-TN, L-TN, R-TN, as well as R-TK. Moreover, R-biomass showed a significant positive correlation ($p < 0.05$) with S-TN, while both L-TP and R-TN exhibited a significant positive correlation ($p < 0.05$). In the case of Inner Mongolia *Pennisetum*, there was a significant positive correlation ($p < 0.05$) between L-chlorophyll and R-TK; similarly, R-biomass displayed a significant positive correlation with soil L-TP ($p < 0.05$). Furthermore, Gansu *Pennisetum* demonstrated a significant positive correlation ($p < 0.05$) between L-chlorophyll and both R-TP and R-TK; additionally, there was a significant positive association ($p < 0.05$) between L-biomass and soil variables such as L-TC, L-TP, R-TK, and R-TC. Finally, the fungal community diversity exhibited a significantly positive correlation ($p < 0.05$) with S-TN.

Structural equation modeling analysis (Figures 12j–l) found that L-biomass and R-biomass were significantly positively correlated in Shaanxi *Pennisetum*, and nitrogen addition significantly affected fungal diversity ($p < 0.05$). In Inner Mongolia *Pennisetum*, L-biomass and temperature significantly affected bacterial diversity ($p < 0.05$). In Gansu *Pennisetum*, temperature and nitrogen had no significant effect on microorganisms, indicating that soil microbial communities were influenced by multiple factors.

Further redundancy analysis (Figures 12d–i) found that soil pH was the main environmental factor affecting bacteria in Shaanxi *Pennisetum*, and soil total phosphorus was the main environmental factor affecting fungi. In Inner Mongolia *Pennisetum*, soil pH and soil total potassium were the main environmental factors affecting bacteria, and R-biomass was the main environmental factor affecting fungi. In Gansu *Pennisetum*, R-biomass, L-biomass, and L-TP were the main environmental factors affecting bacteria, and R-TC and R-TP were the main environmental factors affecting fungi.

4 Discussion

4.1 Effects of different nitrogen fertilizers and temperatures on the characteristics of microbial communities in *Pennisetum* soils

Soil microorganisms exhibit diminutive morphology, wide distribution, relatively short life cycles, remarkable diversity, prompt response to environmental perturbations, and the ability to swiftly adapt to environmental changes while upholding ecosystem stability (Xiong et al., 2017). This study showed that *Proteobacteria* in the soil of Shaanxi and Inner Mongolia *Pennisetum* significantly decreased under high temperature and high nitrogen treatments, while *Acidobacteriota* had higher relative abundance under low

10.3389/fmicb.2024.1483150

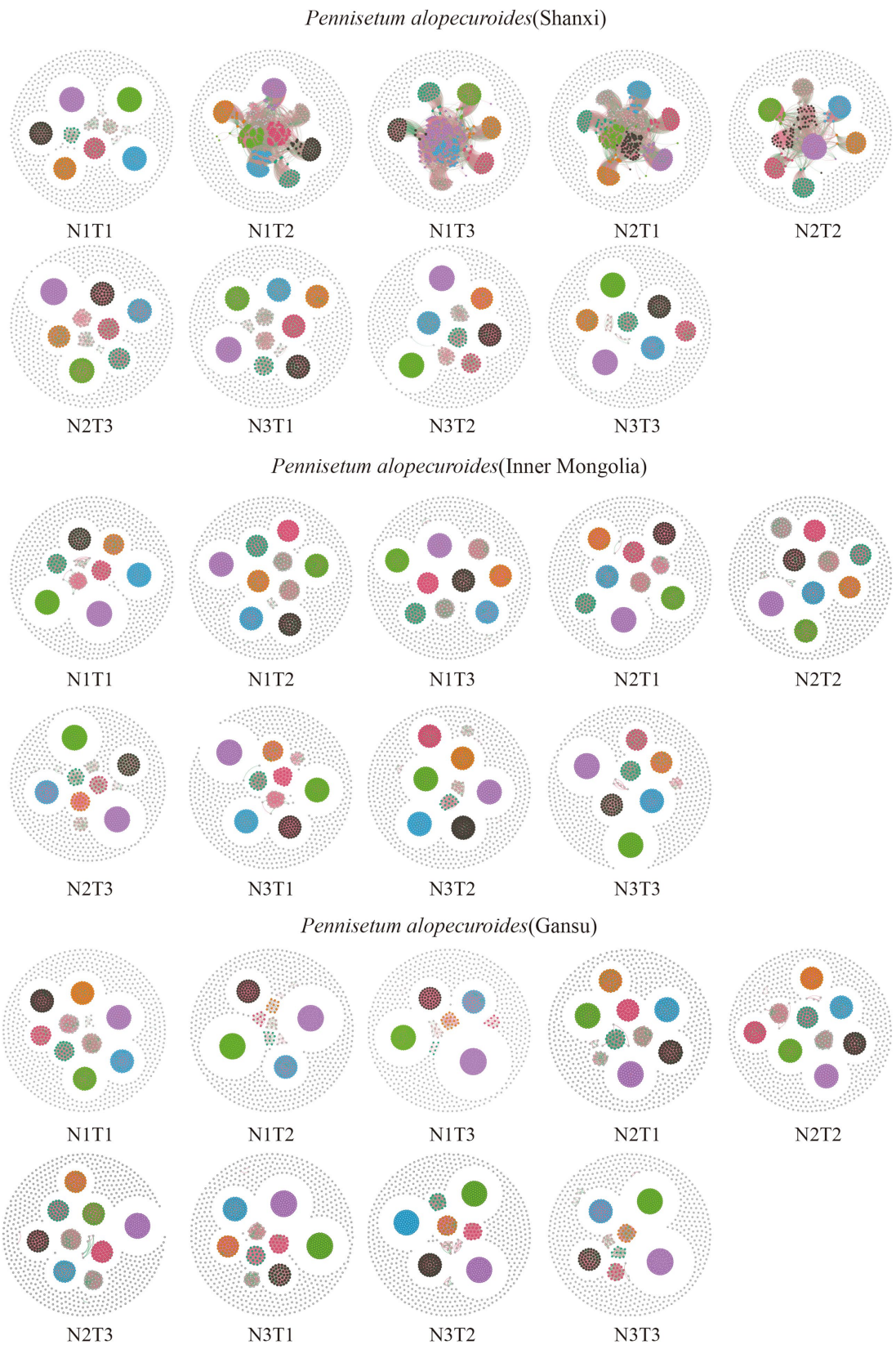


FIGURE 11
Co-linear network analysis of soil microbial communities. The node size represents the degree (or the number of nodes connected to it). Red connection lines are positive connections, green connection lines are negative connections. The number of nodes is colored according to the different classifications.

TABLE 2 Topological parameters of microbial co-occurrence network in Shaanxi *Pennisetum* soil.

Topological parameters	N1T1	N1T2	N1T3	N2T1	N2T2	N2T3	N3T1	N3T2	N3T3
Node	992	996	957	998	998	916	938	982	995
Edge	17,033	16,571	16,017	16,356	16,595	14,633	13,138	17,600	18,955
Positive edge	52.17%	66.92%	70.04%	63.84%	75.14%	69.7%	58.32%	86.45%	70.82%
Negative edge	47.83%	33.08%	29.96%	36.16%	24.86%	30.3%	41.68%	13.55%	29.18%
Average weighting	17.17	17.101	17.798	17.067	17.067	15.975	14.006	17.923	19.05
Graph density	0.017	0.017	0.018	0.016	0.017	0.017	0.015	0.018	0.019
Modularity	0.800	0.742	0.646	0.713	0.755	0.763	0.829	0.764	0.77

TABLE 3 Topological parameters of the microbial co-occurrence network of *Pennisetum* soil in Inner Mongolia.

Topological parameters	N1T1	N1T2	N1T3	N2T1	N2T2	N2T3	N3T1	N3T2	N3T3
Node	996	992	996	998	994	908	998	1,000	998
Edge	18,828	13,891	14,257	15,818	13,945	16,480	19,189	17,325	19,875
Positive edge	69.11%	68.00%	67.03%	62.83%	75.15%	57.49%	77.66%	54.81%	78.03%
Negative edge	30.89%	32.00%	32.97%	37.17%	24.85%	42.51%	22.34%	45.19%	21.97%
Average weighting	18.904	14.003	14.314	15.85	14.029	18.15	19.227	17.325	19.915
Graph density	0.019	0.014	0.014	0.016	0.014	0.02	0.019	0.017	0.02
Modularity	0.756	0.855	0.85	0.796	0.841	0.719	0.740	0.827	0.755

TABLE 4 Topological parameters of microbial co-occurrence network of *Pennisetum* soil in Gansu.

Topological parameters	N1T1	N1T2	N1T3	N2T1	N2T2	N2T3	N3T1	N3T2	N3T3
Node	998	988	980	926	1,000	998	944	986	974
Edge	15,033	27,004	30,222	13,776	14,334	15,629	17,470	21,136	24,318
Positive edge	69.07%	65.61%	64.04%	70.2%	79.98%	78.26%	87.49%	67.37%	58.48%
Negative edge	30.93%	34.39%	35.96%	29.8%	20.02%	21.74%	12.51%	32.63%	41.52%
Average weighting	15.063	27.332	30.839	14.877	14.334	15.66	18.506	21.436	24.967
Graph density	0.015	0.028	0.032	0.016	0.014	0.016	0.02	0.022	0.026
Modularity	0.839	0.65	0.516	0.819	0.855	0.762	0.728	0.75	0.633

nitrogen treatment. This may be due to the poor adaptability of *Proteobacteria* to high temperature and high nitrogen environments, inhibiting their metabolic activities and affecting their physiological activities. In contrast, *Acidobacteriota* has a strong adaptability to low nitrogen environments, possibly being more competitive in resource-scarce environments (Li et al., 2022). Additionally, *Cyanobacteriota* in Inner Mongolia *Pennisetum* soil was significantly higher under high temperature and high nitrogen treatments, possibly due to the nitrogen-fixing ability of *Cyanobacteriota*, which helps improve soil nitrogen utilization efficiency under high nitrogen treatments, benefiting their growth and reproduction (Cole et al., 2016). *Cyanobacteriota* can survive and reproduce at higher temperatures. High temperatures may promote the growth and metabolic activities of *Cyanobacteriota*, increasing their relative abundance in high temperature environments (Tang et al., 2002). In Gansu *Pennisetum* soil, *Proteobacteria* had the lowest relative abundance under medium temperature and medium nitrogen treatments, while *Cyanobacteriota* had the highest relative abundance, possibly due to the higher altitude of Gansu *Pennisetum*, causing different adaptability to environmental conditions, resource utilization efficiency, and competition with other microorganisms. Additionally, *Ascomycota* was significantly higher under low temperature and high nitrogen treatments, while *Basidiomycota* and *Glomeromycota* were significantly higher under high temperature and low nitrogen treatments in the soil of the three provenances of *Pennisetum*. This may be due to high nitrogen treatments promoting the secretion of more amino acids and sugars by plant roots, increasing soil nutrient content and further enhancing the reproduction and growth of *Ascomycota*. Low temperature environments cause fungi to produce cold-tolerant enzymes and antifreeze proteins, enabling them to adapt to lower temperature environments and occupy ecological advantages. Low temperature environments may inhibit the growth of some other fungi, allowing *Ascomycota* to dominate in competition (Chen et al., 2017; Hu et al.,

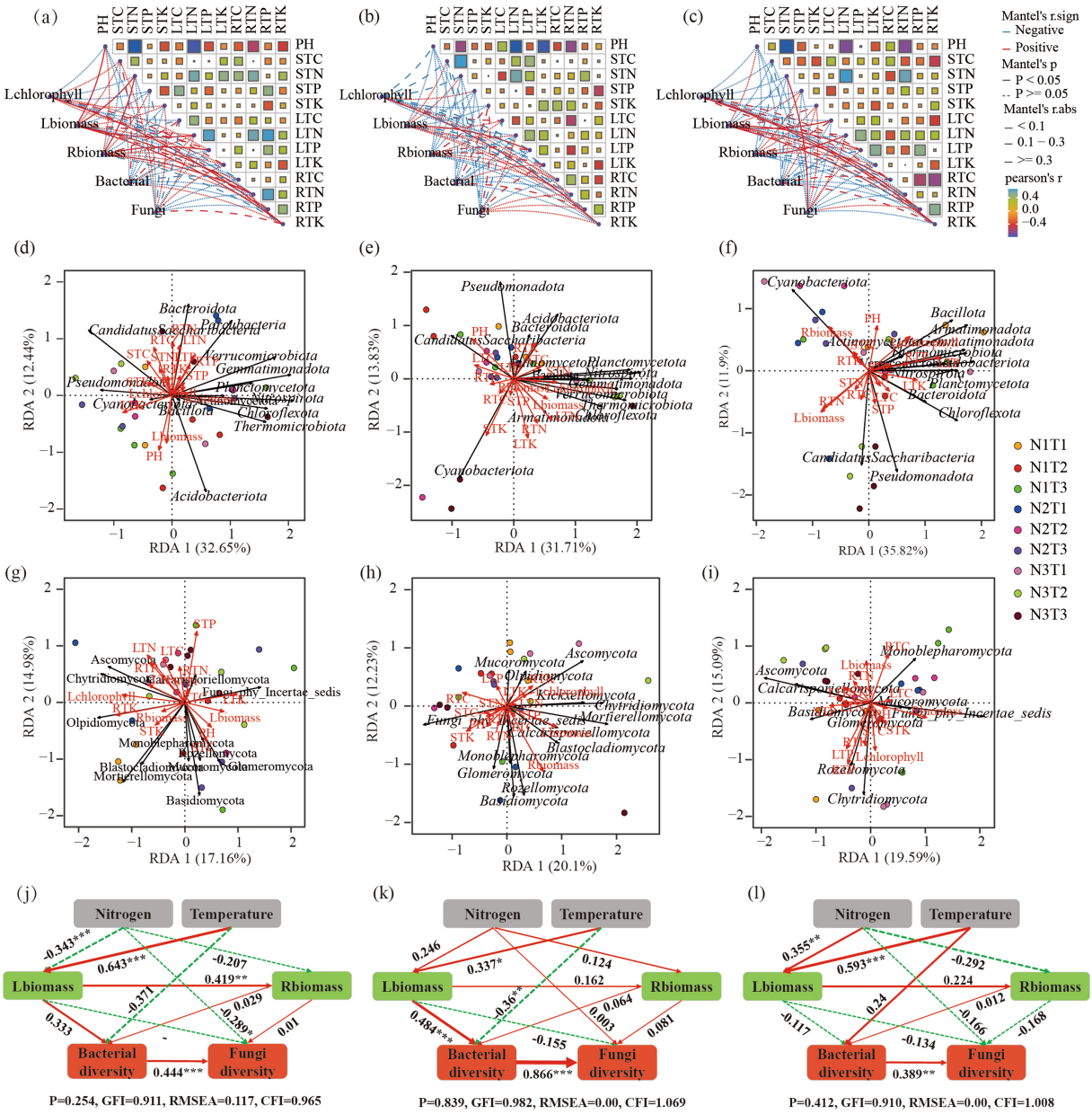


FIGURE 12
Panels **(a–c)** display the Mantel analysis for Pennisetum in Shaanxi, Inner Mongolia, and Gansu, respectively. Panels **(d–f)** show the redundancy analysis (RDA) of bacterial communities and physicochemical factors for Pennisetum in Shaanxi, Inner Mongolia, and Gansu, respectively. Panels **(g–i)** illustrate the RDA of fungal communities and physicochemical factors in Shaanxi, Inner Mongolia, and Gansu, respectively. Panels **(j–l)** depict the structural equation models for Pennisetum in Shaanxi, Inner Mongolia, and Gansu, respectively.

2014; Tedersoo et al., 2014). Many species of *Basidiomycota* can grow and reproduce in high temperature environments. These fungi can tolerate higher temperature conditions through heat shock proteins and other protective mechanisms, occupying ecological advantages in high temperature environments. Similarly, some fungi in *Glomeromycota* can maintain activity and reproductive capacity under high temperature conditions (Huang et al., 2023; Vedenicheva, et al., 2018). Low nitrogen treatments reduce the available nitrogen content in soil, benefiting fungi that can efficiently utilize limited nitrogen sources. Many species in *Basidiomycota* and *Glomeromycota* can obtain the necessary nitrogen from organic matter through efficient nitrogen metabolism pathways, gaining advantages under low nitrogen conditions (Hestrin et al., 2021; Pellitier and Zak, 2018). Additionally, high temperature and low nitrogen treatments may change the physical and chemical properties of soil, such as pH, moisture content, and organic matter decomposition rate. These changes affect the ecological niches and competition relationships of different fungal groups. *Basidiomycota* and *Glomeromycota* may have strong adaptability under these changing conditions, gaining competitive advantages in high temperature and low nitrogen environments (Classen et al., 2016; Harrower and Gilbert, 2021).

Redundancy analysis found that soil pH was the main factor affecting soil bacterial communities in Shaanxi and Inner Mongolia *Pennisetum*. Changes in soil acidity and alkalinity can broadly affect bacterial survival and metabolic activities, altering the physiological

activities, nutrient forms, and availability of soil microorganisms, indirectly affecting their growth (Ullah et al., 2020). Redundancy analysis found that soil pH was the main factor affecting soil bacterial communities in Shaanxi and Inner Mongolia *Pennisetum*. Changes in soil acidity and alkalinity can broadly affect bacterial survival and metabolic activities, altering the physiological activities, nutrient forms, and availability of soil microorganisms, indirectly affecting their growth (Clayton et al., 2021) Root biomass and aboveground biomass also significantly impact soil microbial communities. Plants provide abundant carbon sources and nutrients for soil microorganisms through root exudates and litter, affecting microbial growth and metabolic activities. Changes in root and aboveground phosphorus content also indirectly affect microbial community structure by altering the distribution and availability of phosphorus in soil (Wang et al., 2023). In summary, the impact of soil environmental factors on microbial communities under different treatments showed significant differences. These differences reflect the characteristics of different treatment soils and reveal the sensitivity and adaptability of microbial communities to environmental changes. Understanding these environmental factors' impact on microbial communities is crucial for soil management and agricultural production. Optimizing soil pH, rationally applying nutrients, and improving plant growth conditions can effectively regulate soil microbial communities, enhancing soil health and agricultural productivity. The Chao1 and Shannon indices for Shaanxi *Pennisetum* soil bacteria in N2T1 treatment were higher than other treatments, possibly because moderate nitrogen and low temperature conditions may enhance nutrient cycling and organic matter decomposition, promoting bacterial species richness and diversity (Hu et al., 2022). Inner Mongolia *Pennisetum* soil bacterial and fungal Chao1 and Shannon indices were higher in N3T2 treatment than other treatments, possibly due to high nitrogen and moderate temperature providing sufficient nutrients and suitable environments for soil bacteria and fungi, promoting species richness and diversity (Conant et al., 2011). The temperature of the soil in the Gansu area is the most suitable environment for the soil bacteria and fungi. The Chao1 and Shannon indices of soil bacteria and fungi in Pennisetum in Gansu were lower in the N2T1 treatment than in the other treatments, which may be due to the increase of competitive pressure or the unmet specific needs of some bacteria and fungi, resulting in the decrease of the abundance and diversity of the bacterial and fungal community (Tang et al., 2020) The above results indicated that there were significant differences in soil bacterial and fungal diversity in response to N fertilizer application and temperature conditions in different regions. This may be related to the soil types, climatic conditions and growth characteristics of Pennisetum in each region.

4.2 Effects of different nitrogen fertilizers and temperatures on microbial interactions in Pennisetum soils

Molecular ecological networks can reflect interactions between different groups within a community and assess the complexity of target communities, successfully applied to analyze environmental characteristics' impact on microbial communities (Carr et al., 2019). Soil microbial co-occurrence networks under different nitrogen and temperature levels showed significant differences. This study showed strong cooperative relationships among microbial species under high nitrogen environments in the soil of three provenances of *Pennisetum*, possibly due to high nitrogen environments promoting ecological niche differentiation among microbial species and the production and transmission of signaling molecules and metabolites in microbial communities, further promoting microbial communication and cooperation (Bernard et al., 2022; Lemaire et al., 2021) Shaanxi and Inner Mongolia *Pennisetum* had strong cooperative relationships among soil microbial species under high temperature conditions, while Gansu *Pennisetum* had strong cooperative relationships under low temperature conditions, possibly due to the adaptation of Shaanxi and Inner Mongolia *Pennisetum* soil microorganisms to high temperature environments and Gansu *Pennisetum* soil microorganisms to low temperature environments (Bardgett and Putten, 2014). The *Pennisetum* may secrete diverse chemicals at varying temperatures, and these inter-root secretions can exert influence on the composition and function of microbial communities; inter-root secretions under high temperatures may facilitate the growth of specific collaborative microorganisms, while those under low temperatures may promote the cooperation among another group of microorganisms (Chaparro et al., 2013). In general, future investigations could delve into the molecular mechanisms underlying alterations in microbial network characteristics across different environmental conditions and elucidate their impacts on *Pennisetum* growth and ecosystem functioning. This will help better understand the role of soil microorganisms in agriculture and ecological restoration and provide scientific evidence for optimizing planting and management strategies.

4.3 Environmental impacts and limitations of this study

This study explored the characteristics of soil microbial communities, and also used microbial co-occurrence network and pathway analysis to explore the effects of nitrogen fertilizer additions and temperature changes on the stability of the soil ecosystems of *Pennisetum*, among others. It found strong cooperative relationships among microbial species under high nitrogen and high temperature treatments for Shaanxi and Inner Mongolia *Pennisetum*, while Gansu *Pennisetum* showed strong competitive relationships. Therefore, it is necessary to determine the effective improvement of soil ecosystem stability under different nitrogen and temperature treatments for different provenances of *Pennisetum*, thereby improving soil moisture retention and nutrient cycling efficiency (Agnihotri et al., 2022). In recent years, no studies have evaluated the ecological stability of soil microorganisms in different provenances of *Pennisetum*. Ecological network structure analysis provides insights into microbial community interactions and system stability (Zeng et al., 2016). Increased connectivity and complexity of microbial networks under high temperature and high nitrogen treatments indicate increased ecosystem stability and enhanced resistance to ecological disturbances (Wang et al., 2019). Therefore, soil microbes play an important role in the ecosystem.

This study unveiled significant impacts of nitrogen fertilizer and temperature fluctuations on the microbial community structure in *Pennisetum* soils located in Northwest China, indicating that moderate levels of nitrogen fertilizer and temperature can enhance arbuscular mycorrhizal fungi (AMF) diversity and ecosystem functionality.

However, improper nitrogen fertilizer application and temperature changes may exert detrimental effects on microbial communities and overall ecosystem health. Therefore, future investigations should prioritize exploring the composition and function of soil microfood webs comprising fungi, bacteria, nematodes, and protozoa to comprehensively comprehend the consequences of nitrogen fertilization and temperature variations on soil microfood webs as well as ecosystem functioning.

5 Conclusion

This study deepened our understanding of the mechanisms of soil microbial changes under different nitrogen and temperature conditions. The dominant bacterial and fungal phyla in the soil of three different provenances of *Pennisetum* were *Proteobacteria* and *Ascomycota*, respectively. Nitrogen and temperature variations significantly affected the richness and diversity of soil microbial communities, leading to significant changes in their structure. Ecological network analysis indicated strong cooperative relationships among microbial species under high nitrogen and temperature treatments for Shaanxi and Inner Mongolia *Pennisetum*, while Gansu *Pennisetum* showed strong competitive relationships. Soil pH, total potassium, and total phosphorus were the main environmental factors affecting microorganisms. This experiment explored the microbial community changes and driving factors under different nitrogen fertilizer and temperature levels, which can provide a theoretical basis for evaluating the sustainable use of *Pennisetum* artificial grassland in Northwest China.

Data availability statement

The bacterial and fungal DNA sequences of the 81 soil samples were deposited in the SRA of the NCBI database under accession nos. PRJNA1137271, PRJNA1137536.

Author contributions

ND: Writing – original draft, Methodology, Investigation. LN: Writing – review & editing, Software, Data curation. SZ: Writing – review & editing, Methodology, Formal analysis. YiL: Writing – review & editing, Supervision, Methodology. HS: Writing – review & editing, Resources. YaL: Writing – review & editing, Investigation. ZM: Writing – review & editing, Project administration, Funding acquisition, Conceptualization.

Funding

The author(s) declare that financial support was received for the research, authorship, and/or publication of this article. This work was supported by "Natural Science Foundation of Science and Technology Department of Shaanxi Province (S2024-JC-YB-2574, 2020ZDLSF06-01)", "National Natural Science Foundation of China (32201588)" and "Xi'an Science Technology Bureau Fund (23NYGG0050, 22NYYF029)", Project of the First Investigation of Wild Plants Resources in Xi'an (K6-2207039).

Conflict of interest

The authors declare that the research was conducted in the absence of any commercial or financial relationships that could be construed as a potential conflict of interest.

Publisher's note

All claims expressed in this article are solely those of the authors and do not necessarily represent those of their affiliated organizations, or those of the publisher, the editors and the reviewers. Any product that may be evaluated in this article, or claim that may be made by its manufacturer, is not guaranteed or endorsed by the publisher.

References

Agnihotri, R., Sharma, M. P., Prakash, A., Ramesh, A., Bhattacharjya, S., Patra, A. K., et al. (2022). Glycoproteins of arbuscular mycorrhiza for soil carbon sequestration: review of mechanisms and controls. *Sci. Total Environ.* 806:150571. doi: 10.1016/j.scitotenv.2021.150571

Bardgett, R. D., and Putten, W. H. V. D. (2014). Belowground biodiversity and ecosystem functioning. *Nature* 515, 505–511. doi: 10.1038/nature13855

Belesky, D. P., and Malinowski, D. P. (2016). Grassland communities in the USA and expected trends associated with climate change. *Acta Agrobot.* 69:1673. doi: 10.5586/aa.1673

Bernard, L., Basile-Doelsch, I., Derrien, D., Fanin, N., Fontaine, S., Guenet, B., et al. (2022). Advancing the mechanistic understanding of the priming effect on soil organic matter mineralisation. *Funct. Ecol.* 36, 1355–1377. doi: 10.1111/1365-2435.14038

Bertola, M., Ferrarini, A., and Visioli, G. (2021). Improvement of soil microbial diversity through sustainable agricultural practices and its evaluation by-omics approaches: a perspective for the environment, food quality and human safety. *Microorganisms* 9:1400. doi: 10.3390/microorganisms9071400

Brookes, P. C., Landman, A., Pruden, G., and Jenkinson, D. S. (1985). Chloroform fumigation and the release of soil nitrogen: a rapid direct extraction method to measure microbial biomass nitrogen in soil. *Soil Biol. Biochem.* 17, 837–842. doi: 10.1016/0038-0717(85)90144-0

Carr, A., Diener, C., Baliga, N. S., and Gibbons, S. M. (2019). Use and abuse of correlation analyses in microbial ecology. *ISME J.* 13, 2647–2655. doi: 10.1038/s41396-019-0459-z

Chaparro, J. M., Badri, D. V., Bakker, M. G., Sugiyama, A., Manter, D. K., and Vivanco, J. M. (2013). Root exudation of phytochemicals in Arabidopsis follows specific patterns that are developmentally programmed and correlate with soil microbial functions. *PLoS One* 8:e55731. doi: 10.1371/journal.pone.0055731

Chen, Y.-L., Xu, T.-L., Veresoglou, S. D., Hu, H. W., Hao, Z. P., Hu, Y. J., et al. (2017). Plant diversity represents the prevalent determinant of soil fungal community structure across temperate grasslands in northern China. *Soil Biol. Biochem.* 110, 12–21. doi: 10.1016/j.soilbio.2017.02.015

Classen, A. T., Sundqvist, M. K., Henning, J. A., Newman, G. S., Moore, J. A. M., Cregger, M. A., et al. (2016). Direct and indirect effects of climate change on soil microbial and soil microbial-plant interactions: what lies ahead? *Ecosphere* 6:1. doi: 10.1890/ES15-00217.1

Clayton, J., Lemanski, K., and Bonkowski, M. (2021). Shifts in soil microbial stoichiometry and metabolic quotient provide evidence for a critical tipping point at 1% soil organic carbon in an agricultural post-mining chronosequence. *Biol. Fertil. Soils* 57, 435–446. doi: 10.1007/s00374-020-01532-2

Cole, B. J., Sayegh, E. T., Yanke, A. B., Chalmers, P. N., and Frank, R. M. (2016). Fixation of soft tissue to bone: techniques and fundamentals. *J. Am. Acad. Orthop. Surg.* 24, 83–95. doi: 10.5435/JAAOS-D-14-00081

Conant, R. T., Ryan, M. G., Ågren, G. I., Birge, H. E., Davidson, E. A., Eliasson, P. E., et al. (2011). Temperature and soil organic matter decomposition rates – synthesis of current knowledge and a way forward. *Glob. Chang. Biol.* 17, 3392–3404. doi: 10.1111/j.1365-2486.2011.02496.x

Dang, J. H., Cho, Y. H., and Lee, C. S. (2017). Effect of soil reinforcement on shear strength by Pennisetum alopecuroides and *Miscanthus sinensis* roots on loamy sand at river banks. *J. Korea Soc. Environ. Restor. Technol.* 20, 79–91. doi: 10.13087/kosert.2017.20.2.79

de Vries, F. T., Griffiths, R. I., Bailey, M., Craig, H., Girlanda, M., Gweon, H. S., et al. (2018). Soil bacterial networks are less stable under drought than fungal networks. *Communications* 9:10.1038/s41467-018-05516-7. doi: 10.1038/s41467-018-05516-7

Duchenne, F., Wüest, R. O., and Graham, C. H. (2022). Seasonal structure of interactions enhances multidimensional stability of mutualistic networks. *Proc. R. Soc. B* 289:20220064. doi: 10.1098/rspb.2022.0064

Goncharov, A. A., Leonov, V. D., Rozanova, O. L., Semenina, E. E., Tsurikov, S. M., Uvarov, A. V., et al. (2023). A meta-analysis suggests climate change shifts structure of regional communities of soil invertebrates. *Soil Biol. Biochem.* 181:109014. doi: 10.1016/j.soilbio.2023.109014

Graham, E. B., and Knelman, J. E. (2023). Implications of soil microbial community assembly for ecosystem restoration: patterns, process, and potential. *Microb. Ecol.* 85, 809–819. doi: 10.1007/s00248-022-02155-w

Guimaraes, H. I. P., Santana, R. H., Silveira, R., Pinto, O. H. B., Quirino, B. F., Barreto, C. C., et al. (2020). Seasonal variations in soil microbiota profile of termite (Syntermes wheeleri) mounds in the Brazilian tropical savanna. *Microorganisms* 8:1482. doi: 10.3390/microorganisms8101482

Harrower, J. T., and Gilbert, G. S. (2021). Parasitism to mutualism continuum for Joshua trees inoculated with different communities of arbuscular mycorrhizal fungi from a desert elevation gradient. *PLoS One* 16:256068. doi: 10.1371/journal.pone.0256068

Hestrin, R., Weber, P. K., Pett-Ridge, J., and Lehmann, J. (2021). Plants and mycorrhizal symbionts acquire substantial soil nitrogen from gaseous ammonia transport. *New Phytol.* 231, 1746–1757. doi: 10.1111/nph.17527

Hu, J., Huang, C., Zhou, S., Liu, X., and Dijkstra, F. A. (2022). Nitrogen addition increases microbial necromass in croplands and bacterial necromass in forests: a global meta-analysis. *Soil Biol. Biochem.* 165:108500. doi: 10.1016/j.soilbio.2021.108500

Hu, Y., Wang, L., Tang, Y., Li, Y., Chen, J., Xi, X., et al. (2014). Variability in soil microbial community and activity between coastal and riparian wetlands in the Yangtze River estuary – potential impacts on carbon sequestration. *Soil Biol. Biochem.* 70, 221–228. doi: 10.1016/j.soilbio.2013.12.025

Huang, B., Zhang, L., Cao, Y., Yang, Y., Wang, P., Li, Z., et al. (2023). Effects of land-use type on soil organic carbon and carbon pool management index through arbuscular mycorrhizal fungi pathways. *Glob. Ecol. Conserv.* 43:e02432. doi: 10.1016/j.gecco.2023.e02432

Jiao, S., Lu, Y., and Wei, G. (2022). Soil multitrophic network complexity enhances the link between biodiversity and multifunctionality in agricultural systems. *Glob. Chang. Biol.* 28, 140–153. doi: 10.1111/gcb.15917

Jordan, P., and Vilter, H. (1991). Extraction of proteins from material rich in anionic mucilages: partition and fractionation of vanadate-dependent bromoperoxidases from the brown algae Laminaria digitata and *L. saccharina* in aqueous polymer two-phase systems. *Biochim. Biophys. Acta* 1073, 98–106. doi: 10.1016/0304-4165(91)90188-M

Kang, X., Sun, Y., Li, L., Kong, X., and Yuan, Z. (2018). Improving methane production from anaerobic digestion of Pennisetum hybrid by alkaline pretreatment. *Bioresour. Technol.* 255, 205–212. doi: 10.1016/j.biortech.2017.12.001

Landi, P., Minoarivelo, H. O., Brännström, Å., Hui, C., and Dieckmann, U. (2018). Complexity and stability of ecological networks: a review of the theory. *Popul. Ecol.* 60, 319–345. doi: 10.1007/s10144-018-0628-3

Layeghifard, M., Hwang, D. M., and Guttman, D. S. (2017). Disentangling interactions in the microbiome: a network perspective. *Trends Microbiol.* 25, 217–228. doi: 10.1016/j.tim.2016.11.008

Lemaire, G., Tang, L., Bélanger, G., Zhu, Y., and Jeuffroy, M. H. (2021). Forward new paradigms for crop mineral nutrition and fertilization towards sustainable agriculture. *Eur. J. Agron.* 125:126248. doi: 10.1016/j.eja.2021.126248

Levine, H., Rowe, J. J., and Grimaldi, F. S. (1954). The molybdenum blue reaction and the determination of phosphorus in waters containing arsenic, silicon, and germanium. *Science* 119, 327–328. doi: 10.1126/science.119.3088.327-a

Li, C., Liao, H., Xu, L., Wang, C., He, N., Wang, J., et al. (2022). The adjustment of life history strategies drives the ecological adaptations of soil microbiota to aridity. *Mol. Ecol.* 31, 2920–2934. doi: 10.1111/mec.16445

Li, L., Luo, Z., Li, L., Niu, Y., Zhang, Y., He, R., et al. (2024). Long-term phosphorus fertilization reveals the phosphorus limitation shaping the soil micro-food web stability in the loess plateau. *Front. Microbiol.* 14:1256269. doi: 10.3389/fmicb.2023.1256269

Li, J., Zhu, T., Singh, B. K., Pendall, E., Li, B., Fang, C., et al. (2021). Key microorganisms mediate soil carbon-climate feedbacks in forest ecosystems. *Sci. Bull.* 66, 2036–2044. doi: 10.1016/j.scib.2021.03.008

Liu, W., Jiang, L., and Yang, S. (2020). Critical transition of soil bacterial diversity and composition triggered by nitrogen enrichment. *Ecology* 101:53. doi: 10.1002/2cy3053

Liu, J., Wang, Y., Li, Y., Peñuelas, J., Zhao, Y., Sardans, J., et al. (2023). Soil ecological stoichiometry synchronously regulates stream nitrogen and phosphorus concentrations and ratios. *Catena* 231:107357. doi: 10.1016/j.catena.2023.107357

Mueller, R. C., Paula, F. S., Mirza, B. S., Rodrigues, J. L. M., Nüsslein, K., and Bohannan, B. J. M. (2014). Links between plant and fungal communities across a deforestation chronosequence in the Amazon rainforest. *ISME J.* 8, 1548–1550. doi: 10.1038/ismej.2013.253

Nelson, D. W., and Sommers, L. E. (1996). "Total Carbon, Organic Carbon, and Organic Matter" in Methods of Soil Analysis. Part 3-Chemical Methods. eds. D. L. Sparks, A. L. Page, P. A. Helmke, R. H. Loeppert, P. N. Soltanpour and M. A. Tabatabaiet al. (Madison: Soil Science Society of America Inc.), 961–1010.

Pellitier, P. T., and Zak, D. R. (2018). Ectomycorrhizal fungi and the enzymatic liberation of nitrogen from soil organic matter: why evolutionary history matters. *New Phytol.* 217, 68–73. doi: 10.1111/nph.14598

Seaton, F. M., Reinsch, S., Goodall, T., White, N., Jones, D. L., Griffiths, R. I., et al. (2022). Long-term drought and warming alter soil bacterial and fungal communities in an upland heathland. *Ecosystems* 25, 1279–1294. doi: 10.1007/s10021-021-00715-8

Shao, P., Han, H., Sun, J., and Xie, H. (2023). Effects of global change and human disturbance on soil carbon cycling in boreal forest: a review. *Pedosphere* 33, 194–211. doi: 10.1016/j.pedsph.2022.06.035

Shen, X., Bai, X., Zhao, C., Tan, Q., Luo, G., Li, C., et al. (2024). Global response of soil biodiversity to climate and land use changes. *J. Clean. Prod.* 471:143381. doi: 10.1016/j.jclepro.2024.143381

Shen, G., Ju, W., Liu, Y., Guo, X., Zhao, W., and Fang, L. (2019). Impact of urea addition and Rhizobium inoculation on plant resistance in metal contaminated soil. *Int. J. Environ. Res. Public Health* 16:1955. doi: 10.3390/ijerph16111955

Sinclair, L., Osman, O. A., Bertilsson, S., and Eiler, A. (2015). Microbial community composition and diversity via 16S rRNA gene amplicons: evaluating the illumina platform. *PLoS One* 10:e0116955. doi: 10.1371/journal.pone.0116955

Tang, D. L., Kawamura, H., and Luis, A. J. (2002). Short-term variability of phytoplankton blooms associated with a cold eddy in the northwestern Arabian Sea. *Remote Sens. Environ.* 81, 82–89. doi: 10.1016/S0034-4257(01)00334-0

Tang, X., Xie, G., Shao, K., Hu, Y., Cai, J., Bai, C., et al. (2020). Contrast diversity patterns and processes of microbial community assembly in a river-lake continuum across a catchment scale in northwestern China. *Environ. Microb.* 15:10. doi: 10.1186/s40793-020-00356-9

Tedersoo, L., Bahram, M., Põlme, S., Kõljalg, U., Yorou, N. S., Wijesundera, R., et al. (2014). Fungal biogeography. Global diversity and geography of soil fungi. *Science* 346:1256688. doi: 10.1126/science.1256688

Ullah, S., He, P., Ai, C., Zhao, S., Ding, W., Song, D., et al. (2020). How do soil bacterial diversity and community composition respond under recommended and conventional nitrogen fertilization regimes? *Microorganisms* 8:1193. doi: 10.3390/microorganisms8081193

Vedenicheva, N. P., al-Maali, G. A., Bisko, N. A., Shcherbatiuk, M. M., and Kosakivska, I. V.M. G. Kholodny Institute of Botany of the NAS of Ukraine, Kyiv (2018). Peculiarities of the growth and the content of endogenous cytokinins in the mycelial biomass of basidial mushrooms Hericium coralloides and Fomitopsis officinalis growing in vitro. *Rep. Natnl. Acad. Sci. Ukraine* 9, 97–104. doi: 10.15407/dopovidi2018.09.097

Wang, S., Chen, J., Yang, G., Gao, W., and Chen, K. (2017). Efficient conversion of Hubrid Pennisetum to glucose by oxygen-aqueous alkaline ionic liquid media pretreatment under benign conditions. *Bioresour. Technol.* 243, 335–338. doi: 10.1016/j.biortech.2017.06.134

Wang, S., Heal, K. V., Zhang, Q., Yu, Y., Tigabu, M., Huang, S., et al. (2023). Soil microbial community, dissolved organic matter and nutrient cycling interactions change along an elevation gradient in subtropical China. *J. Environ. Manag.* 345:118793. doi: 10.1016/j.jenvman.2023.118793

Wang, L., Liu, D., and Bai, E. (2018). Decreasing soil microbial diversity is associated with decreasing microbial biomass under nitrogen addition. *Soil Biol. Biochem.* 120, 126–133. doi: 10.1016/j.soilbio.2018.02.003

Wang, C., Ma, L., Zuo, X., Ye, X., Wang, R., Huang, Z., et al. (2022). Plant diversity has stronger linkage with soil fungal diversity than with bacterial diversity across grasslands of northern China. *Glob. Ecol. Biogeogr.* 31, 886–900. doi: 10.1111/geb.13462

Wang, G., Schultz, P., Tipton, A., Zhang, J., Zhang, F., and Bever, J. D. (2019). Soil microbiome mediates positive plant diversity-productivity relationships in late successional grassland species. *Ecol. Lett.* 22, 1221–1232. doi: 10.1111/ele.13273

Wen, Z., Han, J., Shang, Y., Tao, H., Fang, C., Lyu, L., et al. (2024). Spatial variations of DOM in a diverse range of lakes across various frozen ground zones in China: insights into molecular composition. *Water Res.* 252:121204. doi: 10.1016/j.watres.2024.121204

Widdig, M., Heintz-Buschart, A., Schleuss, P. M., Guhr, A., Borer, E. T., Seabloom, E. W., et al. (2020). Effects of nitrogen and phosphorus addition on microbial community composition and element cycling in a grassland soil. *Soil Biol.* 151:108041. doi: 10.1016/j.soilbio.2020.108041

Xie, L., Lin, G., Wang, Q.-W., and Yin, C. (2024). Tree species-specific differences in carbon allocation to ectomycorrhizal symbionts tightly relate to ectomycorrhizal fungal community composition. *For. Ecol. Manag.* 562:121935. doi: 10.1016/j.foreco.2024.121935

Xiong, W., Jousset, A., Guo, S., Karlsson, I., Zhao, Q., Wu, H., et al. (2017). Soil protist communities form a dynamic hub in the soil microbiome. *ISME J.* 12, 634–638. doi: 10.1038/ismej.2017.171

Yan, D., Bissett, A., Gellie, N., Mills, J. G., Lowe, A. J., and Breed, M. F. (2020). Soil bacterial community differences along a coastal restoration chronosequence. *Plant Ecol.* 221, 795–811. doi: 10.1007/s11258-019-00979-0

Yang, Y., Dou, Y., Huang, Y., and An, S. (2017). Links between soil fungal diversity and plant and soil properties on the loess plateau. *Front. Microbiol.* 8:2198. doi: 10.3389/fmicb.2017.02198

Yang, J., Park, J.-H., and Yoon, Y.-H. (2020). Comparison of the high concentration calcium chloride (CaCl 2) salt reduction effect of soil amendment agent and planting *Pennisetum alopecuroides*. *Korean J. Environ. Ecol.* 34, 345–354. doi: 10.13047/KJEE.2020.34.4.345

Yao, B., and Zhou, Y. (2022). "Biochars' potential role in the remediation, revegetation, and restoration of contaminated soils" in Biochar in Agriculture for Achieving Sustainable Development Goals. eds. C. W. Tsang and Y. S. Ok (Amsterdam: Elsevier), 381–399.

Yu, W., Hayat, K., Ma, J., Fan, X., Yang, Y., Zhang, Z., et al. (2024). Effect of antibiotic perturbation on nitrous oxide emissions: an in-depth analysis. *Crit. Rev. Environ. Sci. Technol.* 54, 1612–1632. doi: 10.1080/10643389.2024.2339795

Zeng, J., Liu, X., Song, L., Lin, X., Zhang, H., Shen, C., et al. (2016). Nitrogen fertilization directly affects soil bacterial diversity and indirectly affects bacterial community composition. *Soil Biol. Biochem.* 92, 41–49. doi: 10.1016/j.soilbio.2015.09.018

Zhan, P., Wang, H., Tang, K. W., Penuelas, J., Huang, J., Liu, N., et al. (2024). Composition and assembly of soil bacterial communities between tidal saltwater and freshwater marshes in China. *Appl. Soil Ecol.* 201:105508. doi: 10.1016/j.apsoil.2024.105508

Zhang, T., Song, B., Han, G., Zhao, H., Hu, Q., Zhao, Y., et al. (2023). Effects of coastal wetland reclamation on soil organic carbon, total nitrogen, and total phosphorus in China: a meta-analysis. *Land Degrad. Dev.* 34, 3340–3349. doi: 10.1002/ldr.4687

Zhang, Y., Zhang, N., Yin, J., Zhao, Y., Yang, F., Jiang, Z., et al. (2020). Simulated warming enhances the responses of microbial N transformations to reactive N input in a Tibetan alpine meadow. *Environ. Int.* 141:105795. doi: 10.1016/j.envint.2020.105795

frontiers | Frontiers in Microbiology

TYPE Original Research
PUBLISHED 06 November 2024
DOI 10.3389/fmicb.2024.1458944

Check for updates

OPEN ACCESS

EDITED BY
Muhammad Zahid Mumtaz,
Gansu Agricultural University, China

REVIEWED BY
Dalia A. Gaber Mahmoud,
University of Applied Sciences Erfurt, Germany
Guohong Liu,
Fujian Academy of Agricultural Sciences, China
Rajeshwari Negi,
Eternal University, India
Muhammad Waqar Alam,
University of Okara, Pakistan

*CORRESPONDENCE
Bo Zhang
✉ zhangbofungi@126.com
Xiao Li
✉ lxmogu@163.com
Yu Li
✉ yuli966@126.com

†These authors have contributed equally to this work

RECEIVED 03 July 2024
ACCEPTED 18 October 2024
PUBLISHED 06 November 2024

CITATION
Li X, Dai D, Tuo Y, Li Y, Hu J, Sossah FL, Zhang B, Li X and Li Y (2024) Two new species and three new records of *Diachea* (Physarales) from China based on morphological and molecular evidence. *Front. Microbiol.* 15:1458944. doi: 10.3389/fmicb.2024.1458944

COPYRIGHT
© 2024 Li, Dai, Tuo, Li, Hu, Sossah, Zhang, Li and Li. This is an open-access article distributed under the terms of the Creative Commons Attribution License (CC BY). The use, distribution or reproduction in other forums is permitted, provided the original author(s) and the copyright owner(s) are credited and that the original publication in this journal is cited, in accordance with accepted academic practice. No use, distribution or reproduction is permitted which does not comply with these terms.

Two new species and three new records of *Diachea* (Physarales) from China based on morphological and molecular evidence

Xuefei Li[1,2†], Dan Dai[1,3†], Yonglan Tuo[1,2], You Li[1,2], Jiajun Hu[1,4], Frederick Leo Sossah[1,5], Bo Zhang[1,2,6*], Xiao Li[1,2,6*] and Yu Li[1,2,6*]

[1]Engineering Research Center of Chinese Ministry of Education for Edible and Medicinal Fungi, Jilin Agricultural University, Changchun, China, [2]College of Mycology, Jilin Agricultural University, Changchun, China, [3]Institute of Agricultural Applied Microbiology, Jiangxi Academy of Agricultural Sciences, Nanchang, China, [4]School of Life Science, Zhejiang Normal University, Jinhua, China, [5]Council for Scientific and Industrial Research (CSIR), Oil Palm Research Institute, Coconut Research Programme, Sekondi, Ghana, [6]Industrial Development Institute for Plants, Animals, and Fungi Integration of Biyang County, Zhumadian, China

Diachea is an important genus of myxomycetes, recognized for its ecological role and wide distribution. This study aimed to expand knowledge of species diversity within this genus in China. We collected *Diachea* specimens from various locations in Shaanxi and Sichuan provinces and characterized them through morphological analysis and phylogenetic analysis using four genetic markers: small subunit ribosomal RNA (nSSU), translation elongation factor 1-alpha (*EF-1α*), mitochondrial small subunit (mtSSU), and alpha-tubulin gene (*α-Tub*). Based on these analyses, we describe two new species, namely, *Diachea plectophylla* and *D. sichuanensis*, discovered in the Shaanxi and Sichuan provinces, respectively. *Diachea plectophylla* is distinguished by its dense, rigid capillitium, spore warts, and distinct separation of capillitium ends from the peridium. *Diachea sichuanensis*, closely related to *D. leucopodia*, is identified by its blunt-headed columella, clustered spore warts, and robust stalks. In addition to these new species, we recorded five previously documented species, including *D. bulbillosa* in Gansu province, *D. leucopodia* in Yunnan and Sichuan provinces, and *D. subsessilis* in Sichuan province. Detailed descriptions, micrographs, taxonomic comparisons, and an identification key are provided to aid in accurate identification. The discovery of these new species not only enhances the known diversity of slime molds in the region but also provides valuable information for future studies on their geographical distribution and ecological relationships.

KEYWORDS

diversity, morphology, multigene phylogeny, new taxa, taxonomy

1 Introduction

Myxogastria, commonly known as true slime molds, are fungal-like eukaryotes classified within the kingdom Protozoa, forming a monophyletic group within the Amoebozoa (Adl et al., 2012; Kang et al., 2017). These organisms typically thrive in damp, cool environments, obtaining nutrients from decaying substrates such as rotting wood, dead leaves, branches, and moss. While myxomycetes can adapt to various vegetation types and environmental

conditions, they show a preference for these specific habitats. According to Lado (2005/2024), over 1,100 species of myxomycetes are currently recognized.

The genus *Diachea* Fr., within the order Physarales, includes only 18 known species worldwide, seven of which have been reported in China. Species within this genus are primarily distinguished by the glittering gold, bronze, or bluish iridescence of their peridium. The capillitium, a network of threads inside the sporotheca, lacks limestone and is dark brown. Both the stalk and columella, a prominent structure at the base of the sporotheca or plasmodiocarp, contain granular or crystalline limestone (Martin and Alexopoulos, 1969; Keller et al., 2004; Kirk et al., 2008; Poulain et al., 2011).

Diachea was established by Fries in 1825 based on *D. leucopodia* (Bull.) Rostaf. (Martin and Alexopoulos, 1969). Historically, researchers have focused on species within *Diachea* that featured a halo-peridium, capillitium without limestone, and a well-developed columella—traits resembling those of the Stemonitidales. As a result, *Diachea* was initially classified in the family *Stemonitaceae*, suggesting a close relationship with *Lamproderma* (Fries, 1829; Martin and Alexopoulos, 1969). However, resemblances to species in the Physarales prompted Rostafiński (1874) and Alexopoulos and Saenz (1975) to reclassify it into the family *Didymiaceae* within the order Physarales (Alexopoulos and Saenz, 1975). Subsequent research by Cavalcanti et al. (2006) supported the placement of *D. leucopodia* within *Didymiaceae* and Physarales.

The classification of *Diachea* has fluctuated between the Physarales and Stemonitidales (Alexopoulos, 1982; Kalyanasundaram and Mubarak, 1989; Lado, 2005/2024). Recent studies by García-García-Martín et al. (2023) and Prikhodko et al. (2023), using multigene phylogenetic analyses, confirmed that *Diachea* belongs to *Didymiaceae* within Physarales. This taxonomic uncertainty may stem from variations in capillitium features during different developmental stages. A comprehensive phylogenetic analysis of *Diachea* remains incomplete due to limited sequence data, leaving its classification unresolved.

China's diverse natural environment contributes to a rich myxomycetes species diversity. However, research on this group in China remains limited. In this study, we describe two new *Diachea* species and confirm the presence of five previously recorded species. We employed four genetic markers (nSSU, *EF-1α*, mtSSU, and *α-Tub*) for our molecular analyses. The discovery of these new and newly recorded species enhances our understanding of myxomycetes diversity and provides essential data for future systematic studies of the genus *Diachea*.

2 Materials and methods

2.1 Morphological studies

Specimens were collected from eight locations across China over a 12-year period (2010–2021). Samples, including dead bark, leaves, branches, and litter, were gathered in the field, air-dried in a ventilated area, and stored in collection boxes. For species description, photographs of mature sporocarps were taken using a Zeiss dissecting microscope (Axio Zoom V16, Carl Zeiss Microscopy GmbH, Göttingen, Germany) and a Leica stereoscopic dissector (Leica M165, Wetzlar, Germany). Light micrographs were captured with a Lab A1 microscope (Carl Zeiss AG, Jena, Germany) and processed using ZEN 2.3 software (Carl Zeiss AG). Dried specimens were mounted in 3% KOH for spore examination under oil immersion, and the diameters of 20 spores were measured. Spore and capillitium dimensions are reported as (minimum–) 25th percentile – 75th percentile (–maximum) (Leontyev et al., 2023). Specimens were also examined using a scanning electron microscope (SEM), and photomicrographs were taken using a Hitachi S-4800 SEM (Japan) at 10–15 kV. All analyzed specimens were deposited in the myxomycete collection of the Herbarium of Mycology at Jilin Agriculture University (HMJAU), China.

2.2 DNA extraction, amplification, and sequencing

Genomic DNA from the putative new species was extracted from dried materials using the TIANamp Micro DNA Kit (TianGen Biotech Co., Ltd., Beijing, China). Four genetic markers were used: nSSU (S2F/SR4DarkR), *EF-1α* (PB1F/PB1R), mtSSU (Kmit-F/Kmit-R), and *α-Tub* (kTub-F2/KTub-R1) (García-Martín et al., 2023; Novozhilov et al., 2013). These markers are commonly used for barcoding in protists (Adl et al., 2014) and myxomycetes (García-Cunchillos et al., 2022; Leontyev and Schnittler, 2022; García-Martín et al., 2023). The PCR mixture composition, sample preparation, and sequencing protocols followed Prikhodko et al. (2023) and García-Martín et al. (2023). PCR products were analyzed via gel electrophoresis and purified using the Universal DNA Purification Kit (TianGen Biotech Co., Ltd., Beijing, China). Purified PCR products were sequenced by Kumei Biotechnology Co., Ltd. (Changchun City, China) using the Sanger method. The resulting sequences were deposited in the National Center for Biotechnology Information (NCBI) GenBank database (Table 1).[1]

2.3 Phylogenetic analysis

For phylogenetic analysis, we used 214 sequences derived from 33 species to construct a concatenated dataset. Raw sequence editing and assembly were performed using BioEdit 7.1.3 (Hall, 1999). Sequences for nSSU, *EF-1α*, mtSSU, and *α-Tub* from GenBank were retrieved for other *Diachea* species, as well as representatives from the families *Didymiaceae* and *Physaraceae*. Single-gene alignments were generated using MAFFT V7.490 (Katoh and Standley, 2013), and manual adjustments were made in BioEdit (Hall, 1999). Phylogenetic analyses were performed separately for each gene and for the concatenated dataset using PhyloSuite v1.2.2 (Zhang et al., 2020; Xiang et al., 2023).

Maximum likelihood (ML) and Bayesian inference (BI) methods were employed for phylogenetic tree construction. ML analyses were conducted using IQ-TREE 1.6.12 with 1,000 non-parametric replicates (Nguyen et al., 2015). BI analyses were performed with MrBayes 3.2.6 (Ronquist and Huelsenbeck, 2003), running two simultaneous chains for 10 million generations; trees were sampled every 1,000 generations, and the first 25% were discarded as burn-in. Convergence of the Markov chain Monte Carlo (MCMC) was assessed with TRACER 1.7.2 (Rambaut et al., 2018). Phylogenetic trees were visualized using ITOL version 6.9 (Bork, 2007) and further edited using Adobe Illustrator (San Jose, CA, United States).

1 http://www.ncbi.nlm.nih.gov/genbank

TABLE 1 Information for the sequences used in this study.

Scientific name	Voucher/ specimen numbers	GenBank accession numbers				Reference
		nSSU	*EF-1α*	mtSSU	*α-Tub*	
Diachea bulbillosa	MM32108	–	–	ON059548	–	Lado et al. (2022)
D. bulbillosa	**HMJAU M10037**	**PP795178**	**PP796508**	**PP833125**	–	**This study**
D. bulbillosa	**HMJAU M10002**	**PP795179**	**PP796509**	**PP833126**	–	**This study**
D. cylindrica	MM46123	ON059420	–	ON059549	–	Lado et al. (2022)
D. cylindrica	TVDH548	–	ON081604	ON059550	OP630984	Lado et al. (2022); García-Martín et al. (2023)
D. dictyospora	MM39407	OP646293	OP631018	OP646253	OP630979	García-Martín et al. (2023)
D. dictyospora	**HMJAU M20124-2**	**PP795180**	**PP796510**	**PP833127**	–	**This study**
D. dictyospora	**HMJAU M20124-1**	**PP795181**	**PP796511**	**PP833128**	–	**This study**
D. leucopodia s. lat.	MCCNNU00043	KF743861	KF743855	–	–	Unpublished
D. leucopodia s. lat.	MCCNNU00134	KF743862	KF743856	–	–	Unpublished
D. leucopodia s. lat.	MA-Fungi 90,990	MG963646	MG963478	MG963551	MG963709	García-Martín et al. (2023)
D. leucopodia s. lat.	MA-Fungi 68,824	–	ON081605	ON059551	OP630985	Lado et al. (2022)
D. leucopodia s. lat.	MA-Fungi 86,466	MG963645	MG963477	MG963550	MG963708	García-Martín et al. (2023)
D. leucopodia s. lat.	MA-Fungi 86,465	MG963644	MG963476	MG963549	MG963707	García-Martín et al. (2023)
D. leucopodia s. lat.	**HMJAU M10086**	**PP795182**	**PP796512**	**PP833129**	**PP796523**	**This study**
D. leucopodia s. lat.	**HMJAU M10005**	**PP795183**	**PP796513**	**PP833130**	**PP796524**	**This study**
D. macroverrucosa	**HMJAU M10039**	**PP795184**	**PP796514**	**PP833131**	–	**This study**
D. macroverrucosa	**HMJAU M10067**	**PP795185**	**PP796515**	**PP833132**	–	**This study**
D. macroverrucosa	**HMJAU M10064**	**PP795186**	**PP796516**	**PP833133**	–	**This study**
D. mitchellii	MA-Fungi 96,696	ON059424	ON081610	ON059556	–	Lado et al. (2022)
D. mitchellii	MA-Fungi 91,212	ON059421	ON081607	ON059553	OP630986	Lado et al. (2022)
D. mitchellii	MA-Fungi 96,407	ON059423	ON081609	ON059555	OP630987	Lado et al. (2022)
D. obovata	MM47920	OP646297	OP631019	OP646257	OP630983	García-Martín et al. (2023)
D. obovata	MM39542	OP646296	–	OP646256	OP630982	García-Martín et al. (2023)
D. obovata	MM37196	OP646295	–	OP646255	OP630981	García-Martín et al. (2023)
D. plectophylla	**HMJAU M10006**	**PP795187**	**PP796517**	**PP833134**	–	**This study**
D. plectophylla	**HMJAU M10004**	**PP795188**	**PP796518**	**PP833135**	–	**This study**
D. sichuanensis	**HMJAU M10022**	**PP795189**	**PP796519**	**PP833136**	–	**This study**
D. sichuanensis	**HMJAU M10044**	**PP795190**	**PP796520**	**PP833137**	–	**This study**
D. silvaepluvialis	MA_Fungi_51360	ON059425	–	ON059558	–	Lado et al. (2022)
D. silvaepluvialis	MA_Fungi_51896	–	MW240029	MW240161	–	García-Martín et al. (2023)
D. subsessilis	MA_Fungi_60512	MW240302	MW240030	OP646258	OP630988	García-Martín et al. (2023)
D. subsessilis	MA_Fungi_82029	ON059427	–	ON059561	–	Lado et al. (2022)
D. subsessilis	MA_Fungi_68835	ON059426	–	ON059560	–	Lado et al. (2022)
D. subsessilis	**HMJAU M10075**	**PP795191**	**PP796521**	**PP833138**	–	**This study**
D. subsessilis	**HMJAU M10032**	**PP795192**	**PP796522**	**PP833139**	–	**This study**
Didymium dubium	MA-Fungi 63,904	MW240326	MW240058	MW240188	MW239915	García-Martín et al. (2023)
D. dubium	MA-Fungi 80,036	MW240327	MW240059	MW240189	MW239916	García-Martín et al. (2023)
D. dubium	MA-Fungi 80,492	MG662512	MW240060	MW240190	MW239917	García-Martín et al. (2023)
D. dubium	K7	AM231294	–	–		Wikmark et al. (2007)
D. melanospermum	MA-Fungi 91,238	MG963668	MG963497	MG963577	MG963736	García-Martín et al. (2023)
D. melanospermum	MA-Fungi 62,790	MG963667	MW240068	MG963576	MG963735	García-Martín et al. (2023)

(Continued)

TABLE 1 (Continued)

Scientific name	Voucher/ specimen numbers	GenBank accession numbers				Reference
		nSSU	*EF-1α*	mtSSU	*α-Tub*	
D. nivicola	MA-Fungi 90,573	MT227090	MT230925	–	–	Janik et al. (2020)
D. nivicola	AH19667	MT227019	MT230908	–	–	Janik et al. (2020)
D. yulii	HMJAU M3002	MF149871	MK905755	–	–	Zhao et al. (2021)
D. yulii	HMJAU M3001	MF149870	MK905754	–	–	Zhao et al. (2021)
Echinostelium coelocephalum	ATCC MYA 2964	AY842033	AY643813	–	–	Fiore-Donno et al. (2005)
E. minutum	ATCC 22345	AY842034	AY643814	–	–	Fiore-Donno et al. (2005)
Enerthenema intermedium	MM 21635	DQ903688	–	–		Fiore-Donno et al. (2008)
E. melanospermum	MM 28388	DQ903689	–	–		Fiore-Donno et al. (2008)
E. papillatum	AMFD141	AY643823	–	–		Fiore-Donno et al. (2005)
Lamproderma aeneum	MA-Fungi 81,947	MW240352	MW240092	MW240217	MW239949	García-Martín et al. (2023)
L. aeneum	MA-Fungi 86,925	MW240353	MW240093	MW240218	–	García-Martín et al. (2023)
L. aeneum	MA-Fungi 90,422	MW240354	MW240094	MW240219	–	García-Martín et al. (2023)
L. ovoideum	Sc30802	MN595543	MN596918	–	–	Shchepin et al. (2024)
Macbrideola oblonga	M. Schnittler	DQ903682	–	–	–	Fiore-Donno et al. (2008)
Meriderma aggregatum	AMFD135	DQ903669	–	–	–	Fiore-Donno et al. (2008)
M. carestiae var. *retisporum*	AMFD173	DQ903671	–	–	–	Fiore-Donno et al. (2008)
M. fuscatum	MM 24907	DQ903668	–	–	–	Fiore-Donno et al. (2008)
Nannengaella globulifera	MA-Fungi 51,647	MF352479	MF352528	MW240269	MW239991	García-Martín et al. (2018)
N. globulifera	MA-Fungi 46,711	MW240379	–	MW240268	MW239990	García-Martín et al. (2023)
N. globulifera	MYX8635	MW693010	MW701657	–	–	Shchepin et al. (2022)
N. globulifera	MYX8695	MW693014	MW701661	–	–	Shchepin et al. (2022)
N. mellea	MA-Fungi 69,850	MF352484	MF352534	MG963629	MG963776	García-Martín et al. (2018)
N. mellea	MA-Fungi 87,986	MF352485	MF352535	MG963630	MG963777	García-Martín et al. (2018)
N. mellea	MA-Fungi 60,322	MW240383	MG963528	MG963628	MG963775	García-Martín et al. (2023)
Physarum didermoides	MA-Fungi 71,195	MW240378	OP650825	MW240267	–	García-Martín et al. (2023)
P. didermoides	MA-Fungi 57,262	MF352488	MF352542	MW240266	MW239988	García-Martín et al. (2018)
P. leucophaeum	MA-Fungi 49,730	MG963686	MG963521	MG963614	MW239996	García-Martín et al. (2023)
P. leucophaeum	MA-Fungi 78,861	MG963688	–	MG963618	MG963767	García-Martín et al. (2023)
P. leucophaeum	MA-Fungi 59,323	MF352477	MF352526	MG963615	MG963765	García-Martín et al. (2018)
P. straminipes	MA-Fungi 70,363	MF352489	MF352543	MW240291	MW240015	García-Martín et al. (2018)
P. straminipes	MA-Fungi 87,865	MW240394	–	MW240292	MW240016	García-Martín et al. (2023)
P. viride	LE302489	MW693022	MW701670	–	–	Shchepin et al. (2022)
P. viride	LE317322	MW693024	MW701672	OP616654	–	Shchepin et al. (2022); Prikhodko et al. (2023)
Symphytocarpus impexus	–	AY230188	–	–		Walkera et al. (2003)

Sequences produced in this study are in bold.

3 Results

3.1 Phylogenetic analyses

We analyzed 167 sequences representing 33 species in this study, including 47 newly acquired sequences from the specimens examined: 15 sequences each for nSSU, *EF-1α*, and mtSSU and 2 sequences for *α-Tub*. The dataset consisted of 72 sequences with 7,606 characters for nSSU, 57 sequences with 2,505 characters for *EF-1α*, 55 sequences with 477 characters for mtSSU, and 29 sequences with 1,007 characters for *α-Tub*, including gaps.

The phylogenetic trees generated using both maximum likelihood (ML) and Bayesian inference (BI) analyses showed consistent topologies across the single-gene datasets. For clarity,

only the ML tree is presented here. In the multigene phylogenetic tree, which combines the alignments of nSSU, *EF-1α*, mtSSU, and *α-Tub* sequences, all 11 specimens of the genus *Diachea* formed a cohesive and well-supported clade (PP = 1, BS = 99.3%). Within this group, *Diachea plectophylla* and *D. sichuanensis* emerged as distinct, strongly supported clades (PP = 1, BS = 100%). These results, along with unique morphological traits, confirm the discovery of these two previously undocumented species, identifying *D. plectophylla* and *D. sichuanensis* as distinct lineages (Figure 1).

Taxonomy

Diachea plectophylla **X.F. Li, D. Dai, B. Zhang & Y. Li, sp. nov.**

MycoBank: MB854209.

(Figure 2)

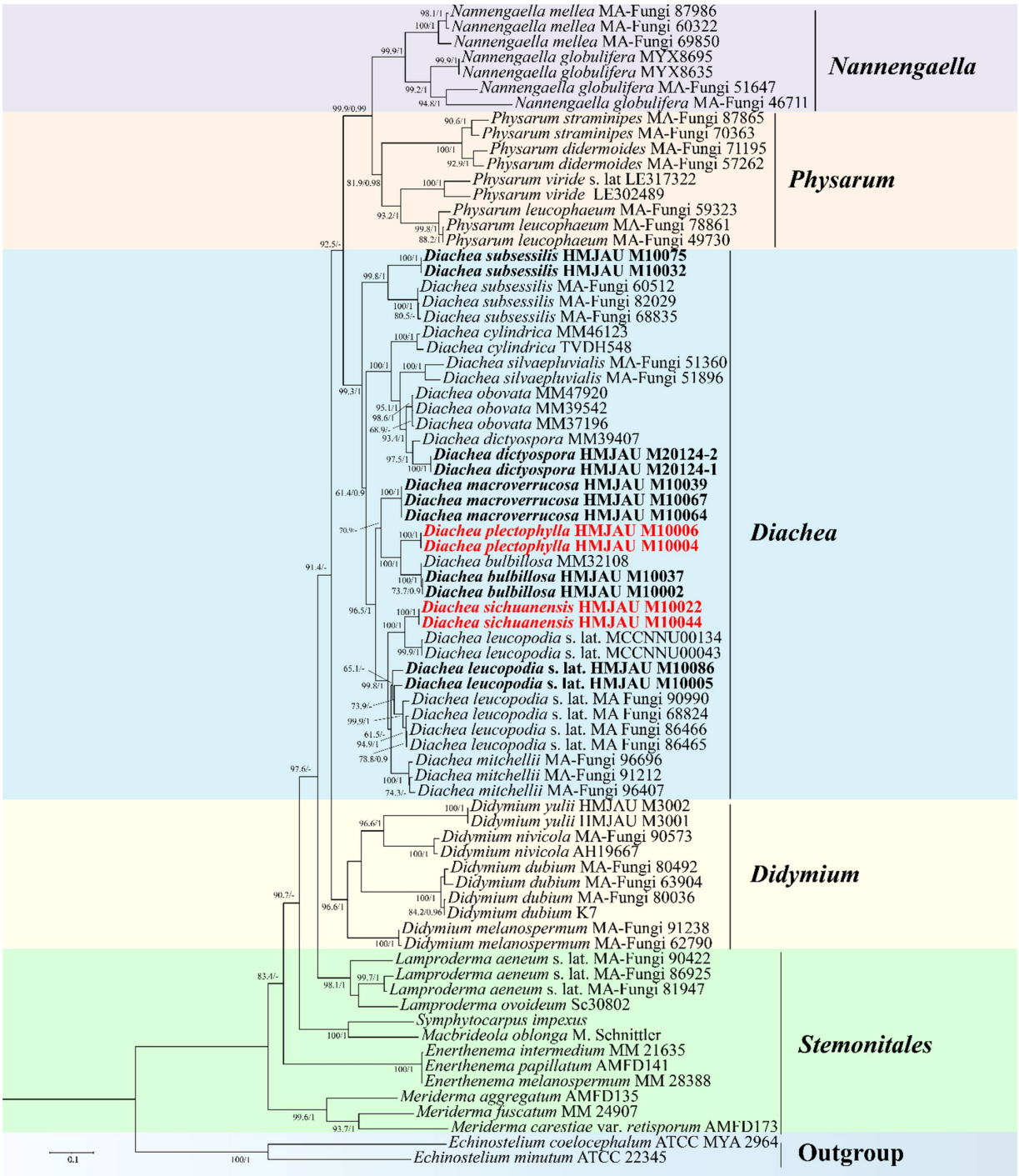


FIGURE 1
Maximum likelihood phylogenetic tree generated from the nSSU, *EF-1α*, mt SSU, and *α-Tub* datasets of the target clade containing the new species from *Diachea*. The two values of internal nodes, respectively, represent the maximum likelihood bootstrap (BS)/Bayesian posterior probability (PP). This study species is in bold and red font.

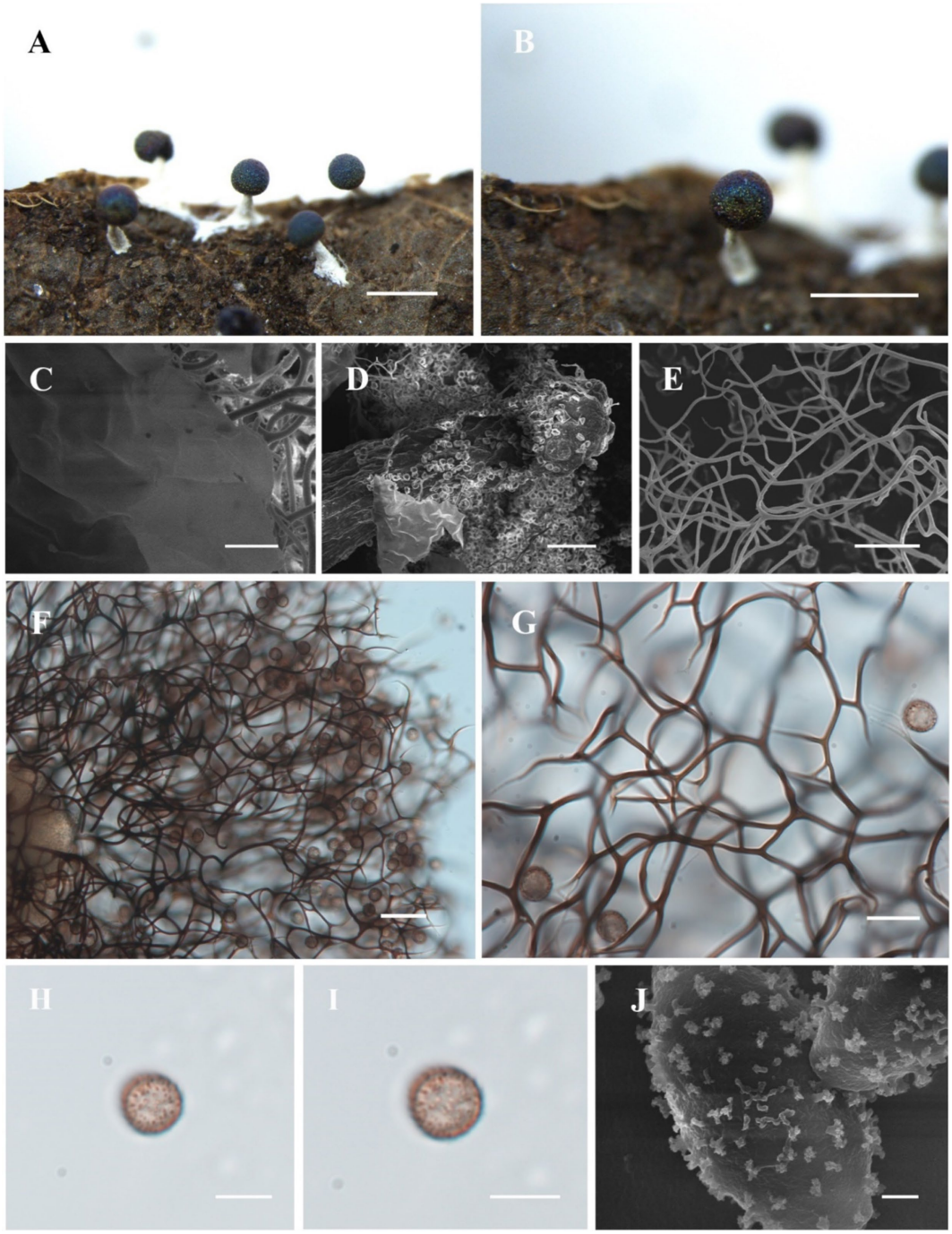


FIGURE 2
Habitat and microstructure of *Diachea plectophylla* (HMJAU M10004). (A,B) Sporocarps; (C) peridium by SEM; (D) columella by SEM; (E–G) capillitium by SEM and TL; (H–J) spores with cluster warts by TL and SEM. Scale bars: (A), B = 1 mm, C = 10 μm, (D), *F* = 40 μm, (E), G = 20 μm, H, I = 10 μm, J = 1 μm.

Diagnosis. Capillitium dense, hard, and straight; ends not connected to the peridium.

Holotype. China, Shaanxi province, Niubeiliang National Nature Reserve, on the rotten leaves, 23 July 2014, B. Zhang, HMJAU M10004.

Etymology. The epithet "*plectophylla*" refers to crude the dense capillitium.

Description. Sporocarp, gregarious, stipitate, spherical, with blue-purple halo, (0.3–) 0.35–0.5 (−0.55) mm in diameter, (0.5–) 0.6–1.2 (−1.3) mm in tall. Stalk calcareous, white, with enlarged at the base, tapering upward, with numerous calcareous particles. Peridium single-layered, thin, halo, persistent, irregular dehiscence. Hypothallus inconspicuous. Columella white, conical, blunt-headed, tapering upward, reaching approximately half of the sporotheca, an extension of the stalk. Capillitium dense, thick, hard, black brown, branched, and connected, radiating from columella, not connected to the peridium. Spores dark in mass, dark brown by transmitted light, with sparse warts, sometimes warts connect to form ridges, 8–9 (−9.5) μm in diameter.

Habitat. On the rotten leaves and branches.

Distribution in China. Shaanxi province.

Distribution in the World. China.

Additional specimens examined. China, Shaanxi province, Niubeiliang National Nature Reserve, on the rotten leaves, 23 July 2014, B. Zhang, HMJAU M10006.

Notes. *Diachea plectophylla* is morphologically similar to *D. bulbillosa*, *D. macroverrucosa*, and *D. splendens* due to its blue halo, subglobose sporocarp, white stalk, and obvious columella (Table 2). However, *D. plectophylla* differs from *D. macroverrucosa* in having relatively large columella and small spores. *Diachea plectophylla* differs from *D. bulbillosa* in its dense capillitium and small spores (Table 2). *Diachea plectophylla* can be distinguished from *D. splendens* by its dense capillitium, where warts connect to form ridges, whereas *D. splendens* has sparse reticular capillitium, and spores have rough nodules and ridges, arranged in a network pattern. From the

TABLE 2 Comparison of morphological characteristics of *Diachea* species in this study.

	Sporocarps	Stalk	Peridium	Hypothallus	Columella	Capillitium	Spores
D. plectophylla	Spherical, with blue-purple halo, (0.3–) 0.35–0.5 (−0.55) mm in diameter, (0.5–) 0.6–1.2 (−1.3) mm in tall.	Stalk calcareous, white	Single-layered, thin, halo, persistent, dehiscence irregular.	Inconspicuous	White, conical, blunt-headed, reaching approximately half of the sporotheca.	Black brown, radiating from various parts of the columella, not connected to the peridium.	With sparse warts, 8–9 (−9.5) μm in diameter.
D. sichuanensis	Cylindrical, metal blue, sometimes purple or bronze halo, blunt-headed, (0.35–) 0.4–0.6 (−0.65) mm in diameter, (0.9–) 1–2 (−2.2) mm in tall.	Stalk calcareous, brittle, snow-white, 1/4–1/2 of full height.	Single-layered, thin, halo, persistent, dehiscence irregular.	Conspicuous, calcareous, white.	White, thick, blunt-headed, calcareous, often close to the top of the sporotheca.	Brown, light-colored at the end, extending from various parts of the columella.	With clustered warts, (7–) 8–11 μm in diameter.
D. dictyospora	Spherical, upper white, lower brown, (0.3–) 0.35–0.4 (−0.45) mm in diameter, (1–) 1.2–1.4 (−1.5) mm in tall.	Stalk calcareous, yellow brown, dark brown at the top.	Single-layered, white or gray, slightly halo, the lower part persistent in a reddish-brown	Membranous, transparent, light brown.	Light brown, rod-shaped, and grows to the center of the sporotheca.	Sparse, lime nodes large, white, presenting a network within the sporotheca.	With obvious coarse warts, 12–13.5 (−16) μm in diameter.
D. bulbillosa	Spherical or subglobose, with blue or purple halo, (0.3–) 0.35–0.5 (−0.55) mm in diameter, (0.8–) 0.9–1.3 (−1.4) mm in tall.	Stalk cylindrical, calcareous, white.	Single-layered, with halo, irregularly cracked.	Inconspicuous, calcareous, white.	White, with an enlarged tip, club-shaped, generally reaching half or more of the sporotheca.	Purple-brown, curved, reticulate.	With sparsely and irregularly warts, (7–) 8–11 μm in diameter.
D. leucopodia	Cylindrical or elliptical, metal blue, or purple or bronze halo, (0.35–) 0.4–0.6 (−0.65) mm in diameter, (0.8–) 1–2 (−2.2) mm in tall.	Stalk slender, calcareous, snow-white, 1/2 of full height.	Single-layered, often falls off and dehiscence irregularly.	White, calcareous, with veins and often forming a network.	White, coniform, calcareous, higher than half of the sporotheca.	Dark brown, colorless at the tips, radiate from various parts of the columella.	With minutely warted, 8–10 (−11) μm in diameter.
D. macroverrucosa	Spherical, haze and blue halo, (0.3–) 0.35–0.4 (−0.45) mm in diameter, (0.7–) 0.75–0.9 (−1) mm in tall.	Stalk coarse and short, (0.35–) 0.4–0.5 (−0.55) mm in length, white, calcareous	Single-layered, with halo, dehiscence irregular.	Membranous, colorless and transparent, sometimes connected into sheets.	White, conical, blunt-headed, approximately 1/4 of the sporotheca.	Black brown, radiating from various parts of the columella, light-colored at the end, and not connected to the peridium.	With sparse dark warts, (8–) 9–13 μm in diameter.
D. subsessilis	Spherical, short-stalked or sessile, gray-green or dark blue halo, (0.35–) 0.4–0.8 (−0.85) mm in diameter, (0.5–) 0.6–1 (−1.2) mm in tall.	Stout, cylindrical, white, calcareous, not exceeding the height of the sporocarp.	Single-layered, with halo.	Network, small, slightly calcium or absent.	Short, calcareous, conical, sometimes absent.	Light brown, radiating from the columella, with light-colored at the end.	With clustered warts, (7–) 8–12 μm in diameter.

phylogenetic tree, *D. plectophylla* is similar to *D. bulbillosa* but has a separate branch.

Diachea sichuanensis **X.F. Li, D. Dai, B. Zhang & Y. Li, sp. nov.**
MycoBank: 854210.
Figure 3

Diagnosis. Clustered warts are present on the surface of spores, and the capillitium is connected to the peridium.

Holotype. China, Sichuan province, Liangshan Yi Autonomous Prefecture, Mianning County, Lingshan Temple, on the branches, rotten leaves, and living plants, 12 July 2013, B. Zhang, HMJAU M10022.

Etymology. The epithet "*sichuanensis*" refers to Sichuan, the location of the holotype.

Description. Sporocarp dense, gregarious, stipitate, metal blue, sometimes with a purple or bronze halo, cylindrical or rarely

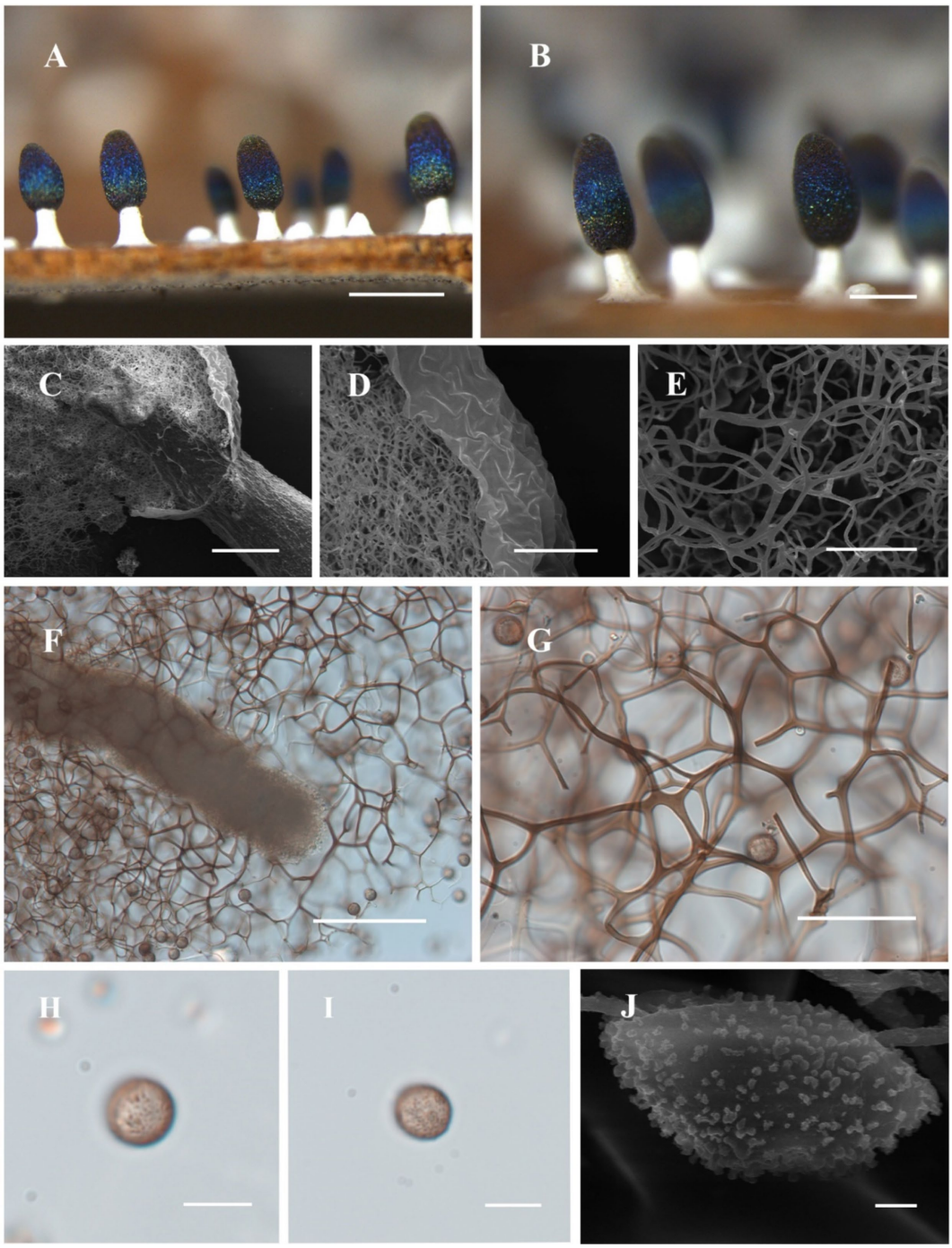


FIGURE 3
Habitat and microstructure of *Diachea sichuanensis* (HMJAU M10022). (A,B) Sporocarps; *C. columella* by SEM; (D,E) peridium and capillitium by SEM; (F) columella and capillitium by TL; (G) capillitium and spores by TL; (H–J) Spores with clustered warts by TL and SEM. Scale bars: A = 1 mm, B = 500 μm, C, *F* = 100 μm, D, G = 40 μm, E = 20 μm, H, I = 10 μm, J = 1 μm.

subspherical, blunt-headed, (0.35–) 0.4–0.6 (−0.65) mm in diameter, (0.9–) 1–2 (−2.2) mm in tall. Stalk robust, calcareous, brittle, snow-white, 1/4–1/2 of full height, tapering upward. Peridium single-layered, thin, halo, persistent, with irregular dehiscence. Hypothallus conspicuous, white, calcareous, with a network of veins. Columella thick, gradually tapering upward, blunt-headed, white, calcareous, higher than half of the sporotheca, often close to the top of the sporotheca. Capillitium curved, branched, and connected, brown, light-colored at the end, radiating from various parts of the columella. Spore dark in mass, light purple under transmitted light, (7–) 8–11 µm in diameter, rough, with clustered warts.

Habitat. On the branches, rotten leaves, and living plants.

Distribution in China. Sichuan province.

Distribution in the World. China.

Additional specimens examined. China, Sichuan province, Liangshan Yi Autonomous Prefecture, Mianning County, Lingshan Temple, on the branches, rotten leaves, and living plants, 12 July 2013, B. Zhang, HMJAU M10044.

Notes. The primary characteristic of this species is the clustered warts on the surface of spores, with capillitium connected to the peridium. *Diachea sichuanensis* shares similarities with *D. leucopodia* in terms of sporocarp size and stalk color. However, *D. sichuanensis* can be distinguished from *D. leucopodia* by its blunt-headed columella, with spores of cluster warts and robust stalks. *Diachea sichuanensis* can be distinguished from *D. bulbillosa* by its spores with clustered warts, while the latter has sparse and large warts (Table 2). From the phylogenetic tree, *D. sichuanensis* is similar to *D. leucopodia*, but the genetic distance between the two is relatively far.

Diachea dictyospora (Rostaf.) J.M. García-Martín, J.C. Zamora & Lado, *Persoonia* 51:106 (2023).

Figure 4

Description. Sporocarp, gregarious or densely crowded, erect, stipitate, spherical, upper white, lower brown, (0.3–) 0.35–0.4 (−0.45) mm in diameter, (1–) 1.2–1.4 (−1.5) mm in tall. Stalk slender, gradually tapering upward, calcareous, yellow brown, dark brown at the top, with longitudinal grooves, lighter, (0.7–) 0.8–1 (−1.1) mm in length. Peridium thin, membranous, irregularly cracked, covered with a layer of small calcareous particles on the surface, white or gray, slightly halo, with the upper part gray, the lower part persistent in a reddish-brown cup-shaped shape. Hypothallus membranous, transparent, light brown. Columella rod-shaped, light brown, and reaching the center of the sporotheca. Capillitium sparse, with large lime nodes, white, forming a network within the sporotheca. Spores dark in mass, red-brown by transmitted light, with coarse warts, sometimes forming an incomplete net of warts fused into shout ridge, 12–13.5 (−16) µm in diameter.

Habitat. On the dead branches.

Distribution in China. Jilin province and Heilongjiang province.

Distribution in the World. China, United States, Spain, France, Portugal, Germany, Italy, Japan.

Specimens examined. China, Jilin province, Baishan City, Fusong County, Lushuihe Town National Forest Park Hunting Ground, on the dead branches, 23 July 2018, B. Zhang, HMJAU M20124, HMJAU M20125, HMJAU M20126; China, Jilin province, Jian City, Wunvfeng National Forest Park, on the dead branches, 19 July 2018, B. Zhang, HMJAU M20127, HMJAU M20128.

Notes. The main characteristics of this species are red-brown or gray-brown sporocarp, large lime nodes, and dark, coarsely warted spores. *Diachea dictyospora* is similar to *D. muscorum* in terms of its sporocarp shape and spore color and size. However, some morphological features of *D. dictyospora* differ from *D. muscorum*, such as a short stalk and spores that have loosely reticulate ridges approximately 1 µm high. In contrast, *D. dictyospora* has a long stalk, with spores marked by an incomplete net of broad fused into short ridges. These two species previously belonged to the genus *Craterium* Trentep.; Lado et al. redefined the genus *Diachea* in 2023. *Diachea dictyospora*, *D. muscorum*, and *D. obovata* were transferred to this genus and classified based on their morphological characteristics (García-Martín et al., 2023).

Diachea bulbillosa (Berk. & Broome) Lister, in Penzig, *Myxomyc. Fl. Buitenzorg* 47 (1898).

Figure 5

Description. Sporocarp, gregarious, stipitate, spherical or subglobose, with blue or purple halo, darkening with age, (0.3–) 0.35–0.5 (−0.55) mm in diameter, (0.8–) 0.9–1.3 (−1.4) mm in tall. Stalk cylindrical, gradually tapering upward, calcareous, white with an enlarged base. Peridium thin, membranous, with halo, irregularly cracked. Hypothallus inconspicuous, white. Columella obvious, white, calcareous, with an enlarged tip, club-shaped, reaching half or more of the sporocyst. Capillitium sparse, purple-brown, curved, reticulate, with membranous enlargement. Spores dark in mass, violet-gray by transmitted light, (7–) 8–11 µm in diameter, large, with sparsely and irregularly warted.

Habitat. On the dead branches and fallen leaves.

Distribution in China. Jilin province, Liaoning province, Gansu province, Beijing City, Hebei province, Inner Mongolia Autonomous Region, Anhui province, Guangdong province, Heilongjiang province, Taiwan, Henan province, Jiangsu province.

Distribution in the World. Widely distributed.

Specimens examined. China, Jilin province, Jiaohe City, Lafashan National Forest Park, on the dead branches and fallen leaves, 6 September 2018, B. Zhang, HMJAU M10037. China, Liaoning province, Fuxin City, Haitangshan National Nature Reserve, on the branches and leaves, 1 September 2012, B. Zhang, HMJAU M10007. China, Gansu province, Tianshui City, Dangchuan Town forest farm, Maiji District, on the dead leaves and branches, 16 August 2010, B. Zhang, HMJAU M10002.

Notes. *Diachea bulbillosa* is morphologically similar to *D. splendens,* sharing features such as a subglobose sporocarp with a halo, long stalk, and conspicuous columella. However, *D. bulbillosa* differs from *D. splendens* by having larger, sparsely, and irregularly distributed warts, while *D. splendens* possesses thick tumorous processes, often connected into irregular lines or incomplete mesh.

Diachea leucopodia (Bull.) Rostaf., *Sluzowce monogr*. 190 (1874).

Figure 6

Description. Sporocarp, gregarious or densely crowded, stipitate, metallic blue, or with a purple or bronze halo, cylindrical or elliptical, occasionally subspherical, with slightly concave navel below, (0.35–) 0.4–0.6 (−0.65) mm in diameter, (0.8–) 1–2 (−2.2) mm in tall. Stalk slender, calcareous, brittle, snow-white, approximately 1/2 the full height, tapering upward. Peridium often dehiscencing irregularly and falling off. Hypothallus white, calcareous, with veins and often forming a network. Columella thick, conical, gradually tapering upward, white, calcareous, extending more than half the height of the sporotheca, often reaching near the top of the sporotheca. Capillitium curved, branched, and interconnected, dark brown, colorless at the

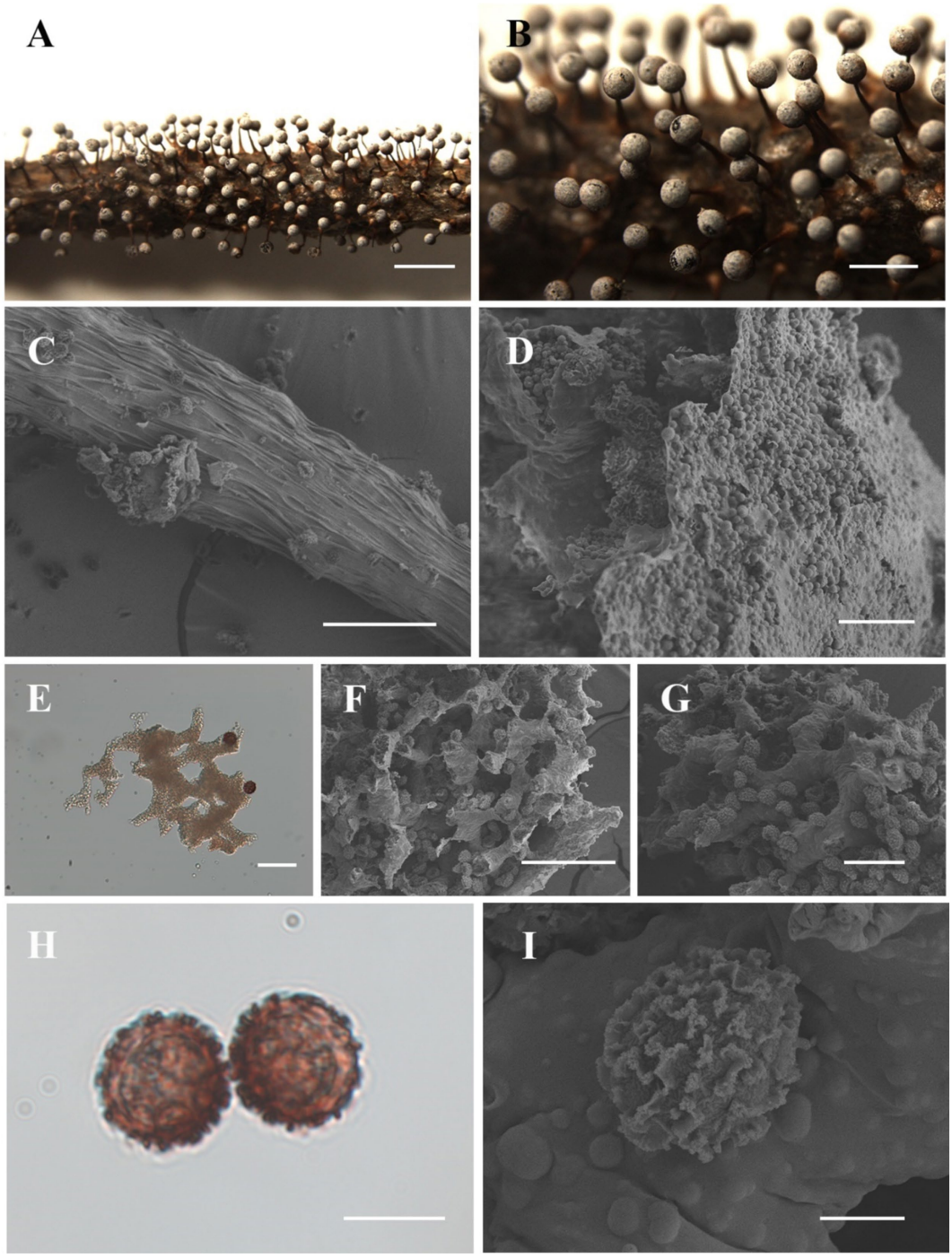


FIGURE 4
Habitat and microstructure of *Diachea dictyospora* (HMJAU M20124). (A,B). Sporocarps; (C) stalk by SEM; (D) peridium by SEM; (E) lime nodes by TL; (E–G) capillitium, lime nodes, and spores by SEM; (H–I) spores with sparse and large ridges by TL and SEM. Scale bars: A = 2 mm, B = 1 mm, C, F = 100 μm, D = 20 μm, E, G = 40 μm, H = 10 μm, I = 5 μm.

tips, radiating from various points of the columella. Spores dark in mass, light purple by transmitted light, rough, with minutely warted, 8–10 (−11) μm in diameter.

Habitat. On the dead branches and fallen leaves.

Distribution in China. Guangdong province, Guangxi Zhuang Autonomous Region, Yunnan province, Jilin province, Sichuan Province, Hebei province, Shanxi province, Inner Mongolia Autonomous Region, Jiangsu province, Fujian province, Shandong province, Hubei province, Shaanxi province, Gansu province, Henan province, Hunan province, Liaoning province, Taiwan, Hong Kong, Heilongjiang province, Beijing City, Ningxia Hui Autonomous Region, Anhui province.

Distribution in the World. Widely distributed.

Specimens examined. China, Guangdong province, Shaoguan City, Zhenjiang District, on the dead branches and fallen leaves, 13 May 2019, D. Dai, HMJAU M10086; China, Guangxi Zhuang Autonomous Region, Nanning City, Liang Feng Jiang National Forest

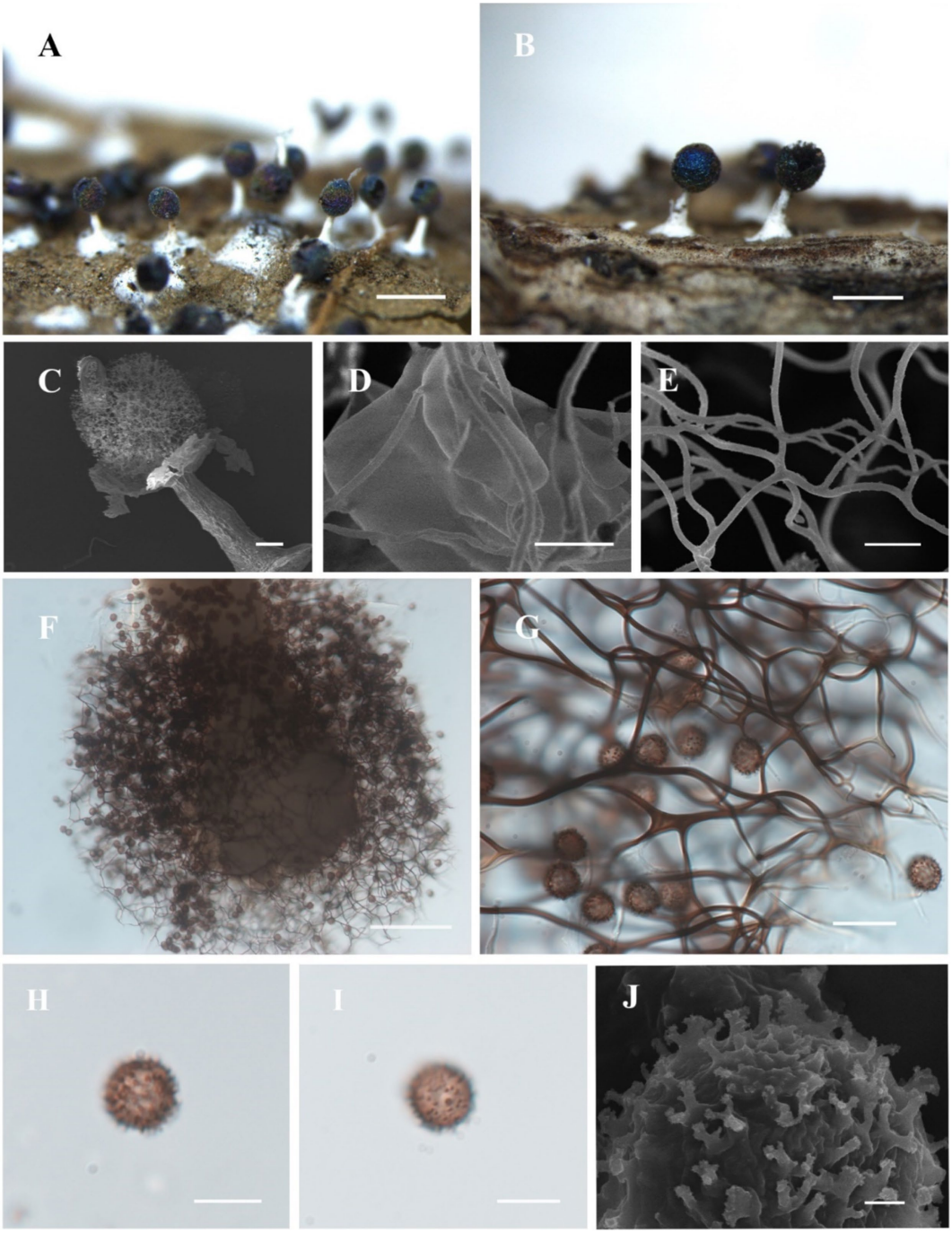


FIGURE 5
Habitat and microstructure of *Diachea bulbillosa* (HMJAU M10002). (A,B) Sporocarps; (C) sporocarp by SEM; (D) peridium and capillitium connected by SEM; (E) capillitium by SEM; (F) columella and capillitium by TL; (G) capillitium and spores by TL; H-J. Spores with sparse and large warts by TL. Scale bars: (A), B = 1 mm, (C), F = 100 μm, D, E = 5 μm, G = 20 μm, (H), I = 10 μm, J = 1 μm.

Park, on the dead branches and fallen leaves, 15 August 2020, D. Dai, HMJAU M10087; China, Yunnan province, Lijiang City, on the dead branches and fallen leaves, 20 August 2012, B. Zhang, HMJAU M10005; China, Jilin province, Lushuihe Town, Changbai Mountain International Hunting Resort, on the dead branches and fallen leaves, 7 August 2014, B. Zhang, HMJAU M10015, HMJAU M10016; China, Jilin province, Jilin Agricultural University campus, on the dead branches and fallen leaves, 28 May 2013, B. Zhang, HMJAU M10018; China, Sichuan province, Ganzi Tibetan Autonomous Prefecture, Yajiang County, Gexigou Nature Reserve, on the dead leaves and branches, 5 August 2015, B. Zhang, HMJAU M10033.

Notes. *Diachea leucopodia* characterized by its white, calcareous hypothallus, stalk, and columella. The conical columella and cylindrical to oval sporocarps, along with light-color spores, and distinguish this species from others.

Diachea macroverrucosa D. Dai & B. Zhang, *Mycology*: 51 (2024).

10.3389/fmicb.2024.1458944

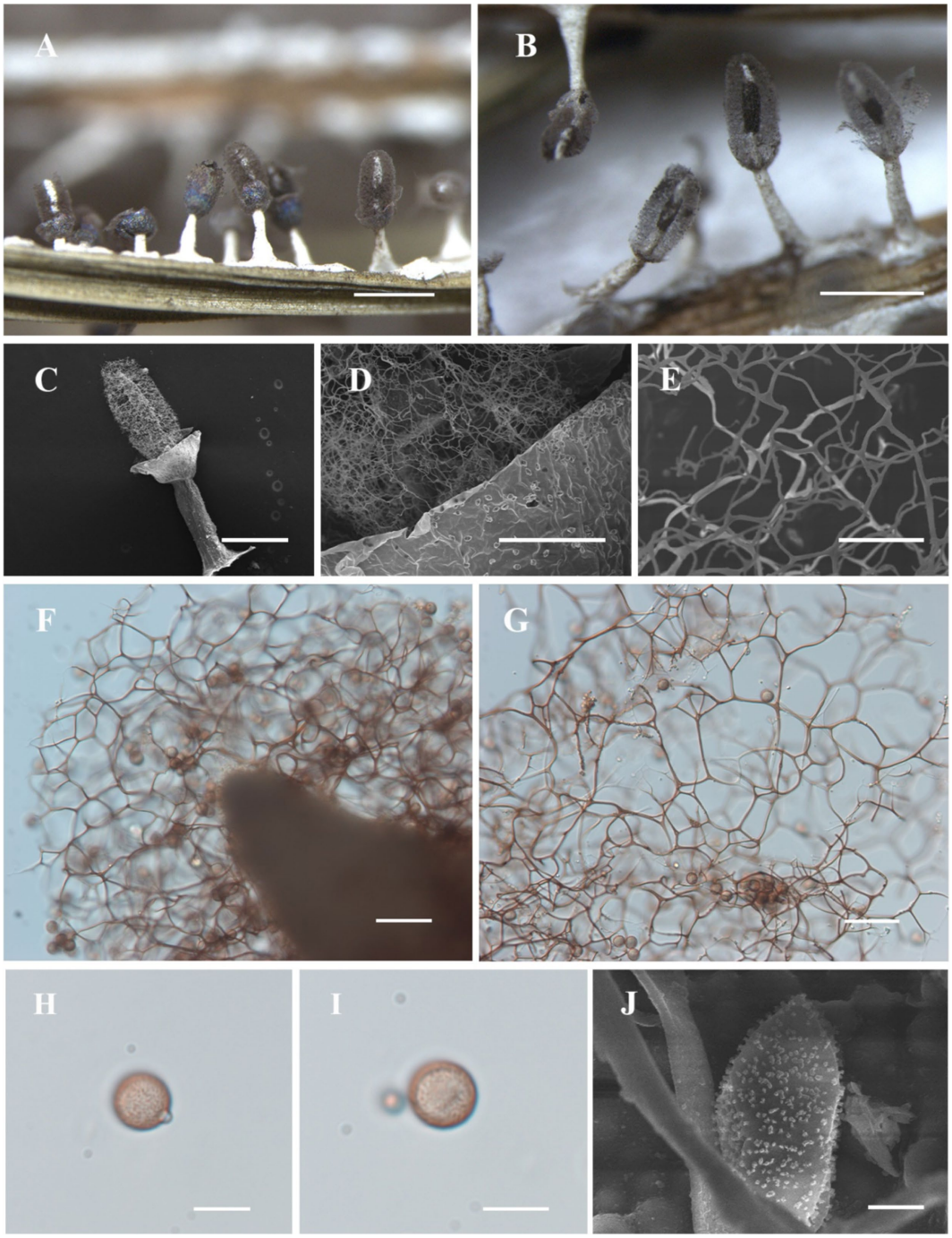


FIGURE 6
Habitat and microstructure of *Diachea leucopodia* (HMJAU M10005). (A,B) Sporocarps; (C) sporocarp by SEM; (D) capillitium and peridium by SEM; (E) capillitium by SEM; (F,G) columella and capillitium by TL; (H–J) spores with cluster warts by TL and SEM. Scale bars: (A), B = 1 mm, C = 400 μm, D = 100 μm, E = 20 μm, (F), G = 40 μm, (H), I = 10 μm, J = 2 μm.

Figure 7

Description. Sporocarp, gregarious to clusterous, stipitate, spherical, with haze and blue halo, (0.3–) 0.35–0.4 (−0.45) mm in diameter, (0.7–) 0.75–0.9 (−1) mm in tall. Stalk coarse and short, (0.35–) 0.4–0.5 (−0.55) mm in length, white, tapering upward, calcareous, containing numerous calcareous particles. Peridium single-layered, with a halo, dehiscencing irregularly. Hypothallus membranous, colorless, and transparent, sometimes forming sheets. Columella white, conical, blunt-headed, approximately 1/4 of the sporotheca. Capillitium dense, thin, hard, dark brown, branched, and interconnected, radiating from various points of the columella, lighter at the end, and not connected to the peridium. Spores black in mass, dark brown by transmitted light (TL), (8–) 9–13 μm in diameter, sparsely covered with large dark warts.

Habitat. On the branches and rotten leaves.

Distribution in China. Shaanxi province, Jilin Province, Liaoning Province.

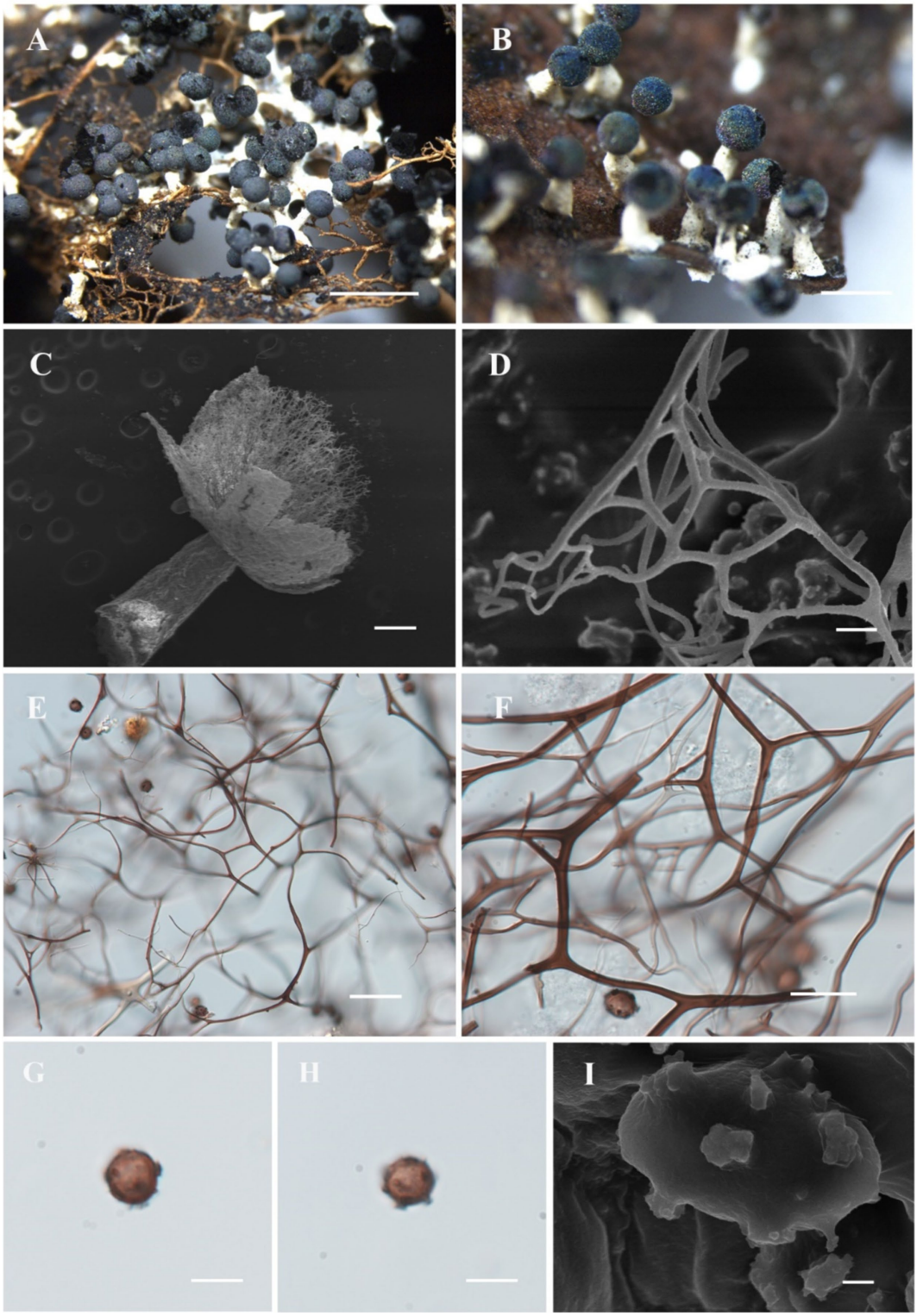


FIGURE 7
Habitat and microstructure of *Diachea macroverrucosa* (HMJAU M10064). (A,B) Sporocarps; (C) sporocarp by SEM; (D–F) capillitium by SEM and TL; (G–I) spores with sparse and large warts by TL and SEM. Scale bars: A = 2 mm, B = 1 mm, C = 100 μm, D = 5 μm, E = 40 μm, *F* = 20 μm, G, H = 10 μm, I = 1 μm.

Distribution in the World. China.

Specimens examined, China, Shaanxi province, Niubeiliang National Nature Reserve, on the rotten leaves, 21 July 2014, B. Zhang, HMJAU M10001; China, Jilin province, Yanbian Korean Autonomous Prefecture, Antu County, Changbai Mountain National Nature Reserve, on the rotten branches and leaves, 25 August 2013, B. Zhang, HMJAU M10027; China, Jilin province, Yanbian Korean Autonomous Prefecture, Longjing City, Tianfo Zhishan National Nature Reserve, on the rotten branches and leaves, 4 September 2011, B. Zhang, HMJAU M10009; China, Liaoning province, Fuxin City, Haitangshan National

Nature Reserve, on the rotten branches and leaves, 1 September 2012, B. Zhang, HMJAU M10039, HMJAU M10057, HMJAU M10064, HMJAU M10067, HMJAU M10069, HMJAU M10073.

Notes. *Diachea macroverrucosa* is characterized by its large warts resembling an inflorescence on the spore surface. The columella is conical and does not exceed 1/2 the height of the sporocarp. Morphologically, *D. macroverrucosa* resembles *D. bulbillosa*, sharing characteristics such as sporangium shape, color, and spore diameter. Both species possess white columellae and stalks. However, *D. macroverrucosa* can be differentiated from *D. bulbillosa* by its shorter overall height and shorter columella, and sparse warts (Table 2).

Diachea subsessilis Peck, Annual Rep. New York State Mus. 31:41 (1878).

Figure 8

Description. Sporocarp, gregarious or densely crowded, short-stalked or sessile, rarely plasmodiocarp, with gray-green or dark blue halo, (0.35–) 0.4–0.8 (−0.85) mm in diameter, (0.5–) 0.6–1 (−1.2) mm in tall. Stalk, when present, stout, cylindrical, white, calcareous,

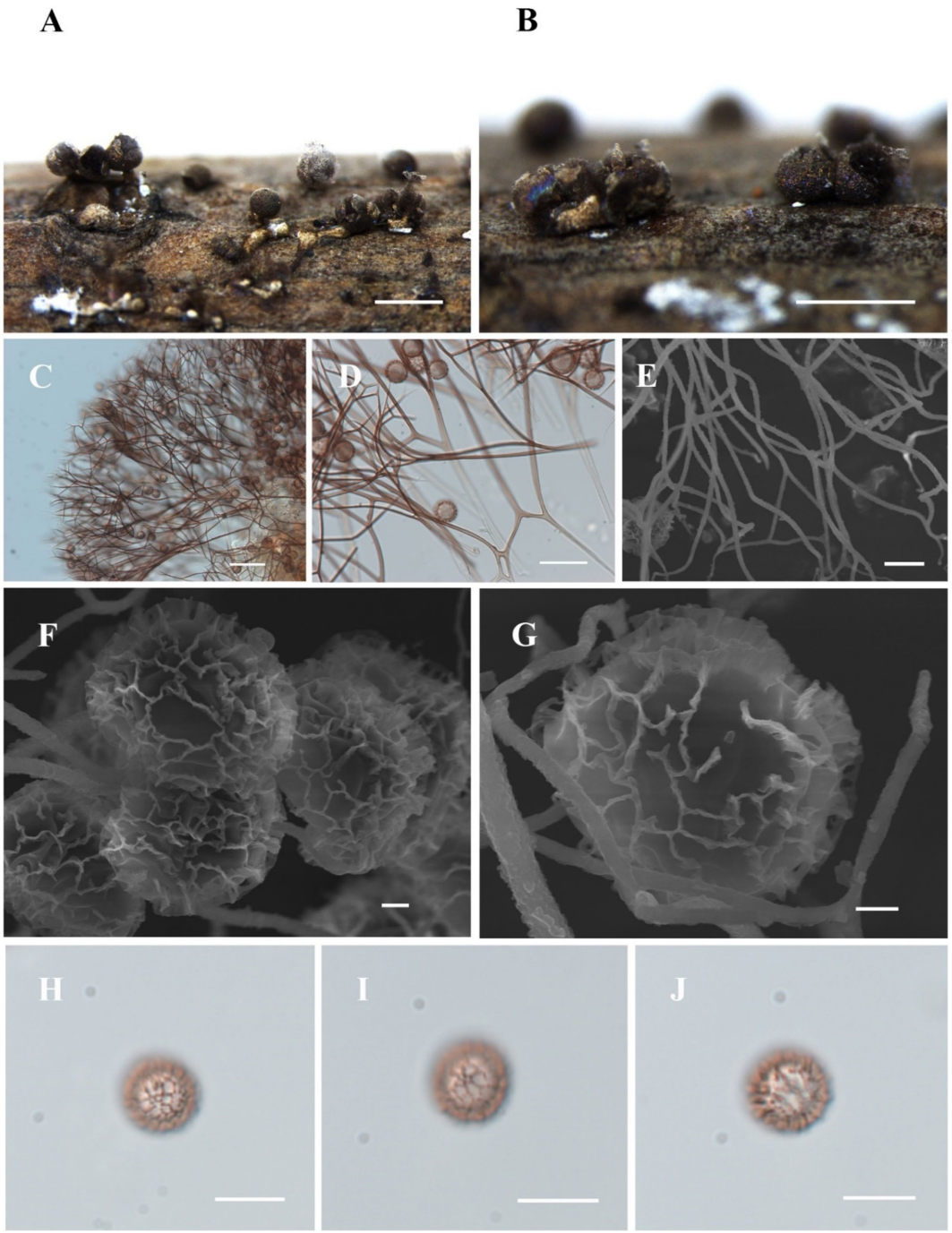


FIGURE 8
Habitat and microstructure of *Diachea subsessilis* (HMJAU M10075). (A,B) Sporocarps; (C–E) capillitium by TL and SEM; (F–J) Spores with clustered and connected into a network wart by SEM and TL. Scale bars: A, B = 1 mm, C = 40 μm, D = 20 μm, E = 5 μm, F, G = 1 μm, H-J = 10 μm.

not exceeding the height of the sporocarp. Peridium single-layered, with halo. Hypothallus small, networked, slightly calcareous, or absent. Columella short, calcareous, conical, and sometimes absent. Capillitium thin, radiating from the columella, light brown, branched and connected, light-colored at the ends. Spores dark in mass, light brown by transmitted light, with clustered warts and lines connected into a network, (7–) 8–12 µm in diameter.

Habitat. On the branches and rotten leaves.

Distribution in China. Sichuan province, Guangxi Zhuang Autonomous Region, Jiangsu province.

Distribution in the World. China, North America, Europe, and Southeast Asia.

Specimens examined. China, Sichuan province, Chengdu city, Tazishan Park, on the branches and rotten leaves, 15 July 2013, B. Zhang, HMJAU M10031, HMJAU M10075.

Notes. *Diachea subsessilis* is characterized by its short-stalked or sessile sporocarp with a gray-green or dark blue halo. It shares morphological similarities with *D. radiata* including a subglobose sporocarp, similar spore size, white columella, and stalk. However, *D. subsessilis* can be differentiated by its short columella. The spores have a spinulose-reticulate surface, often forming a complete net on one side, whereas *D. radiata* has small spinulose warts.

Taxonomic key to the species of *Diachea*.

1. Capillitium with limestone……...……
……...……*Diachea dictyospora.*
1. Capillitium without limestone……
...……...……...…2.
2. Hypothallus, stalk, and columella are orange……...……
……...… *Diachea silvaepluvialis.*
2. Hypothallus, stalk, and columella are white……
……...…...……3.
3. Sporocarp generally cylindrical or oval, rarely subglobose……...…...…….4.
3. Sporocarp spherical……
……...…...…….5.
4. Spores are light in color and nearly smooth……...…
……...…*Diachea leucopodia.*
4. Spores are light in color, with warts and dark clusters……...……
……...…*Diachea sichuanensis.*
5. Spores with reticular patterns and capillitium are soft and slender……...*Diachea subsessilis.*
5. Spores with warts or nodular protrusion……
……...……...……6.
6. Spores with less nodular protrusion, large……
……...…*Diachea macroverrucosa.*
6. Spores with more nodular protrusion, small……
……...……7.
7. Capillitium are sparse and curly.……
……...…...…*Diachea bulbillosa.*
7. Capillitium dense, hard, and straight……
……...…*Diachea plectophylla.*

4 Discussion

This study significantly advances our understanding of *Diachea* by providing detailed descriptions of two newly identified species, namely, *D. plectophylla* and *D. sichuanensis*, supported by robust phylogenetic analysis. In addition, we report new distribution records for five previously known species: *D. bulbillosa* in Gansu province, *D. leucopodia* in Yunnan and Sichuan provinces, and *D. subsessilis* in Sichuan province, China. Morphologically, *D. plectophylla* resembles *D. bulbillosa* with its sparse warts, iridescent sporocarps, white stalk, and prominent columella. However, it differs in having smaller spores and occasionally interconnected warts forming ridges. *D. sichuanensis* can be distinguished from *D. leucopodia* by its blunt-headed columella, spores with clustered warts, and thicker stalks. A detailed comparison of species characteristics is provided in Table 2.

Traditionally, species identification in myxomycete has relied on morphological traits. However, advances in molecular biology have greatly improved the accuracy of species identification, helping resolve discrepancies caused by morphology alone. Our morphological distinctions are further validated by the unique placements of these species, which confirms their taxonomic status. In our phylogenetic analysis, *Diachea* species formed a distinct branch within the family *Physaraceae*, contrasting with some recent research (Prikhodko et al., 2023). Studies by Fiore-Donno et al. (2012) and Cainelli et al. (2020) suggested that *Diachea* and *Didymium* are sister branches, albeit with weak support. Our results, however, suggest that *Diachea*, *Nannengaella*, and *Physarum* are more closely related sister branches.

Lado et al. (2022), who used the 18S rRNA, 17S rRNA, and *EF-1α* genes, faced challenges with incomplete data, leading to weak support in the ML analysis for six species. Discrepancies between our study and previous research may arise from the use of different gene markers. For instance, García-Martín et al. (2023) redefined *Diachea* to include species previously classified in *Physaraceae*, such as *Craterium* spp., but placed *Diachea* within *Didymiaceae*, divided into two groups, which diverges from our findings. Similarly, Prikhodko et al. (2023) used three gene markers to analyze *Didymiaceae*, resulting in some reclassifications. We believe that these differences stem from the varying gene markers, sample size, and available sequences used in each study. In addition, factors such as collection area, climate, and vegetation type may have contributed to the variations observed.

The taxonomic classification of the genus *Diachea* has historically been contentious. Despite its wide geographical distribution and the growing number of reported species, the limited availability of specimens and genetic sequences has hindered accurate classification. The scarcity of known *Diachea* sequences, along with unidentified sequences uploaded to NCBI, may lead to misinterpretations when using BLAST search. In recent studies, *Diachea* has been classified within the order Physarales; but its placement has oscillated between the families *Physaraceae* (Lister, 1925) and *Didymiaceae* (Keller and Braun, 1999; García-Martín et al., 2023; Prikhodko et al., 2023).

Our research identified five species forming a distinct evolutionary branch, which we tentatively assigned to the family *Didymiaceae* based on recent systematic research on Physarales (García-Martín et al., 2023). However, due to the limited number of specimens, we did not conduct a comprehensive analysis of the entire genus, focusing instead on the discovery of two new species. The limited data leave their taxonomic status somewhat uncertain. Nonetheless, our findings provide valuable sequences and preliminary insights for future systematic studies of this genus.

The recent discovery of new *Diachea* species, such as *D. mitchellii* (Lado et al., 2022), *D. racemosa* (Novozhilov et al., 2023), and *D. macroverrucosa* (Liu et al., 2024), underscores the greater species richness within the genus than previously documented. Looking

ahead, we plan to expand our sampling range, enhance morphological observations, increase the number of sequences, and employ additional gene markers to deepen our understanding of the relationships among *Diachea*, *Didymiaceae*, and *Physaraceae*. Future research should incorporate more gene markers (nSSU, *EF-1α*, mtSSU, *COI*, and *α-Tub*) and aim to obtain complete sequences of these genes for a more comprehensive study. To minimize variations caused by regional and environmental factors, collaboration with international researchers to broaden the sampling area is recommended. In addition, increasing specimen collection from extreme environments will facilitate a more thorough and systematic study of this genus and its relatives, ultimately clarifying its taxonomic status.

5 Conclusion

This study identifies two newly discovered species of *Diachea* and provides a detailed morphological description of these species, along with five previously known ones. An identification key for these species is also included. Given the limited research and sequence data available for this genus, our findings offer valuable foundational information to support future systematic research. Furthermore, the discovery of these new and newly recorded species enhances our understanding of *Diachea* diversity, contributing to broader research on the community composition ecological roles, and spatiotemporal distribution of myxomycetes and their substrates.

Data availability statement

The datasets presented in this study can be found in https://www.ncbi.nlm.nih.gov/nuccore. The accession number(s) can be found in the article/supplementary material.

Author contributions

XL: Conceptualization, Data curation, Formal analysis, Investigation, Methodology, Visualization, Writing – original draft, Writing – review & editing. DD: Methodology, Visualization, Writing – original draft. YT: Formal analysis, Writing – review & editing. YoL: Investigation, Writing – review & editing. JH: Formal analysis, Investigation, Methodology, Writing – review & editing. FS: Writing – review & editing. BZ: Project administration, Resources, Supervision, Writing – review & editing. XL: Project administration, Resources, Supervision, Writing – review & editing. YuL: Project administration, Resources, Supervision, Writing – review & editing.

Funding

The author(s) declare that financial support was received for the research, authorship, and/or publication of this article. This study was funded by several programs: the Jilin Provincial Key Research and Development Program (nos. 20230202121NC and 20240303101NC), the National Key R & D of Ministry of Science and Technology (no. 2023YFD1201601-2), the Modern Agroindustry Technology Research System (CARS20), and the 111 Program (no. D17014).

Acknowledgments

We gratefully acknowledge Xiaolan He from the Sichuan Edible Fungi Research Institute and Haixia Ma from the Chinese Academy of Tropical Agricultural Sciences for their invaluable assistance with fieldwork.

Conflict of interest

The authors declare that the research was conducted in the absence of any commercial or financial relationships that could be construed as a potential conflict of interest.

Publisher's note

All claims expressed in this article are solely those of the authors and do not necessarily represent those of their affiliated organizations, or those of the publisher, the editors and the reviewers. Any product that may be evaluated in this article, or claim that may be made by its manufacturer, is not guaranteed or endorsed by the publisher.

References

Adl, S. M., Habura, A., and Eglit, Y. (2014). Amplification primers of SSU rDNA for soil protists. *Soil Biol. Biochem.* 69, 328–342. doi: 10.1016/j.soilbio.2013.10.024

Adl, S. M., Simpson, A. G., Lane, C. E., Lukeš, J., Bass, D., Bowser, S. S., et al. (2012). The revised classification of eukaryotes. *J. Eukaryot. Microbiol.* 59, 429–514. doi: 10.1111/j.1550-7408.2012.00644.x

Alexopoulos, C. J. (1982). Cell biology of Physarum and Didymium V1: Organisms, nucleus, and cell cycle: 3–21. New York, USA: Academic Press.

Alexopoulos, C. J., and Saenz, J. A. (1975). The myxomycetes of Costa Rica. *Mycotaxon* 2, 223–271.

Bork, P. (2007). Interactive tree of life (iTOL): an online tool for phylogenetic tree display and annotation. *Bioinformatics* 23, 127–128. doi: 10.1093/bioinformatics/btl529

Cainelli, R., Haan, M. D., Meyer, M., Bonkowski, M., and Fiore-Donno, A. M. (2020). Phylogeny of Physarida (Amoebozoa, Myxogastria) based on the small-subunit ribosomal RNA gene, redefinition of Physarum pusillum s. str. And reinstatement of P. Gravidum Morgan. *J. Eukaryot. Microbiol.* 67, 327–336. doi: 10.1111/jeu.12783

Cavalcanti, L. H., Ponte, M. P. M. P., and Mobin, M. (2006). Myxomycetes, state of Piauí, Northeast Brazil. *Check List.* 2, 70–74. doi: 10.15560/2.2.70

Fiore-Donno, A. M., Berney, C., Pawlowski, J., and Baldauf, S. L. (2005). Higher-order phylogeny of plasmodial slime molds (Myxogastria) based on elongation factor 1-a and small subunit rRNA gene sequences. *J. Eukaryot. Microbiol.* 52, 201–210. doi: 10.1111/j.1550-7408.2005.00032.x

Fiore-Donno, A. M., Kamono, A., Meyer, M., Schnittler, M., Fukui, M., and Cavalier-Smith, T. (2012). 18S rDNA phylogeny of Lamproderma and allied genera (Stemonitales, Myxomycetes, Amoebozoa). *PLoS One* 7:e35359. doi: 10.1371/journal.pone.0035359

Fiore-Donno, A. M., Meyer, M., Baldauf, S. L., and Pawlowski, J. (2008). Evolution of dark-spored Myxomycetes (slime-molds): molecules versus morphology. *Mol. Phylogenet. Evol.* 46, 878–889. doi: 10.1016/j.ympev.2007.12.011

Fries, E. M. (1829). Systema mycologicum, sistens fungorum ordines, genera et species. Germany: Greifswald.

García-Cunchillos, I., Zamora, J. C., Ryberg, M., and Lado, C. (2022). Phylogeny and evolution of morphological structures in a highly diverse lineage of fruiting-body-forming amoebae, order Trichiales (Myxomycetes, Amoebozoa). *Mol. Phylogenet. Evol.* 177:107609. doi: 10.1016/j.ympev.2022.107609

García-Martín, J. M., Mosquera, J., and Lado, C. (2018). Morphological and molecular characterization of a new succulenticolous Physarum (Myxomycetes, Amoebozoa) with

unique polygonal spores linked in chains. *Eur. J. Protistol.* 63, 13–25. doi: 10.1016/j.ejop.2017.12.004

García-Martín, J. M., Zamora, J. C., and Lado, C. (2023). Multigene phylogeny of the order Physarales (Myxomycetes, Amoebozoa): shedding light on the dark-spored clade. *Persoonia* 51, 89–124. doi: 10.3767/persoonia.2023.51.02

Hall, T. (1999). BioEdit: a user-friendly biological sequence alignment editor and analysis program for windows 95/98/NT. *Nucleic Acids Symp. Ser.* 734, 95–98. doi: 10.1021/bk-1999-0734.ch008

Janik, P., Lado, C., and Ronikier, A. (2020). Range-wide Phylogeography of a nivicolous protist Didymium nivicola Meyl. (Myxomycetes, Amoebozoa): striking contrasts between the northern and the southern hemisphere. *Protist* 171:125771. doi: 10.1016/j.protis.2020.125771

Kalyanasundaram, I., and Mubarak, A. N. (1989). Taxonomic note on the myxomycete genus Diachea. *Mycol. Res.* 93, 233–235. doi: 10.1016/S0953-7562(89)80124-8

Kang, S., Tice, A. K., Spiegel, F. W., Silberman, J. D., Pánek, T., Cepicka, I., et al. (2017). Between a pod and a hard test: the deep evolution of amoebae. *Mol. Biol. Evol.* 34, 2258–2270. doi: 10.1093/molbev/msx162

Katoh, K., and Standley, D. M. (2013). MAFFT multiple sequence alignment software version 7: improvements in performance and usability. *Mol. Biol. Evol.* 30, 772–780. doi: 10.1093/molbev/mst010

Keller, H. W., and Braun, K. L. (1999). Myxomycetes of Ohio: their systematics, biology, and use in teaching. *Ohio Biol. Surv. Bull. New Series* 13, 1–182.

Keller, H. W., Skrabal, M., Eliasson, U. H., and Gaither, T. W. (2004). Tree canopy biodiversity in the Great Smoky Mountains National Park: ecological and developmental observations of a new myxomycete species of Diachea. *Mycologia* 96, 537–547. doi: 10.1080/15572536.2005.11832952

Kirk, P. M., Cannon, P. F., Minter, D. W., and Stalpers, J. A. (2008). Dictionary of the fungi. *10th* Edn. Wallingford, CT: CAB International, 759–771.

Lado, C. (2005/2024). *An on line nomenclatural information system of Eumycezotozoa*. Available at: http://www.nomen.eumycetozoa.com.

Lado, C., Treviño-Zevallos, I., García-Martín, J. M., and Wrigley, B. D. (2022). Diachea mitchellii: a new myxomycete species from high elevation forests in the tropical Andes of Peru. *Mycologia* 114, 798–811. doi: 10.1080/00275514.2022.2072140

Leontyev, D., Ishchenko, Y., and Schnittler, M. (2023). Fifteen new species from the myxomycete genus Lycogala. *Mycologia* 115, 524–560. doi: 10.1080/00275514.2023.2199109

Leontyev, D. V., and Schnittler, M. (2022). The phylogeny and phylogenetically based classification of myxomycetes. *Myxomycetes* 2022, 97–124. doi: 10.1016/B978-0-12-824281-0.00008-7

Lister, A. (1925). A monograph of the Mycetozoa: A descriptive catalogue of the species in the herbarium of the British museum. *3rd* Edn. London, UK: Printed by order of the Trustees.

Liu, S. L., Zhao, P., Cai, L., Shen, S., Wei, H. W., Na, Q., et al. (2024). Catalogue of fungi in China 1. New taxa of plant-inhabiting fungi. *Mycology.*, 1–58. doi: 10.1080/21501203.2024.2316066

Martin, G. W., and Alexopoulos, C. J. (1969). The Myxomycetes. Iowa City: University of Iowa Press.

Nguyen, L. T., Schmidt, H. A., Haeseler, A. V., and Minh, B. Q. (2015). IQ-TREE: a fast and effective stochastic algorithm for estimating maximum-likelihood phylogenies. *Mol. Biol. Evol.* 32, 268–274. doi: 10.1093/molbev/msu300

Novozhilov, Y. K., Okun, M. V., Erastova, D. A., Shchepin, O. N., Zemlyanskaya, I. V., García-Carvajal, E., et al. (2013). Description, culture and phylogenetic position of a new xerotolerant species of Physarum. *Mycologia* 105, 1535–1546. doi: 10.3852/12-284

Novozhilov, Y. K., Prikhodko, I. S., Bortnikov, F. M., Shchepin, O. N., Luptakova, A. D., Dobriakova, K. D., et al. (2023). Diachea racemosa (Myxomycetes = Myxogastrea): a new species with cespitose sporocarps from southern Vietnam and its position within the phylogenetic clade Diachea sensu lato (Physarales). *Protistology* 17, 189–204. doi: 10.21685/1680-0826-2023-17-4-1

Poulain, M., Meyer, M., and Bozonnet, J. (2011). *Les Myxomycetes*. Fédération mycologique et botanique Dauphiné-Savoie, Sévrier.

Prikhodko, I. S., Shchepin, O. N., Bortnikova, N. A., Novozhilov, Y. K., Gmoshinskiy, V. I., Moreno, G., et al. (2023). A three-gene phylogeny supports taxonomic rearrangements in the family Didymiaceae (Myxomycetes). *Mycol. Prog.* 22:11. doi: 10.1007/s11557-022-01858-1

Rambaut, A., Drummond, A. J., Xie, D., Baele, G., and Suchard, M. A. (2018). Posterior summarization in Bayesian phylogenetics using Tracer 1.7. *Syst. Biol.* 67, 901–904. doi: 10.1093/sysbio/syy032

Ronquist, F., and Huelsenbeck, J. P. (2003). MrBayes 3: Bayesian phylogenetic inference under mixed models. *Bioinformatics (Oxford, England)* 19, 1572–1574. doi: 10.1093/bioinformatics/btg180

Rostafiński, J. T. (1874). Śluzowce (Mycetozoa) Monografia. *Pamiętnik Towarzystwa Nauk Ścisłych Paryżu* 5, 1–215.

Shchepin, O. N., López, V. Á., Inoue, M., Prikhodko, I. S., Erastova, D. A., Okun, M. V., et al. (2024). DNA barcodes reliably differentiate between nivicolous species of Diderma (Myxomycetes, Amoebozoa) and reveal regional differences within Eurasia. *Protist* 175:126023. doi: 10.1016/j.protis.2024.126023

Shchepin, O., Novozhilov, Y., Woyzichovski, J., Bog, M., Prikhodko, I., Fedorova, N., et al. (2022). Genetic structure of the protist Physarum albescens (Amoebozoa) revealed by multiple markers and genotyping by sequencing. *Mol. Ecol.* 31, 372–390. doi: 10.1111/mec.16239

Walkera, G., Silbermanb, J. D., Karpovc, S. A., Preisfeld, A., Foster, P., Frolov, A. O., et al. (2003). An ultrastructural and molecular study of Hyperamoeba dachnaya, n. sp. and its relationship to the mycetozoan slime moulds - ScienceDirect. *Eur. J. Protistol.* 39, 319–336. doi: 10.1078/0932-4739-00906

Wikmark, O. G., Haugen, P., Lundblad, E. W., Haugli, K., and Johansen, S. D. (2007). The molecular evolution and structural organization of group I introns at position 1389 in nuclear small subunit rDNA of myxomycetes. *J. Eukaryot. Microbiol.* 54, 49–56. doi: 10.1111/j.1550-7408.2006.00145.x

Xiang, C. Y., Gao, F. L., Jakovlić, I., Lei, H. P., Hu, Y., Zhang, H., et al. (2023). Using PhyloSuite for molecular phylogeny and tree-based analyses. *Imeta* 2:e87. doi: 10.1002/imt2.87

Zhang, D., Gao, F., Jakovlić, I., Zou, H., Zhang, J., Li, W. X., et al. (2020). PhyloSuite: an integrated and scalable desktop platform for streamlined molecular sequence data management and evolutionary phylogenetics studies. *Mol. Ecol. Resour.* 20, 348–355. doi: 10.1111/1755-0998.13096

Zhao, F. Y., Liu, S. Y., Stephenson, S. L., Hsiang, T., Qi, B., and Li, Z. (2021). Morphological and molecular characterization of the new aethaloid species Didymium yulii. *Mycologia* 113, 926–937. doi: 10.1080/00275514.2021.1922224

frontiers | Frontiers in Microbiology

TYPE Original Research
PUBLISHED 20 November 2024
DOI 10.3389/fmicb.2024.1466300

Check for updates

OPEN ACCESS

EDITED BY
Elena Tamburini,
University of Cagliari, Italy

REVIEWED BY
Manish Kumar,
Amity University, Gwalior, India
Francesco Vitali,
Council for Agricultural Research and Agricultural Economy Analysis | CREA, Italy

*CORRESPONDENCE
Yanling Chen
✉ chenyanling21@163.com

†These authors have contributed equally to this work

RECEIVED 17 July 2024
ACCEPTED 31 October 2024
PUBLISHED 20 November 2024

CITATION
Zhu L, Zhang P, Ma S, Yu Q, Wang H, Liu Y, Yang S and Chen Y (2024) Enhancing carrot (*Daucus carota* var. sativa Hoffm.) plant productivity with combined rhizosphere microbial consortium.
Front. Microbiol. 15:1466300.
doi: 10.3389/fmicb.2024.1466300

COPYRIGHT
© 2024 Zhu, Zhang, Ma, Yu, Wang, Liu, Yang and Chen. This is an open-access article distributed under the terms of the Creative Commons Attribution License (CC BY). The use, distribution or reproduction in other forums is permitted, provided the original author(s) and the copyright owner(s) are credited and that the original publication in this journal is cited, in accordance with accepted academic practice. No use, distribution or reproduction is permitted which does not comply with these terms.

Enhancing carrot (*Daucus carota* var. sativa Hoffm.) plant productivity with combined rhizosphere microbial consortium

Liping Zhu[1,2†], Peiqiang Zhang[1†], Shunan Ma[1], Quan Yu[1], Haibing Wang[1], Yuexuan Liu[1], Song Yang[1] and Yanling Chen[1*]

[1]Shandong Provincial Key Laboratory of Applied Mycology, School of Life Sciences, College of Resource and Environment Science, Qingdao Agricultural University, Qingdao, Shandong, China, [2]Postdoctoral Research Station, Rushan Hanwei Bio-Technical & Science CO., LTD., Weihai, Shandong, China

Background: Plant growth-promoting rhizobacteria (PGPR) are an integral part of agricultural practices due to their roles in promoting plant growth, improving soil conditions, and suppressing diseases. However, researches on the PGPR in the rhizosphere of carrots, an important vegetable crop, is relative limited. Therefore, this study aimed to isolate and characterize PGPR strains from the rhizosphere soil of greenhouse-grown carrots, with a focus on their potential to stimulate carrot growth.

Methods: Through a screening process, 12 high-efficiency phosphorus-solubilizing bacteria, one nitrogen-fixing strain, and two potassium-solubilizing strains were screened. Prominent among these were *Bacillus firmus* MN3 for nitrogen fixation ability, *Acinetobacter pittii* MP41 for phosphate solubilization, and *Bacillus subtilis* PK9 for potassium-solubilization. These strains were used to formulate a combined microbial consortium, N3P41K9, for inoculation and further analysis.

Results: The application of N3P41K9, significantly enhanced carrot growth, with an increase in plant height by 17.1% and root length by 54.5% in a pot experiment, compared to the control group. This treatment also elevated alkaline-hydrolyzable nitrogen levels by 72.4%, available phosphorus by 48.2%, and available potassium by 23.7%. Subsequent field trials confirmed the efficacy of N3P41K9, with a notable 12.5% increase in carrot yields. The N3P41K9 treatment had a minimal disturbance on soil bacterial diversity and abundance, but significantly increased the prevalence of beneficial genera such as *Gemmatimonas* and *Nitrospira*. Genus-level redundancy analysis indicated that the pH and alkali-hydrolyzable nitrogen content were pivotal in shaping the bacterial community composition.

Discussion: The findings of this study highlight the feasibility of combined microbial consortium in promoting carrot growth, increasing yield, and

enriching the root environment with beneficial microbes. Furthermore, these results suggest the potential of the N3P41K9 consortium for soil amelioration, offering a promising strategy for sustainable agricultural practices.

KEYWORDS

carrot, phosphorus-solubilization, potassium-solubilization, nitrogen fixation, rhizosphere, microbial consortium, soil property

1 Introduction

Nitrogen (N), phosphorus (P), and potassium (K) are essential macronutrients for the growth and development of higher plants. However, conventional agricultural practices that heavily utilize chemical fertilizers have been linked to environmental challenges, including soil compaction and aquatic eutrophication (Bhardwaj et al., 2014; Rahman and Dunfu, 2018). The efficiency of N fertilizer uptake by plants is relatively low, at 30–40%, with the remainder contributing to soil acidification, reduced organic matter, and the escalation of serious diseases and pests (Taurian et al., 2013; Ahmed et al., 2017; Rahman and Dunfu, 2018). Phosphorus, critical for plant growth and crop yield, is often limited in agricultural ecosystems, with the majority of applied chemical phosphate becoming fixed in the soil, resulting in a P utilization efficiency of only 5–25% (Kochian, 2012; Alori et al., 2017; George et al., 2017; Timofeeva et al., 2022; Pan and Cai, 2023). Excessive P application not only limits plant uptake but also risks the accumulation of residual P in the soil, and the subsequent eutrophication of water bodies (Powers et al., 2016). Potassium, the third most important plant nutrient after N and P, is involved in plant resistance to biotic and abiotic stresses and is required to activate most different enzymes involved in plant processes (Bakki et al., 2024). With only 2% of soil K in a free soluble form, the need for sustainable fertilization practices is acute. These practices should aim to enhance nutrient bioavailability and reduce environmental impact. Soil microorganisms offer a promising avenue for achieving these goals, presenting a critical breakthrough for sustainable agriculture. Abundant and essential to ecosystem functions, soil microbial communities are the driving force behind biogeochemical cycling. The rhizosphere, the dynamic zone surrounding plant roots, is a hub of microbial diversity and complexity. Within this ecosystem, plant growth-promoting rhizobacteria (PGPR), play a pivotal role in soil health, fertility, and the sustainability production of crops (Saha et al., 2008; Sangoquiza-Caiza et al., 2023). PGPR strains enhance plant growth and yield through a variety of direct mechanisms, including the production of phytohormone production, nitrogen fixation, phosphate and potassium-solubilization, siderophores, and ammonia, as well as by indirect pathways such as hyperparasitism, antibiosis, and generation of lytic enzymes (Backer et al., 2018; Basu et al., 2021; Grover et al., 2021; Fiodor et al., 2023). The application of microbial inoculants containing PGPR has been demonstrated to significantly increase crop production by 12–20% (Glick, 2014; Pérez-Jaramillo et al., 2016; Shi et al., 2023), underscoring their potential as a sustainable agricultural strategy.

Phosphorus solubilizing bacteria (PSB), a subset of PGPR, have been identified as pivotal for promoting plant growth and disease resistance (Billah et al., 2019; Kumar et al., 2021; Shultana et al., 2022). Predominantly isolated from the rhizosphere, these strains are metabolically active and capable of transforming insoluble P into bioavailable forms, garnering attention for their role in sustainable agriculture (Hanif et al., 2015; Timofeeva et al., 2022; Wang S. et al., 2022). The solubilization mechanism involve the secretion of organic acids such as malic, lactic, acetic, citric, and succinic, alongside enzymes like phytase and phosphatase, and chelation through siderophores and extracellular polysaccharides (Rodríguez and Vidal, 1999; Hanif et al., 2015; Wang et al., 2017; Liang et al., 2020). Notably, certain PSBs produce plant growth regulators, including indole acetic acid (IAA) and gibberellin (GA), which significantly influence vegetative growth characteristics (Singh et al., 2011; Narendra Babu et al., 2015; Azaroual et al., 2020). The inoculation of PSB, exemplified by *Acinetobacter pittii* gp-1, has markedly improved soybean growth through increased enzymatic activities and phytohormone levels (He and Wan, 2021). Similarly, *Bacillus* sp. LTAD-52, isolated from rapeseed, has demonstrated a substantial yield increase ranging from 21 to 44% under greenhouse conditions (Valetti et al., 2018). Seven endophytic PBS strains from *Cunninghamia lanceolata* have been found to increase plant height, stem diameter, and biomass by 20 to 40% (Chen J. et al., 2021). The function of nitrogen-fixing bacteria (NFB) as a component of microbial fertilizers is influenced by various factors such as crop type, soil moisture, and organic matter content (Shi et al., 2023). While NFB can benefit certain crops, their efficiency is sometimes limited due to low compatibility with host plants, and weak competitive ability against indigenous rhizosphere bacteria. Without an adequate supply of K, plants will have poorly developed roots, grow slowly, and have lower yields (Meena et al., 2014). Potassium solubilizing bacteria (KSB) can solubilize insoluble potassium minerals such as biotite, feldspar, muscovite, vermiculite, smectite, orthoclase, and mica into soluble forms that are available to plants. In this process, the production of organic acid by microorganisms leads to the dissolution of mineral potassium. In addition, KSB can provide beneficial effects by suppressing pathogens, reducing root-knot nematode, and improving soil nutrients and structure (El-Hadad et al., 2011; Meena et al., 2014). Identified KSB, including *Bacillus mucilaginosus*, *B. edaphicus*, *B. circulans*, *Acidithiobacillus ferrooxidans* and *Paenibacillus* spp have shown positive effects on various crops like wheat (Wang et al., 2020), maize, tomato, apple, and so on (Liu et al., 2012; Meena et al., 2014; Feng et al., 2019; Raji and Thangavelu, 2021; Muthuraja and Muthukumar, 2022; Jiao et al., 2024).

Despite these advancements in PGPR research, a disproportionate focus has been placed on cereals like wheat and maize (Nawaz et al., 2020; Kálmán et al., 2023), and legumes such as soybean (Kuzmicheva et al., 2017), with root crops like carrots receiving comparatively less attention. Carrots are

recognized for their health benefits, including antioxidants, fiber, and vitamins that may contribute to cancer prevention (Yi et al., 2023), and they also respond positively to mycorrhizal fungi inoculants, which improve their morphological and biochemical traits (Yadav et al., 2021). However, the impact of PGPR on the agronomic and rhizosphere soil characteristics of carrots remains understudied. On the other hand, although PGPR are naturally present in the soil, their populations are often insufficient to compete with other established bacteria in the rhizosphere. Given that successful rhizosphere colonization is a prerequisite for PGPR to exert their effects on plants (Lodeiro, 2015), inoculating with PGPR is a critical step to increase their numbers within the soil, thus optimizing their agricultural benefits. Recent advances have shown that formulations incorporating diverse strains with multiple functions are increasingly recognized for their superior efficiency in improving soil quality and increasing crop yields compared to single-strain microbial fertilizers with limited functions (Beneduzi et al., 2012). This has led to adoption of a strategic approach of selecting multifunctional PGPR strains native to the plant as active components of inoculants, aiming to increase yield potential.

Therefore, in this study, we isolated PGPR strains native to the carrot rhizosphere and evaluated their effects on carrot growth and soil properties. Three dominant PGPR strains with exceptional abilities in P solubilization, N fixation, and K solubilization, were identified and used in single-strain inoculation tests. The study further investigated the effects of single and combined microbial consortia, as well as their integration with chemical fertilizers, on carrot growth parameters and soil enzymatic activities. Additionally, through sequencing analysis, the impact of microbial fertilizers on soil microbial community structure was evaluated. By employing a sustainable strategy based on a combined microbial consortium, this research provides an innovative approach to carrot cultivation, and offers a holistic solution to contemporary agricultural challenges.

2 Materials and methods

2.1 Site description and sampling

Sampling sites were from carrot rhizosphere soil at Laixi Carrot Science and Technology College, Qingdao Agricultural University, China (E120° 21′, N36° 39′). The soil, characterized as mortar black, exhibited properties of pH 6.99, 7.16 g/kg organic matter, 175.70 mg/kg alkali-hydrolyzable nitrogen (N), 27.75 mg/kg available phosphorus (P), and117.58 mg/kg available potassium (K).

2.2 Isolation and screening of PGPR strains with phosphorus solubilizing, nitrogen-fixing, and potassium solubilizing abilities from the rhizosphere of carrot

Productive carrots with adhering soil were transferred into a sterile bench, and then the non-rhizosphere soil was removed by gentle shaking. The rhizosphere soil collected from 10 samples was mixed into a 50 ml sterile tube. 1 g of rhizosphere soil was mixed with 9 ml of sterile water thoroughly for 30 min and serial dilutions of 10^{-1} to 10^{-7} were performed. Subsequently, 100 μL aliquots of each dilution were spread onto plates of Ashby (per 1 L containing 10 g mannitol, 5.0 g $CaCO_3$, 0.2 g KH_2PO_4, 0.2 g $MgSO_4{\cdot}7H_2O$, 0.2 g NaCl, 0.1 g $CaSO_4{\cdot}2H_2O$ and 15 g agar), phosphate-solubilizing medium [per 1 L containing 10 g glucose, 10 g $Ca_3(PO4)_2$, 0.5 g $(NH_4)_2SO_4$, 0.3 g $MgSO_4{\cdot}7H_2O$, 0.3 g $FeSO_4{\cdot}7H_2O$, 0.3 g KCl, 0.3 g NaCl, 0.03 g $MnSO_4{\cdot}4H_2O$, and 15 g agar], and potassium-solubilizing medium [per 1 L containing 10 g sucrose, 0.5 g yeast extract, 1.0 g $(NH_4)_2SO_4$, 2.0 g Na_2HPO_4, 0.5 g $MgSO_4{\cdot}7H_2O$, 1.0 g $CaCO_3$, 1.0 g potassium feldspar powder, and 15 g agar], to isolate nitrogen-fixing, phosphorus-solubilizing, and potassium-solubilizing bacteria (Chen J. et al., 2021; Jiao et al., 2024). These plates were incubated at 28°C for 3 days and the relative bacterial colonies were selected based on the appearance of hyaline circles (Valetti et al., 2018). The isolates were subjected to successive purification steps and the purified strain was then stored in glycerol stock at −80°C. The solubility index (SI) was determined by measuring hyaline circles and colony diameters at 4 days of culture according to the following formula: SI = (colony diameter + halo diameter)/(colony diameter) (Ibáñez et al., 2021).

2.3 Evaluation of the growth-promoting properties of the PGPR strains

2.3.1 Phosphate solubility assay

The phosphate solubility assay was conducted in quadruplicate to ensure accuracy. PSB strains with higher SI values were subjected to further testing in the NBRIP liquid medium (Hanane et al., 2008), which incorporated tricalcium phosphate as the sole source of phosphorus. Inoculations were made into 500 mL Erlenmeyer flasks containing 100 mL of the NBRIP liquid medium, achieving a final concentration of 5×10^4 colony-forming units per mL (CFU/mL) for each bacterial strain. The cultures were incubated at 30°C and 150 rpm for 8 days, with the soluble P content being measured at every 48 h interval as follows: a small volume of the fermentation broth was centrifuged at 10,000 rpm/min for 10 min and the supernatant was collected and diluted if necessary; the reaction mixture was prepared by sequentially adding 1 mL Mo Sb antibody solution and 0.5 mL of ascorbic acid solution, followed by thorough mixing and a 15-min incubation at room temperature. The *P* concentration was measured using the molybdate blue method, with P-free samples serving as blank controls in this study (Jiao et al., 2024).

2.3.2 Determination of nitrogen fixation efficiency

The screened NFB strain was incubated in a 150 mL conical flask with 50 ml of liquid Ashby medium for 7 days at 28°C. The culture was centrifuged (10,000 r/min) for 20 min, and the supernatant was taken for N concentration detection using the micro-Kjeldahl method (Shi et al., 2023). The test was repeated three times with the uninoculated medium as a control.

2.3.3 Determination of potassium solubility

The screened KSB stains were incubated in 50 mL of K solubilizing medium at 28°C with shaking at 180 rpm for

5 days. After incubation, the fermentation broth was centrifuged at 500 rpm for 10 min to remove the insoluble particles. The supernatant was then collected by centrifugation at 10,000 r/min for 10 min. This process was conducted in triplicate, with a control group using an uninoculated medium. Then flame spectrophotometry was used to calculate the effective K content of the supernatant (Jiao et al., 2024).

2.4 Strain identification and phylogenetic analysis

The bacteria strains were chosen for molecular identification based on full 16S rRNA sequence, using universal primers, 27F (5′-AGAGTTTGATCCTGGCTCAG-3′) and 1492R (5′-TACGACTTAACCCCAATCGC-3′). The sequencing results were aligned against 16S rDNA homologous sequences in the NCBI database and a high percentage of sequence identity (usually > 97%) is considered indicative of the same species. Subsequently, a phylogenetic tree was constructed using MEGA 6 software and iTOL network (Tamura et al., 2007).[1]

2.5 Verification of screened strains on the growth of carrot

2.5.1 Potted experiment design

The experimental procedures were conducted with slight modifications to the method previously described (He and Wan, 2021). Carrot seeds of full viability were selected and subjected to surface disinfection, followed by a soak in a 1% sodium hypochlorite for 5 min, and then thoroughly rinsed with sterile water at least 4 times to remove the disinfectant. These seeds were then placed on two layers of moistened filter paper and incubated at 28°C in the dark for 48 h to germinate. The germinated seeds were sown in sterilized potting soil within containers measuring 20 cm × 20 cm × 15 cm, with each pot receiving 2 kg of soil and 10 seeds, and the seed surface was covered with a thin layer of about 1 cm of soil.

Meanwhile, bacterial strains were inoculated into 250 mL Erlenmeyer flasks containing 100 mL of LB liquid medium and cultured at 25°C, 200 rpm for 48 h. The bacterial cells were harvested by centrifugation at 8,000 *g* for 10 min at room temperature. The pelleted cells were resuspended with sterile water to achieve a bacterial density of 3×10^7 colony-forming units (CFU/mL), which was used for inoculation purposes. Subsequently, two treatments were established: (1) CK, where plants were inoculated with 50 mL of sterile water serving as a control group; (2) the bacterial strain treatment, where plants were treated with 50 ml of bacterial inoculant with 3×10^7 CFU/mL. Each treatment was conducted in triplicate. In addition, the combined microbial consortium and commercial biofertilizer were also treated for the pot experiment, designated as groups N3P41K9, WZF, BSW, and PGA. The N3P41K9 treatment featured a combined microbial consortium comprising MN3, M6P41, and PK9. The WZF, BSW, and PGA treatments involved the application of commercially available microbial biofertilizers. WZF for Wuzhoufeng, contains *Trichoderma harzianum*, *B. subtilis*, and *Paenibacillus* spp, with a product specification of 25 kg/bag, and an effective viable count of at least 200 million/g, purchased by Wuzhoufeng Agricultural Science and Technology Co., LTD.; BSW, for Baisiwang, contains *B. subtilis* and *Bacillus thuringiensis*, comes in 500 g/bag with an effective viable count of at least 1×10^{10} CFU/g/g, containing, purchased from Shandong Shigaode Plant Nutrition Technology Co., LTD.; PGA, for Pea-based polyglutamic-acid enhanced microbial agent, is a package in 40 kg/bag with an effective viable count exceeding 5×10^8 CFU/g, containing soybean meal, saprophytic fungi, nitrogen-fixing bacteria, phosphorus-solubilizing bacteria, and potassium-solubilizing bacteria and purchased from Shandong Muyu Shi Biotechnology Co., LTD. Each treatment was standardized to an effective viable count of 200 million/g.

The potted plants were placed in a greenhouse with a photoperiod of 16 h light/8 h darkness and a temperature regime of 25°C/18°C. The soil moisture was meticulously maintained at 40% following the emergence of the carrot seedings. Growth parameters including plant height, fresh weight, root length and root diameter were recorded at 20, 30, and 40 days post-emergence. After 40 days, soil samples were collected from the pots for analysis of available element contents and enzymatic activities.

2.5.2 Field test of combined microbial consortium

This research was conducted in Houtun Village, Dianbu Town, West City, Qingdao City, Shandong Province, China (E120°21', N36°39'), from July to December 2023. The study region, characterized by a temperate semi-humid monsoon climate, has an average annual temperature of 11.3 °C and receives a mean annual rainfall of 732.5 mm. The test soil used was Shajiang black soil, which has been part of a long-term crop rotation of carrots. The carrot cultivar selected for testing was Outehong 2. The experimental design included ten treatments, each with equal N application and viable bacteria groups: a control (CK) without fertilizer, a complex microbial consortium (N3P41K9), and commercially available microbial biofertilizers (WZF, BSW, PGA), as well as an optimized treatment (OPT: with N 274.5 kg/ha, P_2O_5 49.5 kg/ha, K_2O 315 kg/ha) combined with each of the microbial agents. Each treatment was replicated three times in a completely randomized layout, with an area of 25 m^2 per replicate. Each treatment group's effective viable bacteria count was 2×10^8 CFU/mL. Fertilization of microbial agents was applied before sowing, followed by three additional fertilizer applications at the seedling establishment, the rosette development, and the early phase of fleshy root expansion, all after sampling for measurement. Finally, samples were taken at the seedling emergence stage (Day 20), the rosette stage (Day 40), the expansion stage (Day 80), and the harvest stage (Day 100) for the determination of carrot growth indicators and soil characteristics.

2.5.3 Analysis of plant biomass

Plant biomass was assessed through the collection and processing of carrot samples. The sampling was conducted at the germination stage, rosette stage, fleshy root expansion stage, and harvest stage, to determine plant height, fresh weight, root length, respectively.

1 https://itol.embl.de/

2.5.4 Determination of soil properties

In the pot experiment, 20 g of soil surrounding the main roots of the carrots after 40 days of growth was collected, sieved through a 2-millimeter mesh, and then used for the analysis of soil properties. In the field, soil sampling was carried out at the four stages mentioned above, collecting surface soil samples (0–20 cm depth). Three replicates were gathered and mixed to create a composition sol sample. Soil physicochemical properties were determined using standard methods (Bao, 2000). A brief procedure involved the placement of an air-dried soil sample into a triangular flask, followed by the addition of distilled water at a soil-to-water ratio of 1:2.5. The mixture was then incubated at 160 rpm for 2 h, centrifuged, and the pH value of the supernatant was measured. The alkaline-hydrolyzable N was ascertained using the diffusion method (DB13/T 843–2007); the available P level was determined by the molybdenum-antimony colorimetry method (NY/T1121.7–2014); and the available K content was determined by ammonium acetate extraction method (NYT 889–2004). By methodology for soil enzyme research (Miao et al., 2019; Zhang et al., 2023), soil sucrase activity was evaluated using the 3,5-dinitrosalicylic acid colorimetry method, with results expressed as milligrams of glucose after 24 h. Similarly, soil urease activity was measured by the sodium phenoxide colorimetry method, expressed as milligrams of NH_3-N per gram of soil over 24 h. The final calculation of the change is to indicate the difference, which is determined by subtracting the relevant value of the original soil from the value of the measured sample. All data was recorded after three repetitions of each test.

2.6 Analysis of soil microbial community structure

To investigate the impact of the inoculated microbial consortium on indigenous soil microbial communities, fresh soil samples after harvesting were extracted for microbial DNA using a Fast DNA SPIN kit (MP Biomedicals, USA). PCR amplification was performed for bacterial 16S rDNA using primer pairs 515F (5′-GTGCCAGCMGCCGCGG-3′) and 907R (5′-CCGTCAATTCTTTTRAGTTT-3′). Sequencing was conducted on the Illumina MiSeq platform (Beijing Nuohe Zhiyuan Technology Co., Ltd.). Operational taxonomic units (OTUs) clustering was performed using USEARCH (version 10.0) at a similarity level of 97% and filtered using a threshold of 0.005% of the total number of sequences (Bokulich et al., 2013).

2.7 Statistical analysis

All data were analyzed by analysis of variance (ANOVA) using SPSS (version 26.0, IBM, Inc.) and expressed as means (± SE; standard error), and the plotting was conducted using GraphPad Prism 8.0. The statistically significant level was set as $P < 0.05$, and the extremely significant level was set as $P < 0.01$. In this study, only results with a $P < 0.05$ are reported, while those that are not statistically significant are omitted. Venn diagram and non-metric multidimensional scaling (NMDS) plot were used to reflect bacterial community composition. Pairwise analysis of similarity (ANOSIM) was applied to quantitatively evaluate differences in bacterial community composition. The Shannon index of bacterial community composition was analyzed. An abundance plot of soil microbial communities featuring the species with higher rankings in relative abundance at the phylum and genus levels was created based on the classification and proportional count of OTUs. Pearson correlation analysis was used to study the relationship between plant physiological indexes, soil physical and chemical properties, enzyme activities, and soil microorganisms. Redundancy analysis (RDA) to evaluate the relationship between soil properties and the microbial communities, was performed using the online tool at www.bioincloud.tech/standalone-task-ui/rda. MEGA 6.0 software was applied for phylogenetic trees, employing the Neighbor-Joining method with a Bootstrap value of 1,000.

3 Results

3.1 Isolation and evaluation of PBS, NFB and KSB strains from the rhizosphere of carrot

From the carrot rhizosphere, a variety of bacteria were isolated, and upon verification considering their growth rates, 15 distinct morphological strains were identified, including 12 PBS, one NFB, and two KSB, as illustrated in Supplementary Figure 1a. The phylogenetic tree constructed from 16S rRNA sequence indicated that these 12 PSB isolates belonged to three genera (two for *Bacillus*, three for *Pseudomonas*, and seven for *Acinetobacter*); the NFB strain MN3 was identified as *Bacillus firmus*; two KSB strains PK9 and MK31 were identified as *B. subtilis* and *Paenibacillus polymyxa*, respectively (Supplementary Figure 1b and Supplementary Table 1).

As seen in Figure 1a, among the 12 PSB strains, OP82 (*B. subtilis*), MP41 (*A. pittii*), and MP117 (*B. velezensis*) displayed the most pronounced hydrolysis halo according to the solubilizing index (SI). The PK9 (*B. subtilis*) showed a higher K SI. Further detection revealed that during the liquid phosphorus fermentation process, the pH value of the medium (with an original pH of 6.8) exhibited an overall trend of "initial decline followed by a gradual rise" in correlation with the duration of phosphorus-solubilization. A marked decrease in pH was observed for most of the strains on Day 2, which was followed by an incline. The highest level of P soluble content was reached on Day 4, with values ranging from 136 to 330 mg/L (Figure 1b), reflecting a notable variance in the solubilization capabilities of the strains. The most effective strains in solubilizing P were MP41, OP61 (*A. pittii*), OP81 (*A. pittii*), OP82, and MP117, and Linear regression analysis between pH and phosphate soluble content revealed a significant negative correlation over the cultivation period (Supplementary Figure 2). Similarly, two KSB strains also showed hydrolytic halos on the medium, with strain PK9 having a higher SI than MK31 (Figure 1a). During the liquid medium cultivation (Figure 1c), the pH significantly decreased on Day 2 from the initial neutrality to around 4.5. The maximum soluble K content also occurred on Day 4, with the strain PK9 at 123.3 mg/L and MK31 at 103.9 mg/L, respectively. It is speculated that phosphate-solubilizing or the potassium-solubilizing ability was related to acid

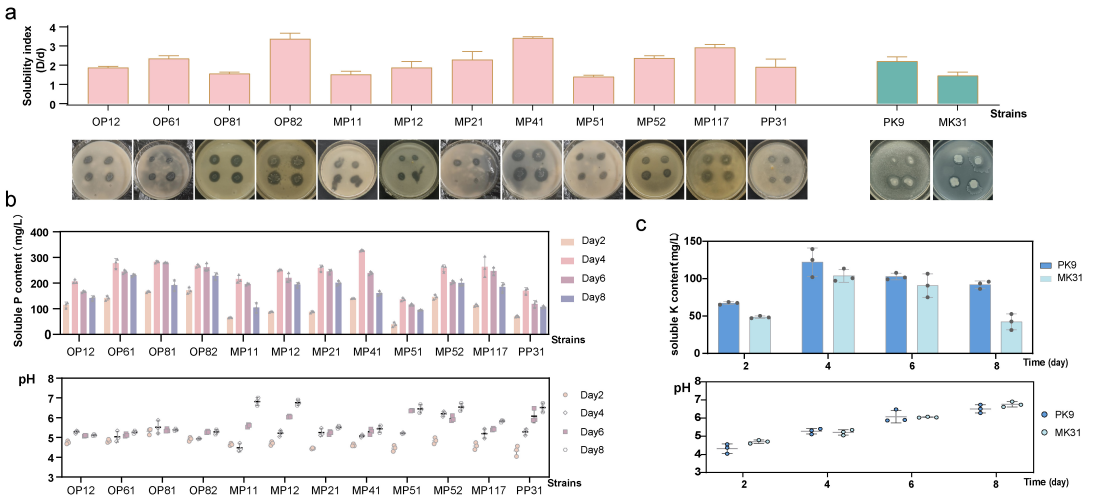


FIGURE 1
Evaluation of the PSB and KSB strains. **(a)** Soluble index (SI) performance of the strains; **(b)** Phosphorus solubilizing effect and pH analysis of PSB strains in liquid media; **(c)** Potassium solubilizing effect and pH analysis of KSB strains in liquid media.

production. However, as the strain metabolizes, the concentration of phosphorus or potassium in the culture decreases and the pH value gradually returns. In addition, after 15 days of cultivation of the NFB strain MN3, the total nitrogen content was measured to reach 21.91 mg/L.

3.2 Effect of different strains on the carrot growth and soil-related elements in the pot experiment

To elucidate the impact of these bacteria strains on carrot growth, we carried out the pot experiment and detected the relative growth indicators of carrots after 20, 30 and 40 days of treatment with different bacterial agents, respectively. As shown in Figure 2a and Supplementary Table 2, plant height, plant fresh weight and root length of most of the treatment groups were significantly higher than the control group. In the early stages of carrot growth (the first 20 days), these strains showed a certain growth-promoting effect, with an average increase in plant height, root length and root fresh weight of 15.5 ± 12.2, 28.4 ± 13.7, and 45.1 ± 23.4%, respectively, compared to the control. Among all the strains, the NFB strain MN3 had the most significant effect, increasing the plant height, root length, and root fresh weight by 54.2 ± 8.9, 39.7 ± 6.8, and 61.6 ± 39.8%, respectively. On Day 30, the growth-promoting effects of the PSB and KSB were more pronounced, such as MP21, OP81, OP82, PP31, PK9, and MK3. However, The PSB strain PK9 had a promoting effect on the plant height, while MK31 had a more obvious promoting effect on the root. On Day 40, the carrot roots began to swell and turn orange, and the growth-promoting effect of the strains was more significant. Among them, MP41, and PK9 showed an advantage in plant height, increasing by 58.4 ± 11.3%, and 56.7 ± 10.7% compared to the control, respectively; OP12, MP41, and PP31 displayed a marked advantage in root fresh weight, increasing by 391.1 ± 101.7, 348.6 ± 78.2, and 267.1 ± 11.5% compared to control, respectively. The NFB strain MN3 also showed a stable growth-promoting effect, increasing plant height, root length, and root fresh weight by 5.2 ± 8.6, 14.8 ± 4.8, and 144.2 ± 8.4%, respectively. OP61 and OP117 were the least significant in promoting growth in all aspects.

Subsequently, the result of the changes in the content of corresponding elements in the soil after Day 40 was illustrated in Figure 2b. The soil's available P content varied significantly with PP31 resulting in the highest level, followed by MP41. In contrast, strains OP12, MP117, and MP52 had the lowest available P content. Regarding the soil's available K content, PK9 was 6.3 ± 1.7% higher than MK31. Compared to the control group, MN3 significantly increased the soil's alkaline-hydrolyzable N content by 94.9 ± 2.7%. Further analysis of growth indicators using the correlation heatmap (Figure 2c) revealed that NFB, as well as PSB and KSB, significantly influenced plant growth at 20, 30, and 40 days post-application of the bacterial agents, respectively. Within the group of PSB, strain MP41 showed a synergistic effect, closely clustered with MN3, PK9, and MK31. Considering the slight superiority of PK9 over MK31, we constructed a microbial consortium N3P41K9 comprising MN3, MP41, and PK9 to assess their collective impact on carrot growth. Additionally, the growth of these three strains did not exhibit any antagonism or inhibition (Supplementary Figure 3).

3.3 Effects of microbial consortium N3P41K9 in the pot experiment

To thoroughly evaluate the impact of the microbial consortium N3P41K9 on carrot growth, we executed a comparative pot fertilization treatment using commercially available microbial fertilizers WZF, BSW and PGA, as positive controls and single strains as negative controls (Figure 3a and Supplementary Table 3). During the initial phase (Day 20 post-inoculation), no significant difference in carrot growth was detected among the various microbial treatments, while a discernible enhancement in both plant height and root length was noted in comparison to the

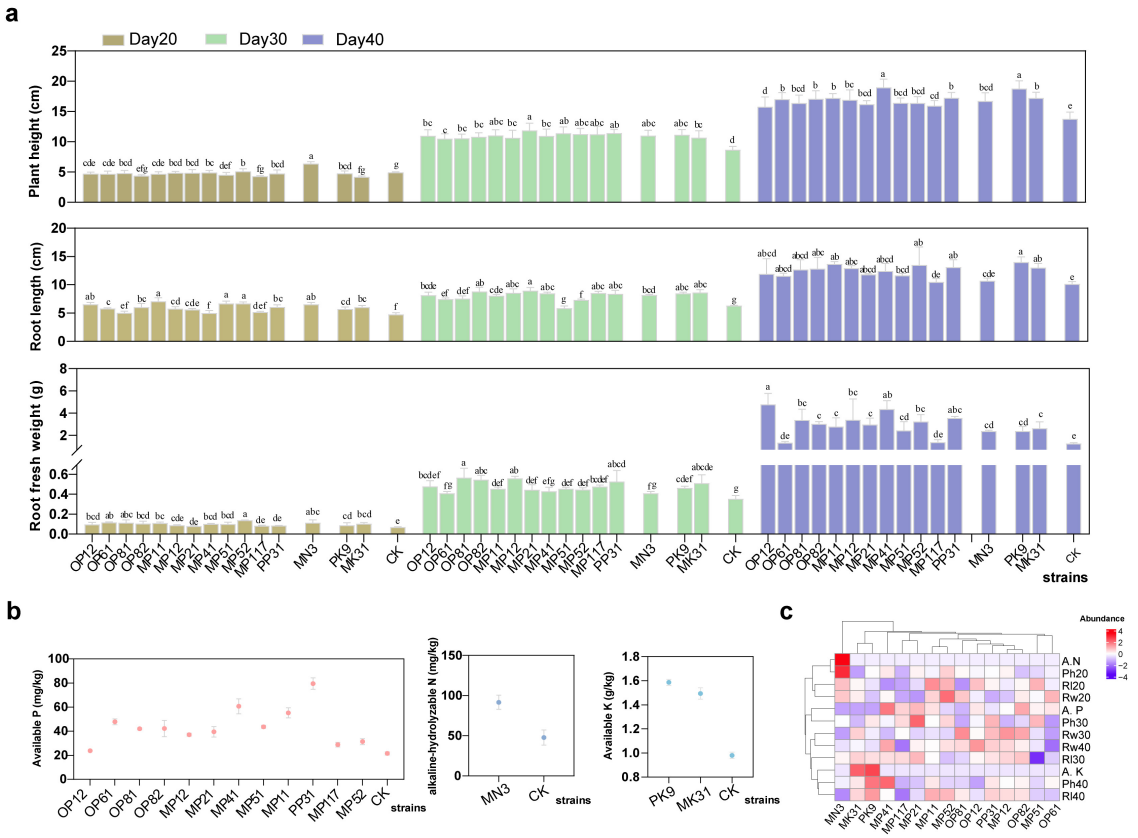


FIGURE 2
Effect of individual strain on the pot experiment's carrot growth and soil nutrients. **(a)** Growth metrics for carrots, including plant height, root length, and root fresh weight were recorded on day 20, 30, 40, respectively. Different lowercase letters indicate significant differences ($P < 0.05$) among treatments of different strains. CK represents the sample without inoculation. **(b)** Soil nutrient levels, the content of available phosphorus (P), potassium (K) and alkaline-hydrolyzable nitrogen (N) in the soil on Day 40. **(c)** A heatmap analysis of the impact of each strain on these parameters.

untreated control. By Day 30, significant differences emerged, with the N3P41K9 group exhibiting the most remarkable increases in plant height (41.8 ± 15.9%) and root length (61.7 ± 19.9%) over the untreated control. The strain MP41 followed, enhancing plant height by 33.7 ± 9.0%, and the strain PK9 notably increased root length by 40.9 ± 9.8%. The impact of MN3, WZF, and PGA microbial agents was comparable, in contrast to BSW, which had a minimal effect. These results suggested that phosphorus-solubilizing bacteria potentially foster root elongation. By Day 40, the microbial treatment showed a discernible impact, with carrot plant height increasing by 17.0 ± 4.8 to 20.7 ± 6.8% and root fresh weight escalating substantially from 137.0 ± 17.8 to 156.1 ± 18.4%. Notably, the consortium N3P41K9 matched the efficacy of commercial microbial agent products. Upon soil sampling and physicochemical analysis after Day 40, it was observed that the application of N3P41K9 resulted in a significant increase in available K by 23.7 ± 2.4%. However, its impact on the availability of P and alkaline-hydrolyzable N in soil was less pronounced compared to commercial microbial products, particularly PGA (Figure 3b and Supplementary Table 3). The PGA, containing multiple strains known for their abilities in P and K solubilization and N fixation, showed a notable increase in available P by 117.9 ± 14.4% and in available K by 20.8 ± 2.7%. Significant increases in phosphatase (from 12.3 ± 3.7 to 44.6 ± 6.6%) and sucrase activity (from 28.3 ± 10.6 to 88.5 ± 12.9%) were observed compared to the control (Figure 3b). The WZF, BSW and PGA groups exhibited the highest phosphatase activity, followed by the N3P41K9 and MP41. In contrast, single strain MN3 and the microbial agent BSW substantially increased sucrase activity by 70.6 ± 10.9 and 88.5 ± 12.9%, respectively. The urease content was increased in all treatment groups compared to the control, except for the WZF. Among them, BSW showed the highest increase, followed by the N3P41K9.

Collectively, these results demonstrated that the microbial consortium N3P41K9 was not only more effective in promoting early carrot growth than individual strains, but also rivals the performance of commercial microbial fertilizers. In terms of soil properties, the consortium N3P41K9 was comparable to the commercial microbial agent PGA, and slightly lower than BSW. The impact of the microbial consortium still requires further validation through field experiments.

3.4 Effects of microbial consortium N3P41K9 in the field experiments

Furthermore, we validated the effect of the combined microbial consortium N3P41K9 on carrot growth in field trials compared

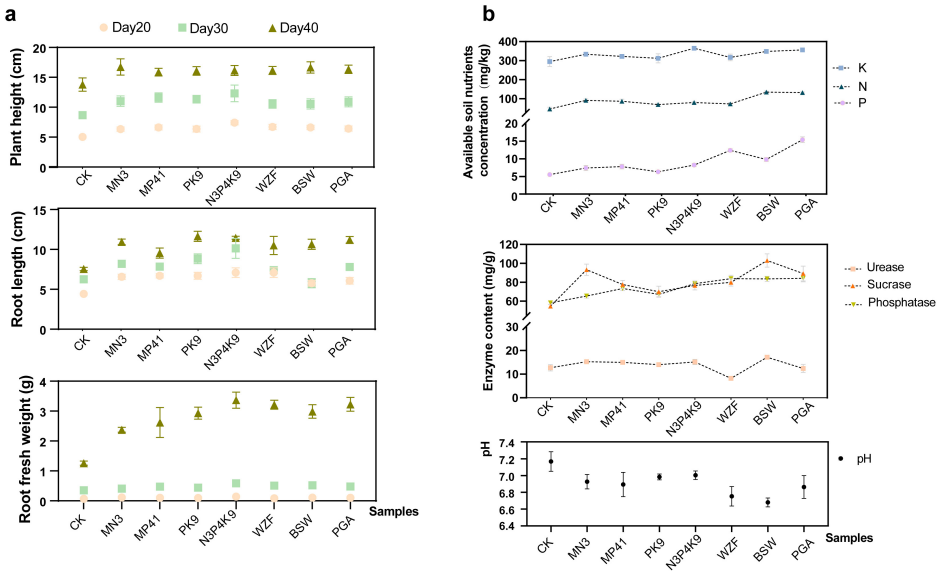


FIGURE 3
Effect of combined microbial consortium N3P41K9 on the pot experiment's carrot growth and soil nutrients. **(a)** Growth metrics for carrots, including plant height, root length, and root fresh weight were recorded on Day 20, 30, 40, respectively. **(b)** Soil nutrient levels, including the content of available P, K, and alkaline-hydrolyzable N, as well as the enzyme contents and the soil pH on Day 40. CK represents the blank control without inoculation. The sample inoculated with a single strain of MN3/MP41/PK9 was used as the negative control, while the samples inoculated with commercial fertilizers, like WZF, BSW, and PGA, were used as the positive control.

to commercially available microbial agents, WZF, BSW, and PGA. Concurrently, we investigated the efficacy of co-applying microbial agents in conjunction with an optimized chemical fertilizer regimen, designated as OPT, which was customized by farmers and the treatments were categorized into groups: OPT+N3P41K9, OPT+WZF, OPT+BSW, OPT+PGA. After fertilizing, the carrot growth indicators, and post-harvest soil physicochemical properties were assessed at four distinct developmental stages: the seedling emergence stage (Day 20), the rosette stage (Day 40), the expansion stage (Day 80), and the harvest stage (Day 100). Figure 4a reflects the growth status of carrots under different treatments at various sampling time points. The growth indicators measured at different stages (Figure 4b and Supplementary Table 4) indicated that the exclusive application of microbial agents significantly enhanced carrot plant height by 2.7 ± 2.8 to 20.3 ± 8.9%, root length by 8.1 ± 12.7 to 26.7 ± 6.0%, and fresh root weight by 3.7 ± 15.2 to 82.2 ± 55.4%. The co-application of chemical fertilizers and microbial agents yielded even more pronounced results, with an increase in fresh root weight ranging from 6.1 ± 13.2 to 151.7 ± 109.4%. Notably, the standalone use of N3P41K9 showed a significant advantage in promoting root elongation; in terms of fresh root weight, its performance was comparable to that of WZF but did not match up to PGA. The combined application of N3P41K9 with OPT exhibited a significant advantage in both root length and fresh weight, exceeding the combination of OPT + WZF. In comparison to the control, the application of microbial fertilizer led to a significant increase in the levels of available P and K, and alkaline-hydrolyzable N, with N3P41K9 showing increases of 25.2 ± 5.2, 27.0 ± 1.5, and 43.2 ± 4.5%, respectively (Figure 4c). The use of N3P41K9 also enhanced the soil's urease, sucrase, and phosphatase content, with increases of 61.3 ± 17.4, 48.9 ± 4.9, and 14.0 ± 4.0%, respectively, without causing a significant drop in soil pH. It is noteworthy that the N3P41K9 treatment outperformed the WZF treatment in terms of alkaline-hydrolyzable N, urease, sucrase, and phosphatase content. These results suggest that the composite microbial consortium developed in this study is competitive with the commercially available microbial agent WZF, slightly less effective than PGA, but markedly superior to BSW.

3.5 Effect of combined microbial consortium N3P41K9 on soil bacterial community

The diversity and composition of the soil bacterial communities from the treatment of consortium N3P41K9 were collected after the harvest of carrots and analyzed based on high-throughput sequencing. It showed that whether it was the application of microbial agents, chemical fertilizers, or the combined use of both, there was a certain impact and fluctuation on the structure and quantity of the soil microbial community. A total of 5,449 OTUs were found across all the samples, and they shared 984 OTUs (Figure 5a). The NMDS result showed a distinct difference in bacterial community composition among the six groups with a stress of 0.0518 (Supplementary Figure 4). The N3P41K9 group showed the closest relation with the CK group and OPT+WZF group. The chemical fertilizer-used groups (OPT, OPT+N3P41K9, OPT+WZF) were separated from the other microbial fertilizer-used groups on the MDS1 dimension. Besides, The WZF and OPT groups are most closely related on the MDS2 dimension. ANOSIM confirmed further the significant difference (R = 0.65, p = 0.001). The bacterial community diversity represented by the Shannon

10.3389/fmicb.2024.1466300

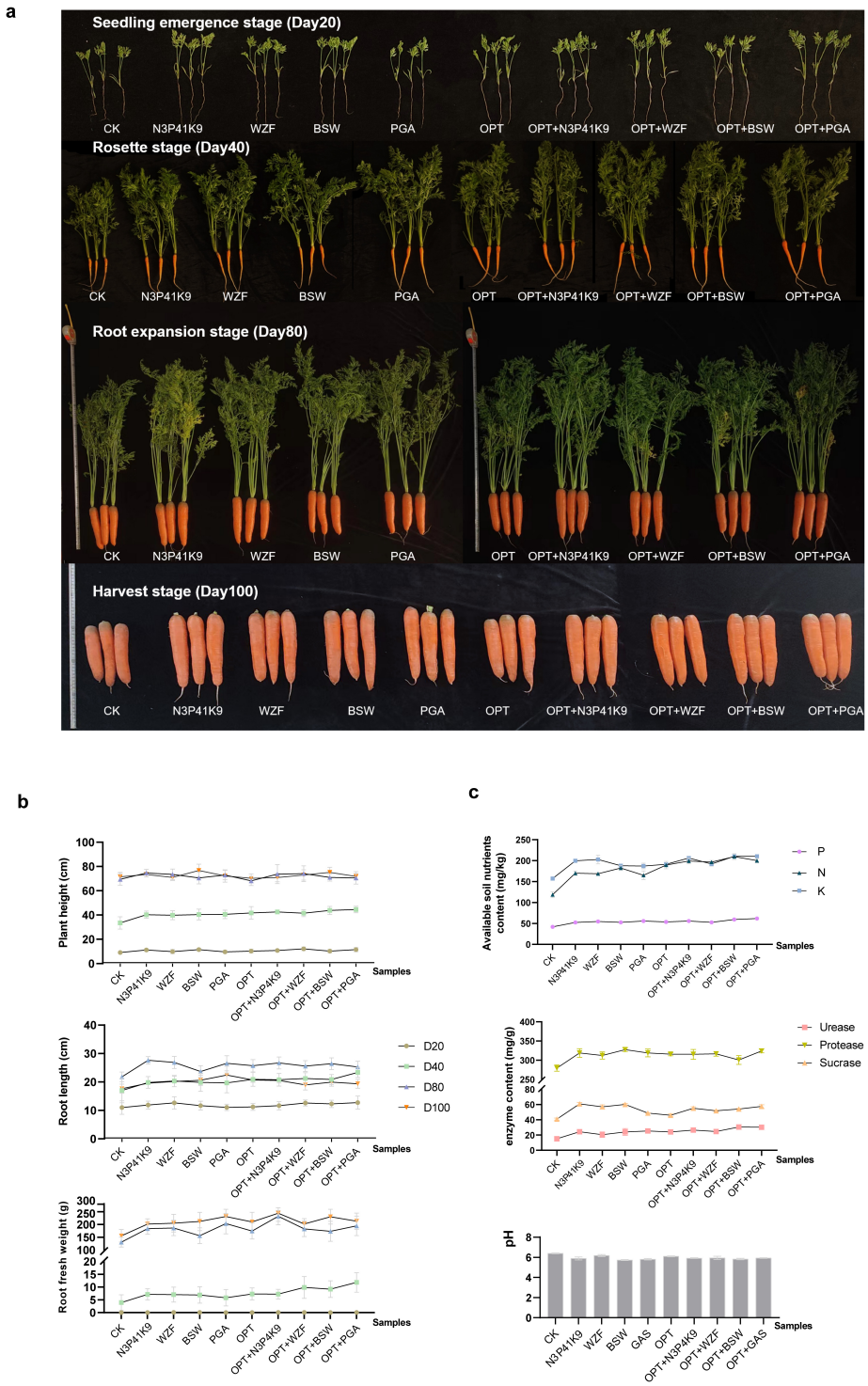


FIGURE 4
Effect of combined microbial consortium N3P41K9 on the carrot growth and soil nutrients in the field trial. **(a)** Growth morphology of the carrots at different stages under different treatments. **(b)** Growth metrics for carrots, including plant height, root length, and root fresh weight were recorded on Day 20, 40, 80, 100, respectively. **(c)** Soil nutrient levels, including the content of available P, K and alkaline-hydrolyzable N, as well as the enzyme contents and the soil pH on Day 100. CK represents the blank control without inoculation. OPT stands for optimized chemical fertilizer regime used by the farmers. The samples inoculated with commercial fertilizers, like WZF, BSW, and PGA, were used as the positive control.

indexes was significantly lower in fertilizer-used groups than in other treatments (Figure 5b).

At the phylum level (Figure 5c), compared to the control group CK, all the treatment groups mainly altered the proportions of the Actinobacteriota, Gemmatimonadota, Chloroflexi, Crenarchaeota, and Nitrospirota. Among them, the group using only chemical fertilizers (OPT) significantly increased the proportion of Crenarchaeota. The application of the microbial agent N3P41K9

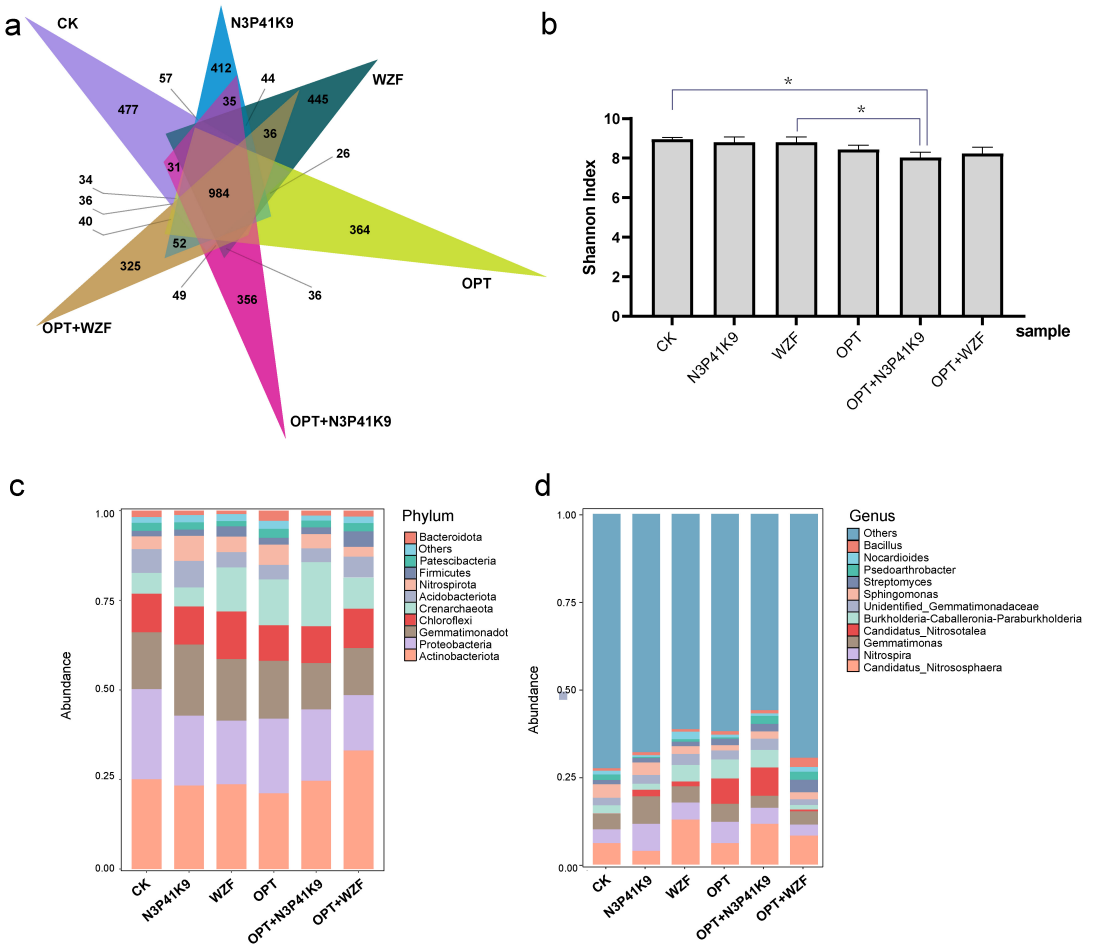


FIGURE 5
Composition of rhizosphere microbial community. **(a)** The Venn diagram shows the unique and shared core microbiomes among six groups. **(b)** Shannon index of the microbial community of different groups. Asterisks denote significance (*$p < 0.05$). The stacking diagram reflects the impact of the microbial fertilizers on the relative abundance of the bacterial communities in the rhizosphere soils, at the phylum level **(c)** and the genus level **(d)**. The top 10 bacterial phyla and top 11 bacterial genera with relative abundance > 1% are displayed.

increased the proportion of Gemmatimonadota, while the WZF group mainly increased the proportion of Crenarchaeota and decreased the proportion of Proteobacteria. The combination of chemical fertilizer and microbial agents, OPT+N3P41K9, significantly increased Crenarchaeota, while OPT+WZF significantly increased the proportion of Actinobacteriota. At the genus level (Figure 5d), compared to the control group CK, all treatment groups increased the genus *Candidatus* Nitrosotalea. In addition, a single use of N3P41K9 was able to increase the proportions of *Nitrospira* and *Gemmatimonas*, and a single use of WZF had a significant impact on the soil, notably increasing the proportion of Candidatus Nitrososphaera. The application of the chemical fertilizer OPT significantly led to an increase in *Candidatus* Nitrosotalea in the soil. Compared with the control OPT, the combination of OPT+ N3P41K9 mainly caused an increase in *Candidatus* Nitrososphaera, while OPT+WZF showed a significant difference in the impact on soil microbial communities. It can be seen that the application of microbial agents alone had the least overall impact on the balance of soil microbial communities. Particularly, N3P41K9 showed a relatively stable characteristic when used alone or in combination with chemical fertilizers, resulting in minimal fluctuations in the soil microbial community. However, WZF caused greater microbial community fluctuations, especially when used in combination with chemical fertilizers.

3.6 Relationships between soil properties and microbial communities

The structure and composition of the soil microbial community are closely linked to soil's physical and chemical properties. Redundancy analysis (RDA) (Figure 6) showed that the soil properties had a significant impact on the soil microbial community structure. Environmental factors on the first ordination axis explained 24.21% of the observed variations, and the second ordination axis explained 17.36%. Among the soil properties, the available K showed the strongest effect, followed by the alkaline-hydrolyzable N and available P. Among the abundance of bacterial genera, *Candidatus* Nitrososphaera showed a certain positive correlation with the alkaline-hydrolyzable N level, and *Nocardioides* was closely correlated with the soil's available K content. Other bacterial genera, such as *Sphingomonas*, *Candidatus*

Solibacter, *Haliangium*, and *Pseudarthrobacter* exhibited a correlation with soil pH, which played a key role in the bacterial community distribution.

4 Discussion

4.1 Effect of the PSB strains screened from the rhizosphere of carrot

Phosphorus is the second most important macronutrient necessary for plants, after N. P compounds are involved in various physiological and biochemical reactions (Timofeeva et al., 2022). PSB are found in most soils and are estimated to account for 40% of the culturable microbial population (Bakki et al., 2024). In this study, the majority of the microorganisms isolated from the rhizosphere of the carrot were capable of phosphorus-solubilizing ability, indicating the importance of rhizosphere PSB for the growth of carrots. 12 PSB strains isolated in this study belonged to the genera of *Acinetobacter* (7 strains), *Pseudomonas* (3 strains), and *Bacillus* (2 strains). Both *Pseudomonas* and *Bacillus*, recognized as well-documented PGPR, have been reported to be powerful phosphate solubilizers (Ullah et al., 2022; Bouizgarne et al., 2023; Janati et al., 2023; Bakki et al., 2024). The beneficial effects of *Pseudomonas* species, including phosphate solubilization, phytohormones production, and the biosynthesis of antifungal and antibacterial agents, positively influence plant size or fruit yield (Yahya et al., 2021; Wang Z. et al., 2022). Strains of *Bacillus* could stimulate plant growth promotion through the production of auxins or by enhancing the availability and uptake of P (Wang Z. et al., 2022; Bakki et al., 2024). Recently, many studies on PGPR have uncovered that certain PSB strains belong to *Acinetobacter*, such as *A. calcoaceticus* (Ren et al., 2013), *A. rhizosphaerae* (Gulati et al., 2009), and *A. pittii* (He and Wan, 2021; Zhao et al., 2023). The soil sequencing in this study also revealed that the most abundant microorganisms in carrot soil samples belonged to the phylum of Acinetobacteriota (Figure 5a). The phosphate solubilization ability of PSB has been approved to improve seed germination of carrot (Fiodor et al., 2023), and enhance salinity stress during carrot growth (Yadav et al., 2021).

The release of insoluble phosphates in the soil is slow and is regulated by several factors, particularly the soil pH (Devau et al., 2009). Most PSB strains produce indole-3-acetic acid (IAA) and low molecular weight organic acids, creating an acidic pH, which is essential for phosphate solubilization (Patel et al., 2011; Alori et al., 2017). Based on the liquid P dissolution experiment, it was found that for most PBS strains selected in this study, the pH of the medium dropped to the lowest on the 2nd day of cultivation, and the highest P solubilization effect was achieved on the 4th day (Figure 1b). Subsequently, the dissolved P was metabolized by the strain, resulting in an increase in pH and a decrease in the available P content (Figure 1b). Therefore, this feature makes it possible to combine PSB with mineral and organic P, which can increase the efficiency of chemical fertilizers (Duarah et al., 2011; Chen Y. et al., 2021). In addition, PSB can also enhance the efficiency of N fixation (Gupta et al., 2021; Timofeeva et al., 2022), which provides a strategy for the combined use of different functional strains, as well as the co-application of microbial and chemical fertilizers.

Additionally, it is worth noticing that the distribution of PSB has an obvious rhizosphere effect, which means the number and activity of PSB in rhizosphere soils were much higher than those in non-rhizosphere soils (Patel et al., 2011; Li et al., 2019). Also, the phosphatase activity was found much higher in rhizosphere soils than in non-rhizosphere soils (Pan and Cai, 2023). Furthermore, PSB can alter the soil microbial community to increase the P content and related enzyme activity in the soil. This rhizosphere effect is crucial for the construction of PSB communities, which in turn significantly impacts soil processes and enhances crop growth and yield (Pan and Cai, 2023).

4.2 Effect of the NFB strain screened from the rhizosphere of carrot

In this study, a rapidly growing strain *B. firmus* MN3 was identified from four NFBs, consistent with previous research that demonstrated the difficulty of isolating NFB from the rhizosphere of non-leguminous plants (Lodeiro, 2015). Studies have shown that NFB strains not only significantly increase plant yields and improve soil fertility, but also affect soil microbial community structure (Stajković-Srbinović et al., 2017). The natural rhizospheric association of *Klebsiella terrigena* E6 and *B. firmus* E3 was reported to have fixed active molecular nitrogen at an effective rate (Zlotnikov et al., 2007). Genome analysis demonstrated that *B. firmus* strain TNAU1 harbors multiple genes related to N fixation (Settu et al., 2024). It has been found that N absorption by the plant could promote the simultaneous absorption of P and K, thus promoting seedling growth (Shi et al., 2023). Also, previously reported effects of strain *B. firmus* SW5 was shown to enhance the uptake of P and K in soybean plants under saline stress (El-Esawi et al., 2018). Similarly, the single use of MN3 strain in this pot experiment was also found to significantly increase the content of soil-available alkaline-hydrolyzable N and P (Figure 3b). Meanwhile, it showed excellent traits in improving the carrot's root length and plant height (Figure 3a). Moreover, *B. firmus* has shown lethal effects against nematodes, as the toxins it produces can inhibit the hatching of nematode eggs (Ghahremani et al., 2020; Settu et al., 2024). This is significant for root vegetables like carrots, and it also had certain improvements in the morphology of the carrots when used in the combined microbial consortium N3P41K9 in this field trial (Figure 4a).

4.3 Effect of the KSB strain screened from the rhizosphere of carrot

Two KSB strains were identified in this study, *B. subtilis* PK9 and *P. polymyxa* MK31. *B. subtilis* is an important biological inoculant with multiple biological functions and multi-stress tolerance (Mehmood et al., 2021). For example, *B. subtilis* PM32 possesses several traits including IAA, phosphate, zinc, and K solubilization, N fixation, siderophore, and extracellular enzyme production, making it a potential biocontrol agent (Mehmood et al., 2021). Other *Bacillus*, such as *B. mucilaginosus* AS1153 (Liu et al., 2017), and *B. amyloliquefaciens* HSE-12 (Li et al., 2023), have also been found to have potassium-solubilizing abilities

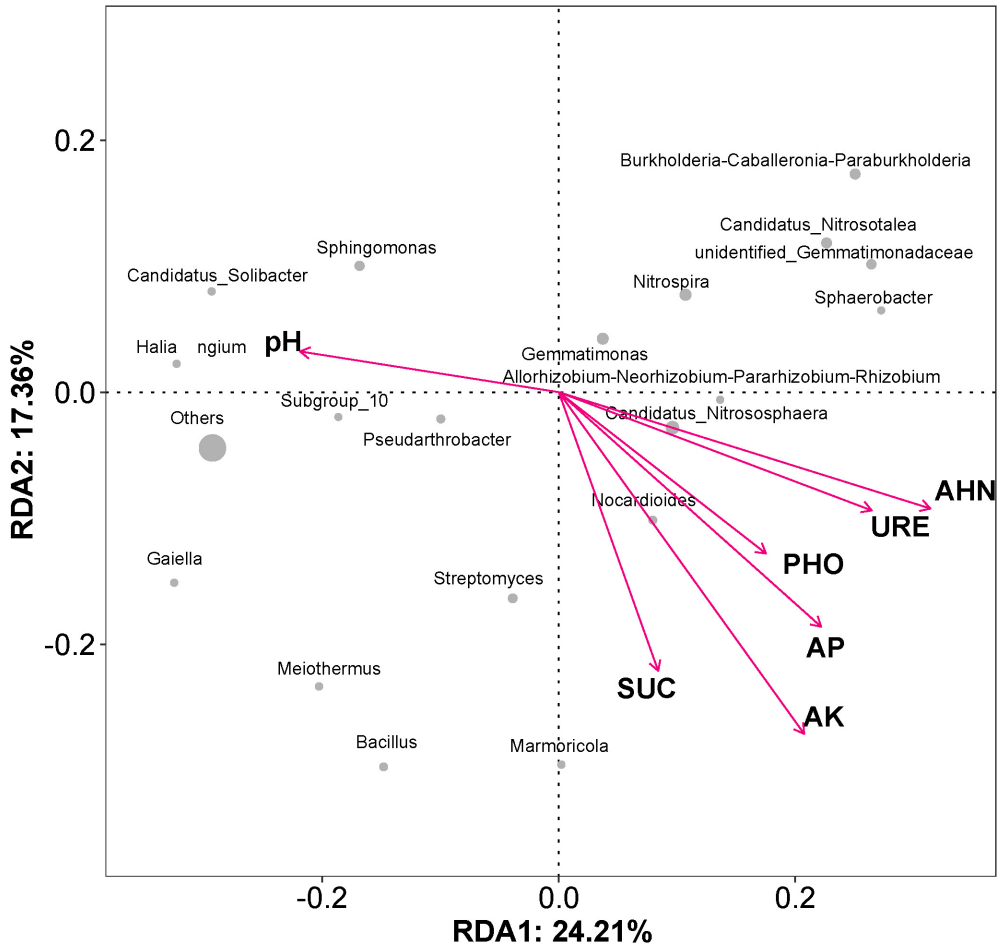


FIGURE 6
Redundancy analysis of the impacts of soil properties on rhizosphere bacterial community structure. The arrow length represents the intensity of the indicated environmental factor's influence on community changes. The angle between the arrow and the axis represents the correlation between the indicated environmental factor and the axis; smaller angles correspond to higher correlations. The distance between each sample point and arrow indicates the strength of the effect of that environmental factor on the sample. The location of a sample in the same direction as an arrow indicates a positive correlation between the environmental factor and changes in the microbial community; conversely, alignment in the opposite direction indicates a negative correlation. AP, available phosphorus; AK, available potassium; AHN, alkaline-hydrolyzable nitrogen; URE, urease; SUC, sucrase; PHO, phosphatase. The gray dots represent the abundance of the dominant genera.

and genes related to potassium-solubilizing have been studied in *B. aryabhattai* SK1-7as well (Chen Y. et al., 2021). However, *P. polymyxa* has been relatively less studied, but several strains have been proven to have potassium-solubilizing activity as well as the ability to control nematodes (El-Hadad et al., 2011; Sherpa et al., 2021). An increasing number of studies are exploring the possibility of KBS as a substitute for chemical K fertilizers (Anjanadevi et al., 2015). In this study, *B. subtilis* PK9 has a slightly better potassium-solubilizing effect than *P. polymyxa* MK31 (Figure 1c). Furthermore, PK9 showed a significant promoting effect on the root length and weight of carrots, compared to MN3 and MP41 (Figure 3a). This suggested that the PK9 strain served as an excellent PGPR. In the pot experiment, inoculation of PK9 did not enhance the available K in the soil compared to the control group (Figure 3b). It was previously reported the enhancement of plant K nutrition might be due to the stimulation of root growth or the elongation of root hairs by bacteria, Thus, no direct increase in the availability of soil solution K is expected (Meena et al., 2014).

4.4 Effect of the combined consortium N3P41K9

Considering the distinct advantages of the strains MN3, MP41, and PK9 in different functional aspects, we attempted to construct a microbial consortium to research the synergistic effect of the combined strains during carrot growth. There is a mutual promotion effect between bacteria with different characteristics among the heterogeneous microbes. For example, PSB can promote biological N fixation, production of phytohormones and various activities related to bio-control (Gupta et al., 2021; Timofeeva et al., 2022). Biofertilizers that contain NFB, PSB and KSB, have high potential for increasing the yield of crops and vegetables (Leaungvutiviroj et al., 2010; Kaur et al., 2024). Therefore, commercial microbial inoculants increasingly adopt the combination of multiple microbial cultures as a consortium, such as WZF, BSW, and PGA used in this study. Moreover, the PGPR can effectively control root-knot nematodes, which is particularly

crucial for root crops like carrots. In this study, the constructed consortium N3P41K9 showed better effects on carrot root length and weight as well as soil properties (available chemical elements content and activities of phosphatase, urease, and sucrase) than individual strains (Figures 3, 4), demonstrating additive effects, and its performance is comparable to, or even better than, the microbial fertilizers used commonly in practice. It was previously reported that microbial inoculants had a significant positive correlation with soil enzyme activities, which are involved in most of the biochemical reactions and beneficial to the stability of soil micro-ecosystem (Akhtar et al., 2018; An et al., 2022). Also, it was discovered that the carrot yield and soil properties in the treatment of OPT+N3P41K9 were significantly higher than in the other treatments when chemical fertilizer (OPT) and the best strains of bacteria N3P41K9 were applied simultaneously (Figure 4). This indicates that this treatment had the best effect on N, P, and K uptake and growth promotion of carrot roots.

Although a single inoculation event can enhance crop yields or improve soil properties, establishing long-term colonization of exogenous bacteria in the *in situ* soil remains a challenge (van Elsas et al., 2012). However, the advancement in microbial sequencing technology has enabled us to observe the changes in the soil microbial communities caused by exogenous microbial inoculation. It is worth mentioning that the microbial inoculant of N3P41K9 caused the least disturbance to the indigenous soil microbial community than the chemical fertilizer OPT or the WZF (Figure 5). The stability of soil microbial community diversity can be used to some extent as an indicator of soil ecosystem stability and health. Compared to the CK group, all other groups treated with microbial fertilizer, chemical fertilizer, or a combination of both, exhibited a decrease in final soil pH values. RDA at the genus level indicated that the pH and alkali-hydrolyzable N content played a key role in the bacterial community distribution. Concurrently, the abundance of the acidophilic ammonia-oxidizing archaea (AOA) *Candidatus* Nitrosotalea increased in all groups. AOA is believed to drive nitrification, with ammonia oxidation being the rate-limiting step of this process (Lehtovirta-Morley et al., 2014). AOA predominates in soils, exceeding bacteria by significant amounts, yet their physiology remains largely unknown due to the scarcity of cultivated strains (Lehtovirta-Morley et al., 2011; Lehtovirta-Morley et al., 2014; Herbold et al., 2017). pH and anoxia appear to be key factors regulating AOA community composition in soil (Herrmann et al., 2012). Furthermore, the increase in the abundance of this genus caused by the chemical fertilizer was significantly greater than that caused by microbial fertilizers (Figure 5b), indicating that the application of chemical fertilizer could significantly promote nitrification, which may lead to substantial fertilizer loss and atmospheric and groundwater pollution (Lehtovirta-Morley et al., 2011). Additionally, the beneficial bacterial genus *Gemmatimonas* was also significantly enriched in the field trial of the N3P41K9 group than other groups (Figure 5b). *Gemmatimonas* belongs to the phylum Gemmatimonadetes, which is known as one of the essential genera in phosphate dissolution (Lu et al., 2020). However, in the group OPT+N3P41K9, the increase in the abundance of this genus was minimal, indicating that the use of chemical fertilizer suppressed the enrichment of the PSB. Nocardioide was closely associated with available K content by the RDA, which may be due to the characteristic of Nocardioide that can withstand various low-nutrient conditions and concurrently degrade pollutants (Ma et al., 2023).

5 Conclusion

In this study, we investigated the impact of specific PGPR strains or consortium on carrot growth and its rhizosphere microbial community. However, unlike the traditional approach of directly using commercial microbial agents, we isolated multiple indigenous PGPR strains from the carrot rhizosphere and identified three highly efficient strains: MP41, MN3, and PK9, based on their exceptional abilities in P solubilization, N fixation, and K solubilization. These strains were strategically combined to form the microbial consortium N3P41K9, which exceeded the effects of single-strain inoculations in promoting carrot growth and amending soil quality in the pot experiment. Subsequent field trials confirmed the impact of the N3P41K9 consortium, resulting in a significant increase in carrot yields, and improved soil properties, comparable to the performance of commercial microbial fertilizers. Crucially, these benefits were achieved with minimal disruption to the soil's indigenous microbial community, while also enriching beneficial microbial populations. In addition, this study compared the fertilization practices commonly used by farmers, including chemical fertilizers and microbial fertilizers. The results highlight the potential of microbial consortium N3P41K9 as a beneficial microbial inoculant for the carrot rhizosphere, providing a sustainable alternative to reduce the use of chemical fertilizers. This approach can also be extended to other root crops with the aim of creating a network of PGPR, which will promote the development of demand-based sustainable agriculture.

Data availability statement

The data presented in this study are deposited in the NCBI repository, accession number PRJNA1161228. Further inquiries can be directed to the corresponding author.

Author contributions

LZ: Conceptualization, Methodology, Writing – original draft, Data curation, Project administration, Writing – review and editing. PZ: Data curation, Investigation, Methodology, Resources, Visualization, Writing – original draft. SM: Data curation, Methodology, Visualization, Writing – review and editing. QY: Data curation, Methodology, Visualization, Writing – review and editing. HW: Investigation, Resources, Writing – review and editing. YL: Investigation, Resources, Writing – review and editing. SY: Formal analysis, Resources, Writing – review and editing. YC: Funding acquisition, Project administration, Supervision, Writing – review and editing.

Funding

The authors declare that financial support was received for the research, authorship, and/or publication of this article. This work was financially supported by the National Science Foundation of Shandong Province (grant No. ZR2023MC110); study on fertilizer application performance in Shandong characteristic crop growing area (grant No. 20220045); and the central government guides local special plans for science and technology development (grant No. 22-1-3-7-zyyd-nsh).

Conflict of interest

LZ was employed by Rushan Hanwei Bio-Technical & Science CO., LTD.

The remaining authors declare that the research was conducted in the absence of any commercial or financial relationships that could be construed as a potential conflict of interest.

Publisher's note

All claims expressed in this article are solely those of the authors and do not necessarily represent those of their affiliated organizations, or those of the publisher, the editors and the reviewers. Any product that may be evaluated in this article, or claim that may be made by its manufacturer, is not guaranteed or endorsed by the publisher.

Supplementary material

The Supplementary Material for this article can be found online at: https://www.frontiersin.org/articles/10.3389/fmicb.2024.1466300/full#supplementary-material

References

Ahmed, M., Rauf, M., Mukhtar, Z., and Saeed, N. (2017). Excessive use of nitrogenous fertilizers: An unawareness causing serious threats to environment and human health. *Environ. Sci. Pollut. Res.* 24, 26983–26987. doi: 10.1007/s11356-017-0589-7

Akhtar, K., Weiyu, W., Guangxin, R., Khan, A., Yongzhong, F., and Gaihe, Y. (2018). Changes in soil enzymes, soil properties, and maize crop productivity under wheat straw mulching in Guanzhong, China. *Soil Tillage Res.* 182, 94–102. doi: 10.1016/j.still.2018.05.007

Alori, E. T., Glick, B. R., and Babalola, O. O. (2017). Microbial phosphorus solubilization and its potential for use in sustainable agriculture. *Front. Microbiol.* 8:971. doi: 10.3389/fmicb.2017.00971

An, X., Liu, J., Liu, X., Ma, C., and Zhang, Q. (2022). Optimizing phosphorus application rate and the mixed inoculation of arbuscular mycorrhizal fungi and phosphate-solubilizing bacteria can improve the phosphatase activity and organic acid content in Alfalfa soil. *Sustainability* 14, 11342–11342. doi: 10.3390/su141811342

Anjanadevi, I. P., John, N. S., John, K. J., Jeeva, M. L., and Misra, R. S. (2015). Rock inhabiting potassium solubilizing bacteria from Kerala, India: Characterization and possibility in chemical K fertilizer substitution. *J. Basic Microbiol.* 56, 67–77. doi: 10.1002/jobm.201500139

Azaroual, S. E., Hazzoumi, Z., Mernissi, N. E., Aasfar, A., Kadmiri, I. M., and Bouizgarne, B. (2020). Role of inorganic phosphate solubilizing bacilli isolated from moroccan phosphate rock mine and rhizosphere soils in wheat (Triticum aestivum L) phosphorus uptake. *Curr. Microbiol.* 77, 2391–2404. doi: 10.1007/s00284-020-02046-8

Backer, R., Rokem, J. S., Ilangumaran, G., Lamont, J. R., Praslickova, D., Ricci, E., et al. (2018). Plant growth-promoting rhizobacteria: Context, mechanisms of action, and roadmap to commercialization of biostimulants for sustainable agriculture. *Front. Plant Sci.* 9:1473. doi: 10.3389/fpls.2018.01473

Bakki, M., Banane, B., Marhane, O., Esmaeel, Q., Hatimi, A., Barka, E. A., et al. (2024). Phosphate solubilizing *Pseudomonas* and *Bacillus* combined with rock phosphates promoting tomato growth and reducing bacterial canker disease. *Front. Microbiol.* 15:1289466. doi: 10.3389/fmicb.2024.1289466

Bao, S. D. (2000). *Soil and Agricultural Chemistry Analysis*, 3rd Edn. Beijing: China Agricultural Press.

Basu, A., Prasad, P., Subha Narayan, D., Kalam, S., Sayyed, R. Z., Reddy, M. S., et al. (2021). Plant growth promoting rhizobacteria (PGPR) as green bioinoculants: Recent developments, constraints, and prospects. *Sustainability* 13:1140. doi: 10.3390/su13031140

Beneduzi, A., Ambrosini, A., and Passaglia, L. M. P. (2012). Plant growth-promoting rhizobacteria (PGPR): Their potential as antagonists and biocontrol agents. *Genet. Mol. Biol.* 35, 1044–1051. doi: 10.1590/s1415-47572012000600020

Bhardwaj, D. K., Ansari, M. W., Sahoo, R. K., and Tuteja, N. (2014). Biofertilizers function as key player in sustainable agriculture by improving soil fertility, plant tolerance and crop productivity. *Microb. Cell Fact.* 13:66. doi: 10.1186/1475-2859-13-66

Billah, M., Khan, M., Bano, A., Hassan, T. U., Munir, A., and Gurmani, A. R. (2019). Phosphorus and phosphate solubilizing bacteria: Keys for sustainable agriculture. *Geomicrobiol. J.* 36, 904–916. doi: 10.1080/01490451.2019.1654043

Bokulich, N. A., Subramanian, S., Faith, J. J., Gevers, D., Gordon, J. I., Knight, R., et al. (2013). Quality-filtering vastly improves diversity estimates from Illumina amplicon sequencing. *Nat. Methods* 10, 57–59. doi: 10.1038/nmeth.2276

Bouizgarne, B., Bakki, M., Boutasknit, A., Banane, B., El Ouarrat, H., Ait, et al. (2023). Phosphate and potash solubilizing bacteria from moroccan phosphate mine showing antagonism to bacterial canker agent and inducing effective tomato growth promotion. *Front. Plant Sci.* 14:970382. doi: 10.3389/fpls.2023.970382

Chen, J., Zhao, G., Wei, Y., Dong, Y., Hou, L., and Jiao, R. (2021). Isolation and screening of multifunctional phosphate solubilizing bacteria and its growth-promoting effect on Chinese fir seedlings. *Sci. Rep.* 11:9081. doi: 10.1038/s41598-021-88635-4

Chen, Y., Yang, H., Shen, Z., and Ye, J. (2021). Whole-genome sequencing and potassium-solubilizing mechanism of *Bacillus aryabhattai* SK1-7. *Front. Microbiol.* 12:722379. doi: 10.3389/fmicb.2021.722379

Devau, N., Cadre, E. L., Hinsinger, P., Jaillard, B., and Gérard, F. (2009). Soil pH controls the environmental availability of phosphorus: Experimental and mechanistic modelling approaches. *Appl. Geochem.* 24, 2163–2174. doi: 10.1016/j.apgeochem.2009.09.020

Duarah, I., Deka, M., Saikia, N., and Deka Boruah, H. P. (2011). Phosphate solubilizers enhance NPK fertilizer use efficiency in rice and legume cultivation. *3 Biotech* 1, 227–238. doi: 10.1007/s13205-011-0028-2

El-Esawi, M. A., Alaraidh, I. A., Alsahli, A. A., Alamri, S. A., Ali, H. M., and Alayafi, A. A. (2018). *Bacillus firmus* (SW5) augments salt tolerance in soybean (Glycine max L.) by modulating root system architecture, antioxidant defense systems and stress-responsive genes expression. *Plant Physiol. Biochem.* 132, 375–384. doi: 10.1016/j.plaphy.2018.09.026

El-Hadad, M. E., Mustafa, M. I., Selim, Sh, M., El-Tayeb, T. S., Mahgoob, A. E., et al. (2011). The nematicidal effect of some bacterial biofertilizers on Meloidogyne incognita in sandy soil. *Braz. J. Microbiol.* 42, 105–113. doi: 10.1590/s1517-83822011000100014

Feng, K., Cai, Z., Ding, T., Yan, H., Liu, X., and Zhang, Z. (2019). Effects of potassium-solubulizing and photosynthetic bacteria on tolerance to salt stress in maize. *J. Appl. Microbiol.* 126, 1530–1540. doi: 10.1111/jam.14220

Fiodor, A., Ajijah, N., Dziewit, L., and Pranaw, K. (2023). Biopriming of seed with plant growth-promoting bacteria for improved germination and seedling growth. *Front. Microbiol.* 14:1142966. doi: 10.3389/fmicb.2023.1142966

George, T. S., Giles, C. D., Menezes-Blackburn, D., Condron, L. M., Gama-Rodrigues, A. C., Jaisi, D. P., et al. (2017). Organic phosphorus in the terrestrial

environment: A perspective on the state of the art and future priorities. *Plant Soil* 427, 191–208. doi: 10.1007/s11104-017-3391-x

Ghahremani, Z., Escudero, N., Beltrán-Anadón, D., Saus, E., Cunquero, M., Andilla, J., et al. (2020). *Bacillus firmus* Strain I-1582, a nematode antagonist by itself and through the plant. *Front. Plant Sci.* 11:796. doi: 10.3389/fpls.2020.00796

Glick, B. R. (2014). Bacteria with ACC deaminase can promote plant growth and help to feed the world. *Microbiol. Res.* 169, 30–39. doi: 10.1016/j.micres.2013.09.009

Grover, M., Bodhankar, S., Sharma, A., Sharma, P. K., Singh, J., and Nain, L. (2021). PGPR mediated alterations in root traits: Way toward sustainable crop production. *Front. Sustainable Food Syst.* 4:618230. doi: 10.3389/fsufs.2020.618230

Gulati, A., Vyas, P., Rahi, P., and Kasana, R. C. (2009). Plant growth-promoting and rhizosphere-competent *Acinetobacter rhizosphaerae* strain BIHB 723 from the cold deserts of the himalayas. *Curr. Microbiol.* 58, 371–377. doi: 10.1007/s00284-008-9339-x

Gupta, R., Anshu, Noureldeen, A., and Darwish, H. (2021). Rhizosphere mediated growth enhancement using phosphate solubilizing rhizobacteria and their tri-calcium phosphate solubilization activity under pot culture assays in rice (Oryza sativa.). *Saudi J. Biol. Sci.* 28, 3692–3700. doi: 10.1016/j.sjbs.2021.05.052

Hanane, H., Brahim, B., Mohamed, H., Ahmed, L., Marie-Joëlle, V., and Yedir, O. (2008). Screening for rock phosphate solubilizing *Actinomycetes* from moroccan phosphate mines. *Appl. Soil Ecol.* 38, 12–19. doi: 10.1016/j.apsoil.2007.08.007

Hanif, M. K., Hameed, S., Imran, A., Naqqash, T., Shahid, M., and Van Elsas, J. D. (2015). Isolation and characterization of a β-propeller gene containing phosphobacterium *Bacillus subtilis* strain KPS-11 for growth promotion of potato (Solanum tuberosum L.). *Front. Microbiol.* 6:583. doi: 10.3389/fmicb.2015.00583

He, D., and Wan, W. (2021). Phosphate-solubilizing bacterium *Acinetobacter pittii* gp-1 affects rhizosphere bacterial community to alleviate soil phosphorus limitation for growth of soybean (Glycine max). *Front. Microbiol.* 12:737116. doi: 10.3389/fmicb.2021.737116

Herbold, C. W., Lehtovirta-Morley, L. E., Jung, M. Y., Jehmlich, N., Hausmann, B., Han, P., et al. (2017). Ammonia-oxidising archaea living at low pH: Insights from comparative genomics. *Environ. Microbiol.* 19, 4939–4952. doi: 10.1111/1462-2920.13971

Herrmann, M., Hädrich, A., and Küsel, K. (2012). Predominance of thaumarchaeal ammonia oxidizer abundance and transcriptional activity in an acidic fen. *Environ. Microbiol.* 14, 3013–3025. doi: 10.1111/j.1462-2920.2012.02882.x

Ibáñez, A., Diez-Galán, A., Cobos, R., Calvo-Peña, C., Barreiro, C., Medina-Turienzo, J., et al. (2021). Using rhizosphere phosphate solubilizing bacteria to improve barley (Hordeum vulgare) plant productivity. *Microorganisms* 9:1619. doi: 10.3390/microorganisms9081619

Janati, W., Bouabid, R., Mikou, K., Ghadraoui, L. E., and Errachidi, F. (2023). Phosphate solubilizing bacteria from soils with varying environmental conditions: Occurrence and function. *PLoS One* 18:e0289127. doi: 10.1371/journal.pone.0289127

Jiao, H., Wang, R., Qin, W., and Yang, J. (2024). Screening of rhizosphere nitrogen fixing, phosphorus and potassium solubilizing bacteria of Malus sieversii (Ldb.) Roem. and the effect on apple growth. *J. Plant Physiol.* 292, 154142. doi: 10.1016/j.jplph.2023.154142

Kálmán, C. D., Nagy, Z., Berényi, A., Kiss, E., and Posta, K. (2023). Investigating PGPR bacteria for their competence to protect hybrid maize from the factor drought stress. *Cereal Res. Commun.* 52, 129–150. doi: 10.1007/s42976-023-00388-0

Kaur, T., Devi, R., Negi, R., Kumar, S., Singh, S., Rustagi, S., et al. (2024). Microbial consortium with multifunctional attributes for the plant growth of eggplant (Solanum melongena L.). *Folia Microbiol.* 69, 1255–1266. doi: 10.1007/s12223-024-01168-x

Kochian, L. V. (2012). Plant nutrition: Rooting for more phosphorus. *Nature* 488, 466–467. doi: 10.1038/488466a

Kumar, M., Giri, V. P., Pandey, S., Gupta, A., Patel, M. K., Bajpai, A. B., et al. (2021). Plant-growth-promoting rhizobacteria emerging as an effective bioinoculant to improve the growth, production, and stress tolerance of vegetable crops. *Int. J. Mol. Sci.* 22:12245. doi: 10.3390/ijms222212245

Yadav, K. V., Krishna Jha, R., Kaushik, P., Altalayan, F. H., Al Balawi, T., and Alam, P. (2021). Traversing arbuscular mycorrhizal fungi and *Pseudomonas fluorescens* for carrot production under salinity. *Saudi J. Biol. Sci.* 28, 4217–4223. doi: 10.1016/j.sjbs.2021.06.025

Kuzmicheva, Y. V., Shaposhnikov, A. I., Petrova, S. N., Makarova, N. M., Tychinskaya, I. L., Puhalsky, J. V., et al. (2017). Variety specific relationships between effects of rhizobacteria on root exudation, growth and nutrient uptake of soybean. *Plant Soil* 419, 83–96. doi: 10.1007/s11104-017-3320-z

Leaungvutiviroj, C., Ruangphisarn, P., Hansanimitkul, P., Shinkawa, H., and Sasaki, K. (2010). Development of a new biofertilizer with a high capacity for N2 fixation, phosphate and potassium solubilization and auxin production. *Biosci. Biotechnol. Biochem.* 74, 1098–1101. doi: 10.1271/bbb.90898

Lehtovirta-Morley, L. E., Ge, C., Ross, J., Yao, H., Nicol, G. W., and Prosser, J. I. (2014). Characterisation of terrestrial acidophilic archaeal ammonia oxidisers and their inhibition and stimulation by organic compounds. *FEMS Microbiol. Ecol.* 89, 542–552. doi: 10.1111/1574-6941.12353

Lehtovirta-Morley, L. E., Stoecker, K., Vilcinskas, A., Prosser, J. I., and Nicol, G. W. (2011). Cultivation of an obligate acidophilic ammonia oxidizer from a nitrifying acid soil. *Proc. Natl. Acad. Sci. U S A.* 108, 15892–15897. doi: 10.1073/pnas.1107196108

Li, H., Li, C., Song, X., Li, J. T., Zhang, Q., Sun, F., et al. (2023). Isolation and identification of antagonistic *Bacillus amyloliquefaciens* HSE-12 and its effects on peanut growth and rhizosphere microbial community. *Front. Microbiol.* 14:1274346. doi: 10.3389/fmicb.2023.1274346

Li, H., Su, J. Q., Yang, X. R., and Zhu, Y. G. (2019). Distinct rhizosphere effect on active and total bacterial communities in paddy soils. *Sci. Total Environ.* 649, 422–430. doi: 10.1016/j.scitotenv.2018.08.373

Liang, J. L., Liu, J., Jia, P., Yang, T. T., Zeng, Q. W., Zhang, S. C., et al. (2020). Novel phosphate-solubilizing bacteria enhance soil phosphorus cycling following ecological restoration of land degraded by mining. *Isme J.* 14, 1600–1613. doi: 10.1038/s41396-020-0632-4

Liu, D., Lian, B., and Dong, H. (2012). Isolation of *Paenibacillu* ssp. and sssessment of its potential for enhancing mineral weathering. *Geomicrobiol. J.* 29, 413–421. doi: 10.1080/01490451.2011.576602

Liu, S., Tang, W., Yang, F., Meng, J., Chen, W., and Li, X. (2017). Influence of biochar application on potassium-solubilizing *Bacillus mucilaginosus* as potential biofertilizer. *Prep. Biochem. Biotechnol.* 47, 32–37. doi: 10.1080/10826068.2016.1155062

Lodeiro, A. R. (2015). Queries related to the technology of soybean seed inoculation with *Bradyrhizobium spp*. *Rev. Argent Microbiol.* 47, 261–273. doi: 10.1016/j.ram.2015.06.006

Lu, H., Wu, Y., Liang, P., Song, Q., Zhang, H., Wu, J., et al. (2020). Alkaline amendments improve the health of soils degraded by metal contamination and acidification: Crop performance and soil bacterial community responses. *Chemosphere* 257:127309. doi: 10.1016/j.chemosphere.2020.127309

Ma, Y., Wang, J., Liu, Y., Wang, X., Zhang, B., Zhang, W., et al. (2023). Nocardioides: "Specialists" for hard-to-degrade pollutants in the environment. *Molecules* 28:7433. doi: 10.3390/molecules28217433

Meena, V. S., Maurya, B. R., and Verma, J. P. (2014). Does a rhizospheric microorganism enhance K? availability in agricultural soils? *Microbiol. Res.* 169, 337–347. doi: 10.1016/j.micres.2013.09.003

Mehmood, S., Muneer, M. A., Tahir, M., Javed, M. T., Mahmood, T., Afridi, M. S., et al. (2021). Deciphering distinct biological control and growth promoting potential of multi-stress tolerant *Bacillus subtilis* PM32 for potato stem canker. *Physiol. Mol. Biol. Plants* 27, 2101–2114. doi: 10.1007/s12298-021-01067-2

Miao, F., Li, Y., Cui, S., Jagadamma, S., Yang, G., and Zhang, Q. (2019). Soil extracellular enzyme activities under long-term fertilization management in the croplands of China: A meta-analysis. *Nutrient Cycling Agroecosyst.* 114, 125–138. doi: 10.1007/s10705-019-09991-2

Muthuraja, R., and Muthukumar, T. (2022). Co-inoculation of halotolerant potassium solubilizing *Bacillus licheniformis* and *Aspergillus violaceofuscus* improves tomato growth and potassium uptake in different soil types under salinity. *Chemosphere* 294:133718. doi: 10.1016/j.chemosphere.2022.133718

Narendra Babu, A., Jogaiah, S., Ito, S., Kestur Nagaraj, A., and Tran, L. S. (2015). Improvement of growth, fruit weight and early blight disease protection of tomato plants by rhizosphere bacteria is correlated with their beneficial traits and induced biosynthesis of antioxidant peroxidase and polyphenol oxidase. *Plant Sci.* 231, 62–73. doi: 10.1016/j.plantsci.2014.11.006

Nawaz, A., Shahbaz, M., Asadullah, Imran, A., Marghoob, M. U., Imtiaz, M., et al. (2020). Potential of salt tolerant PGPR in growth and yield augmentation of wheat (Triticum aestivum L.) under saline conditions. *Front. Microbiol.* 11:2019. doi: 10.3389/fmicb.2020.02019

Pan, L., and Cai, B. (2023). Phosphate-solubilizing bacteria: Advances in their physiology, molecular mechanisms and microbial community effects. *Microorganisms* 11:2904. doi: 10.3390/microorganisms11122904

Patel, D. K., Murawala, P., Archana, G., and Kumar, G. N. (2011). Repression of mineral phosphate solubilizing phenotype in the presence of weak organic acids in plant growth promoting fluorescent pseudomonads. *Bioresour. Technol.* 102, 3055–3061. doi: 10.1016/j.biortech.2010.10.041

Pérez-Jaramillo, J. E., Mendes, R., and Raaijmakers, J. M. (2016). Impact of plant domestication on rhizosphere microbiome assembly and functions. *Plant Mol. Biol.* 90, 635–644. doi: 10.1007/s11103-015-0337-7

Powers, S. M., Bruulsema, T. W., Tim, B., Chan, N. L., Elser, J. J., Haygarth, P. M., et al. (2016). Long-term accumulation and transport of anthropogenic phosphorus in three river basins. *Nat. Geosci.* 9, 353–356. doi: 10.1038/ngeo2693

Rahman, K. M. A., and Dunfu, Z. (2018). Effects of Fertilizer Broadcasting on the Excessive Use of inorganic fertilizers and environmental sustainability. *Sustainability* 10:759. doi: 10.3390/su10030759

Raji, M., and Thangavelu, M. (2021). Isolation and screening of potassium solubilizing bacteria from saxicolous habitat and their impact on tomato growth in different soil types. *Arch. Microbiol.* 203, 3147–3161. doi: 10.1007/s00203-021-02284-9

Ren, Y. X., Zhu, X. L., Fan, D. D., Ma, P., and Liang, L. H. (2013). Inoculation of phosphate solubilizing bacteria for the improvement of lead accumulation by *Brassica juncea*. *Environ. Technol.* 34, 463–469. doi: 10.1080/09593330.2012.701234

Rodríguez, H., and Vidal, R. F. (1999). Phosphate solubilizing bacteria and their role in plant growth promotion. *Biotechnol. Adv.* 17, 319–339. doi: 10.1016/s0734-9750(99)00014-2

Saha, S., Mina, B. L., Gopinath, K. A., Kundu, S., and Gupta, H. S. (2008). Relative changes in phosphatase activities as influenced by source and application rate of organic composts in field crops. *Bioresour. Technol.* 99, 1750–1757. doi: 10.1016/j.biortech.2007.03.049

Sangoquiza-Caiza, C. A., Pincay-Verdezoto, A. K., Park, C. H., and Zambrano-Mendoza, J. L. (2023). Diversity of nitrogen-fixing and phosphorus-solubilizing bacteria associated with the rhizosphere of Andean maize in Ecuador. *Braz. J. Biol.* 83:e273632. doi: 10.1590/1519-6984.273632

Settu, V., Annaiyan, S., and Mannu, J. (2024). Revealing the genetic arsenal of *Bacillus firmus* TNAU1: Unleashing nematicidal and plant growth promotion traits. *Physiol. Mol. Plant Pathol.* 129:102177. doi: 10.1016/j.pmpp.2023.102177

Sherpa, M. T., Sharma, L., Bag, N., and Das, S. (2021). Isolation, Characterization, and evaluation of native rhizobacterial consortia developed from the rhizosphere of rice grown in organic state Sikkim, India, and their effect on plant growth. *Front. Microbiol.* 12:713660. doi: 10.3389/fmicb.2021.713660

Shi, Z., Guo, X., Lei, Z., Wang, Y., Yang, Z., Niu, J., et al. (2023). Screening of high-efficiency nitrogen-fixing bacteria from the traditional Chinese medicine plant Astragalus mongolicus and its effect on plant growth promotion and bacterial communities in the rhizosphere. *BMC Microbiol.* 23:292. doi: 10.1186/s12866-023-03026-1

Shultana, R., Zuan, A. T. K., Naher, U. A., Islam, A. K. M. M., Rana, M. M., Rashid, H., et al. (2022). The PGPR mechanisms of salt stress adaptation and plant growth promotion. *Agronomy* 12:2266. doi: 10.3390/agronomy12102266

Singh, A., Prasad, B., and Shah, S. (2011). Influence of phosphate solubilizing bacteria for enhancement of plant growth and seed yield in lentil. *J. Crop Weed* 7, 1–4.

Stajković-Srbinović, O., Delić, D., Nerandžić, B., Andjelović, S., Sikirić, B., Kuzmanović, D, et al. (2017). Alfalfa yield and nutrient uptake as influenced by co-inoculation with rhizobium and rhizobacteria. *Romanian Biotechnol. Lett.* 22, 12834–12841.

Tamura, K., Dudley, J., Nei, M., and Kumar, S. (2007). MEGA4: Molecular evolutionary genetics analysis (MEGA) software version 4.0. *Mol. Biol. Evol.* 24, 1596–1599. doi: 10.1093/molbev/msm092

Taurian, T., Anzuay, M. S., Ludueña, L. M., Angelini, J. G., Muñoz, V., Valetti, L., et al. (2013). Effects of single and co-inoculation with native phosphate solubilising strain *Pantoea sp J49* and the symbiotic nitrogen fixing bacterium *Bradyrhizobium sp SEMIA 6144* on peanut (*Arachis hypogaea* L.) growth. *Symbiosis* 59, 77–85. doi: 10.1007/s13199-012-0193-z

Timofeeva, A., Galyamova, M., and Sedykh, S. (2022). Prospects for using phosphate-solubilizing microorganisms as natural fertilizers in agriculture. *Plants* 11:2119. doi: 10.3390/plants11162119

Ullah, S., Bano, A., Asadullah, Shahidnd, M. A., and Khan, N. (2022). A comparative study of plant growth promoting rhizobacteria (PGPR) and sowing methods on nutrient availability in wheat and rhizosphere soil under salinity stress. *Rhizosphere* 23:100571. doi: 10.1016/j.rhisph.2022.100571

Valetti, L., Iriarte, L., and Fabra, A. (2018). Growth promotion of rapeseed (Brassica napus) associated with the inoculation of phosphate solubilizing bacteria. *Appl. Soil Ecol.* 132, 1–10. doi: 10.1016/j.apsoil.2018.08.017

van Elsas, J. D., Chiurazzi, M., Mallon, C. A., Elhottova, D., Kristufek, V., and Salles, J. F. (2012). Microbial diversity determines the invasion of soil by a bacterial pathogen. *Proc. Natl. Acad. Sci. U S A.* 109, 1159–1164. doi: 10.1073/pnas.1109326109

Wang, J., Li, R., Zhang, H., Wei, G., and Li, Z. (2020). Beneficial bacteria activate nutrients and promote wheat growth under conditions of reduced fertilizer application. *BMC Microbiol.* 20:38. doi: 10.1186/s12866-020-1708-z

Wang, S., Li, Y., Zhang, J., Wang, X., Hong, J., Qiu, C., et al. (2022). Transcriptome profiling analysis of phosphate-solubilizing mechanism of *Pseudomonas* Strain W134. *Microorganisms* 10:1998. doi: 10.3390/microorganisms10101998

Wang, Z., Xu, G., Ma, P., Lin, Y., Yang, X., and Cao, C. (2017). Isolation and characterization of a phosphorus-solubilizing bacterium from rhizosphere soils and its colonization of Chinese cabbage (*Brassica campestris ssp. chinensis*). *Front. Microbiol.* 8:1270. doi: 10.3389/fmicb.2017.01270

Wang, Z., Zhang, H., Liu, L., Li, S., Xie, J., Xue, X., et al. (2022). Screening of phosphate-solubilizing bacteria and their abilities of phosphorus solubilization and wheat growth promotion. *BMC Microbiol.* 22:296. doi: 10.1186/s12866-022-02715-7

Yahya, M., Islam, E. U., Rasul, M., Farooq, I., Mahreen, N., Tawab, A., et al. (2021). Differential root exudation and architecture for improved growth of wheat mediated by phosphate solubilizing bacteria. *Front. Microbiol.* 12:744094. doi: 10.3389/fmicb.2021.744094

Yi, X., Jin, L., Liao, D., Peng, G., Zheng, X., Xu, H., et al. (2023). Carrot and carotene and multiple health outcomes: An umbrella review of the evidence. *J. Sci. Food Agric.* 103, 2251–2261. doi: 10.1002/jsfa.12425

Zhang, Y., Gao, W., Ma, L., Luan, H., Tong, J., Li, R., et al. (2023). Long-term partial substitution of chemical fertilizer by organic amendments influences soil microbial functional diversity of phosphorus cycling and improves phosphorus availability in greenhouse vegetable production. *Agric. Ecosyst. Environ.* 341:108193. doi: 10.1016/j.agee.2022.108193

Zhao, R., Huang, L., Peng, X., Fan, L., Chen, S., Qin, P., et al. (2023). Effect of different amounts of fruit peel-based activator combined with phosphate-solubilizing bacteria on enhancing phytoextraction of Cd from farmland soil by ryegrass. *Environ. Pollut.* 316:120602. doi: 10.1016/j.envpol.2022.120602

Zlotnikov, A. K., Kazakov, M. L., Zlotnikov, K. M., Kazakov, A. V., and Umarov, M. M. (2007). Physiological and biochemical properties of the bacterial association of *Klebsiella terrigena* E6 and *Bacillus firmus* E3. *Prikl. Biokhim. Mikrobiol.* 43, 338–346. doi: 10.1134/s000368380703012x

frontiers | Frontiers in Microbiology

TYPE Original Research
PUBLISHED 16 December 2024
DOI 10.3389/fmicb.2024.1507798

Check for updates

OPEN ACCESS

EDITED BY
Brahim Bouizgarne,
Ibn Zohr University, Morocco

REVIEWED BY
Mohamed Ait-El-Mokhtar,
University of Hassan II Casablanca, Morocco
Ouahmane Lahcen,
Cadi Ayyad University, Morocco

*CORRESPONDENCE
Yongmei He
✉ heyongmei06@126.com
Fangdong Zhan
✉ zfd97@ynau.edu.cn

RECEIVED 08 October 2024
ACCEPTED 04 December 2024
PUBLISHED 16 December 2024

CITATION
Yang Y, Li Y, Li X, Yan J, Wu L, Tang Z, He Y and Zhan F (2024) Mycorrhizal extraradical mycelium can reduce cadmium uptake by maize and cadmium leaching from contaminated soil: based on an in-growth core experiment.
Front. Microbiol. 15:1507798.
doi: 10.3389/fmicb.2024.1507798

COPYRIGHT
© 2024 Yang, Li, Li, Yan, Wu, Tang, He and Zhan. This is an open-access article distributed under the terms of the Creative Commons Attribution License (CC BY). The use, distribution or reproduction in other forums is permitted, provided the original author(s) and the copyright owner(s) are credited and that the original publication in this journal is cited, in accordance with accepted academic practice. No use, distribution or reproduction is permitted which does not comply with these terms.

Mycorrhizal extraradical mycelium can reduce cadmium uptake by maize and cadmium leaching from contaminated soil: based on an in-growth core experiment

Yijie Yang[1], Yang Li[1], Xiaoyi Li[1], Jie Yan[1], Longhua Wu[2], Zhenwu Tang[3], Yongmei He[1]* and Fangdong Zhan[1]*

[1]College of Resources and Environment, Yunnan Agricultural University, Kunming, China, [2]Nanjing Institute of Soil Science, Chinese Academy of Sciences, Nanjing, China, [3]College of Resources and Environment, Southwest University, Chongqing, China

Arbuscular mycorrhizal fungi (AMF) are commonly found in heavy metal-contaminated environments and form extraradical mycelium (ERM), but knowledge of their ecological functions is limited. In the present study, a soil column was filled with sterilized cadmium (Cd)-contaminated soil and contained an in-growth core for AMF-inoculated maize seedling growth. The in-growth core was static to maintain or rotated to disrupt ERM growth. Compared with the static treatment, the rotation treatment caused significant decreases in the content of glomalin-related soil protein (GRSP), the photosynthetic physiology of leaves, and maize growth, while increasing the Cd content in shoots and roots by 64 and 82%, respectively; additionally, the rotation treatment resulted in increases in the Cd concentration of the soil solution inside and outside the growth core by 30–38 and 17–52%, respectively, and Cd leaching loss by 29–39%. Moreover, the rotation treatment significantly altered the Cd forms in the soil solution and leachate, increasing the proportion of free Cd^{2+} by 0.8–2.1% and decreasing the proportions of $CdSO_4$(aq) and $CdOH^+$ by 6.1–56.1% and 26.1–48.7%, respectively. The structural equation model indicated that AMF directly and indirectly reduced maize Cd uptake and Cd leaching loss by decreasing Cd availability in the soil and soil solution through the GRSP secreted by ERM. Thus, AMF plays a crucial role in inhibiting Cd migration in soil through mycelial exudates.

KEYWORDS

arbuscular mycorrhizal fungi, extraradical mycelium, ingrowth core, soil solution, cadmium form, leaching loss

1 Introduction

Heavy metal (HM) pollution in soil is currently one of the most prominent environmental problems (Mohammed et al., 2011). According to the National Soil Pollution Survey Bulletin, the area of HM-contaminated farmland accounts for 1/5 of the arable land (Zhao et al., 2015). Moreover, surface runoff and leaching under rainfall or irrigation conditions led to the downward migration of HMs such as cadmium (Cd) that accumulated in the soil surface layer, which in turn triggered Cd leaching loss and pollution diffusion into deeper soil and groundwater (Gray et al., 2017). Cd contamination in soil can induce adverse effects such as

soil degradation, reduced fertility, and hindered plant growth and development (Haider et al., 2021).

Cd migration from contaminated soil can be affected by soil microorganisms (NaziaTahir et al., 2021). Arbuscular mycorrhizal fungi (AMF) are crucial soil microorganisms that engage in symbiotic relationships with over 80% of terrestrial plants, offering beneficial effects on plant growth and Cd uptake (Riaz et al., 2021). AMF not only improved the physical and chemical properties of contaminated soil but also promoted nutrient and water uptake by the host plant and promoted plant performance under Cd stress (Kavadia et al., 2020; Ghobadi et al., 2020; Zhan et al., 2019). AMF colonizes plant roots and forms mycorrhizae, which can alleviate Cd toxicity in plants and inhibit Cd uptake by blocking Cd transfer from roots to shoots (Riaz et al., 2021). Moreover, AMF altered root growth, including root length and biomass, and consequently affected Cd transfer and uptake (Guo et al., 2023). Additionally, a large number of mycorrhizal extraradical mycelium (ERM) can bind to Cd ions through mycelial exudates, thus significantly impacting Cd migration in soil (Ferrol et al., 2016). ERM can bind Cd by secreting glomalin-related soil protein, which can increase Cd adsorption in soil and reduce Cd leaching loss (He et al., 2020; Gonzalez-Chavez et al., 2004). However, most of the related research has focused on the effects of AMF on plant growth by improving the uptake of nutrients and water under Cd stress (Yu et al., 2021; Chang et al., 2018). However, the understanding of the effects of ERM and its underlying mechanisms on Cd migration in soil is limited.

Some experimental devices have been developed to investigate ERM function. The in-growth core is a special experimental device consisting of a transparent container or tube that simulates the real growth environment of plants in soil and is usually used to study the effects of ERM on plant growth (Leifheit et al., 2014; Wu et al., 2016). The in-growth core can effectively separate the root and fungal mycelium via microporous mesh with a pore diameter of 20–50 μm to maintain internal root growth and allow the ERM to grow to the outside of the core. Furthermore, the in-growth core remained static to maintain or rotate to disrupt the growth of ERM outside the core. Previous studies revealed that the disruption of ERM by rotation of the in-growth core led to a decrease in the level of glomalin-related soil protein (GRSP) and a significant decrease in the growth and nutrient uptake of maize, suggesting that ERM is critical for plant growth (Wu et al., 2016; Liu et al., 2014).

In the present study, an in-growth core was developed according to the method of Johnson et al. (2001), and it was put into a soil column filled with sterilized Cd-contaminated soil. The in-growth core was static or rotated to maintain or disrupt ERM growth in the soil column. The effects of ERM on maize growth, the Cd concentration and form in the soil solution inside and outside the in-growth core, and the loss of Cd from the soil column were investigated. It was hypothesized that ERM plays a crucial role in inhibiting Cd uptake by plants and Cd leaching loss from soil by reducing the Cd concentration and form in soil solution.

2 Materials and methods

2.1 Materials

Soil samples were collected from Cd-contaminated farmland near the lead-zinc mining region in Huize County, Qujing City, Yunnan Province, China (latitude 26°31′10″N, longitude 103°34′56″E). After natural air-drying, the soil was sieved through a sieve with a pore diameter of 2 mm and autoclave sterilized at 120°C for 2 h. The physical and chemical properties of the soil are shown in Supplementary Table S1.

The AMF inoculant was *Funneliformis mosseae* (BGC YN05, 1511C0001BGCAM0013), which was provided by the Institute of Plant Nutrition and Resources, Beijing Academy of Agricultural and Forestry Sciences. The AMF inoculant contained approximately 18 spores per gram.

Seeds (variety of Huidan 4) of *Zea mays* L. were used in the present study. After surface disinfection with 75% ethanol (soaking for 1 min) and 10% sodium hypochlorite (soaking for 2 min), the maize seeds were placed in a constant temperature incubator at 28°C for 3 days to germinate into a 0.5–1 cm long seedling.

2.2 Experimental device

In the research, a soil column was filled with sterilized Cd-contaminated soil and contained an in-growth core for maize seedling growth (Supplementary Figure S1). The soil column was made of polyvinyl chloride (PVC) with a diameter of 110 mm and a height of 300 mm, and a drainage tap was installed at the bottom to drain the leachate. Within the soil column, an in-growth core with a diameter of 50 mm and a height of 240 mm was produced according to the method of Johnson et al. (2001). There were holes with a diameter of 3 cm around the in-growth core, which was covered by a nylon mesh of 400 mesh (37 μm) that allowed the ERM but prevented the root from passing through. Additionally, samplers were installed inside the in-growth core and the soil column at 10 and 20 cm depths for sampling the soil solution.

2.3 Experimental design

The sterilized soil in the in-growth core was planted with a maize seedling and inoculated with 50 g of AMF inoculant. The treatments included static (the in-growth core remained static to maintain ERM growth inside the soil column) and rotated (the in-growth core rotated every 3 days to disrupt ERM growth inside the soil column) treatments. Thus, there were 5 pots per treatment and 10 pots in total.

The experiment was carried out in a greenhouse. After the maize seedlings had grown to a height of 5 cm for 5 days, the in-growth core began to rotate every 3 days, rotating about 45° along the vertical axis to deter mycorrhizal extraradical mycelium (ERM) penetration into the core.

After 30 days of maize seedlings grown, 3 leaching events were conducted every 7 days on Days 31, 38, and 45. The soil column received 3 L of deionized water over 1 h at a drip irrigation rate of 50 mL/min. After irrigation, the soil solution was sampled from the inside and outside of the in-growth core at depths of 10 cm and 20 cm, respectively, in the soil column using a solution sampler (Rhizon 19.21.23F, Environment Purification Science and Technology Limited Company, Beijing, China). The leachate was collected through a drainage tap at the bottom of the soil column. Subsequently, the soil solution and leachate were filtered through a 0.45 μm membrane for subsequent analyses.

2.4 Evaluation of maize photosynthesis, height, and biomass traits

After 45 days of maize growth, plant height was measured with steel tape. The photosynthesis of the third leaf at the top of maize, including the photosynthetic rate, intercellular CO_2 concentration, and transpiration rate, was measured by a portable photosynthesis analyzer (LCpro T, ADC Bioscientific Ltd., Hoddesdon, UK). Fresh leaves (0.5 g) were weighed and placed in a centrifuge tube, ground with 80% ethanol solution to extract the chlorophyll, filtered through filter paper, and transferred to a 25 mL volumetric flask. The absorbance was measured at 645 nm and 663 nm via spectrophotometry, and the content of chlorophyll a and b in the leaves was calculated according to the formula (Porra et al., 1989).

After harvesting, the maize plants were divided into roots and shoots. These parts were initially subjected to 105°C for 30 min in an oven, then dried to a constant weight at 75°C, with their biomasses subsequently recorded.

2.5 Determination of the mycorrhizal colonization rate, spore number, and glomalin-related soil protein (GRSP) content

After the maize plants were harvested on Day 45, the soil adhering to the maize roots was collected as the rhizosphere soil. After the rhizosphere soil was kept indoors for 7 days and air-dried, a 20.0 g sample was weighed. Then, the AMF spores were separated by the wet sieving decantation-sucrose centrifugation method (Daniels and Skipper, 1982). The AMF spore number was counted via a stereomicroscope, and the number was calculated.

Moreover, 1.0 g of air-dried soil was weighed and placed into a centrifuge tube. The total glomalin-related soil protein (T-GRSP) was isolated from the soil using 8 mL of 50 mmol/L sodium citrate buffer (pH 8.0) at 121°C for 90 min, followed by centrifugation at 10,000 rpm for 6 min. This process was repeated 5 times. Similarly, the easily extractable glomalin-related soil protein (EE-GRSP) was obtained by treating the soil with 8 mL of 20 mmol/L citric acid buffer (pH 7.0) at 121°C for 30 min and centrifuging at 10,000 rpm for 6 min, also repeated 5 times. Finally, the supernatants were centrifuged again at 10,000 rpm for 10 min to obtain a new supernatant. Then, the concentrations of T-GRSP and EE-GRSP in the supernatant were determined by the Coomassie brilliant blue method, and the contents of T-GRSP and EE-GRSP in the rhizosphere soil were calculated (Wright and Upadhyaya, 1998).

After the maize roots were separated and cleaned thoroughly, some fibrous roots were sampled randomly and cut to approximately 1 cm in length for at least 80 segments. Then, these root segments were transferred into a tube with 10% (weight/volume) potassium hydroxide solution for dissociation at 90°C for 1 h in a water bath. At least 50 root segments were picked and placed on glass slides for staining with 0.1% acid fuchsin for 30 min and then destained with 50% lactoglycerin for 48 h. AMF colonization was observed under a microscope (Leica DM2000 LED, Leica Microsystems, Wetzlar, Germany), and the AMF colonization rate was calculated by the cross method (McGonigle et al., 1990).

2.6 Determination of cadmium contents in maize

Maize roots and shoots samples were crushed into powder smaller than 0.25 mm. A powder sample of 0.5 g was digested in 6 mL of nitric acid and 2 mL of perchloric acid into a transparent digestive liquid according to the wet digestion method and transferred into a volumetric bottle to a volume of 50 mL with distilled water. The Cd concentration in the solution was determined by a flame atomic absorption spectrophotometer (ICE-3000-SERIESThermo Scientific, Franklin, MA, USA). Then, the Cd content in maize was calculated according to the relevant formula. Cd uptake in maize (μg/plant) = biomass of maize (g/plant) × Cd content in maize (mg/kg).

2.7 Determination of cadmium availability and speciation in soil

Five grams of air-dried rhizosphere soil was weighed and placed into an Erlenmeyer flask (100 mL) filled with 0.01 mM $CaCl_2$ solution (25 mL). Then, the flask was shaken at 120 revolutions per minute (rpm) for 120 min and filtered using quantitative filter paper into a volumetric flask to a volume of 50 mL with distilled water. Finally, the Cd concentration in solution was determined by a flame atomic absorption spectrophotometer, and the Cd availability ($CaCl_2$-extracted) was calculated according to the relevant formula (Bao, 2000).

A 1.0 g of air-dried soil was used to determine the Cd speciation according to the Community Bureau of Reference (BCR) extraction method (Quevauviller et al., 1994). A 1.0 g soil sample was shaken at 22°C for 16 h with 40 mL of a 0.11 mol/L acetic acid (HAc) solution and centrifuged at 3000 rpm for 20 min. The supernatant was used to determine the acid-extractable Cd content. The residue was extracted with 40 mL of 0.5 mol/L NH_2HCl solution at 22°C for 16 h and centrifuged at 3000 rpm for 20 min. The supernatant was used to determine the reducible Cd content. The residue was shaken with 10 mL of 8.8 mol of H_2O_2 at 22°C for 1 h and digested at 85°C to a volume of 1 mL. Then, 50 mL of 1.0 mol/L NH_4Ac solution was added, and the mixture was oscillated at 22°C for 16 h. The mixture was subsequently centrifuged at 3000 rpm for 20 min, after which the supernatant was collected for determination of the oxidizable Cd content. After the above steps, 0.10 g of residue was weighed, 3 mL of HCl, 2 mL of HNO_3, 1 mL of $HClO_4$, and 5 mL of hydrofluoric acid (HF) solution were added. The residue was digested using the wet digestion method to yield a transparent digest for assessing the residual Cd content.

2.8 Determination of cadmium concentration and form in soil solution and leachate

The pH values of the soil solution and leachate were determined by a pH meter. Following filtration, 5 mL of the filtrate underwent digestion with 5 mL of HNO_3 and 5 mL of H_2O_2 at 90–95°C on an electric heating plate. The digestion mixture was transferred to a volumetric flask to a volume of 50 mL with distilled water. The Cd concentration was determined by a graphite

furnace atomic absorption spectrophotometer (ICE 3000 Series, Thermo Scientific, Franklin, MA, USA), and then the Cd concentrations in the soil solution and leachate were calculated. Cd leaching loss (μg) = Cd concentration (μg/mL) × volume of leachate (mL).

Ion chromatography was used to determine the ions in the leachate and soil (Michalski, 2006), and the instrument used was an Aquion instrument (Thermo Fisher Scientific, Waltham, MA, United States). The anions used an AG19 chromatographic column and an AS19 protective column equipped with a KOH automatic elution device (concentration of 20 mM), and the flow rate was 1 mL/min to determine the ion concentrations of SO_4^{2-}, Cl^-, and F^-. To determine the ion concentrations of Na^+, Mg^{2+}, Ca^{2+}, and NH_4^+, an AG12 chromatographic column, AS12 protective column, and methylsulfonic acid eluent (concentration of 20 mM) were used, and the flow rate was 1 mL/min.

The pH, cation content, anion content, and cadmium content were recorded with visual MINTEQ3.1 software (Environmental Protection Agency, United States) to calculate the occurrence of cadmium in the soil solution and leachate, including Cd^{2+}, $CdSO_4$ (aq), $CdOH^+$, CdF^+, and $CdCl^+$.

2.9 Data analysis

The experimental data were the average of 5 replicates. IBM SPSS Statistics 21 was used for significance analysis and correlation analysis of the data. The mean value and standard error of the data were analyzed by one-way ANOVA. Differences were tested by Duncan's multiple comparison test. The significance level was set at $p < 0.05$. The Pearson correlation coefficient was used to analyze the correlation, Origin 2022 was used for chart drawing, and IBM SPSS Amos 26 was used to construct the structural equation model.

3 Results

3.1 Characteristics of ERM infestation in maize roots

Maize root infection rates ranged from 20.7 to 39.6% when inoculated with AMF, with spore counts per gram of soil ranging from 10.5 to 18.3, indicating that AMF effectively infected maize roots.

Compared with the static treatment, the rotation treatment caused a decrease in the content of easily extracted glomalin-related soil protein (EE-GRSP) inside and outside the in-growth core from 1.15 and 0.96 mg/g to 0.85 and 0.81 mg/g, a decrease of 16 and 5%, respectively, but had no significant effect on the total glomalin-related soil protein (T-GRSP) content (Supplementary Figure S2).

3.2 Effect of ERM on maize plant height, biomass, and photosynthetic physiology

Compared with the static treatment, the rotation treatment reduced the plant height of maize from 32.54 cm to 27.52 cm, with a decrease of 15%. But had no significant effect on the maize total biomass or the shoot or root biomass.

Compared with the static treatment, the rotation treatment caused a significant decrease in the chlorophyll b content and net photosynthetic rate of maize leaves, by 30 and 43%, respectively, while the transpiration rate increased by 51% (Table 1).

3.3 Effect of ERM on cd content and uptake in maize

Compared with the static treatment, the rotation treatment caused a significant increase in the Cd content in the shoot and root of maize, by 64 and 82%, respectively (Figure 1A), while it increased the Cd uptake in the root by 46% (Figure 1B).

3.4 Effects of ERM on the form and $CaCl_2$-extraction of cd in soil

Compared with the static treatment, the rotation treatment caused a significant increase in the proportion of acid-extractable Cd in the rhizosphere soil of maize by 13%, a significant decrease in the proportion of residual Cd by 8%, a significant increase in the proportion of acid-extractable Cd in the non-rhizosphere soil by 15%, and a significant decrease in the proportion of residual Cd by 8% (Figure 2A).

Compared with the static treatment, the rotation treatment caused a significant increase in the $CaCl_2$-extracted Cd content in the rhizosphere and non-rhizosphere soils by 13 and 12%, respectively (Figure 2B).

3.5 Effect of AMF on soil solution cd concentration and leaching loss

Compared with the static treatment, the rotation treatment caused a significant increase in the Cd concentration in the soil solution within the growing core, the 10 cm depth soil solution, the 20 cm depth soil solution, and the leachate by 38, 49, 52, and 26%, respectively, under the first leaching; the Cd concentrations in the 10 cm and 20 cm depth soil solutions increased by 50 and 36%, respectively, under the second leaching; and the Cd concentrations in the soil solution in the in-growth core, 20 cm depth soil solution, and

TABLE 1 Effects of static and rotated treatments on photosynthetic physiology of maize.

Treatment	Photosynthetic rate ($\mu mol\ CO_2 \cdot m^{-2} \cdot s^{-1}$)	Intercellular CO_2 concentration ($\mu mol \cdot mol^{-1}$)	Transpiration rate (mmol $H_2O \cdot m^{-2} \cdot s^{-1}$)	Chlorophyll a Content ($mg \cdot g^{-1}$)	Chlorophyll b Content ($mg \cdot g^{-1}$)
Static	7.31 ± 1.42**	243.2 ± 26.02	2.16 ± 0.2	2.55 ± 0.34	2.27 ± 0.1**
Rotated	4.19 ± 0.41	225 ± 23.82	3.25 ± 0.45**	2.10 ± 0.35	1.58 ± 0.25

All values represent the mean ± error (SE), $n = 5$. "**" indicates highly significant correlation at $p < 0.01$ level.

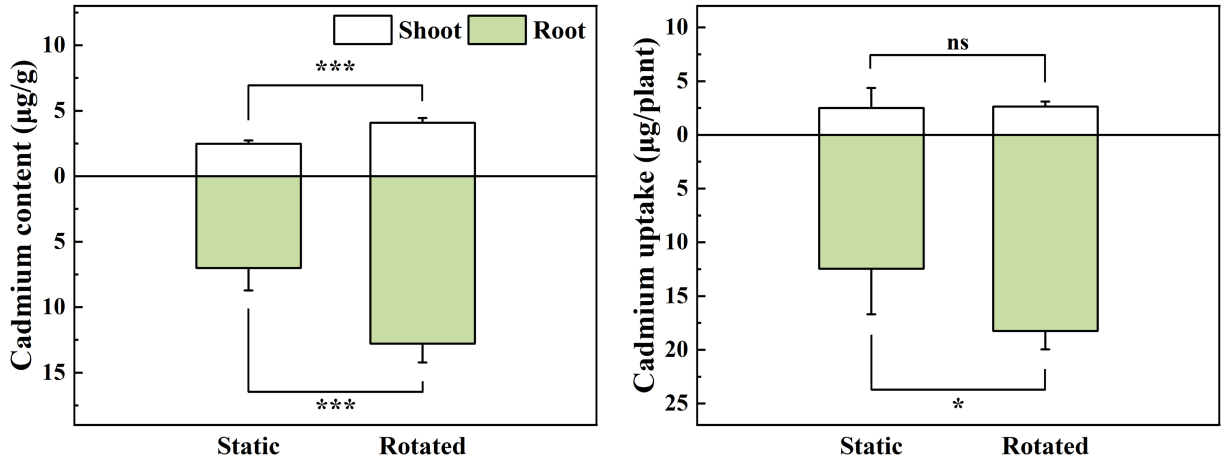


FIGURE 1
Effects of static and rotated treatments on **(A)** Cd content and **(B)** uptake in maize. All values represent the mean ± error (SE), n = 5. "*" indicates significant correlation at $p < 0.05$ level, "***" indicates highly significant correlation at $p < 0.001$ level; "ns" indicate no significant differences between treatments.

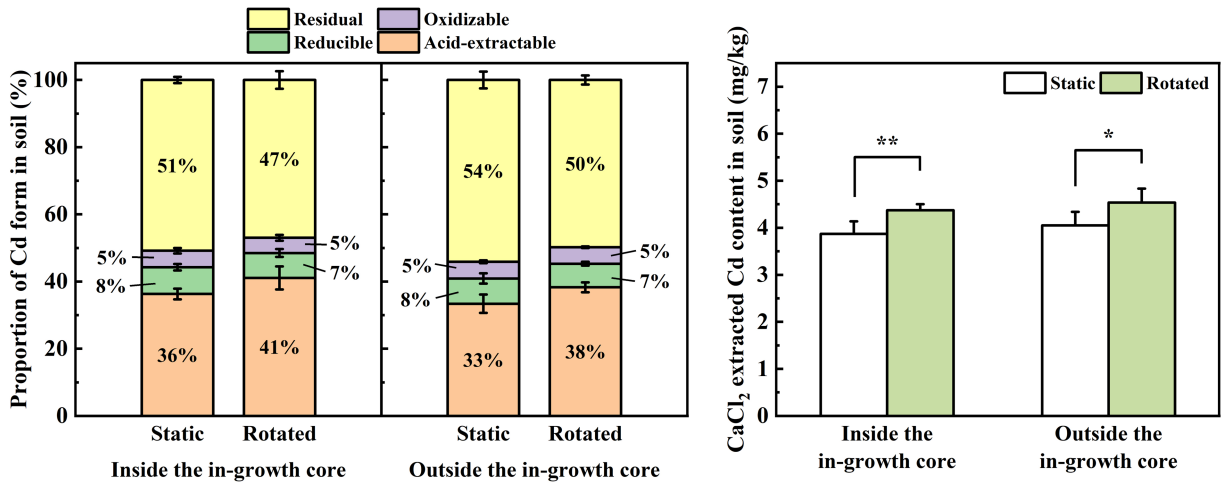


FIGURE 2
Effects of static and rotated treatments on **(A)** form and **(B)** $CaCl_2$-extracted Cd in soil. All values represent the mean ± error (SE), n = 5. "*" indicates significant correlation at $p < 0.05$ level, "**" indicates highly significant correlation at $p < 0.01$ level.

leachate under the third leaching increased by 30, 17, and 30%, respectively (Figures 3A–C).

The rotation treatment caused a significant increase in the leaching loss of Cd by 29, 39, and 39%, respectively, in the three leaching tests (Figure 3D).

3.6 Effects of ERM on the form of cd in soil solution and leachate

In the three leaching tests, Cd^{2+} predominated, comprising 93.04 to 99.04% of the concentration; $CdSO_4$ (aq) ranked next, at 0.71 to 6.68%; while CdF^+ was least, ranging from 0.02 to 0.07%.

Within in-growth cores, compared with the static treatment, rotational treatment induced significant variations in the proportions of different Cd ion forms during leaching. Specifically, Cd^{2+} proportion increased by 2.1% during the first leaching, while $CdSO_4$(aq) proportion decreased by 56.1 and 6.1% during the first and third leaching, respectively. Moreover, the $CdOH^+$ proportion decreased by 47.9 and 48.7% during the first and second leaching, and the $CdCl^+$ proportion increased by 40.5% during the third leaching (Figure 4).

At the sampling point at 10 cm depth outside the in-growing core, rotational treatment caused a 1.9% increase in Cd^{2+} proportion during the first leaching, a decrease in $CdSO_4$(aq) proportion by 34.7 and 29.6% during the first and third leaching, a 26.1% decrease in $CdOH^+$ proportion during the second leaching, and a 51.4% increase in $CdCl^+$ proportion during the third leaching (Figure 5).

At the sampling point at the 20 cm depth outside the in-growth core, rotational treatment caused a 1.7% increase in Cd^{2+} proportion during the second leaching, a 44.5% decrease in $CdSO_4$(aq) proportion

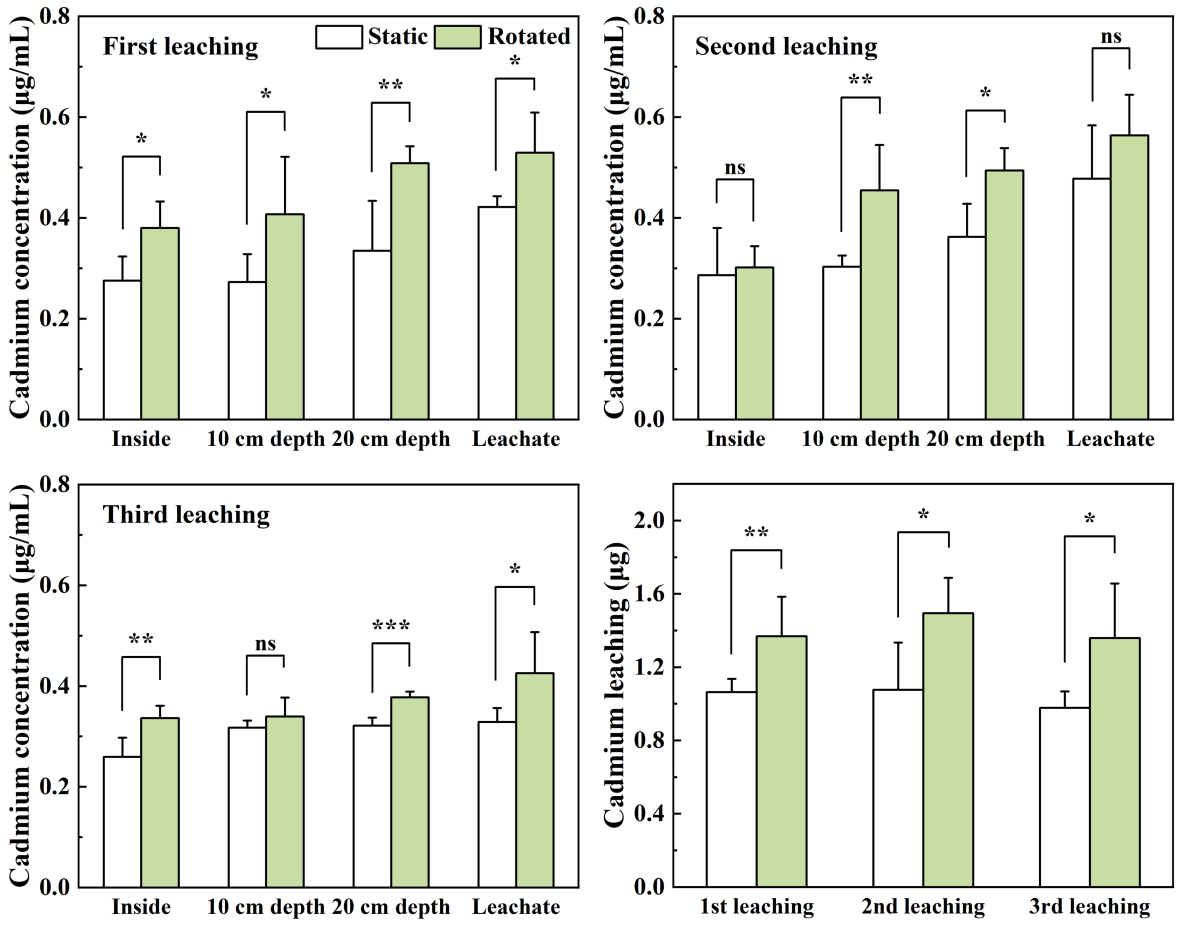


FIGURE 3
Effects of static and rotated treatments on **(A)** Cd concentration and **(B)** leaching loss from soil solution and leachate. All values represent the mean ± error (SE), $n = 5$. "*" indicates significant correlation at $p < 0.05$ level, "**" indicates highly significant correlation at $p < 0.01$ level, "***" indicates highly significant correlation at $p < 0.001$ level; "ns" indicate no significant differences between treatments.

during the second leaching, and a 32.1% decrease in $CdOH^+$ proportion during the second leaching (Figure 5).

In the leachate, rotational treatment caused a 0.8% increase in Cd^{2+} proportion during the first leaching, a 39.3% decrease in $CdSO_4$(aq) proportion during the first leaching, and a 36.0% decrease in $CdOH^+$ proportion during the third leaching (Figure 6).

3.7 Analysis of the effect of ERM on the migration of cd from contaminated soil

Correlation analysis (Figure 7) revealed that the contents of EE-GRSP and T-GRSP in contaminated soil were significantly negatively correlated with Cd leaching loss ($p < 0.001$) and were significantly ($p < 0.001$) or significantly ($p < 0.05$) positively correlated with the Cd content in shoots and roots and with Cd uptake in roots. These results indicate that GRSP secreted by AMF through its mycelium helped reduce Cd leaching loss in contaminated soil and Cd uptake by plants.

The content of EE-GRSP in contaminated soil was significantly negatively correlated with the content of acid-extractable Cd, $CaCl_2$-extractable Cd, and solution Cd^{2+} in soil ($p < 0.01$) and significantly positively correlated with the content of reducible Cd, residual Cd and solution $CdSO_4$ (aq) in soil ($p < 0.01$). GRSP secreted by AMF mycelium reduces the content of Cd^{2+} in solution, acid-extractable Cd and $CaCl_2$-extractable Cd in soil, and increases the content of residual Cd in soil and $CdSO_4$ (aq) in solution.

The acid-extractable Cd, $CaCl_2$-extractable Cd, and solution-extractable Cd^{2+} in contaminated soil were significantly ($p < 0.05$) or extremely significantly ($p < 0.01$) positively correlated with the Cd content in shoots and roots, Cd uptake in roots, and Cd leaching loss. The contents of reducible Cd, residual Cd, and solution $CdSO_4$ (aq) in contaminated soil were significantly ($p < 0.05$) or extremely significantly ($p < 0.01$) negatively correlated with the Cd content in the shoot and root and with the Cd uptake in the root. These results indicate that the reducible and residual Cd in soil and the solution of $CdSO_4$ (aq) helped reduce plant Cd uptake and Cd leaching loss in contaminated soil.

The structural equation model (Figure 8) showed that the path coefficient of ERM to GRSP was 0.653 ($p < 0.001$), and the path coefficients of GRSP to acid-extractable Cd, $CaCl_2$-extractable Cd, and shoot Cd uptake were − 0.361 ($p < 0.001$), −0.735 ($p < 0.001$), and − 0.457 ($p < 0.001$), respectively, indicating that GRSP directly

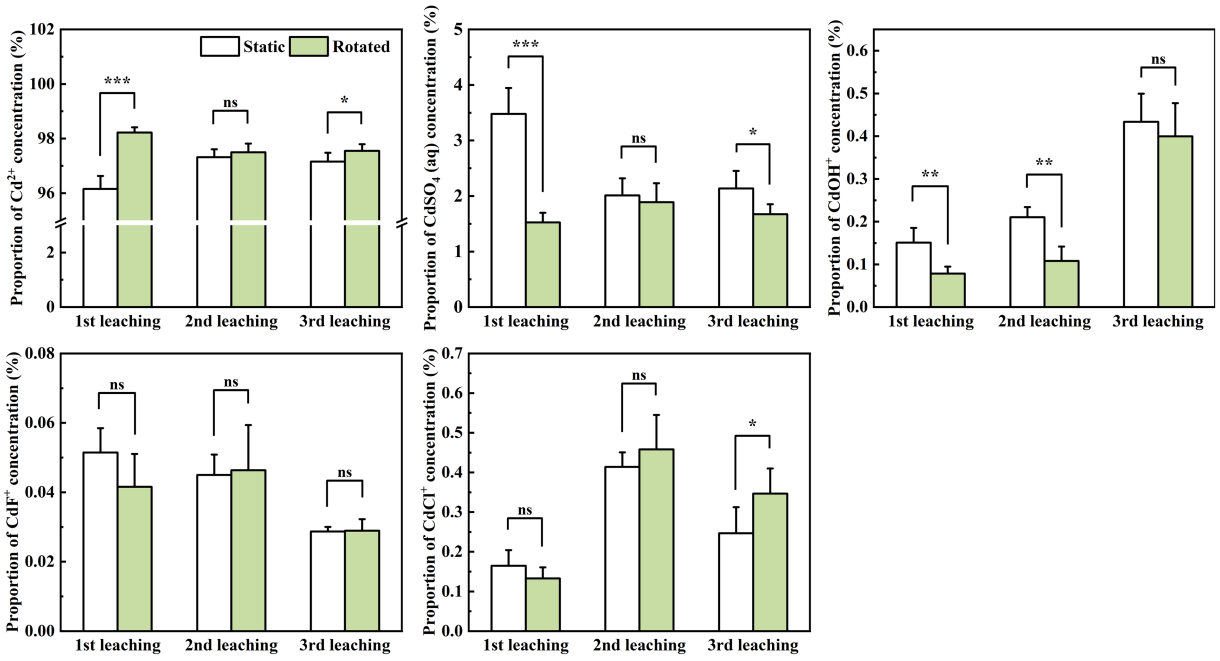


FIGURE 4
Effects of static and rotated treatments on the form of Cd in soil solution within the in-growth core. All values represent the mean ± error (SE), $n = 5$. "*" indicates significant correlation at $p < 0.05$ level, "**" indicates highly significant correlation at $p < 0.01$ level, "***" indicates highly significant correlation at $p < 0.001$ level; "ns" indicate no significant differences between treatments.

had a significant or very significant negative effect on available Cd in soil and maize Cd uptake. Moreover, the path coefficients of the GRSP to the Cd concentration in the soil solution and the free Cd^{2+} and Cd leaching losses were − 0.212 ($p < 0.05$), −0.276 ($p < 0.01$) and − 0.550 ($p < 0.001$), respectively, indicating that the GRSP directly reduced the Cd concentration, the proportion of free Cd^{2+} in the soil solution and its leaching loss.

Moreover, the path coefficient of acid-extractable Cd and shoot Cd uptake was 0.380 ($p < 0.001$), and that of $CaCl_2$-extractable Cd in soil to root Cd uptake was 0.299 ($p < 0.01$), indicating that the available Cd in soil had a very significant positive effect on maize Cd uptake. The path coefficients of the Cd concentration and free Cd^{2+} in the soil solution for Cd leaching loss were 0.269 ($p < 0.01$) and 0.167 ($p < 0.05$), respectively, indicating that the Cd concentration in the soil solution contributed to Cd leaching loss. Thus, AMF can directly and indirectly reduce Cd uptake by plants and Cd leaching loss by decreasing Cd availability in soil and soil solution through the GRSP secreted by ERM.

4 Discussion

AMF, as soil fungi that can colonize roots and form symbiotic relationships with host plants, have a remarkable impact on plant growth and performance (Yang et al., 2015). AMF establishes a symbiotic relationship with plant roots, enhancing root surface area, facilitating nutrient absorption and transport, and improving nutrient utilization efficiency, thus promoting photosynthesis and growth of the plant (Song et al., 2021; Bhantana et al., 2021). ERM helps to increase the plant's ability to absorb and retain water, maintain the water balance in the plant, and promote photosynthesis, growth, and development (Begum et al., 2019). Additionally, ERM can supply a portion of the plant's carbon needs, promoting the accumulation and distribution of photosynthetic products within the plant, thereby augmenting growth and metabolic functions (Wahab et al., 2023). Together, these mechanisms optimize nutrient absorption, water regulation, and carbon supply in plants, ultimately advancing plant growth and development. Disruption of the ERM hampers the functionality of AMF, leading to detrimental impacts on plant growth (Bahadur et al., 2019). In the present study, compared with the static treatment with an undisrupted ERM, the rotation treatment to disrupt the ERM outside the in-growth core caused significant decreases in the plant height and photosynthetic physiology of the maize plants. These findings indirectly underscore the beneficial role of ERM in promoting maize growth.

Under abiotic stresses such as Cd pollution in soil, the presence of AMF enhanced plant resistance to Cd stress with the help of ERM in soil (Wu et al., 2014; Bargaz et al., 2018). First, ERM reduced the amount of Cd entering plant roots through adsorption, thereby reducing Cd toxicity to plants (Pan et al., 2023). In addition, the ERM produced a special glycoprotein, glomalin-related soil protein (GRSP), which is secreted on the surface of the extraradical mycelium of symbionts. GRSP can bind or chelate heavy metals and therefore plays an important role in fixing heavy metal ions such as Cd in soil (Gujre et al., 2021; Wang et al., 2012). Thus, GRSP contributed to reducing Cd bioavailability in soil and Cd uptake by plants (Xiao et al., 2021; Li et al., 2018). In the present study, compared with the static treatment, the rotation treatment caused significant increases in the Cd content in the shoots and roots of maize plants grown in the in-growth core. The structural equation model (SEM) also indicated that the GRSP

10.3389/fmicb.2024.1507798

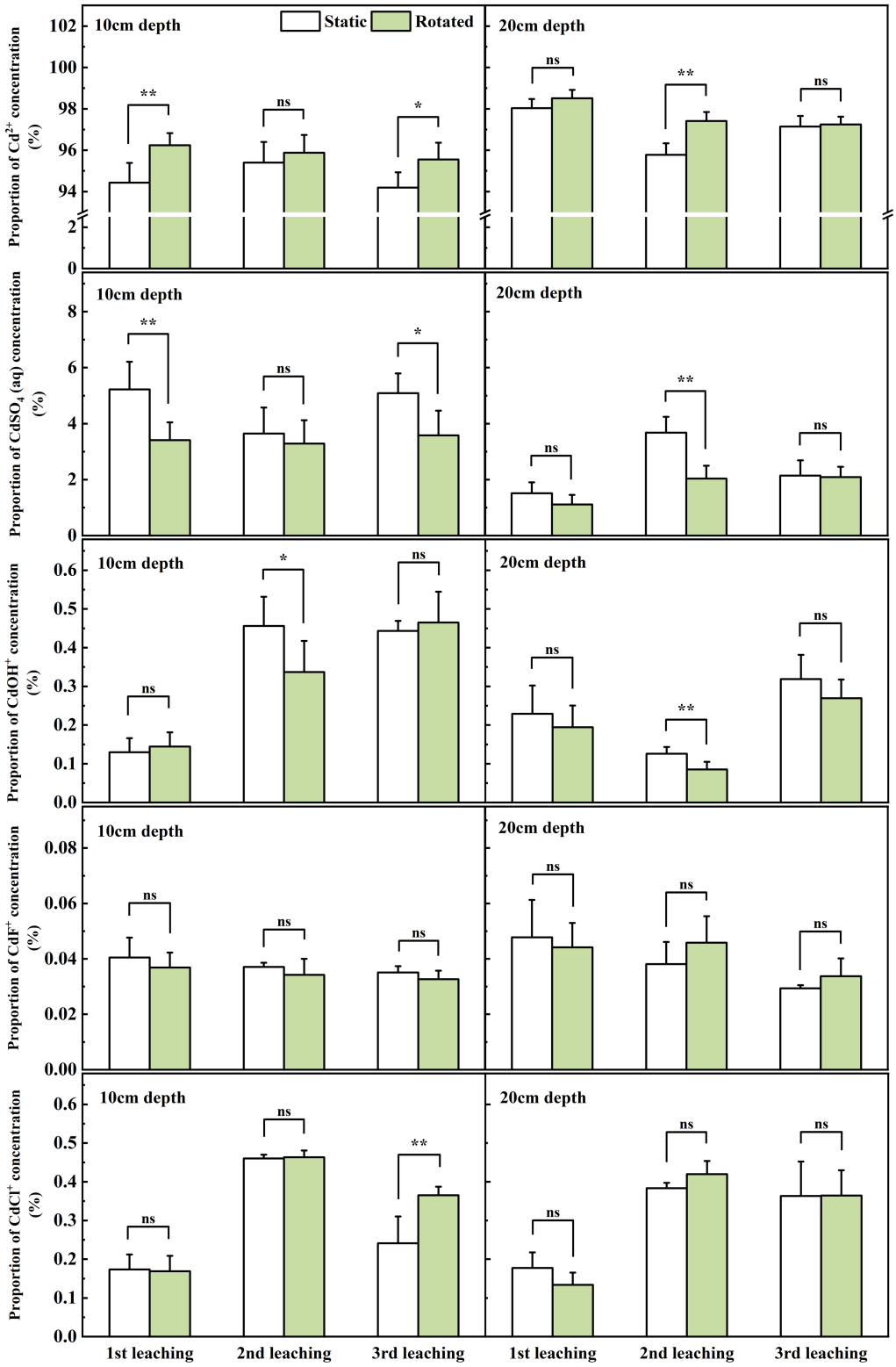


FIGURE 5
Effects of static and rotated treatments on the form of Cd in soil solution outside the in-growth core. All values represent the mean ± error (SE), n = 5. "*" indicates significant correlation at $p < 0.05$ level, "**" indicates highly significant correlation at $p < 0.01$ level; "ns" indicate no significant differences between treatments.

was a key factor that was negatively correlated with the Cd content in maize. Therefore, the present study also confirmed that ERM secreted GRSP to inhibit Cd availability and uptake by plants.

Many studies have shown that AMF immobilizes Cd in soil through ERM and mycorrhizal structures, which convert active Cd ions into inactive species and reduce Cd bioavailability in soil (Fang

10.3389/fmicb.2024.1507798

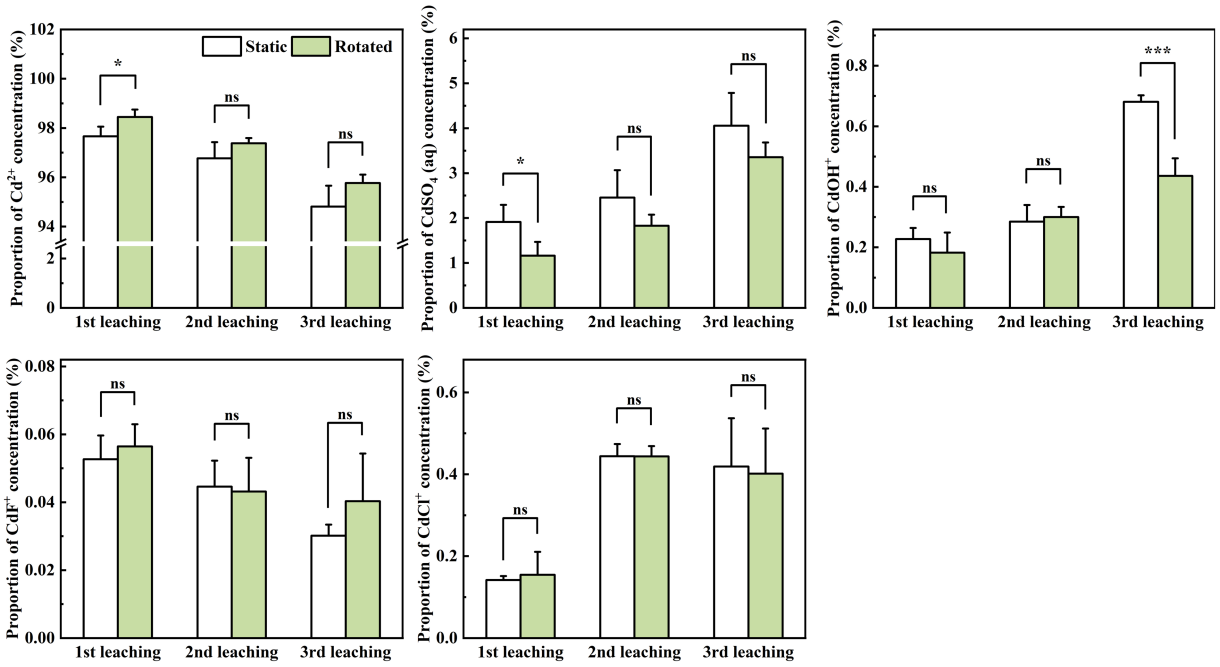
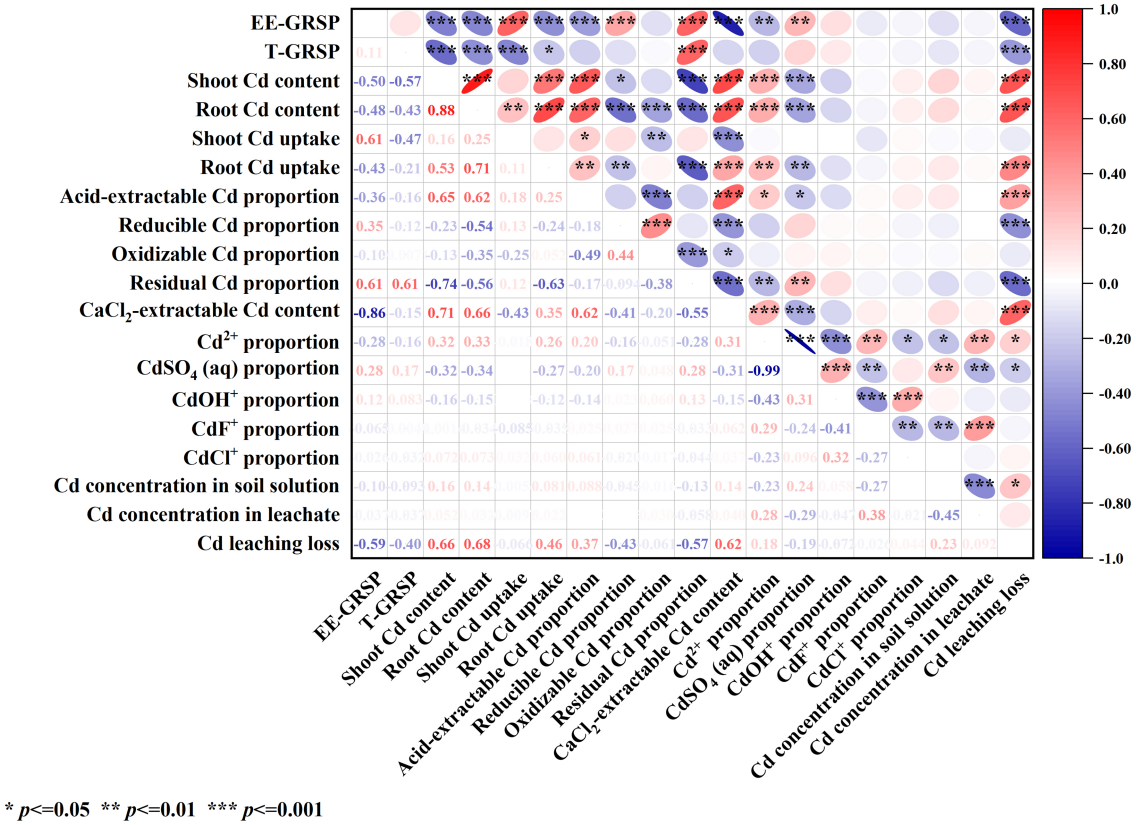


FIGURE 6
Effects of static and rotated treatments on the form of Cd in the leachate. All values represent the mean ± error (SE), n = 5. "*" indicates significant correlation at $p < 0.05$ level, "***" indicates highly significant correlation at $p < 0.001$ level; "ns" indicate no significant differences between treatments.



* p<=0.05 ** p<=0.01 *** p<=0.001

FIGURE 7
Correlation analysis of the effects of AMF on the morphology and migration of Cd in contaminated soil-maize.

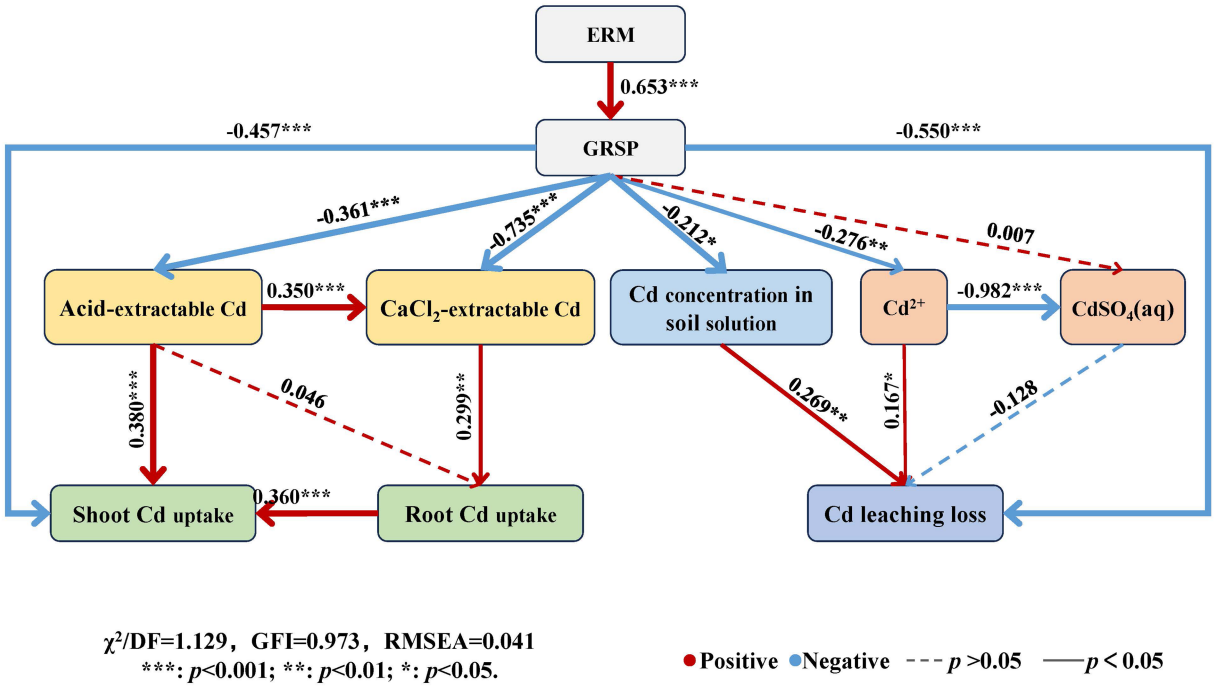


FIGURE 8
Structural equation model of influencing factors of Cd migration in contaminated soil. Note: The red line indicates a positive relationship, the blue line indicates a negative relationship, and the path with insignificant coefficients is represented by a dotted line. The online numbers represent the total effect of standardization.

et al., 2024; Zhang et al., 2019). The GRSP secreted by ERM immobilizes various heavy metals, including Cd, Pb, Cu, etc., and plays an important role in alleviating the bioavailability and toxicity of heavy metals in soil (Ai et al., 2022). In the present study, the rotation treatment increased the proportion of acid-extractable Cd and reduced the proportion of residual Cd in the soil, and the $CaCl_2$-extracted Cd content was significantly greater in the rotation treatment than in the static treatment. These results indicated that ERM disruption resulted in the transformation of Cd speciation from a low activity (residual) to a higher activity (acid-extractable), and ERM reduced the $CaCl_2$-extracted Cd content in the soil. The rotation of the in-growth core to break the ERM outside led to a decrease in the GRSP content in the soil.

Additionally, previous studies have shown that the GRSP secreted by ERM has a strong adsorption capacity for Cd ions and effectively adsorbs 76% of Cd ions in water (Wang et al., 2019; Yuan et al., 2022; Zhan et al., 2023). Therefore, GRSP significantly reduced the solubility and migration of Cd ions from water. In the present study, the ERM disruption in the Rotated treatment caused significant increases in the Cd concentration in the soil solution, indirectly indicating that the ERM significantly limited the bioavailability and migration of Cd ions in the soil solution. Therefore, the rotation treatment significantly increased Cd leaching loss from the soil, indicating that ERM plays a functional role in inhibiting Cd leaching loss.

Furthermore, ERM growth and nutrient absorption from soil transform the chemical composition and forms of Cd ions in the soil solution (Ullah et al., 2023). For example, ERM can absorb nutrients such as nitrogen, phosphorus, potassium, calcium, and magnesium from the soil solution, resulting in a change in the chemical properties of the soil solution (Fall et al., 2022). Studies have shown that ERM can affect the forms of Cd ions in soil solution through adsorption, chelation, and precipitation (Zhang et al., 2021). On the one hand, the surface of ERM is negatively charged, and these negative charges can interact with the positive charges of Cd ions so that Cd ions are adsorbed on the surface of the mycelium (Han et al., 2021). This adsorption can reduce the concentration of free Cd ions in soil solution, thereby reducing its toxicity and bioavailability. On the other hand, ERM also secretes some organic substances, such as low molecular weight organic acids, into the soil solution and then promotes the transformation of active Cd ions into inactive forms, such as Cd oxides or Cd chelates, which helps to reduce the bioavailability and mobility of Cd ions. In addition, the substances secreted by ERM can react with Cd ions to form insoluble precipitates. These precipitates can cause Cd ions to exist in the soil solution in a precipitated state, reducing its dissolved concentration (Jiang et al., 2021; Wang et al., 2022). In the present study, the ERM disruption in the rotation treatment increased the proportion of Cd^{2+} ions and decreased the proportions of $CdSO_4$(aq) and $CdOH^+$ in the soil solution and leachate. Furthermore, the Cd^{2+} proportion in the soil solution was significantly positively correlated with Cd leaching loss, and the $CdSO_4$(aq) proportion was significantly negatively correlated with Cd leaching loss. These results indirectly indicated that ERM contributed to the transformation of Cd^{2+} with greater activity to $CdSO_4$ (aq) and $CdOH^+$ with lower activity and to reducing Cd leaching loss from the soil solution.

Based on the in-growth core experiment, the present study indicated that ERM can potentially promote plant growth and inhibit Cd uptake by plants and Cd leaching loss by changing the Cd form

and reducing the Cd concentration in the soil solution. This study aims to investigate the ERM in Cd contaminated soil by disrupting its growth. Understanding this role is crucial for comprehending the potential of ERM in remediating soil pollution. The experimental outcomes will serve as a foundation for crafting strategies to mitigate Cd contamination, enhancing soil quality and reducing crop toxicity. However, the effects of ERM on Cd migration in the field are still unclear. The mechanisms underlying the effects of ERM on the chemical properties of soil solutions are poorly understood. Therefore, more studies on the ecological effects of ERM on soil and soil solutions in the field should be conducted. Additionally, the mechanisms underlying the effects of ERM on soil properties and Cd migration in soil solutions should be further explored. Therefore, the potential functions of ERM should be further utilized in the ecological remediation and management of heavy metal-polluted soil.

5 Conclusion

Based on the in-growth-core experiment, the ERM disruption of the rotation treatment significantly reduced the photosynthetic physiology of leaves, and maize growth, and the GRSP content in the soil but increased the Cd availability in the soil, caused an increase in the percentage of acid-extractable Cd in the soil and a decrease in the percentage of residual Cd, which resulted in increases in the Cd content and uptake by maize. Additionally, ERM disruption increased the Cd concentration and the proportion of free Cd^{2+} in the soil solution, which caused an increase in Cd leaching loss from the soil. These results indirectly indicated that AMF plays a crucial role in inhibiting Cd uptake by plants and Cd leaching loss through the GRSP secreted by ERM in soil.

Data availability statement

The original contributions presented in the study are included in the article/Supplementary material, further inquiries can be directed to the corresponding authors.

Author contributions

YY: Data curation, Formal analysis, Visualization, Writing – original draft. YL: Conceptualization, Resources, Writing – original draft. XL: Resources, Visualization, Writing – original draft. JY: Investigation, Methodology, Writing – original draft. LW: Methodology, Resources, Supervision, Writing – review & editing. ZT: Formal analysis, Methodology, Writing – review & editing. YH: Conceptualization, Funding acquisition, Supervision, Writing – review & editing. FZ: Funding acquisition, Project administration, Writing – review & editing.

Funding

The author(s) declare that financial support was received for the research, authorship, and/or publication of this article. This work was financially supported by the National Natural Science Foundation of China (Nos. 42,177,381 and 42,267,002), the Key Project of the Basic Research Plan of Yunnan Province (202401AS070087), and the Expert Workstation Project of Yunnan Province (202305AF150042).

Conflict of interest

The authors declare that the research was conducted in the absence of any commercial or financial relationships that could be construed as a potential conflict of interest.

Generative AI statement

The author(s) declare that no Generative AI was used in the creation of this manuscript.

Publisher's note

All claims expressed in this article are solely those of the authors and do not necessarily represent those of their affiliated organizations, or those of the publisher, the editors and the reviewers. Any product that may be evaluated in this article, or claim that may be made by its manufacturer, is not guaranteed or endorsed by the publisher.

Supplementary material

The Supplementary material for this article can be found online at: https://www.frontiersin.org/articles/10.3389/fmicb.2024.1507798/full#supplementary-material

References

Ai, Y. J., Li, F. P., Yang, J. Q., Lu, S., and Gu, H. H. (2022). Research progress and potential functions of AMF and GRSP in the ecological remediation of metal tailings. *Sustain. For.* 14:9611. doi: 10.3390/su14159611

Bahadur, A., Jin, Z., Long, X., Jiang, S., Zhang, Q., Pan, J., et al. (2019). Arbuscular mycorrhizal fungi alter plant interspecific interaction under nitrogen fertilization. *Eur. J. Soil Biol.* 93:103094. doi: 10.1016/j.ejsobi.2019.103094

Bao, S. D. (2000). *Soil and agricultural chemistry analysis*. Beijing: China Agriculture Press, 370–375.

Bargaz, A., Lyamlouli, K., Chtouki, M., Zeroual, Y., and Dhiba, D. (2018). Soil microbial resources for improving fertilizers efficiency in an integrated plant nutrient management system. *Front. Microbiol.* 9:1606. doi: 10.3389/fmicb.2018.01606

Begum, N., Ahanger, M. A., Su, Y., Lei, Y., Mustafa, N. S. A., Ahmad, P., et al. (2019). Improved drought tolerance by AMF inoculation in maize (*Zea mays*) involves physiological and biochemical implications. *Plan. Theory* 8:579. doi: 10.3390/plants8120579

Bhantana, P., Rana, M. S., Sun, X. C., Moussa, M. G., Saleem, M. H., Syaifudin, M., et al. (2021). Arbuscular mycorrhizal fungi and its major role in plant growth, zinc nutrition, phosphorous regulation and phytoremediation. *Symbiosis* 84, 19–37. doi: 10.1007/S13199-021-00756-6

Chang, Q., Diao, F. W., Wang, Q. F., Pan, L., Dang, Z. H., and Guo, W. (2018). Effects of arbuscular mycorrhizal symbiosis on growth, nutrient and metal uptake by maize seedlings (*Zea mays* L.) grown in soils spiked with lanthanum and cadmium. *Environ. Pollut.* 241, 607–615. doi: 10.1016/j.envpol.2018.06.003

Daniels, B. A., and Skipper, H. D. (1982). Methods for the recovery and quantitative estimation of propagules from soil. *Methods & Principles of Mycorrhizal Research*. 29–35.

Fall, A. F., Nakabonge, G., Ssekandi, J., Founoune-Mboup, H., Apori, S. O., Ndiaye, A., et al. (2022). Roles of arbuscular mycorrhizal fungi on soil fertility: contribution in the improvement of physical, chemical, and biological properties of the soil. *Front. Fung. Biol.* 3:723892. doi: 10.3389/ffunb.2022.723892

Fang, X., Lee, X., Twagirayezu, G., Cheng, H., Lu, H., Huang, S., et al. (2024). A critical review of the effectiveness of biochar coupled with arbuscular mycorrhizal Fungi in soil cadmium immobilization. *J. Fungi* 10:182. doi: 10.3390/jof10030182

Ferrol, N., Tamayo, E., and Vargas, P. (2016). The heavy metal paradox in arbuscular mycorrhizas: from mechanisms to biotechnological applications. *J. Exp. Bot.* 67, 6253–6265. doi: 10.1093/jxb/erw403

Ghobadi, M., Dehnavi, M. M., Yadavi, A. R., Parvizi, K., and Zafari, D. (2020). Reduced P fertilization improves Fe and Zn uptake in potato when inoculated with AMF in P, Fe and Zn deficient soil. *Rhizosphere* 15:100239. doi: 10.1016/j.rhisph.2020.100239

Gonzalez-Chavez, M. C., Carrillo-Gonzalez, R., Wright, S. F., and Nichols, K. A. (2004). The role of glomalin, a protein produced by arbuscular mycorrhizal fungi, in sequestering potentially toxic elements. *Environ. Pollut.* 130, 317–323. doi: 10.1016/j.envpol.2004.01.004

Gray, C. W., Monaghan, R. M., Orchiston, T., Laurenson, S., and Cavanagh, J. A. (2017). Cadmium losses in overland flow from an agricultural soil. *Environ. Sci. Pollut. Res.* 24, 24046–24053. doi: 10.1007/s11356-017-0117-9

Gujre, N., Agnihotri, R., Rangan, L., Sharma, M. P., and Mitra, S. (2021). Deciphering the dynamics of glomalin and heavy metals in soils contaminated with hazardous municipal solid wastes. *J. Hazard. Mater.* 416:125869. doi: 10.1016/j.jhazmat.2021.125869

Guo, J., Chen, J., Li, C., Wang, L., Liang, X., Shi, J., et al. (2023). Arbuscular mycorrhizal fungi promote the degradation of the fore-rotating crop (*Brassica napus* L.) straw, improve the growth of and reduce the cadmium and lead content in the subsequent maize. *Agronomy* 13:767. doi: 10.3390/agronomy13030767

Haider, F. U., Liqun, C., Coulter, J. A., Cheema, S. A., Wu, J., Zhang, R., et al. (2021). Cadmium toxicity in plants: impacts and remediation strategies. *Ecotoxicol. Environ. Saf.* 211:111887. doi: 10.1016/j.ecoenv.2020.111887

Han, Y., Zveushe, O. K., Dong, F., Ling, Q., Chen, Y., Sajid, S., et al. (2021). Unraveling the effects of arbuscular mycorrhizal fungi on cadmium uptake and detoxification mechanisms in perennial ryegrass (*Lolium perenne*). *Sci. Total Environ.* 798:149222. doi: 10.1016/j.scitotenv.2021.149222

He, Y. M., Yang, R., Lei, G., Li, B., Jiang, M., Yan, K., et al. (2020). Arbuscular mycorrhizal fungi reduce cadmium leaching from polluted soils under simulated heavy rainfall. *Environ. Pollut.* 263:114406. doi: 10.1016/j.envpol.2020.114406

Jiang, Y., Huang, R., Jiang, L., Chen, K., and Zhu, W. (2021). Alleviation of cadmium toxicity to *medicago truncatula* by AMF involves the changes of cd speciation in rhizosphere soil and subcellular distribution. *Phyton* 90, 403–415. doi: 10.32604/phyton.2021.014376

Johnson, D., Leake, J. R., and Read, D. J. (2001). Novel in-growth core system enables functional studies of grassland mycorrhizal mycelial networks. *New Phytol.* 152, 555–562. doi: 10.1046/J.0028-646X.2001.00273.X

Kavadia, A., Omirou, M., Fasoula, D., Trajanoski, S., Andreou, E., and Ioannides, I. M. (2020). Genotype and soil water availability shape the composition of AMF communities at chickpea early growth stages. *Appl. Soil Ecol.* 150:103443. doi: 10.1016/j.apsoil.2019.103443

Leifheit, E. F., Verbruggen, E., and Rillig, M. C. (2014). Rotation of hyphal in-growth cores has no confounding effects on soil abiotic properties. *Soil Biol. Biochem.* 79, 78–80. doi: 10.1016/j.soilbio.2014.09.006

Li, J., Sun, Y., Jiang, X., Chen, B., and Zhang, X. (2018). Arbuscular mycorrhizal fungi alleviate arsenic toxicity to *Medicago sativa* by influencing arsenic speciation and partitioning. *Ecotoxicol. Environ. Saf.* 157, 235–243. doi: 10.1016/j.ecoenv.2018.03.073

Liu, W., Zheng, C., Fu, Z., Gai, J., Zhang, J., Christie, P., et al. (2014). Facilitation of seedling growth and nutrient uptake by indigenous arbuscular mycorrhizal fungi in intensive agroecosytems. *Biol. Fertil. Soils* 50, 381–394. doi: 10.1007/s00374-013-0859-6

McGonigle, T. P., Miller, M. H., Evans, D. G., Fairchild, G. L., and Swan, J. A. (1990). A new method which gives an objective measure of colonization of roots by vesicular—arbuscular mycorrhizal fungi. *New Phytol.* 115, 495–501. doi: 10.1111/j.1469-8137.1990.tb00476.x

Michalski, R. (2006). Ion chromatography as a reference method for determination of inorganic ions in water and wastewater. *Crit. Rev. Anal. Chem.* 36, 107–127. doi: 10.1080/10408340600713678

Mohammed, A. S., Kapri, A., and Goel, R. (2011). Heavy metal pollution: source, impact, and remedies. *Biomanag. Metal Contamin. Soils* 20, 1–28. doi: 10.1007/978-94-007-1914-9_1

NaziaTahir, Ullah, A., Tahir, A., Rashid, H. U., Rehman, T., Danish, S., et al. (2021). Strategies for reducing cd concentration in paddy soil for rice safety. *J. Clean. Prod.* 316:128116. doi: 10.1016/j.jclepro.2021.128116

Pan, J., Cao, S., Xu, G., Rehman, M., Li, X., Luo, D., et al. (2023). Comprehensive analysis reveals the underlying mechanism of arbuscular mycorrhizal fungi in kenaf cadmium stress alleviation. *Chemosphere* 314:137566. doi: 10.1016/j.chemosphere.2022.137566

Porra, R. J., Thompson, W. A., and Kriedemann, P. E. (1989). Determination of accurate extinction coefficients and simultaneous equations for assaying chlorophylls a and b extracted with four different solvents: verification of the concentration of chlorophyll standards by atomic absorption spectroscopy. *Biochimica et Biophysica Acta* 975, 384–394. doi: 10.1016/S0005-2728(89)80347-0

Quevauviller, P., Rauret, G., Muntau, H., Ure, A. M., Rubio, R., López-Sánchez, J. F., et al. (1994). Evaluation of a sequential extraction procedure for the determination of extractable trace metal contents in sediments. *Fresenius J. Anal. Chem.* 349, 808–814. doi: 10.1007/BF00323110

Riaz, M., Kamran, M., Fang, Y., Wang, Q., Cao, H., Yang, G., et al. (2021). Arbuscular mycorrhizal fungi-induced mitigation of heavy metal phytotoxicity in metal contaminated soils: a critical review. *J. Hazard. Mater.* 402:123919. doi: 10.1016/j.jhazmat.2020.123919

Song, C., Sarpong, C. K., Zhang, X., Wang, W., Wang, L., Gan, Y., et al. (2021). Mycorrhizosphere bacteria and plant-plant interactions facilitate maize P acquisition in an intercropping system. *J. Clean. Prod.* 314:127993. doi: 10.1016/j.jclepro.2021.127993

Ullah, S., Liu, Q., Wang, S., Jan, A. U., Sharif, H. M. A., Ditta, A., et al. (2023). Sources, impacts, factors affecting Cr uptake in plants, and mechanisms behind phytoremediation of Cr-contaminated soils. *Sci. Total Environ.* 899:165726. doi: 10.1016/j.scitotenv.2023.165726

Wahab, A., Muhammad, M., Munir, A., Abdi, G., Zaman, W., Ayaz, A., et al. (2023). Role of arbuscular mycorrhizal fungi in regulating growth, enhancing productivity, and potentially influencing ecosystems under abiotic and biotic stresses. *Plan. Theory* 12:3102. doi: 10.3390/plants12173102

Wang, Q., Mei, D., Chen, J., Lin, Y., Liu, J., Lu, H., et al. (2019). Sequestration of heavy metal by glomalin-related soil protein: implication for water quality improvement in mangrove wetlands. *Water Res.* 148, 142–152. doi: 10.1016/j.watres.2018.10.043

Wang, F. Y., Wang, L., Shi, Z. Y., Li, Y. J., and Song, Z. M. (2012). Effects of AM inoculation and organic amendment, alone or in combination, on growth, P nutrition, and heavy-metal uptake of tobacco in Pb-cd-contaminated soil. *J. Plant Growth Regul.* 31, 549–559. doi: 10.1007/s00344-012-9265-9

Wang, H. R., Zhao, X. Y., Zhang, J. M., Lu, C., and Feng, F. J. (2022). Arbuscular mycorrhizal fungus regulates cadmium accumulation, migration, transport, and tolerance in *Medicago sativa*. *J. Hazard. Mater.* 435:129077. doi: 10.1016/j.jhazmat.2022.129077

Wright, S. F., and Upadhyaya, A. (1998). A survey of soils for aggregate stability and glomalin, a glycoprotein produced by hyphae of arbuscular mycorrhizal fungi. *Plant Soil* 198, 97–107. doi: 10.1023/A:1004347701584

Wu, Q. S., Cao, M. Q., Zou, Y. N., and He, X. H. (2014). Direct and indirect effects of glomalin, mycorrhizal hyphae and roots on aggregate stability in rhizosphere of trifoliate orange. *Sci. Rep.* 4:5823. doi: 10.1038/srep05823

Wu, Q. S., Wang, S., and Srivastava, A. K. (2016). Mycorrhizal hyphal disruption induces changes in plant growth, glomalin-related soil protein and soil aggregation of trifoliate orange in a core system. *Soil Tillage Res.* 160, 82–91. doi: 10.1016/j.still.2016.02.010

Xiao, Y., Zhao, Z., Chen, L., and Li, Y. (2021). Arbuscular mycorrhizal fungi mitigate the negative effects of straw incorporation on *Trifolium repens* in highly cd-polluted soils. *Appl. Soil Ecol.* 157:103736. doi: 10.1016/j.apsoil.2020.103736

Yang, H., Zhang, Q., Dai, Y., Liu, Q., Tang, J., Bian, X., et al. (2015). Effects of arbuscular mycorrhizal fungi on plant growth depend on root system: a meta-analysis. *Plant Soil* 389, 361–374. doi: 10.1007/s11104-014-2370-8

Yu, Z., Zhao, X., Su, L., Yan, K., Li, B., He, Y., et al. (2021). Effect of an arbuscular mycorrhizal fungus on maize growth and cadmium migration in a sand column. *Ecotoxicol. Environ. Saf.* 225:112782. doi: 10.1016/j.ecoenv.2021.112782

Yuan, B., Li, H., Hong, H., Wang, Q., Tian, Y., Lu, H., et al. (2022). Immobilization of lead (II) and zinc (II) onto glomalin-related soil protein (GRSP): adsorption properties and interaction mechanisms. *Ecotoxicol. Environ. Saf.* 236:113489. doi: 10.1016/j.ecoenv.2022.113489

Zhan, F., Li, B., Jiang, M., Li, T., He, Y., Li, Y., et al. (2019). Effects of arbuscular mycorrhizal fungi on the growth and heavy metal accumulation of bermudagrass [*Cynodon dactylon* (L.) Pers.] grown in a lead–zinc mine wasteland. *Int. J. Phytoremediation* 21, 849–856. doi: 10.1080/15226514.2019.1577353

Zhan, F., Zeng, W., Li, B., Li, Z., Chen, J., He, Y., et al. (2023). Inhibition of native arbuscular mycorrhizal fungi induced increases in cadmium loss via surface runoff and interflow from farmland. *Int. Soil Water Conserv. Res.* 11, 213–223. doi: 10.1016/J.ISWCR.2022.05.006

Zhang, X. F., Hu, Z. H., Yan, T. X., Lu, R. R., Peng, C. L., Li, S. S., et al. (2019). Arbuscular mycorrhizal fungi alleviate cd phytotoxicity by altering cd subcellular distribution and chemical forms in *Zea mays*. *Ecotoxicol. Environ. Saf.* 171, 352–360. doi: 10.1016/j.ecoenv.2018.12.097

Zhang, J., Su, L., Yan, K., Li, M., He, Y., Zu, Y., et al. (2021). An arbuscular mycorrhizal fungus increased the macroaggregate proportion and reduced cadmium leaching from polluted soil. *Int. J. Phytoremediation* 23, 1–9. doi: 10.1080/15226514.2020.1849014

Zhao, F. J., Ma, Y., Zhu, Y. G., Tang, Z., and McGrath, S. P. (2015). Soil contamination in China: current status and mitigation strategies. *Environ. Sci. Technol.* 49, 750–759. doi: 10.1021/es5047099

frontiers | Frontiers in Microbiology

TYPE Original Research
PUBLISHED 17 January 2025
DOI 10.3389/fmicb.2024.1487323

Check for updates

OPEN ACCESS

EDITED BY
Tereza Castellane,
São Paulo State University, Brazil

REVIEWED BY
Everlon Cid Rigobelo,
São Paulo State University, Brazil
Agnieszka Kuźniar,
The John Paul II Catholic University of Lublin, Poland
Poonam Singh,
LaserLeap Technologies (Portugal), Portugal

*CORRESPONDENCE
Zhouping Sun
✉ sunzp@syau.edu.cn
Hongdan Fu
✉ fuhongdan@syau.edu.cn

RECEIVED 27 August 2024
ACCEPTED 28 October 2024
PUBLISHED 17 January 2025

CITATION
Li X, Awais M, Wang S, Zhang Z, Zhao S, Liu Y, Sun Z, Fu H and Li T (2025) The process of nitrogen-adaptation root endophytic bacterial rather than phosphorus-adaptation fungal subcommunities construction unveiled the tomato yield improvement under long-term fertilization.
Front. Microbiol. 15:1487323.
doi: 10.3389/fmicb.2024.1487323

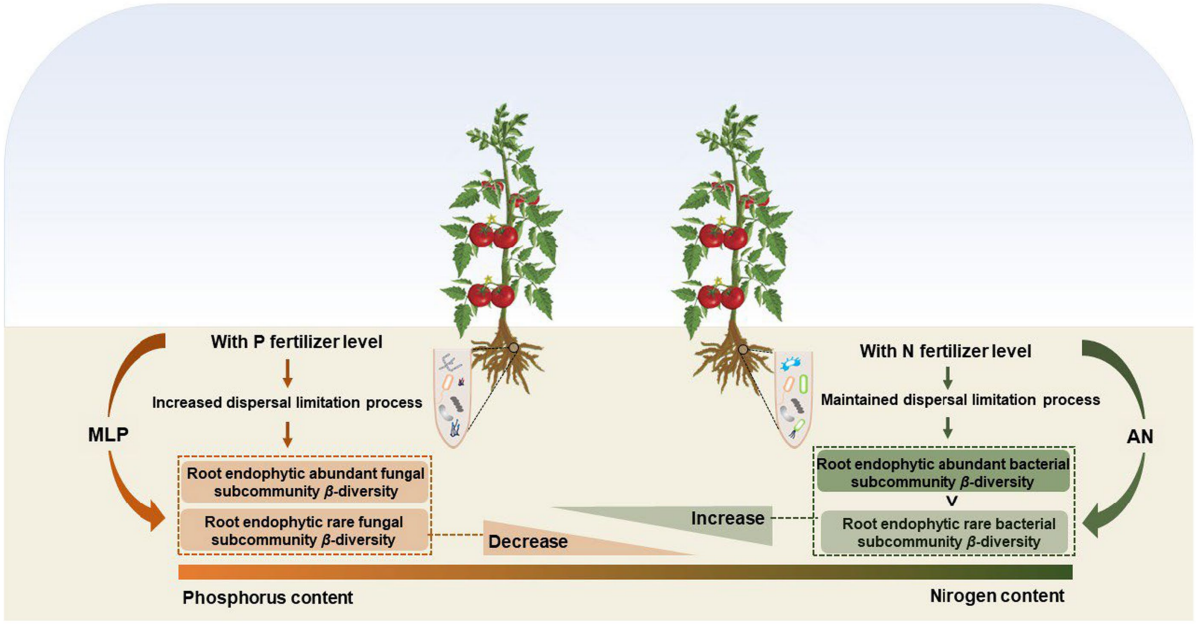
COPYRIGHT
© 2025 Li, Awais, Wang, Zhang, Zhao, Liu, Sun, Fu and Li. This is an open-access article distributed under the terms of the Creative Commons Attribution License (CC BY). The use, distribution or reproduction in other forums is permitted, provided the original author(s) and the copyright owner(s) are credited and that the original publication in this journal is cited, in accordance with accepted academic practice. No use, distribution or reproduction is permitted which does not comply with these terms.

The process of nitrogen-adaptation root endophytic bacterial rather than phosphorus-adaptation fungal subcommunities construction unveiled the tomato yield improvement under long-term fertilization

Xiaoxia Li[1,2,3], Muhammad Awais[1,2,3], Shuang Wang[1,2,3,4], Zhu Zhang[1,2,3], Shuning Zhao[1,2,3], Yufeng Liu[1,2,3], Zhouping Sun[1,2,3]*, Hongdan Fu[1,2,3]* and Tianlai Li[1,2,3]

[1]College of Horticulture, Shenyang Agricultural University, Shenyang, China, [2]Key Laboratory of Protected Horticulture of Education Ministry and Liaoning Province, Shenyang, China, [3]National and Local Joint Engineering Research Center of Northern Horticultural Facilities Design and Application Technology, Shenyang, China, [4]College of Agriculture, Eastern Liaoning University, Dandong, Liaoning, China

Interactions between endophytes (endophytic bacteria and fungi) and plants are crucial in maintaining crop fitness in agricultural systems, particularly in relation to abundant and rare subcommunities involved in community construction. However, the influence of long-term fertilization on heterogeneous rhizosphere nitrogen and phosphorus environments and how these conditions affect the key subcommunities of root endophytes and their community assembly mechanisms remain unclear. We studied the 26th year of a field experiment conducted in a greenhouse with varying levels of nitrogen and phosphorus (CKP0, CKP1, CNP0, CNP1, ONP0, and ONP1) to assess the composition of tomato root endophytes and their impact on yield. We employed 16S rRNA and fungal ITS region amplicon sequencing to investigate the assembly mechanisms of abundant and rare endophytic subcommunities, network correlations, core subcommunity structures, and key species that enhance crop yield. The results indicated that organic manure and phosphorus fertilizers significantly increased the rhizosphere soil nitrogen content, phosphorus content, and phosphorus availability (labile P, moderately labile P, and non-labile P). These fertilizers also significantly affected the composition (based on Bray-Curtis distance) and community assembly processes (βNTI) of endophytic microbial subcommunities. The assembly of both bacterial and fungal subcommunities was primarily governed by dispersal limitation, with community structures being significantly regulated by the content of rhizosphere soil available nitrogen (AN) and moderately labile P (MLP). Rare bacterial and fungal subcommunities complemented the ecological niches of abundant subcommunities in the co-occurrence network, supporting community functions and enhancing network stability. Nitrogen-adapting abundant and rare bacterial subcommunities provided a stronger predictive correlation for tomato yield than phosphorus-adapting fungal subcommunities. Additionally, three core genera of rare endophytic bacteria such as *Arthrobacter*, *Microbacterium*, and *Sphingobium* were identified as potentially



GRAPHICAL ABSTRACT

involved in improving crop yield improvement. These findings revealed the distinct assembly mechanisms of endophytic microbial subcommunities affected by fertilization, enhancing our understanding of better management practices and controlling endophytes to improve crop yield in intensive agricultural ecosystems.

KEYWORDS

endophyte, community assembly, abundant microbial taxa, rare microbial taxa, solar greenhouse

1 Introduction

Endophytes are a group of living microorganisms that can successfully colonize various plant tissues without causing disease symptoms (Adeleke and Babalola, 2021; Santoyo et al., 2016). Plants develop complex coexistence and mutualistic relationships with various endophytes (Battu and Ulaganathan, 2020; Harman and Uphoff, 2019) due to the essential functions provided by these endophytes, such as nutrient acquisition (Bolan, 1991; Burragoni and Jeon, 2021; Xie et al., 2024), stress tolerance (Ali et al., 2014; Battu and Ulaganathan, 2020; Harman and Uphoff, 2019; Zhang et al., 2024), and disease suppression (Adeleke et al., 2021; Card et al., 2016; Omomowo and Babalola, 2019; Sena et al., 2024). The mutualistic benefits between plants and endophytes also depend on the genetic and environmental conditions of the host (Meng et al., 2022). In particular, plant root endophytes are inherited through host genes and successfully colonize after filtrating through rhizosphere microorganisms (Meng et al., 2022; Xie et al., 2024). Hence, plant root endophytes exhibit survival strategies similar to those of rhizosphere soil microorganisms, offering significant benefits for healthy plant growth and improved yield (Guo et al., 2024; Harman and Uphoff, 2019). Root endophyte symbiosis, which improves plant adaptability under stress conditions, is increasingly important. Notably, some root endophytes have developed strategies to adapt to the unique soil dynamic environments (Beltran-Garcia et al., 2021; Byregowda et al., 2022; Collavino et al., 2020; Edwards et al., 2015). For instance, root endophytic fungi play fundamental ecological roles in substituting phosphorus strategies in non-mycorrhizal crops or nitrogen availability (Mehta et al., 2019; Sindhu et al., 2024; Sun et al., 2022; Xie et al., 2024). These root endophytes served as a more accurate and effective microbial indicators for evaluating plant resistance to environmental disturbances (Rani et al., 2022; Sun et al., 2021). Although the understanding of microbial community composition in different soil environments has rapidly increased, it remains unclear whether the resistance of root endophytic bacteria and fungi to soil environments influences their beneficial effects on crop yield.

In the natural ecosystem, local microbial communities generally comprise a few dominant species (abundant taxa) and numerous low-abundance species (rare taxa) (Ma et al., 2024; Zheng et al., 2021). The assembly dynamics of abundant and rare taxa in different ecosystems are complex and inconsistent (Gschwend et al., 2021), especially in the context of soil nutrient imbalance in agricultural ecosystems, where they exhibit different distribution patterns and functional characteristics (Jiao et al., 2019a; Ma et al., 2022a; Wu et al., 2023). These differences are attributed to varying microbial survival strategies and substrate preferences (Long and Yao, 2020; Wan et al., 2021). Understanding community assembly process is vital for

elucidating the coexistence status among soil microorganisms and preserving species diversity (Chen et al., 2020; Liu et al., 2024). The community assembly process has been categorized into deterministic process, including homogeneous and variable selection, and stochastic process, including homogenizing dispersal, dispersal limitation, and undominated (Chase and Myers, 2011; Stegen et al., 2015). Due to diverse ecological functions and collaborative capabilities of species, the assembly of abundant taxa communities often shows greater stochasticity (Xiong et al., 2020), which underpins the overall stability of the microbial community (Wan et al., 2021). Rare taxa, with high genetic diversity, can adapt to specific environments and play key roles in stabilizing microbial communities and ecosystem functions (Cui et al., 2023; Jia et al., 2022; Ma et al., 2024; Xue et al., 2020; Yu et al., 2024; Zhang et al., 2023). Some key taxa variations of the rare subcommunity have shown ecological potential for mediating microbial interactions, dominating community stability, and contributing to the complexity of symbiotic networks (Jousset et al., 2017; Liang et al., 2020; Xiong et al., 2020). Changes in the proportion and diversity of abundant and rare endophytic subcommunities inevitably affect the stability and ecological function of endophytic communities (Xi et al., 2024; Xiong et al., 2020; Zhang et al., 2024). Thus, understanding the distribution characteristics, assembly processes, and symbiosis patterns of abundant and rare subcommunities is crucial for examining how long-term fertilization affects endophytic microbial diversity and ecological stability.

The use of excessive inorganic nitrogen and phosphorus fertilizers in greenhouse cultivation, driven by yield and economic benefit, is a widespread practice (Wang et al., 2022; Zhang et al., 2017). This practice has led to excessive nutrient accumulation in the soil (Han et al., 2015; Tian et al., 2022) and exacerbated the negative effects on soil microbial community assembly (Bai et al., 2022; Banerjee et al., 2019; Liu et al., 2023b). Traditionally, manure has helped mitigate the harmful effects of chemical fertilizers on microbial communities, thereby contributing to the yield (Zhang et al., 2021). This positive and effective agronomic practice may be key to determining facility crop yield and maintaining agricultural sustainability. Increasing evidence suggests that environmental changes, such as variations in soil nitrogen and phosphorus levels, play a significant role in driving niche variation of root endophytic microbial species and determining the assembly process of root endophytic microbial communities (Bai et al., 2022; Long and Yao, 2020; Sindhu et al., 2024). Appropriate nitrogen levels are conducive to the dominant characteristics of endophytic fungi and endophytic bacterial communities, as well as higher diversity and richness (Liu et al., 2023b; Miranda-Carrazco et al., 2022; Sindhu et al., 2024). The composition and structural changes of rice root endophytic bacterial communities are affected by chemical phosphorus fertilizer (Long and Yao, 2020). Differences in the community structure of root endophytic bacteria and fungi in response to fertilization may be closely related to the host's nutrient utilization. Therefore, it is essential to identify external environmental factors, particularly nitrogen and phosphorus availability, that influence the assembly of abundant and rare root endophytic subcommunities and their contribution to the yield. Understanding these factors can shed light on the co-evolution of different niche endophytic subcommunities with plants and help develop targeted strategies to manipulate key subcommunities and species to improve crop yields. In this study, we conducted a long-term experiment with nitrogen, phosphorus, and organic manure application in a solar greenhouse. The aims of this study were to (i) identify the relative contributions of the environmental factors in shaping root endophytes and assess how deterministic and stochastic processes influence abundant and rare subcommunities; and (ii) explore the species traits, ecological functions, and co-occurrence patterns of abundant and rare endophytic microbial taxa. We hypothesized the following: (i) The availability of nitrogen and phosphorus in the rhizosphere soil are potential key environmental variables driving stochastic process (dispersal limitation) in endophytic bacterial and fungal assembly, causing structural changes in subcommunities. (ii) Phosphorus-adapting endophytic fungi may occupy niches that complement nitrogen-adaption endophytic bacterial subcommunities, each contributing to main ecological functions. (iii) Rare bacterial subcommunities provide core species that maintain the stability of the endophytic microbial network and complement the functions of abundant bacterial subcommunities, ultimately enhancing crop yield potential.

2 Materials and methods

2.1 Field site and experimental design

The long-term targeted fertilization experiment was designed in 1996 as a solar greenhouse field at the Shenyang Agricultural University of Liaoning Province, China (41°480 N, 123°250 E). The experimental soil was classified as Glesol (FAO and ISRIC, 1988). The initial basic chemical properties were as follows: pH = 6.75, soil organic matter (SOM) = 24.30 g·kg^{-1}, total P (TP) = 1.37 g·kg^{-1}, available P (AP) = 70.80 mg·kg^{-1}, labile P (LP) = 333.90 mg·kg^{-1}, moderately labile P (MLP) = 364.73 mg·kg^{-1}, non-labile P (NLP) = 1163.38 mg·kg^{-1}, and total N (TN) = 1.16 g·kg^{-1}. The fertilization experiment site has a cropping system of continuous tomato cultivation in spring and autumn every year. The fertilization experiment consisted of six treatments arranged in a completely randomized block design (1.5 * 1.0 * 0.8 m^3 for each pool): (1) CKP0 (unfertilized), (2) CKP1 (chemical phosphorus fertilizer), (3) CNP0 (chemical nitrogen fertilizer), (4) CNP1 (chemical nitrogen plus phosphorus), (5) ONP0 (organic manure), and (6) ONP1 (organic manure plus phosphorus). Each treatment was replicated in three independent cement pools. The fertilizers application rate per year are shown in Supplementary Table S1. Chemical nitrogen fertilizer was applied twice during the tomato whole growing season. Chemical phosphorus fertilizers and organic manure (horse manure obtained 8.69% organic matter, 0.45% total N, and 0.30% total phosphorus) were evenly spread on the surface and incorporated into the plow layer by manual hoeing before planting. The fertilization experiment was conducted in the autumn season of the 26th year from August 2022 to December 2022. Each tomato ("Meisheng") plant had a single branch after pruning, and there were four clusters of fruits on the branch and five fruits per cluster.

2.2 Root and rhizosphere soil sampling

Four rhizosphere soils were randomly collected from each pool and then merged into one rhizosphere soil sample (Bulgarelli et al., 2012). Four tomato root samples were randomly collected from each pool, washed, and merged into one root sample, which was stored in sterilized

1 × PBS (pH = 7.0). All samples were promptly transported to the laboratory. The rhizosphere soil samples were stored at −80°C, while root samples for processed further to prepare for the isolation of root endophytic fungi and bacteria. A total of 2.0 g mixed roots of each sample were surface sterilized in 75% ethanol (1 min), 3.25% sodium hypochlorite (3 min), and 75% ethanol (30 s), followed by three rinses in distilled water (Guo et al., 2000). Root samples were then stored in liquid nitrogen immediately. The key difference was that all solutions used were sterile and the last sterile washed water of each root sample was placed in a PDA medium for 1 week at 28°C to confirm the effectiveness of surface sterilization. A total of 36 experimental samples, including 18 rhizosphere soil samples and 18 root samples (6 treatments × 3 duplicates), were stored at −80°C for subsequent DNA extraction.

2.3 Soil chemical parameters determination

Soil pH was measured using 1:2.5 (w/v) soil-to-water suspension. Soil organic carbon (SOC) was determined using the H_2SO_4-$K_2Cr_2O_7$ oxidation capacity method (Mebius, 1960). Available phosphorus (AP) was determined through 0.5 M $NaHCO_3$ extraction, while total phosphorus (TP) was measured through H_2SO_4-$HClO_4$ digestion. Soil phosphorus fractions were prepared and analyzed as reported by Hedley et al. (1982) and Tiessen and Moir (1993). These phosphorus fractions were classified into LP (resin-Pi, $NaHCO_3$-Pi, and $NaHCO_3$-Po), MLP (NaOH-Pi and NaOH-Po), and NLP (HCl-Pi, concentrated HCl-Pi, concentrated HCl-Po, and residual P) (Maranguit et al., 2017; Shi et al., 2023). Total nitrogen (TN) was quantified using an automatic Kjeldahl distillation–titration method (Cabrera and Beare, 1993). Available nitrogen (AN) was measured using the alkali-hydrolyzed diffusion method, while soil nitrate (NO_3^--N) and ammonium (NH_4^+-N) were quantified using a flow-injection autoanalyzer (Skalar San^{++} CFA, Erkelenz, Germany) (Bornemisza et al., 1988).

2.4 DNA extraction and high-throughput sequencing

Total DNA was isolated from 0.5 g of pooled root samples (which were created by randomly collecting four surface-sterilized roots and mixing them into a single sample from each pool) using the CretMag™ Plant DNA Mini Kit: CretBiotech, Suzhou, China, following the manufacturer's instructions. The DNA samples obtained from root samples were amplified using PCR with specific primer sets that included adaptors and barcodes. Fungal ITS1 region amplification was as follows: ITS1F (5′-CTTGGTCATTTAGAGGAAGTAA-3′) and ITS2 (5′- GCTGCGTTCTTCATCGATGC-3′). *16S rDNA* gene V5-V7 region amplification was as follows: 799F (5′- AACMGGATTAG ATACCCKG-3′) and 1193R (5′-ACGTCATCCCCACCTTCC-3′) (Liu et al., 2023b). Additionally, to ensure efficiency and accuracy, PCR amplification was performed using TaKaRa Premix Taq® Version 2.0 (TaKaRa Biotechnology Co., Dalian, China), and the reactions took place in the thermocycler PCR system BioRad S1000 (Bio-Rad Laboratory, CA) under the following thermal cycling program for fungi: 95°C/3 min (initial denaturation) followed by 34 cycles of 95°C/20 s, 56°C/20 s, 72°C/30 s, 72°C/5 min (final extension), and lastly held at 12°C. The following thermal cycling program for bacteria is as follows: 98°C/30 s (initial denaturation) followed by 32 cycles of 98°C/10 s, 53°C/20 s, 72°C/30 s, 72°C/2 min (final extension), and lastly hold at 12°C. The PCR mixtures for fungi contain 25 μL of 2 × ES Taq MasterMix(Dye), 2 μL of forward primer (10 μM), 2 μL of reverse primer (10 μM), 50 ng of template DNA, and ddH_2O added to a final volume of up to 50 μL. The PCR mixtures for bacteria contain 25 μL of Q5, 5 μL of forward primer (10 μM), 5 μL of reverse primer (10 μM), 50 ng of template DNA, and ddH_2O added to a final volume of up to 50 μL. PCR reactions were performed in triplicate. DNA integrity of isolated DNA was visually inspected using 1.5% agarose gel electrophoresis, and DNA concentration and volume were determined using the NanoDrop2000 (Thermo Fisher Scientific, United States) (For detailed information, refer Supplementary Table S2). During the PCR process, negative controls with water and positive control tests were set. After comparing the concentration of PCR products, the required volume of each sample was calculated based on the principle of equal mass, and the PCR products were mixed accordingly. Target strips were cut and purified using the E.Z.N.A.® Gel Extraction Kit (Omega, United States) and quantified using GeneTools Analysis Software (Version4.03.05.0, SynGene), following the manufacturer's instructions. The cDNA library was constructed using the NEBNext® Ultra™ II DNA Library Prep Kit for Illumina® (New England Biolabs, United States), according to the manufacturer's instruction. Purified amplicons were pooled in equimolar and paired-end sequenced by the Shanghai Biotree Biotech Co., Ltd. (Shanghai, China) on the Illumina HiSeq PE250 sequencing platform. The resulting paired sequence reads were merged, trimmed, filtered, and clustered into zero-radius operational taxonomic units using USEARCH (version 0.2.7) with a sequence similarity threshold of 0.97 (Edgar, 2016a; Rognes et al., 2016). The UNITE (ITS) database and the Ribosomal Database Project (RDP) (16S) database were used for taxonomical alignment at a threshold of 0.8 using the SINTAX algorithm (Edgar, 2016b). These databases were used to align multiple sequences, remove annotation for chloroplasts or mitochondria, analyze the phylogenetic relationship between different operational taxonomic units (OTUs), and investigate the differences between the dominant microbial community species across different groups. All of raw reads data are available in the NCBI Sequence Read Archive (SRA) database (Accession Number: PRJNA1182544).

2.5 Data analyses

A one-way ANOVA ($p < 0.05$) test was performed to analyze differences in the rhizosphere soil environment factors, yield, and the dominant microbial abundances among different fertilizations using IBM SPSS Statistics (version 22.0, IBM Corporation, Armonk, N.Y., United States) software. The analysis of microbial subcommunity characteristics were performed using R software (version 4.3.0), and some histograms were generated using Origin 2024. Abundant and rare OTUs were defined based on cutoffs above 0.1% and below 0.01% of total sequences, as described in previous studies (Jiao et al., 2017; Jiao and Lu, 2020; Zheng et al., 2021). The "abundant subcommunity" included OTUs with a mean relative abundance >0.1% in root endophytic bacterial and fungal communities across all samples, while the "rare subcommunity" included OTUs with a mean relative abundance <0.01%. The relative abundance of bacterial and fungal subcommunities at the phylum level was constructed using the

"*microtable*" package in R (Liu et al., 2020). The Kruskal–Wallis test for α-diversity indexes (Shannon and Richness), non-metric multidimensional scaling (NMDS), and analysis of similarities (ANOSIM) were performed using the "*vegan*" package in R (Liu et al., 2015; Oksanen et al., 2012; Yu et al., 2024). The beta diversity was analyzed using the "*betapart*" package in R (Baselga and Orme, 2012). In this study, the Bray–Curtis-based Raup-Crick (RCbray) and the β-nearest taxon index (βNTI) were used to calculate the variations in phylogenetic and taxonomic diversity using the "comdistnt" function from the "*picante*" R package (Jiao and Lu, 2020). Quantitatively, the proportion of inferred bacterial and fungal subcommunity assembly ecological processes in root endophytes was analyzed using a phylogenetic bin-based null model analysis (with 999 randomizations), implemented via the "icamp.big" function in R (Ma et al., 2022a; Ning et al., 2020; Wu et al., 2023). Both homogeneous and variable selections were considered as forms of species sorting (deterministic process) (Jiao et al., 2019b). Based on the co-occurrence networks to explore the interrelationships of all OTUs in bacterial and fungal subcommunities, except for the rare and abundant subcommunities, the remaining OTUs were classified as "Others." Robust correlations were identified using Spearman's correlation coefficients (r) > 0.6 and false discovery rate-corrected p values <0.05 (p value corrected by FDR multiple test). These metrics were applied to construct random networks of root endophytes and four endophytic subcommunities using the "*igraph*" package in R (Hartman et al., 2018; Jiao et al., 2019b). The topological characteristics of the networks were calculated based on the following metrics: average clustering coefficient, average connectivity, average path distance, and modularity. Furthermore, the keystone species for endophytic subcommunity networks were identified based on the threshold values of Zi (measuring how well a node was connected to other nodes within its module) and Pi (measuring how well a node was connected to nodes between different modules), set at 2.5 and 0.62, respectively (Guimerà and Nunes Amaral, 2005; Lang et al., 2021; Liang et al., 2016; Wu et al., 2023). To identify the key root endophytic subcommunity and taxa predictors for yield, the "*randomForest*" package in R was used, and each predictor was assessed using the "*rfPermute*" package. A Mantel test was conducted to determine the correlation between community composition and rhizosphere soil environment factors. A structural equation model (SEM) was analyzed using IBM SPSS Amos 26 to quantify the direct and indirect effects of the rhizosphere environment factors (such as pH, AN, and MLP) and the α and β diversities of the bacterial subcommunities on the yield. All variables were standardized using Z transformation (mean = 0, standard deviation = 1) with the 'scale' function in the R package. The maximum likelihood method was employed to fit the model (Jin et al., 2020). The standardized total effects (STEs) of the rhizosphere soil nutrients and root endophytic bacterial subcommunities on the yield were calculated.

3 Results

3.1 Response of the rhizosphere soil physicochemical parameters to long-term fertilization

Long-term fertilization significantly increased the total nutrient content of the rhizosphere soil excluding NH_4^+-N (Table 1). The contents of SOC, TN, AN, and NO_3^--N significantly increased in ONP0 and ONP1, by 175%–214%, 71%–84%, 362%–506%, and 956%–1,672%, respectively, compared with CKP0. Different fractions of phosphorus increased with the application of phosphorus and organic manure, with the highest increases in the contents of TP, AP, LP, and NLP observed in ONP1, by 284%, 426%, 330%, and 155%, respectively. The MLP content in ONP1, CKP1, and CNP1 significantly increased by 539%, 587%, and 756%, respectively, compared to CKP0. Soil pH significantly decreased across all treatments compared to CKP0, except in ONP0.

3.2 Response of the endophytic microbial subcommunity characteristics to long-term fertilization

In tomato roots, the total number of 3,122 bacterial OTUs and 487 fungal OTUs were observed (Supplementary Table S3). A high

TABLE 1 Effects of long-term fertilization on rhizosphere soil physicochemical parameters.

Treatment	CKP0	CKP1	CNP0	CNP1	ONP0	ONP1
pH (1:2.5 v/w)	7.19 (0.04)a	6.87 (0.04)c	6.84 (0.03)c	6.56 (0.08)d	7.21 (0.02)a	7.00 (0.01)b
SOC (g kg^{-1})	7.85 (0.58)c	8.51 (0.27)c	7.18 (0.40)c	7.58 (0.00)c	21.55 (1.06)b	24.61 (0.53)a
TP (g kg^{-1})	1.12 (0.03)d	3.32 (0.14)b	0.99 (0.01)d	3.30 (0.08)b	1.85 (0.03)c	4.29 (0.15)a
AP (mg kg^{-1})	31.46 (1.51)b	135.94 (2.59)a	23.23 (2.13)b	142.70 (3.58)a	150.11 (13.13)a	165.59 (18.73)a
LP (mg kg^{-1})	247.81 (10.59)e	929.73 (52.35)b	144.42 (14.57)e	801.18 (28.33)c	526.76 (30.63)d	1064.73 (64.31)a
MLP (mg kg^{-1})	163.60 (13.65)c	1125.49 (51.67)b	179.21 (6.61)c	1401.08 (140.42)a	272.29 (8.23)c	1046.20 (64.63)b
NLP (mg kg^{-1})	1132.53 (45.66)c	1906.99 (109.87)b	1000.73 (50.06)c	1671.50 (76.37)b	1518.79 (87.28)b	2884.05 (251.78)a
TN (g kg^{-1})	1.45 (0.15)b	1.29 (0.07)b	1.41 (0.04)b	1.48 (0.04)b	2.49 (0.10)a	2.68 (0.09)a
AN (mg kg^{-1})	9.33 (2.54)c	21.00 (1.75)bc	19.83 (2.33)bc	27.42 (4.21)bc	43.17 (15.47)ab	56.58 (7.10)a
NO_3^--N (mg kg^{-1})	0.80 (0.21)d	1.18 (0.19)d	1.61 (0.52)d	19.51 (0.06)a	8.42 (1.96)c	14.12 (0.56)b
NH_4^+-N (mg kg^{-1})	1.43 (0.29)a	1.16 (0.12)a	1.20 (0.13)a	1.87 (0.42)a	1.78 (0.39)a	1.27 (0.09)a

The pH, SOC, TP, AP, LP, MLP, NLP, TN, AN, NO_3^--N, and NO_4^+-N refer to rhizosphere soil pH, soil organic carbon, total phosphorus, available phosphorus, labile phosphorus, moderately labile phosphorus, non-labile phosphorus, total nitrogen, available nitrogen, nitrate nitrogen, and ammonium nitrogen, respectively. Lowercase letters denote significant differences based on the Duncan's one-way analysis of variance among different treatments ($n = 3$, $p < 0.05$).

percentage of OTUs were recognized as rare taxa, constituting rare subcommunities of bacteria and fungi. These rare taxa represented an average of 84.30% and 55.44% of bacterial and fungal OTUs, respectively, but contributed only 6.04% and 0.91% to the average relative abundance in all samples. Conversely, abundant bacterial and fungal taxa constituted a small proportion of OTUs with mean values of 2.85% and 8.00% but accounted for 81.01% and 94.07% of the average relative abundance in all samples, respectively. The rare bacterial subcommunity exhibited higher α-diversity, in terms of both richness and Shannon indexes, compared to the abundant subcommunity under the same treatments. The rare fungal subcommunity showed only a higher Shannon index compared to abundant subcommunity under the same treatments (Figure 1). The Shannon index of abundant bacterial and fungal subcommunities significantly decreased in CNP0 and ONP0 compared to CKP0 ($p < 0.05$; Figures 1A,C). The richness of abundant and rare fungi in CNP1 and ONP0 also significantly decreased compared to CKP0 ($p < 0.05$; Figures 1G,H). There was no significant difference in the Shannon index of rare bacterial and fungal subcommunities or the richness of abundant and rare bacterial subcommunities across other treatments, compared to CKP0 ($p < 0.05$; Figures 1B,D–F).

Root endophyte OTUs were classified into 10 bacterial and five fungal phyla, excluding unclassified sequences. The abundant bacterial subcommunity was predominantly Proteobacteria (2.81%–54.50%), whereas the rare bacterial subcommunity was also dominated by Proteobacteria (22.15%–36.75%) (Figures 2A,B). The relative abundance of Proteobacteria in the abundant bacterial subcommunity was significantly decreased by nitrogen application (CNP0 and ONP0) compared to CKP0 ($p < 0.05$; Supplementary Table S4). The relative abundance of Actinobacteriota, Chloroflexi, and Gemmatimonadota in rare bacterial subcommunity was significantly increased in ONP1, CNP1, and CNP1, respectively, compared to CKP0 ($p < 0.05$; Supplementary Table S4). The relative abundance of Acidobacteriota was significantly increased in CKP1, CNP0, and CNP1 compared to CKP0 ($p < 0.05$; Supplementary Table S4). The abundant fungal subcommunity was dominated by Ascomycota (0.8%–13.36%) (Figure 2C), while the rare fungal subcommunity was dominated by Ascomycota (25.23%–51.43%) and Basidiomycota (8.8%–29.63%) (Figure 2D). There was no significant difference in the relative abundance of endophytic fungal phyla among different treatments ($p < 0.05$; Supplementary Table S4). The NMDS analysis of Bray–Curtis distances revealed a distinct separation of all OTUs composition between treatments (beta-diversity). This revealed a clear separation between treatments of the bacterial and fungal subcommunities (Figures 2E–H). The ANOSIM analysis further indicated that the composition of bacterial subcommunity significantly varied with N levels, whereas the composition of the fungal subcommunity significantly varied with P levels rather than among different treatments ($p \leq 0.05$; Supplementary Table S5).

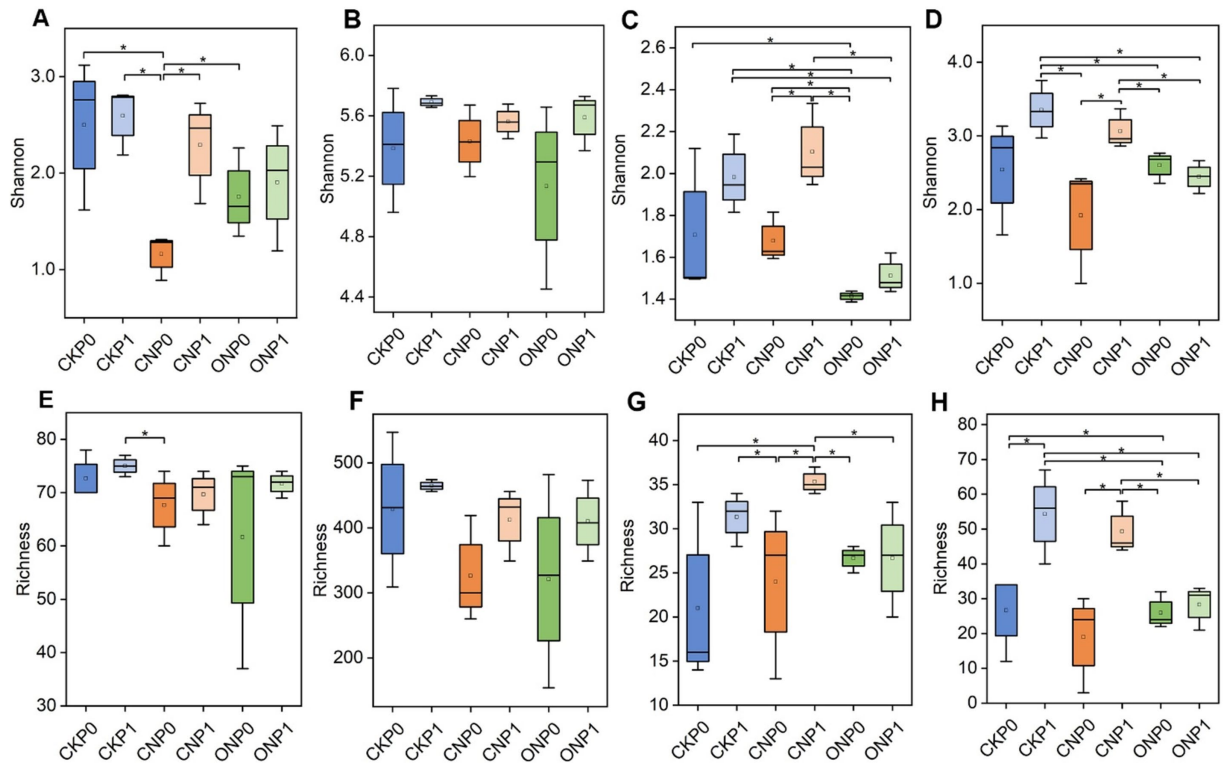


FIGURE 1
Shannon and richness indexes of root endophytic abundant bacteria **(A,E)**, rare bacteria **(B,F)**, abundant fungi **(C,G)**, and rare fungi **(D,H)** under different treatments. CKP0, Unfertilized; CKP1, Chemical phosphorus applied; CNP0, Chemical nitrogen applied; CNP1, Chemical nitrogen plus phosphorus; ONP0, Organic manure supply nitrogen; ONP1, Organic manure supply nitrogen plus phosphorus. *$p < 0.05$, as tested by multiple comparisons using the Kruskal–Wallis test, and only significant differences are displayed. The treatment denotations are the same as those in Figure 1.

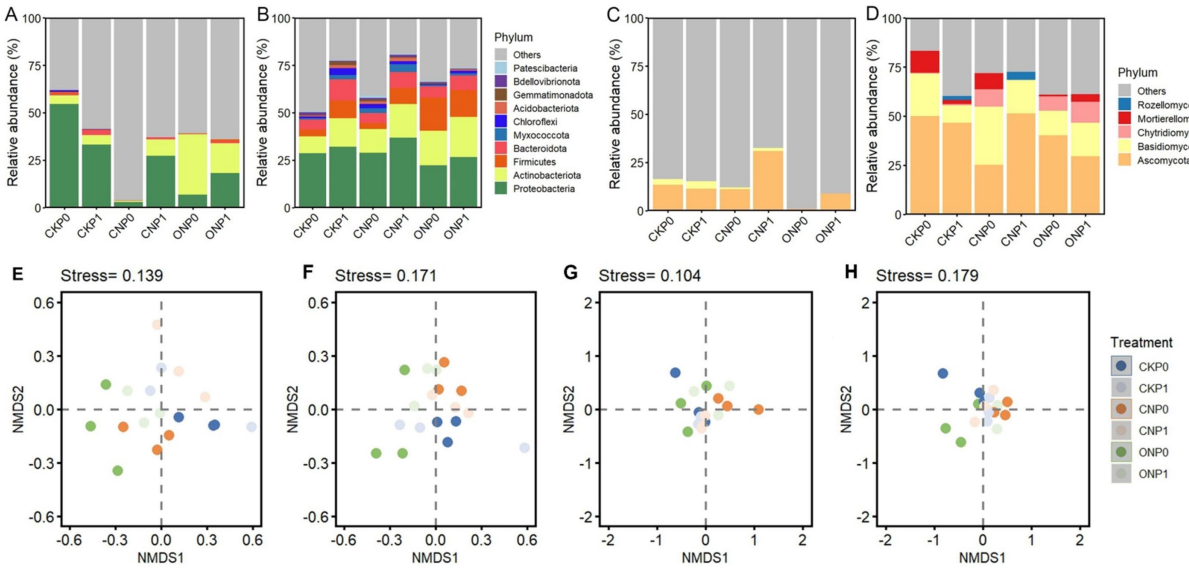


FIGURE 2
Subcommunity composition at the phylum level and non-metric multidimensional scaling (NMDS) plots of root endophytic abundant bacteria **(A,E)**, rare bacteria **(B,F)**, abundant fungi **(C,G)**, and rare fungi **(D,H)** under different treatments. Unclassified bacterial and fungal OTUs were labeled as "Others." The treatment denotations are the same as those in Figure 1.

3.3 Community assembly of root endophytic abundant and rare microbial subcommunities

β-nearest taxon index values were used to quantify the relative contributions of ecological processes in different fertilization treatments (Figures 3A–D). A significant discrepancy in βNTI values of rare fungal and abundant bacterial subcommunities was caused by different N and P levels, respectively ($p \leq 0.05$). There was no significant discrepancy in βNTI of different microbial subcommunities under different treatments and were all between −2 and + 2. Furthermore, the null model analysis revealed that the ecological assembly of root endophytic abundant and rare subcommunities varied with different treatments. Phosphorus levels mainly governed the abundant bacterial subcommunity through dispersal limitation (23.42%–96.79%), which, and an undominated process (0%–76.58%), which gradually increased ($p < 0.05$; Figures 3A,E). Dispersal limitation (12.26%–50.22%) and undominated (39.82%–77.72%) processes mainly governed the rare bacterial subcommunity (Figure 3F). The abundant fungal subcommunity was entirely governed by stochastic processes, mainly shaped by the undominated process in CKP0, CNP0, and ONP0 and increase dispersal limitation process in P level (CKP1, CNP1, and ONP1) (Figure 3G). The rare fungal subcommunity was mainly governed by nitrogen levels through decreased dispersal limitation (13.73%–72.07%) and increased undominated process (24.82%–84.56%) (Figure 3H). In summary, the assembly of abundant bacterial, abundant fungal, and rare fungal subcommunities was governed by dispersal limitation and undominated processes, while stochastic processes dominated the rare bacterial subcommunity and gradually replaced deterministic processes completely under different treatments (Figure 3).

3.4 Keystone species and network topological properties of endophytic microbial subcommunities

Co-occurrence networks under different treatments revealed that the endophytic rare subcommunities, with a higher number of nodes, played a more important role than abundant subcommunities (Figures 4A–F). Rare bacterial nodes accounted for 53.88% to 58.80%, whereas abundant bacterial nodes accounted for only 3.92% to 5.57%. Rare fungal nodes accounted for 4.02% to 7.50%, whereas abundant fungal nodes accounted for 2.10% to 3.03%. A co-occurrence network was also constructed for root endophytic abundant and rare subcommunities that conformed to the power-law distribution (Supplementary Figure S2). We observed that the numbers of nodes, edges, and average degree in the root endophytic microbial network decreased with nitrogen application (CNP0, CNP1, ONP0, and ONP1), while the modularity increased and the graph density decreased with phosphorus application (CKP1, CNP1, and ONP1) (Supplementary Figure S1). The observed potential interactions at root endophytes were predominantly positive, accounting for 78.12%–87.38% of the total linkages (Figure 4). The proportion of negative correlations in the root endophytic network of ONP1 was the highest (21.88%) compared to CKP0 (Figure 4F).

Nitrogen application reduced the modularity and average path length of the abundant bacterial subcommunity network, while increasing the clustering coefficient and average path length and reducing the average degree in the rare bacterial subcommunity network. Phosphorus application increased the modularity and average path length in the network of the abundant fungal subcommunity, while decreasing the clustering coefficient. In the rare fungal subcommunity, phosphorus application increased the clustering coefficient and average degree, but decreased the modularity and average path length (Supplementary Table S6). The topological

10.3389/fmicb.2024.1487323

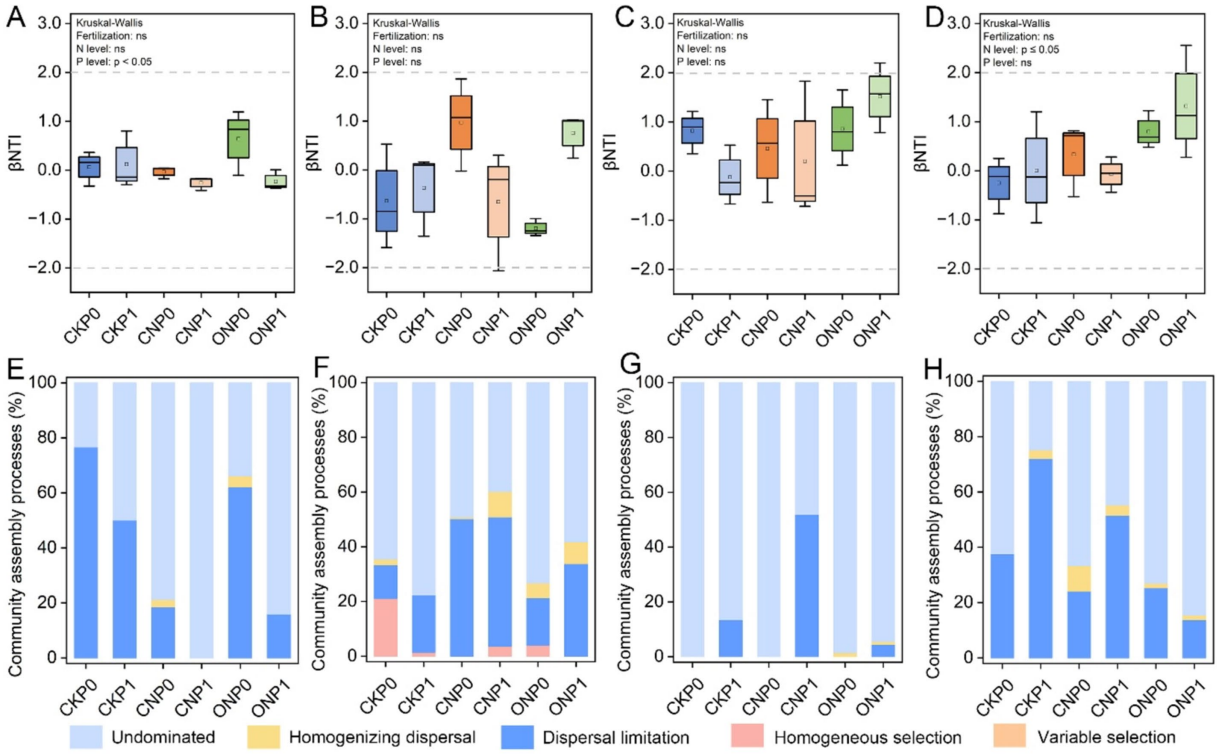


FIGURE 3
Root endophytic bacterial and fungal subcommunities assembly processes (based on *β*NTI and RCBray). βNTI of root endophytic abundant bacteria **(A)**, rare bacteria **(B)**, abundant fungi **(C)**, and rare fungi **(D)** subcommunities. Proportions of deterministic and stochastic assembly processes in governing root endophytic abundant bacteria **(E)**, rare bacteria **(F)**, abundant fungi **(G)**, and rare fungi **(H)** subcommunities under different treatments.

roles of the individual subcommunity network nodes were shown in a Zi-Pi plot (Figure 5). Peripherals were completely occupied by total nodes in abundant bacterial and abundant fungal subcommunities (Figures 5A,C). We found a total of 63 keystone species in the root endophytic rare bacterial subcommunity network; one was identified as a module hub, while the remaining species served as connectors (Figure 5B). These keystone species play a significant role (2.45%) in the network, and they mainly belong to *Proteobacteria*, *Actinobacteriota*, *Bacteroidota*, *Firmicutes*, *Myxococcota*, *Chloroflex*, *Acidobacteriota*, and *Gemmatimonadota* (Supplementary Table S7). These phyla were highly enriched under ONP1, followed by CKP1. Two keystone species belonging to Ascomycota played a 0.85% role in the rare fungal subcommunity network (Figure 5D; Supplementary Table S7).

3.5 Specific subcommunity composition and taxa as predictors of yield under long-term fertilization

Compared with the CKP0, fertilization treatments significantly increased the yield except CKP1 ($p < 0.05$; Figure 6A). The random forest regression model was used to identify the structure of the root endophytic subcommunity, including abundant bacteria, rare bacteria, abundant fungi, and rare fungi that could predict the yield across different fertilization treatments (Figure 6B). The structure of abundant bacteria and rare bacteria significantly contribute to yield ($p < 0.05$; Figure 6B). Moreover, the structure of the abundant bacterial subcommunity explained 22.03% of yield variation, whereas the rare bacterial subcommunity accounted for 3.09% (Figure 6B). Additionally, the structures of bacterial subcommunities were positively related to AN content ($p < 0.05$; Figure 6B). On the contrary, abundant fungi and rare fungi were positively associated with soil phosphorus especially MLP ($p < 0.01$; Figure 6B), and both of them have no significant positive contribution to yield (Figure 6A). These four subcommunities, except the abundant subcommunity, were negatively correlated to soil pH ($p < 0.05$; Figure 6B). The random forest regression model further predicted the top 10 genera of the rare subcommunity (54.93%) had a greater impact than on yield variation compared to those in the abundant subcommunity (19.32%), indicating that they are more important drivers to yield variation (Figure 6). No key role genus of abundant subcommunity was identified from network, though top 10 abundant genus could predict the yield variation (Figure 6C; Supplementary Table S7). Three keystone species *Arthrobacter*, *Microbacterium*, and *Sphingobium* have been found in the rare microbial subcommunity. These species contribute to increased yield in response to soil nutrient changes and also serve as connectors in the network (Figure 6D; Supplementary Table S7).

Structural equation model was employed to quantify the correlations among key soil characters (AN, pH, and MLP) in

10.3389/fmicb.2024.1487323

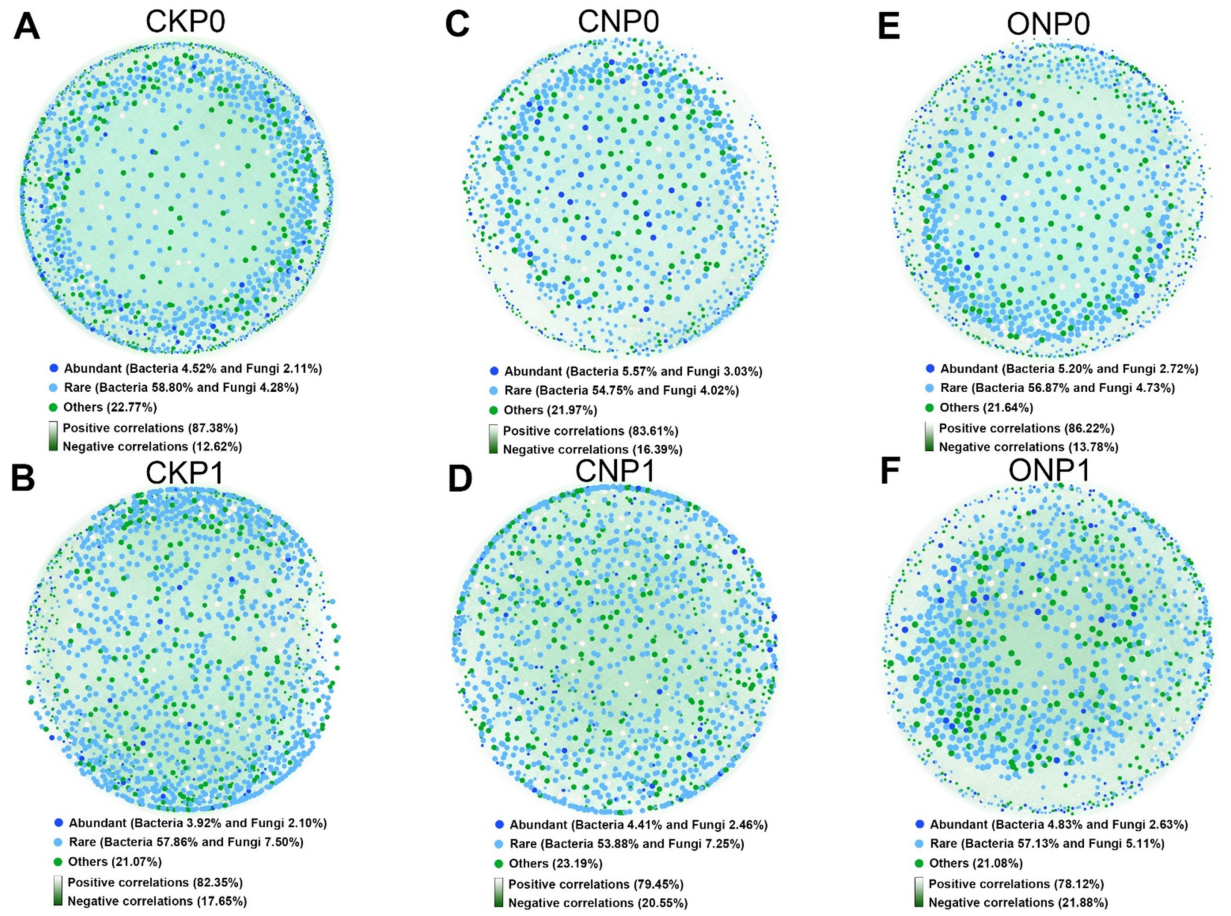


FIGURE 4
Co-occurrence networks of bacterial and fungal coexistence communities under different fertilizations **(A–F)**. The networks were established by calculating correlations among abundant, rare, and other OTUs.

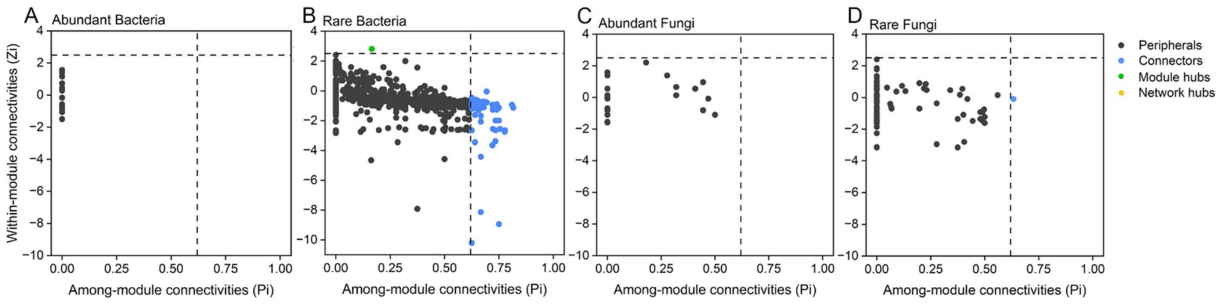


FIGURE 5
Distributions of network roles by analyzing module features, within-module connectivities (Zi) and among-module connectivities (Pi), in the endophytic abundant bacterial **(A)**, rare bacterial **(B)**, abundant fungal **(C)**, and rare fungal **(D)** co-occurrence networks of root, respectively.

response to amounts of N and P fertilizers, the most important root endophytic bacterial subcommunities, and yield (Figure 7). The soil AN, pH, and MLP explained much more variation of the β-diversity ($r^2 = 0.47$) than α-diversity ($r^2 = 0.30$) in abundant bacterial subcommunity, but much more variation of α-diversity ($r^2 = 0.54$) than β-diversity ($r^2 = 0.38$) in rare bacterial subcommunity. Soil AN had a positive direct and indirect effect by influencing the β-diversity of abundant and rare bacterial subcommunity on yield. It should be noted that the α-diversity of abundant and rare bacterial subcommunities showed no direct effect on yield. The contrasting results were observed for yield, being directly negatively affected by pH and MLP, while through the α-diversity of rare bacteria directly related to MLP (Figure 7A). The soil pH and MLP had a positive effect and AN had a negative effect on the α-diversity of abundant and rare

10.3389/fmicb.2024.1487323

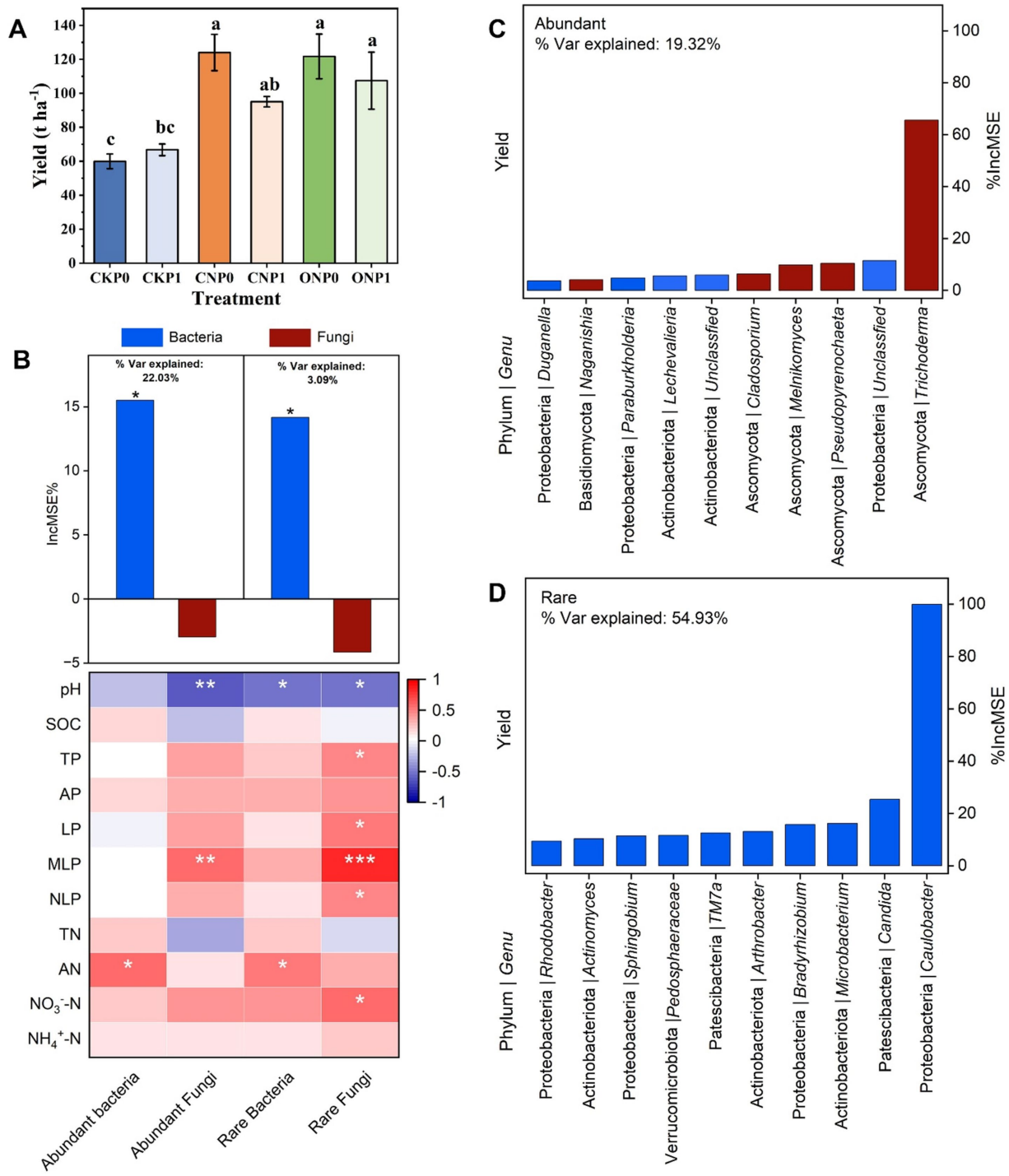


FIGURE 6
Changes in tomato yield **(A)**. The random forest regression model shows the root endophytic subcommunity structures as drivers of yield. A correlation between the structure of microbial subcommunities and soil nutrients was identified using Spearman's test **(B)**. The random Forest regression model identifies the top 10 most important taxa of abundant **(C)** and rare **(D)** subcommunities at the genus level, along with their respective phylum, as key drivers of tomato yield. The bars illustrate the increase in mean squared error (%IncMSE) scores for the contribution of root endophytes at the genus level among six fertilization treatments, affecting the tomato yield. Significance levels are denoted with $*p < 0.05$, $**p < 0.01$, and $***p < 0.001$.

subcommunities, but its effects were contrary on the β-diversity of abundant and rare bacterial subcommunities. The soil AN was found to have the largest standardized positive effect on yield, followed by the β-diversity of abundant and rare bacterial subcommunities, while the contribution of the abundant bacterial β-diversity was greater compared to that of the rare bacterial β-diversity (Figure 7B).

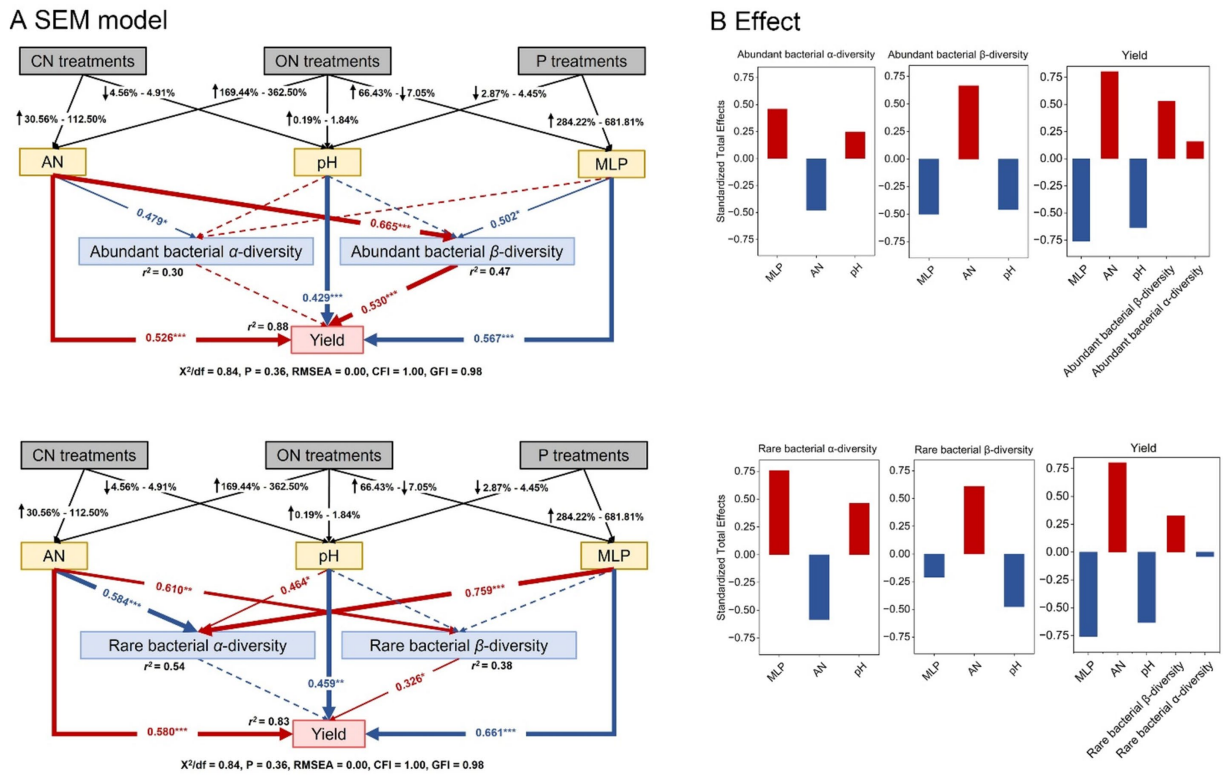


FIGURE 7
Structural equation model (SEM) illustrating how the root endophytic bacterial subcommunities influenced yield by responding to soil AN, pH, and MLP **(A)**. The total standardized effects of these factors on yield, α-diversity (Shannon diversity), and β-diversity are shown **(B)**. Red arrows, black arrows, and dashed arrows indicate the positive significant, negative significant, and nonsignificant relationships between different variables. The width of the arrows indicates the strength of the standardized path coefficient. Adjacent values near the arrows indicate path coefficients. r^2 values indicate the proportion of variance explained by each variable. Significance levels are denoted with $*p < 0.05$, $**p < 0.01$, and $***p < 0.001$.

4 Discussion

4.1 Long-term fertilization affected the construction processes in distribution characters of root endophytes subcommunities

The abundant endophytic bacterial and fungal subcommunities were prevalent in most fertilization treatments with an average relative abundance of 81.01% and 94.07%, respectively. Abundant species may occupy wider niches, competitively utilize more enriched resources, have high growth rates, and effectively adapt to the environment. All of these supported their persistence and their widespread distribution (Jiao and Lu, 2020; Liu et al., 2023a). In addition, the relative abundance of root endophytic rare bacterial and fungal subcommunities that contributed less to the total community abundance was unevenly distributed among different fertilization treatments. The different distribution patterns of root endophytic abundant and rare taxa may be attributed to their distinct life strategies. The rare subcommunities usually exhibited dormancy or low growth rates and competitiveness. Hence, root endophytic microbial subcommunities showed limitations but not extinction in nutrient-enriched environments caused by long-term fertilization (Jia et al., 2018; Jousset et al., 2017). Notably, the rare subcommunities had the highest abundance and diversity compared with abundant subcommunities, which supported the fact that the rare subcommunity was an important contributor to the microbial diversity (du et al., 2020; Li et al., 2021; Lynch and Neufeld, 2015). This trend may be attributed to the fact that a community has a limited capacity and excessive diversity was formed by species competition. Rare taxa can become abundant members of a community in response to favorable environmental conditions (Jia et al., 2022). Few rare species dominated the root samples in our study, but rare bacterial taxa were more susceptible to environmental heterogeneity and with ability to grow fast were affected by nutrient concentration increasing as conditionally rare taxa (Jia et al., 2022; Jiao et al., 2019a). This is possibly due to the selective pressure of resources in the rhizosphere soil environment driving the aggregation of root endophytic rare microbial communities (Liu et al., 2024). It is known that soil environment factors such as carbon, nitrogen, and phosphorus concentrations could across compartments affect root species abundance and interactions (Zhang et al., 2019). These findings suggest that the aggregation process of microbiome with different nutritional strategies can affect the diversity and abundance of endophytic microbial subcommunities (Li et al., 2021; Liu et al., 2023a). Similar evidence has been found in previous studies to explain this change (Dos Santos et al., 2022), where the alpha diversity of endophytic microorganisms increases with the application of fertilizers. However, the α-diversity of fungal subcommunities, especially the α-diversity of the rare fungal subcommunity, was mainly

increased by the application of chemical nitrogen and phosphorus fertilizers in our study ($p < 0.05$). Similarly, we found that different N levels and P levels shaped complex rhizosphere soil nutrient heterogeneity that significantly affected the structure of root endophytic bacterial and fungal subcommunities (Ma et al., 2021; Ma et al., 2022b; Zhang et al., 2019). This may have mediated a richer diversity of the rare subcommunity and enhanced their involvement in nutrient cycling processes between environments (Liu et al., 2023a; Shu et al., 2021).

The microbial community assembly processes, which determine the presence and abundance of species, are generally divided into deterministic and stochastic processes (Feng et al., 2018; Jiao et al., 2019b). The null model suggested that the construction of root endophytic bacterial and fungal subcommunities are mainly dominated by stochastic processes especially dispersal limitation (Zhong et al., 2022). More importantly, the assembly process of abundant and rare subcommunities of endophytic bacteria and fungi exhibited different trade-off patterns, reflecting varying relative contributions in response to changes in nitrogen and phosphorus levels (Xing et al., 2023). The proportion of stochastic processes in microbial community assembly can also increase through the functional redundancy generated by biological interactions and spatial and environmental processes (Li and Gao, 2023). Under different fertilization treatments of nitrogen and phosphorus levels, rhizosphere environmental filtration emphasizes the stochastic process of dispersal limitation, which may be involved in determining the development of different sub community systems, which was a very novel finding. Previous studies have revealed that determinism seems to be related to low nutrient levels, and stochasticity increases with nutrient levels (Chase, 2010; Zhou et al., 2014). Therefore, the current nutritional strategy for microbial community assembly processes may be more important than the priority effects shaped by host selection (Li and Gao, 2023). In particular, as the subcommunity rarity increases, dispersal limitation was more conducive to driving the assembly and construction of root endophytic bacterial and fungal subcommunities in enough nitrogen and phosphorus environments, respectively. This validation showed that rare microbial subcommunities were not a random taxonomic cluster; instead, most of these rare subcommunities show restricted distribution or migratory diffusion (Cui et al., 2023; Liu et al., 2015; Long and Yao, 2020). Compared to rare taxa, more individuals in abundant taxa were likely to be involved in dispersal limitation (Liu et al., 2015), such as abundant bacterial subcommunities in our study. From this perspective, abundant taxa are likely to adopt growth yield or resource acquisition strategies that enable them to outcompete other microorganisms for broader niche space and nutrients (Cui et al., 2023; Delgado-Baquerizo et al., 2018; Dong et al., 2021; Jiao and Lu, 2020; Ma et al., 2022a). Consequently, we concluded that long-term fertilization indeed affected the specific niche differentiation of phosphorus-sensitive fungal and nitrogen-sensitive root endophytic bacterial, both abundant and rare subcommunities (Hamonts et al., 2018; Leach et al., 2017; Niu et al., 2017).

The rare fungal subcommunity exhibited a more intense and significant response to phosphorus than the abundant fungal subcommunity, possibly due to the long-life cycle, low community turnover rate, and differences in metabolic activity and diffusion ability of fungi (Jiao and Lu, 2020; Omomowo and Babalola, 2019). Higher nutrient levels increased the importance of stochastic processes (Chase, 2010; Chen et al., 2020), providing insights into the assembly patterns of root endophytic fungal subcommunities promoted by phosphorus. Nitrogen application maintained the control of the dispersal limitation on the enrichment of both abundant and rare bacterial subcommunities, significantly impacting their structure. Previous studies found that short-term high nitrogen levels have a greater effect on the interactions among endophytic fungal communities in maize than on endophytic bacteria (Bai et al., 2022). We found community assembly processes and ANOSIM analysis suggested that endophytic bacteria respond more strongly to nitrogen fertilizer than endophytic fungi. This difference may be partly because nutrient supplementation reduces the competitive advantage of fungi over bacteria (Michalska-Smith et al., 2022) and increases bacterial abundance (Wu et al., 2019), especially in rare bacterial subcommunity. On the other hand, bacteria rely more on fixed sources of nitrogen and carbon than fungi (Schmidt et al., 2014), and organic fertilizers also compensate for the relative lack of carbon when achieving nitrogen supply in this process. These indicated that these subcommunities were formed by more complex assembly processes, especially rare subcommunities, which may also be important metabolic strategies for microbial cells to cope with environmental pressures and be less susceptible to deterministic processes (Fujii et al., 2012; Lennon and Jones, 2011; Nemergut Diana et al., 2013). It is worth noting that stochastic process plays more importance in community assembly, leading to higher β-diversity of microorganisms and higher yield (Chase, 2010). The altered community aggregation characteristics of different subcommunities of root endophytic bacteria and fungi have improved the overall adaptability of microbial communities to their environment, potentially enhancing our understanding of ecosystem sustainability through various means. Rare subcommunities may serve as sensitive biological indicators for regulating their assembly mechanisms and reflecting environmental change risks, closely related to the composition of the entire endophytic microbial community. They may also be a key factor in enhancing the resistance of microbial networks through functional redundancy (Li et al., 2021; Lynch and Neufeld, 2015).

4.2 Co-occurrence network of root endophytes subcommunities and keystone species response to long-term fertilization

Network analysis has been identified as a powerful tool for exploring the role of microbial symbiotic interactions in coping with environmental stress (Michalska-Smith et al., 2022; Shu et al., 2021). Fertilizations have affected the network structural characteristics, providing insights into how symbiotic patterns of microbe form different endophytic microbial communities (Liu et al., 2023a) and helping to identify potential keystone taxa in network (Wu et al., 2022; Zhong et al., 2022). Our finding indicated that the frequency, intensity, and distribution patterns of OTU interactions within subcommunities of root endophytic bacteria and fungi vary in response to different fertilization treatments, particularly changed with nitrogen and phosphorus levels. These findings are consistent with previous studies, showing that the cross soil and plant compartments of nutrient concentrations significantly altered overall community dynamics by affecting niche differentiation and

colonization of root endophytic bacteria and fungi (Michalska-Smith et al., 2022; Sun et al., 2022; Xu et al., 2022). This niche dispersal selectively recruits microbial subcommunities and formed stable coexistence through root interactions (Ernst et al., 2011). After phosphorus application (CKP1, CNP1, and ONP1), root endophytic microbial communities exhibited higher modularity and lower graph density topological parameters, with an increased proportion of negative cohesion, indicative of a more stable and complex symbiotic pattern. Positive correlations among microbial species have indicated cooperative relationships or niche overlap, while negative correlations have indicated competitive relationships or niche separation (Ernst et al., 2011; Ghoul and Mitri, 2016). Due to higher soil nutrient levels, the highest network complexity and microbial growth diversity have been observed in ONP1, suggesting high nutrient competition among taxa under ONP1 (Deng et al., 2016). This has been verified by the enhanced negative cohesion in the root endophytic symbiotic network under ONP1 (increased by 9.26% and 8.10% compared to CKP0 and ONP0, respectively). Such a complex symbiotic network increased community structure stability, enabling resistance to long-term chemical fertilizer-induced disturbances.

The topological characteristics of the subnetwork indicated that rare subcommunities exhibited more complex and stable symbiotic associations compared to abundant subcommunities (Li et al., 2021). We found that rare bacterial and fungal subcommunities have shown stronger clustering with nitrogen and phosphorus applications, respectively, reflecting the importance of ecological assembly processes and cooperative nutrient metabolism pathways among taxa in the endophytic microbiome (Cui et al., 2023; Fabiańska et al., 2019; Ma et al., 2022b; Sun et al., 2022). The tight associations in the symbiotic network may be the contribution of rare bacterial and rare fungal subcommunities, which were driven by dispersal limitation processes and achieved functional complementarity from different taxonomic compositions. Moreover, under nitrogen level treatments (CN, ON), although the number of nodes and interactions in the subnetwork have decreased, a higher proportion of negative cohesion helped to form more robust competitive relationships and more stable subnetwork, which can be explained by enrichment-dominated and depletion-supplemented patterns (Liu et al., 2024). The complex network structures indicated a more efficient potential for resource and information transmission within the community, allowing it to withstand environmental stress.

Studies have shown that chemical nitrogen fertilizer has significantly affected the structure of root endophytic bacterial communities (Miranda-Carrazco et al., 2022) and reduced the diversity and stability of soil microbial networks (Zhang et al., 2021). Our findings are similar to previous studies, but happened in rare bacterial subnetwork rather than abundant bacterial subnetwork, possibly because the subnetwork structure changes of abundant bacteria have not weakened the core subcommunities or species dominance. Compared to chemical nitrogen fertilizer, long-term organic manure application has likely supported taxonomic groups with similar functions, thereby increasing functional redundancy (Fan et al., 2019). This has a stronger positive effect on maintaining the complexity and stability of the root endophytic bacterial symbiotic network (Zhang et al., 2021), which further enhances the resistance toward the negative effect caused by chemical fertilizers. In general, the root endophytic abundant microbial subcommunities had high stability under different fertilization treatments, which indicated that it could play a dominant role in the symbiotic network. At the same time, the rare subcommunities and their key species may interact with abundant subcommunities under environmental disturbances, forming more stable symbiotic network and performing specific ecological functions (Jiao et al., 2017; Jiao et al., 2019a; Li et al., 2021).

Previous research has also provided evidence that the presence or loss of rare subcommunity and their key species under environmental disturbances can affect the stability of interactions within the entire community, leading to significant structural and functional changes (Cui et al., 2023; Ma et al., 2024). We found that the topological characters of nitrogen-adaption rare bacterial subcommunity tend to align with the structural changes of the entire endophytic microbiome. This further verify that rare endophytic bacterial subcommunity play a significantly more important role than endophytic fungal subcommunities (Liu et al., 2024). The rare bacterial subcommunity contained the most of key species occupying the nodes of module hubs and connectors in the network, and their abundance increases with the application of nitrogen and phosphorus fertilizers. These keystone species can disproportionately and significantly impact ecosystems, with their activity and abundance determining community integrity (Wu et al., 2023). At the phylum level, keystone species in rare bacterial subcommunities belong primarily to *Proteobacteria*, *Actinobacteriota*, *Bacteroidota*, *Firmicutes*, *Myxococcota*, *Chloroflex*, *Acidobacteriota*, *Gemmatimonadota*, and unclassified bacteria.

High nitrogen and phosphorus nutrient concentrations have been unfavorable for the growth of oligotrophic bacteria such as *Acidobacteriota* and *Chloroflexi* (Fierer et al., 2012). Long-term nitrogen and phosphorus fertilizer application has increased the relative abundance of copiotrophic bacteria, including *Alphaproteobacteria*, *Gammaproteobacteria*, *Firmicutes* (Ho et al., 2017), *Bacteroidota*, and *Actinobacteriota* (Dai et al., 2018; Fierer et al., 2012; Sun et al., 2023). Similarly, nitrogen and phosphorus fertilizers have significantly promoted the growth of *Ascomycota*, a hub in the root endophytic fungal subcommunity network, which is considered an r-strategy copiotrophic fungus (Guo et al., 2020). *Ascomycota* is often reported to harbor a high number of genes relevant to stress tolerance and nutrition uptake (e.g., nitrogen immobilization and phosphate transporter) (Egidi et al., 2019). Our results indicated that long-term nitrogen and phosphorus fertilizer applications enriched copiotrophic root endophytic nitrogen-adaption bacteria and phosphorus-adaption fungi, which may possess symbiotic ecological functions (Wu et al., 2023). This enrichment may benefit crop health and high yield in agricultural ecosystems. The most direct reason is that nitrogen and phosphorus fertilizers increased nutrient availability, which may differentially impact communication within bacterial subcommunities in the network, subsequently inducing the transformation of various key groups within the entire microbial community. Therefore, we concluded that long-term balanced fertilization with nitrogen and phosphorus, especially with organic manure and chemical phosphorus fertilizer (ONP1), may enrich more beneficial and important tomato root endophytes, thereby improving microbial network stability and crop yield.

4.3 The importance of endophytic bacterial subcommunity structure driven by AN and MLP to yield

Rhizosphere soil nutrient characteristics, particularly nitrogen, phosphorus, and their availability, are potential key factors influencing

composition and aggregation of root endophytic microbial community (Liu et al., 2023b; Long and Yao, 2020; Meng et al., 2022; Sindhu et al., 2024). Studies indicated that soil changes are the initial step affecting root endophyte colonization. Although the impact of soil is relatively smaller than that of the host, nitrogen and phosphorus availability still influence endophytic microbial community aggregation and structure (Almario et al., 2017; Edwards et al., 2015). Previous research has shown that different nitrogen levels lead to differences in root endophytic bacteria (Beltran-Garcia et al., 2021). We discovered that different nitrogen supplements caused inconsistent changes in endophytic bacterial community diversity, but structures of endophytic bacteria had similar responses to same rhizosphere soil physicochemical parameters. Long-term different nitrogen fertilizer significantly increased AN content, which showed a significant positive correlation with the structure of both abundant and rare endophytic bacterial subcommunities. Additionally, the reduction in pH was strongly negatively correlated with the structure of rare endophytic bacterial subcommunities, suggesting that pH involved in determining specific endophytic bacterial communities (Lin et al., 2020; Zhang et al., 2024). Previous studies have indicated that endophytic fungal communities are closely related to phosphorus content (Wu et al., 2022). Chemical phosphorus fertilizer provided substantial amounts of labile and moderately labile phosphorus (Maranguit et al., 2017; Shi et al., 2023), and continuous changes in phosphorus availability promote the turnover of endophytic fungal subcommunity structures (Long and Yao, 2020). In non-mycorrhizal crops like tomatoes, it has been found that root endophytic fungi may serve as an alternative strategy for phosphorus utilization, supporting a significant response of endophytic fungal subcommunity to changes in rhizosphere soil MLP content.

Random forest model regression analysis revealed that the most important endophytic subcommunities for predicting crop yield were abundant endophytic bacterial subcommunities, followed by rare bacterial subcommunity, accounting for 22.03% and 3.09% of the variance in predictive factors, respectively. This finding differs from studies on maize-wheat/barley rotation systems (Xiong et al., 2020). In tomato roots affected by long-term fertilization, rare subcommunities structures and species that promote higher network stability may synergistically assist the positive effects of abundant subcommunities with environmental resistance on crop yield. Consequently, the associations between rhizosphere soil nitrogen and phosphorus availability and root endophytic bacterial and fungal subcommunities suggest a pattern of endophytic microbial structural succession, which optimizes microbial communities to influence the relative contributions of different subcommunities to crop yield. Notably, among the top 10 rare subcommunity predictors of yield, three key species were identified that *Arthrobacter*, *Microbacterium*, and *Sphingobium*. Interestingly, both *Arthrobacter* and *Microbacterium* belong to the *Actinobacteriota*, while *Sphingobium* belongs to *Proteobacteria*. These key rare taxa, as plant growth-promoting endophytes (PGPE), have potential to enhance plant resilience to environmental stress and improve crop health and yield, possessing specific functions such as nitrogen fixation and phosphorus solubilization (Machado et al., 2020; Walitang et al., 2017).

5 Conclusion

This study provided a systematic understanding of how root endophytic microbial subcommunities, adapted to different ecological niches under long-term fertilization, contribute to maintaining tomato yield. Long-term nitrogen and phosphorus fertilizers increased the proportion of negative cohesion in the root endophytic microbial co-occurrence network, forming ecological niche complementarity between rare bacterial subcommunities and fungal subcommunities. This effect was particularly pronounced in the ONP1 treatment, which led to a more complex, tighter, and stable network structure. The assembly of rare and abundant subcommunities of endophytic bacteria and fungi were dominated by stochastic processes. Nitrogen applications maintained the dispersal limitation ecological process, influencing the assembly process of endophytic rare and abundant bacterial subcommunities, while phosphorus applications controlled the assembly of rare and abundant subcommunities of endophytic fungi by increasing the proportion of the dispersal limitation process. The AN and MLP content in rhizosphere soil significantly affected the community structure changes of nitrogen-adaption root endophytic bacteria and phosphorus-adaption endophytic fungi. The nitrogen-adaption endophytic bacterial subcommunity, particularly the abundant bacterial subcommunity, had a higher explanatory power for tomato yield than the phosphorus-adaption fungal subcommunity. *Arthrobacter*, *Microbacterium*, and *Sphingobium* from the rare subcommunity can potentially serve as beneficial symbiotic endophytes to enhance crop yield. Overall, the application of organic manure combined with chemical phosphorus fertilizer favored the survival strategy of abundant subcommunities and the diversity of rare subcommunities. Ecological complementarity among different subcommunities contributes to forming a more complex and tighter symbiotic network, thereby driving functional redundancy in rare subcommunities potential for high crop yield. The findings have significant implications for sustainable fertilization practices to control root endophytic microbial communities for achieving high crop yield.

Data availability statement

The datasets from this study are available in online repositories, with repository names and accession numbers provided in the article.

Author contributions

XL: Conceptualization, Data curation, Formal analysis, Writing – original draft. MA: Writing – review & editing. SW: Formal analysis, Writing – review & editing. ZZ: Investigation, Formal analysis, Writing – original draft. SZ: Investigation, Visualization, Writing – review & editing. YL: Writing – review & editing. ZS: Funding acquisition, Supervision, Writing – review & editing. HF: Supervision, Writing – review & editing. TL: Writing – review & editing.

Funding

The author(s) declare that financial support was received for the research, authorship, and/or publication of this article. This study was financially supported by the National Key R&D Program of China (2022YFD1602110) and the China Agriculture Research System

(CARS-23). The funders had no role in the execution of the study or the decision to publish the findings.

Acknowledgments

The authors thank Lijun Chen for his contributions in revising the manuscript.

Conflict of interest

The authors declare that the research was conducted in the absence of any commercial or financial relationships that could be construed as a potential conflict of interest.

Publisher's note

All claims expressed in this article are solely those of the authors and do not necessarily represent those of their affiliated organizations, or those of the publisher, the editors and the reviewers. Any product that may be evaluated in this article, or claim that may be made by its manufacturer, is not guaranteed or endorsed by the publisher.

Supplementary material

The Supplementary material for this article can be found online at: https://www.frontiersin.org/articles/10.3389/fmicb.2024.1487323/full#supplementary-material

References

Adeleke, B. S., and Babalola, O. O. (2021). The endosphere microbial communities, a great promise in agriculture. *Int. Microbiol.* 24, 1–17. doi: 10.1007/s10123-020-00140-2

Adeleke, B. S., Babalola, O. O., and Glick, B. R. (2021). Plant growth-promoting root-colonizing bacterial endophytes. *Rhizosphere* 20:100433. doi: 10.1016/j.rhisph.2021.100433

Ali, S., Charles, T. C., and Glick, B. R. (2014). Amelioration of high salinity stress damage by plant growth-promoting bacterial endophytes that contain ACC deaminase. *Plant Physiol. Biochem.* 80, 160–167. doi: 10.1016/j.plaphy.2014.04.003

Almario, J., Jeena, G., Wunder, J., Langen, G., Zuccaro, A., Coupland, G., et al. (2017). Root-associated fungal microbiota of nonmycorrhizal Arabis alpina and its contribution to plant phosphorus nutrition. *Proc. Natl. Acad. Sci. USA* 114, E9403–e9412. doi: 10.1073/pnas.1710455114

Bai, L., Zhang, X., Li, B., Sun, F., Zhao, X., Wang, Y., et al. (2022). Fungal communities are more sensitive to nitrogen fertilization than bacteria in different spatial structures of silage maize under short-term nitrogen fertilization. *Appl. Soil Ecol.* 170:104275. doi: 10.1016/j.apsoil.2021.104275

Banerjee, S., Walder, F., Büchi, L., Meyer, M., Held, A. Y., Gattinger, A., et al. (2019). Agricultural intensification reduces microbial network complexity and the abundance of keystone taxa in roots. *ISME J.* 13, 1722–1736. doi: 10.1038/s41396-019-0383-2

Baselga, A., and Orme, C. D. L. (2012). Betapart: an R package for the study of beta diversity. *Methods Ecol. Evol.* 3, 808–812. doi: 10.1111/j.2041-210X.2012.00224.x

Battu, L., and Ulaganathan, K. (2020). Whole genome sequencing and identification of host-interactive genes in the rice endophytic Leifsonia sp. ku-ls. *Funct. Integr. Genomics* 20, 237–243. doi: 10.1007/s10142-019-00713-z

Beltran-Garcia, M. J., Martínez-Rodríguez, A., Olmos-Arriaga, I., Valdes-Salas, B., Di Mascio, P., and White, J. F. (2021). Nitrogen fertilization and stress factors drive shifts in microbial diversity in soils and plants. *Symbiosis* 84, 379–390. doi: 10.1007/s13199-021-00787-z

Bolan, N. S. (1991). A critical review on the role of mycorrhizal fungi in the uptake of phosphorus by plants. *Plant Soil* 134, 189–207. doi: 10.1007/BF00012037

Bornemisza, E., Blakemore, LC, Searle, PL, and Daly, BK (1988). Methods for chemical analysis of soils. New Zealand soil bureau scientific report, 1987, 103 p.

Bulgarelli, D., Rott, M., Schlaeppi, K., Loren, V., van Themaat, E., Ahmadinejad, N., et al. (2012). Revealing structure and assembly cues for Arabidopsis root-inhabiting bacterial microbiota. *Nature* 488, 91–95. doi: 10.1038/nature11336

Burragoni, S. G., and Jeon, J. (2021). Applications of endophytic microbes in agriculture, biotechnology, medicine, and beyond. *Microbiol. Res.* 245:126691. doi: 10.1016/j.micres.2020.126691

Byregowda, R., Prasad, S. R., Oelmüller, R., Nataraja, K. N., and Prasanna Kumar, M. K. (2022). Is endophytic colonization of host plants a method of alleviating drought stress? Conceptualizing the hidden world of endophytes. *Int. J. Mol. Sci.* 23:9194. doi: 10.3390/ijms23169194

Cabrera, M. L., and Beare, M. H. (1993). Alkaline persulfate oxidation for determining total nitrogen in microbial biomass extracts. *Soil Sci. Soc. Am. J.* 57, 1007–1012. doi: 10.2136/sssaj1993.03615995005700040021x

Card, S., Johnson, L., Teasdale, S., and Caradus, J. (2016). Deciphering endophyte behaviour: the link between endophyte biology and efficacious biological control agents. *FEMS Microbiol. Ecol.* 92, 1–19. doi: 10.1093/femsec/fiw114

Chase, J. M. (2010). Stochastic community assembly causes higher biodiversity in more productive environments. *Science* 328, 1388–1391. doi: 10.1126/science.1187820

Chase, J. M., and Myers, J. A. (2011). Disentangling the importance of ecological niches from stochastic processes across scales. *Philos. Trans. R. Soc. Lond. Ser. B Biol. Sci.* 366, 2351–2363. doi: 10.1098/rstb.2011.0063

Chen, G., Wang, W., Zhang, Y., Liu, Y., Gu, X., Shi, X., et al. (2020). Abundant and rare species may invoke different assembly processes in response to climate extremes: implications for biodiversity conservation. *Ecol. Indic.* 117:106716. doi: 10.1016/j.ecolind.2020.106716

Collavino, M. M., Cabrera, E. V. R., Bruno, C., and Aguilar, O. M. (2020). Effect of soil chemical fertilization on the diversity and composition of the tomato endophytic diazotrophic community at different stages of growth. *Braz. J. Microbiol.* 51, 1965–1975. doi: 10.1007/s42770-020-00373-3

Cui, W., Li, R., Fan, Z., Wu, L., Zhao, X., Wei, G., et al. (2023). Weak environmental adaptation of rare phylotypes sustaining soil multi-element cycles in response to decades-long fertilization. *Sci. Total Environ.* 871:162063. doi: 10.1016/j.scitotenv.2023.162063

Dai, Z., Su, W., Chen, H., Barberán, A., Zhao, H., Yu, M., et al. (2018). Long-term nitrogen fertilization decreases bacterial diversity and favors the growth of Actinobacteria and Proteobacteria in agro-ecosystems across the globe. *Glob. Chang. Biol.* 24, 3452–3461. doi: 10.1111/gcb.14163

Delgado-Baquerizo, M., Oliverio, A. M., Brewer, T. E., Benavent-González, A., Eldridge, D. J., Bardgett, R. D., et al. (2018). A global atlas of the dominant bacteria found in soil. *Science* 359, 320–325. doi: 10.1126/science.aap9516

Deng, Y., Zhang, P., Qin, Y., Tu, Q., Yang, Y., He, Z., et al. (2016). Network succession reveals the importance of competition in response to emulsified vegetable oil amendment for uranium bioremediation. *Environ. Microbiol.* 18, 205–218. doi: 10.1111/1462-2920.12981

Dong, Y., Wu, S., Deng, Y., Wang, S., Fan, H., Li, X., et al. (2021). Distinct functions and assembly mechanisms of soil abundant and rare bacterial taxa under increasing pyrene stresses. *Front. Microbiol.* 12:689762. doi: 10.3389/fmicb.2021.689762

Dos Santos, R. M., Cueva-Yesquén, L. G., Garboggini, F. F., Desoignies, N., and Rigobelo, E. C. (2022). Inoculum concentration and mineral fertilization: effects on the endophytic microbiome of soybean. *Front. Microbiol.* 13:900980. doi: 10.3389/fmicb.2022.900980

du, S., Dini-Andreote, F., Zhang, N., Liang, C., Yao, Z., Zhang, H., et al. (2020). Divergent co-occurrence patterns and assembly processes structure the abundant and rare bacterial communities in a salt marsh ecosystem. *Appl. Environ. Microbiol.* 86:e00322. doi: 10.1128/AEM.00322-20

Edgar, R C. (2016a). UNOISE2: improved error-correction for Illumina 16S and ITS amplicon sequencing. bioRxiv [Preprint]. doi: 10.1101/081257

Edgar, R C. (2016b). SINTAX: a simple non-Bayesian taxonomy classifier for 16S and ITS sequences. bioRxiv [Preprint]. doi: 10.1101/074161

Edwards, J., Johnson, C., Santos-Medellín, C., Lurie, E., Podishetty, N. K., Bhatnagar, S., et al. (2015). Structure, variation, and assembly of the root-associated microbiomes of rice. *Proc. Natl. Acad. Sci.* 112, E911–E920. doi: 10.1073/pnas.1414592112

Egidi, E., Delgado-Baquerizo, M., Plett, J. M., Wang, J., Eldridge, D. J., Bardgett, R. D., et al. (2019). A few Ascomycota taxa dominate soil fungal communities worldwide. *Nat. Commun.* 10:2369. doi: 10.1038/s41467-019-10373-z

Ernst, M., Neubert, K., Mendgen, K. W., and Wirsel, S. G. R. (2011). Niche differentiation of two sympatric species of Microdochium colonizing the roots of common reed. *BMC Microbiol.* 11:242. doi: 10.1186/1471-2180-11-242

Fabiańska, I., Sosa-Lopez, E., and Bucher, M. (2019). The role of nutrient balance in shaping plant root-fungal interactions: facts and speculation. *Curr. Opin. Microbiol.* 49, 90–96. doi: 10.1016/j.mib.2019.10.004

Fan, K., Delgado-Baquerizo, M., Guo, X., Wang, D., Wu, Y., Zhu, M., et al. (2019). Suppressed N fixation and diazotrophs after four decades of fertilization. *Microbiome* 7:143. doi: 10.1186/s40168-019-0757-8

FAO and ISRIC. (1988). Soil map of the world, revised legend. Food and agriculture organization of the united nations, Rome, Italy.

Feng, M., Adams, J. M., Fan, K., Shi, Y., Sun, R., Wang, D., et al. (2018). Long-term fertilization influences community assembly processes of soil diazotrophs. *Soil Biol. Biochem.* 126, 151–158. doi: 10.1016/j.soilbio.2018.08.021

Fierer, N., Lauber, C. L., Ramirez, K. S., Zaneveld, J., Bradford, M. A., and Knight, R. (2012). Comparative metagenomic, phylogenetic and physiological analyses of soil microbial communities across nitrogen gradients. *ISME J.* 6, 1007–1017. doi: 10.1038/ismej.2011.159

Fujii, M., Kojima, H., Iwata, T., Urabe, J., and Fukui, M. (2012). Dissolved organic carbon as major environmental factor affecting Bacterioplankton communities in Mountain Lakes of eastern Japan. *Microb. Ecol.* 63, 496–508. doi: 10.1007/s00248-011-9983-8

Ghoul, M., and Mitri, S. (2016). The ecology and evolution of microbial competition. *Trends Microbiol.* 24, 833–845. doi: 10.1016/j.tim.2016.06.011

Gschwend, F., Hartmann, M., Hug, A.-S., Enkerli, J., Gubler, A., Frey, B., et al. (2021). Long-term stability of soil bacterial and fungal community structures revealed in their abundant and rare fractions. *Mol. Ecol.* 30, 4305–4320. doi: 10.1111/mec.16036

Guimerà, R., and Nunes Amaral, L. A. (2005). Functional cartography of complex metabolic networks. *Nature* 433, 895–900. doi: 10.1038/nature03288

Guo, L. D., Hyde, K. D., and Liew, E. C. Y. (2000). Identification of endophytic fungi from *Livistona chinensis* based on morphology and rDNA sequences. *New Phytol.* 147, 617–630. doi: 10.1046/j.1469-8137.2000.00716.x

Guo, Z., Wan, S., Hua, K., Yin, Y., Chu, H., Wang, D., et al. (2020). Fertilization regime has a greater effect on soil microbial community structure than crop rotation and growth stage in an agroecosystem. *Appl. Soil Ecol.* 149:103510. doi: 10.1016/j.apsoil.2020.103510

Guo, B., Zhang, H., Liu, Y., Chen, J., and Li, J. (2024). Assembly of cereal crop fungal communities under water stress determined by host niche. *Environ. Exp. Bot.* 219:105650. doi: 10.1016/j.envexpbot.2024.105650

Hamonts, K., Trivedi, P., Garg, A., Janitz, C., Grinyer, J., Holford, P., et al. (2018). Field study reveals core plant microbiota and relative importance of their drivers. *Environ. Microbiol.* 20, 124–140. doi: 10.1111/1462-2920.14031

Han, J., Shi, J., Zeng, L., Xu, J., and Wu, L. (2015). Effects of nitrogen fertilization on the acidity and salinity of greenhouse soils. *Environ. Sci. Pollut. Res.* 22, 2976–2986. doi: 10.1007/s11356-014-3542-z

Harman, G. E., and Uphoff, N. (2019). Symbiotic root-endophytic soil microbes improve crop productivity and provide environmental benefits. *Australas. Sci.* 2019, 9106395–9106325. doi: 10.1155/2019/9106395

Hartman, K., van der Heijden, M. G. A., Wittwer, R. A., Banerjee, S., Walser, J.-C., and Schlaeppi, K. (2018). Cropping practices manipulate abundance patterns of root and soil microbiome members paving the way to smart farming. *Microbiome* 6:14. doi: 10.1186/s40168-017-0389-9

Hedley, M. J., Stewart, J. W. B., and Chauhan, B. S. (1982). Changes in inorganic and organic soil phosphorus fractions induced by cultivation practices and by laboratory incubations. *Soil Sci. Soc. Am. J.* 46, 970–976. doi: 10.2136/sssaj1982.03615995004600050017x

Ho, A., Di Lonardo, D. P., and Bodelier, P. L. E. (2017). Revisiting life strategy concepts in environmental microbial ecology. *FEMS Microbiol. Ecol.* 93:fix006. doi: 10.1093/femsec/fix006

Jia, X., Dini-Andreote, F., and Falcão Salles, J. (2018). Community assembly processes of the microbial rare biosphere. *Trends Microbiol.* 26, 738–747. doi: 10.1016/j.tim.2018.02.011

Jia, X., Dini-Andreote, F., and Salles, J. F. (2022). Unravelling the interplay of ecological processes structuring the bacterial rare biosphere. *ISME Commun.* 2:96. doi: 10.1038/s43705-022-00177-6

Jiao, S., Chen, W., and Wei, G. (2017). Biogeography and ecological diversity patterns of rare and abundant bacteria in oil-contaminated soils. *Mol. Ecol.* 26, 5305–5317. doi: 10.1111/mec.14218

Jiao, S., and Lu, Y. (2020). Abundant fungi adapt to broader environmental gradients than rare fungi in agricultural fields. *Glob. Chang. Biol.* 26, 4506–4520. doi: 10.1111/gcb.15130

Jiao, S., Wang, J., Wei, G., Chen, W., and Lu, Y. (2019a). Dominant role of abundant rather than rare bacterial taxa in maintaining agro-soil microbiomes under environmental disturbances. *Chemosphere* 235, 248–259. doi: 10.1016/j.chemosphere.2019.06.174

Jiao, S., Yang, Y., Xu, Y., Zhang, J., and Lu, Y. (2019b). Balance between community assembly processes mediates species coexistence in agricultural soil microbiomes across eastern China. *ISME J.* 14, 202–216. doi: 10.1038/s41396-019-0522-9

Jin, S., Vegelius, J., and Yang-Wallentin, F. (2020). A marginal maximum likelihood approach for extended quadratic structural equation modeling with ordinal data. *Struct. Equ. Model. Multidiscip. J.* 27, 864–873. doi: 10.1080/10705511.2020.1712552

Jousset, A., Bienhold, C., Chatzinotas, A., Gallien, L., Gobet, A., Kurm, V., et al. (2017). Where less may be more: how the rare biosphere pulls ecosystems strings. *ISME J.* 11, 853–862. doi: 10.1038/ismej.2016.174

Lang, M., Zou, W., Chen, X., Zou, C., Zhang, W., Deng, Y., et al. (2021). Soil microbial composition and phoD gene abundance are sensitive to phosphorus level in a Long-term wheat-maize crop system. *Front. Microbiol.* 11:605955. doi: 10.3389/fmicb.2020.605955

Leach, J. E., Triplett, L. R., Argueso, C. T., and Trivedi, P. (2017). Communication in the Phytobiome. *Cell* 169, 587–596. doi: 10.1016/j.cell.2017.04.025

Lennon, J. T., and Jones, S. E. (2011). Microbial seed banks: the ecological and evolutionary implications of dormancy. *Nat. Rev. Microbiol.* 9, 119–130. doi: 10.1038/nrmicro2504

Li, T., and Gao, J. (2023). Attribution of dispersal limitation can better explain the assembly patterns of plant microbiota. *Front. Plant Sci.* 14:1168760. doi: 10.3389/fpls.2023.1168760

Li, G.-l., Wu, M., Li, P.-f., Wei, S.-p., Liu, J., Jiang, C.-y., et al. (2021). Assembly and co-occurrence patterns of rare and abundant bacterial sub-communities in rice rhizosphere soil under short-term nitrogen deep placement. *J. Integr. Agric.* 20, 3299–3311. doi: 10.1016/S2095-3119(20)63462-1

Liang, Y., Xiao, X., Nuccio, E. E., Yuan, M., Zhang, N., Xue, K., et al. (2020). Differentiation strategies of soil rare and abundant microbial taxa in response to changing climatic regimes. *Environ. Microbiol.* 22, 1327–1340. doi: 10.1111/1462-2920.14945

Liang, Y., Zhao, H., Deng, Y., Zhou, J., Li, G., and Sun, B. (2016). Long-term oil contamination alters the molecular ecological networks of soil microbial functional genes. *Front. Microbiol.* 7:60. doi: 10.3389/fmicb.2016.00060

Lin, G.-Y., Lin, C.-Y., Chang, S.-J., and And Lin, W.-Y. (2020). The dynamics of endophytic bacterial community structure in Rice roots under different field management systems. *Agronomy* 10:1623. doi: 10.3390/agronomy10111623

Liu, Y., Chu, G., Stirling, E., Zhang, H., Chen, S., Xu, C., et al. (2023b). Nitrogen fertilization modulates rice seed endophytic microbiomes and grain quality. *Sci. Total Environ.* 857:159181. doi: 10.1016/j.scitotenv.2022.159181

Liu, C., Cui, Y., Li, X., and Yao, M. (2020). Microeco: an R package for data mining in microbial community ecology. *FEMS Microbiol. Ecol.* 97, 1–9. doi: 10.1093/femsec/fiaa255

Liu, S., Liu, R., Zhang, S., Shen, Q., Chen, J., Ma, H., et al. (2024). The contributions of sub-communities to the assembly process and ecological mechanisms of bacterial communities along the cotton soil–root continuum niche gradient. *Microorganisms* 12:869. doi: 10.3390/microorganisms12050869

Liu, L., Yang, J., Yu, Z., and Wilkinson, D. M. (2015). The biogeography of abundant and rare bacterioplankton in the lakes and reservoirs of China. *ISME J.* 9, 2068–2077. doi: 10.1038/ismej.2015.29

Liu, L., Zhu, L., Yan, R., Yang, Y., Adams, J. M., and Liu, J. (2023a). Abundant bacterial subcommunity is structured by a stochastic process in an agricultural system with P fertilizer inputs. *Sci. Total Environ.* 871:162178. doi: 10.1016/j.scitotenv.2023.162178

Long, X.-E., and Yao, H. (2020). Phosphorus input alters the assembly of Rice (*Oryza sativa* L.) root-associated communities. *Microb. Ecol.* 79, 357–366. doi: 10.1007/s00248-019-01407-6

Lynch, M. D. J., and Neufeld, J. D. (2015). Ecology and exploration of the rare biosphere. *Nat. Rev. Microbiol.* 13, 217–229. doi: 10.1038/nrmicro3400

Ma, J., Ma, K., Liu, J., and Chen, N. (2022a). Rhizosphere soil microbial community under ice in a high-latitude wetland: different community assembly processes shape patterns of rare and abundant microbes. *Front. Microbiol.* 13:783371. doi: 10.3389/fmicb.2022.783371

Ma, L., Niu, W., Li, G., Du, Y., Sun, J., Zhang, Q., et al. (2024). Crucial role of rare taxa in preserving bacterial community stability. *Land Degrad. Dev.* 35, 1397–1410. doi: 10.1002/ldr.4994

Ma, Y., Wang, D., Guo, X., Zhu, Y.-G., Delgado-Baquerizo, M., and Chu, H. (2022b). Root stoichiometry explains wheat endophytes and their link with crop production after four decades of fertilization. *Sci. Total Environ.* 846:157407. doi: 10.1016/j.scitotenv.2022.157407

Ma, Y., Weisenhorn, P., Guo, X., Wang, D., Yang, T., Shi, Y., et al. (2021). Effect of long-term fertilization on bacterial communities in wheat endosphere. *Pedosphere* 31, 538–548. doi: 10.1016/S1002-0160(19)60838-6

Machado, P. C., Andrade, P. H. M., Sousa, C. P. D., Souza, C. W. O. D., and And Lacava, P. T. (2020). In vitro characterization of endophytic bacteria associated with physic nut (*Jatropha curcas* L.) and their potential for plant-growth promotion and biocontrol / Caracterização in vitro de bactérias endofíticas associadas ao pinhão-manso (*Jatropha curcas* L.) e seu potencial de promoção de crescimento vegetal e biocontrole. *Braz. J. Dev.* 6, 88572–88589. doi: 10.34117/bjdv6n11-326

Maranguit, D., Guillaume, T., and Kuzyakov, Y. (2017). Land-use change affects phosphorus fractions in highly weathered tropical soils. *Catena* 149, 385–393. doi: 10.1016/j.catena.2016.10.010

Mebius, L. J. (1960). A rapid method for the determination of organic carbon in soil. *Anal. Chim. Acta* 22, 120–124. doi: 10.1016/S0003-2670(00)88254-9

Mehta, P., Sharma, R., Putatunda, C., and Walia, A. (2019). "Endophytic fungi: role in phosphate solubilization" in Advances in Endophytic Fungal Research: Present Status and Future Challenges. ed. B. P. Singh (Cham: Springer International Publishing), 183–209.

Meng, Y., Zhang, Q., Shi, G., Liu, Y., Du, G., and Feng, H. (2022). Can nitrogen supersede host identity in shaping the community composition of foliar endophytic fungi in an alpine meadow ecosystem? *Front. Microbiol.* 13:895533. doi: 10.3389/fmicb.2022.895533

Michalska-Smith, M., Song, Z., Spawn-Lee, S. A., Hansen, Z. A., Johnson, M., May, G., et al. (2022). Network structure of resource use and niche overlap within the endophytic microbiome. *ISME J.* 16, 435–446. doi: 10.1038/s41396-021-01080-z

Miranda-Carrazco, A., Navarro-Noya Yendi, E., Govaerts, B., Verhulst, N., and Dendooven, L. (2022). Nitrogen fertilizer application alters the root endophyte bacterial microbiome in maize plants, but not in the stem or rhizosphere soil. *Microbiol. Spectr.* 10, e0178522–e0101722. doi: 10.1128/spectrum.01785-22

Nemergut Diana, R., Schmidt Steven, K., Fukami, T., O'Neill Sean, P., Bilinski Teresa, M., Stanish Lee, F., et al. (2013). Patterns and processes of microbial community assembly. *Microbiol. Mol. Biol. Rev.* 77, 342–356. doi: 10.1128/mmbr.00051-12

Ning, D., Yuan, M., Wu, L., Zhang, Y., Guo, X., Zhou, X., et al. (2020). A quantitative framework reveals ecological drivers of grassland microbial community assembly in response to warming. *Nat. Commun.* 11:4717. doi: 10.1038/s41467-020-18560-z

Niu, B., Paulson, J. N., Zheng, X., and Kolter, R. (2017). Simplified and representative bacterial community of maize roots. *Proc. Natl. Acad. Sci. USA* 114, E2450–e2459. doi: 10.1073/pnas.1616148114

Oksanen, J., Blanchet, F., Kindt, R., Legendre, P., Minchin, P., O'Hara, R., et al. (2012). Vegan: community ecology package: ordination, diversity and dissimilarities, version 2.0-4. (Reprinted from: Reprint E dition).

Omomowo, O. I., and Babalola, O. O. (2019). Bacterial and fungal endophytes: tiny giants with immense beneficial potential for plant growth and sustainable agricultural productivity. *Microorganisms* 7:481. doi: 10.3390/microorganisms7110481

Rani, S., Kumar, P., Dahiya, P., Maheshwari, R., Dang, A. S., and Suneja, P. (2022). Endophytism: a multidimensional approach to plant–prokaryotic microbe interaction. *Front. Microbiol.* 13:861235. doi: 10.3389/fmicb.2022.861235

Rognes, T. F. T., Nichols, B., Quince, C., and Mahé, F. (2016). VSEARCH: a versatile open source tool for metagenomics. *PeerJ* 4:e2584. doi: 10.7717/peerj.2584

Santoyo, G., Moreno-Hagelsieb, G., del Carmen Orozco-Mosqueda, M., and Glick, B. R. (2016). Plant growth-promoting bacterial endophytes. *Microbiol. Res.* 183, 92–99. doi: 10.1016/j.micres.2015.11.008

Schmidt, S. K., Nemergut, D. R., Darcy, J. L., and Lynch, R. (2014). Do bacterial and fungal communities assemble differently during primary succession? *Mol. Ecol.* 23, 254–258. doi: 10.1111/mec.12589

Sena, L., Mica, E., Valè, G., Vaccino, P., and Pecchioni, N. (2024). Exploring the potential of endophyte-plant interactions for improving crop sustainable yields in a changing climate. *Front. Plant Sci.* 15:1349401. doi: 10.3389/fpls.2024.1349401

Shi, Q., Song, Q., Shan, X., Li, X., Wang, S., Fu, H., et al. (2023). Microorganisms regulate soil phosphorus fractions in response to low nocturnal temperature by altering the abundance and composition of the pqqC gene rather than that of the phoD gene. *Biol. Fertil. Soils* 59, 973–987. doi: 10.1007/s00374-023-01766-w

Shu, D., Guo, Y., Zhang, B., Zhang, C., Van Nostrand, J. D., Lin, Y., et al. (2021). Rare prokaryotic sub-communities dominate the complexity of ecological networks and soil multinutrient cycling during long-term secondary succession in China's loess plateau. *Sci. Total Environ.* 774:145737. doi: 10.1016/j.scitotenv.2021.145737

Sindhu, L., Song, Y., Li, L., Dong, Z., Yang, Q., Mangi, S. S., et al. (2024). Meta-omics revealed that nitrogen fertilization alters the endophytic fungi divergence in maize field ecosystem. *Ecol. Indic.* 160:111852. doi: 10.1016/j.ecolind.2024.111852

Stegen, J. C., Lin, X., Fredrickson, J. K., and Konopka, A. E. (2015). Estimating and mapping ecological processes influencing microbial community assembly. *Front. Microbiol.* 6:370. doi: 10.3389/fmicb.2015.00370

Sun, A., Jiao, X.-Y., Chen, Q., Wu, A.-L., Zheng, Y., Lin, Y.-X., et al. (2021). Microbial communities in crop phyllosphere and root endosphere are more resistant than soil microbiota to fertilization. *Soil Biol. Biochem.* 153:108113. doi: 10.1016/j.soilbio.2020.108113

Sun, K., Lu, F., Huang, P.-W., Tang, M.-J., Xu, F.-J., Zhang, W., et al. (2022). Root endophyte differentially regulates plant response to NO3− and NH4+ nutrition by modulating N fluxes at the plant–fungal interface. *Plant Cell Environ.* 45, 1813–1828. doi: 10.1111/pce.14304

Sun, C., Wang, R., Tang, G., Cai, S., Shi, H., Liu, F., et al. (2023). Integrated 16S and metabolomics revealed the mechanism of drought resistance and nitrogen uptake in rice at the heading stage under different nitrogen levels. *Front. Plant Sci.* 14:1120584. doi: 10.3389/fpls.2023.1120584

Tian, K., Xing, Z., Kalkhajeh, Y. K., Zhao, T., Hu, W., Huang, B., et al. (2022). Excessive phosphorus inputs dominate soil legacy phosphorus accumulation and its potential loss under intensive greenhouse vegetable production system. *J. Environ. Manag.* 303:114149. doi: 10.1016/j.jenvman.2021.114149

Tiessen, H., and Moir, J. (1993). "Characterization of available P by sequential extraction" in Soil Sampling and Methods of Analysis, 75–86. doi: 10.1201/9781420005271.ch25

Walitang, D. I., Kim, K., Madhaiyan, M., Kim, Y. K., Kang, Y., and Sa, T. (2017). Characterizing endophytic competence and plant growth promotion of bacterial endophytes inhabiting the seed endosphere of Rice. *BMC Microbiol.* 17:209. doi: 10.1186/s12866-017-1117-0

Wan, W., Gadd, G. M., Yang, Y., Yuan, W., Gu, J., Ye, L., et al. (2021). Environmental adaptation is stronger for abundant rather than rare microorganisms in wetland soils from the Qinghai-Tibet plateau. *Mol. Ecol.* 30, 2390–2403. doi: 10.1111/mec.15882

Wang, S., Zheng, S., Bian, T., Wu, T., Li, X., Fu, H., et al. (2022). Photosynthetic characteristics combined with metabolomics analysis revealed potential mechanisms of cucumber (*Cucumis sativus*) yield reduction induced by different phosphorus stresses. *Sci. Hortic.* 302:111156. doi: 10.1016/j.scienta.2022.111156

Wu, J., Liu, W., Zhang, W., Shao, Y., Duan, H., Chen, B., et al. (2019). Long-term nitrogen addition changes soil microbial community and litter decomposition rate in a subtropical forest. *Appl. Soil Ecol.* 142, 43–51. doi: 10.1016/j.apsoil.2019.05.014

Wu, D., Ma, Y., Yang, T., Gao, G., Wang, D., Guo, X., et al. (2022). Phosphorus and zinc are strongly associated with belowground fungal communities in wheat field under Long-term fertilization. *Microbiol. Spectr.* 10:e0011022. doi: 10.1128/spectrum.00110-22

Wu, C., Yan, B., Wei, F., Wang, H., Gao, L., Ma, H., et al. (2023). Long-term application of nitrogen and phosphorus fertilizers changes the process of community construction by affecting keystone species of crop rhizosphere microorganisms. *Sci. Total Environ.* 897:165239. doi: 10.1016/j.scitotenv.2023.165239

Xi, M., Wang, Y., Yang, J., Bi, X., Zhong, S., Duan, T., et al. (2024). Spatial distribution and community composition of endophytic fungi within Mussaenda pubescens stems. *Fungal Biol.* 128, 1815–1826. doi: 10.1016/j.funbio.2024.05.001

Xie, H., Chai, Y., Liu, Z., Hao, W., and Gai, J. (2024). Community assembly of endophytic bacteria and fungi differs in soil-root continuum of Carex cepillacea. *Appl. Soil Ecol.* 194:105206. doi: 10.1016/j.apsoil.2023.105206

Xing, W., Gai, X., Ju, F., and Chen, G. (2023). Microbial communities in tree root-compartment niches under cd and Zn pollution: structure, assembly process and co-occurrence relationship. *Sci. Total Environ.* 860:160273. doi: 10.1016/j.scitotenv.2022.160273

Xiong, C., He, J. Z., Singh, B. K., Zhu, Y. G., Wang, J. T., Li, P. P., et al. (2020). Rare taxa maintain the stability of crop mycobiomes and ecosystem functions. *Environ. Microbiol.* 23, 1907–1924. doi: 10.1111/1462-2920.15262

Xu, R., Li, K., Zhang, W., Chen, A., Hou, H., Wei, W., et al. (2022). Responses of endophytic bacterial communities in rice roots to phosphorus deficiency at the seedling stages. *Eur. J. Soil Biol.* 110:103405. doi: 10.1016/j.ejsobi.2022.103405

Xue, M., Guo, Z., Gu, X., Gao, H., Weng, S., Zhou, J., et al. (2020). Rare rather than abundant microbial communities drive the effects of long-term greenhouse cultivation on ecosystem functions in subtropical agricultural soils. *Sci. Total Environ.* 706:136004. doi: 10.1016/j.scitotenv.2019.136004

Yu, Z., Zhang, W., Duo, P., Zhang, Y., Tian, X., Sun, L., et al. (2024). Assembly processes of rare and abundant taxa are closely related to the bacterial and fungal functionality during desert vegetation reestablishment. *Pedosphere*. doi: 10.1016/j.pedsph.2024.03.004

Zhang, H., Huang, B., Dong, L., Hu, W., Akhtar, M. S., and Qu, M. (2017). Accumulation, sources and health risks of trace metals in elevated geochemical background soils used for greenhouse vegetable production in southwestern China. *Ecotoxicol. Environ. Saf.* 137, 233–239. doi: 10.1016/j.ecoenv.2016.12.010

Zhang, J., Na, M., Wang, Y., Ge, W., Zhou, J., and Zhou, S. (2024). Cadmium levels and soil pH drive structure and function differentiation of endophytic bacterial communities in Sedum plumbizincicola: a field study. *Sci. Total Environ.* 912:168828. doi: 10.1016/j.scitotenv.2023.168828

Zhang, M., Zhang, X., Zhang, L., Zeng, L., Liu, Y., Wang, X., et al. (2021). The stronger impact of inorganic nitrogen fertilization on soil bacterial community than organic fertilization in short-term condition. *Geoderma* 382:114752. doi: 10.1016/j.geoderma.2020.114752

Zhang, X., Zhao, W., Kou, Y., Fang, K., Liu, Y., He, H., et al. (2023). The contrasting responses of abundant and rare microbial community structures and co-occurrence networks to secondary forest succession in the subalpine region. *Front. Microbiol.* 14:1177239. doi: 10.3389/fmicb.2023.1177239

Zhang, X., Zhong, Z., Gai, X., Du, X., Bian, F., Yang, C., et al. (2019). Changes of root endophytic bacterial community along a Chronosequence of intensively managed lei bamboo (Phyllostachys praecox) forests in subtropical China. *Microorganisms* 7:616. doi: 10.3390/microorganisms7120616

Zheng, W., Zhao, Z., Lv, F., Wang, R., Wang, Z., Zhao, Z., et al. (2021). Assembly of abundant and rare bacterial and fungal sub-communities in different soil aggregate sizes in an apple orchard treated with cover crop and fertilizer. *Soil Biol. Biochem.* 156:108222. doi: 10.1016/j.soilbio.2021.108222

Zhong, Y., Sorensen, P. O., Zhu, G., Jia, X., Liu, J., Shangguan, Z., et al. (2022). Differential microbial assembly processes and co-occurrence networks in the soil-root continuum along an environmental gradient. *iMeta* 1:e18. doi: 10.1002/imt2.18

Zhou, J., Deng, Y., Zhang, P., Xue, K., Liang, Y., Van Nostrand, J. D., et al. (2014). Stochasticity, succession, and environmental perturbations in a fluidic ecosystem. *Proc. Natl. Acad. Sci.* 111, E836–E845. doi: 10.1073/pnas.1324044111

frontiers | Frontiers in Microbiology

TYPE Original Research
PUBLISHED 22 January 2025
DOI 10.3389/fmicb.2024.1485353

Check for updates

OPEN ACCESS

EDITED BY
Izzah Shahid,
Public University of Navarre, Spain

REVIEWED BY
Digvijay Verma,
Babasaheb Bhimrao Ambedkar University, India
Rafael A. Rojas-Herrera,
Universidad Autónoma de Yucatán, Mexico

*CORRESPONDENCE
Anastasiia K. Kimeklis
akimeklis@arriam.ru

†These authors have contributed equally to this work and share first authorship

RECEIVED 23 August 2024
ACCEPTED 30 December 2024
PUBLISHED 22 January 2025

CITATION
Kimeklis AK, Gladkov GV, Orlova OV, Lisina TO, Afonin AM, Aksenova TS, Kichko AA, Lapidus AL, Abakumov EV and Andronov EE (2025) Metagenomic insights into the development of microbial communities of straw and leaf composts. *Front. Microbiol.* 15:1485353. doi: 10.3389/fmicb.2024.1485353

COPYRIGHT
© 2025 Kimeklis, Gladkov, Orlova, Lisina, Afonin, Aksenova, Kichko, Lapidus, Abakumov and Andronov. This is an open-access article distributed under the terms of the Creative Commons Attribution License (CC BY). The use, distribution or reproduction in other forums is permitted, provided the original author(s) and the copyright owner(s) are credited and that the original publication in this journal is cited, in accordance with accepted academic practice. No use, distribution or reproduction is permitted which does not comply with these terms.

Metagenomic insights into the development of microbial communities of straw and leaf composts

Anastasiia K. Kimeklis[1,2*†], Grigory V. Gladkov[1†], Olga V. Orlova[1], Tatiana O. Lisina[1], Alexey M. Afonin[1,3], Tatiana S. Aksenova[1], Arina A. Kichko[1], Alla L. Lapidus[4], Evgeny V. Abakumov[1,2] and Evgeny E. Andronov[1]

[1]Laboratory of Microbiological Monitoring and Bioremediation of Soils, All-Russian Research Institute of Agricultural Microbiology, Saint Petersburg, Russia, [2]Department of Applied Ecology, Saint-Petersburg State University, Saint Petersburg, Russia, [3]A.I. Virtanen Institute for Molecular Sciences, University of Eastern Finland, Kuopio, Finland, [4]Independent Researcher, Saint-Petersburg, Russia

Introduction: Soil microbiome is a major source of physiologically active microorganisms, which can be potentially mobilized by adding various nutrients. To study this process, a long-term experiment was conducted on the decomposition of oat straw and leaf litter using soil as a microbial inoculum.

Methods: Combined analyses of enzymatic activity and NGS data for 16S rRNA gene amplicon and full metagenome sequencing were applied to study taxonomic, carbohydrate-active enzyme (CAZy), and polysaccharide utilization loci (PULs) composition of microbial communities at different stages of decomposition between substrates.

Results: In straw degradation, the microbial community demonstrated higher amylase, protease, catalase, and cellulase activities, while peroxidase, invertase, and polyphenol oxidase were more active in leaf litter. Consistent with this, the metagenome analysis showed that the microbiome of straw compost was enriched in genes for metabolic pathways of simpler compounds. At the same time, there were more genes for aromatic compound degradation pathways in leaf litter compost. We identified nine metagenome-assembled genomes (MAGs) as the most promising prokaryotic decomposers due to their abnormally high quantity of PULs for their genome sizes, which were confirmed by 16S rRNA gene amplicon sequencing to constitute the bulk of the community at all stages of substrate degradation. MAGs from Bacteroidota (*Chitinophaga* and *Ohtaekwangia*) and Actinomycetota (*Streptomyces*) were found in both composts, while those from Bacillota (*Pristimantibacillus*) were specific for leaf litter. The most frequently identified PULs were specialized on xylans and pectins, but not cellulose, suggesting that PUL databases may be underrepresented in clusters for complex substrates.

Discussion: Our study explores microbial communities from natural ecosystems, such as soil and lignocellulosic waste, which are capable of decomposing lignocellulosic substrates. Using a comprehensive approach with chemical analyses of the substrates, amplicon, and full metagenome sequencing data, we have shown that such communities may be a source of identifying the highly effective decomposing species with novel PULs.

KEYWORDS

straw, leaf litter, soil of Chernevaya taiga, cellulose decomposition, PUL, MAG, amplicon sequencing, metagenome

1 Introduction

Majority of the organic carbon storage in terrestrial ecosystems is located in the soil and plants, where it is involved in the global carbon cycle between living and dead biomass, atmosphere, and geosphere (Kayler et al., 2017). Annually, several hundred billion tons of lignocellulosic biomass in the form of agricultural and forestry residues, food, and industrial wastes are produced (Singh et al., 2022; Ojo, 2023). Thus, its decomposition is a major part of organic carbon circulation in terrestrial biomes (Liao et al., 2022). Recently, plant residue decomposition became the focus of metagenomic studies, but due to the high diversity of types of lignocellulosic substrates, the process is highly variable. Thus, the specific features of a particular plant waste decomposition are still insufficiently highlighted (Huang et al., 2023). While the recirculation of plant litter in agricultural ecosystems receives increasing attention (Sun et al., 2023; Liu et al., 2023; Wang et al., 2022), the knowledge about biomass turnover in natural ecosystems remains limited (Giweta, 2020). Yet, leaf litter, as a major component of the annual forest litterfall (Thakur et al., 2022) and the primary component of soil formation, takes longer periods to decompose than straw, a part of agricultural waste, which is linked to the differences in their chemical composition (Manzoni, 2017; Liu et al., 2022).

Lignocellulosic biomass is a complex substrate, mainly consisting of recalcitrant cellulose, hemicellulose, and lignin in varying proportions (Toushik et al., 2017; Chen, 2014). Majority of these compounds are degraded by enzymes, encoded by genes united in the CAZy database, including families of glycoside hydrolases (GHs), glycosyltransferases (GTs), polysaccharide lyases (PLs), carbohydrate esterases (CEs), auxiliary activities (AAs), and carbohydrate-binding modules (CBMs) (Drula et al., 2022). These genes are often combined in gene clusters, providing a full decomposition of a carbohydrate polymer (Zhang et al., 2018). Historically, Bacteroidota exhibited a cluster organization (Bjursell et al., 2006), which was referred to as polysaccharide utilization loci (PUL), which represented the set of physically linked genes organized around a *sus*CD gene pair (Terrapon et al., 2015). Later, cluster organization was shown for other phyla, not obligatorily linked with these genes (Terrapon et al., 2018). Therefore, for the automatic search of such structures, CAZyme gene clusters (CGC) were proposed, which encode at least one CAZyme, one transporter, one transcriptional regulator, and one signaling transduction protein (Zhang et al., 2018). Still, while PULs are curated and experimentally accredited working gene clusters with known substrates, CGCs are not. Thus, PULs are highly sought after in natural ecosystems, but they are mostly described for gut microbiota (Hao et al., 2021). The most frequent carriers of PULs belong to Bacteroidota and Bacillota (Grondin et al., 2017). Whether PULs are limited to these environments and phyla is unclear.

In natural ecosystems, the initial sequestration of carbon is accomplished by soil microorganisms (Wu et al., 2024). Soils represent a global diversity storage of microbiota capable of decomposing lignocellulosic substrates. It was shown that communities from carbon-rich soils are more capable of assimilating organic matter (Nayak et al., 2022). Thus, such soils can be used as a source for the mobilization of active microbiota. For this, we have chosen the soil of Chernevaya taiga (Tomsk, Russia), which forms in the mid-mountainous area in the conditions of low eluviation of nutrients and low erosion (E. V. Abakumov et al., 2020). The unique combination of environmental factors leads to the gigantism of the perennial grass cover (Kravchenko et al., 2022; Achat et al., 2013), which annually leaves up to 400 g/m^2 of lignocellulosic biomass to be processed by soil microorganisms. This results in the accumulation of the thick humic layer, reaching up to 70 cm in depth. The microbiota from this soil has great potential in decomposing cellulosic substrates, but this issue has not been studied before. Hence, the goal of our study was to reveal this potential by setting up a long-term decomposing experiment, where the soil of Chernevaya taiga was enriched with two contrasting lignocellulosic substrates (straw and leaf litter) to reveal which parts of the microbial community would be more advanced in the new conditions and to reveal differences in the functional potential of these communities. Two substrates of totally different hemicellulose composition were chosen to see to what extent different microbial communities would be mobilized from one soil microbiome under the influence of different substrates. This process was monitored by evaluating the shift of chemical composition of the substrates, taxonomic composition, and metagenome composition of the decomposing microbial communities with a focus on CAZy and PULs organization. The combination of Illumina sequencing of the 16S rRNA gene and Oxford Nanopore metagenome sequencing was used to reveal the most probable active bacterial members of these communities.

2 Materials and methods

2.1 Experiment setup

As a model of the decomposition of two contrasting cellulosic substrates, we set up the experiment of composting oat straw and leaf litter with the soil-based inoculum (Figure 1).

The soil of Chernevaya taiga was collected near Tomsk, Russia (N 56.30693, E 85.47063) in 2019. The forest is formed by a stable population of *Populus tremula* and *Abies sibirica*. The forbs are comprised of Siberian and Asia-specific tall-herbaceous perennials—*Euphorbia lutescens*, *Saussurea latifolia*, *Heracleum dissectum*, and *Alfredia cernua*. The soil type is Umbric Retisol, and its chemical characteristics and microbial composition were reported earlier (E. V. Abakumov et al., 2020; Kravchenko et al., 2022; Polyakov et al., 2022; Abakumov et al., 2023). Briefly, the topsoil was slightly acidic (pH = 5.8–6.2), with high organic carbon (2.4–9.9%) and nitrogen (0.2–0.6%) content. The phosphorus content reached 1,000 mg/kg, comparable to the soils from tropical rainforests—one of the most productive ecosystems (Reed et al., 2011). Two starter inoculates for the main experiment were prepared by making enrichment cultures by adding cellulose substrates to the soil twice to activate and later increase the number of cellulolytic microorganisms. For this, 500 g of topsoil was mixed with 25 g (20:1 in mass, 1:1 in volume) of air-dry substrates (shredded oat straw or birch leaf litter) in 1-l containers and incubated in a thermostat at 28 ± 2°C with a moisture content of 60%. After 8 months, an additional 12.5 g of the substrates were mixed in. The resulting composts were used as starter inoculates for the main experiment to accelerate the decomposition process.

For the experiment, two types of lignocellulosic biomass were used: (1) oat straw and (2) a mixture of fallen leaves of birch, oak, aspen, and willow ("leaf litter"). The chemical characteristics of the substrates are given in Supplementary Table S1. The substrates were shredded into particles 1–3 cm in size. For each type of lignocellulosic biomass, 3 kg

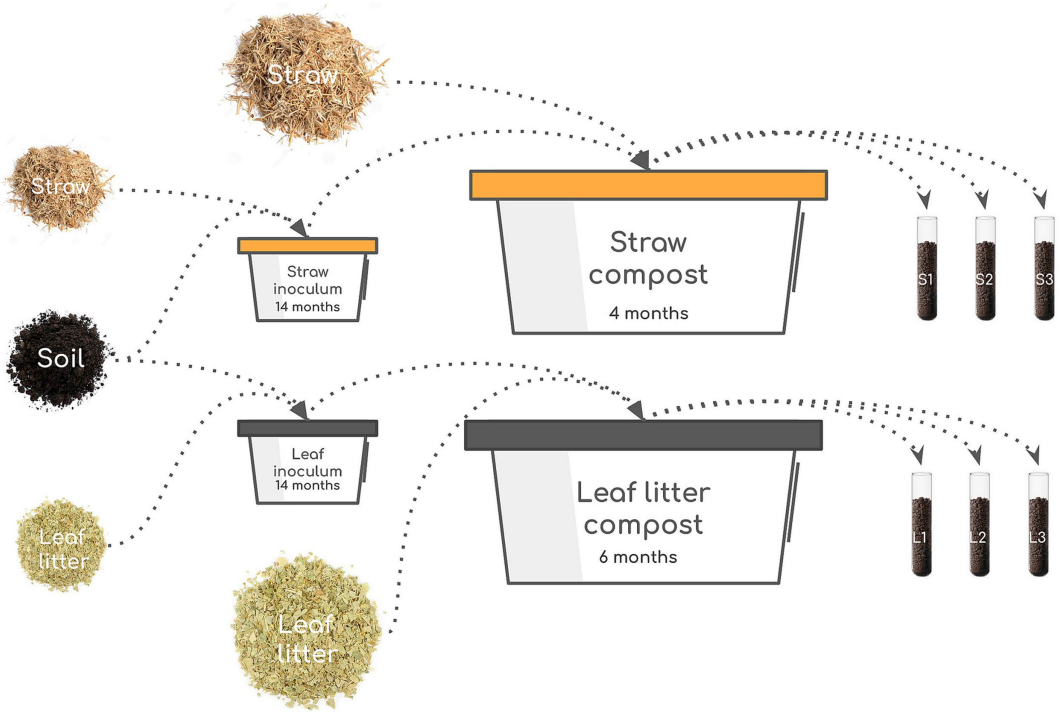


FIGURE 1
Scheme of the experiment. The starting culture was prepared by mixing soil and substrate (straw or leaves) and incubating for 14 months. The resulting inoculum was mixed with the fresh batch of substrates and incubated for 4 months (straw) or 6 months (leaves). Three samples were taken from each compost: 9, 61, and 111 days for straw and 9, 111, and 174 days for leaves.

of air-dry substrate, 300 g of compost inoculum, and 9 L of water were mixed in a 60-l polypropylene tub. Nine nylon bags with 5 g of air-dry substrate were placed inside the mixed mass for subsequent assessment of mass loss during composting. The top surface of the composted substrates was covered with plastic film to prevent drying out. Composting was carried out at a constant temperature of 28 ± 2°C in a thermostat room. Moisture content was controlled once a week, and the substance was stirred once every 2 weeks. Important to note is that while the decomposition of lignocellulosic biomass in the soil is accomplished both by fungi and bacteria, the conditions of our experiment favored the growth of the prokaryotic component more than the eukaryotic component since we aimed at exploring the genomic structure of the bacterial decomposers.

Sampling was carried out three times during the experiment based on the external signs of the decomposition stage, which differed for the two substrates: straw on days 9, 61, and 111 and leaf litter on days 9, 111, and 174, for a total of six samples. Furthermore, these dates are referred to as the early phase (day 9 for straw and leaf litter), middle phase (day 61 for straw and day 111 for leaf litter), and late phase (day 111 for straw and day 174 for leaf litter). The chemical analyses of samples were performed immediately after collection, while samples for enzymatic and molecular analyses were stored at −20°C until the end of the experiment.

2.2 Sample processing

As a measure of the decomposition process, we evaluated mass loss of the substrate, respiration rates, chemical composition, and enzyme activity for six collected samples. The amount of the decomposed substrate was quantified by measuring the dry weight of the contents of nylon bags at the time of sample collection. The activity of the microbial biomass was assessed through the respiration of the substrate, expressed in the amount of the release of carbon dioxide using the alkali absorption method (Cleve et al., 1979). Enzymatic analyses included amylase, catalase, exocellulase, endocellulase, peroxidase, polyphenol oxidase, invertase, and protease activity (Khaziev, 1976), which were carried out at the Agrophysical Research Institute. Other chemical analyses included the determination of pH, total carbon, nitrogen, cellulose, hemicellulose, and humic compound content (Tsyplenkov et al., 1997; Sharkov et al., 1976), which were conducted both for the samples of composts and of substrates before the decomposition. The pH values were measured using pH meter F690 (Beckman Coulter, Inc., United States). The content of organic carbon (TOC) was expressed through the ash content in the substrates. The content of total nitrogen (TN) was measured on an automatic nitrogen analyzer (Boshu, Switzerland).

For the amplicon sequencing, total DNA was extracted from the six experimental samples in triplicate using the RIAM protocol (Pinaev et al., 2022). Pair-ended libraries were prepared using primers F515 (5'-GTGCCAGCMGCCGCGGTAA-3′) and R806 (5'-GGAC TACVSGGGTATCTAAT-3′) (Bates et al., 2011) for the 16S rRNA gene and ITS3 (5'-GCATCGATGAAGAACGCAGC-3′) and ITS4 (5'-TCCTCCGCTTATTGATATGC-3′) (White et al., 1990) for the ITS2 fragment and sequenced on the Illumina Miseq platform (Illumina, Inc., United States).

DNA for the metagenome sequencing was extracted from the same six experiment samples, pre-stirred in liquid nitrogen, using the NucleoSpin® Soil Kit (Macherey-Nagel GmbH & Co. KG, Germany).

The metagenome libraries were prepared using the Ligation Sequencing Kit 1D (Oxford Nanopore Technologies, United Kingdom) and sequenced on the MinION platform with the Flow Cell 9.4.1 rev D (Oxford Nanopore Technologies, Oxford, United Kingdom).

2.3 Data analysis

The amplicon sequencing data were processed in Rstudio (R Core Team, 2024) using the DADA2 pipeline (Callahan et al., 2016) as described earlier (Kimeklis et al., 2023), including analysis of alpha-diversity (observed and Shannon (Shannon and Weaver, 1949) indices) and beta-diversity (NMDS (Kruskal, 1964) with Bray–Curtis distances (Bray and Curtis, 1957)). Taxonomic identification of isolated ASVs (amplicon sequencing variants) was performed using Silva 138.1 (for 16S rRNA gene) (Quast et al., 2013) and Unite ver8_02.02.2019 (for ITS2 fragment) (Nilsson et al., 2019) databases. The canonical correspondence analysis (CCA) (Braak et al., 1995) was performed to connect the microbiome composition of the composting substrates with the variability of their chemical characteristics. The data analyses of amplicon sequencing and analysis of chemical characteristics were performed using vegan (Oksanen et al., 2012), phyloseq (McMurdie and Holmes, 2013), and ANCOM-BC (H. Lin and Peddada, 2020) packages.

Metagenomes of the microbial decomposer communities of straw and leaf litter were basecalled by Guppy (Wick et al., 2019), assembled with Flye 2.9 using modifiers meta-and nano-raw (Kolmogorov et al., 2020), and polished with medaka (Medaka, 2024). The program kraken2 (Wood et al., 2019) in combination with the taxonkit utility (Shen and Ren, 2021) was used to determine the taxonomic composition of the metagenomes. The GTDB 214 database (Parks et al., 2022) was used as a reference base for prokaryotes (using the kraken2 struo2 database creation utility), and the PlusPF database based on the RefSeq NCBI database was used to identify eukaryotes. The results obtained were combined with the GTDB database, being prioritized for prokaryote taxonomy divergence. The functional annotation of the metagenomes was performed using EggNOG-mapper v2 (Cantalapiedra et al., 2021) via Diamond with the --frameshift parameter (Buchfink et al., 2021). The annotation results were normalized by the sequencing depth, acquired by minimap2 (Li, 2018) and samtools (Li et al., 2009), and contigs with length less than 10,000 were filtered out. The differences in gene composition between metagenomes of different substrates were assessed using differential expression analysis in limma/voom from the edgeR library (Law et al., 2014). Significantly different KO (KEGG Orthology) identifiers (Kanehisa et al., 2016) between substrates were further processed using the MinPath (Ye and Doak, 2009) program. DRAM annotator data were used to select genes responsible for lignocellulosic substrate decomposition based on functional annotation.

MAGs were isolated from the metagenome assemblies using Semibin2 software (Pan et al., 2023). After polishing the obtained draft bins by the medaka program, the bins were filtered by quality [medium (Genome QC Criteria, 2024) and high (Bowers et al., 2017)] using the CheckM2 program. Taxonomic annotation of MAGs was performed using GTDB-Tk (Chaumeil et al., 2022). PUL search in MAGs was performed using dbCAN in dbCAN-PUL (Ausland et al., 2021). The rRNA genes were isolated from the MAGs using the Barrnap program (Seemann, 2013) and aligned to the amplicon sequencing results. The results were visualized in the R software environment.

The package versions and scripts used in the study are available at the repository https://github.com/crabron/clusters.

3 Results

3.1 The chemical characteristics of the composting process

The initial difference between composted substrates was assessed by the differences in the dynamics of chemical and enzyme parameters it feels redundant. The decomposition process was evidenced by a decrease in respiration and the loss of substrate mass, carbon, cellulose, and hemicellulose content, with differing dynamics for two substrates (Figure 2A). During the oat straw decomposition, the microbial activity (accessed by the carbon dioxide emission from substrates) was the highest in the early and middle phases and rapidly declined toward the end, indicating the completion of the decomposition of the most available organic compounds. The leaf litter rates in the early and late phases were not significantly different, which may be linked to the initial smaller content of available nutrients. Along with the microbial activity, the process of decomposition for both substrates was marked by the mass loss of the decomposing substrate, which coincides with the loss of organic compounds. For the oat straw, 72.65% of the mass was decomposed by the late phase of the experiment, whereas the leaf mass loss by the late phase amounted to only 47.55%. In both substrates, the hemicellulose undergoes decomposition by the early phase, while the cellulose content in the substrate remains practically unchanged. A significant decrease in cellulose content was detected in the middle phase for the oat straw and the late phase for the leaf litter. This also could be linked to a higher content of humic compounds in straw compared to leaf compost.

The total carbon content decreased gradually in both substrates as they decomposed, while the total nitrogen content shifted in waves: an increase followed by a decrease, indicating succession in the microbial communities. The leaf compost at the beginning of composting had a pH value slightly more acidic than the straw compost due to differences in substrate acidity. During the composting process, an increase in pH was observed for leaf litter and a slight decrease for straw.

The dynamics of the enzyme groups of interest were shown to shift according to the stage of degradation and substrate (Figure 2B). Both oat straw and leaf litter were characterized by a decrease in the activity of peroxidase, invertase, amylase, and protease by the late stages of decomposition. Agreeing with the data of chemical analysis, higher enzyme activity was shown in the decomposition of oat straw. Straw compost showed higher activity of catalases, endocellulases, exocellulases, peroxidases, and proteases. Invertase was more active in leaf litter. Polyphenol oxidase in straw compost was the most active in the middle phase, while in leaf litter, it was in the last. Thus, significant differences in the rate and efficiency were observed in the decomposition of cellulose-containing substrates differing in nutrient availability.

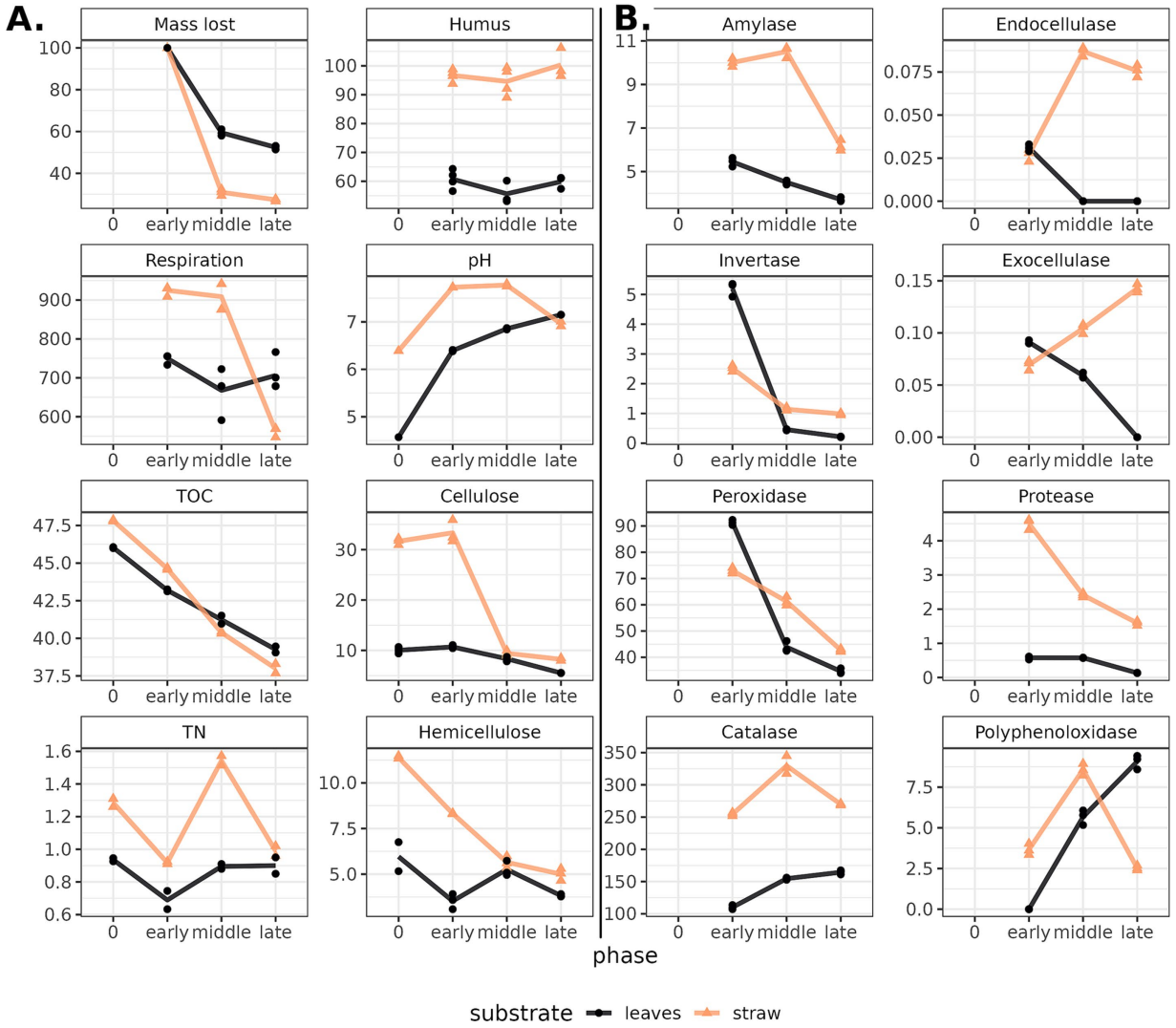


FIGURE 2
(A) Chemical characteristics and **(B)** enzyme activity in composts (leaves—black line, straw—yellow) during decomposition. Phase "0" stands for the characteristics of the cellulosic substrate without the soil-based inoculum. The Y-axis corresponds with the absolute values of the parameters (see Supplementary Table S1). Dots show replications (n = 3) within samples. Lines connect the means. TOC—total organic carbon, TN—total nitrogen.

3.2 The composts' taxonomic composition

We attempted to link the previously discussed differences in the chemical composition of composts with the dynamics of their taxonomic composition. After filtering unidentified phylum-level ASVs and organelle reads, a total of 2,244 phylotypes were identified for the 16S rRNA gene and 250 for the ITS2 fragment libraries. We observed a different pattern in taxonomic dynamics for prokaryotes and eukaryotes of microbial communities during plant residue decomposition. For prokaryotes, there was an increase in the richness (number of observed ASV) of both composting substrates from early to late stages (Figure 3A). Evenness (inverted Simpson index) increased in leaf litter compost and decreased in straw compost. Both richness and evenness of the eukaryotic component were characterized by a decline in diversity from the early to the late decomposition stages. The richness values were different in the beginning (in leaf litter higher), but at the late stage, they were equally low. Initially, the evenness values were similar, but in straw, at the later stages, values were higher. Thus, the prokaryotic and eukaryotic components of the decomposing community were characterized by reverse dynamics—an increase in the richness of the former and a decrease in the latter.

The beta-diversity of the microbiomes showed that the prokaryotic communities from the early phases of both composts were the most distinct from each other, while the middle and late phases for each substrate were similar (Figure 3B). The same was observed for eukaryotic communities, except that all phases of straw compost were quite close in composition (Supplementary Figure S1). According to the CCA, carbon content coincided with the dynamics of the decomposition, while respiration, pH, TN, cellulose, and humus content were associated with the substrate differences.

Since the experiment used a soil-based microbial inoculum for the initiation of the decomposition, the taxonomic composition of the composts' prokaryotic community was very diverse at the phylum level. The early phase consisted mostly of Pseudomonadota and Bacteroidota phyla, but during the composting process, their relative representation decreased in favor of other phyla (Acidobacteriota,

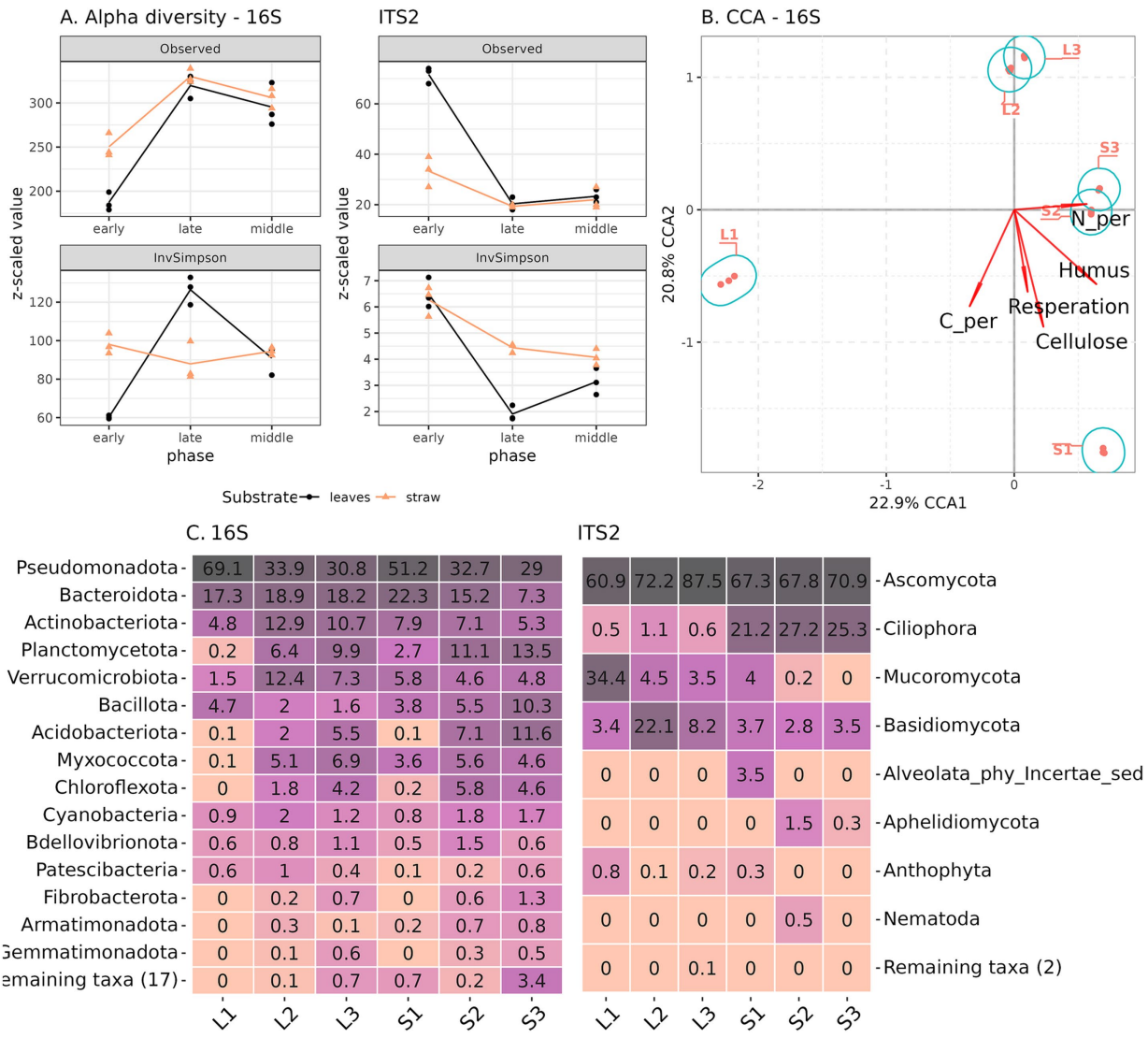


FIGURE 3
Prokaryotic and eukaryotic composition of composts accessed by 16S rRNA gene and ITS2 fragment Illumina sequencing. **(A)** Alpha-diversity, **(B)** CCA for 16S rRNA, and **(C)** Phylum composition (relative abundance). S1–S3—samples from straw compost, L1—L3—from leaf litter.

Planctomycetota, Myxococcota, Chloroflexota, and Cyanobacteria) (Figure 2C). In the straw compost, Bacillota increased their abundance during decomposition, while in leaf litter, they decreased. On the genus level in the early phase, both composts were dominated by *Flavobacterium*, *Pseudomonas*, *Pseudoxanthomonas*, and *Chitinophaga* (Supplementary Figure S2). In addition, in straw compost, we detected *Devosia*, *Luteimonas*, and *Sphingobacterium*; in leaf, we detected *Paenibacillus*, *Novosphingobium*, *Allorhizobium*, and *Galbitalea*. In the later phases, both composts were inhabited by *Ohtaekwangia*, *Acidibacter*, and *Steroidobacter*. Straw was characteristic of *Bacillus*, *Sphaerisporangium*, and *Clostridium*; leaf was characteristic of *Terrimonas*, *Verrucomicrobium*, and *Bauldia*. The diverse eukaryotic community of the early phases of decomposition was gradually replaced by *Ovatospora* (Ascomycota) in both composts, which was especially characteristic of leaf litter (Figure 3C; Supplementary Figure S2). The late phase of the straw compost became inhabited by ciliates *Gastrostyla* and *Gonostomum*. Potentially pathogenic fungi *Alternaria*, *Pyrenophora*, *and Lichtheimia* were present at the early phases of decomposition but not detected in the mature composts.

3.3 The composts' metagenome analysis and functional composition

After nanopore sequencing, six metagenomes (three for straw and three for leaf litter) with a total read length of 190.4 Gb were obtained. The technical information on the quality of reads after basecalling and the quality of the resulting assemblies is presented in the Supplementary Table S2. To characterize functional differences between composts, we compared full metagenome annotations, specifically CAZy genes. The composition of CAZy genes, linked to the polysaccharide's utilization, did not show significant variability either between substrate types or phases of decomposition, except for the early phase of leaf compost, which had the lowest values across all samples and DRAM categories (Figure 4A). The most abundant CAZy

gene categories were amorphous cellulose, mixed-linkage glucans, xylans, xyloglucan, and chitin.

Following assembly and subsequent annotation, 14,691 KO categories were identified in the metagenomes. After filtration by the representation, 5,793 KO categories were used for the differential analysis to assess significant differences between substrates, treating all phases from one substrate as replicates. As a result, 263 KO categories were significantly increased in straw and 258 KO categories were significantly increased in leaf litter (Supplementary Figure S3). The most represented category was the two-component system; each substrate was more abundant in specific KOs from this category (Figure 4B). Differences in the two-component system suggest that the leaf compost microbiome may experience catabolite repression, low nitrogen availability, and oxygen limitation (Supplementary Figure S4). The second most abundant category was ABC transporters, and the leaf compost had more than twice the amount of KO compared to straw. Notably, leaf litter compost was more abundant in taurine and alkanesulfonate uptake, which coincides with the fact that it was also more abundant in KO from sulfur metabolism. Straw compost was enriched in the metabolism of simpler compounds (starch and sucrose, amino sugar, fructose, and mannose), while leaf litter was more abundant in KO from pathways of aromatic compounds degradation (xylene, benzoate, aminobenzoate, furfural, dioxin, and hydroxy phthalate) (Figure 4B; Supplementary Table S3). The metagenome of the straw compost had more KO, indicating the presence of microbial interaction—bacterial chemotaxis, antibiotic resistance, and flagellar assembly. Both composts were enriched in nitrogen metabolism, but straw compost had a pronounced denitrification pathway. Diversification in secretion-type systems was also noted—while straw compost was more prevalent in types II, III, and VI, leaf litter was more prevalent in types I and IV. Straw was enriched in biotin and zinc uptake.

Consistent with the Illumina data, a considerable amount of contigs in the metagenomic assembly of early phases of composting was annotated as belonging to the Pseudomonadota phylum, which decreased in later phases (Supplementary Figure S5). Yet, even in the early phases, the proportion of genes associated with cellulose degradation in this phylum in the metagenomes was lower in both substrates compared to other phyla, e.g., Actinobacteriota, Planctomycetota, Bacteroidota, and Bacillota (Supplementary Figure S5). The most characteristic was the difference between the earliest phase and the rest for both substrates. Oat straw was characterized by a high proportion of endocellulases in Bacillota and Verrucomicrobiota representatives. Furthermore, the representation of these gene groups in the minor communities only continues to increase. For the leaf litter community, lower diversity of these genes (cellulase, catalase, and amylase) in minor phyla was observed, with higher representation in representatives of Actinobacteriota and Bacteroidota. Therefore, during the decomposition, we observed an increase in the taxonomic diversity of the functional genes.

3.4 MAGs and PULs from the compost's metagenomes

After we did not detect significant differences in CAZy composition between the composts, we shifted the analysis from the level of full metagenomes to metagenome-assembled genomes

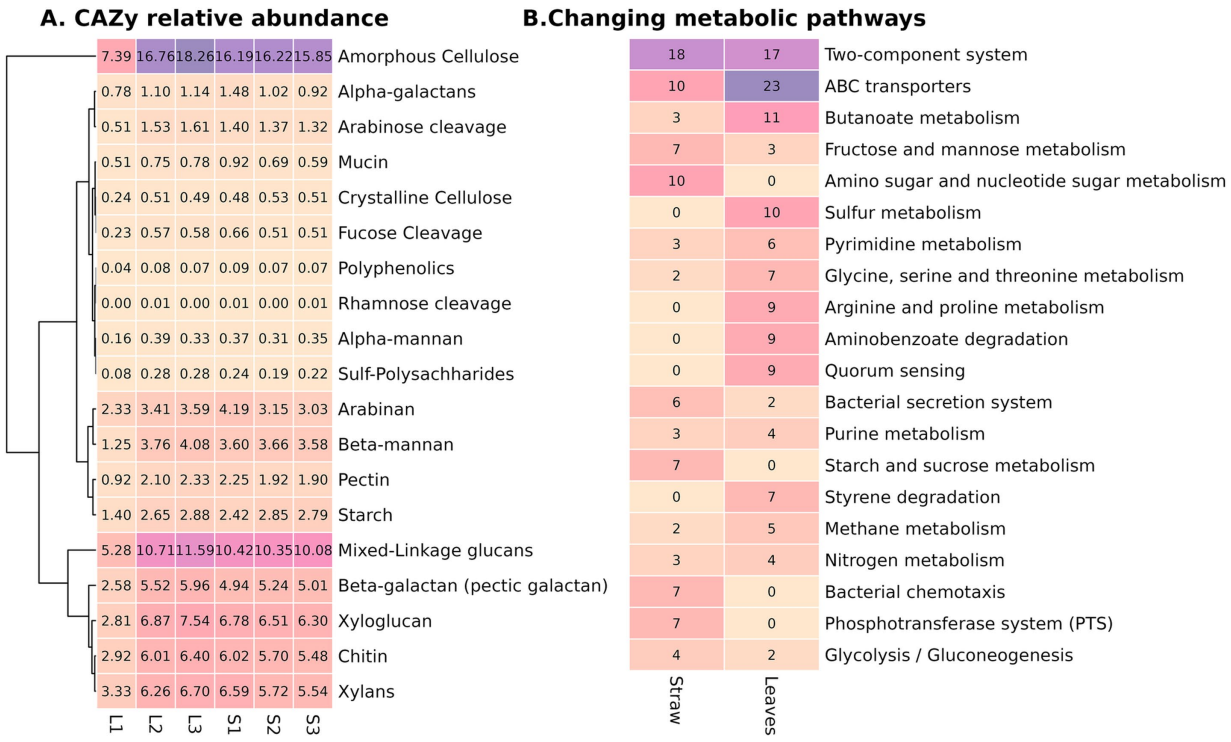


FIGURE 4
Metagenome characteristics of the contrasting composts: **(A)** Relative abundance (in percentiles from the ORFs from the metagenome) of CAZY genes united in DRAM categories in the six samples, **(B)** Number of KO (KEGG orthology) categories in the 20 most abundant metabolic pathways, significantly different between compost types.

(MAGs) and polysaccharide utilization loci (PULs). A total of 57 high and 240 medium-quality MAGs were obtained from the metagenomes. Of these, 254 contained clusters of carbohydrate-active genes (CGCs). In turn, PULs were identified in 188 genomes, of which 135 had clusters capable of cleaving the β-1,4 bond between glucose residues, which is characteristic of cellulose and hemicellulose. We compared the CGC/PUL ratio in MAGs from different phyla (Supplementary Figure S6) to elucidate possible distortions in the data we obtained, connected with the underrepresentation of non-Bacteroidota phyla in the dbCAN-PUL. All ratios strived toward 50%, except MAGs from Acidobacteriota and Verrucomicrobiota, although it may be caused by a small number of CGCs in them. The completeness of the genome assemblies did not affect these results. Thus, PUL quantities should adequately describe cellulolytic potential in the observed MAGs.

The highest number of PULs among all composts was observed in the representatives of Bacteroidota, Pseudomonadota, Actinomycetota, Bacillota, and Chloroflexota (Supplementary Table S4). The most numerous target substrates of their PULs were pectin, xylan, and arabinan. Pseudomonadota were also abundant in PULs for target substrates, not directly connected with cellulose degradation, such as capsule polysaccharide synthesis, glycosaminoglycan, and starch.

The data obtained allowed us to identify the most potentially active cellulolytic organisms from the microbial communities of both composts. These were nine MAGs, containing an abnormally high proportion of PULs relative to their genome size (Figure 5A). They attributed to Bacteroidota (*Chitinophaga* in straw and *Ohtaekwangia* in straw and leaf litter), Actinobacteriota (*Streptomyces* in straw), and Bacillota (*Pristimantibacillus* in leaf litter). There were other bacteria, mostly belonging to the Pseudomonadota, which contained high amounts of PUL, but their PULs used pectin as a target substrate or were involved in cell capsid degradation. We found a match for these MAGs with five phylotypes from 16S rRNA gene amplicon sequencing data (Figure 5B). Two bacilli genomes belonged to the same phylotype, and one representative of *Chitinophaga* aligned to a minor phylotype, probably due to nanopore sequencing error. The remaining phylotypes belonged to the major component of the community. *Bacillus* and *Streptomyces* were characteristic of the early stages of leaf decomposition, and *Chitinophaga* was most represented in the early stages of straw decomposition. The representative of *Ohtaekwangia* did not show substrate specificity in relative representation and appeared only at the late stages of decomposition.

The identified PUL target substrates varied between genera of MAGs. *Chitinophaga* was the most abundant in PULs specific for pectin, *Ohtaekwangia*—xylan, *Pristimantibacillus*—arabinan, and *Streptomyces*—beta-glucan (Figure 5C, Supplementary Table S5). Other target substrates, for which PULs were present, included arabinoxylan, mucin, glycosaminoglycan, chitin, and starch. "PULs of simpler polysaccharide compounds from MAGs assembled in this study shared high similarity with the reference ones, e.g., in *Chitiniphaga* – glucomannan, Streptomyces – beta-glucan, *Ohtaekwangia,* and *Pristimantibacillus* – pectin (Supplementary Figure S7). At the same time, PULs for xylans were mostly different in organization from the reference ones.

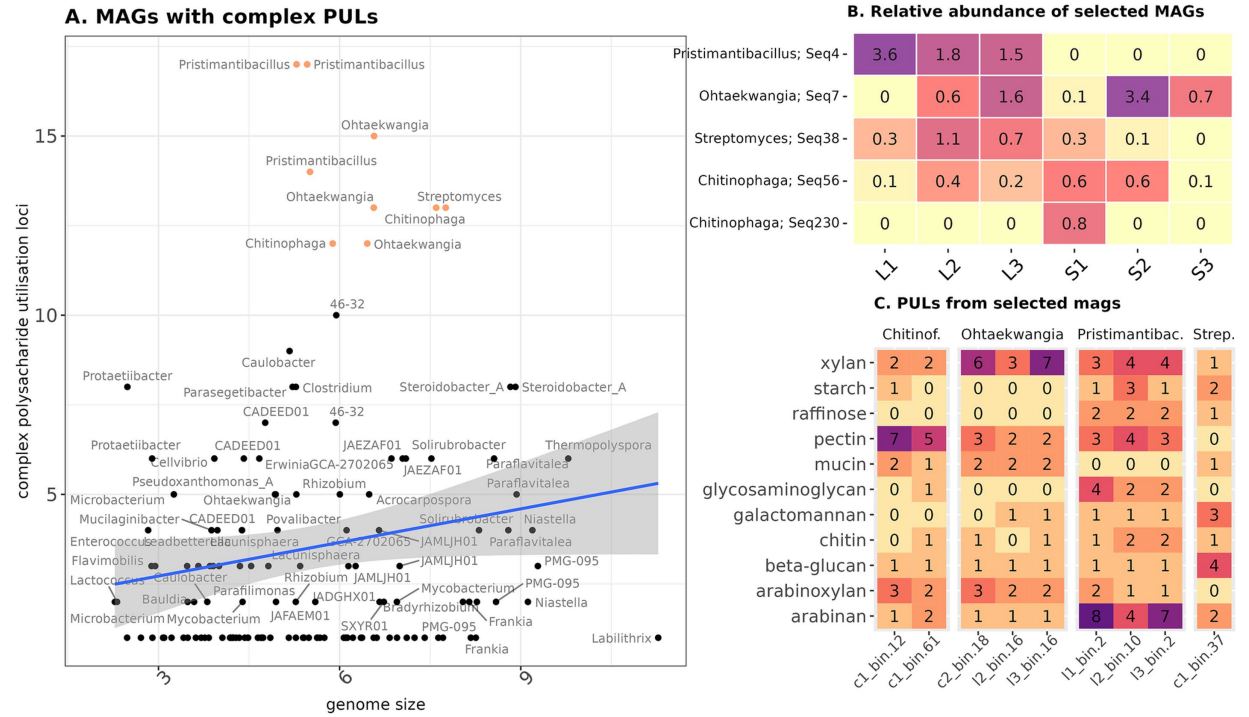


FIGURE 5
Characteristics of the most potential cellulolytic MAGs. **(A)** Ratio of PULs linked with lignocellulose degradation to the genome size. The group selected for further analysis is highlighted in color. **(B)** Presence of the chosen MAGs in the composts according to the Illumina data. **(C)** PUL substrates found in the selected MAGs. Genus names are given according to the GTDB annotation and match those on the left plot.

4 Discussion

In the present study, cellulolytic communities of different decomposition stages of oat straw and leaf litter were selected as the objective of the investigation. The use of a compost based on the soil of Chernevaya taiga soil as an inoculum was motivated by the fact that, although a significant number of active cellulolytic organisms have been described in the literature, majority of them have been isolated from rumen and intestinal microbiomes (Chassard et al., 2010), and soil microorganisms are extremely underrepresented in the databases. The advantage of soil microbiota over rumen is in the potentially higher adaptation to the decomposition of a wider range of plant residue types (Bao et al., 2021). Understanding which part of the microbial community has the greatest potential for lignocellulosic complex decomposition may allow a shift from microbial preparations based on individual strains to more effective ones based on microbial consortia (Bradáčová et al., 2019; Liu et al., 2023). This is specifically important because soil communities are highly diverse and relatively stable, which complicates the integration of microbial preparations based on single strains (Kaminsky et al., 2019; Ke et al., 2021). The soil of Chernevaya taiga, formed in unique environmental and geochemical conditions, is specifically promising in finding such microbiota.

We used two contrasting lignocellulosic substrates—oat straw and leaf litter. The dynamics of chemical characteristics and differences in the activity of the enzymes in both composts may indicate that oat straw in the experiment was more saturated with water-soluble hydrocarbons and proteins relative to leaf litter, while the latter was more recalcitrant due to higher content of resilient materials, not covered by our analyses. In addition, while organic carbon content was similar, nitrogen content was higher in straw, so the C/N ratio, which affects the activity of microbiota (Azis et al., 2023; Guo et al., 2018), was more favorable in straw than in leaf litter. The lower C/N ratio could also explain the release of mineral nitrogen in the middle phase of oat straw decomposition (Janssen, 1996), which additionally facilitated the endo-and exo-cellulolytic activity of the microbiota. The presence of bacterivorous ciliates in straw compost may serve as further evidence of the faster turnover of the organic material (Bick and Müller, 1973). Consistent with this, in our experiment, straw turned out to be a more accessible substrate and decomposed much faster than leaf litter.

As stated above, while both straw and leaf litter are cellulosic substrates, their resistance to decomposition is different due to chemical characteristics. This establishes conditions for the mobilization of different parts of the initial microbial soil community into the enrichment culture. We observed this effect in the taxonomic structure of the compost microbial communities, which shifted significantly between the types of substrates. However, both composts shared similar patterns of microbiome development. Our choice of longer periods of sample incubation had a significant effect on the outcome: we detected long-term shifts in microbial and functional composition, with an increase in bacterial diversity and a decrease in fungi, coinciding with one of our previous experiments (Kimeklis et al., 2023). The observations of dynamics at the taxonomic level are consistent with the earlier findings, specifically the prevalence of Pseudomonadota during the initial stages of straw colonization from soil and the diversification of the community in the later phases (X. Wang et al., 2022; Kimeklis et al., 2023). Genera detected by Illumina sequencing in both types of composts—*Pseudomonas*, *Bacillus*, *Flavobacterium, Sphingobacterium, and Novosphingobium*—were reported multiple times to contain potentially active cellulolytic species (Lednická et al., 2000; Kim and Yu, 2020; Cheng et al., 2019; Goswami et al., 2022). Cellulose-degrading strains from *Pseudoxanthomonas suwonensis* (Hou et al., 2015) and *Luteimonas* (Lin et al., 2020) were isolated from the soil. Hence, while both composts were diversified in major microbiota, majority of them comprised potential decomposers. Despite this, on the taxonomy level of analysis, we cannot determine which members of the community had this predisposition, especially considering that the microbiomes of the middle and late phases in both composts were very close, but the enzymatic activity between these phases shifted very prominently. Moreover, earlier findings showed that only a minority of a bacterial community in the compost may be associated with lignocellulosic substrate degradation (Sun et al., 2023). Therefore, we used metagenomic data to look for potential active decomposers in both communities.

Despite the strong variation in the activity of cellulolytic-related enzymes between the phases of decomposition and substrate types, we did not detect significant shifts in CAZy categories between the six analyzed metagenomes. Consistent with this, no enrichment of any CAZy families was shown between metagenomes of microbial communities isolated from different substrates (Gladkov et al., 2022). The activity of catalytic enzymes decreased by the late phases of decomposition, while the relative content of genes associated with lignocellulose decomposition remains stable. While we did not dwell on this matter more closely, we can speculate that this regulation is performed on the level of gene expression, which, in turn, is regulated at the cellular level by regulatory systems (e.g., two-component systems) responding to the substrate representation in the environment. This assumption is evidenced by the overrepresentation of diverse KO groups from two-component metabolic pathways between compost types. Another important observation is that although Pseudomonadota contributed a lot to the metagenome on the level of all annotated genes, their contribution to the genes associated with cellulose decomposition was smaller. Therefore, we can assume that members of minor phyla were potentially more involved in cellulose-degrading activity than members of Pseudomonadota (Supplementary Figure S5). This effect is particularly evident in the late stages of decomposition and is substrate-dependent. A similar effect was shown previously, as we detected that a significant part of microbial taxonomic diversity at the later phases of straw colonization does not participate in cellulose degradation because it does not have genes for the corresponding enzymes in its genomes, while these groups of microorganisms can make a serious contribution to the community by shifting the representation of effective cellulolytic microorganisms (Kimeklis et al., 2023).

To identify the most probable active decomposers of the microbial communities of the composts, we searched for MAGs with an abnormally high content of PULs relative to their genome size. The previous study on lignocellulose biomass decomposition indicated that the most promising degraders, according to the GH gene content, belong to Bacteroidota and Bacillota (Huang et al., 2023). Consistent with their findings, according to Illumina sequencing, Bacteroidota and Bacillota phyla were abundant in both composts, and out of nine MAGs, which we selected as promising active decomposers according to our criteria, five belonged to the first and three to the latter. Notably, Actinobacteriota was also reported to play an important role in the lignocellulose degradation (C. Wang et al., 2016), but only one potentially cellulolytic MAG from this phylum was assembled, which may be linked to its genome size (Seshadri et al., 2022). All these

MAGs were the representatives of both minor and major microbiota, indicating the involvement of the diverse ecological groups in the process of decomposition.

These data could not be checked for significance, but the PULs specificity seems to be connected to the MAG taxonomic attribution, not the phase of decomposition from which it was detected. Since we observed the taxonomic differentiation of potentially active MAGs between composts, we can assume that PUL specificity is also highly linked with the substrate type. Interestingly, Huang et al. (2023) used CGCs instead of validated PULs because majority of their data were not indexed in dbCAN-PUL. We managed to work on the PUL level, but majority of their target substrates were compounds, accompanying cellulose fibrils. Along with that, the PULs, specific for cellulose degradation, were absent in almost all MAGs, selected as potentially active degraders. This may be a consequence of the fact that the PUL database mostly covers compounds, usually found in the gastrointestinal tract, which is the most frequent object for studying polysaccharide degradation. Thus, our study demonstrates that soil communities decomposing lignocellulose can also be a valuable source for the identification of novel PULs.

All the above shows that the design of effective lignocellulosic communities requires an integrated approach, which is not limited only to the analysis of individual enzyme groups or individual taxa. It is important to understand the principles of formation and functioning of the cellulolytic microbial consortium to apply this knowledge to the formulation of highly effective microbial preparations.

5 Conclusion

The composts based on two types of lignocellulosic biomass were studied with a comprehensive approach using the combination of analyses of enzyme activities, Illumina Miseq read-based sequencing of the 16S rRNA gene and ITS2 fragment amplicon libraries, and metagenome analysis using Oxford Nanopore MinION long-read technology to search for promising cellulolytic prokaryotes. The complementarity and convergence of the two sequencing methods in the context of soil metagenomics were demonstrated. We have shown that in a long-term experiment on the decomposition of plant residues, despite the use of an inoculum prepared from one soil, succession of different microorganisms occurs in different composts. The rates of dynamics of chemical parameters and changes in taxonomic composition do not coincide, which indicates an incomplete correspondence between the functional potential and the taxonomic composition of the community. The same is confirmed by the fact that in the studied composts, the dynamics of enzymatic activity associated with the decomposition of plant residues did not coincide with the dynamics of the CAZy genes. However, the analysis showed that functional differences between composts were revealed not at the level of individual genes but at the level of their organization into clusters. Moreover, the analysis of MAGs of potential cellulolytic microorganisms showed that some of them are substrate-specific and are major representatives of the microbial community.

Data availability statement

The datasets presented in this study can be found in online repositories. The names of the repository/repositories and accession number(s) can be found in the article/Supplementary material.

Author contributions

AKK: Conceptualization, Investigation, Validation, Visualization, Writing – original draft, Writing – review & editing. GVG: Conceptualization, Data curation, Formal Analysis, Investigation, Methodology, Software, Validation, Visualization, Writing – original draft, Writing – review & editing. OVO: Formal Analysis, Methodology, Writing – review & editing. TOL: Methodology, Writing – review & editing. AMA: Formal Analysis, Software, Validation, Writing – review & editing. TSA: Resources, Writing – review & editing. AAK: Methodology, Resources, Writing – review & editing. AL: Resources, Writing – review & editing. EVA: Resources, Writing – review & editing. EEA: Funding acquisition, Project administration, Supervision, Writing – review & editing.

Funding

The author(s) declare that financial support was received for the research, authorship, and/or publication of this article. This research was funded by the Russian Science Foundation, grant no. 23–16-00147.

Acknowledgments

We thank the Center for Genomic Technologies, Proteomics and Cell Biology (ARRIAM, Russia) for performing the preparation and sequencing of gene and genomic libraries and the Agrophysical Research Institute for performing the enzymatic analysis. We also thank Sergei V. Loiko and Georgy I. Istigechev for organizing the field research of soil from the Chernevaya taiga under the leadership of Lapidus AL.

Conflict of interest

The authors declare that the research was conducted in the absence of any commercial or financial relationships that could be construed as a potential conflict of interest.

Publisher's note

All claims expressed in this article are solely those of the authors and do not necessarily represent those of their affiliated organizations, or those of the publisher, the editors and the reviewers. Any product that may be evaluated in this article, or claim that may be made by its manufacturer, is not guaranteed or endorsed by the publisher.

Supplementary material

The Supplementary material for this article can be found online at: https://www.frontiersin.org/articles/10.3389/fmicb.2024.1485353/full#supplementary-material

References

Abakumov, E. V., Loyko, S. V., Istigechev, G. I., Kulemzina, A. I., Lashchinskiy, N. N., Andronov, E. E., et al. (2020). Soils of Chernevaya taiga of Western Siberia — morphology, agrochemical features, microbiota. *Agric. Biol.* 55, 1018–1039. doi: 10.15389/agrobiology.2020.5.1018eng

Abakumov, E., Nizamutdinov, T., Lapidus, A., Istigechev, G., and Loiko, S. (2023). Micromorphological characteristics of soils in the Chernevaya taiga (Western Siberia, Russia). *Geosciences* 13:186. doi: 10.3390/geosciences13060186

Achat, D. L., Bakker, M. R., Augusto, L., Derrien, D., Gallegos, N., Lashchinskiy, N., et al. (2013). Phosphorus status of soils from contrasting forested ecosystems in southwestern Siberia: effects of microbiological and physicochemical properties. *Biogeosciences* 10, 733–752. doi: 10.5194/bg-10-733-2013

Ausland, C., Zheng, J., Yi, H., Yang, B., Li, T., Feng, X., et al. (2021). DbCAN-PUL: a database of experimentally characterized CAZyme gene clusters and their substrates. *Nucleic Acids Res.* 49, D523–D528. doi: 10.1093/nar/gkaa742

Azis, F. A., Choo, M., Suhaimi, H., and Abas, P. E. (2023). The effect of initial carbon to nitrogen ratio on kitchen waste composting maturity. *Sustain. For.* 15:6191. doi: 10.3390/su15076191

Bao, Y., Dolfing, J., Guo, Z., Chen, R., Meng, W., Li, Z., et al. (2021). Important Ecophysiological roles of non-dominant Actinobacteria in plant residue decomposition, especially in less fertile soils. *Microbiome* 9:84. doi: 10.1186/s40168-021-01032-x

Bates, S. T., Donna Berg-Lyons, J., Caporaso, G., Walters, W. A., Knight, R., and Fierer, N. (2011). Examining the global distribution of dominant archaeal populations in soil. *ISME J.* 5, 908–917. doi: 10.1038/ismej.2010.171

Bick, H., and Müller, H. P. (1973). Population dynamics of Bacteria and Protozoa associated with the decay of organic matter. *Bull. Ecol. Res. Comm.* 17, 379–386.

Bjursell, M. K., Martens, E. C., and Gordon, J. I. (2006). Functional genomic and metabolic studies of the adaptations of a prominent adult human gut symbiont, *Bacteroides Thetaiotaomicron*, to the suckling period. *J. Biol. Chem.* 281, 36269–36279. doi: 10.1074/jbc.M606509200

Bowers, R. M., Kyrpides, N. C., Stepanauskas, R., Harmon-Smith, M., Devin Doud, T. B. K., Reddy, R., et al. (2017). Minimum information about a single amplified genome (MISAG) and a metagenome-assembled genome (MIMAG) of Bacteria and Archaea. *Nat. Biotechnol.* 35, 725–731. doi: 10.1038/nbt.3893

Braak, T., Cajo, J. F., and Verdonschot, P. F. M. (1995). Canonical correspondence analysis and related multivariate methods in aquatic ecology. *Aquat. Sci.* 57, 255–289. doi: 10.1007/BF00877430

Bradáčová, K., Florea, A., Bar-Tal, A., Minz, D., Yermiyahu, U., Shawahna, R., et al. (2019). Microbial consortia versus single-strain inoculants: an advantage in PGPM-assisted tomato production? *Agronomy* 9:105. doi: 10.3390/agronomy9020105

Bray, J. R., and Curtis, J. T. (1957). An ordination of the upland Forest communities of southern Wisconsin. *Ecol. Monogr.* 27, 325–349. doi: 10.2307/1942268

Buchfink, B., Reuter, K., and Drost, H.-G. (2021). Sensitive protein alignments at tree-of-life scale using DIAMOND. *Nat. Methods* 18, 366–368. doi: 10.1038/s41592-021-01101-x

Callahan, B. J., McMurdie, P. J., Rosen, M. J., Han, A. W., Johnson, A. J., and Holmes, S. P. (2016). DADA2: high-resolution sample inference from Illumina amplicon data. *Nat. Methods* 13, 581–583. doi: 10.1038/nmeth.3869

Cantalapiedra, C. P., Hernández-Plaza, A., Letunic, I., Bork, P., and Huerta-Cepas, J. (2021). EggNOG-mapper v2: functional annotation, Orthology assignments, and domain prediction at the metagenomic scale. *Mol. Biol. Evol.* 38, 5825–5829. doi: 10.1093/molbev/msab293

Chassard, C., Delmas, E., Robert, C., and Bernalier-Donadille, A. (2010). The cellulose-degrading microbial Community of the Human gut Varies According to the presence or absence of methanogens: cellulolytic microbiota and CH4 production in the human gut. *FEMS Microbiol. Ecol.* 74, 205–213. doi: 10.1111/j.1574-6941.2010.00941.x

Chaumeil, P.-A., Mussig, A. J., Hugenholtz, P., and Parks, D. H. (2022). GTDB-Tk v2: memory friendly classification with the genome taxonomy database. *Bioinformatics* 38, 5315–5316. doi: 10.1093/bioinformatics/btac672

Chen, H. (2014). Biotechnology of lignocellulose: Theory and practice. Dordrecht: Springer Netherlands.

Cheng, J. F., Guo, J. X., Bian, Y. N., Chen, Z. L., Li, C. L., Li, X. D., et al. (2019). Sphingobacterium Athyrii Sp. Nov., a cellulose-and Xylan-degrading bacterium isolated from a decaying Fern (Athyrium Wallichianum Ching). *Int. J. Syst. Evol. Microbiol.* 69, 752–760. doi: 10.1099/ijsem.0.003231

Cleve, V., Keith, P. I., Coyne, E. G., Johnson, C., and Kelley, M. (1979). A comparison of four methods for measuring respiration in organic material. *Soil Biol. Biochem.* 11, 237–246. doi: 10.1016/0038-0717(79)90068-3

Drula, E., Garron, M.-L., Dogan, S., Lombard, V., Henrissat, B., and Terrapon, N. (2022). The carbohydrate-active enzyme database: functions and literature. *Nucleic Acids Res.* 50, D571–D577. doi: 10.1093/nar/gkab1045

Genome QC Criteria. (2024) *Ecogenomic Methods*. Available at: https://gtdb.ecogenomic.org/methods (Accessed July 29, 2024).

Giweta, M. (2020). Role of litter production and its decomposition, and factors affecting the processes in a tropical Forest ecosystem: a review. *J. Ecol. Environ.* 44:11. doi: 10.1186/s41610-020-0151-2

Gladkov, G. V., Kimeklis, A. K., Afonin, A. M., Lisina, T. O., Orlova, O. V., Aksenova, T. S., et al. (2022). The structure of stable cellulolytic consortia isolated from natural lignocellulosic substrates. *Int. J. Mol. Sci.* 23:10779. doi: 10.3390/ijms231810779

Goswami, K., Boruah, H. P. D., and Saikia, R. (2022). Purification and characterization of Cellulase produced by Novosphingobium Sp. Cm1 and its waste hydrolysis efficiency and bio-stoning potential. *J. Appl. Microbiol.* 132, 3618–3628. doi: 10.1111/jam.15475

Grondin, J. M., Tamura, K., Guillaume Déjean, D., Abbott, W., and Brumer, H. (2017). Polysaccharide utilization loci: fueling microbial communities. *J. Bacteriol.* 199:16. doi: 10.1128/JB.00860-16

Guo, T., Zhang, Q., Ai, C., Liang, G., He, P., and Zhou, W. (2018). Nitrogen enrichment regulates straw decomposition and its associated microbial Community in a Double-Rice Cropping System. *Sci. Rep.* 8:1847. doi: 10.1038/s41598-018-20293-5

Hao, Z., Wang, X., Yang, H., Tao, T., Zhang, J., Luo, H., et al. (2021). PUL-mediated plant Cell Wall polysaccharide utilization in the gut Bacteroidetes. *Int. J. Mol. Sci.* 22:3077. doi: 10.3390/ijms22063077

Hou, L., Jiang, J., Zhihui, X., Zhou, Y., and Leung, F. C.-C. (2015). Complete genome sequence of *Pseudoxanthomonas Suwonensis* strain J1, a cellulose-degrading bacterium isolated from leaf-and Wood-enriched soil. *Genome Announc.* 3, e00614–e00615. doi: 10.1128/genomeA.00614-15

Huang, J., Gao, K., Yang, L., and Lu, Y. (2023). Successional action of Bacteroidota and Firmicutes in decomposing straw polymers in a Paddy soil. *Environ. Microbiome* 18:76. doi: 10.1186/s40793-023-00533-6

Janssen, B. H. (1996). Nitrogen mineralization in relation to C:N ratio and decomposability of organic materials. *Plant Soil* 181, 39–45. doi: 10.1007/BF00011290

Kaminsky, L. M., Trexler, R. V., Malik, R. J., Hockett, K. L., and Bell, T. H. (2019). The inherent conflicts in developing soil microbial inoculants. *Trends Biotechnol.* 37, 140–151. doi: 10.1016/j.tibtech.2018.11.011

Kanehisa, M., Sato, Y., Kawashima, M., Furumichi, M., and Tanabe, M. (2016). KEGG as a reference resource for gene and Protein annotation. *Nucleic Acids Res.* 44, D457–D462. doi: 10.1093/nar/gkv1070

Kayler, Z., Janowiak, M., and Swanston, C. (2017). *Global carbon*. (June, 2017). U.S. Department of Agriculture, Forest Service, climate change resource center. Available at: https://www.fs.usda.gov/ccrc/topics/global-carbon.

Ke, J., Wang, B., and Yoshikuni, Y. (2021). Microbiome engineering: synthetic biology of plant-associated microbiomes in sustainable agriculture. *Trends Biotechnol.* 39, 244–261. doi: 10.1016/j.tibtech.2020.07.008

Khaziev, F. K. (1976). Enzymatic activity of soils. Toolkit. Moscow: Nauka.

Kim, H., and Yu, S. M. (2020). *Flavobacterium nackdongense* Sp. Nov., a cellulose-degrading bacterium isolated from sediment. *Arch. Microbiol.* 202, 591–595. doi: 10.1007/s00203-019-01770-5

Kimeklis, A. K., Gladkov, G. V., Orlova, O. V., Afonin, A. M., Gribchenko, E. S., Aksenova, T. S., et al. (2023). The succession of the cellulolytic microbial community from the soil during oat straw decomposition. *Int. J. Mol. Sci.* 24:6342. doi: 10.3390/ijms24076342

Kolmogorov, M., Bickhart, D. M., Behsaz, B., Gurevich, A., Rayko, M., Shin, S. B., et al. (2020). metaFlye: scalable Long-read metagenome assembly using repeat graphs. *Nat. Methods* 17, 1103–1110. doi: 10.1038/s41592-020-00971-x

Kravchenko, I., Rayko, M., Tikhonova, E., Konopkin, A., Abakumov, E., and Lapidus, A. (2022). Agricultural crops grown in laboratory conditions on Chernevaya taiga soil demonstrate unique composition of the rhizosphere microbiota. *Microorganisms* 10:2171. doi: 10.3390/microorganisms10112171

Kruskal, J. B. (1964). Multidimensional scaling by optimizing goodness of fit to a nonmetric hypothesis. *Psychometrika* 29, 1–27. doi: 10.1007/BF02289565

Law, C. W., Chen, Y., Shi, W., and Smyth, G. K. (2014). Voom: precision weights unlock linear model analysis tools for RNA-Seq read counts. *Genome Biol.* 15:R29. doi: 10.1186/gb-2014-15-2-r29

Lednická, D., Mergaert, J., Cnockaert, M. C., and Swings, J. (2000). Isolation and identification of cellulolytic Bacteria involved in the degradation of natural cellulosic Fibres. *Syst. Appl. Microbiol.* 23, 292–299. doi: 10.1016/S0723-2020(00)80017-X

Li, H. (2018). Minimap2: pairwise alignment for nucleotide sequences. *Bioinformatics* 34, 3094–3100. doi: 10.1093/bioinformatics/bty191

Li, H., Handsaker, B., Wysoker, A., Fennell, T., Ruan, J., Homer, N., et al. (2009). The sequence alignment/map format and SAMtools. *Bioinformatics* 25, 2078–2079. doi: 10.1093/bioinformatics/btp352

Liao, C., Long, C., Zhang, Q., and Cheng, X. (2022). Stronger effect of litter quality than Micro-organisms on leaf and root litter C and N loss at different decomposition stages following a subtropical land use change. *Funct. Ecol.* 36, 896–907. doi: 10.1111/1365-2435.13999

Lin, H., and Peddada, S. D. (2020). Analysis of compositions of microbiomes with Bias correction. *Nat. Commun.* 11:3514. doi: 10.1038/s41467-020-17041-7

Lin, P., Yan, Z.-F., and Li, C.-T. (2020). *Luteimonas cellulosilyticus* Sp. Nov., cellulose-degrading bacterium isolated from soil in Changguangxi National Wetland Park, China. *Curr. Microbiol.* 77, 1341–1347. doi: 10.1007/s00284-020-01934-3

Liu, L., Cheng, M., Yang, L., Xinyue, G., Jin, J., and Minjie, F. (2023). Regulation of straw decomposition and its effect on soil function by the amount of returned straw in a cool zone Rice crop system. *Sci. Rep.* 13:15673. doi: 10.1038/s41598-023-42650-9

Liu, J., Ding, C., Zhang, W., Wei, Y., Zhou, Y., and Zhu, W. (2022). Litter mixing promoted decomposition rate through increasing diversities of Phyllosphere microbial communities. *Front. Microbiol.* 13:1009091. doi: 10.3389/fmicb.2022.1009091

Liu, X., Mei, S., and Salles, J. F. (2023). Inoculated microbial consortia perform better than single strains in living soil: a meta-analysis. *Appl. Soil Ecol.* 190:105011. doi: 10.1016/j.apsoil.2023.105011

Manzoni, S. (2017). Flexible carbon-use efficiency across litter types and during decomposition partly compensates nutrient imbalances—results from analytical stoichiometric models. *Front. Microbiol.* 8:661. doi: 10.3389/fmicb.2017.00661

McMurdie, P. J., and Holmes, S. (2013). Phyloseq: an R package for reproducible interactive analysis and graphics of microbiome census data. *PLoS One* 8:e61217. doi: 10.1371/journal.pone.0061217

Medaka. (2024). *Sequence Correction Provided by ONT Research*. Available at: https://github.com/nanoporetech/medaka (Accessed July 5, 2024).

Nayak, N., Mehrotra, R., and Mehrotra, S. (2022). Carbon biosequestration strategies: a review. *Carbon Capture Sci. Technol.* 4:100065. doi: 10.1016/j.ccst.2022.100065

Nilsson, R. H., Larsson, K.-H., Taylor, A. F. S., Bengtsson-Palme, J., Jeppesen, T. S., Schigel, D., et al. (2019). The UNITE database for molecular identification of Fungi: handling dark taxa and parallel taxonomic classifications. *Nucleic Acids Res.* 47, D259–D264. doi: 10.1093/nar/gky1022

Ojo, A. (2023). An overview of lignocellulose and its biotechnological importance in high-value product production. *Fermentation* 9:990. doi: 10.3390/fermentation9110990

Oksanen, J., Blanchet, F. G., Kindt, R., Legendre, P., Minchin, P. R., O'Hara, R. B., et al. (2012). *Vegan: Community ecology package*. Available at: http://CRAN.R-project.org/package=vegan.

Pan, S., Zhao, X.-M., and Coelho, L. P. (2023). SemiBin2: self-supervised contrastive learning leads to better MAGs for short-and Long-read sequencing. *Bioinformatics* 39, i21–i29. doi: 10.1093/bioinformatics/btad209

Parks, D. H., Chuvochina, M., Rinke, C., Mussig, A. J., Chaumeil, P.-A., and Hugenholtz, P. (2022). GTDB: an ongoing census of bacterial and archaeal diversity through a phylogenetically consistent, rank normalized and complete genome-based taxonomy. *Nucleic Acids Res.* 50, D785–D794. doi: 10.1093/nar/gkab776

Pinaev, A. G., Kichko, A. A., Aksenova, T. S., Safronova, V. I., Kozhenkova, E. V., and Andronov, E. E. (2022). RIAM: a universal accessible protocol for the isolation of high purity DNA from various soils and other humic substances. *Methods Protoc.* 5:99. doi: 10.3390/mps5060099

Polyakov, V., Abakumov, E., Lodygin, E., Vasilevich, R., and Lapidus, A. (2022). Distribution of molecular weight of humic substances isolated from soils of tallgrass temperate rainforests (Chernevaya taiga). *Agronomy* 12:1760. doi: 10.3390/agronomy12081760

Quast, C., Pruesse, E., Yilmaz, P., Gerken, J., Schweer, T., Yarza, P., et al. (2013). The SILVA ribosomal RNA gene database project: improved data processing and web-based tools. *Nucleic Acids Res.* 41, D590–D596. doi: 10.1093/nar/gks1219

R Core Team. (2024). *R: A Language and Environment for Statistical Computing*. Available at: https://www.R-project.org/ (Accessed July 29, 2024).

Reed, S. C., Townsend, A. R., Taylor, P. G., and Cleveland, C. C.. (2011). Phosphorus cycling in tropical forests growing on highly weathered soils. In: Bünemann, E., Oberson, A., and Frossard, E. Phosphorus in action. *26*. Berlin, Heidelberg: Springer Berlin Heidelberg, 339–369.

Seemann, T. (2013). *Barrnap 0.8: Rapid ribosomal RNA prediction*.

Seshadri, R., Roux, S., Huber, K. J., Dongying, W., Sora, Y., Udwary, D., et al. (2022). Expanding the genomic encyclopedia of Actinobacteria with 824 isolate reference genomes. *Cell Genom.* 2:100213. doi: 10.1016/j.xgen.2022.100213

Shannon, C. E., and Weaver, W. (1949). The mathematical theory of communication. Champaign, IL: University of Illinois Press.

Sharkov, V. I., Kuibina, N. I., Solovieva, Y. P., and Pavlova, T. A. (1976). Quantitative chemical analysis of plant materials. Moscow: Forestry industry.

Shen, W., and Ren, H. (2021). TaxonKit: a practical and efficient NCBI taxonomy toolkit. *J. Genet. Genomics* 48, 844–850. doi: 10.1016/j.jgg.2021.03.006

Singh, N., Singhania, R. R., Nigam, P. S., Dong, C.-D., Patel, A. K., and Puri, M. (2022). Global status of lignocellulosic biorefinery: challenges and perspectives. *Bioresour. Technol.* 344:126415. doi: 10.1016/j.biortech.2021.126415

Sun, R., Wang, X., Hamoud, Y. A., Mengxing, L., Shaghaleh, H., Zhang, W., et al. (2023). Dynamic variation of bacterial community assemblage and functional profiles during Rice straw degradation. *Front. Microbiol.* 14:1173442. doi: 10.3389/fmicb.2023.1173442

Terrapon, N., Lombard, V., Drula, É., Lapébie, P., Al-Masaudi, S., Gilbert, H. J., et al. (2018). PULDB: the expanded database of polysaccharide utilization loci. *Nucleic Acids Res.* 46, D677–D683. doi: 10.1093/nar/gkx1022

Terrapon, N., Lombard, V., Gilbert, H. J., and Henrissat, B. (2015). Automatic prediction of polysaccharide utilization loci in *Bacteroidetes* species. *Bioinformatics* 31, 647–655. doi: 10.1093/bioinformatics/btu716

Thakur, T. K., Eripogu, K. K., Thakur, A., Kumar, A., Sanjeev Bakshi, S. L., Swamy, A. B., et al. (2022). Disentangling Forest dynamics for litter biomass production in a biosphere Reserve in Central India. *Front. Environ. Sci.* 10:940614. doi: 10.3389/fenvs.2022.940614

Toushik, S. H., Lee, K.-T., Lee, J.-S., and Kim, K.-S. (2017). Functional applications of Lignocellulolytic enzymes in the fruit and vegetable processing industries. *J. Food Sci.* 82, 585–593. doi: 10.1111/1750-3841.13636

Tsyplenkov, P. V., Fedotov, A. S., Bankina, T. A., and Fedorova, N. N. (1997). Determination of the chemical composition of plant materials. Saint-Petersburg: Publishing house St. Petersburg University.

Wang, C., Dong, D., Wang, H., Müller, K., Qin, Y., Wang, H., et al. (2016). Metagenomic analysis of microbial consortia enriched from compost: new insights into the role of Actinobacteria in lignocellulose decomposition. *Biotechnol. Biofuels* 9:22. doi: 10.1186/s13068-016-0440-2

Wang, X., He, P., Xinpeng, X., Qiu, S., and Zhao, S. (2022). Characteristics of Rice straw decomposition and bacterial community succession for 2 consecutive years in a Paddy field in southeastern China. *Sci. Rep.* 12:20893. doi: 10.1038/s41598-022-25229-8

White, T. J., Bruns, T., Lee, S., and Taylor, J. (1990). "Amplification and direct sequencing of fungal ribosomal RNA genes for Phylogenetics" in PCR Protocols. ed. T. J. White (Amsterdam, Netherlands: Elsevier), 315–322.

Wick, R. R., Judd, L. M., and Holt, K. E. (2019). Performance of neural network Basecalling tools for Oxford Nanopore sequencing. *Genome Biol.* 20:129. doi: 10.1186/s13059-019-1727-y

Wood, D. E., Jennifer, L., and Langmead, B. (2019). Improved metagenomic analysis with kraken 2. *Genome Biol.* 20:257. doi: 10.1186/s13059-019-1891-0

Wu, H., Cui, H., Chenxi, F., Li, R., Qi, F., Liu, Z., et al. (2024). Unveiling the crucial role of soil microorganisms in carbon cycling: a review. *Sci. Total Environ.* 909:168627. doi: 10.1016/j.scitotenv.2023.168627

Ye, Y., and Doak, T. G. (2009). A parsimony approach to biological pathway reconstruction/inference for genomes and metagenomes. *PLoS Comput. Biol.* 5:e1000465. doi: 10.1371/journal.pcbi.1000465

Zhang, H., Yohe, T., Huang, L., Entwistle, S., Peizhi, W., Yang, Z., et al. (2018). dbCAN2: a Meta server for automated carbohydrate-active enzyme annotation. *Nucleic Acids Res.* 46, W95–W101. doi: 10.1093/nar/gky418

frontiers | Frontiers in Microbiology

TYPE Original Research
PUBLISHED 28 January 2025
DOI 10.3389/fmicb.2025.1538117

Check for updates

OPEN ACCESS

EDITED BY
Muhammad Zahid Mumtaz,
Gansu Agricultural University, China

REVIEWED BY
Abhinav Aeron,
Chonbuk National University, Republic of Korea
Chengqiang Wang,
Shandong Agricultural University, China

*CORRESPONDENCE
Susu Fan
✉ fanss@qlu.edu.cn
Xinjian Zhang
✉ zhangxj@qlu.edu.cn

RECEIVED 02 December 2024
ACCEPTED 10 January 2025
PUBLISHED 28 January 2025

CITATION
Tang Y, Wang L, Fu J, Zhou F, Wei H, Wu X, Fan S and Zhang X (2025) Unraveling the microecological mechanisms of phosphate-solubilizing *Pseudomonas asiatica* JP233 through metagenomics: insights into the roles of rhizosphere microbiota and predatory bacteria.
Front. Microbiol. 16:1538117.
doi: 10.3389/fmicb.2025.1538117

COPYRIGHT
© 2025 Tang, Wang, Fu, Zhou, Wei, Wu, Fan and Zhang. This is an open-access article distributed under the terms of the Creative Commons Attribution License (CC BY). The use, distribution or reproduction in other forums is permitted, provided the original author(s) and the copyright owner(s) are credited and that the original publication in this journal is cited, in accordance with accepted academic practice. No use, distribution or reproduction is permitted which does not comply with these terms.

Unraveling the microecological mechanisms of phosphate-solubilizing *Pseudomonas asiatica* JP233 through metagenomics: insights into the roles of rhizosphere microbiota and predatory bacteria

Yuhan Tang[1], Linlin Wang[1], Jing Fu[1], Fangyuan Zhou[1], Hailei Wei[2], Xiaoqing Wu[1], Susu Fan[1]* and Xinjian Zhang[1]*

[1]Shandong Provincial Key Laboratory of Applied Microbiology, Ecology Institute, Qilu University of Technology (Shandong Academy of Sciences), Ji'nan, China, [2]Key Laboratory of Microbial Resources Collection and Preservation, Ministry of Agriculture and Rural Affairs, Institute of Agricultural Resources and Regional Planning, Chinese Academy of Agricultural Sciences, Beijing, China

The effects of phosphate-solubilizing bacteria (PSB) on plant productivity are high variable under field conditions. Soil phosphorus (P) levels are proposed to impact PSB performance. Furthermore, the effect of exogenous PSB on rhizosphere microbial community and their functions are largely unexplored. Our study examined how different P background and fertilization affected the performance of PSB *Pseudomonas asiatica* JP233. We further conducted metagenomic sequencing to assess its impact on rhizosphere microbiota and functions, with a focus on genes related to soil P cycling. We found that JP233 could enhance P solubilization and tomato growth to different extent in both high and low P soils, irrespective of P fertilization. It was particularly effective in high P soil without extra fertilization. JP233 altered the rhizosphere microbial community, boosting taxa known for plant growth promotion. It also changed soil gene profiling, enriching pathways related to secondary metabolite biosynthesis, amino acids, carbon metabolism, and other key processes. Particularly, JP233 increased the abundance of most P cycle genes and strengthened their interconnections. Populations of certain predatory bacteria increased after JP233 inoculation. Our findings provide valuable insights into PSB's mechanisms for P solubilization and plant growth promotion, as well as potential adverse impacts of resident microbes on bioinoculants.

KEYWORDS

phosphate-solubilizing bacteria, *Pseudomonas asiatica*, soil P cycling, metagenomics, predatory bacteria

1 Introduction

Macroelements in soil participate in various physiological activities of crop growth and development, and are closely related to crop yield (Wang F. et al., 2022; Wang L. L. et al., 2022; Wang Z. H. et al., 2022; Pan and Cai, 2023; Zhang et al., 2023). After nitrogen, phosphorus (P) is the second nutritional element that limits terrestrial ecosystems the most (Yang and Post, 2011). The amount of P that is currently directly absorbed and utilized by plants is less than 2.5% of the total P concentration in the world's soil, which severely limits plant growth and development (Pan and Cai, 2023; Pang et al., 2024). Nevertheless, conventional P application techniques not only fail to address this issue, but also lead to critical environmental consequences, such as eutrophication (Zhang et al., 2017; Feng et al., 2019). Phosphate-solubilizing bacteria (PSB) can liberate soluble P from recalcitrant P sources in the soil, providing plants with directly utilizable P. This microbial inoculant has been widely studied as an eco-friendly strategy to promote P uptake by plants (Luo et al., 1993; Feng et al., 2019; Huang K. et al., 2024; Huang Y. L. et al., 2024).

PSB, recognized as plant growth promoting rhizobacteria (PGPR), can be inoculated into the plant rhizosphere to enhance soil available phosphorus (AP) content and promote plant growth, and there have been many successful cases using PSB as P bio-fertilizers to enhance plant productivity (Bargaz et al., 2021; Elhaissoufi et al., 2022). However, there are also many studies report that effects of PSB in improving plant growth is variable, particularly under field conditions and their performances are influenced by many environmental factors (Raymond et al., 2021). For example, the soil total P and AP were found to have relations with PSB populations (Li et al., 2021). Furthermore, colonization and persistence of PSB in soil was proposed to be as a prerequisite for expression of P-solubilization and PGPR traits (Raymond et al., 2021).

A vast array of microbes resides within the rhizosphere, where their interactions with plants are crucial for nutrient acquisition and growth enhancement (Trivedi et al., 2020). Recently, considerable efforts have been directed toward understanding whether exogenous bioinoculants can successfully colonize in the rhizosphere and the subsequent effects they may have on the indigenous microbial community (Da Silva et al., 2022; Swiatczak et al., 2023; Sierra-García et al., 2024). Many studies have revealed that, although bioinoculants do not dominate the soil microbiome, they can indirectly foster plant growth by modulating the structure of the rhizosphere microbiome (Liu et al., 2020; Hu et al., 2021). However, due to the bioinoculants' intricate roles in the rhizosphere, their impacts on the resident microbiome remain largely unexplored (Swiatczak et al., 2023). Specifically, most research has centered on the impact of inoculants on the structure of the resident microbiota, with no studies yet reporting on the effects of exogenous PSB on microbiome functions (Kong and Liu, 2022). PSB are pivotal in soil P cycling, which are mainly regulated by four gene groups related to P-starvation response regulation, P-uptake and transport, inorganic P-solubilization, and organic P-mineralization (Liu et al., 2023). As of now, the influence of exogenous PSB on the P cycle gene profiles of resident microbiome remains unknown.

Pseudomonas asiatica JP233 is an efficient PSB isolated in our laboratory. Previous studies have demonstrated its ability to solubilize P and promote plant growth, with 2-keto gluconic acid (2KGA) serving as the primary functional factor for P solubilization *in vitro* (Yu et al., 2022). The *gcd* gene, which is crucial for the production of 2KGA, has been identified in its genome (Wang F. et al., 2022; Wang L. L. et al., 2022; Wang Z. H. et al., 2022). To devise optimal application strategies for JP233 in agricultural settings, the primary objectives of this study are as follows: Firstly, to investigate how varying P levels in soil affect the P solubilization and growth-promotion capabilities of JP233. Secondly, to utilize metagenomics sequencing to elucidate the impact of exogenous PSB on the structure and functional genes of plant rhizosphere microbiomes, with special emphasis on the effects on genes associated with soil P cycling.

2 Materials and methods

2.1 Plant and bacterial

P. asiatica JP233, isolated from the soil of vegetable greenhouse in Shouguang, Shandong Province, has been proved to be a potentially efficient Phosphate-solubilizing bacteria (PSB) (Wang F. et al., 2022; Wang L. L. et al., 2022; Wang Z. H. et al., 2022; Yu et al., 2022). Bacterial strains were streaked and purified on Luria-Bertani (LB) solid medium, single colonies were selected and transferred to LB liquid medium for shake culture at 180 rpm and 28°C for 24 h. The bacterial culture was then centrifuged, with the supernatants being discarded, and washed and re-suspended with sterile water as inoculant. Two kinds of soil with different phosphorus (P) (Supplementary Tables S1, S2), high-P soil and low-P soil, were used in the plant pot experiment, and Dutch hard powder tomato varieties were purchased from local suppliers.

2.2 Effect of different phosphorus levels on the solubility of phosphorus

The experiment involved 12 treatments, utilizing two different P levels soils [low-P (L) and high-P (H)]. Three levels of P application at 0, 50, and 100 mg kg^{-1} were applied under varying P levels soils. The experimental group was inoculated with the JP233 strain, while the control group received an equal amount of water. Each treatment included 12 biological replicates. The seeds were disinfected with alcohol and sodium hypochlorite, then placed in sterile water-soaked petri dishes at 28°C to aid germination. Subsequently, the tomato seedlings were transplanted into planting cups. When the tomato reached true leaf stage, the experimental group was inoculated with JP233 bacterial solution by root irrigation, and each plant received a 6 mL bacterial suspension with 10^8 CFU mL^{-1}. The control group received the same amount of sterile water. The pot experiment was run in a controlled environment at 25°C in full light in the greenhouse. Samples were collected at 7, 14, 21, 28 days post-inoculation of the bacterial solution to measure plant height, stem diameter, fresh weight/dry weight of the above/underground plant parts, total P content in the plant parts, total phosphorus (TP) content in the soil, and available phosphorus (AP) content in the soil. Plant total P was analyzed using the H_2SO_4-H_2O_2 digestion method and vanadium molybdate blue colorimetric method (Bao, 2000), soil TP was determined using the potassium persulfate digestion method (Su and Chen, 2010), and soil AP was assessed using the Olsen method (Bao, 2000).

2.3 DNA extraction and metagenomic sequencing

The H0 (0 mg kg^{-1} P added in high P soil) level, which is the most significant level of increase in soil AP content, was selected and the tomato rhizosphere soil was sampled for metagenomic sequencing analysis. The rhizosphere soil was collected by taking tomato root from its pot and gently shaking off the loosely attached bulk soil. The soil firmly adhering to the roots, with a thickness of approximately 1 mm, was deemed as rhizosphere soil and gathered through a washing and centrifugation process. DNA from rhizosphere soil samples of H0 tomato was isolated and purified with magnetic bead genomic DNA extraction kit (Beijing, Bioteke, China). Using the truSeq nano DNA LT library preparation kit (Illumina, United States), a DNA library was created. LC Bio Technology CO., Ltd. (Hangzhou, China) used the Illumina NovaseqTM 6000 platform to sequence DNA libraries. PE150 was the sequencing mode used. Using the fastqc program,[1] quality control of the original data was carried out. To eliminate host contamination, reads were aligned to the host genome using bowtie2.[2] To ensure that the subsequent assembly and analysis results were microbial sequences (Langmead and Salzberg, 2012). Valid data of each sample assembled by MEGAHIT software[3] to acquire FASTA format file (Li et al., 2015). Coding Region (CDS) prediction was carried out using MetaGeneMark software to retain contigs sequences with a length greater than 500 bp. Sequences with CDS length less than 100 nt were filtered according to the predicted results (Zhu et al., 2010; Gurevich et al., 2013). To extract non-redundant unigenes, CD-HIT[4] was used to cluster the CDS sequences of all samples. In the meantime, the longest sequence was chosen as the representative sequence to build the Unigenes collection, and identity 95% and coverage 90% were employed for clustering (Fu et al., 2012). The different annotation information taxonomic levels of species were obtained by using DIAMOND software[5] to compare the Unigenes protein sequence and Non-Redundant Protein Sequence Database (NR) meta library. Compared with Kyoto Encyclopedia of Genes and Genomes (KEGG), Gene Ontology (GO), Evolutionary genealogy of genes: Non-supervised Orthologous Groups (eggNOG), functional databases to obtain annotation information of each functional database (Buchfink et al., 2015). Finally, the abundance informations of various species and functional taxonomic levels were obtained based on the abundance statistics of Unigenes. Statistical analysis was performed based on species, function and Unigenes among the comparison groups. The difference threshold was $p < 0.05$ and $|\log_2(\text{fold change})| \geq 1$ ($\log_2$FC), which was applied for subsequent analysis.

2.4 Functional annotation and species classification of soil P cycle genes

Based on the genes related to P cycle in soil microorganisms reported in the literature (Dai et al., 2020; Liang et al., 2020; Huang K. et al., 2024; Huang Y. L. et al., 2024; Wang et al., 2024), a total of 33 genes involved in P cycle were collected by comparing the gene name and functional classification with KEGG annotation information of metagenomic clustering Unigene set, excluding genes involved in intracellular phosphatase production in microbial metabolic activities. According to the function of genes, they can be divided into three categories: (1) Genes involved in P-starvation response regulation; (2) Genes involved in P-uptake and transport system; (3) Genes involved in inorganic P-solubilization; (4) Genes involved in organic P-mineralization. The names, functions and classifications of genes related to P cycle in soil microorganisms are shown in (Supplementary Table S3). Based on the corresponding relationship between species and function in the samples, the correlation between species abundance and functional abundance was analyzed. DIAMOND software was used to compare Unigenes protein sequence with NR database (blastp, evalue≤1e−5). Each Unigene with the best comparison result index was selected as the species classification (Buchfink et al., 2015), and Unigene, species (all hierarchical species) and function (all hierarchical annotation results) were annotated accordingly.

2.5 Statistical analysis

Student's *t* test (*T*-test) and homogeneity of Variance Test were performed using IBM SPSS 25.0 (IBM Corporation, Armonk, NY, United States) to examine the significant differences between different P treatments. Metagenomic data using OmicStudio tools for bioinformatics analysis.[6] The functional abundance tables of all Unigenes and eight functional databases were statistically analyzed by Mann Whitney U test, and the threshold value of $|\log_2\text{FC}| \geq 1$, ($p < 0.05$) was used to determine the significant differences. The four types of genes involved in P-cycling were mapped with Unigenes and visualized in the volcano map. The results of KEGG Pathway Definition functional nonparametric difference analysis were visualized in STAMP plot. The gene abundance of four major types of microorganisms involved in P-cycling, as identified in metagenomic data sets, was normalized using Z-score transformation in R (Wu et al., 2022). The differences were then evaluated using a two-sample *T*-test, and GraphPad Prism 10.0 (GraphPad Software, La Jolla, CA, United States) was used to show the results. Spearman was used for correlation calculation, and the correlation threshold was $|\text{rho}| > 0.5$ and $p < 0.05$. The correlation network map was used to compare the complexity of gene association between the two groups.

3 Results

3.1 Effect of different P levels on JP233 efficacy

To investigate the impacts of P status on PSB, strain JP233 was inoculated to tomato plants cultivated in two kinds of soil with low (L) and high (H) P background. Different P fertilization levels were also included for both soils by amending 0, 50, 100 mg kg^{-1} of KH_2PO_4 (designated as L0, L50, L100, H0, H50, H100). In low P soil, JP233 could enhance soil AP within 28 days post inoculation (dpi) across all

1 http://www.bioinformatics.babraham.ac.uk/projects/fastqc/, V0.10.1.
2 https://www.sbgrid.org/software/titles/bowtie-2, V2.2.0.
3 https://github.com/voutcn/megahit, V1.2.9.
4 http://www.bioinformatics.org/cd-hit/, V4.6.1.
5 https://github.com/bbuchfink/diamond, V0.9.14.
6 https://www.omicstudio.cn/tool

three P fertilization levels (Figure 1A). Generally, the growth of tomato was much better under L50 and L100 compared to L0. Although JP233 could also promote plant growth, the increase of aboveground dry weight was not statistically significant after 14 dpi (Figure 1B; Supplementary Table S4). Strain JP233 could increase the P content of aboveground plant, and the increment was significant within 7 dpi (Figure 1C). Similarly, it could also increase the P content of tomato root, albeit the increment was not significant (Figure 1D). Notably, the root P content under L0 was much higher than the roots under L50 and L100 after 14 dpi, potentially due to the stressed growth conditions of the tomato plants under L0 (Figures 1B,D).

In high P soil (Supplementary Table S4), strain JP233 could also enhance soil AP during 28 dpi across all three P fertilization levels (Figure 2A). It is worth noting that extra P fertilization was not beneficial for tomato plant growth, as showed by the reduced aboveground dry weight under H50 and H100 compared with H0 (Figure 2B; Supplementary Table S5). Similar to in low P soil, JP233 could also promote plant growth and enhance the P content of aboveground plant parts and root, albeit the increment was not significant after 7 dpi (Figures 2B–D; Supplementary Table S5). After a comprehensive comparison, the H0 treatment was selected for further metagenomics analysis, as JP233 demonstrated effective P solubilization and plant growth promotion, and the influence of exogenous P could also be minimized under H0 conditions.

3.2 Effect of JP233 inoculation on microbial community structure

As indicated by Chao1, Shannon and Simpson indices, JP233 inoculation did not significantly change the α-diversity of microbial community (Supplementary Figure S1). However, the Anosim analysis revealed that the JP233 inoculation significantly altered the β-diversity ($p < 0.05$). The Principal Coordinate Analysis (PCoA) showed that JP233-treated soil samples clustered separately from the

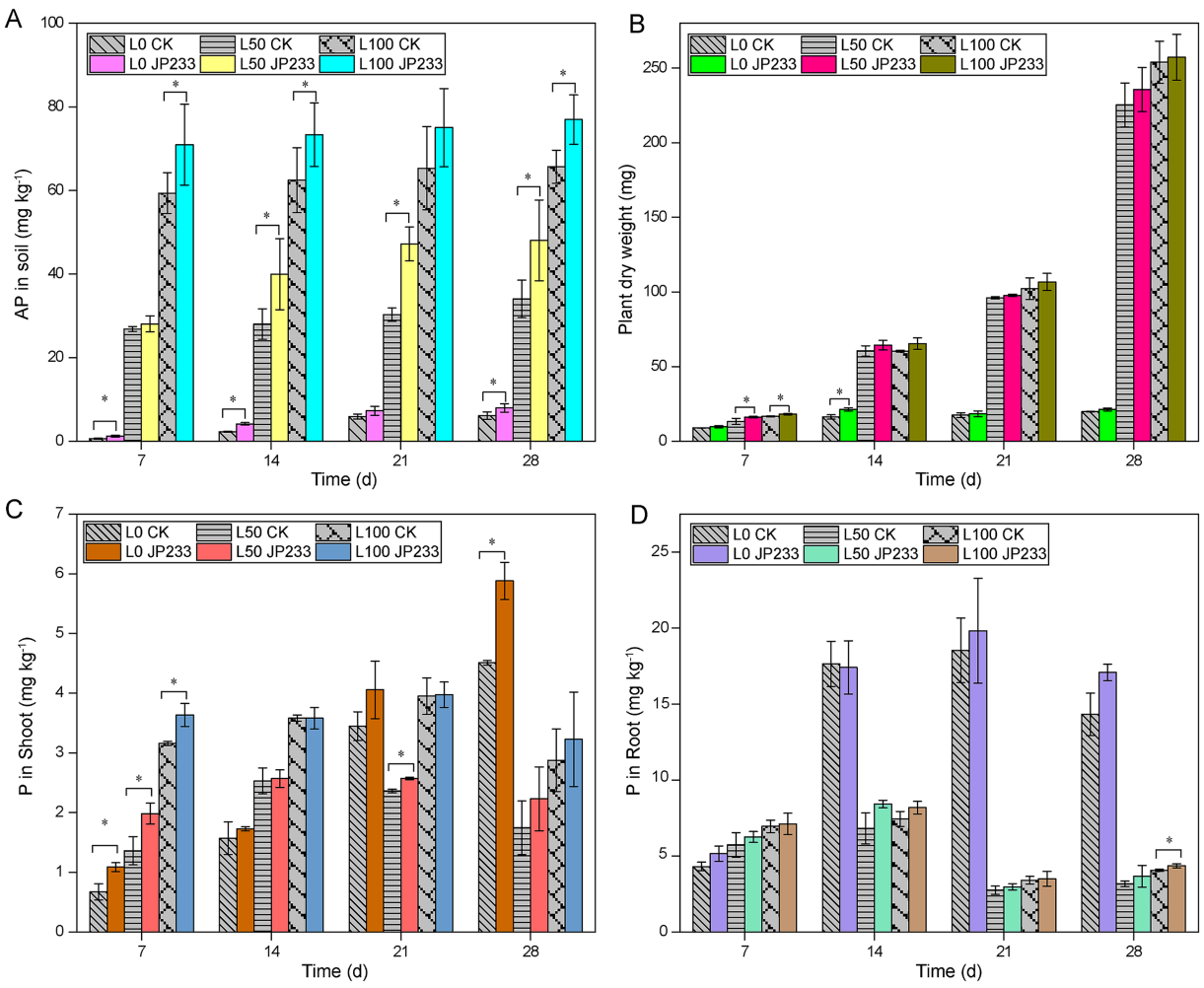


FIGURE 1
Available phosphorus (AP) content in low phosphorus (P) soil **(A)**; Aboveground dry weight in low-P **(B)**; Content of total phosphorus (TP) in aboveground **(C)**/ underground **(D)** of plants in low-P soil; Results represent means ± Standard Deviation (SD). Homogeneity of Variance Test and Student's *t* test (*T*-test) analysis were performed for each P level in the experimental group and the control group for the same culture time. * Significant difference was present at $p < 0.05$. L0, L50, L100 (low-P soil supplemented with 0, 50, 100 mg kg^{-1} of KH_2PO_4).

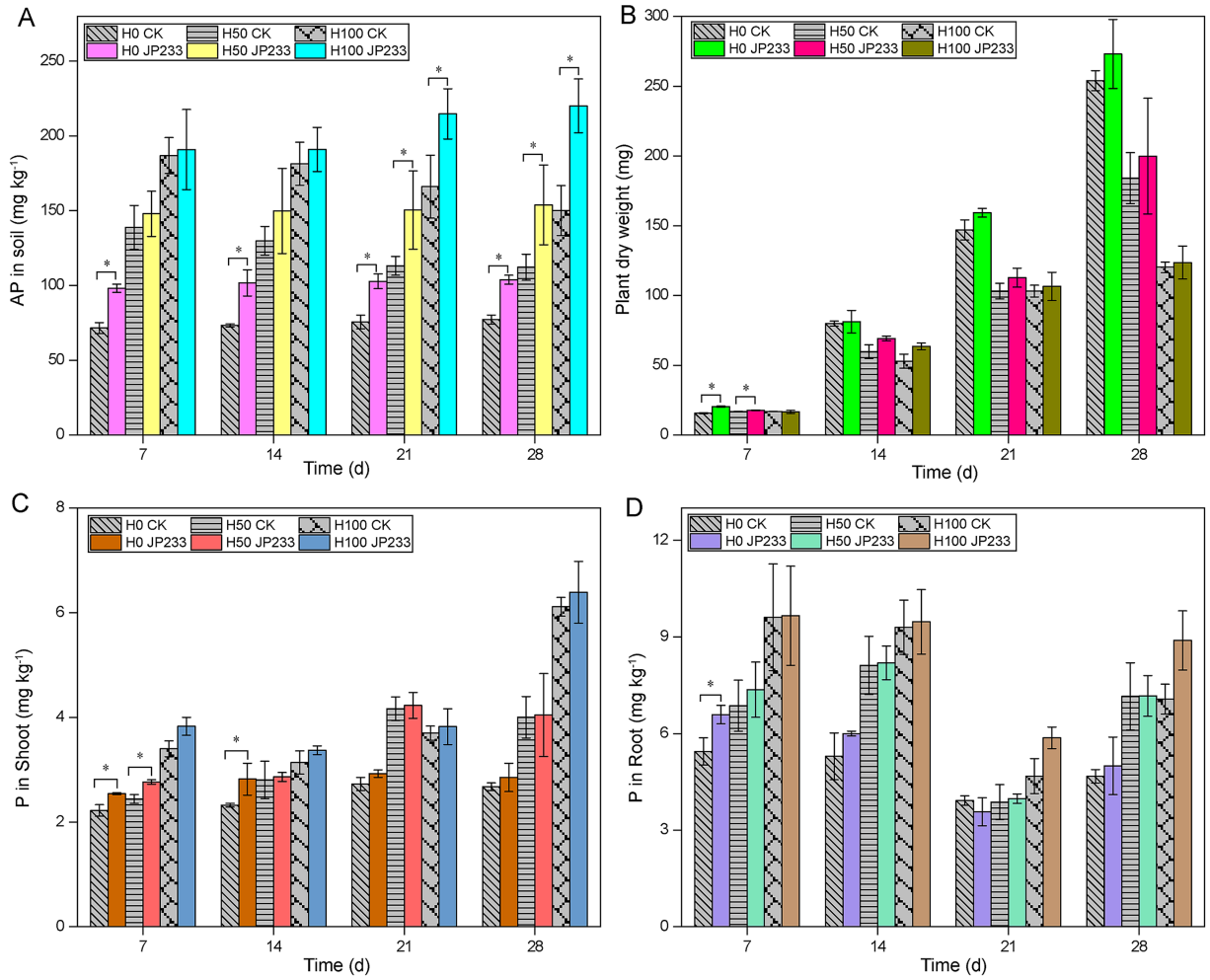


FIGURE 2
Available phosphorus (AP) content in high phosphorus (P) soil **(A)**; Aboveground dry weight in high-P **(B)**; Content of total phosphorus (TP) in aboveground **(C)**/ underground **(D)** of plants in high-P soil; Results represent means ± SD. Homogeneity of Variance Test and *T*-test analysis was performed for each P level in the experimental group and the control group for the same culture time. * Significant difference was present at $p < 0.05$. H0, H50, H100 (high-P soil supplemented with 0, 50, 100 mg kg^{-1} of KH_2PO_4).

control (CK), with PCo1 explained 30.11% variance (Figure 3A). Species annotation based on Unigene sequence assembly discovered that the majority of Unigenes in tomato rhizosphere soil (>83%) originated from bacteria. Following JP233 inoculation, the relative abundance of bacteria was enhanced, while the abundance of viruses and eukaryotes were both significantly depressed ($p < 0.05$) (Figures 3B,C). The top 20 abundant species that were altered by JP233 are shown in Figure 3D. As expected, the relative abundance of *P. asiatica* was found enhanced significantly ($p < 0.05$). *Pseudomonas putida* was also found to be elevated, but there is reason to speculate that the reads may have originated from JP233, given the very close phylogenetic relationship between *P. putida* and *P. asiatica* (Wang F. et al., 2022; Wang L. L. et al., 2022; Wang Z. H. et al., 2022). It is noteworthy that the relative abundance of *Bdellovibrio bacteriovorus* significantly increased after JP233 inoculation (Figure 3D). Given that *B. bacteriovorus* is a predatory bacterium that invades and preys on other Gram-negative bacteria (Strauch et al., 2007), the increase has a detrimental effect on the survival of JP233.

3.3 Effect of JP233 on rhizosphere soil gene profiling

The inoculation of JP233 induced modifications in the rhizosphere soil gene profiling, resulting in a total of 134,184 unigenes with increased abundance and 164,550 unigenes with decreased abundance (Supplementary Figure S2). According to KEGG annotation, these unigenes with significant abundance changes can be categorized into 33 pathways (Figure 4A). Among them, biosynthesis of cofactors, fatty acid metabolism, and ribosome, among others, were enhanced, whereas pathways such as monobactam biosynthesis, lysine biosynthesis, ascorbate and aldarate metabolism exhibited decreases. Enrichment analysis revealed that the unigenes exhibiting significant abundance alterations were predominantly enriched in pathways including the biosynthesis of secondary metabolites, amino acids, carbon metabolism, and others (Figure 4B). Given the advantageous roles of secondary metabolites, amino acids, and organic carbon in

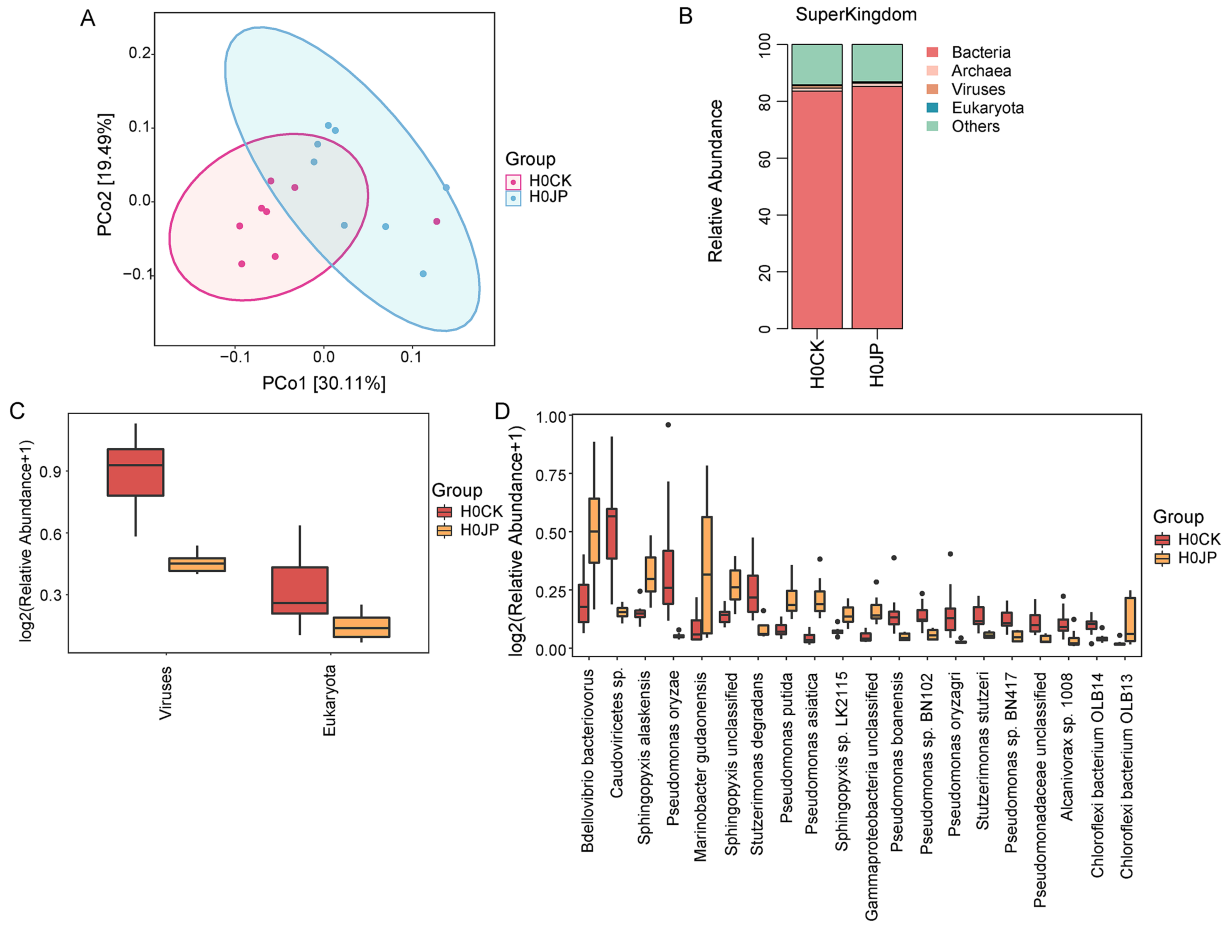


FIGURE 3
Principal Coordinate Analysis (PCoA) of tomato rhizosphere bacterial community **(A)**; Comparison of differences between two groups of JP (JP233) and CK at super-kingdom level **(B)**; Changes in relative abundance of eukaryotes and viruses with significant differences at super-kingdom level **(C)**; Relative abundance of differentiated species across treatments in both JP and CK groups at the species level **(D)**. Threshold screening is based on $|\log_2$ Fold Change$| \geq 1$ ($\log_2$FC), $p < 0.05$.

fostering plant health and growth, these alterations in gene profiling could potentially be attributed to the enhancement of plant growth.

3.4 Effect of JP233 on genes related to soil P-cycling

The processes of the soil P cycle are primarily governed by four distinct gene groups, which are associated with the regulation of P-starvation response, P-uptake and transport, inorganic P-solubilization, and organic P-mineralization (Liu et al., 2023). Based on KEGG annotation, our focus was on 33 genes involved in P cycle (Supplementary Table S3), excluding genes related to intracellular phosphatase production during microbial metabolism (Bergkemper et al., 2016). Notably, the inoculation of JP233 resulted in a significant 3.4% increase in the total relative abundance of P cycle genes ($p < 0.05$). Furthermore, approximately 79% of these P cycle genes exhibited a heightened abundance. According to PCoA analysis, there were significant difference in the profiling of soil P cycle genes attributable to the inoculation of JP233 (Figure 5A).

The most prominent P cycle genes identified in the soil samples were *phoR*, *pstB*, *ppk*, *pstS* and *gcd* (Figure 5B). Specifically, *phoR*, which encodes the phosphate regulon sensor histidine kinase, is associated with the P-starvation response. The *pstB* and *pstS* genes encode components of the high-affinity phosphate-specific transporter *PstSABC*, while the *ppk* gene, which encodes polyphosphate kinase, is also involved in P-uptake and transport. Additionally, the *gcd* gene, encoding quinoprotein glucose dehydrogenase, is linked to inorganic P-solubilization through gluconic acid production. Despite JP233 possessing the *gcd* gene, it did not significantly increase its abundance in the soil ($p > 0.05$). However, JP233 did enhance the abundance of the *ppx* gene, which encodes exopolyphosphatase (PPX), playing a crucial role in the degradation of inorganic polyphosphate into phosphate (Song et al., 2020). Additionally, JP233 increased the abundances of two genes related to organic P-mineralization: *ugpQ* and *phnO*, which encode glycerophosphodiester phosphodiesterase (GDPD) and a C-P lyase subunit, respectively ($p < 0.05$). Conversely, JP233 also decreased the abundances of two P cycle genes, *ugpC* and *phoN*, which encode components of the Ugp transport system and C-P lyase, respectively ($p < 0.05$).

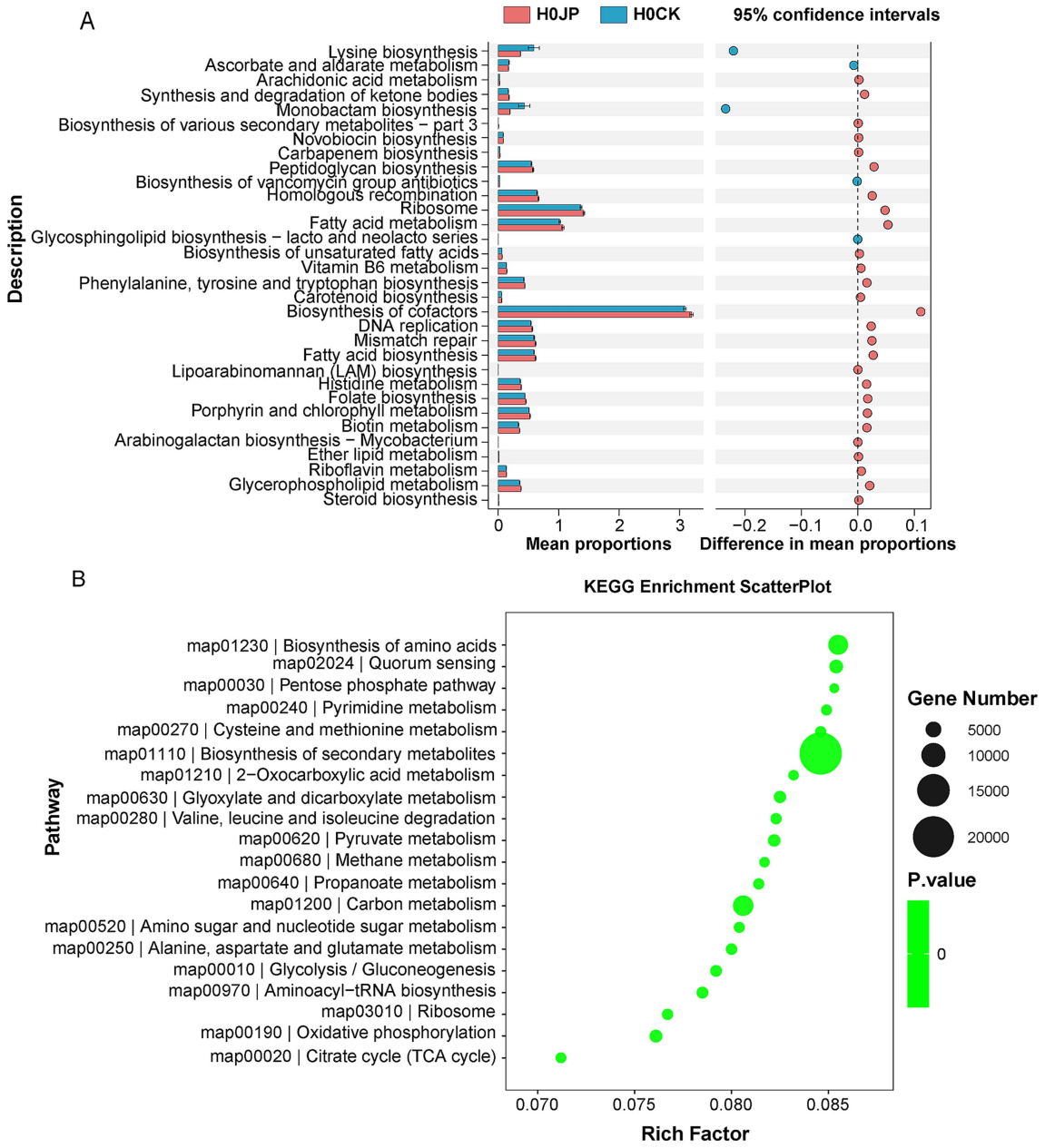


FIGURE 4
Differences in gene and pathway expression in rhizosphere soil inoculated with JP233 (JP). Kyoto Encyclopedia of Genes and Genomes (KEGG) Pathway Definition entries with significant differences **(A)**; KEGG enrichment analysis was performed for genes with different abundance **(B)**. There were eight samples replicates in each group, and the threshold was $|\log_2$ Fold Change$| \geq 1$ ($\log_2$FC), $p < 0.05$.

In addition to the individual P cycle genes, the inoculation of JP233 also modified their co-occurrence network. Specifically, JP233 boosted the connectivity among soil P cycle genes. Comparing with the JP233-treated soil samples, the P gene network in control (CK) soil exhibited lower complexity and sparser linkage density (Figure 5C). The inoculation of JP233 significantly improved key topological parameters, including the average degree and the interconnections among P cycle genes. Notably, genes implicated in P-uptake and transport (*phnCDE*, *pstB*), inorganic P-solubilization and organic P-mineralization (*gcd*, *phnJLHMNP*), as well as the regulation of P-starvation response (*phoB*) demonstrated a substantial increase in node degree and interaction patterns (Figure 5D).

3.5 Effect of JP233 on the taxonomic compositions of P cycle genes

To ascertain the origins of the alterations in the abundance and co-occurrence network of soil P cycle genes following the inoculation of JP233, their taxonomic compositions were traced. Figure 6 displays the top 20 most abundant genera of the P cycle genes that underwent significant alterations due to JP233. Notably, the abundances of the *ppx* gene from *Sphingopyxis*, *Sphingosinicella*, and *Bdellovibrio* increased significantly ($p < 0.05$). Similarly, the abundances of the *ugpQ* gene from *Sphingopyxis* and *Marinobacter* also showed a significant increase ($p < 0.05$). However, for the genes *phnO*, *ugpC*,

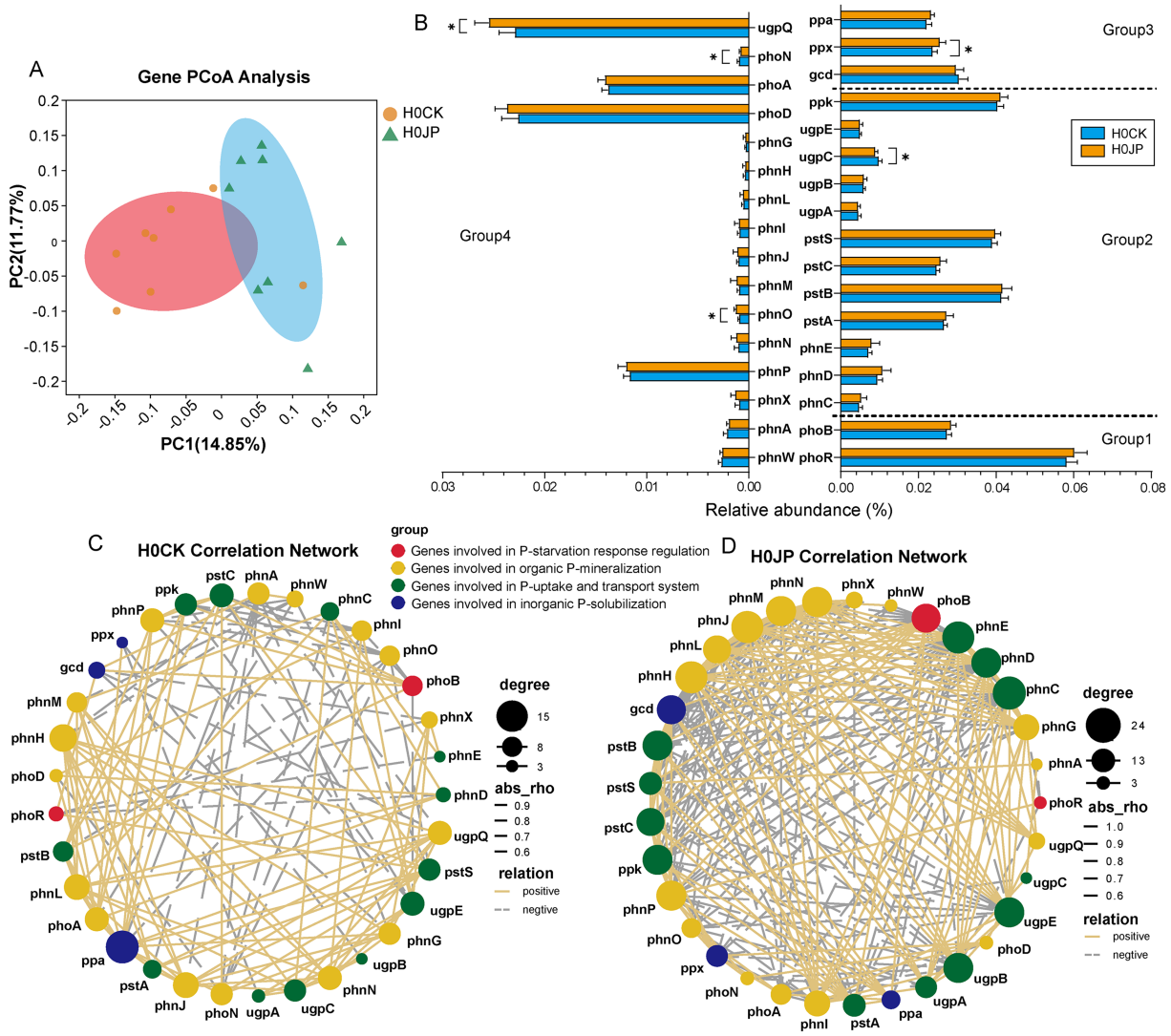


FIGURE 5
PCoA analysis of P cycle genes **(A)**; Changes in abundance and interaction complexity of genes associated with P cycle gene under JP and CK treatments. Under different treatments, relative abundance of genes involved in (1) P-starvation response regulation, (2) P-uptake and transport system, (3) inorganic P-solubilization, (4) organic P-mineralization **(B)**; Network co-occurrence of genes involved in P cycle between the two groups **(C,D)**. * Indicates a significant difference in the relative abundance of genes between the two groups ($p < 0.05$). Node size and color shade indicate the number of related objects between genes. The thickness of the lines indicates the strength of the correlation between genes. The shape of the lines indicates positive and negative correlations between genes.

and *phoN*, no individual genus within the top 20 showed significant alterations. While the abundances of other P cycle genes remained largely unchanged, their taxonomic compositions did shift, as evidenced by PCoA analysis (Figure 6F).

4 Discussion

In this study, we investigated the influence of various phosphorus (P) conditions and P fertilization on the performance of PSB, specifically *P. asiatica* JP233. Our findings revealed that high P soil without additional P amendment (H0) provides an optimal environment for JP233 to exhibit P solubilization and plant growth promotion. Subsequently, we employed metagenomic sequencing to analyze the effects of JP233 on the microbial community structure and functional gene profiles. Special attention was given to genes associated with soil P cycling, in order to elucidate the impacts of JP233 on these critical processes. To our knowledge, this represents the first report utilizing a metagenomics strategy to study the effects of exogenous PSB on the resident rhizosphere microbiome.

The inoculation of JP233 increased the abundance of most P cycle genes and enhanced the connectivity of the gene co-occurrence network, particularly for the genes related to organic P-mineralization (*phnJLHMNP*), P-uptake and transport system genes (*pstB*, *phnCDE*). To different degrees, JP233 induced an increase in the abundance of genes involved in P-starvation response regulation (*phoB*), inorganic P-solubilization (*ppx*, *ppa*), organic P-mineralization (*ugpQ*), alkaline phosphatase (*phoAD*) and other related genes. In soils with long-term high-P inputs, the richness of soil P cycle genes and their interconnections decreased (Liu et al., 2023). Our result demonstrated

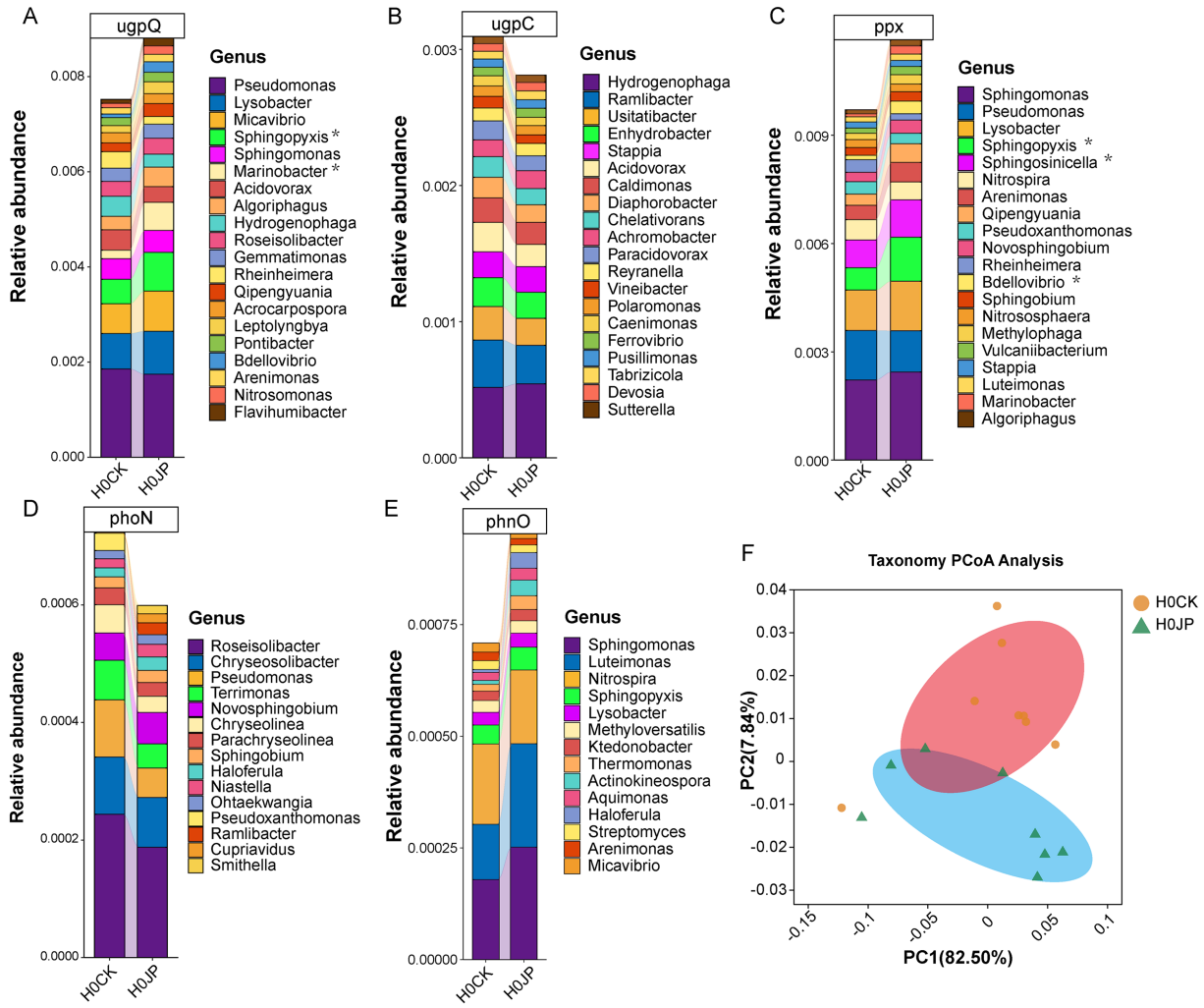


FIGURE 6
Changes in species corresponding to genes associated with rhizosphere soil P cycle. After the inoculation of JP233, the top 20 genera with the highest content in the significantly altered P cycle genes *ugpQ* **(A)**, *ugpC* **(B)**, *ppx* **(C)**, *phoN* **(D)**, *phnO* **(E)**. PCoA analysis based on Bray-Curtis distance **(F)**.

that the inoculation of PSB, specifically JP233, could alleviate these detrimental effects. In PSB JP233, the *gcd* gene plays a crucial role in producing 2-keto gluconic acid, which is the key functional agent for P solubilization by JP233 *in vitro* (Yu et al., 2022). Surprisingly, despite the enhancement of *gcd* gene abundance from *Pseudomonas* and changes in its distribution pattern among different genera (Supplementary Figure S3), the inoculation of JP233 did not significantly increase the overall abundance of the *gcd* gene ($p > 0.05$). The *gcd* gene serves as a pivotal biomarker for soil P cycle (Wu et al., 2022), and it is proposed that important ecosystem functions should remain preserved even as the microbial community structure undergoes changes (Allison and Martiny, 2008).

After inoculating with PSB JP233, significant differences were observed in the microbial community structure of tomato rhizosphere soil (Figure 3A). The influence of exogenous PSB inoculants on the structure of soil microbiota has been widely investigated (Dong et al., 2019; Liu et al., 2020). In this study, the main bacterial phylum in tomato rhizosphere soil, including Pseudomonadota, Acidobacteriota, Bacteroidota, Gemmatimonadota, Chloroflexota, Actinomycetota, Verrucomicrobiota, Myxococcota, Bdellovibrionota, and Planctomycetota, collectively accounted for nearly 81% of the bacterial sequences (Supplementary Figure S4A). Comparable dominant phylum compositions have been reported in other rhizosphere soils (Bejarano et al., 2021; Gao et al., 2023). At the genus level, numerous strains known for their plant-beneficial properties increased following treatment with JP233, including *Sphingomonas* (Wang F. et al., 2022; Wang L. L. et al., 2022; Wang Z. H. et al., 2022), *Lysobacter* (Expósito et al., 2015), *Sphingopyxis* (Dias et al., 2009; Zhang et al., 2019), and *Nitrospira* (Tao et al., 2024) (Figure 4B). In addition to these dominant genera, MetagenomeSeq analysis revealed an enhancement in the relative abundance of various species belonging to *Bacillota* (Figure 7). Notably, among these, species such as *Bacillus* spp. (Probanza et al., 2002), *Paenibacillus* spp. (Li et al., 2021), *Virgibacillus* spp., *Oceanobacillus* spp., *Halobacillus* spp. (Mukhtar et al., 2018), and *Metabacillus* spp. (Yin et al., 2022) have been recognized for their beneficial effects on plants.

Although the inoculation of JP233 significantly increased the abundance of *P. asiatica*, the overall abundance of *Pseudomonas* declined (Supplementary Figure S4B). This reduction may be partially attributed to the significant surge in *Bdellovibrio bacteriovorus*, a

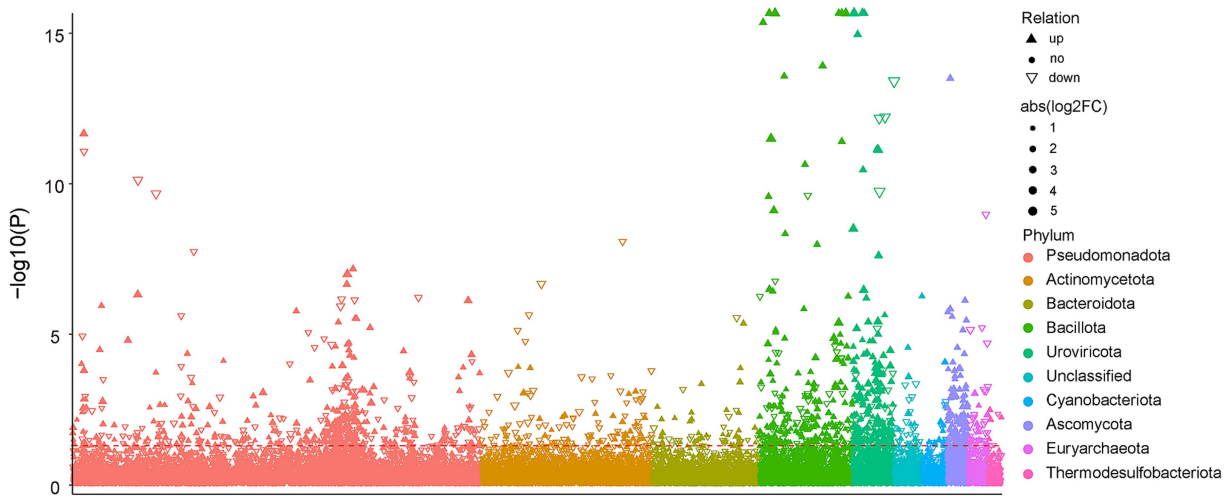


FIGURE 7
Manhattan plot displays the abundance of enriched bacterial phyla in soil under JP vs. CK treatment at the H0 level. Significantly increased abundance phyla are represented as filled triangles, while significantly decreased abundance phyla are shown as hollow triangles; non-significantly phyla are indicated by circles. The dashed line represents the significance threshold at $p = 0.05$. The color of each point denotes the distinction of the phylum, and the size of each point corresponds to the relative abundance of the phylum.

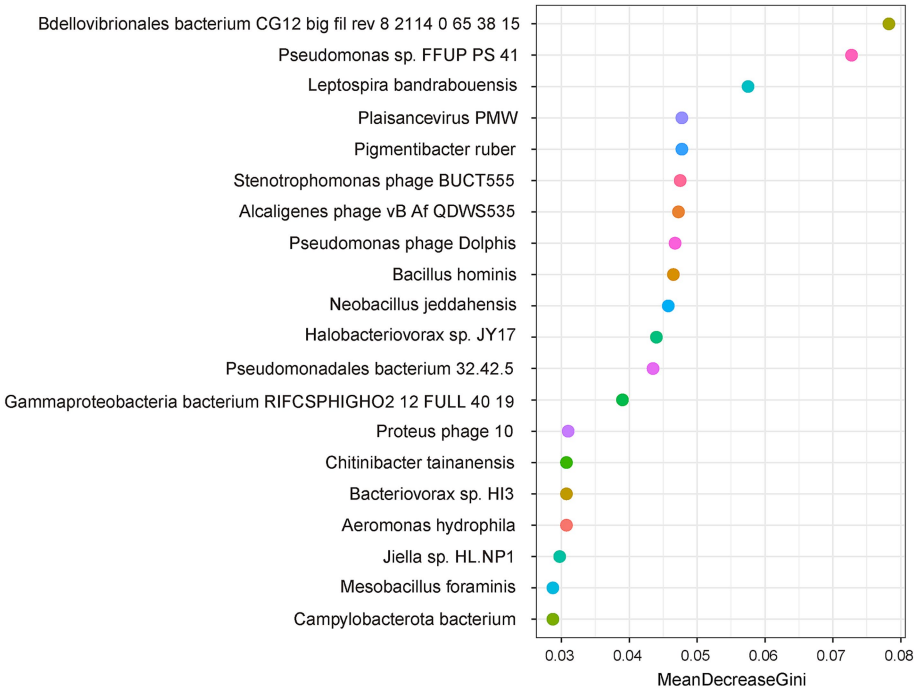


FIGURE 8
Random Forest analysis revealed the species that play a major role in the classification effect of the JP vs. CK group at the H0 level. The larger the MeanDecreaseGini value, the greater importance of the corresponding variable.

predatory bacterium. At genus level, *Bdellovibrio*, along with *Bacteriovorax*, *Halobacteriovorax* and an unclassified genus from *Bdellovibronales* (Supplementary Figure S5), all exhibited enhanced abundance. Given that many strains from these genera prey on susceptible gram-negative bacteria (Williams et al., 2016; Inoue et al., 2023), their increase could also be a consequence of the JP233 inoculation. The results of random forest analysis indicated that a species from *Bdellovibronales* was the most significant predictor, followed by a species from *Pseudomonas*, for distinguishing the grouping of microbial communities between the non-inoculated control and JP233-treated soil samples (Figure 8). These findings may partially explain the lack of *gcd* gene abundance surge and the weakened effect of JP233 in later stages. Although many studies found the exogenous PGPR could not become the dominant strains, and propose they could indirectly enhance plant growth and health by altering the composition and functionality of the rhizosphere microbial

community (Kong and Liu, 2022). Our findings provide deeper insights into the potential adverse impacts of resident microbes on bioinoculants.

5 Conclusion

The inoculation of the exogenous PSB strain *P. asiatica* JP233 enhanced P solubilization and promoted tomato growth in soils with both high and low P backgrounds, irrespective of P fertilization levels. Particularly, its impact was potent in high-P soil without additional P fertilization. This inoculation markedly altered the composition of the rhizosphere microbial community, resulting in a decrease in the relative abundances of viruses and eukaryotes. Specifically, the abundances of *Sphingomonas*, *Lysobacter*, *Sphingopyxis*, *Nitrospira*, and certain species from *Bacillota* were elevated. Notably, many strains from these genera and species are known to possess plant growth-promoting traits. Furthermore, the introduction of JP233 altered the soil gene profiling, with the modulated genes predominantly enriched in pathways related to the biosynthesis of secondary metabolites, amino acids, carbon metabolism, and other vital processes. This inoculation also increased the abundance of most P cycle genes and strengthened the interconnections among these genes, thereby contributing to improved P solubilization. The populations of certain predatory bacteria, including those from *Bdellovibrio*, *Bacteriovorax*, and *Halobacteriovorax*, increased after the inoculation of JP233, which may have a detrimental effect on the survival of JP233. The stimulatory impact observed can be attributed to the selective competitive effects of the rhizosphere microbiota, which are directly or indirectly influenced by the inoculated PSB strain JP233. Our findings offer valuable insights into the microecological mechanisms by which PSB solubilize P in soil and promote plant growth.

Data availability statement

The datasets analyzed for this study can be found in the NCBI Sequence Read File (SRA) under project numbers PRJNA1136594.

Author contributions

YT: Data curation, Methodology, Writing – original draft, Writing – review & editing. LW: Formal analysis, Writing – review & editing. JF: Investigation, Writing – review & editing. FZ: Software, Writing – review & editing. HW: Writing – review & editing. XW: Resources, Writing – review & editing. SF: Supervision, Writing – review & editing. XZ: Conceptualization, Funding acquisition, Project administration, Writing – review & editing.

Funding

The author(s) declare financial support was received for the research, authorship, and/or publication of this article. This work was supported by National key research and development plan project (2023YFD1902704-3), Shandong Province Key Agricultural Project for Application Technology Innovation (SDAIT-31-04), the Science and Education Integration of Qilu University of Technology (grant numbers 2024ZDZX10, 2023PY017), Shandong Province small and medium-size enterprise innovation ability improvement project (2022TSGC2060).

Conflict of interest

The authors declare that the research was conducted in the absence of any commercial or financial relationships that could be construed as a potential conflict of interest.

The author(s) declared that they were an editorial board member of Frontiers, at the time of submission. This had no impact on the peer review process and the final decision.

Generative AI statement

The authors declare that no Gen AI was used in the creation of this manuscript.

Publisher's note

All claims expressed in this article are solely those of the authors and do not necessarily represent those of their affiliated organizations, or those of the publisher, the editors and the reviewers. Any product that may be evaluated in this article, or claim that may be made by its manufacturer, is not guaranteed or endorsed by the publisher.

Supplementary material

The Supplementary material for this article can be found online at: https://www.frontiersin.org/articles/10.3389/fmicb.2025.1538117/full#supplementary-material

References

Allison, S. D., and Martiny, J. B. H. (2008). Resistance, resilience, and redundancy in microbial communities. *Proc. Natl. Acad. Sci. USA* 105, 11512–11519. doi: 10.1073/pnas.0801925105

Bao, S. D. (2000). Soil agrochemical analysis. *3rd* Edn. Beijing: China Agriculture Press, 70–282.

Bargaz, A., Elhaissoufi, W., Khourchi, S., Benmrid, B., Borden, K. A., and Rchiad, Z. (2021). Benefits of phosphate solubilizing bacteria on belowground crop performance for improved crop acquisition of phosphorus. *Microbiol. Res.* 252:126842. doi: 10.1016/j.micres.2021.126842

Bejarano, A., Perazzolli, M., Pertot, I., and Puopolo, G. (2021). The perception of rhizosphere bacterial communication signals leads to transcriptome reprogramming in *Lysobacter capsici* AZ78, a plant beneficial bacterium. *Front. Microbiol.* 12:725403. doi: 10.3389/fmicb.2021.725403

Bergkemper, F., Schöler, A., Engel, M., Lang, F., Krüger, J., Schloter, M., et al. (2016). Phosphorus depletion in forest soils shapes bacterial communities towards phosphorus recycling systems. *Environ. Microbiol.* 18, 1988–2000. doi: 10.1111/1462-2920.13188

Buchfink, B., Xie, C., and Huson, D. H. (2015). Fast and sensitive protein alignment using DIAMOND. *Nat. Methods* 12, 59–60. doi: 10.1038/nmeth.3176

Da Silva, M. L. P., Moen, F. S., Liles, M. R., Feng, Y. C., and Sanz-Saez, A. (2022). The response to inoculation with PGPR plus Orange Peel amendment on soybean is cultivar and environment dependent. *Plants (Basel)* 11:1138. doi: 10.3390/plants11091138

Dai, Z. M., Liu, G. F., Chen, H. H., Chen, C. R., Wang, J. K., Ai, S. Y., et al. (2020). Long-term nutrient inputs shift soil microbial functional profiles of phosphorus cycling in diverse agroecosystems. *ISME J.* 14, 757–770. doi: 10.1038/s41396-019-0567-9

Dias, A. C. F., Costa, F. E. C., Andreote, F. D., Lacava, P. T., Teixeira, M. A., Assumpçao, L. C., et al. (2009). Isolation of micropropagated strawberry endophytic bacteria and assessment of their potential for plant growth promotion. *World J. Microbiol. Biotechnol.* 25, 189–195. doi: 10.1007/s11274-008-9878-0

Dong, C. J., Wang, L. L., Li, Q., and Shang, Q. M. (2019). Bacterial communities in the rhizosphere, phyllosphere and endosphere of tomato plants. *PLoS One* 14:e0223847. doi: 10.1371/journal.pone.0223847

Elhaissoufi, W., Ghoulam, C., Barakat, A., Zeroual, Y., and Bargaz, A. (2022). Phosphate bacterial solubilization: a key rhizosphere driving force enabling higher P use efficiency and crop productivity. *J. Adv. Res.* 38, 13–28. doi: 10.1016/j.jare.2021.08.014

Expósito, R. G., Postma, J., Raaijmakers, J. M., and De Bruijn, I. (2015). Diversity and activity of *Lysobacter* species from disease suppressive soils. *Front. Microbiol.* 6:1243. doi: 10.3389/fmicb.2015.01243

Feng, G., Gai, J., Feng, X., Haigang, L. I., Zhang, L., Yi, K., et al. (2019). Strategies for improving fertilizer phosphorus use efficiency in Chinese cropping systems. *Engineering* 6, 341–347. doi: 10.15302/J-FASE-2019280

Fu, L. M., Niu, B. F., Zhu, Z. W., Wu, S. T., and Li, W. Z. (2012). CD-HIT: accelerated for clustering the next-generation sequencing data. *Bioinformatics* 28, 3150–3152. doi: 10.1093/bioinformatics/bts565

Gao, R. X., Dong, H. H., Liu, Y., Yao, Q., Li, H. P., and Zhu, H. H. (2023). *Sphingomonas lycopersici* sp. nov., isolated from tomato rhizosphere soil. *Int. J. Syst. Evol. Microbiol.* 73:5920. doi: 10.1099/ijsem.0.005920

Gurevich, A., Saveliev, V., Vyahhi, N., and Tesler, G. (2013). QUAST: quality assessment tool for genome assemblies. *Bioinformatics* 29, 1072–1075. doi: 10.1093/bioinformatics/btt086

Hu, J., Yang, T. J., Friman, V. P., Kowalchuk, G. A., Hautier, Y., Li, M., et al. (2021). Introduction of probiotic bacterial consortia promotes plant growth via impacts on the resident rhizosphere microbiome. *Proc. Biol. Sci.* 288:20211396. doi: 10.1098/rspb.2021.1396

Huang, Y. L., Lin, J. H., Tang, C. X., and Xu, J. M. (2024). Organic carbon inputs shift the profiles of phosphorus cycling-related genes in maize rhizosphere. *Plant Soil* 503, 595–609. doi: 10.1007/s11104-024-06605-x

Huang, K., Yin, H. Y., Zheng, Q. R., Lv, W., Shen, X. T., Ai, M., et al. (2024). Microbial inoculation alters rhizoplane bacterial community and correlates with increased rice yield. *Pedobiologia* 104:150945. doi: 10.1016/j.pedobi.2024.150945

Inoue, D., Nakamura, S., Sugiyama, T., and Ike, M. (2023). Potential of predatory Bacteria to colonize the duckweed microbiome and change its structure: a model study using the obligate predatory bacterium, *Bacteriovorax* sp. HI3. *Microbes Environ.* 38:23040. doi: 10.1264/jsme2.ME23040

Kong, Z. Y., and Liu, H. G. (2022). Modification of rhizosphere microbial communities: a possible mechanism of plant growth promoting Rhizobacteria enhancing plant growth and fitness. *Front. Plant Sci.* 13:920813. doi: 10.3389/fpls.2022.920813

Langmead, B., and Salzberg, S. L. (2012). Fast gapped-read alignment with bowtie 2. *Nat. Methods* 9, 357–359. doi: 10.1038/nmeth.1923

Li, D. H., Liu, C. M., Luo, R. B., Sadakane, K., and Lam, T. W. (2015). MEGAHIT: an ultra-fast single-node solution for large and complex metagenomics assembly via succinct *de Bruijn* graph. *Bioinformatics* 31, 1674–1676. doi: 10.1093/bioinformatics/btv033

Li, J. T., Lu, J. L., Wang, H. Y., Fang, Z., Wang, X. J., Feng, S. W., et al. (2021). A comprehensive synthesis unveils the mysteries of phosphate-solubilizing microbes. *Biol. Rev.* 96, 2771–2793. doi: 10.1111/brv.12779

Liang, J. L., Liu, J., Jia, P., Yang, T. T., Zeng, Q. W., Zhang, S. C., et al. (2020). Novel phosphate-solubilizing bacteria enhance soil phosphorus cycling following ecological restoration of land degraded by mining. *ISME J.* 14, 1600–1613. doi: 10.1038/s41396-020-0632-4

Liu, L., Gao, Z. Y., Yang, Y., Gao, Y., Mahmood, M., Jiao, H. J., et al. (2023). Long-term high-P fertilizer input shifts soil P cycle genes and microorganism communities in dryland wheat production systems. *Agric. Ecosyst. Environ.* 342:108226. doi: 10.1016/j.agee.2022.108226

Liu, J., Qi, W. Y., Li, Q., Wang, S. G., Song, C., and Yuan, X. Z. (2020). Exogenous phosphorus-solubilizing bacteria changed the rhizosphere microbial community indirectly. *3 Biotech* 10:164. doi: 10.1007/s13205-020-2099-4

Luo, A. C., Sun, X., and Zhang, Y. S. (1993). Species of inorganic phosphate solubilizing Bacteria in red soil and the mechanism of Solubilization. *Pedosphere* 3, 285–288.

Mukhtar, S., Mehnaz, S., Mirza, M. S., Mirza, B. S., and Malik, K. A. (2018). Diversity of *Bacillus*-like bacterial community in the rhizospheric and non-rhizospheric soil of halophytes (Salsola *stocksii* and *Atriplex amnicola*), and characterization of osmoregulatory genes in halophilic *Bacilli*. *Can. J. Microbiol.* 64, 567–579. doi: 10.1139/cjm-2017-0544

Pan, L., and Cai, B. Y. (2023). Phosphate-solubilizing Bacteria: advances in their physiology, molecular mechanisms and microbial community effects. *Microorganisms* 11:2904. doi: 10.3390/microorganisms11122904

Pang, F., Li, Q., Solanki, M. K., Wang, Z., Xing, Y. X., and Dong, D. F. (2024). Soil phosphorus transformation and plant uptake driven by phosphate-solubilizing microorganisms. *Front. Microbiol.* 15:1383813. doi: 10.3389/fmicb.2024.1383813

Probanza, A., García, J. A. L., Palomino, M. R., Ramos, B., and Mañero, F. J. G. (2002). *Pinus pinea* L. seedling growth and bacterial rhizosphere structure after inoculation with PGPR *Bacillus* (*Blicheniformis* CECT 5106 and *Bpumilus* CECT 5105). *Appl. Soil Ecol.* 20, 75–84. doi: 10.1016/s0929-1393(02)00007-0

Raymond, N. S., Gómez-Muñoz, B., van der Bom, F. J. T., Nybroe, O., Jensen, L. S., Müller-Stöver, D. S., et al. (2021). Phosphate-solubilising microorganisms for improved crop productivity: a critical assessment. *New Phytol.* 229, 1268–1277. doi: 10.1111/nph.16924

Sierra-García, I. N., Ferreira, M. J., Torres-Ballesteros, A., Louvado, A., Gomes, N., and Cunha, A. (2024). Brevibacterium EB3 inoculation enhances rhizobacterial community interactions leading to improved growth of *Salicornia europaea*. *Appl. Soil Ecol.* 196:105306. doi: 10.1016/j.apsoil.2024.105306

Song, H., Dharmasena, M. N., Wang, C., Shaw, G. X., Cherry, S., Tropea, J. E., et al. (2020). Structure and activity of PPX/GppA homologs from *Escherichia coli* and *Helicobacter pylori*. *FEBS J.* 287, 1865–1885. doi: 10.1111/febs.15120

Strauch, E., Schwudke, D., and Linscheid, M. (2007). Predatory mechanisms of *Bdellovibrio* and like organisms. *Future Microbiol.* 2, 63–73. doi: 10.2217/17460913.2.1.63

Su, W. H., and Chen, Y. R. (2010). Determination of total phosphorus in soil by potassium persulfate digestion. *Light Text. Ind. Fujian* 6, 43–45. doi: 10.3969/j.issn.1007-550X.2010.06.004

Swiatczak, J., Kalwasinska, A., Szabó, A., and Brzezinska, M. S. (2023). The effect of seed bacterization with *Bacillus paralicheniformis* 2R5 on bacterial and fungal communities in the canola rhizosphere. *Microbiol. Res.* 275:127448. doi: 10.1016/j.micres.2023.127448

Tao, R., Ding, W. Y., Zhang, K. Y., Li, Y. Y., Li, J., Hu, B. W., et al. (2024). Response of comammox *Nitrospira* clades a and B communities to long-term fertilization and rhizosphere effects and their relative contribution to nitrification in a subtropical paddy field of China. *J. Environ. Manag.* 367:121939. doi: 10.1016/j.jenvman.2024.121939

Trivedi, P., Leach, J. E., Tringe, S. G., Sa, T. M., and Singh, B. K. (2020). Plant-microbiome interactions: from community assembly to plant health. *Nat. Rev. Microbiol.* 18, 607–621. doi: 10.1038/s41579-020-0412-1

Wang, X. W., Guo, H., Wang, J. N., He, P., Kuzyakov, Y., Ma, M. J., et al. (2024). Microbial phosphorus-cycling genes in soil under global change. *Glob. Chang. Biol.* 30:e17281. doi: 10.1111/gcb.17281

Wang, F., Wei, Y. L., Yan, T. Z., Wang, C. C., Chao, Y. H., Jia, M. Y., et al. (2022). *Sphingomonas* sp. Hbc-6 alters physiological metabolism and recruits beneficial rhizosphere bacteria to improve plant growth and drought tolerance. *Front. Plant Sci.* 13:1002772. doi: 10.3389/fpls.2022.1002772

Wang, Z. H., Zhang, H. H., Liu, L., Li, S. J., Xie, J. F., Xue, X., et al. (2022). Screening of phosphate-solubilizing bacteria and their abilities of phosphorus solubilization and wheat growth promotion. *BMC Microbiol.* 22:296. doi: 10.1186/s12866-022-02715-7

Wang, L. L., Zhou, F. Y., Zhou, J. B., Harvey, P. R., Yu, H. Y., Zhang, G. Z., et al. (2022). Genomic analysis of *Pseudomonas asiatica* JP233: an efficient phosphate-solubilizing bacterium. *Genes* 13:1290. doi: 10.3390/genes13122290

Williams, H. N., Lymperopoulou, D. S., Athar, R., Chauhan, A., Dickerson, T. L., Chen, H., et al. (2016). *Halobacteriovorax*, an underestimated predator on bacteria: potential impact relative to viruses on bacterial mortality. *ISME J.* 10, 491–499. doi: 10.1038/ismej.2015.129

Wu, X. J., Rensing, C., Han, D. F., Xiao, K. Q., Dai, Y. X., Tang, Z. X., et al. (2022). Genome-resolved metagenomics reveals distinct phosphorus acquisition strategies between soil microbiomes. *Msystems* 7:e0110721. doi: 10.1128/msystems.01107-21

Yang, X., and Post, W. M. (2011). Phosphorus transformations as a function of pedogenesis: a synthesis of soil phosphorus data using Hedley fractionation method. *Biogeosciences* 8, 2907–2916. doi: 10.5194/bg-8-2907-2011

Yin, Z. Q., Wang, X., Hu, Y. J., Zhang, J. K., Li, H., Cui, Y. R., et al. (2022). *Metabacillus dongyingensis* sp. nov. is represented by the plant growth-promoting bacterium BY2G20 isolated from saline-alkaline soil and enhances the growth of *Zea mays* L. under salt stress. *Msystems* 7:e0142621. doi: 10.1128/msystems.01426-21

Yu, H. Y., Wu, X. Q., Zhang, G. Z., Zhou, F. Y., Harvey, P. R., Wang, L. L., et al. (2022). Identification of the phosphorus-solubilizing Bacteria strain JP233 and its effects on soil phosphorus leaching loss and crop growth. *Front. Microbiol.* 13:892533. doi: 10.3389/fmicb.2022.892533

Zhang, Y., Gao, X., Shen, Z. Z., Zhu, C. Z., Jiao, Z. X., Li, R., et al. (2019). Pre-colonization of PGPR triggers rhizosphere microbiota succession associated with crop yield enhancement. *Plant Soil* 439, 553–567. doi: 10.1007/s11104-019-04055-4

Zhang, W., Liu, D. Y., Liu, Y. M., Chen, X. P., and Zou, C. Q. (2017). Overuse of phosphorus fertilizer reduces the grain and flour protein contents and zinc bioavailability of winter wheat (*Triticum aestivum* L.). *J. Agric. Food Chem.* 65, 1473–1482. doi: 10.1021/acs.jafc.6b04778

Zhang, B., Wang, Y., Liu, H., Yang, X., Yuan, P., Wang, C., et al. (2023). Optimal phosphorus management strategies to enhance crop productivity and soil phosphorus fertility in rapeseed-rice rotation. *Chemosphere* 337:139392. doi: 10.1016/j.chemosphere.2023.139392

Zhu, W. H., Lomsadze, A., and Borodovsky, M. (2010). *Ab initio* gene identification in metagenomic sequences. *Nucleic Acids Res.* 38:e132. doi: 10.1093/nar/gkq275

frontiers | Frontiers in Microbiology

TYPE Original Research
PUBLISHED 22 April 2025
DOI 10.3389/fmicb.2025.1564159

Check for updates

OPEN ACCESS

EDITED BY
Tereza Castellane,
São Paulo State University, Brazil

REVIEWED BY
Luziane Sales,
São Paulo State University, Brazil
Rattan Deep Singh,
Lovely Professional University, India

*CORRESPONDENCE
Jianfeng Li
✉ lijianfeng@gznc.edu.com

RECEIVED 21 January 2025
ACCEPTED 01 April 2025
PUBLISHED 22 April 2025

CITATION
Zhang S, Guo J, Li J, Yang Y and Zhang Q (2025) Effects of tea plant endophytic phosphate-solubilizing bacteria on the growth and selenium uptake of maize seedlings in selenium-rich soil. *Front. Microbiol.* 16:1564159. doi: 10.3389/fmicb.2025.1564159

COPYRIGHT
© 2025 Zhang, Guo, Li, Yang and Zhang. This is an open-access article distributed under the terms of the Creative Commons Attribution License (CC BY). The use, distribution or reproduction in other forums is permitted, provided the original author(s) and the copyright owner(s) are credited and that the original publication in this journal is cited, in accordance with accepted academic practice. No use, distribution or reproduction is permitted which does not comply with these terms.

Effects of tea plant endophytic phosphate-solubilizing bacteria on the growth and selenium uptake of maize seedlings in selenium-rich soil

Shuqing Zhang[1,2,3], Jinmei Guo[1,2,3], Jianfeng Li[2,3]*, Yousu Yang[1] and Qiuyue Zhang[1]

[1]School of Geography and Resources, Guizhou Education University, Guiyang, China, [2]Institute of Soil and Environment Bioremediation in Karst Habitats, Guizhou Education University, Guiyang, China, [3]Key Laboratory of Biological Resources Exploitation and Utilization in Colleges and Universities of Guizhou, Guiyang, China

Phosphorus (P) is an important nutrient required for plant growth. In this study, seven phosphate-solubilizing bacterial (PSB) strains isolated from tea plant (*Camellia sinensis*) roots were used as test inoculants. After inoculating maize (*Zea mays* L.) seedlings for 45 days, we measured the available AN, AP, AK and available Se contents in the rhizosphere soil, as well as the N, P, K, and Se contents in the plants, along with growth and physiological parameters. The study aimed to explore the effects of endophytic PSB from tea plants on maize seedling growth and the uptake of nutrients such as N, P, K, and Se. The results showed that the endophytic PSB enhanced the P content in maize leaves and the AP content in rhizosphere soil. They also significantly increased seedling fresh weight, dry weight, plant height, and root length. Treatment with *P. fungorum* PMS-05 significantly increased the dry weight, fresh weight, and plant height of seedlings by 103.79, 77.69, and 51.27%, respectively. Inoculation with *P. fungorum* PMS-20 significantly increased plant height and root length by 70.89 and 223.45%, respectively. Furthermore, treatment with *P. fungorum* PMS-05 significantly increased the available Se contents in the rhizosphere soil and the plants by 144.47 and 97.77%, respectively. In conclusion, tea plant endophytic PSB can increase the contents of AP and available Se in rhizosphere soil, promote nutrient absorption, and positively impact seedling growth. *P. fungorum* PMS-05 and *P. fungorum* PMS-20 showed superior growth-promoting effects on seedlings compared with the other strains tested and can be used to develop high-quality PSB agents tailored for crops grown in selenium-rich red soils in Guizhou.

KEYWORDS

phosphate-solubilizing bacteria, biomass, plant height, chlorophyll, nitrogen (N), phosphorus (P), potassium (K), selenium (Se)

1 Introduction

Phosphorus (P) is an essential nutrient element for plants and plays an important role in metabolism (Oldroyd and Leyser, 2020; Isidro et al., 2023). In China, two-thirds of arable land suffers from severe phosphorus deficiency. However, most traditional phosphorus fertilizers applied to the soil are fixed by calcium, iron, and aluminum ions in the soil and thus converted into insoluble phosphates that are difficult for plants to directly absorb and utilize (Chi et al., 2021). Phosphate-solubilizing microorganisms (PSMs) can convert insoluble phosphorus into soluble phosphorus, thereby increasing the availability of phosphorus in the soil and improving the efficiency of phosphorus uptake and utilization by crops (Zhang et al., 2024).

Currently, more than 20 genera of PSM have been identified, including bacteria, fungi, and actinomycetes, with bacteria being the most abundant, followed by fungi and actinomycetes (Chi et al., 2021). Commonly applied phosphate-solubilizing bacteria (PSB) include *Bacillus*, *Burkholderia*, *Azotobacter*, and *Pseudomonas* (Li et al., 2024). PSMs decompose insoluble phosphorus by secreting organic acids, lowering soil pH, and releasing phosphatases. Additionally, they promote crop growth by producing plant growth regulators (Chi et al., 2021). Research has shown that PSB can promote the growth of Chinese cabbage rapa and establish long-term colonization in rhizosphere soil (Wang et al., 2016). In rice, rhizosphere PSB can produce auxins and gibberellins, which exhibit strong nutrient conversion and growth-promoting abilities (Liu et al., 2018). Rhizosphere PSB in camellia plants can enhance the enzymatic activity of leaves and soil, as well as the available phosphorus content in the soil (Xue et al., 2024). PSB in the rhizosphere of maize can produce siderophores, organic acids, zeatin, and auxins, which significantly improve maize plant height, stem diameter, dry weight, and fresh weight (Hou and Hu, 2024). Thus, utilizing PSMs as biofertilizers can enhance fertilizer utilization efficiency, increase crop yields, and improve the soil environment, playing a crucial role in promoting sustainable agricultural development.

In previous studies (Zhang et al., 2024; Guo et al., 2024), after inoculating tea plant endophytic PSB into tea seedlings, it was found that all tested strains significantly increased the available nitrogen (AN) and available phosphorus (AP) content in the rhizosphere soil of "Longjing 43," enhanced the zinc (Zn) and selenium (Se) content in the aboveground parts of the tea plants, and most strains also improved the available Zn and Se content in the rhizosphere soil. This demonstrated that tea plant endophytic PSB have a positive effect on promoting nutrient absorption in host plants. However, can these strains also promote the growth of non-host plants and improve their nutrient content?

In this study, seven tea plant endophytic PSB were used as the test strains. After inoculating maize seedlings for 45 days, the physiological growth parameters of the seedlings were measured, along with the soil AN, AP, AK and available Se contents and the plant N, P, K, and Se concentrations. The effects of PSB on seedling growth and the uptake of N, P, K, Se, and other nutrients were analyzed. The main goals were: (1) to analyze the effects of PSB on the growth and nutrient uptake of maize seedlings; (2) to evaluate the influence of PSB on rhizosphere soil nutrient dynamics; (3) to compare the differential impacts of tea plant-derived endophytic PSB on growth and nutrient absorption between host (tea) and non-host (maize) plants. This study aims to provide microbial resources and a theoretical foundation for the further development and application of plant growth-promoting bacterial agents.

2 Materials and methods

2.1 Test materials

2.1.1 Test soil

The soil was collected from the Masson pine-wild oil tea mixed forest in Anping Village, Kaiyang County, Guiyang City, Guizhou Province, China (longitude: 106°59′48.77″, latitude: 27°12′ 10.04″, altitude: 1,086 m). The soil type was red soil. The soil type is red soil. 0-30 cm soil was collected by five-point sampling method and brought back to the laboratory, where impurities were removed, after which the samples were air-dried, homogenized, and prepared for the pot experiment. At the same time, fresh soil samples were analyzed for the total nitrogen (TN), total phosphorus (TP), total potassium (TK), and organic matter contents and soil pH (Zhang et al., 2024; Bao, 2008). The test soil contained 0.40 $g{\cdot}kg^{-1}$ TN, 0.52 $g{\cdot}kg^{-1}$ TP, 4.89 $g{\cdot}kg^{-1}$ TK, 1.44 $mg{\cdot}kg^{-1}$ total Se, and 27.99 $g{\cdot}kg^{-1}$ organic matter and had a pH of 4.6 (Zhang et al., 2024).

2.1.2 Test plant

The maize seeds used in this study were of the variety "Zhongnongtian 488," purchased from the Cricket Agricultural Technology Extension Service Center (Shouguang City, Shandong Province, China). The seed purity was greater than 95%.

2.1.3 Test strains

The PSB strains (PMS05, PCF06, PSt07, PMS-08, PSt09, PSt12, and PMS-20) were isolated from tea plant roots. These strains were obtained from the Microbial Fertilizer Research Group at the Key Laboratory of Biological Resource Development and Utilization in Guizhou Higher Education Institutions. The strains were isolated from tea plant root tissues collected from tea plantations in Fenggang County (Guizhou Province, China) using PKO (Pikovskaya's inorganic phosphate-solubilizing medium), Mongina organic phosphate-solubilizing medium, and Winogradsky's nitrogen-free medium. Based on 16S rRNA sequencing, the strains were identified as *Paraburkholderia fungorum*, *Kluyvera intermedia*, *Paraburkholderia fungorum*, *Paraburkholderia fungorum*, *Enterobacter wuhouensis*, *Kluyvera intermedia*, and *Paraburkholderia fungorum*. Among these strains, PMS05 and PCF06 have dual functions of inorganic phosphorus solubilization and nitrogen fixation; PSt07 and PSt12 can solubilize only inorganic phosphorus; PMS-08 and PMS-20 can solubilize only organic phosphorus; and PSt09 can solubilize both organic and inorganic phosphorus.

2.1.4 Culture medium

LB medium (Liu et al., 2015) was used for cultivation and short-term preservation of the PSB.

2.2 Pot Experiment

Maize seeds with full grains and intact seed coats were selected and evenly placed in Petri dishes lined with double-layered filter paper, with 30 seeds per dish and 6 dishes prepared per crop. An appropriate amount of distilled water was added to each dish, and the seeds were placed in a 25°C incubator for uniform germination.

Several flowerpots with a diameter of 18 cm were prepared, and approximately 2,400 g of test soil was added to each pot. Maize seeds with sprouts longer than 1 cm were transplanted into the pots and covered with an appropriate amount of soil. A total of 24 pots were planted, with 4–5 plants per pot. The pots were watered thoroughly the first time, and subsequent watering was adjusted based on weather conditions. The pots were placed outdoors in the experimental cultivation field.

2.3 Preparation of PSB suspensions

The seven activated test strains were individually inoculated into LB liquid medium to prepare PSB suspensions. The bottles were sealed with sterile sealing film, labeled, and cultured at 28°C with shaking at 200 r·min^{-1} for 20 h. The optical density (OD) of the PSB suspensions at a wavelength of 600 nm was measured using a spectrophotometer. If the $OD_{600\ nm}$ value was $\geq$ 1.0, the PSB suspension was transferred to sterile centrifuge tubes and centrifuged at 4,000 r·min^{-1} for 10 min. The supernatant was discarded, and an appropriate amount of sterile water was added. The PSB pellet at the bottom of the centrifuge tube was resuspended by shaking, and sterile distilled water was added to adjust the $OD_{600\ nm}$ of the PSB suspension to 0.8 (Zhang et al., 2024).

2.4 PSB inoculation and index measurements

Fifteen days after maize seedling emergence, 100 mL of the prepared PSB suspensions was applied to the root zone of each plant for treatment, with three replicates. The control group received an equal amount of distilled water. After 45 days of inoculation, the entire seedlings were carefully removed, ensuring minimal damage to the roots. The soil attached to the roots was gently shaken off, and soil particles adhering to the root surface were brushed off with a soft brush to obtain rhizosphere soil for this study. The plant height, root length, dry weight, and fresh weight were measured according to the method described by Ke and Pan (2022). The chlorophyll content in the leaves was determined following Wang (2006). The soluble sugar and malondialdehyde (MDA) contents were measured using the thiobarbituric acid method (Zhang, 2004). Root activity was assessed using the TTC method (Zou, 1979). The ammonium nitrogen (NH_4^+-N), nitrate nitrogen (NO_3^--N), available phosphorus (AP), and available potassium (AK) contents in the soil and plants were determined according to Bao (2008). The available Se in the soil and the Se content in the plants were measured following the method described by Gou et al. (2013). The available nitrogen (AN) content was calculated as the sum of the ammonium nitrogen and nitrate nitrogen contents. Each sample was analyzed in triplicate.

2.5 Data processing

The standard error and average value of three replicates of the test data were calculated. Their one-way ANOVA (analysis of variance) and the Duncan multiple comparison method were implemented using SPSS 23.0 software. Origin 2021 software was used to draw the graphs.

3 Results

3.1 Effects of tea plant endophytic PSB on fresh and dry weight of maize seedlings

Inoculation with different PSB strains significantly promoted biomass accumulation in maize seedlings (Figure 1). The fresh weight of the plants in the PSB treatment increased by more than 36.16% compared to the control. The fresh weight of seedlings inoculated with strain PMS-05 was significantly higher than that of the control by 77.69% ($P < 0.05$) and exceeded that of the other PSB treatments by more than 15.63%. Along with the increase in fresh weight, the dry weight of the maize seedlings also increased significantly after PSB inoculation. The increase ranged from 102.12 to 191.78% ($P < 0.05$). Notably, the dry weight of seedlings treated with strain PSt12 reached 202.12% that of the control group ($P < 0.05$).

3.2 Effects of tea plant endophytic PSB on the root length and plant height of maize seedlings

Inoculation with PSB significantly increased the root length of maize seedlings by 129.66-223.45% ($P < 0.05$) (Figure 2). Among the tested strains, PMS-20 had the most pronounced effect, with the root length significantly exceeding that of the other treatments by 13.83-40.84% ($P < 0.05$).

Inoculation with PSB significantly increased the plant height of maize seedlings by 13.33-70.89% ($P < 0.05$) (Figure 2). The plant height of seedlings treated with strain PMS-20 reached 170.89% of that of the control and was significantly higher than that of seedlings treated with other PSB strains by 12.97-28.57% ($P < 0.05$). These findings indicate that inoculation with the tested PSB strains can promote the growth of aboveground and underground parts of maize seedlings.

3.3 Effects of tea plant endophytic PSB on root activity of maize seedlings

After inoculation with different PSB strains, there were no significant changes in root activity of maize seedlings (Figure 3). Only the root activity of seedlings treated with strain PMS-05 was slightly lower than that of the control and the other treatments, but the difference was not significant ($P > 0.05$). These findings suggest that PSB did not cause any damage to the roots.

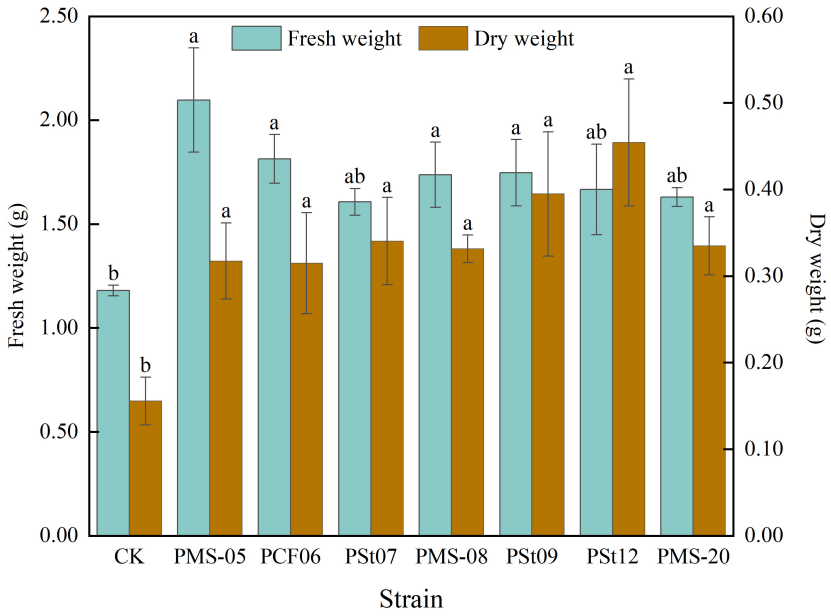


FIGURE 1
Effects of different strains on fresh and dry weight of maize seedlings. Different lowercase letters in the figure indicate significant differences in maize seedling parameters between different strains ($P < 0.05$). The same applies below.

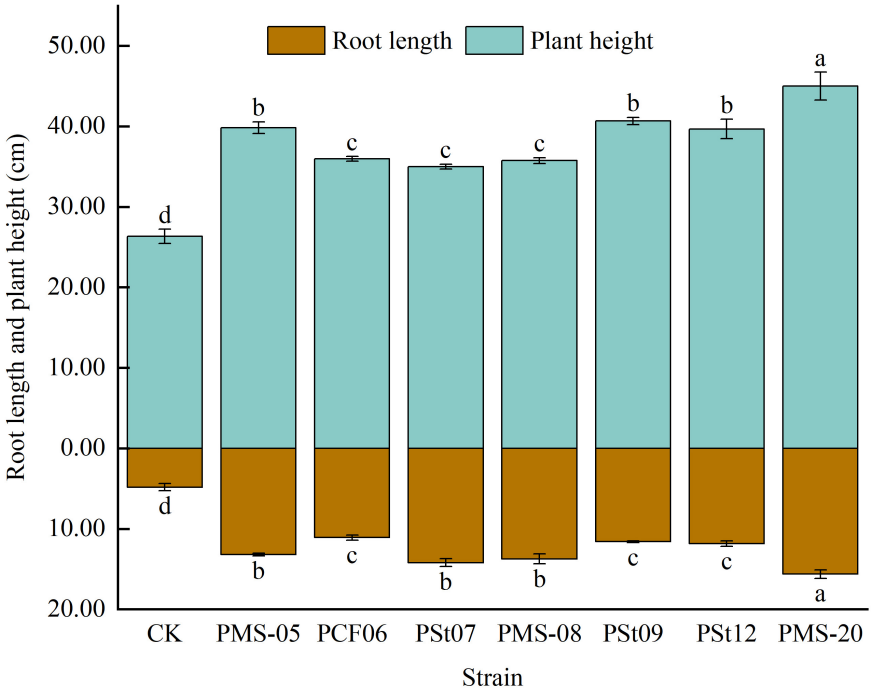


FIGURE 2
Effect of different strains on root length and plant height of maize seedlings.

3.4 Effects of tea plant endophytic PSB on chlorophyll content in maize seedling leaves

The chlorophyll content in maize seedling leaves treated with different PSB strains was 6.08-48.61% higher than that in the control (Figure 4). Among the treatments, strain PSt12 had the most significant effect on increasing the chlorophyll content ($P < 0.05$), which was 39-148.61% of control and other treatments. This strain was followed by strain PMS-05, which results in a chlorophyll content 133.42% that of the control ($P < 0.05$). These results indicate that inoculation with PSB strains can effectively

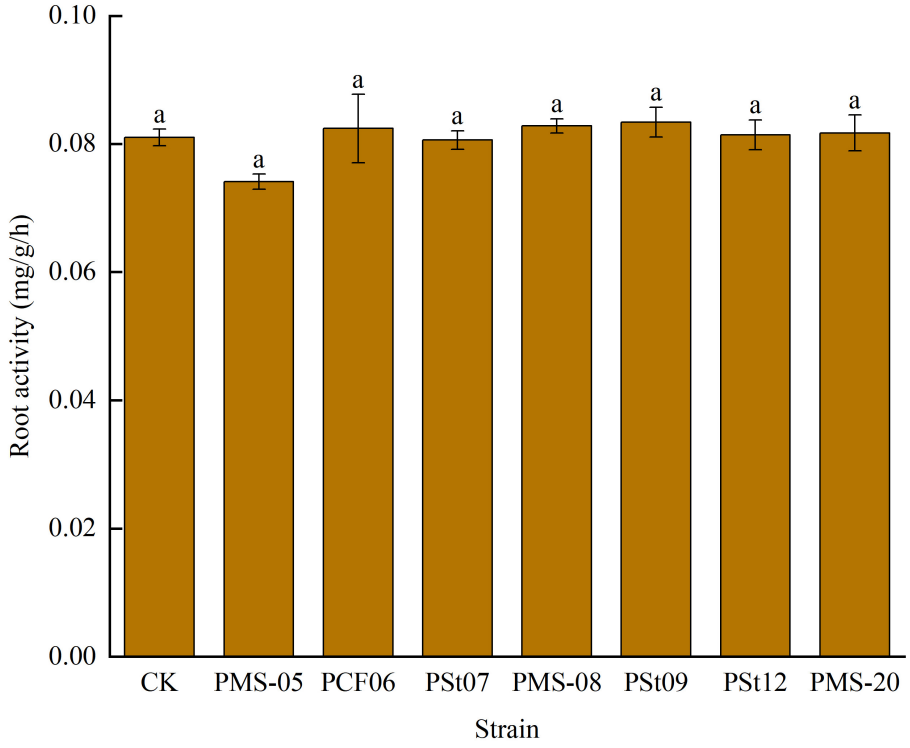


FIGURE 3
Effect of different strains on root activity of maize seedlings.

enhance the chlorophyll content in maize seedling leaves, thereby improving photosynthesis in the leaves.

3.5 Effects of tea plant endophytic PSB on soluble sugar content in maize seedling leaves

The rapid accumulation of soluble sugars in leaves is typically a response to mitigate membrane system damage caused by external stresses. The soluble sugar content in maize seedling leaves after inoculation with PSB was significantly lower than that in the control (Figure 5), by 28.17-52.01% ($P < 0.05$). Among the treatments, strain PSt12 caused the smallest change in soluble sugar content. These results suggest that the introduction of PSB as exogenous microbes into the soil temporarily reduced the stress tolerance of maize seedlings.

3.6 Effects of tea plant endophytic PSB on malondialdehyde (MDA) content in maize seedling leaves

The MDA content in maize seedling leaves significantly increased under all PSB treatments (Figure 6), with an increase ranging from 209.54 to 365.59% ($P < 0.05$). Among the treatments, strain PSt12 caused the greatest increase in MDA content, indicating that this strain had the most significant effect on the stress tolerance of maize seedlings.

3.7 Effects of tea plant endophytic PSB on AN, AP, and AK contents in the rhizosphere soil of maize seedlings

After inoculation with PSB, there was no significant change in the AN content in the rhizosphere soil (Figure 7). However, all PSB strains increased the AP content in the rhizosphere soil. Among them, strain PMS-08 significantly enhanced the AP content, which was 27.99-141.47% higher than those in the control and the other treatments ($P < 0.05$). The trend for AK was consistent with that for AP, with all treatments showing increases compared with the control. Strains PSt07, PMS-08, and PSt09 demonstrated the most prominent effects, they were 34.20, 33.99 and 37.58% higher than the control.

3.8 Effects of tea plant endophytic PSB on the N P K content of Longjing tea plants

After inoculation with different PSB strains, the N content in maize seedlings increased slightly but showed no significant differences (Figure 8). The P content increased by 13.33-24.24%,

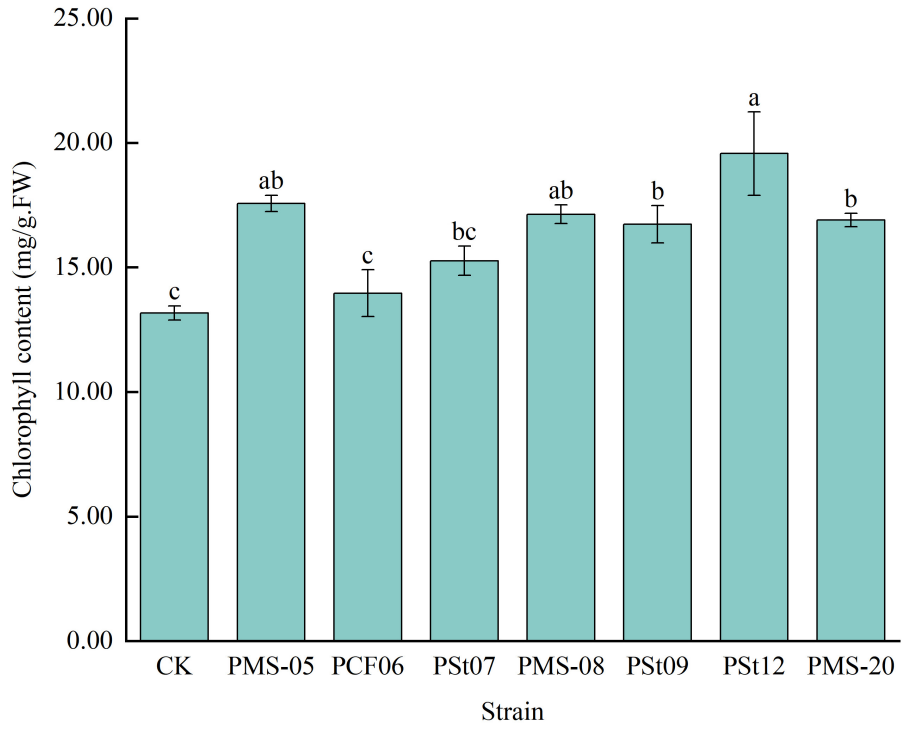


FIGURE 4
Effect of different strains on chlorophyll content of maize seedling leaves.

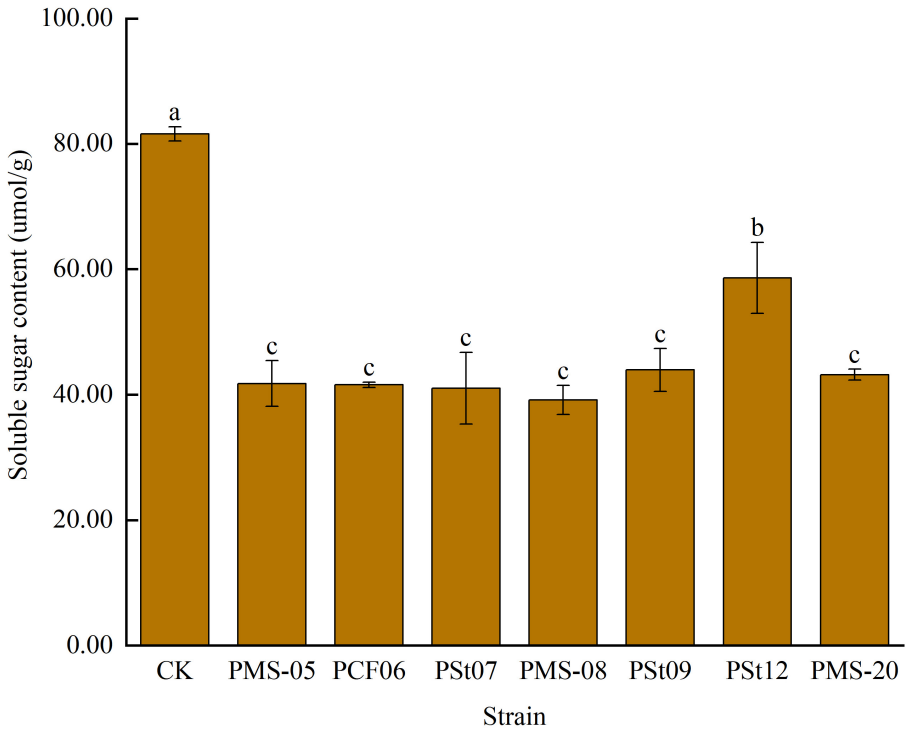


FIGURE 5
Effects of different strains on soluble sugar content in leaves of maize seedlings.

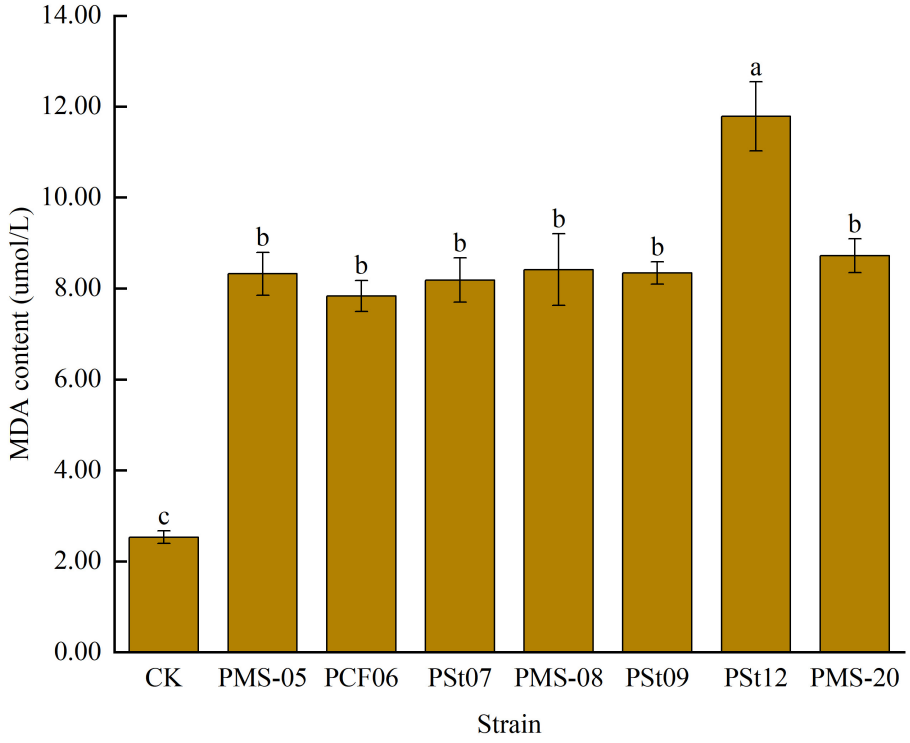


FIGURE 6
Effect of different strains on MDA content in leaves of maize seedlings.

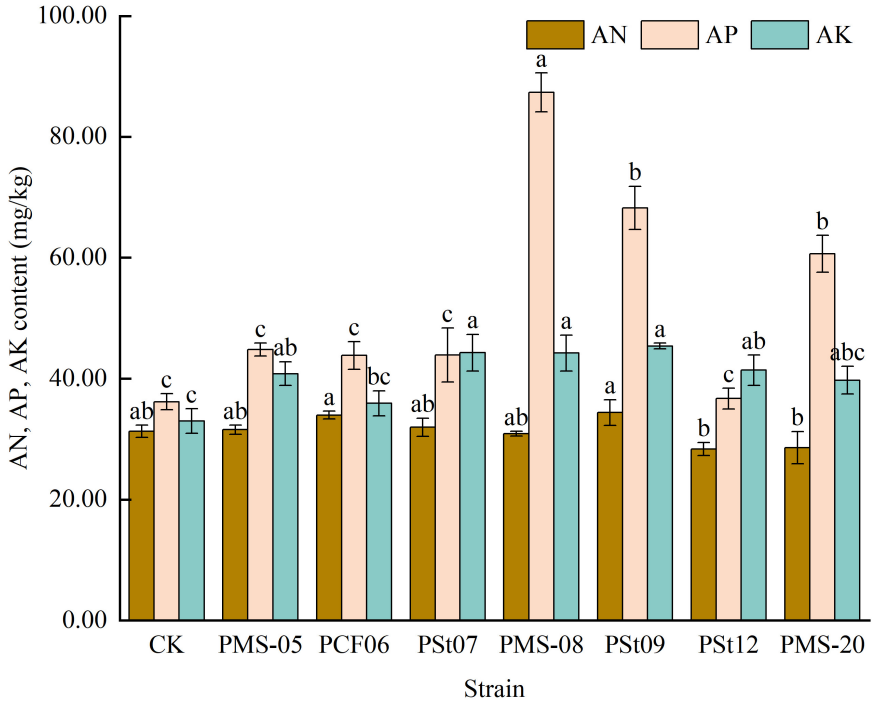


FIGURE 7
Effect of different strains on the content of AN, AP, and AK in rhizosphere soil of maize seedlings.

with significant differences observed ($P < 0.05$). Strains PMS-08 and PSt09 were particularly effective at promoting P uptake in seedlings. The K content in the seedlings also increased to varying degrees under all PSB treatments, with strain PSt07 being the most effective in enhancing K absorption, higher than control 26.35%.

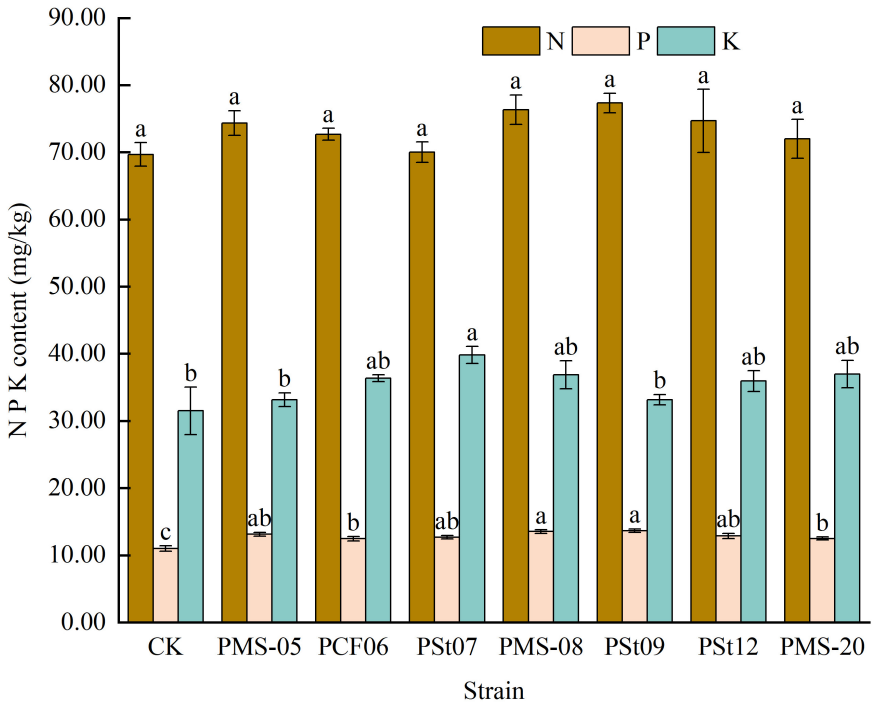


FIGURE 8
Effect of different strains on N, P, and K contents of maize seedlings.

3.9 Effects of tea plant endophytic PSB on available Se content in rhizosphere soil of maize seedlings

Forty-five days after inoculation with different PSB strains, the available Se content in the rhizosphere soil of the maize seedlings showed significant changes (Figure 9). Compared with the control, the rhizosphere soils treated with strains PMS-20 and PMS-05 presented significantly higher available Se contents, with increases of 195.73 and 144.47%, respectively ($P < 0.05$). In contrast, the available Se content under all the other PSB treatments was significantly lower than that of the control ($P < 0.05$).

3.10 Effects of tea plant endophytic PSB on Se content in maize seedlings

The effects of different PSB strains on Se absorption in maize seedlings varied significantly (Figure 10). Four strains noticeably promoted Se uptake in the plants, while two strains inhibited it. Seedlings treated with PMS-05, PCF06, PSt07, and PMS-08 exhibited significant increases in Se content compared to the control, with increases of 97.77, 49.50, 48.27, and 138.61%, respectively ($P < 0.05$). Among these strains, PMS-05 not only significantly increased the available Se content in the rhizosphere soil (Figure 9) but also enhanced the translocation of Se from soil to plants. In contrast, strains PCF06, PSt07, and PMS-08 improved the ability of maize seedlings to absorb and transport Se to leaves, despite reducing the available Se content in the rhizosphere soil.

4 Discussion

4.1 Effects of tea plant endophytic PSB on the growth and physiology of maize

Exogenous soluble P introduced into the soil is easily adsorbed and fixed by the soil, forming insoluble phosphate compounds. Excessive application of phosphorus fertilizer not only reduces phosphorus use efficiency but also exacerbates soil compaction (Chi et al., 2021). Phosphate-solubilizing and nitrogen-fixing functional microorganisms, as excellent growth-promoting bacterial resources, exhibit strong growth-promoting effects and are environmentally friendly, making them highly promising for development into microbial inoculants. Zhang et al. (2025) found that plant growth-promoting rhizobacteria (PGPR) from the maize rhizosphere can enhance maize biomass accumulation and effectively improve soil nutrient content. Similarly, Hou and Hu (2024) reported that multifunctional growth-promoting bacteria isolated from maize rhizosphere soil significantly promoted the root length, maximum leaf area, chlorophyll content, plant height, stem diameter, dry weight, and fresh weight of maize. Furthermore, Luo et al. (2024) demonstrated that PSB from the maize rhizosphere promoted maize growth to varying degrees and significantly altered the structure of the rhizosphere soil microbial community.

Endophytic bacteria, as one of the sources of PSB, can directly synthesize or promote host-synthesized phytohormones to regulate plant growth (Liu, 2019). Li et al. (2013) demonstrated that PSB isolated from *Anaphalis lactea* significantly enhanced maize growth parameters, including plant height, fresh weight, and dry weight. Wu et al. (2023) demonstrated that inoculation

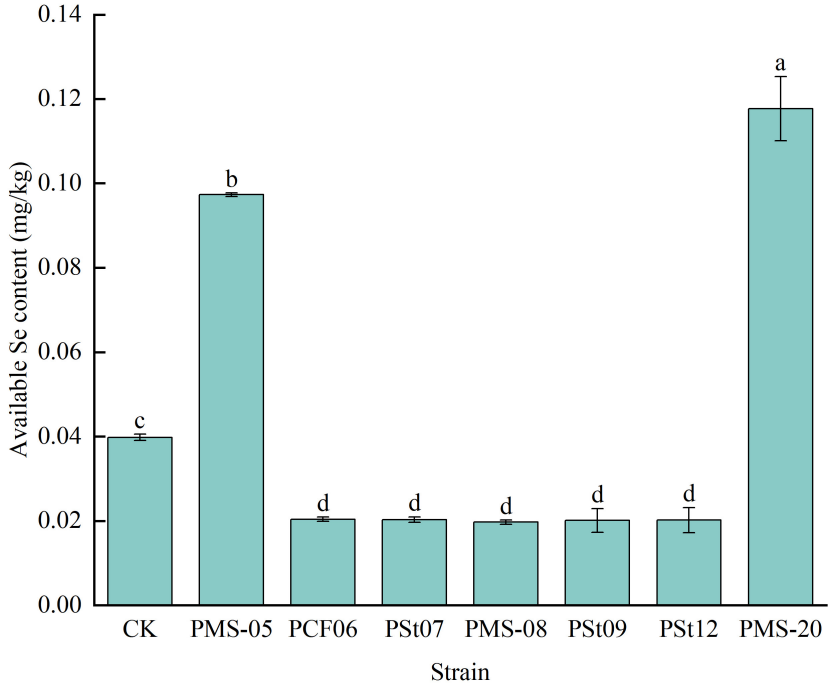


FIGURE 9
Effect of different strains on the content of available Se in rhizosphere soil of maize seedlings.

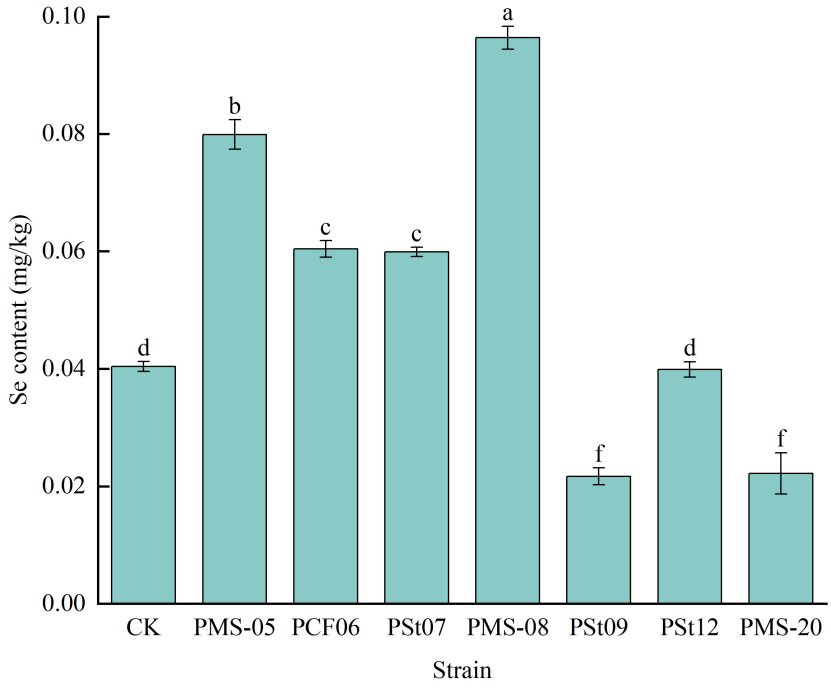


FIGURE 10
Effects of different strains on Se content of maize seedlings.

with endophytic fungi increased plant height, stem diameter, leaf number, nitrogen balance index, net photosynthetic rate, transpiration rate of *Camelia Oleifera*. In this study, the phosphorus solubilization and nitrogen fixation effect of the tested strains significantly increased the fresh and dry weight of maize, promoted increases in plant height and root length in maize seedlings, and enhanced chlorophyll synthesis in the leaves, the growth rates were 36.16-77.69%, 102.12-191.78%, 13.33-70.89%, 129.66-223.45% and 6.08-48.61%, respectively.

MDA is the final decomposition product of membrane lipid peroxidation in plant cell membranes under stress, and it serves as a crucial biochemical indicator for evaluating plant tolerance to adversity by reflecting the extent of cellular damage. Soluble sugars, as important osmotic regulators in plants, also play a role in assessing the degree of cell injury (Zhang et al., 2020). Zhou et al. (2022) reported that inoculating mung bean seedlings with PSB isolated from the rhizosphere soils of *Leymus chinensis* and *Suaeda salsa* reduced the MDA content in the seedlings. Similarly, Zhao et al. (2022) found that inoculating *Paris polyphylla* seedlings with PSB at the seedling stage enhanced root activity, increased the soluble sugar content in leaves, and reduced MDA levels. An et al. (2019) demonstrated that inoculating chili pepper seedlings with high-efficiency PSB isolated from the rhizosphere of tobacco significantly increased stem diameter, leaf number, biomass, and soluble protein content but had no significant effect on soluble sugar content. Liu et al. (2024) observed that Bacillus strains increased the soluble sugar content and reduced MDA levels in maize leaves under drought stress conditions.

In this study, maize seedlings were maintained under non-stress conditions without exposure to abiotic stresses such as salinity/alkalinity or drought throughout the experiment. Inoculation with endophytic PSB significantly increased soil available P content, effectively alleviating P deficiency. The enhanced P supply maintained cell membrane integrity, consequently reducing the need for osmotic adjustment through accumulation of compatible solutes like soluble sugars that would otherwise compensate for membrane damage-induced stress (Li et al., 2014). This mechanism explains the observed decrease in soluble sugar content alongside increased MDA levels. An alternative explanation may involve host-specific effects, as the tested PSB strains were originally isolated from tea plant roots, potentially exhibiting differential physiological impacts on host versus non-host plants (Gao et al., 2019).

4.2 Effects of tea plant endophytic PSB on the absorption of N, P, and K nutrients in maize

N, P, and K are essential elements for plant growth, with P also being a critical factor influencing photosynthesis and respiration (Liu et al., 2024). Arbuscular mycorrhizal fungi have been shown to promote maize growth and enhance the absorption of N, P, and K by the plant (Chen et al., 2023). Bacillus strains with nitrogen-fixing and phosphate-solubilizing capabilities can also increase the N, P, and K nutrient contents in maize plants (Liu et al., 2024). The contents of nitrate N, AP and organic carbon in rhizosphere soil of *Camelia Oleifera* were increased by inoculation of endophytic fungi (Wu et al., 2023). In previous studies, inoculating host tea plant seedlings with selected PSB strains revealed that PSB could enhance the availability of N, P, and K in the rhizosphere soil of "Longjing 43" tea seedlings (Zhang et al., 2024; Guo et al., 2024). In this study, seven strains of endophytic PSB isolated from tea plants were found to increase the AP and AK contents in rhizosphere soil, while no significant changes were observed in AN content. The effects of different strains on the AN, AP, and AK contents in the rhizosphere soils of host and non-host plants varied. This phenomenon may be due to differences in root exudates between non-host and host plants, which could affect the colonization of the tested strains in the rhizosphere soil, thereby leading to nutrient changes that differ between the two types of plants. Whether these results change with the growth period of the inoculated plants requires further investigation. The increased chlorophyll contents in the maize leaves further indicates that the inoculated PSB promoted the absorption of nutrients by the plants (Liu et al., 2024).

4.3 Effects of tea plant endophytic PSB on Se absorption in maize

Se is an essential trace element for humans, and agricultural products are the primary source of Se for the human diet. The Se content in agricultural products largely depends on the available Se content in the soil. PSB can increase the AP content in soil; this AP competes for adsorption sites on soil colloids, activating and releasing SeO_3^{2-}, and consequently increasing the available Se content in soil (Zhang et al., 2024). Durána et al. (2015) reported that endophytic bacteria could significantly increase the Se content in wheat crops.

In a separate experiment, inoculation of the tested strains into host tea plant seedlings revealed that five strains of PSB significantly increased the available Se content in the rhizosphere soil and the Se content in tea plant roots. Among them, the PSt12 strain notably increased the available Se content in the rhizosphere soil and Se content in tea plant roots by 573.07 and 397.26%, respectively, compared to the control ($P < 0.05$) (Zhang et al., 2024; Guo et al., 2024). However, in this study, the PSt12 strain had no significant effect on the Se content in maize leaves and even significantly reduced the available Se content in the rhizosphere soil of maize. These findings suggest that, as an endophyte originating from tea plant tissues, the strain has different effects on Se absorption and transport in host and non-host plants. This discrepancy may also be attributed to the differences in nutrient uptake characteristics between tea plants and maize. Additionally, the Se content in the aboveground parts of maize is influenced by soil texture, plant variety, and growth stage (Placzek and Barbara, 2020).

5 Conclusion

In this study, seven strains of endophytic PSB isolated from tea plant roots were inoculated into maize seedlings to analyze their effects on maize seedling growth, physiology, and soil nutrients. The results showed that all seven strains of tea plant endophytic PSB significantly increased the fresh weight, dry weight, plant height, and root length of maize seedlings. Fresh weight increased the most under *P. fungorum* PMS-05 treatment, plant height and root length increased the most under *P. fungorum* PMS-20 treatment. All strains enhanced the AP content in the rhizosphere soil and the P content in the maize plants. Specifically, treatment with *P. fungorum* PMS-05 significantly increased the available Se content in the rhizosphere soil and the Se content in the maize plants ($P < 0.05$).

In conclusion, tea plant endophytic PSB promote the growth of maize seedlings, improve rhizosphere soil nutrients, and enhance

nutrient uptake by plants. *P. fungorum* PMS-05 and *P. fungorum* PMS-20 can be considered potential growth-promoting bacterial resources for the early growth stages of maize.

Data availability statement

The original contributions presented in this study are included in this article/supplementary material, further inquiries can be directed to the corresponding author.

Author contributions

SZ: Data curation, Formal Analysis, Writing – original draft. JG: Formal Analysis, Writing – original draft. JL: Funding acquisition, Writing – review & editing. YY: Methodology, Validation, Writing – original draft. QZ: Methodology, Validation, Writing – original draft.

Funding

The author(s) declare that financial support was received for the research and/or publication of this article. The author(s) declare that financial support was received for the research, authorship, and/or publication of this article. This work was funded by the Natural Science Research Projects of the Education Department of Guizhou Province [QJJ(2024)337], Natural Science Foundation of China [32360353, 32360352], Guizhou Sci-Tech Support Plan [QKHZC(2023)Y223], Special project of innovative talent team of Guizhou Education University (2024RCTD003), and Guizhou Key Laboratory of Biological Resources Develop-Utilization in Universities [(2022)031].

Acknowledgments

We would like to thank the Key Laboratory of Biological Resources Exploitation and Utilization in Universities of Guizhou, and Institute of Soil and Environment Bioremediation in Karst Habitats, Guizhou Education University, Guiyang, China.

Conflict of interest

The authors declare that the research was conducted in the absence of any commercial or financial relationships that could be construed as a potential conflict of interest.

Generative AI statement

The authors declare that no Generative AI was used in the creation of this manuscript.

Publisher's note

All claims expressed in this article are solely those of the authors and do not necessarily represent those of their affiliated organizations, or those of the publisher, the editors and the reviewers. Any product that may be evaluated in this article, or claim that may be made by its manufacturer, is not guaranteed or endorsed by the publisher.

References

An, D., Che, Y. M., Zhao, F. G., Li, Y. H., Yang, D. C., and Liu, X. (2019). Physiological mechanisminthe growth promotiong effect of phosphate solubilizing bacteria 3P29 on pepper. *Northern Hortic.* 22, 8–16. doi: 10.11937/bfyy.20191118

Bao, S. D. (2008). *Soil Agrochemical Analysis*, 3rd Edn. Beijing: China Agricultural Press.

Chen, J. X., Yan, J., You, Y. H., Li, B., He, C. Z., and Tu, C. L. (2023). Effects of AMF on growth, low-molecular-weight organic acids secreted by roots, and Cd uptake in maize. *J. Agric. Resour. Environ.* 40, 1329–1338. doi: 10.13254/j.jare.2022.0658

Chi, J. L., Hao, M., Wang, Z. X., and Li, Y. (2021). Advances in research and application of phosphorus-solubilizing microorganism. *J. Microbiol.* 41, 1–7. doi: 10.3969/j.issn.1005-7021.2021.01.001

Durána, P., Acuñaa, J. J., Gianfredab, L., Azcónc, R., Funes-Colladod, V., and Mora, M. L. (2015). Endophytic selenobacteria as new inocula for selenium biofortification. *Appl. Soil Ecol.* 96, 319–326. doi: 10.1016/j.apsoil.2015.08.016

Gao, Y. M., Yao, T., Li, H. Y., Luo, H. Q., Zhang, J. G., and Yang, Y. S. (2019). Isolation, screening, and growth-promoting characteristics of plant growth promoting rhizobacteria in the rhizosphere of *Kobresia myosuroides* and *Polygonum viviparum* in alpine meadow pasture. *Acta Pratacult. Sin.* 28, 114–123. doi: 10.11686/cyxb2018754

Gou, T. Z., Xu, S. Q., and Sun, D. F. (2013). Selenium content of tea and its influencing factors in Liping county. *Guizhou Agric. Sci.* 41, 42–44. doi: 10.3969/j.issn.1001-3601.2013.11.0646

Guo, J. M., Zhang, S. Q., and Li, J. F. (2024). Impact of three exogenous phosphorus-solubilizing bacteria on zinc and selenium contents and rhizosphere soil nutrients of Longjing and Huangjinya tea plants. *Front. Microbiol.* 15:1413538. doi: 10.3389/fmicb.2024.1413538

Hou, Y. Y., and Hu, X. M. (2024). Screening and identification of three strains of phosphate-solubilizing bacteria from maize rhizosphere and their roles in plant growth promoting effect. *J. Northeast Agric. Univ.* 55, 46–55. doi: 10.19720/j.cnki.issn.1005-9369.2024.05.005

Isidro, B. M., Felipe, R. P., Lady, M. C., Angelica, Y. G., Antonio, M. M. S., and German, E. B. (2023). Inoculation of phosphate-solubilizing bacteria improves soil phosphorus mobilization and maize productivity. *Nutr. Cycl. Agroecosyst.* 126, 21–34. doi: 10.1007/s10705-023-10268-y

Ke, Y. Q., and Pan, T. G. (2022). Effects of NaCl stress on seedling growth and IAA metabolism of sweet potato and its relation to salt-tolerance. *Chin. J. Appl. Ecol.* 10, 1303–1306. doi: 10.13287/j.1001-9332.2002.0301

Li, J., Zhang, B. L., Zhao, Y., Xin, S. G., Chen, Q., Song, N. N., et al. (2014). Progress in endophyte improving plant salt and alkali resistance. *Biotechnol. Bull.* 4, 14–18. doi: 10.13560/j.cnki.biotech.bull.1985.2014.04.018

Li, X. T., Zhang, D., Zhao, F. P., Jjang, Y. F., Zeng, X., and Wang, X. D. (2024). Screening and analysis of two strains of high efficiency phosphor-soluble bacteria. *J. Microbiol.* 44, 60–69. doi: 10.3969/j.issn.1005-7021.2024.03.007

Li, Z. D., Chen, X. R., Yang, C. D., and Li, P. (2013). Screening, identification and solubilizing properties of the endophytic phosphate-solubilizing bacteria isolated from *Anaphalis lactea*. *Acta Pratacult. Sin.* 22, 150–158. doi: 10.11686/cyxb20130619

Liu, C. (2019). *Effects of Endophyte on Metabonomics and WRKY Gene Expression of Rice Seedlings Under Salt Stress*. Shenyang: Shenyang Normal University.

Liu, J., Luo, W. Q., Ming, L. W., Ma, L., Qi, X. K., and Fu, J. (2024). Growth promotion effects of two *Bacillus* specieson maize seedlings under drought stress. *Agric. Res. Arid Areas* 42, 35–43. doi: 10.7606/j.issn.1000-7601.2024.03.04

Liu, P., Zhao, H., Lin, G. X., and Che, L. W. (2015). Screening of phosphate-solubilizing strain and effects of medium components on its phosphate-solubilizing ability. *J. Tianjin Univ. Sci. Technol.* 30, 17–22. doi: 10.13364/j.issn.1672-6510.20140162

Liu, Z. P., Wang, Z. G., Xu, W. H., Chen, W. J., Lv, Z. H., and Wang, C. L. (2018). Screen, identification and analysis on the growth -promoting ability for the rice growth -promoting rhizobacteria. *J. Agric. Resour. Environ.* 35, 119–125. doi: 10.13254/j.jare.2017.0251

Luo, D., Shi, J., Li, M., Chen, J., Wang, T., and Zhang, Q. (2024). Consortium of phosphorus-solubilizing bacteria promotes maize growth and changes the microbial community composition of rhizosphere soil. *Agronomy* 14:1535. doi: 10.3390/agronomy14071535

Oldroyd, G. E. D., and Leyser, O. (2020). A plant's diet, surviving in a variable nutrient environment. *Science* 368:6486. doi: 10.1126/science.aba0196

Placzek, A., and Barbara, P. P. (2020). Changes in the selenium content in aerial parts of maize varieties, depending on the growing period and soil texture. *J. Elementol.* 25, 787–800. doi: 10.5601/jelem.2020.25.1.1944

Wang, X. K. (2006). *Experimental Principles and Techniques of Plant Physiology and Biochemistry*. Beijing: Higher Education Press.

Wang, Z., Cao, C. L., Ku, Y. L., Xu, G. Y., Lin, Y. B., and Liu, X. D. (2016). *Bacillus megatherium* WY4 labeled by GFP and its colonization in chinese cabbage (*Brassica chinensis*). *J. Agric. Biotechnol.* 24, 1925–1934. doi: 10.3969/j.issn.1674-7968.2016.12.015

Wu, W. J., Wang, F. L., Han, M. Z., Liu, Y. Y., Liu, R. C., Zou, Y. N., et al. (2023). Effects of root endophytic fungi on growth, gas exchange, and soil properties of field *Camellia oleifera* plants. *Non-wood For. Res.* 41:190. doi: 10.14067/j.cnki.1003-8981.2023.04.018

Xue, Y., Luo, D., Zhou, G. Y., Liu, J. A., and Deng, X. J. (2024). Screening of high-efficiency phosphorus-solubilizing bacteria in the rhizosphere of *Camellia oleifera* and their phosphorus solubilizing characteristics. *J. Central South Univ. For. Technol.* 44, 94–104. doi: 10.14067/j.cnki.1673-923x.2024.10.010

Zhang, S. Q., Guo, J. M., Li, J. F., Wu, L., Wang, X., and Zeng, Z. Q. (2024). Effects of phosphate solubilizing bacteriaand phosphatesolubilizing and nitrogen-fixing bacteria on selenium and zinc contents in selenium-rich soil and *Camellia sinensis* seedlings in Guizhou. *J. Tea Sci.* 44, 431–442. doi: 10.13305/j.cnki.jts.2024.03.011

Zhang, S. Q., Zang, D. D., Li, J. F., and Guo, J. M. (2020). Effects of drought-tolerance Rhizobium on the *Dolichos lablab* growth under drought stress. *Agric. Res. Arid Areas* 38, 39–45. doi: 10.7606/j.issn.1000-7601.2020.06.06

Zhang, T., Wan, Y. X., Xu, W. H., Wang, Z. G., Chen, W. J., and Hu, Y. L. (2025). Growth-promoting effects of a rhizosphere growth-promoting bacterium *Leclercia adecarboxylata* LN01 in maize plants and its whole-genome analysis. *Biotechnol. Bull.* 41, 41–53. doi: 10.13560/j.cnki.biotech.bull.1985.2024-0487

Zhang, Z. A. (2004). *Experimental Guidance of Plant Physiology*. Beijing: China Agricultural Science and Technology Press.

Zhao, J. J., Guo, D. Q., Yang, M., Zhang, J., and Zhou, N. (2022). Effect of different dosage of dissolving phosphorus bacteria on growth and development in *Paris polyphylla var. Yunnanensis*. *Environ. Chem.* 41, 761–769. doi: 10.7524/j.issn.0254-6108.2020091702

Zhou, Y., Wang, L. N., Zhang, M. Z., Liu, Q., and Yin, K. D. (2022). Screening and identification of phosphate solubilizing bacteria tolerant to salt-alkali and its growth-promoting effecton mung bean. *Acta Agric. Boreali-occidentalis Sin.* 31, 488–497. doi: 107.606/ji.ssn1.004-13892.0220.40.10

Zou, Q. (1979). *Experimental Guidance of Plant Physiology*. Beijing: China Agriculture Press.

frontiers | Frontiers in Microbiology

TYPE Original Research
PUBLISHED 12 May 2025
DOI 10.3389/fmicb.2025.1590686

Check for updates

OPEN ACCESS

EDITED BY
Elena Tamburini,
University of Cagliari, Italy

REVIEWED BY
Kusum Dhakar,
Academy of Sciences of the Czech Republic (ASCR), Czechia
Jialin Hu,
Texas A&M AgriLife Research, United States

*CORRESPONDENCE
Ju-Lin Gao
✉ nmgaojulin@163.com
Qinggeer Borjigin
✉ qinggeer001@163.com

RECEIVED 10 March 2025
ACCEPTED 22 April 2025
PUBLISHED 12 May 2025

CITATION
Liu R-Z, Zhao X-Y, Feng B, Zhao W-S, Li M-Y, Yu X-F, Hu S-P, Li R-P, Gao J-L and Borjigin Q (2025) Research on soil bacterial community assembly and function under different straw returning practices in arid and semi-arid agricultural ecosystems over multiple years.
Front. Microbiol. 16:1590686.
doi: 10.3389/fmicb.2025.1590686

COPYRIGHT
© 2025 Liu, Zhao, Feng, Zhao, Li, Yu, Hu, Li, Gao and Borjigin. This is an open-access article distributed under the terms of the Creative Commons Attribution License (CC BY). The use, distribution or reproduction in other forums is permitted, provided the original author(s) and the copyright owner(s) are credited and that the original publication in this journal is cited, in accordance with accepted academic practice. No use, distribution or reproduction is permitted which does not comply with these terms.

Research on soil bacterial community assembly and function under different straw returning practices in arid and semi-arid agricultural ecosystems over multiple years

Rui-Zhi Liu[1,2,3], Xiao-Ya Zhao[1,2,3], Biao Feng[1,2,3], Wen-Shan Zhao[1,2,3], Ming-Yu Li[1,2,3], Xiao-Fang Yu[1,2,3], Shu-Ping Hu[2,3,4], Rui-Ping Li[1,2,3], Ju-Lin Gao[1,2,3]* and Qinggeer Borjigin[1,2,3]*

[1]College of Agriculture, Inner Mongolia Agricultural University, Hohhot, China, [2]Key Laboratory of Crop Cultivation and Genetic Improvement of Inner Mongolia Autonomous Region, Hohhot, China, [3]Inner Mongolia Autonomous Region Engineering Research Centre of Microorganisms for In Situ Corn Straw Return, Hohhot, China, [4]Vocational and Technical College, Inner Mongolia Agricultural University, Baotou, China

Introduction: Straw return has gained attention for its potential to improve soil quality and crop yields, particularly in semi-arid regions like the Tumu Chuan Plain Irrigation Area. Soil bacteria play a crucial role in regulating soil biological processes, and understanding how straw return affects bacterial populations can guide better agricultural management practices.

Methods: We investigated the impact of continuous straw return on soil bacterial communities using 16S rRNA gene sequencing. Four treatments were applied: Farmers' shallow rotation (CK), straw incorporated with deep tillage (DPR), straw incorporated with subsoiling (SSR), and no-tillage mulching straw return (NTR). Bacterial community structure, metabolic pathways, and assembly mechanisms were analyzed using Bugbase and PICRUSt2 for phenotypic and metabolic pathway predictions.

Results: The study found that straw return practices significantly altered the relative abundance and life history strategies of bacterial phyla, mainly influenced by soil organic matter (SOM) and enzyme activity. The K-strategist to r-strategist ratio was highest in CK (2.06) and lowest in SSR (1.89). DPR and NTR treatments significantly changed bacterial community structure compared to CK ($p < 0.05$), resembling SSR. Predictions showed that DPR and NTR enhanced carbohydrate and amino acid metabolism and promoted more stable bacterial networks, with homogenous selection and drift effects. Bacterial aggregation in all treatments was driven by random processes, with varying aggregation levels: CK (20%), DPR (38.6%), SSR (16.5%), and NTR (30.7%).

Discussion: The study demonstrates that continuous straw return practices significantly impact soil bacterial communities. DPR and NTR notably improved microbial diversity, bacterial cooperation, and ecosystem stability. These findings provide valuable insights for sustainable agricultural practices in semi-arid regions, enhancing soil microbial ecology and soil health through strategic straw return.

KEYWORDS

straw return practices, soil microbial community assembly, bacterial lifestyle, ecosystem stability, semi-arid agriculture

1 Introduction

Approximately 40% of the world's land area is located in arid or semi-arid regions, which are home to approximately one-third of the global agricultural population resides (Bernardino et al., 2025). These areas are crucial for global agricultural production but face challenges such as water scarcity, soil degradation, and environmental deterioration, which significantly limit the sustainability of agriculture. With increasing climate change and growing land resource pressures, enhancing agricultural productivity, restoring soil functions, and achieving ecological sustainability have become critical topics in current agricultural research (Yu et al., 2024). Straw return, as an effective agricultural management measure, has been widely used to improve soil physical structure, enhance water retention capacity, and promote nutrient cycling, which is key to improving soil quality and crop yield (Liu Q. et al., 2024). However, the long-term effects of different straw return practices on soil microbial communities, especially soil bacterial communities, remain unclear, particularly in dry and semi-arid regions where the effectiveness of straw return is influenced by various environmental factors.

Soil microorganisms, particularly bacteria, play a vital role in soil ecosystems by participating in organic matter decomposition, nutrient cycling, and maintaining soil health (Wang et al., 2024). Diverse tillage practices combined with straw return can regulate microbial dynamics in continuous cropping fields, thereby promoting crop nutrient uptake and productivity (Wang et al., 2025). Previous studies have shown that straw return provides a rich carbon sources for microbial communities, enhancing microbial activity and diversity (Liu et al., 2025). However, the mechanisms by which different straw return practices (e.g., deep plowing, no-tillage covering, straw composting) affect microbial communities are not well understood, particularly with respect to their long-term impact on soil health (Zhang J. et al., 2024). Straw direct covering promotes short-term microbial activity by providing labile organic matter, whereas deep plowing improves soil structure and long-term organic matter stability, ultimately influencing microbial community composition and function (Song et al., 2024). These changes may affect microbial ecological functions, such as nitrogen-fixing bacteria abundance or the microbial populations involved in cellulose and lignin decomposition. Microbial community assembly is driven by a combination of environmental selection, crop interactions, and random processes (Tian et al., 2024). Compared to non-straw return, straw return not only changes microbial community structure but also increases soil microbial resistance (Hao et al., 2019). The response of soil microbial communities to drought varies significantly among different straw return practices. In arid regions of northern China, straw return has been shown to significantly alter the complexity and stability of microbial symbiotic networks (Kang et al., 2025). Straw return, by improving soil health and microbial-host compatibility, positively impacts root-soil-microbe interactions and drought-resistant crops (Liu X. et al., 2023). Existing studies have primarily focused on the short-term effects of straw return on microbial community composition and diversity, with a lack of systematic analysis of the combined and long-term effects of different straw return practices on microbial community structure. Microbial responses to environmental selection affect life history strategies and community assembly processes, playing key roles in natural resource utilization and interspecies interactions (Kinnunen et al., 2020; Jiao et al., 2022; Yang et al., 2023), this response can, in turn, influence agricultural productivity under various straw return practices. However, the ecological function of soil bacterial communities, their adaptability to environmental stress, and their interspecies interactions in multi-year straw return practices in semi-arid/arid systems remain inadequately explored.

Maize is an important food crop (Zong et al., 2024), and straw return has significant effects on its yield and soil health (Liu R.-Z. et al., 2024; Chen et al., 2025). Previous studies have shown that straw return can alter the composition and function of soil microbial communities and enhance the activity of beneficial microbes (Yang et al., 2021). This study investigates on the long-term regulation of soil bacterial communities under different straw return practices in a continuous maize cropping system on the Tumu Chuan Plain Irrigation Area. The aim is to explore the effects of continuous straw return practices on bacterial community assembly mechanisms and functional traits, and to investigate the feedback relationships between straw return and soil microbial communities. Our hypotheses are: (1) continuous different straw return practices regulate bacterial community composition, structure, and life history strategies by altering soil physical and chemical properties and microbial habitats, (2) continuous deep plowing with straw incorporation and no-tillage straw covering enhance bacterial adaptation to environmental stress by improving soil conditions. By deeply analyzing the long-term effects of different straw return practices, this study provides scientific evidence for straw management in semi-arid and arid regions and contributes to the sustainable development of agricultural ecosystems.

2 Materials and methods

2.1 Experimental site

This study is based on the pre-constructed straw return trial platform of the group (the straw returning platform test site was established in 2018) conducted in 2020–2024 and was carried out in the China Chilechuan Modern Agricultural Expo Park (Beizhitu Village, Goumen Town, Tumet Right Banner, Baotou City, Inner Mongolia, latitude 40°28′28″N, longitude 110°29′5″E), where perennial straw return to the experimental field has been implemented starting in 2018. This area has a semi-arid mesothermal temperate continental monsoon climate, with an average annual temperature of 6–8°C, 400 mm of annual precipitation, a frost-free period of 140 days, an elevation of 1,015 m, 2,806 h of annual sunshine, and an annual active cumulative temperature ranging from 3,000–3,500°C. The site is used for continuous maize cultivation. In the absence of tillage, the soil texture is sandy loam, and the soil fertility is characterized by an organic matter content of 22.04 g/kg, an alkali-hydrolysable nitrogen content of 57.82 mg/kg, an available phosphorus content of 3.57 mg/

kg, and an available potassium content of 84.97 mg/kg. The soil nutrient data collected before sowing and tillage (0–45 cm soil layer) are shown in Supplementary Table S1, and the main meteorological data collected during the test period are shown in Supplementary Figure S1.

2.2 Experimental design

The experiment used a one-factor experimental design, where the plowing method was applied in the central zone. Farmers' shallow rotation (CK): refers to the sowing method used by local farmers. During the fall land preparation phase, the straw is crushed and baled, then removed from the field. In spring, after the stubble is processed, conventional shallow rotation sowing is carried out. Three treatments were established for comparison, straw incorporated with deep tillage (DPR): in autumn, straw is shredded and plowed into the soil to a depth of 30–40 cm. In spring, sowing is done using a conventional planter. Straw incorporated with subsoiling (SSR): in autumn, straw is shredded and mixed with the soil after subsoiling to a depth of 35–40 cm. In spring, sowing is done using a conventional planter. No-tillage mulching straw return (NTR): in autumn, straw is shredded and left on the soil surface as mulch. In spring, sowing is done using a no-till planter. All straw return treatments included full corn straw return at 135–150 kg ha^{-1}. The maize variety planted was Xianyu 696 at a planting density of 825 plants/ha. Ammonium dihydrogen phosphate (N 18%, P 46%) was applied at a rate of 375 kg ha^{-1}, and potassium sulfate (K 22%) was applied at a rate of 150 kg ha^{-1}. Urea (N 46%) was applied utilized as a supplementary fertilizer with application rates of 30% at V6 (sixth leaf), 60% at V12 (twelfth leaf), and 10% at R2 (blister), resulting in a total nitrogen application of 345 kg/ha. Drip irrigation was performed four times during the growing season: at V6, V12, R1 (silking), and R2. Each irrigation event covered 750 m^3/ha. All remaining management practices followed standard procedures commonly used in large-scale agricultural production.

The experiment was conducted annually during the maize pre-sowing period from 2020 to 2024. Soil samples were collected each May, totaling four sampling events. In each experimental plot, soil was collected from the 0–45 cm layer using an imported auger in an "S"-shaped sampling pattern. A total of 12 subsamples were taken per plot, thoroughly mixed, and passed through a 2 mm mesh sieve to remove plant debris, root fragments, and other impurities. The homogenized soil was then subjected to the quartering method to obtain a representative sample, sealed in sterile bags, and immediately transported to the laboratory. Each composite sample was divided into three parts: the first portion was air-dried for determining soil physicochemical properties and measuring the activity of alkaline phosphatase (ALP) (Tan et al., 2017; Wang et al., 2017) and catalase, the latter being assessed by back-titration of residual H_2O_2 with $KMnO_4$ (Johnson and Temple, 1964). The second portion was stored at 4°C for analysis of glutamine synthetase (Glu) activity (Haghighat, 2005), the third portion was stored at −80°C for DNA extraction and high-throughput sequencing.

2.3 Soil properties analysis

Soil Moisture (SM,%) was measured using the JL-01 multi-point soil temperature and humidity recorder (JL-01, Jingyi Electronic Company). Soil Bulk Density (g/cm^3, BD) was determined by the core method (VanRemortel and Shields, 1993). Soil alkaline nitrogen (AN) was measured using the alkaline hydrolysis diffusion method (Bremner, 1960). Available phosphorus (AP) was determined with the Smartchem140 automated chemical analyzer (SMARTCHEM450, AMS, France) (Olsen and Sommers, 1982). Available potassium (AK) was measured using a flame photometer (M410, Sherwood Scientific, United States) (Allen and Grimshaw, 1986). Soil organic matter (SOM) was determined by the potassium dichromate method (Walkley and Black, 1934). Alkaline phosphatase (ALP) was determined by the phenylphosphate colorimetric method (Liu et al., 2020). Hydrogen peroxide decomposing enzyme (H_2O_2) was measured by the potassium permanganate titration method (Borràs-Brull et al., 2021). Glutamine synthetase (GS) was determined using visible spectrophotometry (Haghighat, 2005).

2.4 Sequencing and bioinformatics analysis

2.4.1 DNA extraction

Genomic DNA was extracted from soil microbial communities using the E.Z.N.A.® Soil DNA Kit (Omega Bio-tek, Norcross, GA, United States), following the manufacturer's instructions. DNA quality was assessed by 1% agarose gel electrophoresis, and DNA concentration and purity were measured using a NanoDrop 2000 spectrophotometer (Thermo Scientific, United States).

2.4.2 PCR amplification and sequencing library construction

The extracted DNA was used as a template, and primers 338F (5′-ACTCCTACGGGAGGCAGCAG-3′) and 806R (5′-GGACTAC HVGGGTWTCTAAT-3′) were used for PCR amplification of the 16S rRNA gene (Liu et al., 2016). Ten nanograms (ng) of DNA were extracted from soil samples for PCR amplification of the V3–V4 region of the 16S rRNA gene. Sequencing was conducted using the Illumina MiSeq PE300 platform. The raw sequencing data were quality controlled using fastp (Chen et al., 2018; https://github.com/OpenGene/fastp, version 0.20.0), and paired-end reads were merged using FLASH (Magoč and Salzberg, 2011; http://www.cbcb.umd.edu/software/flash, version 1.2.7). A total of 22,243,836 high-quality sequences were obtained. To minimize sequencing depth effects on subsequent alpha and beta diversity analyses, all sample sequence numbers were rarefied to 24,845. Sequence rarefaction is recommended to ensure comparability across samples. After rarefaction, the average sequence coverage (Good's coverage) of each sample remained at 99.09%. OTU-level taxonomic annotation was performed using the RDP Classifier (Wang et al., 2007; http://rdp.cme.msu.edu/, version 2.11) against the SILVA 16S rRNA gene database (v138), with a confidence threshold of 70%, to assign taxonomic classifications. The community composition of each sample was statistically analyzed at various taxonomic levels. The 16S functional prediction analysis was conducted using PICRUSt2 (Douglas et al., 2020; version 2.2.0) software.

2.5 Functional and life history trait analysis

The functional potential of bacterial communities was predicted using BugBase and PICRUSt 2 (Wang S. et al., 2022; Zhu et al., 2022).

Phenotypic predictions of the bacterial communities were made using BugBase.[1] Functional characteristics of the bacterial communities were predicted using PICRUSt2,[2] referencing the KEGG pathway database.[3] Life history traits were calculated by selecting K-strategist and r-strategist members within the bacterial communities (Shi et al., 2023). K-strategists primarily include Acidobacteriota, Actinobacteriota, and Chloroflexi, while r-strategists are mainly represented by Firmicutes, Gemmatimonadota, and Proteobacteria.

2.6 Assembly processes analysis

To classify bacterial community assembly into underlying deterministic and stochastic processes, the β-nearest taxon index (βNTI) was calculated using null model generated through 999 randomizations based on the observed data (OTU table and genetic development tree) (Shi et al., 2023; Jiao et al., 2022). βNTI <−2 and βNTI >2 indicated homogeneous and heterogeneous selection (deterministic processes), respectively. |βNTI| <2 indicated that bacterial community assembly was the dominance of stochastic processes. To quantitatively analyze the mechanisms of bacterial community assembly, phylogenetic bin-based null model analysis (iCAMP) was conducted to further segregate the contribution of ecological processes to bacterial assembly (Ning et al., 2020).

2.7 Co-occurrence network analysis and ZiPi analysis

Bacterial co-occurrence network at the OTU level was assessed using the Spearman rank correlation (Shi et al., 2023). Only OTUs with relative abundance >0.1% were used in the analyses. Statistical correlations were identified when Spearman's $r > 0.7$ or <-0.7, and $p < 0.05$ and were then incorporated into the co-occurrence network construction. The node and edge numbers, average clustering coefficient, average degree and graph density were used to evaluate network complexity in this study. Positive and negative correlations between nodes represented cooperative and competitive behaviors (Wang C. et al., 2024).

For the ZiPi analysis, the igraph package and the NetCoMi package (version 1.0.4) in R were used (Olesen, et al., 2007). Based on the Zi value (within-module connectivity) and Pi value (among-module connectivity) of each node, the network nodes were classified into four categories: (1) module hubs (Zi >2.5, Pi ≤0.62), which occupy important positions within modules but have weak associations with other modules, (2) connectors (Zi >2.5, Pi >0.62), which play a significant role in the functional connectivity of the entire network, (3) within-module non-hubs (Zi ≤2.5, Pi ≤0.62), and (4) module outside connectors (Zi ≤2.5, Pi >0.62; Guimerà and Nunes Amaral, 2005).

1 https://bugbase.cs.umn.edu/index.html
2 https://github.com/picrust/picrust2
3 http://www.genome.jp/kegg/

2.8 Statistical analysis

Basic parameters were visualized using the "ggplot2" package in R (version 4.3.1). Statistical analysis was performed using SPSS 23.0 software (SPSS Inc., Chicago, IL), including one-way analysis of variance (ANOVA). A p-value <0.05 was considered statistically significant. One-way ANOVA with Duncan's test was used to assess differences in soil properties, bacterial diversity, life history strategies, and βNTI among the three treatments. Using UPARSE software (Stackebrandt and Goebel, 1994; Edgar, 2013; http://drive5.com/uparse/, version 7.1), sequences were clustered into OTUs based on 97% similarity. Alpha diversity metrics such as Chao 1 and Shannon index were calculated using mothur software (Schloss et al., 2009; http://www.mothur.org/wiki/Calculators), and inter-group differences in alpha diversity were analyzed using the Wilcoxon rank-sum test; principal coordinate analysis (PCoA) based on Bray–Curtis distance algorithm was used to examine the similarity of microbial community structure between samples, and PERMANOVA non-parametric test was performed to analyze whether there were significant differences in microbial community structure between sample groups. The proportion (%) and number of shared and unique OTUs among the four treatments were visualized using the "VennDiagram" package in R. Heatmap analysis was conducted using the "pheatmap" package in R. βNTI and community assembly processes were calculated using the "NST" and "iCAMP" R packages, respectively. Co-occurrence networks were constructed using the "WGCNA" package in R and visualized with Gephi (version 0.10.1). Mantel test and Pearson analysis were performed using the "linkET" package in R to determine the factors influencing bacterial communities and life history strategies. Partial least squares (PLS) regression was conducted using Simca 14.0 (Umetrics, Umeå, Sweden) to distinguish the relative importance of soil physicochemical properties and bacterial characteristics in bacterial community assembly. The direction and magnitude of each factor's influence on microbial carbon were analyzed using the PLS standardized coefficients. The variable importance in projection (VIP) values were used to assess the relative importance of these variables, with VIP >1 indicating significant influence ($p < 0.05$).

3 Results

3.1 Soil bacterial community composition and diversity in different straw return methods

The main bacterial phyla identified in each treatment were Acidobacteriota, Actinobacteriota, Chloroflexi, Gemmatimonadota, Firmicutes, and Proteobacteria (Supplementary Figure S2). The relative abundance of these phyla varied significantly across treatments (Figure 1A). Compared with other treatments, the relative abundance of r-strategist bacteria was the highest in the DPR treatment. At the phylum level, Proteobacteria showed a noticeable increase under the DPR treatment ($p < 0.05$). At the genus level, *Nitrosospira* was the most prominent under the DPR treatment (Supplementary Figure S3). In contrast, K-strategy organisms, such as Actinobacteriota, Chloroflexi, Arthrobacter, and Blastococcus, were less abundant in the

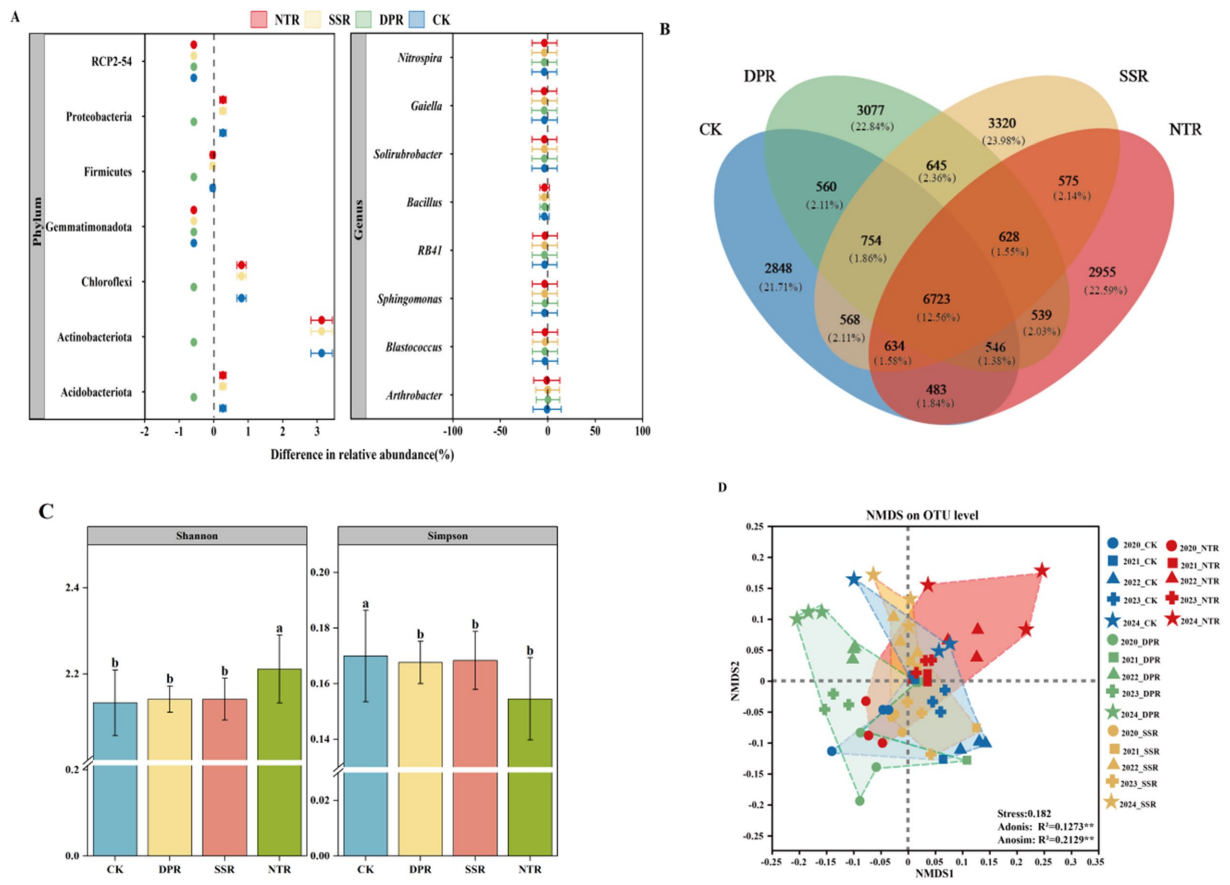


FIGURE 1
Composition and diversity of soil bacterial communities. **(A)** Differences in relative abundance of soil bacterial communities at phylum and genus levels among different straw-returning practices. **(B)** Venn diagram of bacterial OTUs in CK, DPR, SSR, and NTR treatments. **(C)** Error lines for bacterial α-diversity in CK, DPR, SSR, and NTR treatments are standard deviations (SD) from the mean. Different lowercase letters indicate significant differences among the three treatments ($p < 0.05$). **(D)** Non-metric multidimensional scaled ordination plots of loam bacterial communities for CK, DPR, SSR, and NTR treatments were tested for significance using Adonis and Anosim tests (**$p < 0.01$). CK, farmer's shallow rotary; DPR, deep rotary straw return; SSR, straw incorporated with subsoiling, and NTR, no-tillage mulching straw return.

DPR treatment, with Blastococcus showing the largest difference, being notably lower by 79.93%. Under SSR and NTR treatments, these organisms also declined, though to a lesser extent. Conversely, r-strategy organisms, including *Bacillus*, *Proteobacteria*, *Sphingomonas*, and *Nitrospira*, showed minimal reductions or remained more stable across all treatments, particularly in SSR and NTR, indicating higher resilience. In the CK treatment, the abundance of species remained stable, with K-strategy organisms more abundant than r-strategy organisms. Under DPR treatment, r-strategy organisms, such as *Bacillus* and *Nitrospira,* showed an increase, with *Bacillus* rising by 92.17%, while Firmicutes decreased by 182.31%. Over time, r-strategy organisms steadily increased, while K-strategy organisms declined. In SSR and NTR treatments, r-strategy organisms showed a more gradual increase or remained stable, while K-strategy genera, such as Actinobacteriota and Chloroflexi, declined, particularly after 2022.

The Venn diagram revealed that the number of core OTUs shared among CK, DPR, SSR, and NTR treatments was 6,723 (12.54% of the total), indicating strong environmental adaptation of these core flora (Figure 1B). The number of unique OTUs varied across treatments. The SSR treatment had the highest number of unique OTUs (3,320, 13.88%), followed by DPR (3,077, 12.84%) and NTR (2,955, 12.35%). The CK treatment had 2,848 unique OTUs (11.71%).

The different treatments significantly affected the α-diversity and β-diversity of soil bacterial communities under long-term straw-returning conditions (Figures 1C,D). Simpson's index showed higher homogeneity in the CK treatment than in the other treatments ($p < 0.05$). No significant differences were observed among the DPR, SSR, and NTR treatments ($p > 0.05$), all showing low homogeneity. Shannon's index indicated that the NTR treatment significantly increased bacterial diversity, while no significant differences were found between the other treatments (Figure 1C, $p < 0.05$).

In the β-diversity analysis, the NMDS ordination revealed significant segregation of soil bacterial community structures among the different treatments (Stress value = 0.182). The NTR treatment had the widest distribution of points, which were significantly separated from the other treatments. These differences were confirmed by Adonis ($R^2 = 0.12$, $p < 0.01$) and Anosim ($R^2 = 0.21$, $p < 0.01$) tests. The community structure of the CK and DPR treatments was closer, while the community structure of the SSR treatment was positioned between CK and NTR (Figure 1D).

10.3389/fmicb.2025.1590686

3.2 Functional and life history characteristics of soil bacteria in different straw return methods

Functional attributes of bacterial communities were predicted by PICRUSt 2 (Supplementary Figure S4). Bacterial communities in the DPR and NTR treatments showed high collaborative metabolic functions, particularly in global metabolic regulation, carbohydrate metabolism and amino acid metabolism pathways, whereas the CK treatment was dominant in specific pathways. The CK treatment showed dominance in specific pathways, such as lipid metabolism, while the SSR treatment had slightly less diversity in metabolic functions but was prominent in some specific functions.

Bugbase predictions showed that different straw return treatments affected the phenotypic characteristics of bacterial communities (Figure 2A). The NTR and DPR treatments favored the growth of adversity-tolerant, biofilm-forming, and anaerobic bacteria. The CK and SSR treatments favored the colonization of Gram-negative and aerobic bacteria. No significant differences were observed in potentially pathogenic bacteria or mobile genetic element bacteria among the treatments.

The ratio of Gram-positive to Gram-negative bacteria differed significantly ($p < 0.05$) among the CK, DPR, SSR, and NTR treatments, with the NTR treatment showing the lowest G+/G− ratio (0.388), significantly lower than the CK (0.486), DPR (0.478), and SSR (0.475) treatments. Overall, the CK, DPR, and SSR treatments favored the growth of Gram-positive bacteria, while the NTR treatment promoted the dominance of Gram-negative bacteria (Figure 2B).

Among the different treatments, the DPR treatment had the best relative abundance of K-strategists (13.36%) and r-strategists (5.36%), where the abundance of r-strategists was significantly increased by 0.99 percentage points over the CK treatment ($p < 0.05$), the NTR treatment was the second most effective in promoting r-strategy bacteria (5.14%), but less favorable to K-strategy bacteria (12.43%), CK and SSR treatments were closer in promoting K-strategy bacteria (12.92 and 13.34%), but relatively weaker in promoting r-strategy bacteria (4.37 and 4.69%). Overall, DPR treatment most significantly enhanced the synergistic development of K-strategy and r-strategy bacteria, while NTR treatment was more inclined to promote the expansion of r-strategy bacteria.

3.3 Soil bacterial assembly process and network analysis in different straw return methods

The results of the null model analysis showed significant differences in the dominant mechanisms of community construction among the different straw-returning methods (Figure 3A; $p < 0.05$). Heterogeneous selection (Hes) was dominant in all treatments, with the proportion ranging from 54.22% (DPR) to 79.11% (SSR). The proportion of stochastic processes varied significantly across treatments ($p < 0.05$). The DPR treatment had the highest proportion of stochastic processes (38.66%), with drift (DL) and diffusion restricted (DR) contributing 12.44 and 26.22%, respectively. The SSR treatment had the lowest proportion of stochastic processes (16.45%), with drift accounting for 0.89%, while heterogeneous selection was 79.11%. CK and NTR treatments were intermediate, with shallow tillage biased towards deterministic processes, while NTR enhanced stochastic processes due to lower soil disturbance. SSR and CK treatments were dominated by deterministic processes, with SSR contributing most to a stable microbial community. NTR treatment increased the contribution of stochastic processes while maintaining soil stability (Figure 3B).

The co-occurrence network showed that the DPR treatment had the highest ecological network complexity, with 169 nodes, 812 edges, 59.11% positive interactions, and a mean degree of 10.15

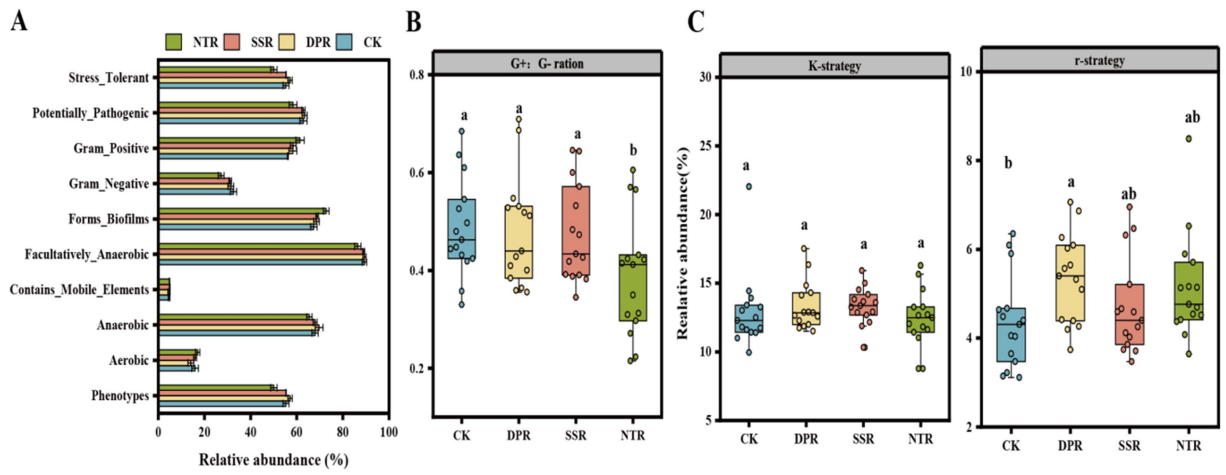


FIGURE 2
Soil bacterial phenotypes and life history characteristics. **(A)** Bacterial community prediction phenotypes obtained with Bugbase in CK, DPR, SSR, and NTR treatments. **(B)** G+:G− ratios in CK, DPR, SSR, and NTR soils. **(C)** Relative abundance of K-strategy and r-strategy bacteria in CK, DPR, SSR, and NTR soils. The error line is the standard deviation (SD) of the mean. Different lowercase letters indicate significant differences ($p < 0.05$) among the three treatments. G+:G− ratio: phenotypic ratio of Gram-positive to Gram-negative bacteria, K-strategy: relative abundance of representative K-strategy clades (Actinobacteriota, Chloroflexi, and Acidobacteriota), r-strategy: relative abundance of representative r-strategy clades (Proteobacteria, Firmicutes, and Gemmatimonadota) relative abundance.

10.3389/fmicb.2025.1590686

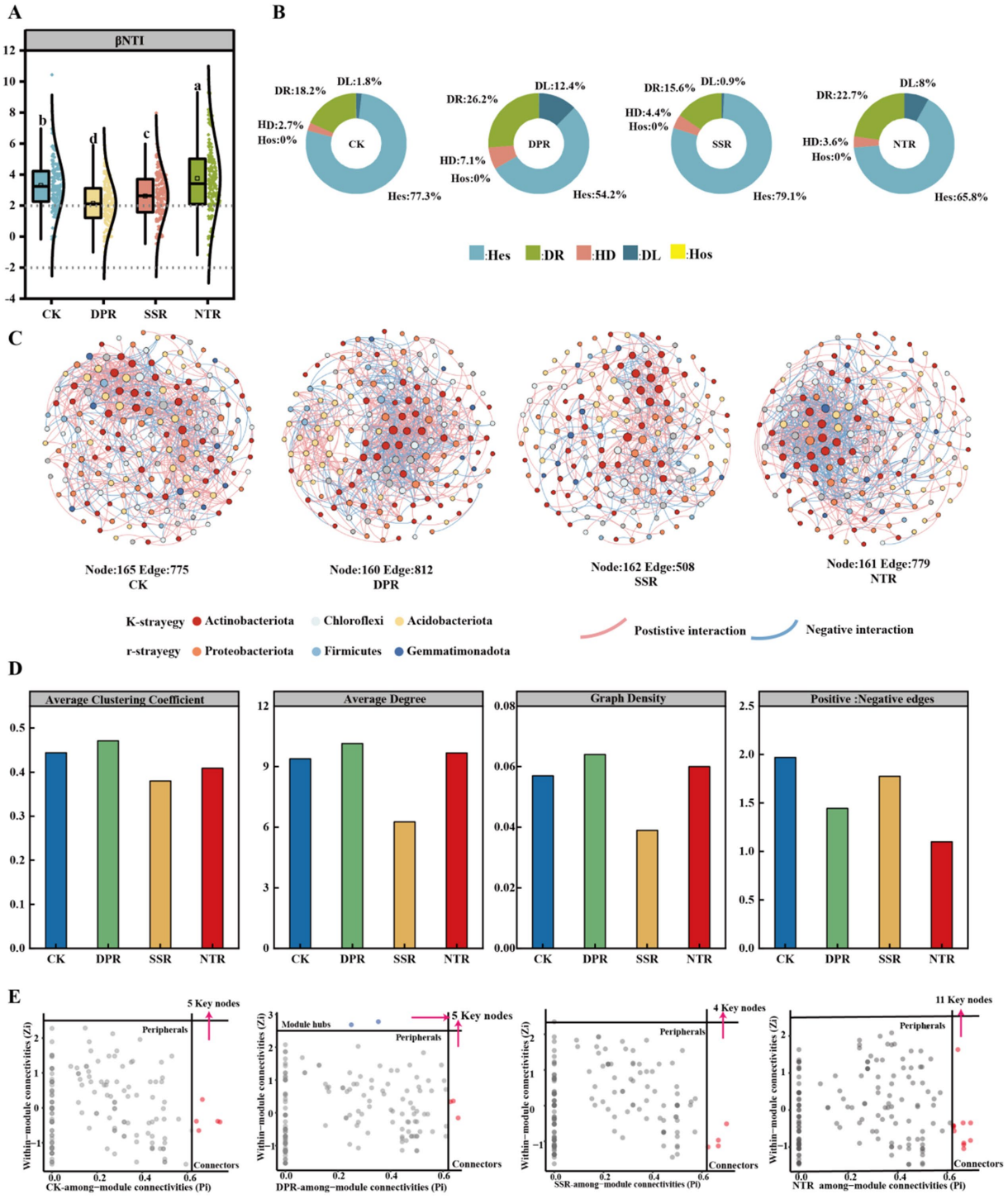


FIGURE 3
Assembly processes and symbiotic networks of soil bacterial communities. **(A)** β-Nearest taxonomy index (βNTI) of CK, DPR, SSR, and NTR soil bacteria with different lower-case letters indicate significant differences among the three treatments ($p < 0.05$). **(B)** Relative contribution of deterministic and stochastic assembly processes in MM, MP, and MS soils. **(C)** Symbiotic network nodes of bacterial communities in MM, MP, and MS soils indicate individual operational taxonomic units (OTUs), while edges indicate significant correlations between OTUs. The colors of the nodes indicate the main gates of K-strategy and r-strategy, and gray nodes indicate other gates. The size of the nodes is proportional to the number of connections. Only nodes that are significantly ($p < 0.05$) and strongly correlated (Spearman correlation coefficient >0.5 or <−0.5) are connected (edges). The thickness of the edge between two nodes is proportional to the value of the Spearman correlation coefficient. Pink and blue edges indicate positive and negative interactions between two individual nodes, respectively. **(D)** Network statistics including average clustering coefficient, average degree, graph density and ratio of positive and negative edges. **(E)** ZiPi analysis to filter out key nodes. Hes, heterogeneous selection; HoS, homogeneous selection; DL, diffusion limit; HD, homogeneous dispersal; DR, drift.

(Figures 3C,D). The K-strategy bacteria (e.g., Actinobacteriota, Chloroflexi) had a relative abundance of 60.62%, while r-strategy bacteria (e.g., Proteobacteria, Firmicutes) had a relative abundance of 29.99%. The NTR treatment had 161 nodes, 779 edges, 52.37% positive interactions, and a mean degree of 9.677. The relative abundance of K-strategy bacteria was 58.79%, and r-strategy bacteria had a relative abundance of 28.58%. The CK treatment had 165 nodes, 775 edges, 66.32% positive interactions, and a mean degree of 9.394. The relative abundance of K-strategy bacteria was 62.61%, and r-strategy bacteria had a relative abundance of 29.7%. The SSR treatment had 162 nodes, 508 edges, 63.98% positive interactions, a mean degree of 6.272, and the lowest relative abundance of K-strategy bacteria at 58.64%, while the relative abundance of r-strategy bacteria was the highest at 30.87%.

ZiPi analysis showed that the DPR treatment exhibited the highest degree of modularity and network complexity (two modular hubs, three connectors), was dominated by K-strategy bacteria, and had the best ecological function and stability. The NTR treatment had the highest number of key nodes (11 connectors), with high colony diversity and network collaboration, and balanced functionality, and the CK had a key node number of five connectors, a dominated by K-strategy bacteria, with moderate stability but low complexity. The SSR treatment, with a minimum of four connectors of key nodes, was dominated by r-strategy bacteria, with the lowest degree of modularity, and the worst collaboration and network stability (Figure 3E).

3.4 Factors influencing soil bacterial community in different straw return methods

Mantel analysis (Figure 4A) showed that soil physicochemical and microbial characteristics significantly influenced soil bacterial community composition and life history strategies in CK, DPR, SSR, and NTR treatments. Soil bacterial community composition was significantly positively correlated with ALP and significantly negatively correlated with BD ($p < 0.05$). Partial least squares (PLS) analysis showed that bacterial assembly processes in the CK, DPR, SSR, and NTR treatments were significantly controlled by AP, SM, ALP, H_2O_2, SOM, and bacterial community composition ($p < 0.05$, VIP >1; Figure 4B).

4 Discussion

4.1 Effects of different straw return methods on the composition, diversity and structure of soil bacterial communities over the years

Soil bacteria are indispensable in regulating ecological processes and functions. Annual straw fertilization can alleviate the pressure on the soil environment and promote the development of the microbiota (Chu et al., 2024). In this study, the relative abundance of major phyla

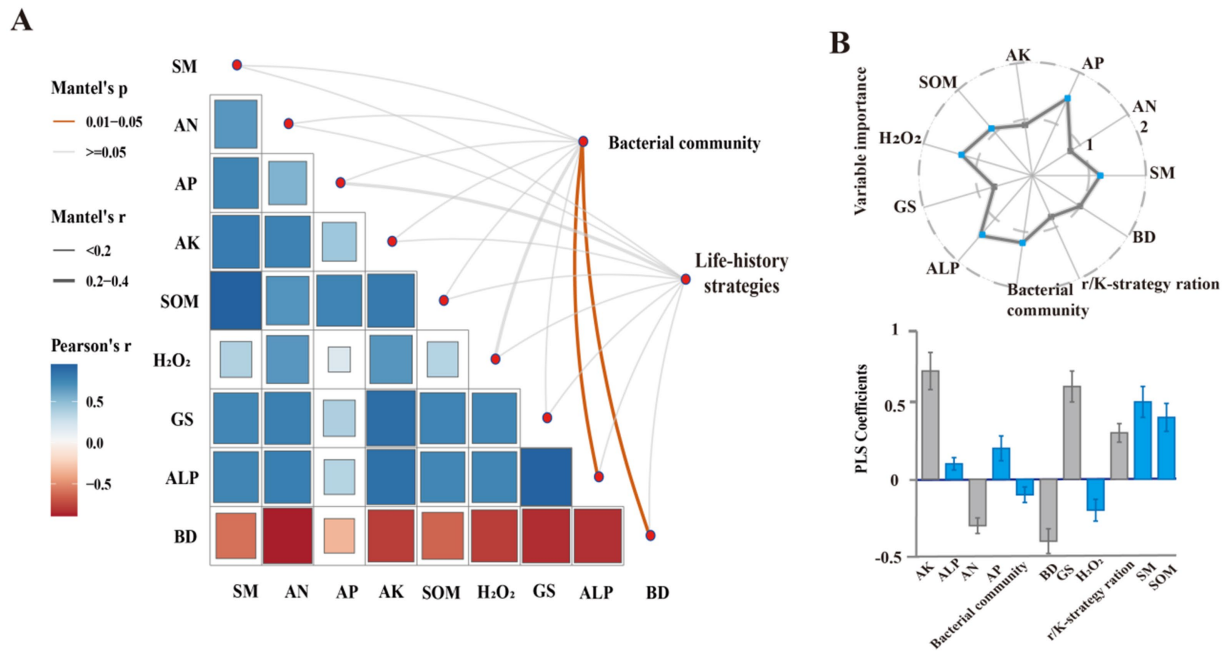


FIGURE 4
Drivers of bacterial community composition, life history and assembly processes. **(A)** Relationships between bacterial communities, life history strategies and soil properties based on Pearson's correlation and Mantel test. **(B)** Relative importance of soil physicochemical and microbiological properties on bacterial assembly processes in CK, DPR, SSR, and NTR treatments. The upper panel shows the variable predicted importance (VIP) values and the lower panel shows the partial least squares (PLS) standardized coefficients (±SEM). The error line is the standard deviation (SD) of the mean. Higher VIP values indicate greater importance in determining the assembly process. Blue dots indicate VIP values greater than 1. PLS standardized coefficients show the direction and magnitude of each variable's impact on the assembly process. Variables with blue bars are significant ($p < 0.05$) where the VIP value is greater than 1. System status: BD, soil bulk density; SM, soil moisture content; AN, soil dissolved alkaline nitrogen; SOM, soil organic matter; AP, soil quick phosphorus; ALP, alkaline phosphatase; Glu, glutamine synthetase; H_2O_2, catalase.

and genera differed between straw-returning conditions in successive years, as did the major bacteria employing r- and K-strategies (Figures 1A, 2C; Supplementary Figures S2, S3, $p < 0.05$). Years can influence soil bacterial community composition in semi-arid cropping systems (Ouverson et al., 2021). Compared to CK, DPR treatment, r-strategy bacteria such as Firmicutes and Proteobacteria and related genera such as *Bacillus* and *Nitrospira* showed stronger adaptation and the relative abundance of *Bacillus* increased by 92.17%. However, K-strategy bacteria such as Actinobacteriota and Chloroflexi and their related genera (e.g., *Arthrobacter* and *Blastococcus*) were significantly reduced, with the abundance of *Blastococcus* decreasing by as much as 79.93%. This suggests that DPR treatment promoted the rapid multiplication and adaptive capacity of r-strategy bacteria (e.g., *Bacillus*) and inhibited the growth of K-strategy bacteria (e.g., *Blastococcus*) by changing the physicochemical properties of the soil (e.g., soil bulkiness, moisture, and nutrient content) due to the fact that the r-strategy bacteria have a greater environmental adaptability and rapid response ability to unstable environment (Yang et al., 2020). It indicated the selective effects of different straw treatments on the life history strategies and functional potential of soil bacterial communities. In addition, successive years of DPR treatments improved nutrient uptake and microbial diversity in corn. Simpson's index showed that soil bacterial community homogeneity was significantly higher in the CK treatment than in the other treatments, suggesting that the community was more homogeneous under the CK treatment ($p < 0.05$). In contrast, the community homogeneity of DPR, SSR and NTR treatments was lower and the difference was not significant. This result supports the theory of Li H.-Z. et al. (2022) that soil management practices may exert selective pressure on bacterial communities, especially under conditions of nutrient excess or environmental instability, where certain bacterial taxa may be dominant, leading to a decrease in community homogeneity. This finding is consistent with Schimel and Schaeffer (2012) who noted that proper nutrient management can support diverse microbial communities and enhance soil ecosystem stability. The increased diversity of the NTR treatment may be due to specific nutrient conditions that promote the survival of more bacterial taxa or reduce environmental competitive pressures, thus providing space for more species to survive. Changes in microbial diversity may depend on soil management strategies, especially nutrient management, under different straw-returning practices, which can lead to healthier and more efficient soil microbial communities, thereby improving soil quality and crop growth (Chen et al., 2021). For example, the core OTUs shared among CK, DPR, SSR and NTR treatments were 6,723, which accounted for 12.54% of the total number of OTUs, suggesting that these core colonies have strong environmental adaptability. In contrast, the number of unique OTUs in the CK treatment was 2,848 (11.71%), which was slightly lower than the other treatments (Figure 1B). These results further demonstrated the different roles of different straw return treatments in microbial community reorganization and selectivity (Song et al., 2020). This study reveals the different responses of soil bacteria to different straw-returning methods in successive years.

In the β-diversity analysis, the NMDS ordination showed that the soil bacterial community structures of different treatments were significantly separated, with the NTR treatment having the most distinctive community structure and being significantly separated from the other treatments (Figure 1D, $p < 0.05$). The significance of this difference was also verified by the results of Adonis and Anosim tests. Overall, the CK treatment maintained high community evenness, the NTR treatment significantly increased community diversity and significantly altered community structure, while the SSR and DPR treatments had relatively little effect. It showed that different straw return methods in successive years led to significant differences in soil bacterial community structure (Li Y. et al., 2022). Soil extracellular enzyme activities were also affected (Yang et al., 2022), especially GS and ALP in DPR soils and H_2O_2 in NTR soils (Supplementary Table S3). In addition, DPR and NTR treatments (with higher average clustering coefficients and graph densities) had higher network complexity (Figure 3D), which is supported by the fact that successive years of DPR and NTR have enhanced microbial interactions between microorganisms (Xu et al., 2023). Moreover, in semi-arid cropping systems, different tillage practices combined with straw return stimulate soil microbial biomass and provide more opportunities for bacterial interactions (Bu et al., 2020), given that bacterial network complexity can also be driven by bacterial r-/K-strategy ratios (Wang C. et al., 2024), soil bacterial network complexity in successive DPR and NTR treatments increased with the r-strategy bacterial ratio increased (Figure 3C and Supplementary Table S4). In addition, the higher the ratio of negative correlation, the smaller the perturbation, which promotes the stability of bacterial network (Shi et al., 2021). The network of bacteria in the DPR treatment was more stable, with a higher mean degree (10.15) and positive connectivity percentage (59.11%). While CK treatment showed opposite trend in terms of network stability, Yang et al. (2016) indicated that under drought conditions, straw return produced less stable bacterial network and more stable fungal network. Therefore, DPR treatment can regulate the sustainability of agriculture under drought conditions through soil microbial response.

4.2 Effects of different straw-returning methods on soil bacterial community structure and function in successive years

In this study, compared with non-returned (CK), straw return significantly enhanced the dominant role of homogenous selection and drift (Figure 3B), especially in the treatments with more organic matter return (e.g., the group of complete straw return). This phenomenon is closely related to resource availability, especially changes in organic matter and nutrient content (e.g., nitrogen and phosphorus content) in the soil that may have facilitated selective microbial acclimation and remodeling of community structure (Liu L. et al., 2024). Differences in acclimatization led to ecological niche partitioning under environmental heterogeneity (Lin et al., 2021), whereas the effects of different straw-returning practices over successive years could shape bacterial symbiosis and community assembly depending on the βNTI values (Figure 3A). Compared with NTR, the CK treatment had a greater deterministic process with significantly lower βNTI values, which is a common phenomenon under relatively low resource conditions (Hao et al., 2023). For example, the bacterial community under low-resource conditions showed stronger deterministic processes in soils with successive years of straw return, which may be related to the gradual accumulation of soil organic matter (Yang et al., 2021). To some extent this bacterial assembly process was related to the higher nutrient content in the

DPR treatment (Supplementary Table S1). Differences in bacterial communities in CK, DPR, SSR, and NTR soils may be attributed to the assembly process, particularly as a result of diffusion limitation at intermediate or short geographic distance differences (Liu, 2023). Thus, DPR and NTR treatments increased the contribution of diffusion limitation to stochastic processes and played a key role in the assembly of soil bacterial communities.

Bacterial phenotypes and related functions of soil were altered to different degrees by different straw-returning practices over the years. The diversity and functional stability of microbial metabolism can be enhanced by stimulating the interactions of bacterial communities under different straw-return practices (Liu X. et al., 2023). Straw return not only affected the composition of the bacterial community, but also significantly altered the bacterial phenotype and tolerance (Wang X. et al., 2022). DPR treatment increased the relative abundance of anaerobic bacteria higher, while SSR treatment significantly increased the abundance of aerobic bacteria. This change may be related to the changes in oxygen supply in the soil after straw return. Siedt et al. (2021) showed that straw return improves soil aeration, which affects microbial life history strategies. In addition, by modulating microbial life-history strategies, straw return increased tolerance to environmental stresses (e.g., hypoxia, changes in pH), which further contributed to the growth of beneficial microorganisms in the soil (Chen et al., 2024).

PICRUSt 2 software was used to analyze the effects of different straw-returning methods on the functional profiles of soil bacterial communities in successive years. Metabolic pathways at the first and second levels showed similarity among different straw return treatments (Supplementary Figure S2). In general, taxonomic diversity and metabolic complexity of microbial communities are related to life history strategies and dependent on resource availability (Lauber et al., 2008). In this study, the relative abundance of genes associated with Meta function was the greatest, especially in the global and overview maps. Moreover, key metabolic pathways such as amino acid metabolism and carbohydrate metabolism were enhanced under DPR and SSR treatments, suggesting that straw return may have promoted the metabolic activity of microorganisms in the soil by providing more organic carbon sources (Shah et al., 2024). Although there were differences in the specific effects of different straw-return treatments on metabolic pathways, it was shown that straw-return promoted the adaptability and tolerance of soil bacterial communities in most cases by enhancing the functional stability of soil microorganisms (Zhang Y. et al., 2024), further supporting the sustainability of soil ecosystems.

ZiPi analysis showed significant differences in the degree of network modularity, complexity, and collaboration among the different treatments (Figure 3E, $p < 0.05$). DPR exhibited the highest degree of modularity and network complexity (two modular hubs, three connectors) and was dominated by K-strategy bacteria, which significantly optimized mycorrhizal collaborative and ecological stability, and is an ideal management practice to enhance soil health and ecological function (Wang et al., 2023). NTR had the highest number of key nodes (11 connectors), which significantly enhanced mycorrhizal diversity and network collaboration, and exhibited good ecological balance and functional stability (Xu et al., 2023). In contrast, the CK treatment had limited network complexity and functional optimization, and weak collaboration despite maintaining the basic functions of the flora, the deep straw return (SSR) treatment had the lowest degree of modularity and complexity, was dominated by r-strategic bacteria, and had enhanced flora competitiveness but poorer collaboration, and limited ecological functions (Khan et al., 2023). Therefore, DPR and NTR have significant advantages in optimizing soil microbial network structure and enhancing soil health, while CK and SSR need to be further optimized in combination with other measures.

4.3 Study on the driving factors of soil bacterial community in different straw return methods in successive years

Changes in biotic and abiotic factors induced by different straw-returning practices control the soil microbial community's response to bacteria, and the soil microbial community is affected by multiple and complex factors that modify the soil habitat (Liu Q. et al., 2024). Similar environmental conditions greatly increase the similarity of soil bacterial communities (Belykh et al., 2024). The composition of soil bacterial communities was significantly positively correlated with ALP and significantly negatively correlated with BD ($p < 0.05$). Elevated ALP was closely associated with enhanced metabolic functions of bacterial communities, which may be attributed to the fact that alkaline phosphatase supports microbial growth and ecological functions by facilitating the release of soil phosphorus, which provides the bacterial community with an abundant source of usable phosphorus (RAES) (Raiesi and Salek-Gilani, 2018). In contrast, higher soil bulk density (BD) suppressed bacterial community diversity and functional activity by limiting soil porosity and water retention capacity (Fang et al., 2024). PLS analysis further revealed that AP, SM, ALP, H_2O_2, and SOC were identified as key driving variables. These factors directly regulate the diversity and life history strategies of bacterial communities by providing sources of organic matter and nutrients (Wang Q. et al., 2024). SOC is a major carbon source for microorganisms, and was significantly elevated in DPR, providing an energy base for r-strategy bacteria (e.g., Proteobacteria and Firmicutes) to rapidly colonize (Zhan et al., 2024). Furthermore, Ma et al. (2022) revealed that biological interactions predicted bacterial communities better than environmental factors, thus driving the assembly of soil bacterial communities in arid ecosystems. Keystone taxa and interactions between bacteria and fungi were significantly associated with community assembly (Shi et al., 2023). An addition, enzymes (ALP and H_2O_2), as biotic factors, influenced the life history strategies of bacteria in CK, DPR, SSR, and NTR soils. There were subtle differences in the composition, diversity and other characteristics of soil bacterial communities in different straw return treatments. In addition, the elevated AP created a more favorable environment for phosphorus metabolism-associated bacteria [e.g., phosphorus solubilizing bacteria (PSB)] to survive, which promoted the ecological functions of K-strategy bacteria (e.g., Actinobacteria and Chloroflexi) (Liu L. et al., 2023). Therefore, this study focused on the factors affecting the common corn field by different straw return methods in successive years. In order to deeply understand the feedback relationship between different straw return methods and soil microbial communities in successive years, future studies should further combine diversified ecological analysis tools to explore the synergistic effects between straw return and other agricultural measures (e.g., fertilizer application, crop rotation, no-tillage), and deeply analyze the mechanism of long-term straw return on the dynamics of soil microbial communities, so as to provide theoretical support for the sustainable development of

agro-ecosystems. Theoretical support for sustainable development of agro-ecosystems.

5 Conclusion

Different straw-returning methods in successive years significantly affected the composition, function, assembly mechanism and network properties of soil bacterial communities by modulating soil physicochemical properties (e.g., ALP, BD, SOC) and enzyme activities ($p < 0.05$). Among them, DPR significantly promoted the synergistic development of K-strategy bacteria and r-strategy bacteria to optimize metabolic functions and network stability, while the opposite was true for CK treatment, no-tillage mulching (NTR) increased community diversity, enhanced environmental adaptation (G+/G− ratio of 0.388), and promoted bacterial collaboration, which was suitable for low-disturbance management, although deep straw removal (SSR) had a significant effect on community reorganization, network DPR and NTR treatments were outstanding in function optimization and low-disturbance management, respectively, while SSR treatment promoted community reorganization effectively but did not enhance long-term ecosystem stability. In the future, it is necessary to comprehensively evaluate the comprehensive effects of straw return methods on sustainable agriculture by combining multi-dimensional indicators such as crop yield, soil quality and resistance, and explore the synergistic effects with other management measures in order to promote the efficient and sustainable development of agroecosystems.

Data availability statement

The original contributions presented in the study are publicly available. All raw sequencing data were deposited in the National Center for Biotechnology Information (NCBI) BioProject database, under accession number PRJNA1222571.

Author contributions

R-ZL: Writing – original draft. X-YZ: Writing – original draft, Data curation, Methodology. BF: Writing – original draft. W-SZ: Data curation, Writing – original draft. M-YL: Writing – original draft. X-FY: Funding acquisition, Project administration, Writing – review & editing. S-PH: Writing – review & editing. R-PL: Writing – review & editing. J-LG: Funding acquisition, Project administration, Writing – review & editing. QB: Funding acquisition, Methodology, Project administration, Writing – review & editing.

Funding

The author(s) declare that financial support was received for the research and/or publication of this article. Inner Mongolia Natural Science Foundation (2024MS03052); National Natural Science Foundation of China (32260532); Basic Research Business Expenses Project for Directly Affiliated Colleges and Universities of Inner Mongolia Autonomous Region (BR22-11-07, BR22-12-02,BR25-10-06); Special Project for Carbon Peak and Carbon Neutrality Research in Colleges and Universities of Inner Mongolia Autonomous Region (STZX202304); Science and Technology Plan Project of Inner Mongolia Autonomous Region (2023KYPT0023); National Maize Industry Technology System (CARS-02-74).

Conflict of interest

The authors declare that the research was conducted in the absence of any commercial or financial relationships that could be construed as a potential conflict of interest.

Generative AI statement

The authors declare that no Gen AI was used in the creation of this manuscript.

Publisher's note

All claims expressed in this article are solely those of the authors and do not necessarily represent those of their affiliated organizations, or those of the publisher, the editors and the reviewers. Any product that may be evaluated in this article, or claim that may be made by its manufacturer, is not guaranteed or endorsed by the publisher.

Supplementary material

The Supplementary material for this article can be found online at: https://www.frontiersin.org/articles/10.3389/fmicb.2025.1590686/full#supplementary-material

At the beginning of the experiment, the basic soil fertility in 2020, the significant analysis of the difference in soil physical and chemical properties enzyme activity from 2020 to 2024, the main bacteria, meteorological factors, relative abundance of phyla and genus levels of K-strategies and r-strategies, and the functional properties of soil bacterial communities are displayed in Supplementary material.

References

Allen, S. E., and Grimshaw, H. M. (1986). Methods of soil analysis, part 2: chemical and microbiological properties. Madison, WI: American Society of Agronomy.

Belykh, E., Maystrenko, T., Velegzhaninov, I., Tavleeva, M., Rasova, E., and Rybak, A. (2024). Taxonomic diversity and functional traits of soil bacterial communities under radioactive contamination: a review. *Microorganisms* 12:733. doi: 10.3390/microorganisms12040733

Bernardino, P. N., de Keersmaecker, W., Horion, S., Oehmcke, S., Gieseke, F., Fensholt, R., et al. (2025). Predictability of abrupt shifts in dryland ecosystem functioning. *Nat. Clim. Change* 15, 86–91. doi: 10.1038/s41558-024-02201-0

Borràs-Brull, M., Blondeau, P., and Riu, J. (2021). The use of conducting polymers for enhanced electrochemical determination of hydrogen peroxide. *Crit. Rev. Anal. Chem.* 51, 204–217. doi: 10.1080/10408347.2020.1718482

Bremner, J. M. (1960). Determination of nitrogen in soil by the kjeldahl method. *Journal of Agricultural Science*. 55, 11–33. doi: 10.1017/S0021859600021572

Bu, R., Ren, T., Lei, M., Liu, B., Li, X., Cong, R., et al. (2020). Tillage and straw-returning practices effect on soil dissolved organic matter, aggregate fraction and bacteria community under rice-rice-rapeseed rotation system. *Agric. Ecosyst. Environ.* 287:106681. doi: 10.1016/j.agee.2019.106681

Chen, H., Chen, Y., Du, B., Wang, Z., Pan, S., Zhang, M., et al. (2025). Mechanism harvesting of main crops straw returning effects on ratooning fragrant rice yield and 2-acetyl-1-pyrroline and their drivers to soil microbial communities. *Plant Physiol. Biochem.* 219:109364. doi: 10.1016/j.plaphy.2024.109364

Chen, Q., Liu, Z., Zhou, J., Xu, X., and Zhu, Y. (2021). Long-term straw mulching with nitrogen fertilization increases nutrient and microbial determinants of soil quality in a maize-wheat rotation on China's loess plateau. *Sci. Total Environ.* 775:145930. doi: 10.1016/j.scitotenv.2021.145930

Chen, Y., Tao, S., Ma, J., Qu, Y., Sun, Y., Wang, M., et al. (2024). New insights into assembly processes and driving factors of urban soil microbial community under environmental stress in Beijing. *Sci. Total Environ.* 947:174551. doi: 10.1016/j.scitotenv.2024.174551

Chen, S., Zhou, Y., Chen, Y., and Gu, J. (2018). fastp: An ultra-fast all-in-one FASTQ preprocessor. *Bioinformatics* 34, i884–i890. doi: 10.1093/bioinformatics/bty560

Chu, J., Wang, L., Jia, R., Zhou, J., Zang, H., Wang, J., et al. (2024). Straw returning with no-tillage alleviates microbial metabolic carbon limitation and improves soil multifunctionality in the northeast plain. *Land Degrad. Dev.* 35, 5149–5161. doi: 10.1002/ldr.5286

Douglas, G. M., Maffei, V. J., Zaneveld, J. R., Yurgel, S. N., Brown, J. R., Taylor, C. M., et al. (2020). PICRUSt2 for prediction of metagenome functions. *Nat. Biotechnol.* 38, 685–688. doi: 10.1038/s41587-020-0548-6

Edgar, R. C. (2013). UPARSE: highly accurate OTU sequences from microbial amplicon reads. *Nat. Methods* 10, 996–998. doi: 10.1038/nmeth.2604

Fang, J., Xu, Z. F., Zhang, T., Chen, C. B., Liu, C. S., Liu, R., et al. (2024). Effects of soil microbial ecology on ginsenoside accumulation in *Panax ginseng* across different cultivation years. *Ind. Crop. Prod.* 215:118637. doi: 10.1016/j.indcrop.2024.118637

Guimerà, R., and Nunes Amaral, L. A. (2005). Functional cartography of complex metabolic networks. *Nature* 433, 895–900. doi: 10.1038/nature03288

Haghighat, N. (2005). Estrogen (17β-estradiol) enhances glutamine synthetase activity in C6-glioma cells. *Neurochem. Res.* 30, 661–667. doi: 10.1007/s11064-005-2754-5

Hao, M., Hu, H., Liu, Z., Dong, Q., Sun, K., Feng, Y., et al. (2019). Shifts in microbial community and carbon sequestration in farmland soil under long-term conservation tillage and straw returning. *Appl. Soil Ecol.* 136, 43–54. doi: 10.1016/j.apsoil.2018.12.016

Hao, J., Xu, W., Song, J., Gao, G., Bai, J., Yu, Q., et al. (2023). Adaptability of agricultural soil microbial nutrient utilization regulates community assembly under mulching measures on the loess plateau. *Agric. Ecosyst. Environ.* 357:108702. doi: 10.1016/j.agee.2023.108702

Jiao, S., Chu, H., Zhang, B., Wei, X., Chen, W., and Wei, G. (2022). Linking soil fungi to bacterial community assembly in arid ecosystems. *iMeta* 1:e2. doi: 10.1002/imt2.2

Johnson, J. L., and Temple, K. L. (1964). Some variables affecting the measurement of "catalase activity" in soil. *Soil Sci. Soc. Am. J.* 28, 207–209. doi: 10.2136/sssaj1964.03615995002800020024x

Kang, P., Pan, Y., Hu, J., Qu, X., Ji, Q., Zhuang, C., et al. (2025). Straw mulch and orchard grass mediate soil microbial nutrient acquisition and microbial community composition in *Ziziphus jujuba* orchard. *Plant Soil*. doi: 10.1007/s11104-024-07144-1

Khan, M. H., Liu, H., Zhu, A., Khan, M. H., Hussain, S., and Cao, H. (2023). Conservation tillage practices affect soil microbial diversity and composition in experimental fields. *Front. Microbiol.* 14:1227297. doi: 10.3389/fmicb.2023.1227297

Kinnunen, P., Guillaume, J. H. A., Taka, M., D'Odorico, P., Siebert, S., Puma, M. J., et al. (2020). Local food crop production can fulfil demand for less than one-third of the population. *Nat. Food* 1, 229–237. doi: 10.1038/s43016-020-0060-7

Lauber, C. L., Strickland, M. S., Bradford, M. A., and Fierer, N. (2008). The influence of soil properties on the structure of bacterial and fungal communities across land-use types. *Soil Biol. Biochem.* 40, 2407–2415. doi: 10.1016/j.soilbio.2008.05.021

Li, Y., Wang, J., Wen, S., and Shao, M. (2022). Effects of different earthworm ecotypes on soil nutrients distribution under straw return management in a maize agroecosystem. *Land Degrad. Dev.* 33, 2327–2339. doi: 10.1002/ldr.4301

Li, H.-Z., Zhu, D., Sun, A. Q., Qin, Y. F., Lindhardt, J. H., and Cui, L. (2022). Effects of soil protists on the antibiotic resistome under long term fertilization. *Environ. Pollut.* 307:119516. doi: 10.1016/j.envpol.2022.119516

Lin, Q., Li, L., Adams, J. M., Heděnec, P., Tu, B., Li, C., et al. (2021). Nutrient resource availability mediates niche differentiation and temporal co-occurrence of soil bacterial communities. *Appl. Soil Ecol.* 163:103965. doi: 10.1016/j.apsoil.2021.103965

Liu, X. (2023). Sustainable intensification: a historical perspective on China's farming system. *Farm. Syst.* 1:100001. doi: 10.1016/j.farsys.2023.100001

Liu, R.-Z., Borjigin, Q., Gao, J.-L., Yu, X.-F., Hu, S.-P., and Li, R. P. (2024). Effects of different straw return methods on soil properties and yield potential of maize. *Sci. Rep.* 14:28682. doi: 10.1038/s41598-024-70404-8

Liu, Q., Dai, H., Wang, L., Qian, X., Gao, Y., Zhang, H., et al. (2024). Microbial community and functions depending on tillage and straw returning management: consequences for soil health and ecosystem services. *Land Degrad. Dev.* 35, 5357–5366. doi: 10.1002/ldr.5301

Liu, L., Liu, D., Ding, X., Chen, M., and Zhang, S. (2024). Straw incorporation and nitrogen fertilization enhance soil carbon sequestration by altering soil aggregate and microbial community composition in saline-alkali soil. *Plant Soil* 498, 341–356. doi: 10.1007/s11104-023-06439-z

Liu, X., Liu, H., Zhang, Y., Chen, G., Li, Z., and Zhang, M. (2023). Straw return drives soil microbial community assemblage to change metabolic processes for soil quality amendment in a rice-wheat rotation system. *Soil Biol. Biochem.* 185:109131. doi: 10.1016/j.soilbio.2023.109131

Liu, B., Wang, S., Wang, J., Zhang, X., Shen, Z., Shi, L., et al. (2020). The great potential for phytoremediation of abandoned tailings pond using ectomycorrhizal *Pinus sylvestris*. *Sci. Total Environ.* 719:137475. doi: 10.1016/j.scitotenv.2020.137475

Liu, L., Yan, R., Zhu, L., Yang, Y., Gao, Z., Yang, W., et al. (2023). Balanced phosphorus fertilization enhances soil bacterial network complexity to maintain multifunctionality and plant production in dryland agricultural systems. *Agric. Ecosyst. Environ.* 356:108647. doi: 10.1016/j.agee.2023.108647

Liu, M., Zhang, Z., He, P., Zhang, Y., and Li, L. J. (2025). Changes in soil microbial community and carbon use efficiency in freeze-thaw period restored after growth season under warming and straw return. *Appl. Soil Ecol.* 205:105779. doi: 10.1016/j.apsoil.2024.105779

Liu, C., Zhao, D., Ma, W., Guo, Y., Wang, A., Wang, Q., et al. (2016). Denitrifying sulfide removal process on high-salinity wastewaters in the presence of Halomonas sp. *Appl. Microbiol. Biotechnol.* 100, 1421–1426. doi: 10.1007/s00253-015-7039-6

Ma, J., Ma, K., Liu, J., and Chen, N. (2022). Rhizosphere soil microbial community under ice in a high-latitude wetland: different community assembly processes shape patterns of rare and abundant microbes. *Front. Microbiol.* 13:783371. doi: 10.3389/fmicb.2022.783371

Magoč, T., and Salzberg, S. L. (2011). FLASH: fast length adjustment of short reads to improve genome assemblies. *Bioinformatics* 27, 2957–2963. doi: 10.1093/bioinformatics/btr507

Ning, D., Yuan, M., Wu, L., Zhang, Y., Guo, X., Zhou, X., et al. (2020). A quantitative framework reveals ecological drivers of grassland microbial community assembly in response to warming. *Nat. Commun.* 11:4717. doi: 10.1038/s41467-020-18560-z

Olesen, J. M., Bascompte, J., Dupont, Y. L., and Jordano, P. (2007). The modularity of pollination networks. *P. Natl. Acad. Sci.* USA. 104, 19891–19896.

Olsen, S. R., and Sommers, L. E. (1982). "Phosphorus" in Methods of soil analysis, part 2: chemical and microbial properties. ed. A. L. Page (Madison, WI: American Society of Agronomy), 401–430.

Ouverson, T., Eberly, J., Seipel, T., Menalled, F. D., and Ishaq, S. L. (2021). Temporal soil bacterial community responses to cropping systems and crop identity in dryland agroecosystems of the northern great plains. *Front. Sustain. Food Syst.* 5:624242. doi: 10.3389/fsufs.2021.624242

Raiesi, F., and Salek-Gilani, S. (2018). The potential activity of soil extracellular enzymes as an indicator for ecological restoration of rangeland soils after agricultural abandonment. *Appl. Soil Ecol.* 126, 140–147. doi: 10.1016/j.apsoil.2018.02.022

Schimel, J. P., and Schaeffer, S. M. (2012). Microbial control over carbon cycling in soil. *Front. Microbiol.* 3:348. doi: 10.3389/fmicb.2012.00348

Schloss, P. D., Westcott, S. L., Ryabin, T., Hall, J. R., Hartmann, M., Hollister, E. B., et al. (2009). Introducing mothur: open-source, platform-independent, community-supported software for describing and comparing microbial communities. *Appl. Environ. Microbiol.* 75, 7537–7541. doi: 10.1128/AEM.01541-09

Shah, T., Khan, Z., Asad, M., Imran, A., Khan Niazi, M. B., Dewil, R., et al. (2024). Straw incorporation into microplastic-contaminated soil can reduce greenhouse gas emissions by enhancing soil enzyme activities and microbial community structure. *J. Environ. Manag.* 351:119616. doi: 10.1016/j.jenvman.2023.119616

Shi, J., Yang, L., Liao, Y., Li, J., Jiao, S., Shangguan, Z., et al. (2023). Soil labile organic carbon fractions mediate microbial community assembly processes during long-term vegetation succession in a semiarid region. *iMeta* 2:e142. doi: 10.1002/imt2.142

Shi, X., Zhao, X., Ren, J., Dong, J., Zhang, H., Dong, Q., et al. (2021). Influence of peanut, sorghum, and soil salinity on microbial community composition in interspecific interaction zone. *Front. Microbiol.* 12:678250. doi: 10.3389/fmicb.2021.678250

Siedt, M., Schäffer, A., Smith, K. E. C., Nabel, M., Roß-Nickoll, M., and van Dongen, J. T. (2021). Comparing straw, compost, and biochar regarding their suitability as agricultural soil amendments to affect soil structure, nutrient leaching, microbial communities, and the fate of pesticides. *Sci. Total Environ.* 751:141607. doi: 10.1016/j.scitotenv.2020.141607

Song, F., Liu, M., Qi, Z., Zhang, Z., Wang, B., Yin, Z., et al. (2024). Straw returning and reducing nitrogen application rates maintain maize yields and reduce gaseous nitrogen emissions from black soil maize fields. *Appl. Soil Ecol.* 203:105637. doi: 10.1016/j.apsoil.2024.105637

Song, K., Sun, Y., Qin, Q., Sun, L., Zheng, X., Terzaghi, W., et al. (2020). The effects of earthworms on fungal diversity and community structure in farmland soil with returned straw. *Front. Microbiol.* 11:594265. doi: 10.3389/fmicb.2020.594265

Stackebrandt, E., and Goebel, B. M. (1994). Taxonomic note: a place for DNA-DNA reassociation and 16S rRNA sequence analysis in the present species definition in bacteriology. *Int. J. Syst. Evol. Microbiol.* 44, 846–849. doi: 10.1099/00207713-44-4-846

Tan, X., Liu, Y., Yan, K., Wang, Z., Lu, G., He, Y., et al. (2017). Differences in the response of soil dehydrogenase activity to cd contamination are determined by the different substrates used for its determination. *Chemosphere* 169, 324–332. doi: 10.1016/j.chemosphere.2016.11.076

Tian, S., Dong, Y., Pang, S., Yuan, G., Cai, S., Zhang, P., et al. (2024). The driving role of acid mine drainage on microbial community assembly and species coexistence in paddy soil profiles. *J. Environ. Sci.* 156, 771–783. doi: 10.1016/j.jes.2024.12.034

VanRemortel, R. D., and Shields, D. A. (1993). Comparison of clod and core methods for determination of soil bulk density. *Commun. Soil Sci. Plant Anal.* 24, 2517–2528. doi: 10.1080/00103629309368972

Walkley, A., and Black, I. A. (1934). An examination of the degtjareff method for determining soil organic matter, and a proposed modification of the chromic acid titration method. *Soil Sci.* 37, 29–38. doi: 10.1097/00010694-193401000-00003

Wang, X., Chi, Y., and Song, S. (2024). Important soil microbiota's effects on plants and soils: a comprehensive 30-year systematic literature review. *Front. Microbiol.* 15:1347745. doi: 10.3389/fmicb.2024.1347745

Wang, Q., Chu, C., Zhao, Z., Zhou, D., and Wu, S. (2024). A study of different agricultural practices over a dozen years: influence on soil CO_2 fixation rates and soil autotrophic microbial communities. *Soil Tillage Res.* 239:106067. doi: 10.1016/j.still.2024.106067

Wang, Q., Garrity, G. M., Tiedje, J. M., and Cole, J. R. (2007). Naïve bayesian classifier for rapid assignment of rRNA sequences into the new bacterial taxonomy. *Appl. Environ. Microbiol.* 73, 5261–5267. doi: 10.1128/AEM.00062-07

Wang, X., Li, Y., Ciampitti, I. A., He, P., Xu, X., Qiu, S., et al. (2022). Response of soil denitrification potential and community composition of denitrifying bacterial to different rates of straw return in north-central China. *Appl. Soil Ecol.* 170:104312. doi: 10.1016/j.apsoil.2021.104312

Wang, Z. Q., Li, Y. B., Tan, X. P., He, W. X., Xie, W., Megharaj, M., et al. (2017). Effect of arsenate contamination on free, immobilized and soil alkaline phosphatases: activity, kinetics and thermodynamics. *Eur. J. Soil Sci.* 68, 126–135. doi: 10.1111/ejss.12397

Wang, C., Shi, Z., Li, A., Geng, T., Liu, L., and Liu, W. (2024). Long-term nitrogen input reduces soil bacterial network complexity by shifts in life history strategy in temperate grassland. *iMeta* 3:e194. doi: 10.1002/imt2.194

Wang, L., Wang, E., Chen, G., Qian, X., Liu, Q., Gao, Y., et al. (2025). Optimizing straw return to enhance grain production and approach carbon neutrality in the intensive cropping systems. *Soil Tillage Res.* 248:106447. doi: 10.1016/j.still.2025.106447

Wang, S., Wang, Y., Liu, H., Li, X., Zhao, J., Dong, Z., et al. (2022). Using PICRUSt2 to explore the functional potential of bacterial community in alfalfa silage harvested at different growth stages. *Chem. Biol. Technol. Agric.* 9:98. doi: 10.1186/s40538-022-00372-6

Wang, X., Wang, Q., Zhang, Y., Zhang, J., Xia, S., Qin, H., et al. (2023). Influence of decomposition agent application and schedule in wheat straw return practice on soil quality and crop yield. *Chem. Biol. Technol. Agric.* 10:8. doi: 10.1186/s40538-022-00362-8

Xu, Z., Sun, R., He, T., Sun, Y., Wu, M., Xue, Y., et al. (2023). Disentangling the impact of straw incorporation on soil microbial communities: enhanced network complexity and ecological stochasticity. *Sci. Total Environ.* 863:160918. doi: 10.1016/j.scitotenv.2022.160918

Yang, Y., Dou, Y., Wang, B., Xue, Z., Wang, Y., An, S., et al. (2023). Deciphering factors driving soil microbial life-history strategies in restored grasslands. *iMeta* 2:e66. doi: 10.1002/imt2.66

Yang, H., Fang, C., Meng, Y., Dai, Y., and Liu, J. (2021). Long-term ditch-buried straw return increases functionality of soil microbial communities. *Catena* 202:105316. doi: 10.1016/j.catena.2021.105316

Yang, H., Feng, J., Zhai, S., Dai, Y., Xu, M., Wu, J., et al. (2016). Long-term ditch-buried straw return alters soil water potential, temperature, and microbial communities in a rice-wheat rotation system. *Soil Tillage Res.* 163, 21–31. doi: 10.1016/j.still.2016.05.003

Yang, Y., Lee, S. H., Jang, I., and Kang, H. (2020). Soil bacterial community structures across biomes in artificial ecosystems. *Ecol. Eng.* 158:106067. doi: 10.1016/j.ecoleng.2020.106067

Yang, L., Muhammad, I., Chi, Y. X., Wang, D., and Zhou, X. B. (2022). Straw return and nitrogen fertilization to maize regulate soil properties, microbial community, and enzyme activities under a dual cropping system. *Front. Microbiol.* 13:823963. doi: 10.3389/fmicb.2022.823963

Yu, K., Zhao, S., Sun, B., Jiang, H., Hu, L., Xu, C., et al. (2024). Enhancing food production through modern agricultural technology. *Plant Cell Environ.* doi: 10.1111/pce.15299

Zhan, Y., Zhou, Y., Wang, E., Miao, X., Zhou, T., Yan, N., et al. (2024). Effects of reductive soil disinfestation combined with different types of organic materials on the microbial community and functions. *Microbiol. Spectr.* 12:e00802. doi: 10.1128/spectrum.00802-23

Zhang, J., Liu, M., Landry, N. B. J., Duan, Y., Li, X., and Zhou, X. (2024). The impact of ricinus straw on tomato growth and soil microbial community. *Front. Microbiol.* 15:1499302. doi: 10.3389/fmicb.2024.1499302

Zhang, Y., Lu, M., Wang, Z., Zhang, K., Zhang, B., Naimaiti, R., et al. (2024). Nutrient supply enhances positive priming of soil organic C under straw amendment and accelerates the incorporation of straw-derived C into organic C pool in paddy soils. *Eur. J. Soil Biol.* 123:103695. doi: 10.1016/j.ejsobi.2024.103695

Zhu, J., Liu, S., Wang, H., Wang, D., Zhu, Y., Wang, J., et al. (2022). Microplastic particles alter wheat rhizosphere soil microbial community composition and function. *J. Hazard. Mater.* 436:129176. doi: 10.1016/j.jhazmat.2022.129176

Zong, M., Manevski, K., Liang, Z., Abalos, D., Jabloun, M., Lærke, P. E., et al. (2024). Diversifying maize rotation with other industrial crops improves biomass yield and nitrogen uptake while showing variable effects on nitrate leaching. *Agric. Ecosyst. Environ.* 371:109091. doi: 10.1016/j.agee.2024.109091

frontiers | Frontiers in Microbiology

TYPE Original Research
PUBLISHED 16 May 2025
DOI 10.3389/fmicb.2025.1586791

Check for updates

OPEN ACCESS

EDITED BY
Muhammad Zahid Mumtaz,
Gansu Agricultural University, China

REVIEWED BY
Shuaimin Chen,
Jilin Academy of Agricultural Sciences, China
Yi Wang,
Chinese Academy of Sciences (CAS), China

*CORRESPONDENCE
Lianzhu Du
✉ dulianzhu99@163.com

RECEIVED 06 March 2025
ACCEPTED 05 May 2025
PUBLISHED 16 May 2025

CITATION
Chang X, Pei Z, Wang X, Wang H, Mu J, Ma Y, Zhang M, Zhang K and Du L (2025) Divergent responses of plant lignin and microbial necromass to the contribution of soil organic carbon under organic and chemical fertilization.
Front. Microbiol. 16:1586791.
doi: 10.3389/fmicb.2025.1586791

COPYRIGHT
© 2025 Chang, Pei, Wang, Wang, Mu, Ma, Zhang, Zhang and Du. This is an open-access article distributed under the terms of the Creative Commons Attribution License (CC BY). The use, distribution or reproduction in other forums is permitted, provided the original author(s) and the copyright owner(s) are credited and that the original publication in this journal is cited, in accordance with accepted academic practice. No use, distribution or reproduction is permitted which does not comply with these terms.

Divergent responses of plant lignin and microbial necromass to the contribution of soil organic carbon under organic and chemical fertilization

Xingping Chang[1], Zhanjiang Pei[2], Xiaofei Wang[3], Hao Wang[1], Jie Mu[1], Yingjun Ma[1], Mingye Zhang[1], Keqiang Zhang[1,4] and Lianzhu Du[1]*

[1]Agro-Environmental Protection Institute, Ministry of Agriculture and Rural Affairs, Tianjin, China, [2]Heilongjiang Academy of Black Soil Conservation & Utilization, Heilongjiang Academy of Agricultural Sciences, Harbin, China, [3]Institute of Plant Nutrition, Agricultural Resources and Environmental Sciences, Henan Academy of Agricultural Sciences, Zhengzhou, China, [4]Key Laboratory of Low-carbon Green Agriculture in North China, Ministry of Agriculture and Rural Affairs, Beijing, China

Introduction: Long-term fertilization strongly influences the formation, turnover and stabilization of soil organic carbon (SOC) in croplands. The underlying mechanism by which chemical fertilizer (CF) and cattle slurry (CS) application influence the dynamics of plant- and microbial-derived carbon (C) remains elusive.

Methods: Lignin phenols and amino sugars as well as microbial carbohydrate-active enzymes (CAZymes) were analyzed in a 10-year field experiment.

Results: CF and CS increased the content of SOC by 26.9% and 88.0% compared with the SOC content of an abandoned land, respectively. CS application increased lignin phenols content by 4.28 times compared with CF application owing to slower oxidative degradation and higher plant inputs. Microbial necromass C (MNC) contents increased by 34.7% in line with an increase in biomass, but its proportion to SOC did not change. In terms of microbial community, the application of CF and CS altered the distribution and structure of microbial community. The dominant bacterial phyla shifted from oligotrophic Actinomycetota to eutrophic Pseudomonadota with change in the application from CF to CS. CS application increased CAZyme genes associated with plant- and bacterial-derived fractions decomposition, suggesting higher degradation potential of plant and bacterial biomass by microorganisms. Availability of substrates and microbial community are important factors affecting SOC accumulation in different fertilization treatments.

Discussion: CS application considerably promoted the accumulation of SOC, mainly via the promotion of plant-derived C. Alterations in microbial communities and CAZyme genes could affect microbial metabolism via "microbial carbon pump", thereby facilitating SOC formation and accumulation.

KEYWORDS

soil organic carbon, plant-derived carbon, microbial-derived carbon, microbial CAZyme families, cattle slurry

1 Introduction

Soil, as the largest terrestrial carbon (C) sink, contains 2–3 times more C than atmosphere and 3–4 times more than vegetation (Friedlingstein et al., 2020; Jackson et al., 2017). Consequently, a slight variation in soil organic carbon (SOC) sink may greatly affect global climate. The formation, turnover and stabilization of SOC are critical processes for C cycling in the terrestrial biosphere, and the accrual of SOC in croplands has a considerable impact on global C storage (Liu et al., 2022; Yang et al., 2023). In traditional perspective, plant residues were considered as the primary contributor to stable C sink, such as lignin, owing to their recalcitrant chemical structure (Liang et al., 2019). Growing studies agree with the view that microbial necromass is a vital source of the stable C sink, which can be transformed from plant residues, and can constitute more than half of SOC in agricultural ecosystems (Camenzind et al., 2023; Chen G. P. et al., 2020). The "microbial carbon pump" framework underlines that microbial metabolism plays a vital role in SOC formation and turnover (Liang et al., 2017; Zhu et al., 2020). Plant components can serve as energy resources for soil microorganisms growth and subsequently be converted to microbial fractions through microbial metabolic pathways: *ex vivo* modification and *in vivo* turnover (Liang et al., 2017; Sokol et al., 2019; Whalen et al., 2022). Microbial residues can bind to soil mineral particles and be physically protected by soil aggregates, which makes them more resistant to be broken down than plant residues (Chen G. P. et al., 2020). Plant-and microbial-derived C are normally quantified by biomarkers, including lignin phenols and amino sugars (Liang et al., 2019; Ma et al., 2018; Su et al., 2023). Therefore, elucidating plant-and microbial-derived C dynamics and their impacts on accumulation of SOC in agricultural ecosystem is essential.

Soil microorganisms participate in the breakdown of plant components and synthesis of microbial compounds, thus affecting terrestrial C cycling processes (Liang, 2020; López-Mondéjar et al., 2018). Recently, carbohydrate-active enzymes (CAZymes) are used to assess microbial metabolic pathways involved in a range of biomolecules (Ren C. J. et al., 2021; Zhang C. et al., 2021). Variations of CAZymes species and abundance can characterize the shift in the ability of soil microbial communities to degrade various organic compounds (Yan et al., 2022). Specific glycoside hydrolases (GHs) and auxiliary enzymes (AAs) have been proven to be responsible for plant necromass breakdown (Bomble et al., 2017; Llado et al., 2019). For example, the cellulolytic enzyme from GH6 is related to cellulose degradation, and peroxidase (POD) from several AAs is responsible for lignin breakdown (López-Mondéjar et al., 2020; Ren C. J. et al., 2021). Chitinases and lysozymes from some GHs are associated with fungal and bacterial residue decomposition (Zifcáková et al., 2017). Soil substrates and environmental variables strongly influence CAZyme activities owing to their effects on microbial communities (Ren C. J. et al., 2021). Cropland management practices, such as fertilization, cause large impacts on soil substrate and environmental factors, further altering microbial utilization of C sources and thus affecting CAZyme genes response for the breakdown of plant and microbial residues (Hu et al., 2020; Liu et al., 2019). Clarifying the shifts of CAZyme gene families and their relevance with organic components decomposition is vital to understand the microbial-mediated SOC dynamics in croplands.

Extensive researches have shown that fertilization is an effective management practice that facilitates the maintenance of soil fertility, improves crop yields, as well as promotes C accumulation in agricultural ecosystem (Ren F. L. et al., 2021; Xiong et al., 2023; Yan et al., 2007). Chemical fertilizer (CF) application can boost crop production, increasing plant inputs and root exudates into the soil and thus substantially influencing C dynamics (Kicklighter et al., 2019). Cattle slurry (CS) application is regarded to be profitable for soil fertility and crop growth due to its abundance of nutrient substrates and organic components (Chen et al., 2024; Lu et al., 2012). However, exogenous C sources imported by CS application and organic components produced by crop, along with C loss from degradation, make the SOC turnover in response to CS application unclear (Peltre et al., 2017; Yang et al., 2015). This study was based on the long-term fertilization experiments in Harbin City and aimed to (1) compare the impacts of CF and CS application on microbial- and plant-derived C and their contributions to SOC, (2) evaluate the distribution and abundance of CAZyme genes involved in microbial and plant components decomposition under different fertilizer applications, and (3) elucidate the main factors driving SOC variations across different fertilizer applications. We hypothesized that (1) long-term CF and CS applications would promote the accumulation of microbial- and plant-derived C, and the increase in SOC under CS application would mainly due to the enhanced contribution of MNC to SOC, (2) CS application would shift the distribution of soil microorganisms and increase the abundance of CAZyme genes responsible for the breakdown of plant and microbial compounds more than CF application, and (3) the bacterial community may be the main factor regulating SOC accumulation owing to its rapid growth in rich-nutrient soil.

2 Materials and methods

2.1 Research site and sample collection

The long-term fertilization study started in 2013 and was located in Harbin City, Heilongjiang Province (45°24′N, 126°22′E), where the soil was categorized as Mollisol. The climate of the study area is characterized as temperate monsoon with a mean annual temperature of 4.2°C and a mean annual precipitation of 523 mm. The planting pattern involved planting maize crop once in a year, with stems and leaves cleared from the field after harvest and in the following spring stubble ploughed into the soil. In the current study, three treatments, each with three replicates, were arranged. The treatments consisted of (1) CF treatment: CF of 245 kg N ha^{-1}, 96 kg P_2O_5 ha^{-1}, and 60 kg K_2O ha^{-1}, (2) CS treatment: cattle slurry of 135 m^3 ha^{-1}, and an abandoned field (CK) that had ceased maize cultivation and fertilization for several years. Due to field and management constraints, a maize-cultivated but unfertilized control treatment was not available. Therefore, CK serves as a background reference reflecting the cessation of fertilization and cultivation.

In April 2023, soil samples were collected from the 0–20 cm topsoil layer of each plot and homogenized. Visible gravel and plant litter were manually removed. After passing through a 2 mm sieve, the soil samples were divided into three sub-samples: one part was for the determination of soil dissolved organic carbon (DOC) and microbial biomass carbon (MBC), which was stored at 4°C; the second part was for the analysis of soil microbial community and stored at −80°C immediately, and the

third part was freeze-dried for the measurements of soil physical and chemical properties, amino sugars, lignin phenols, and enzyme activities.

2.2 Soil physical and chemical property analysis

SOC was quantified using a total organic carbon (TOC) analyzer (Vario TOC Select; Elementar, Germany). MBC was evaluated using the chloroform fumigation method, with a factor of 0.45 applied for calculation. DOC was determined using the TOC analyzer after extraction from the suspension of a 1:5 soil to water ratio. Soil total nitrogen (TN), nitrate nitrogen (NN), ammonium nitrogen (AN), total phosphorus (TP), soil available phosphorus (AP), and soil pH were analyzed via standard analytical processes, with details available in the Supplementary material.

Four soil extracellular enzymes related to C cycling, including peroxidase (POD), polyphenol oxidase (PPO), β-1,4-glucosidase (BG), and β-1,4-d-cellobiohydrolase (CBH) enzymes, were measured following the methods described in the Supplementary material. POD and PPO are oxidative enzymes with the ability to break down resistant organic compounds, such as lignin (Sinsabaugh, 2010). BG and CBH are hydrolytic enzymes capable of decomposing polysaccharides into monosaccharides, including cellulose and hemicellulose (Chen J. et al., 2020).

2.3 Lignin phenol analysis

Lignin phenols were quantified by the CuO oxidation method (Otto et al., 2005). Briefly, 0.5 g of soil, CuO, ammonium iron sulfate, and NaOH solution were mixed in Teflon vessels. After heating at 150°C, the solution was acidified to pH 1 and centrifuged. The supernatant was extracted with addition of Ethyl acetate, and the mixture was blown to near dryness. Ethylvanillin was used as the internal standard, and a methanol and dichloromethane (V:V = 1:1) solution was added to dissolve the mixture, then dried under nitrogen. The mixture was derivatized with methoxyamine hydrochloride and MATFA at 37°C. The derivatized compounds were analyzed using an Agilent 5,977 GC–MS equipped with a DB-35MS column (30 m × 0.25 mm × 0.25 μm).

Total lignin phenol (TLP) contents were the sum of vanillyls (V), syringyls (S), and cinnamyls (C). Vanillin, acetovanillone, and vanillic acid are included in V-typer phenols, syringaldehyde, acetosyringone, and syringic acid in S-typer phenols and p-coumaric and ferulic acid in C-typer phenols. Additionally, the S/V and C/V ratios were applied for the assessment of lignin biotransformation, and the acid-to-aldehyde ratios of vanillyls (Ad/Al) v and syringyls (Ad/Al) s were applied to evaluate the degree of lignin decomposition.

2.4 Amino sugar analysis

Amino sugars were extracted according to the method of Zhang and Amelung (1996). Soil samples were hydrolyzed, purified and derivatized, and the products were determined. Briefly, soil samples were hydrolyzed at 105°C, and then inositol was added as an internal standard. Subsequently, the hydrolysate was rotary evaporated, dissolved and adjusted pH to remove acids. In order to remove the salts, the residue was freeze-dried, dissolved in methanol, and freeze-dried again. After the addition of derivatization reagent to freeze-dried residue, the mixture was further acetylated with acetic anhydride at 80°C. Amino sugar derivatives were subsequently cleaned with HCl and water, dried under nitrogen and dissolved in hexane and ethyl acetate solution. Finally, the derivatized compounds were measured on a Thermo Scientific Trace 1,300 equipped with a TG-5SILMS column (30 m × 0.25 mm × 0.25 μm) and a flame ionization detector (FID).

Total amino sugar (TAS) contents were determined as the sum of glucosamine (GluN), galactosamine (GalN), and muramic acid (MurA). Microbial necromass C (MNC) contains fungal necromass C (FNC) and bacterial necromass C (BNC). FNC and BNC was calculated via GluN and MurA. The calculations were carried out using Equations 1–3:

$$BNC = MurA \times 45 \tag{1}$$

$$FNC = \left(\frac{GluN}{179.2} - 2 \times \frac{MurA}{251.2}\right) \times 179.2 \times 9 \tag{2}$$

$$MNC = BNC + FNC \tag{3}$$

Where 45 and 9 are the factors for converting MurA and GluN into BNC and FNC, respectively. 179.2 and 251.2 are the molecular weight of GluN and MurA, respectively.

2.5 Phospholipid fatty acid analysis

Phospholipid fatty acids (PLFAs) were employed for quantification of soil microbial biomass and were measured according to Frostegard and Baath (1996). In brief, freeze-dried soil samples were mixed with chloroform–methanol–citrate (V:V:V = 2:1:0.8) buffer and the solid-phase extraction column was used for separation of phospholipids. After phospholipids methylation, PLFAs methyl esters were quantified on an Agilent 7890B GC equipped with an FID and a 19091B-102 column (25 m × 0.2 mm × 0.33 μm). Specific PLFA peaks were identified using MIDI Sherlock Microbial Identification System (MIDI Inc., Newark, Delaware, USA).

The specific PLFAs selected as representative markers for various groups of microorganisms are shown in Supplementary Table S1. Total PLFAs were quantified by the summation of bacteria PLFAs, fungal PLFAs, and unspecified PLFAs, and the bacterial PLFAs consisted of gram-positive (G^+) and gram-negative (G^-) bacterial PLFAs. The ratios of G^+/G^- bacterial PLFAs (G^+/G^-) and fungal/bacterial PLFAs (F/B) were applied to analyze microbial community composition.

2.6 DNA extraction, sequencing, and metagenomic analysis

Soil DNA was extracted using an E.Z.N.A.™ Soil DNA Kit (Omega Bio-Tek, Norcross, Georgia, USA). After examination of DNA purity and integrity and construction of paired-end libraries, the metagenomic sequencing was conducted on an Illumina Hiseq 2000 by Majorbio Biopharm Technology (Shanghai, China). The sequences have been uploaded to the National Center for Biotechnology Information, and

RPJNA1166725 is the BioProject accession number. The metagenomic data was assembled with MEGAHIT (version 1.1.2), and then the nonredundant gene catalog was constructed with selection of contigs with overlap length over 300 bp for open reading frame prediction. The gene catalog was annotated according to the NR database[1] to obtain microbial annotation and taxonomic information and the CAZyme database[2] to identify specific functional gene families involved in organic compounds degradation. The reads per kilobase million (RPKM) was used to calculate the normalized abundance value. The detailed information of genes encoding microbial- and plant-derived component decomposition is shown in Supplementary Table S2.

2.7 Statistical analysis

Data normality was examined via the Shapiro–Wilk test. Significant differences of parameters among different fertilizer treatments were compared using one-way ANOVA based on the Duncan's test ($p < 0.05$). Principal Coordinate Analysis (PCoA) was employed to analyze the similarity in the composition of soil bacterial and fungal community under different fertilization based on Bray–Curtis distance, and the significance of dissimilarity was tested by ANOSIM. Mantel test analysis was applied to assess the correction between CAZyme genes associated with the breakdown of microbial and plant compounds, soil enzyme activities and microbial community properties. Pearson correlation analysis was performed to explore the relationship between MNC (FNC and BNC), lignin phenols and soil environmental factors. Random forest analysis was used to assess the impacts of environmental variables on SOC, MNC, and lignin phenols. The percentage increase of the mean squared error (%IncMSE) was used to rank the relative importance of the environmental variables. All statistical analyses were performed in R software (R 4.3.3).

3 Results

3.1 SOC content and physical and chemical properties

CF and CS application led to 26.9 and 88.0% increase in SOC content compared with CK, respectively (Table 1). The enhancement effect was more pronounced in CS treatment. Similarly, the DOC contents increased by 53.8 and 221.0%, respectively. The MBC content reduced by 57.6% in CF treatment and enhanced by 233.8% in CS treatment. In addition, the amounts of TN, TP, and AP showed increasing trends, and CS application was more conducive to the improvement of soil nutrients.

TABLE 1 Soil physical and chemical properties in different treatments.

Properties	CK	CF	CS
SOC (g kg^{-1})	15.5 ± 0.7 c	19.4 ± 0.9 b	29.9 ± 2.5 a
DOC (mg kg^{-1})	41.5 ± 5.4 b	59.3 ± 8.1 b	175.6 ± 18.9 a
MBC (mg kg^{-1})	178.0 ± 22.5 b	75.4 ± 7.6 c	594.0 ± 67.3 a
pH	7.91 ± 0.04 a	5.47 ± 0.07 c	7.14 ± 0.16 b
TN (g kg^{-1})	1.29 ± 0.07 b	1.64 ± 0.02 b	3.02 ± 0.30 a
NN (mg kg^{-1})	9.82 ± 0.97 b	22.86 ± 1.26 a	38.07 ± 2.80 a
AN (mg kg^{-1})	0.58 ± 0.07 a	0.22 ± 0.02 b	0.48 ± 0.03 a
MBN (mg kg^{-1})	1.57 ± 0.17 b	2.23 ± 0.17 b	5.75 ± 0.31 a
C/N	12.0 ± 0.2 a	11.8 ± 0.4 a	10.0 ± 0.5 a
TP (g kg^{-1})	0.48 ± 0.02 b	0.55 ± 0.04 b	1.13 ± 0.05 a
AP (mg kg^{-1})	48.0 ± 1.8 b	55.2 ± 3.6 b	114.4 ± 4.3 a
PPO (μmol g^{-1} h^{-1})	0.32 ± 0.02 b	0.28 ± 0.02 b	0.51 ± 0.08 a
POD (μmol g^{-1} h^{-1})	1.20 ± 0.03 c	1.57 ± 0.02 a	1.33 ± 0.07 b
BG (μmol g^{-1} h^{-1})	1.17 ± 0.11 c	1.54 ± 0.05 b	2.05 ± 0.06 a
CBH (μmol g^{-1} h^{-1})	0.09 ± 0.01 b	0.14 ± 0.01 a	0.16 ± 0.01 a

SOC, soil organic carbon; DOC, dissolved organic carbon; MBC, microbial biomass carbon; TN, total nitrogen; NN, nitrate nitrogen; AN, ammonium nitrogen; MBN, microbial biomass nitrogen; C/N, the ratio of soil organic carbon to total nitrogen; TP, total phosphorus; AP, available phosphorus; PPO, polyphenol oxidase; POD, peroxidase; BG, β-1,4-glucosidase; CBH, β-1,4-D-cellobiohydrolases. Different letters indicate significant differences among different treatments ($p < 0.05$, Duncan's test).

3.2 Amino sugars and microbial necromass in soil

The TAS concentration in different treatments were in the range of 0.97–2.05 g kg^{-1}. The TAS contents in CF and CS treatments were 1.25–1.77 times larger than those in CK treatment (Supplementary Figure S1), with CS treatment having the highest content of TAS. GluN, GalN, and MurA showed a similar trend. The content of MNC ranged from 6.27 to 12.5 g kg^{-1} (Figure 1A). Compared with CF application, CS application increased FNC by 35.0% and BNC by 29.4%, resulting in a 34.7% rise in the MNC content ($p < 0.05$, Figure 1A). However, the contribution of MNC to SOC and FNC/BNC ratios showed no difference between the two fertilization treatments ($p > 0.05$, Figure 1).

3.3 Soil lignin phenols

The contents of TLP ranged from 27.9 to 459 mg kg^{-1}. The CS treatment showed the highest content, which was 4.28 times greater than CF treatment. CS treatment demonstrated a notable increase in the contribution of V-, S-, and C-type phenols to SOC compared with CF treatment ($p < 0.05$, Figures 2A,B). C-type phenols were predominant in lignin phenols, accounting for 43.6–49.9%, followed by S-type phenols (26.8–30.9%) and V-type phenols (22.8–25.1%) in CF and CS treatments. Fertilization affected lignin biotransformation. There was a 1.13 times greater ratio of C/V in CS application compared with CF treatment, while the (Ad/Al)v ratio reduced by 13.4% (Figures 2C,D). No difference was found in the ratios of S/V and (Ad/Al)s between the two treatments.

3.4 Characteristics of soil microbial community

CS application considerably enhanced the total microbial biomass compared with CF application. Similar trends were

1 https://www.ncbi.nlm.nih.gov/
2 http://www.CAZy.org

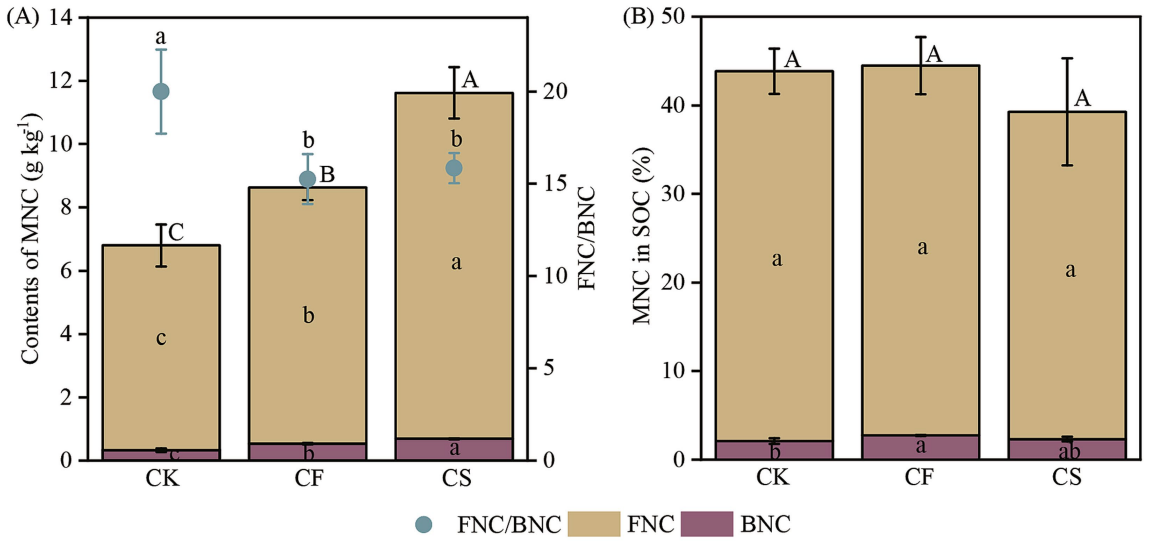


FIGURE 1
Contents of microbial necromass C and the ratio of fungal to bacterial necromass C **(A)**, and their contributions to SOC **(B)** in different treatments. Error bars represent standard errors of the means (n = 3). Different lowercase letters indicate significant differences in fungal and bacterial necromass C, and different uppercase letters indicate significant differences in total microbial necromass C among the treatments ($p < 0.05$, Duncan's test).

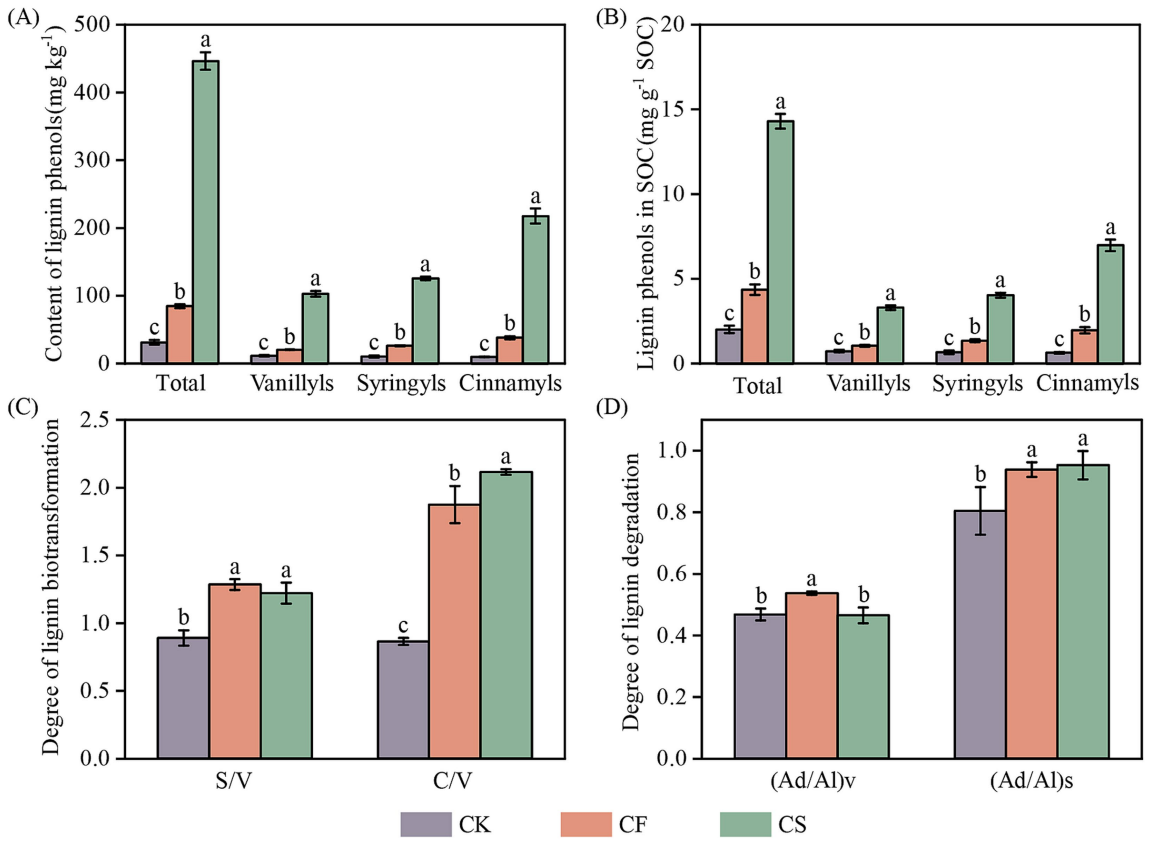


FIGURE 2
Contents of total and individual lignin phenols **(A)**, and their contributions to SOC **(B)**, the degree of lignin biotransformation **(C)** and degradation **(D)** in different treatments. The degree of lignin biotransformation was represented by the ratio of syringyl-type to vanillyl-type monomer (S/V) and cinnamyl-type to vanillyl-type monomer (C/V). The degree of lignin degradation was represented by acid/aldehyde ratio of vanillyl-type monomer (Ad/Al)v and acid/aldehyde ratio of syringyl-type monomer (Ad/Al)s. Error bars represent standard errors of the means (n = 3). Different letters indicate significant differences in total and individual lignin phenols, the degree of lignin biotransformation and degradation among the treatments ($p < 0.05$, Duncan's test).

observed in the biomass of G^+ bacteria, G^- bacteria, bacteria, and fungi (Figure 3A). Compared with CF treatment, CS application increased the total microbial biomass by 64.2%, of which bacterial and fungal biomasses increased by 56.7 and 127%, respectively. The increase in bacterial biomass in CS treatment was mainly due to the increase in the amount of G^- bacteria, which increased by 106%. The application of CS increased the F/B ratio but reduced the G^+/G^- ratio (Figure 3B). The number of CAZymes and gene families identified in the entire metagenome was 180,463 and 491, respectively. Among these CAZymes and gene families, bacteria and fungi accounted for 97.9 and 0.05%, respectively. The ACE indexes of bacterial and fungal communities were 11.4 and 27.1% higher in CF treatment than those in CS treatment, respectively ($p < 0.05$, Supplementary Figure S2A), while the Shannon index showed no difference ($p > 0.05$, Supplementary Figure S2B). PCoA demonstrated that the compositions of soil bacterial and fungal community were clearly distinguished under different fertilizer addition with 50.12 and 42.75% explanations of the first axis, respectively ($p < 0.001$, Figures 3C,D). CS application considerably changed soil bacterial and fungal community compositions compared to the CF treatment. The dominant phyla for bacteria were Pseudomonadota, Actinomycetota, and Acidobacteriota. The relative abundance of Actinomycetota was the highest in CF treatments, while that of Pseudomonadota became the highest in CS treatment. In addition, microbial biomarker species were noted to be more abundant in CS treatment (LDA > 3, $p < 0.05$, Figure 3E). Vicinamibacteraceae, Steroidobacteraceae, Lysobacteraceae and Ilumatobacteraceae were identified as biomarkers at the family level in CS treatment, exhibiting the increase by 10.6, 1.30, 22.5 and 12.5 fold compared with CF treatment, respectively. Ascomycota was the dominant fungal phylum, exhibiting a further increase in relative abundance in the CS treatment (Supplementary Figure S2D). While no significant difference was found for fungal biomarkers at the phylum level, primary enrichments were noted within family groups, including Podosporaceae and Nectriaceae (Figure 3F).

3.5 CAZymes related to the decomposition of plant and microbial necromass

The abundance of CAZymes related to the breakdown of plant-derived compounds was higher than that related to microbial-derived compounds decomposition (Figures 4A–F). Among plant-derived components, the abundance of CAZyme families encoding breakdown of hemicellulose surpassed those encoding cellulose and lignin decomposition. The highest abundance of gene families associated with the breakdown of plant residues were CE1 and GH74, both of which showed a significant enhancement with CS application ($p < 0.05$, Figure 4B). The most abundant CAZymes encoding fungal necromass breakdown was GH20 in CF and CS treatments and GH18 in CK treatment (Figure 4D), and the dominant CAZyme responsible for the breakdown of bacterial necromass was GH23 (Figure 4F).

The specific CAZymes encoding the breakdown of plant and microbial residue fractions varied in different treatments. The CAZymes associated with plant-and bacterial-derived compounds decomposition increased, whereas those encoding fungal-derived components decomposition reduced in CS treatment compared with CF treatment. The abundance of gene families CE1, GH74, and CE7 related to hemicellulose degradation increased by 468, 536, and 253 RPKM, respectively (Figure 4B). The abundance of gene families AA1 and AA5 encoding the breakdown of lignin was lower in CF treatment than in CS treatment (Figure 4C). GH3 and GH1 were the main gene families for cellulose degradation, and no significant difference in abundance was observed between CS and CF treatments. For the CAZymes responsible for decomposition of microbial residue fractions, the abundance values of GH20 and GH18, which are responsible for chitin degradation, were 128 and 76.9 RPKM lower in CS treatment than in CF treatment, respectively (Figure 4D). A similar trend was noted for the abundance values of GH24 and GH25 gene families related to peptidoglycan decomposition, with reductions of 66.3 and 59.0 RPKM, respectively, while the abundance values of the GH23 and GH103 gene families increased by 131 and 63.4 RPKM, respectively (Figure 4F).

The CAZymes encoding the plant and microbial necromass decomposition were primarily attributed to the bacterial communities, with Acidobacteriota, Pseudomonadota, and Actinomycetota being the dominant phyla (Figures 5A–F). The abundance of species associated with the breakdown of fungal-derived peptidoglycan and plant-derived hemicellulose increased in CF and CS treatments compared with CK ($p < 0.05$, Figures 5B,F). CS application enhanced the abundance of species responsible for cellulose, hemicellulose, lignin, and peptidoglycan decomposition and reduced that for chitin and glucan degradation compared with CF application. The abundance of cellulose-degrading species in CS application increased owing to Pseudomonadota, Nitrososphaerota, and Chloroflexota (Figure 5A). Acidobacteriota and Chloroflexota mainly contributed to the increase of hemicellulose, lignin, and peptidoglycan degradation (Figure 5B). The abundance Actinomycetota and Bacteroidota for each residue component decomposition showed a similar decreasing trend in CS treatment compared with CF treatment.

3.6 Relation between soil environmental factors, specific CAZyme genes, and SOC accumulation

Soil enzyme activities had a positive and strong association with bacterial and fungal biomass, with the exception of POD activity ($p < 0.05$, Figure 6A). CAZymes responsible for the breakdown of bacterial-derived components was strongly correlated with soil enzyme activities and microbial biomass. There was a close relation between BG activity and the CAZymes responsible for the plant-derived fractions degradation. However, the abundance of CAZymes responsible for fungal-derived component degradation demonstrated no correlation with any enzyme activity (Figure 6A).

Pearson correlation analysis revealed that the contents of SOC and SOC fractions increased with the increasing TN, TP, and AP contents. Additionally, MNC and TLP were positively correlated with PPO, BG, and CBH activities but showed no significant correlation with POD activity (Figure 6B). Based on the random forest model, these variables explained 80.2, 75.6, and 92.2% of the total variance for SOC, MNC, and TLP, respectively

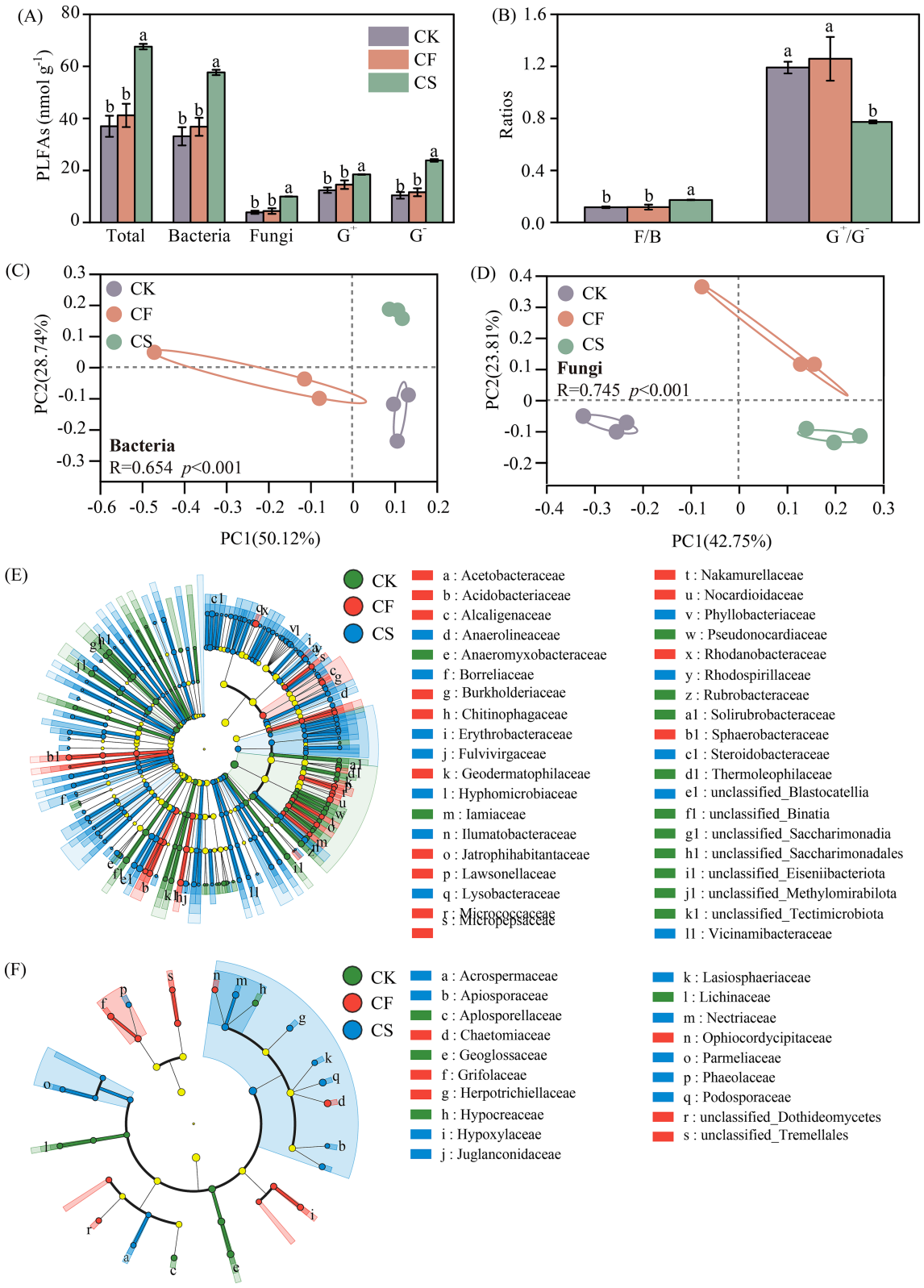


FIGURE 3
Contents of total, bacterial, fungal, gram-positive (G^+) bacterial and gram-negative (G^-) bacterial PLFAs **(A)**, and the ratio of fungal to bacterial PLFAs and gram-positive to gram-negative bacterial PLFAs **(B)** in different treatments. Difference of bacterial **(C)** and fungal **(D)** community structure based on the principal coordinate analysis (PCoA) and biomarker taxa compositions at the family level (LDA > 3, $p < 0.05$) of bacterial **(E)** and fungal **(F)** community. Error bars represent standard errors of the means ($n = 3$). Different letters indicate significant differences in total and individual PLFAs among the treatments ($p < 0.05$, Duncan's test).

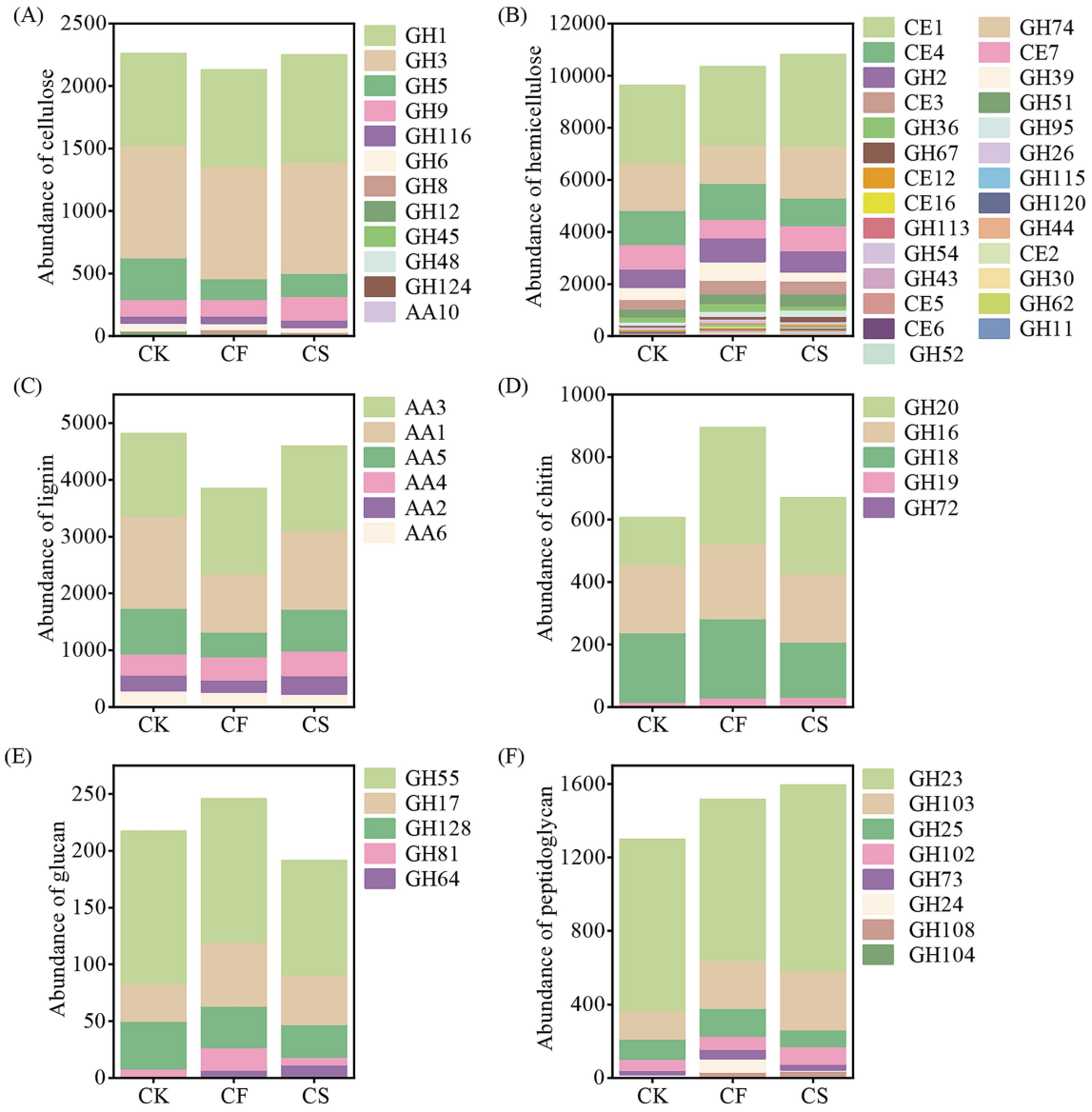


FIGURE 4
Abundance of specific CAZymes encoding the decomposition of plant-derived and microbial-derived components. Cellulose **(A)**, hemicellulose **(B)** and lignin **(C)** were components derived from plants. Chitin **(D)** and glucan **(E)** were components derived from fungus and peptidoglycan **(F)** was a component derived from bacteria.

(Figure 6C). DOC, TN, AP, MBN, BG, BPL, and FPL were the important factors of SOC, MNC, and TLP contents, suggesting that nutrients might be acquired by microbes to promote C accrual. The F/B ratio was the main predictor of MNC and TLP contents.

4 Discussion

4.1 Long-term application of CS had no impact on the contribution of MNC to SOC

In agricultural ecosystems, microbial necromass is essential for long-term conservation and sequestration of SOC and plays a vital role in SOC accumulation (Jia et al., 2017; Zhou et al., 2023). The application of CF and CS increased the MNC contents, including BNC and FNC in our study (Figure 1A), which was in line with the first hypothesis. Fertilizers might promote root biomass inputs and microbial proliferation, as well as increase N availability to enhance microbial C use efficiency, thereby promoting microbial necromass enrichment (Chen J. G. et al., 2020; Hu et al., 2022). The use of CS further enhanced the MNC content in comparison with the utilization of CF, possibly due to the following three reasons. Firstly, CS provided abundant bioavailable organic matter and nutrients, which was beneficial for microbial growth, resulting in larger microbial biomass (Fox et al., 2017; Zhou et al., 2023). Secondly, CS application supplied abundant nutrient substrates and was conducive to microbial

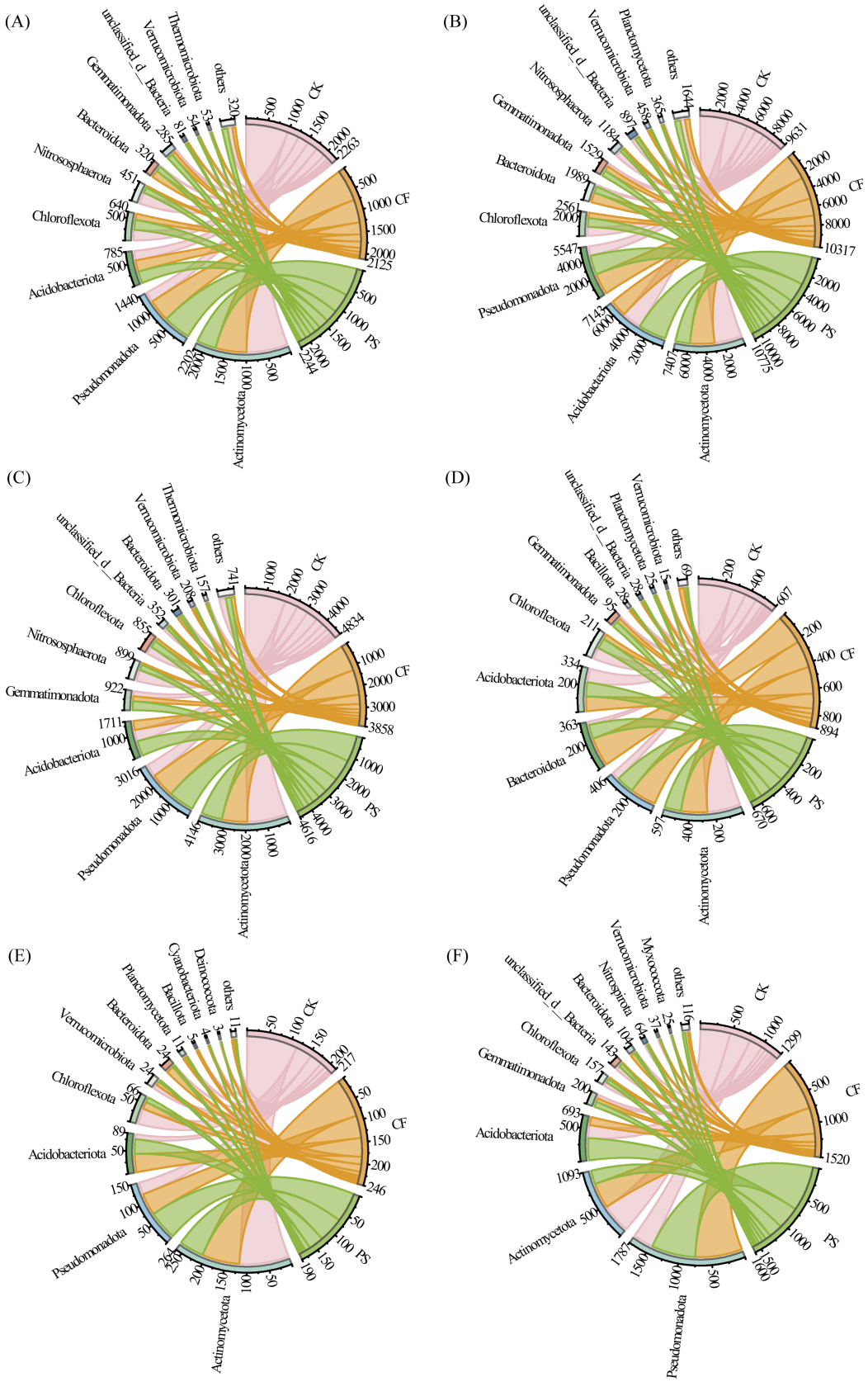


FIGURE 5
Contribution of microbial (bacterial and fungal) phyla to CAZyme genes for the decomposition of plant-and microbial-derived components. Cellulose **(A)**, hemicellulose **(B)** and lignin **(C)** were components derived from plants. Chitin **(D)** and glucan **(E)** were components derived from fungus and peptidoglycan **(F)** was a component derived from bacteria.

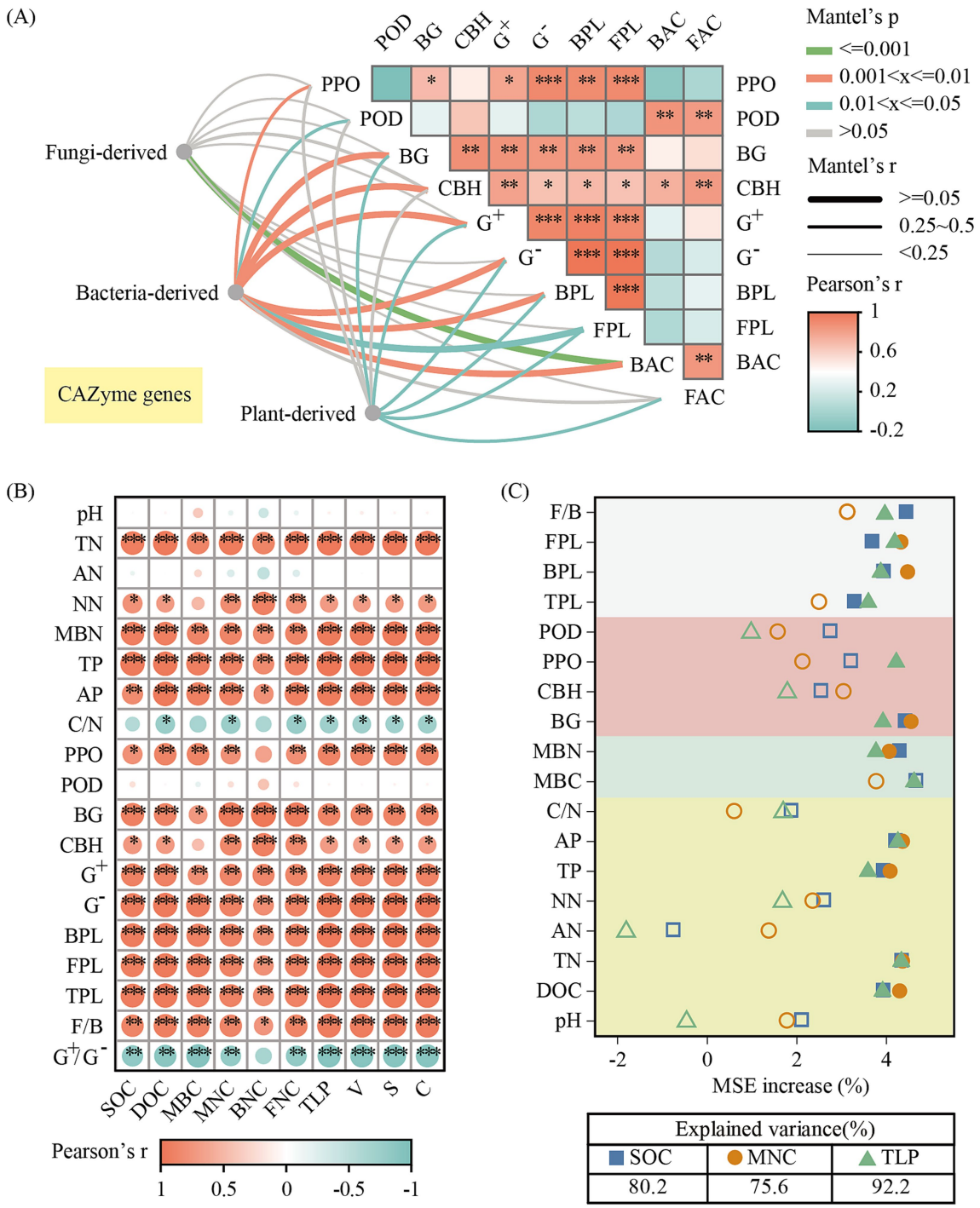


FIGURE 6
Mantel test analysis between the abundance of the CAZyme genes encoding the decomposition of plant- derived (cellulose, hemicellulose and lignin) and microbial-derived (chitin, glucan and peptidoglycan) components and soil enzyme activities **(A)**. Mantel's p and r values are represented by the color and width of the connection line specified in the legend. Pearson correlation analysis between soil physical–chemical properties, soil enzyme activity, soil microbial biomass and the contents of SOC fractions **(B)**. Relative importance of independent variables controlling SOC, MNC and LP as represented by the percentage increase of the mean squared error (MSE%) based on random forest model **(C)**. The significant factors ($p < 0.05$) are indicated as solid colored symbols. BPL, bacterial PLFAs; FPL, fungal PLFAs; BAC, ACE index of bacterial communities; FAC, ACE index of fungal communities.

proliferation (Table 1 and Figure 3A), thereby facilitating enrichment of microbial necromass (Chen et al., 2024; Yang et al., 2022; Ye et al., 2019). MNCs were positively correlated with PLFAs in this study, verifying that the increase in microbial biomass promoted microbial residue accrual (Supplementary Figure S3). Finally, the microorganisms and microbial residues in CS and soil are sources of amino sugars; thus, CS application directly and indirectly promotes long-term MNC accumulation (Chen X. B. et al., 2020; Jost et al., 2011). However, the contribution of MNC to SOC showed no difference

among treatments (Figure 1B), indicating that CS application did not enhance the proportion of MNC to SOC, which contradicted our hypothesis. This might be explained by the simultaneous increase in MNC, combined with the dilution effect of increased plant necromass contribution to SOC, leading to the MNC contribution unchanged.

The content and proportion of FNC in MNC were far higher than those of BNC in our study (Figure 1A), demonstrating that FNC was dominant over BNC for MNC formation. The result may be partly explained by the fact that fungal necromass exhibit greater recalcitrance than bacterial necromass. The bacterial cell wall primarily comprises relatively labile components such as peptidoglycan, whereas the fungal cell wall primarily comprises less decomposable components such as chitin (Chen X. B. et al., 2020; Li et al., 2015). This stability of components facilitated the accumulation of fungal necromass, although fungi having lower biomass than bacteria in this study. In addition, the strong sorption of fungal hyphae in soil minerals could protect it from decomposition by soil enzymes and increase fungal necromass retention (Joergensen, 2018; Luo et al., 2022).

4.2 Long-term application of CS increased lignin phenols content

Accumulation of plant-derived C may be determined by the balance between the input and decomposition of plant-derived necromass (Wang et al., 2022). TLP content significantly increased under fertilization (Figure 2A), which might be explained by the enhancement of lignin input with the increased root biomass and unfavorable habitats for lignin major decomposers in croplands such as white-rot fungi (Su et al., 2023). Compared with CF treatment, the content and contribution to SOC of lignin phenols in CS treatment remarkably increased, as well as V-, S-, and C-type phenols (Figures 2A,B). CS application might facilitate lignin preservation but suppress lignin degradation. Greater S/V and C/V ratios indicate less microbial transformation, while the enhancement in the ratios of (Ad/Al)v and (Ad/Al)s show more side chain oxidation (Ma et al., 2018; Yang et al., 2022). Increased C/V and decreased (Ad/Al)v in CS treatment showed reduced lignin degradation in our study (Figures 2C,D). CS application enhanced lignin decomposition with higher plant inputs but less degradation of preserved lignin in the soil, thus increasing the selective retention of plant lignin. In addition, CS supplied high-available and preferred C sources for microorganisms, thereby reducing the attack from microbes and preserving more lignin (Li et al., 2020). Therefore, the organic components from CS application increased the lignin retention and accrual in soil.

SOC is generally comprised of microbial- and plant-derived C (Huang et al., 2022; Whalen et al., 2022). The unchanged contribution of MNC to SOC suggested that there might be no alteration in the contribution of plant-derived C as expected. Meng et al. (2024) found that despite the positive relationship of lignin phenols with SOC, they are not suitable as the sole biomarker for plant residues alone. Therefore, some other sources of plant necromass should be considered when evaluating the contribution of plant-derived C to SOC.

4.3 Long-term application of CS altered the microbial community and C-degrading genes

The application of CF and CS resulted in a notable separation of microbial community structure and differences in microbial community composition (Figures 3C–F and Supplementary Figure S2). CS application significantly promoted G^- bacteria growth and decreased the G^+/G^- ratio. As biomass varied, the dominant bacterial phyla shifted from Actinomycetota (G^+ bacteria) to Pseudomonadota (G^- bacteria) from CF treatment to CS treatment, with a notable enhancement of Acidobacteriota (G^- bacteria). Pseudomonadota are rapid-growing eutrophs that thrive in C-rich habitats and proficient in decomposing labile plant necromass C, such as cellulose and lignin (Fierer et al., 2007; Wang et al., 2023; Wiseschart et al., 2019). Acidobacteriota can produce various extracellular enzymes and possess an outstanding metabolic capacity to break down organic compounds (Richy et al., 2024; Zifcáková et al., 2016). For fungi, Ascomycota was the dominant phylum, and CS application remarkably enhanced its relative abundance. Ascomycota are effective in the breakdown of plant-derived cellulose and hemicellulose due to their abundant enzyme pool (Li et al., 2022; Manici et al., 2024). These variations in microbial communities indicated CS application accelerated plant residue conversion to microbial necromass.

Changes in microbial communities could drive shifts in microbial ecological functions, such as organic substrates degradation capacity and preference (Cheng et al., 2017). CAZyme genes assignment for degrading complex and simple C sources varied across treatments. The abundance of CAZyme genes encoding the breakdown of plant necromass was larger in CS than that in CF. The abundance of gene families CE1, GH47, and CE7 encoding for hemicellulose degradation (Figure 4B) and gene families AA1 and AA5 encoding for lignin degradation increased (Figure 4C), suggesting higher plant-derived necromass degradation into small C fractions. This might be due to the fact that the production of C-degrading enzymes is to a large extent dependent on energy substance adequacy (Chen Q. L. et al., 2020). A stronger ability of microorganisms to break down hemicellulose and lignin for obtaining more C resources corresponded with increased the biosynthesis of CAZyme genes (Huang et al., 2024; Trivedi et al., 2016). For microbial-derived fractions, the gene families GH16, GH17, GH23, and GH103 confirmed their functions in microbial necromass decomposition (Zifcáková et al., 2017). The elevated abundance of GH23 and GH103, which are associated with peptidoglycan decomposition (Figure 4F), suggests a higher potential for bacterial necromass degradation. In addition, the pool of CAZyme genes encoding breakdown of plant and microbial necromass was distinct, with higher abundance of CAZymes for plant necromass breakdown than that for microbial necromass breakdown. These results indicated a larger investment of plant necromass for C pool and corresponded with the previous viewpoint that plant necromass is rich in organic substance and most likely constitutes a substantial portion of soil C sink (Ren C. J. et al., 2021; Zhang B. G. et al., 2021).

4.4 Mechanism of long-term application of CS affecting SOC accumulation

The contents of SOC, MNC, and TLP increased from the application of CF to CS. Substrate availability, microbial communities, and enzyme activities are significant factors leading to the SOC enhancement

(Figure 6C). The probable mechanism by which CS application improved SOC accumulation is depicted in Figure 7. CS application may boost plant residue input and exogenous C sources, increasing soil nutrients and DOC content. Higher DOC content might promote microbial biomass synthesis by improving microbial metabolism, which was conducive to MNC enrichment (Zifcáková et al., 2017). Furthermore, the shifts of dominant microbial phylum from oligotrophic to eutrophic reflected the alterations of microbial community functions (Domeignoz-Horta et al., 2021). Microbial community features were vital factors affecting MNC and TLP. The correlation between microbial community features and functional CAZyme genes explained the regulative role of soil microorganisms in soil C cycling and the vital role of dominant CAZyme families in C source turnover. Changes in CAZyme genes encoding plant and microbial necromass decomposition would affect microbial metabolism via a "microbial carbon pump," thereby facilitating SOC formation and accumulation. The CK treatment in this study involved abandoned land restored from former maize cultivation without fertilization, rather than maize fields without fertilizer application. This limitation of our work might have introduced variability in SOC conditions, although the primary focus of this study was on the relative differences between CS and CF treatments. Future studies should address the limitation and aim to include a strict maize-without-fertilizer control to further isolate fertilization effects on SOC dynamics. Although this CK treatment differed from the conventional definition of a control, it provided a valuable baseline for assessing SOC dynamics under conditions of minimal anthropogenic inputs. This study offered valuable insights into the underlying connection between SOC degradation and microbial CAZyme genes under the long-term application of cattle slurry.

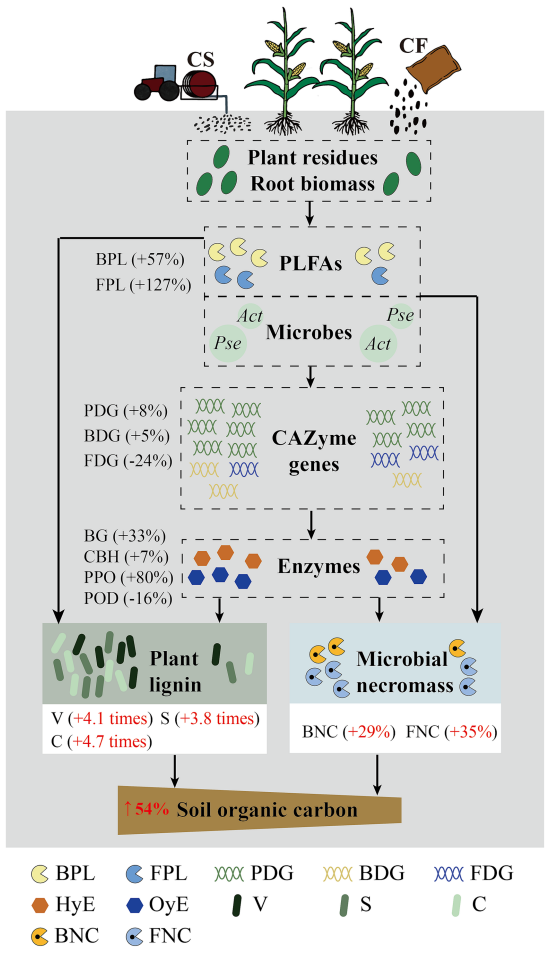


FIGURE 7
A conceptual figure of the influence of cattle slurry (CS) and chemical fertilizer (CF) application on SOC formation. The numerical labels indicates the effect of CS for each indicator compared with CF. HyE, hydrolase (BG and CBH); OyE, oxidase (PPO and POD); PDG, CAZyme genes encoding the decomposition of plant-derived components; BDG, CAZyme genes encoding the decomposition of bacterial-derived components; FDG, CAZyme genes encoding the decomposition of fungal-derived components.

5 Conclusion

Long-term application of CS substantially enhanced SOC accumulation compared with CF treatment, primarily through increased microbial- and plant-derived C. CS application promoted plant biomass input and reduced the oxidative degradation of lignin, leading to a higher lignin phenol content in soil. Although CS stimulated microbial biomass production and MNC accumulation, the contribution of MNC to total SOC remained stable. Compared to CF, CS application induced shifts in microbial community composition, favoring eutrophic bacterial groups such as Pseudomonadota, and enhanced the abundance of CAZyme genes involved in plant and bacterial biomass degradation. These changes suggest a greater potential for substrate turnover and carbon stabilization under CS management. Overall, the availability of substrates, microbial community, and enzyme activities are significant factors attributing to the increase of SOC contents. Our findings offered support for the underlying connection between SOC degradation and microbial CAZyme genes and provide important scientific evidence to support the sustainable recycling of livestock manure in cropland systems.

Data availability statement

The datasets presented in this study can be found in online repositories. The names of the repository/repositories and accession number(s) can be found in the article/Supplementary material.

Author contributions

XC: Conceptualization, Writing – original draft, Writing – review & editing. ZP: Investigation, Writing – review & editing. XW: Investigation, Writing – review & editing. HW: Methodology, Writing – review & editing. JM: Investigation, Writing – review & editing. YM: Software, Writing – review & editing. MZ: Validation, Writing – review & editing. KZ: Writing – review & editing. LD: Funding acquisition, Supervision, Writing – review & editing.

Funding

The author(s) declare that financial support was received for the research and/or publication of this article. This work was supported by the National Key Research and Development Program of China

(2023YFD1702000), Key Research and Development Program of Heilongjiang Province (2023ZX02B03), and the Science and Technology Innovation Project of the Chinese Academy of Agricultural Sciences.

Conflict of interest

The authors declare that the research was conducted in the absence of any commercial or financial relationships that could be construed as a potential conflict of interest.

Generative AI statement

The authors declare that no Gen AI was used in the creation of this manuscript.

Publisher's note

All claims expressed in this article are solely those of the authors and do not necessarily represent those of their affiliated organizations, or those of the publisher, the editors and the reviewers. Any product that may be evaluated in this article, or claim that may be made by its manufacturer, is not guaranteed or endorsed by the publisher.

Supplementary material

The Supplementary material for this article can be found online at: https://www.frontiersin.org/articles/10.3389/fmicb.2025.1586791/full#supplementary-material

References

Bomble, Y. J., Lin, C. Y., Amore, A., Wei, H., Holwerda, E. K., Ciesielski, P. N., et al. (2017). Lignocellulose deconstruction in the biosphere. *Curr. Opin. Chem. Biol.* 41, 61–70. doi: 10.1016/j.cbpa.2017.10.013

Camenzind, T., Mason-Jones, K., Mansour, I., Rillig, M. C., and Lehmann, J. (2023). Formation of necromass-derived soil organic carbon determined by microbial death pathways. *Nat. Geosci.* 16, 115–122. doi: 10.1038/s41561-022-01100-3

Chen, Q. L., Ding, J., Li, C. Y., Yan, Z. Z., He, J. Z., and Hu, H. W. (2020). Microbial functional attributes, rather than taxonomic attributes, drive top soil respiration, nitrification and denitrification processes. *Sci. Total Environ.* 734:139479. doi: 10.1016/j.scitotenv.2020.139479

Chen, J., Elsgaard, L., van Groenigen, K. J., Olesen, J. E., Liang, Z., Jiang, Y., et al. (2020). Soil carbon loss with warming: new evidence from carbon-degrading enzymes. *Glob. Chang. Biol.* 26, 1944–1952. doi: 10.1111/gcb.14986

Chen, J. G., Ji, C. J., Fang, J. Y., He, H. B., and Zhu, B. (2020). Dynamics of microbial residues control the responses of mineral-associated soil organic carbon to N addition in two temperate forests. *Sci. Total Environ.* 748:141318. doi: 10.1016/j.scitotenv.2020.141318

Chen, Z. M., Ma, J. C., Ma, J. W., Ye, J., Yu, Q. G., Zou, P., et al. (2024). Long-term biogas slurry application increases microbial necromass but not plant lignin contribution to soil organic carbon in paddy soils as regulated by fungal community. *Waste Manag.* 175, 254–264. doi: 10.1016/j.wasman.2024.01.011

Chen, G. P., Ma, S. H., Tian, D., Xiao, W., Jiang, L., Xing, A. J., et al. (2020). Patterns and determinants of soil microbial residues from tropical to boreal forests. *Soil Biol. Biochem.* 151:108059. doi: 10.1016/j.soilbio.2020.108059

Chen, X. B., Xia, Y. H., Rui, Y. C., Ning, Z., Hu, Y. J., Tang, H. M., et al. (2020). Microbial carbon use efficiency, biomass turnover, and necromass accumulation in paddy soil depending on fertilization. *Agric. Ecosyst. Environ.* 292:106816. doi: 10.1016/j.agee.2020.106816

Cheng, L., Zhang, N. F., Yuan, M. T., Xiao, J., Qin, Y. J., Deng, Y., et al. (2017). Warming enhances old organic carbon decomposition through altering functional microbial communities. *ISME J.* 11, 1825–1835. doi: 10.1038/ismej.2017.48

Domeignoz-Horta, L. A., Shinfuku, M., Junier, P., Poirier, S., Verrecchia, E., Sebag, D., et al. (2021). Direct evidence for the role of microbial community composition in the formation of soil organic matter composition and persistence. *ISME Commun.* 1:64. doi: 10.1038/s43705-021-00071-7

Fierer, N., Bradford, M. A., and Jackson, R. B. (2007). Toward an ecological classification of soil bacteria. *Ecology* 88, 1354–1364. doi: 10.1890/05-1839

Fox, A., Ikoyi, I., Creamer, R., Lanigan, G., and Schmalenberger, A. (2017). Microbial community structure and function respond more strongly to temporal progression than to the application of slurry in an Irish grassland. *Appl. Soil Ecol.* 120, 97–104. doi: 10.1016/j.apsoil.2017.07.032

Friedlingstein, P., O'Sullivan, M., Jones, M. W., Andrew, R. M., Hauck, J., Olsen, A., et al. (2020). Global Carbon Budget 2020. *Earth Syst. Sci. Data Discuss.* 12, 3269–3340. doi: 10.5194/essd-12-3269-2020

Frostegard, A., and Baath, E. (1996). The use of phospholipid fatty acid analysis to estimate bacterial and fungal biomass in soil. *Biol. Fertil. Soils* 22, 59–65. doi: 10.1007/bf00384433

Hu, J. X., Huang, C. D., Zhou, S. X., Liu, X., and Dijkstra, F. A. (2022). Nitrogen addition increases microbial necromass in croplands and bacterial necromass in forests: a global meta-analysis. *Soil Biol. Biochem.* 165:108500. doi: 10.1016/j.soilbio.2021.108500

Hu, Y. T., Zheng, Q., Noll, L., Zhang, S. S., and Wanek, W. (2020). Direct measurement of the in situ decomposition of microbial-derived soil organic matter. *Soil Biol. Biochem.* 141:107660. doi: 10.1016/j.soilbio.2019.107660

Huang, X. L., Jia, Z. X., Jiao, X. Y., Wang, J. L., and Huang, X. F. (2022). Long-term manure applications to increase carbon sequestration and macroaggregate-stabilized carbon. *Soil Biol. Biochem.* 174:108827. doi: 10.1016/j.soilbio.2022.108827

Huang, Q., Wang, B. R., Shen, J. K., Xu, F. J., Li, N., Jia, P. H., et al. (2024). Shifts in C-degradation genes and microbial metabolic activity with vegetation types affected the surface soil organic carbon pool. *Soil Biol. Biochem.* 192:109371. doi: 10.1016/j.soilbio.2024.109371

Jackson, R. B., Lajtha, K., Crow, S. E., Hugelius, G., Kramer, M. G., and Piñeiro, G. (2017). The ecology of soil carbon: pools, vulnerabilities, and biotic and abiotic controls. *Annu. Rev. Ecol. Evol. Syst.* 48, 419–445. doi: 10.1146/annurev-ecolsys-112414-054234

Jia, J., Feng, X. J., He, J. S., He, H. B., Lin, L., and Liu, Z. G. (2017). Comparing microbial carbon sequestration and priming in the subsoil versus topsoil of a Qinghai-Tibetan alpine grassland. *Soil Biol. Biochem.* 104, 141–151. doi: 10.1016/j.soilbio.2016.10.018

Joergensen, R. G. (2018). Amino sugars as specific indices for fungal and bacterial residues in soil. *Biol. Fertil. Soils* 54, 559–568. doi: 10.1007/s00374-018-1288-3

Jost, D. I., Indorf, C., Joergensen, R. G., and Sundrum, A. (2011). Determination of microbial biomass and fungal and bacterial distribution in cattle faeces. *Soil Biol. Biochem.* 43, 1237–1244. doi: 10.1016/j.soilbio.2011.02.013

Kicklighter, D. W., Melillo, J. M., Monier, E., Sokolov, A. P., and Zhuang, Q. L. (2019). Future nitrogen availability and its effect on carbon sequestration in northern Eurasia. *Nat. Commun.* 10:3024. doi: 10.1038/s41467-019-10944-0

Li, T., Cui, L. Z., Song, X. F., Cui, X. Y., Wei, Y. L., Tang, L., et al. (2022). Wood decay fungi: an analysis of worldwide research. *J. Soils Sediments* 22, 1688–1702. doi: 10.1007/s11368-022-03225-9

Li, N., Xu, Y. Z., Han, X. Z., He, H. B., Zhang, X. D., and Zhang, B. (2015). Fungi contribute more than bacteria to soil organic matter through necromass accumulation under different agricultural practices during the early pedogenesis of a Mollisol. *Eur. J. Soil Biol.* 67, 51–58. doi: 10.1016/j.ejsobi.2015.02.002

Li, J., Zhang, X. C., Luo, J. F., Lindsey, S., Zhou, F., Xie, H. T., et al. (2020). Differential accumulation of microbial necromass and plant lignin in synthetic versus organic fertilizer-amended soil. *Soil Biol. Biochem.* 149:107967. doi: 10.1016/j.soilbio.2020.107967

Liang, C. (2020). Soil microbial carbon pump: mechanism and appraisal. *Soil Ecol. Lett.* 2, 241–254. doi: 10.1007/s42832-020-0052-4

Liang, C., Amelung, W., Lehmann, J., and Kästner, M. (2019). Quantitative assessment of microbial necromass contribution to soil organic matter. *Glob. Chang. Biol.* 25, 3578–3590. doi: 10.1111/gcb.14781

Liang, C., Schimel, J. P., and Jastrow, J. D. (2017). The importance of anabolism in microbial control over soil carbon storage. *Nat. Microbiol.* 2:17105. doi: 10.1038/nmicrobiol.2017.105

Liu, X. T., Tan, S. W., Song, X. J., Wu, X. P., Zhao, G., Li, S. P., et al. (2022). Response of soil organic carbon content to crop rotation and its controls: a global synthesis. *Agric. Ecosyst. Environ.* 335:108017. doi: 10.1016/j.agee.2022.108017

Liu, X., Zhou, F., Hu, G. Q., Shao, S., He, H. B., Zhang, W., et al. (2019). Dynamic contribution of microbial residues to soil organic matter accumulation influenced by maize straw mulching. *Geoderma* 333, 35–42. doi: 10.1016/j.geoderma.2018.07.017

Llado, S., Vetrovsky, T., and Baldrian, P. (2019). Tracking of the activity of individual bacteria in temperate forest soils shows guild-specific responses to seasonality. *Soil Biol. Biochem.* 135, 275–282. doi: 10.1016/j.soilbio.2019.05.010

López-Mondéjar, R., Brabcová, V., Stursová, M., Davidová, A., Jansa, J., Cajthaml, T., et al. (2018). Decomposer food web in a deciduous forest shows high share of generalist microorganisms and importance of microbial biomass recycling. *ISME J.* 12, 1768–1778. doi: 10.1038/s41396-018-0084-2

López-Mondéjar, R., Tláskal, V., Vetrovsky, T., Stursová, M., Toscan, R., da Rocha, U. N., et al. (2020). Metagenomics and stable isotope probing reveal the complementary contribution of fungal and bacterial communities in the recycling of dead biomass in forest soil. *Soil Biol. Biochem.* 148:107875. doi: 10.1016/j.soilbio.2020.107875

Lu, J., Jiang, L. N., Chen, D. J., Toyota, K., Strong, P. J., Wang, H. L., et al. (2012). Decontamination of anaerobically digested slurry in a paddy field ecosystem in Jiaxing region of China. *Agric. Ecosyst. Environ.* 146, 13–22. doi: 10.1016/j.agee.2011.10.011

Luo, R. Y., Kuzyakov, Y., Zhu, B., Qiang, W., Zhang, Y., and Pang, X. Y. (2022). Phosphorus addition decreases plant lignin but increases microbial necromass contribution to soil organic carbon in a subalpine forest. *Glob. Chang. Biol.* 28, 4194–4210. doi: 10.1111/gcb.16205

Ma, T., Zhu, S. S., Wang, Z. H., Chen, D. M., Dai, G. H., Feng, B. W., et al. (2018). Divergent accumulation of microbial necromass and plant lignin components in grassland soils. *Nat. Commun.* 9:3480. doi: 10.1038/s41467-018-05891-1

Manici, L. M., Caputo, F., Fornasier, F., Paletto, A., Ceotto, E., and De Meo, I. (2024). Ascomycota and Basidiomycota fungal phyla as indicators of land use efficiency for soil organic carbon accrual with woody plantations. *Ecol. Indic.* 160:111796. doi: 10.1016/j.ecolind.2024.111796

Meng, X. T., Zhang, X. C., Li, Y. N., Jiao, Y. P., Fan, L. C., Jiang, Y. J., et al. (2024). Nitrogen fertilizer builds soil organic carbon under straw return mainly via microbial necromass formation. *Soil Biol. Biochem.* 188:109223. doi: 10.1016/j.soilbio.2023.109223

Otto, A., Shunthirasingham, C., and Simpson, M. J. (2005). A comparison of plant and microbial biomarkers in grassland soils from the prairie Ecozone of Canada. *Org. Geochem.* 36, 425–448. doi: 10.1016/j.orggeochem.2004.09.008

Peltre, C., Gregorich, E. G., Bruun, S., Jensen, L. S., and Magid, J. (2017). Repeated application of organic waste affects soil organic matter composition: evidence from thermal analysis, FTIR-PAS, amino sugars and lignin biomarkers. *Soil Biol. Biochem.* 104, 117–127. doi: 10.1016/j.soilbio.2016.10.016

Ren, F. L., Misselbrook, T. H., Sun, N., Zhang, X. B., Zhang, S. X., Jiao, J. H., et al. (2021). Spatial changes and driving variables of topsoil organic carbon stocks in Chinese croplands under different fertilization strategies. *Sci. Total Environ.* 767:144350. doi: 10.1016/j.scitotenv.2020.144350

Ren, C. J., Zhang, X. Y., Zhang, S. H., Wang, J. Y., Xu, M. P., Guo, Y. X., et al. (2021). Altered microbial CAZyme families indicated dead biomass decomposition following afforestation. *Soil Biol. Biochem.* 160:108362. doi: 10.1016/j.soilbio.2021.108362

Richy, E., Cabello-Yeves, P. J., Hernandes-Coutinho, F., Rodriguez-Valera, F., González-Alvarez, I., Gandois, L., et al. (2024). How microbial communities shape peatland carbon dynamics: new insights and implications. *Soil Biol. Biochem.* 191:109345. doi: 10.1016/j.soilbio.2024.109345

Sinsabaugh, R. L. (2010). Phenol oxidase, peroxidase and organic matter dynamics of soil. *Soil Biol. Biochem.* 42, 391–404. doi: 10.1016/j.soilbio.2009.10.014

Sokol, N. W., Sanderman, J., and Bradford, M. A. (2019). Pathways of mineral-associated soil organic matter formation: integrating the role of plant carbon source, chemistry, and point of entry. *Glob. Chang. Biol.* 25, 12–24. doi: 10.1111/gcb.14482

Su, Z. X., Zhong, Y. Q. W., Zhu, X. Y., Wu, Y., Shen, Z. F., and Shangguan, Z. P. (2023). Vegetation restoration altered the soil organic carbon composition and favoured its stability in a *Robinia pseudoacacia* plantation. *Sci. Total Environ.* 899:165665. doi: 10.1016/j.scitotenv.2023.165665

Trivedi, P., Delgado-Baquerizo, M., Trivedi, C., Hu, H. W., Anderson, I. C., Jeffries, T. C., et al. (2016). Microbial regulation of the soil carbon cycle: evidence from gene-enzyme relationships. *ISME J.* 10, 2593–2604. doi: 10.1038/ismej.2016.65

Wang, X. Y., Liang, C., Mao, J. D., Jiang, Y. J., Bian, Q., Liang, Y. T., et al. (2023). Microbial keystone taxa drive succession of plant residue chemistry. *ISME J.* 17, 748–757. doi: 10.1038/s41396-023-01384-2

Wang, Q. C., Yang, L. M., Song, G., Jin, S. S., Hu, H. W., Wu, F. Z., et al. (2022). The accumulation of microbial residues and plant lignin phenols are more influenced by fertilization in young than mature subtropical forests. *For. Ecol. Manag.* 509:120074. doi: 10.1016/j.foreco.2022.120074

Whalen, E. D., Grandy, A. S., Sokol, N. W., Keiluweit, M., Ernakovich, J., Smith, R. G., et al. (2022). Clarifying the evidence for microbial- and plant-derived soil organic matter, and the path toward a more quantitative understanding. *Glob. Chang. Biol.* 28, 7167–7185. doi: 10.1111/gcb.16413

Wiseschart, A., Mhuantong, W., Tangphatsornruang, S., Chantasingh, D., and Pootanakit, K. (2019). Shotgun metagenomic sequencing from Manao-pee cave, Thailand, reveals insight into the microbial community structure and its metabolic potential. *BMC Microbiol.* 19:144. doi: 10.1186/s12866-019-1521-8

Xiong, L., Drosos, M., Wang, P., Zhang, W. X., Jin, W., Wang, S. X., et al. (2023). The divergent accumulation mechanisms of microbial necromass C in paddy soil under different long-term fertilization regimes. *Geoderma* 439:116688. doi: 10.1016/j.geoderma.2023.116688

Yan, Z. Q., Kang, E. Z., Zhang, K. R., Hao, Y. B., Wang, X. D., Li, Y., et al. (2022). Asynchronous responses of microbial CAZymes genes and the net CO_2 exchange in alpine peatland following 5 years of continuous extreme drought events. *ISME Commun.* 2:115. doi: 10.1038/s43705-022-00200-w

Yan, D. Z., Wang, D. J., and Yang, L. Z. (2007). Long-term effect of chemical fertilizer, straw, and manure on labile organic matter fractions in a paddy soil. *Biol. Fertil. Soils* 44, 93–101. doi: 10.1007/s00374-007-0183-0

Yang, Y., Dou, Y. X., Wang, B. R., Wang, Y. Q., Liang, C., An, S. S., et al. (2022). Increasing contribution of microbial residues to soil organic carbon in grassland restoration chronosequence. *Soil Biol. Biochem.* 170:108688. doi: 10.1016/j.soilbio.2022.108688

Yang, J., Gao, W., and Ren, S. R. (2015). Long-term effects of combined application of chemical nitrogen with organic materials on crop yields, soil organic carbon and total nitrogen in fluvo-aquic soil. *Soil Tillage Res.* 151, 67–74. doi: 10.1016/j.still.2015.03.008

Yang, L., Luo, Y., Lu, B. L., Zhou, G. P., Chang, D. N., Gao, S. J., et al. (2023). Long-term maize and pea intercropping improved subsoil carbon storage while reduced greenhouse gas emissions. *Agric. Ecosyst. Environ.* 349:108444. doi: 10.1016/j.agee.2023.108444

Ye, G. P., Lin, Y. X., Kuzyakov, Y., Liu, D. Y., Luo, J. F., Lindsey, S., et al. (2019). Manure over crop residues increases soil organic matter but decreases microbial necromass relative contribution in upland Ultisols: results of a 27-year field experiment. *Soil Biol. Biochem.* 134, 15–24. doi: 10.1016/j.soilbio.2019.03.018

Zhang, X. D., and Amelung, W. (1996). Gas chromatographic determination of muramic acid, glucosamine, mannosamine, and galactosamine in soils. *Soil Biol. Biochem.* 28, 1201–1206. doi: 10.1016/0038-0717(96)00117-4

Zhang, B. G., Cai, Y. J., Hu, S. J., and Chang, S. X. (2021). Plant mixture effects on carbon-degrading enzymes promote soil organic carbon accumulation. *Soil Biol. Biochem.* 163:108457. doi: 10.1016/j.soilbio.2021.108457

Zhang, C., Du, X. P., Zeng, Y. H., Zhu, J. M., Zhang, S. J., Cai, Z. H., et al. (2021). The communities and functional profiles of virioplankton along a salinity gradient in a subtropical estuary. *Sci. Total Environ.* 759:143499. doi: 10.1016/j.scitotenv.2020.143499

Zhou, R. R., Liu, Y., Dungait, J. A. J., Kumar, A., Wang, J. S., Tiemann, L. K., et al. (2023). Microbial necromass in cropland soils: a global meta-analysis of management effects. *Glob. Chang. Biol.* 29, 1998–2014. doi: 10.1111/gcb.16613

Zhu, X. F., Jackson, R. D., DeLucia, E. H., Tiedje, J. M., and Liang, C. (2020). The soil microbial carbon pump: from conceptual insights to empirical assessments. *Glob. Chang. Biol.* 26, 6032–6039. doi: 10.1111/gcb.15319

Zifcáková, L., Vetrovsky, T., Howe, A., and Baldrian, P. (2016). Microbial activity in forest soil reflects the changes in ecosystem properties between summer and winter. *Environ. Microbiol.* 18, 288–301. doi: 10.1111/1462-2920.13026

Zifcáková, L., Vetrovsky, T., Lombard, V., Henrissat, B., Howe, A., and Baldrian, P. (2017). Feed in summer, rest in winter: microbial carbon utilization in forest topsoil. *Microbiome* 5:122. doi: 10.1186/s40168-017-0340-0

frontiers | Frontiers in Microbiology

TYPE Original Research
PUBLISHED 20 May 2025
DOI 10.3389/fmicb.2025.1590788

Check for updates

OPEN ACCESS

EDITED BY
Muhammad Zahid Mumtaz,
Gansu Agricultural University, China

REVIEWED BY
Lajos Ács-Szabó,
University of Debrecen, Hungary
Denver Inladchang Walitang,
Romblon State University, Philippines
Muhammad Saqlain Zaheer,
Khwaja Fareed University of Engineering and Information Technology (KFUEIT), Pakistan

*CORRESPONDENCE
Wen-tao Sun
✉ wentaosw@163.com

RECEIVED 10 March 2025
ACCEPTED 02 May 2025
PUBLISHED 20 May 2025

CITATION
Jia S, Li Y-D, Qu H, Li B, Juan Y-h, Xing Y-h, Liu Y, Bao H-j and Sun W-t (2025) Straw retention drives microbial community succession to improve soil C/N cycling: insights from a multi-year rice-based system. *Front. Microbiol.* 16:1590788. doi: 10.3389/fmicb.2025.1590788

COPYRIGHT
© 2025 Jia, Li, Qu, Li, Juan, Xing, Liu, Bao and Sun. This is an open-access article distributed under the terms of the Creative Commons Attribution License (CC BY). The use, distribution or reproduction in other forums is permitted, provided the original author(s) and the copyright owner(s) are credited and that the original publication in this journal is cited, in accordance with accepted academic practice. No use, distribution or reproduction is permitted which does not comply with these terms.

Straw retention drives microbial community succession to improve soil C/N cycling: insights from a multi-year rice-based system

Shu Jia[1], Yue-Dong Li[2], Hang Qu[1], Bo Li, Ying-hua Juan[1], Yue-hua Xing[1], Yan Liu[1], Hong-jing Bao[1] and Wen-tao Sun[1]*

[1]Institute of Plant Nutrition and Environmental Resources, Liaoning Academy of Agricultural Sciences, Shenyang, China, [2]Liaoning Rice Research Institute, Liaoning Academy of Agricultural Sciences, Shenyang, China

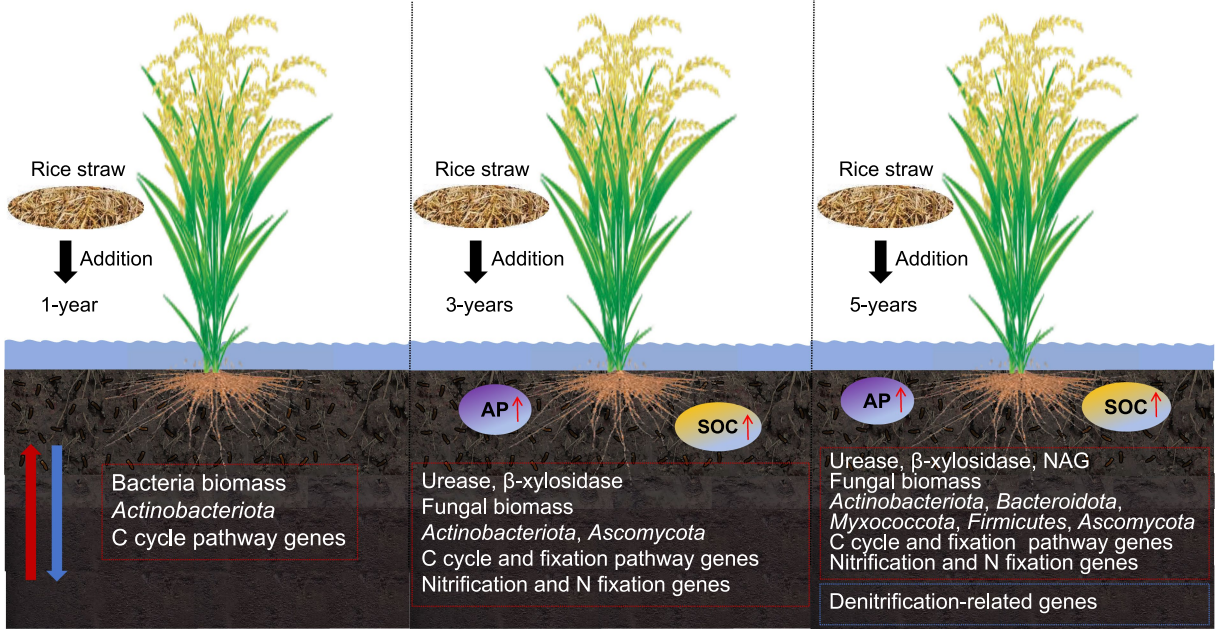
The soil microbial community plays a crucial role in driving the decomposition and mineralization of plant residues, thereby affecting carbon (C) and nitrogen (N) cycling and storage. Straw retention provides soil with C and N sources, which enhances microbial community composition and nutrient cycling. While long-term straw retention has been shown to improve soil quality and nutrient-use efficiency, the impacts of short-term straw-return treatment on soil quality and the underlying microbiological mechanism of straw in improving soil fertility and nutrient-use efficiency remain unclear. The present study aimed to elucidate the dynamic responses of soil microbial community structure and function to rice straw retention using a multi-year field experiment. The findings revealed that rice straw returned for 3 and 5 consecutive years (S3 and S5, respectively), enhanced soil organic carbon (SOC) and available phosphorous (AP) contents, increased fungal biomass, and stimulated the growth of cellulose-decomposing microbial communities. Furthermore, S3 and S5 treatments increased the activities of C cycling enzymes (β-xylosidase) and N cycling enzymes (N-acetyl-glucosaminidase and urease). These treatments also increased the genes abundance associated with C-cycling (*sdimo*), nitrification (*amoA* and *amoB*), and N fixation (*nifH*), while enriched genes related to C cycling and N metabolism pathways (nitrification and nitrate reduction). In contrast, the abundance of genes involved in denitrification (*nirS*) was reduced. However, S3 and S5 treatments led to an increased abundance of the plant pathogens *Magnaporthe oryzae* and *Ustilaginoidea virens*. This work demonstrates that short-term straw retention effectively enhances soil microecological environment and microbial functionality and also underscores the need for strategies to mitigate pathogen accumulation for sustainable agricultural practices.

KEYWORDS

rice straw retention, soil microbial community, microbial function, carbon cycle, nitrogen cycle

1 Introduction

Soil microorganisms are vital biological indicators for assessing agricultural soil quality and ecosystem functionality (Coban et al., 2022; Yuan et al., 2024; Pang et al., 2024). They play a crucial role in sustainable crop productivity by facilitating nutrient cycling and organic matter decomposition, enhancing plant immunity, and contributing to soil remediation (Klimasmith and



GRAPHICAL ABSTRACT

Kent, 2022). As the most active components of soil microecosystems, microorganisms are highly sensitive to environmental changes and agricultural interventions, such as tillage and fertilization (Liu et al., 2020; Yin et al., 2025; Zhang et al., 2023). Different fertilizer application patterns and management practices directly impact crop yields and significantly drive changes in the composition and function of soil microbial communities (Tang et al., 2023; Yang et al., 2025).

Rice is one of the most important food crops globally and serves as the main source of food for more than half of global population. The stable production of rice is crucial for global food security. With the continuous growth of the world economy and population, the demand for both rice yield and quality has steadily increased (Yang et al., 2019). To enhance rice production, large quantities of fertilizers are widely utilized. However, the prolonged use of chemical fertilizers in agriculture adversely impacts soil quality and microecology (Huang Y. P. et al., 2021; Yang et al., 2022), ultimately affecting soil productivity and health (Wang et al., 2022).

Several studies have shown that the prolonged use of chemical fertilizers, particularly nitrogen (N), significantly reduces soil microbial diversity and biomass, disrupts the stability of the bacterial community structures (Wang et al., 2018), and adversely affects soil microbial N fixation and signal transduction functions (Li et al., 2020). Furthermore, excessive fertilizer application can enrich ammonia oxidation functional genes in soil microorganisms, leading to nitrate accumulation, leaching, and increased N2O emissions, ultimately affecting soil nutrient-use efficiency and farmland productivity (Bai et al., 2022; Lin et al., 2025). Therefore, achieving sustainable agricultural production requires the implementation of scientific fertilization techniques that can improve soil quality and soil microecological environment while ensuring rice yield.

The long-term application of organic fertilizers, including animal manure, green manure, and crop straw, can significantly increase soil nutrient content (Cui et al., 2024) and microbial biomass (Cui et al., 2023), improve soil microbial structures, and promote soil nutrient cycling and utilization (Zhou J. S. et al., 2024; Zhou G. P. et al., 2024). In China, crop straw resources are abundant, and straw is rich in essential nutrients, such as N, phosphorus (P), and potassium (K). When returned to the field, straw can mitigate the need for extensive chemical fertilizer application (Liu J. A. et al., 2021). Straw retention facilitates the transport of carbon (C) and nitrogen (N) sources to the soil, thereby improving microbial activity, composition, and function (Yuan et al., 2023). This process increases microbial functional diversity (Xu et al., 2023) and improves soil nutrient availability (Wang Y. J. et al., 2020), making it an effective strategy for sustainable agriculture.

Despite the positive effects of returning straw to the field, existing research has primarily focused on long-term (more than 10 years) straw-return treatment, while studies investigating the impacts of short-term (less than 10 years) straw-return treatments on soil quality and microecology remain limited. Additionally, the microbiological mechanisms through which straw improves soil fertility and nutrient-use efficiency are still poorly understood. The objective of this study was to evaluate the effects of rice straw retention on soil properties, soil microbial activities, and the dynamic responses of soil microbial community structures and potential functions under continuous straw retention using a 1-, 3-, and 5-year rice straw retention field experiment. We aimed to characterize straw-responsive microbial communities that drive soil nutrient cycling and elucidate their functional mechanisms in improving soil fertility and nutrient-use efficiency. Genomic DNA extracted from soil samples was subjected to: (i) quantitative PCR (qPCR) for microbial abundance quantification, (ii) Illumina MiSeq platform-based 16S rRNA gene sequencing for microbial community profiling, and (iii) shotgun metagenomic sequencing for functional gene analysis, enabling comprehensive tracking of microbial succession and characterization of key genes involved in carbon and nitrogen cycling processes. The soil physicochemical properties and enzyme activities related to C and N cycling were also elucidated. Furthermore, we assessed changes in

the abundance of potential plant pathogens. This study provides a theoretical foundation for the fertilizer utilization of straw resources and promotes sustainable agricultural development.

2 Materials and methods

2.1 Experimental design and sample collection

The experimental field was in Tongerpu Town, Dengta City, Liaoyang City, Liaoning Province, China (41° 45′N, 123° 04′E). The region is characterized by a temperate, northern continental climate with an average annual precipitation of 500–700 mm, an average annual temperature of 6–8°C, and a frost-free period of approximately 150 days. The tested field soil comprised Hydragric Anthrosols; its physical and chemical properties are listed in Supplementary Table S1.

The experimental field involved four treatments (each treatment area was 348.84 m^2, i.e., 22.80 × 15.30 m): (1) control (SCK): rice straw was not returned to the field; (2) S1: rice straw was returned to the field for 1 year (2022); (3) S3: rice straw was returned to the field consecutively for 3 years (2020–2022); and (4) S5: the straw was returned consecutively to the field for 5 years (2018–2022). The experiment was arranged in a randomized complete block design (RCBD) with three replicates, where all treatments were randomly assigned within each block to account for field variability. This study used the rice variety Liaojing 401, which was planted using a rice transplanter. Seedlings were transplanted at a row spacing of 33.33 × 18.00 cm. Each year, rice seedlings were transplanted in early May, and rice plants were harvested in early October. After harvest, the rice straw was chopped into approximately 10 cm pieces and then directly returned to the field for rotational tillage. The amount of returned straw was 9.0 t ha^{-1} with the following fertilizer application rates: N 210 kg ha^{-1}, P_2O_5 60 kg ha^{-1}, and K_2O 120 kg ha^{-1}. Chemical N fertilizer was applied as a basal, tillering, and panicle fertilizer (application ratio: 5:3:2). Chemical K_2O and P_2O_5 were also applied as basal fertilizers. The chemical N, P, and K fertilizers were urea, potassium dihydrogen phosphate, and potassium chloride. In mid-October 2023, five topsoil cores (5 cm diameter × 20 cm depth; free from visible crop roots) were systematically collected from inter-rows of each plot using a stainless steel corer and homogenized to form one composite sample per plot. A total of 12 fresh soil samples were collected (four treatments × three replicates), transported on ice to the laboratory within 1 h, and immediately passed through a 2-mm mesh to remove roots and rocks. The soil was then divided into three parts: (1) immediately stored at −80°C for molecular analyses (high-throughput sequencing analysis, metagenomic sequencing, and qRT-PCR analysis), (2) preserved at 4°C for enzyme activity assays within 2 h; and (3) air-dried (25°C, 7 d) for physicochemical characterization.

For enzyme activity measurements, we quantified the activities of carbon-cycling enzymes (β-glucosidase [BG], cellobiohydrolase [CBH], and β-xylosidase) and nitrogen-cycling enzymes (N-acetyl-glucosaminidase [NAG], L-leucine aminopeptidase [LAP], and urease) using commercial kits (Shanghai Enzyme-linked Biotechnology, China) following the manufacturer's protocol with the following modifications: soil suspensions (1:10 w/v in 50 mM acetate buffer, pH 5.5) were incubated at 37°C for 2–4 h depending on the enzyme, with reactions terminated by alkaline solution (0.5 M NaOH) before spectrophotometric analysis.

2.2 DNA extraction and qRT-PCR

Soil DNA was extracted from fresh soil (0.5 g) using an E.Z.N.A.® soil DNA Kit (Omega Bio-tek, Norcross, GA, United States) according to the manufacturer's instructions. The concentration and quality of extracted DNA were evaluated using an ND-2000 spectrophotometer (Thermo Fisher Scientific, Wilmington, DE, United States).

The gene absolute abundance of the bacteria, fungi, and other functional microorganisms related to C and N cycling were evaluated using qRT-PCR. The selected genes for this evaluation included 16S rRNA and ITS rRNA, as well as genes associated with C cycling, specifically *cbhI* (encoding cellobiohydrolase I, EC 3.2.1.91, catalyzing cellulose hydrolysis), *GH48* (glycoside hydrolase family 48 gene, involved in crystalline cellulose degradation), and *sdimo* (soluble diiron monooxygenase gene, mediating aromatic compound oxidation). For N cycling, the examined genes included *nifH* (nitrogenase reductase, EC 1.18.6.1, for biological N_2 fixation), *amoA* and *amoB* (ammonia monooxygenase subunits, EC 1.7.3.4, for nitrification), *narG* (respiratory nitrate reductase, EC 1.7.99.4, for nitrate reduction), *nirK* and *nirS* (copper- and cytochrome cd_1-type nitrite reductases, EC 1.7.2.1, for denitrification), and *nosZ* (nitrous oxide reductase, EC 1.7.2.4, for N_2O reduction). To evaluate the effects of continuous straw return on the abundance of rice pathogenic fungi in soil, we quantified the gene copy number of *Magnaporthe oryza* and *Ustilaginoidea virens*. Gene copy numbers (absolute abundance) were determined using qRT-PCR with a Line-Gene 9600 Plus real-time PCR detection system (Bioer, Hangzhou, China). Detailed information regarding the primers and qRT-PCR conditions is provided in the Supplementary Table S2 (Li et al., 2011, Sun et al., 2013, Yang et al., 2021). Each sample was amplified in triplicate. Gene copy numbers were calculated using standard curves generated by amplifying known DNA quantities from recombinant plasmids carrying each target.

2.3 High-throughput sequencing analysis

To explore the diversity and structures of the soil bacteria and fungi, DNA from the soil samples was sequenced using an Illumina MiSeq 300 platform (Illumina, San Diego, United States). The primer pairs 338F/806R and ITS1/ITS2 were used for bacteria and fungi, respectively (Supplementary Table S2). Sequence reads were demultiplexed, quality-filtered using fastp (version 0.20.0; Chen et al., 2018), and merged using FLASH (version 1.2.11[1]). The operational taxonomic units (OTUs) were clustered with a 97% similarity cutoff using UPARSE (version 7.1[2]). Chimeric sequences were identified and removed using UCHIME (Edgar 2013). The taxonomy of each gene sequence was analyzed using the RDP Classifier (version 2.11[3]) against the Silva (Release138) and Unite (Release 8.0[4]) databases, with a 70% [5]confidence threshold.

1 https://sourceforge.net/projects/flashpage/
2 http://drive5.com/uparse/
3 http://rdp.cme.msu.edu/
4 http://unite.ut.ee/index.php
5 http://www.arbsilva.de

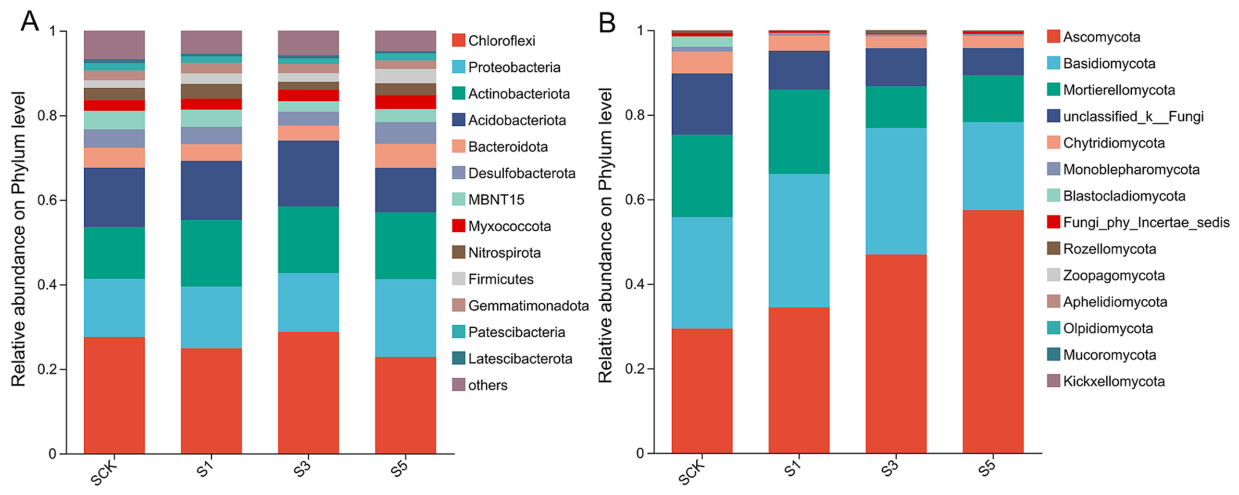


FIGURE 1
Relative abundances of the bacterial **(A)** and fungal **(B)** phyla in different treatments. SCK, the straw was not returned to the field; S1, S3, and S5, the straw was returned to the field consecutively for 1, 3, and 5 years, respectively.

2.4 Shotgun metagenomic sequencing

DNA extracts were fragmented to an average of 400 bp using Covaris M220 (Gene Company Limited, China) for paired-end library construction. The paired-end library was constructed using NEXTFLEX® Rapid DNA-Seq (Bioo Scientific, Austin, TX, United States). Adapters containing the full complement of sequencing primer hybridization sites were ligated to the blunt-ends of the fragments. Paired-end sequencing was performed on Illumina NovaSeq (Illumina Inc., San Diego, CA, United States) at Majorbio Bio-Pharm Technology Co., Ltd. (Shanghai, China) using a NovaSeq 6000 S4 Reagent Kit v1.5 (300 cycles) according to the manufacturer's instructions.[6]

2.5 Statistical analyses

The data were analyzed using the freely available Majorbio Cloud Platform.[7] The Mothur software was used to calculate the alpha diversity index using random sampling. Alpha diversity and richness were determined at the OTU level using the Shannon and Chao1 indices, respectively. Analysis of variance was used to compare the statistical differences among groups. Significant differences were identified at the 95% confidence level. The p value was corrected using a multiple test with false discovery rate (FDR) and results with $p < 0.05$ were considered statistically significant. Similarities in the samples in terms of microbial taxa (bacteria and fungi) and profiles of gene family relative abundance (Kyoto Encyclopedia of Genes and Genomes [KEGG] and Carbohydrate-Active Enzyme [CAZy] databases) were measured using the unweighted UniFrac distance for phylogenetic relationships and the Bray–Curtis dissimilarity index for gene families. A one-way analysis of the similarity test with 999 permutations was conducted to evaluate statistical significance. The Mann–Whitney U-test was used to evaluate differences in two-group comparisons. The p-value was corrected using multiple tests with a false discovery rate. Redundancy analysis (RDA) and Spearman's correlation analysis were used to study the correlations between soil environmental factors, microbial community modifications, and microbial functionality induced by straw return over several consecutive years. Unless otherwise stated, statistical analyses were conducted, and plots were generated using R software (version 3.3.1).

3 Results

3.1 Soil physicochemical properties and enzyme activities under straw retention

Total N (TN), total P (TP), total K (TK), and available N (AN; $p > 0.05$) tended to improve with straw return, whereas soil organic C (SOC) and available phosphorous (AP) contents were significantly increased in S3 and S5 ($p < 0.05$; Supplementary Table S1). Straw retention also had a significant positive effect on the activities of C and N cycle-related enzymes (Supplementary Table S3), and β-xylosidase, NAG, and urease were increased by 69.39, 45.12, and 17.41% compared with the levels in the CK, respectively ($p < 0.05$).

3.2 Microbial communities under straw retention

Compared with CK, the gene copy number of the 16S rRNA in S1 increased significantly ($p < 0.05$), while S3 and S5 returned to levels comparable to CK, with no significant differences ($p > 0.05$, Supplementary Table S4). In S3 and S5, the absolute abundance of the ITS rRNA gene was significantly higher ($p < 0.05$). These results

6 http://www.illumina.com
7 http://www.majorbio.com

revealed that straw retention for 3 and 5 years significantly increased fungal biomass but not bacterial biomass.

After quality filtering, a total of 574,880 bacteria 16Sv3-v4 and 782,583 fungal ITS1 high-quality sequences were obtained for the soil samples from four treatments. Subsequently, 49,124 bacterial and 5,517 fungal operational taxonomic units (OTUs) were assembled at a 97% confidence interval (Supplementary Table S5). For bacterial communities, S1 exhibited significantly reduced richness compared to CK ($p < 0.05$, Supplementary Figure S1), while no significant differences were observed in either richness or diversity among CK, S3, and S5 ($p > 0.05$). For fungal communities, the diversity and evenness in S5 was significantly lower than that in CK ($p < 0.05$), with no significant differences in richness or diversity detected among CK, S1, and S3 ($p > 0.05$).

The predominant bacterial phyla (>1%) in the soil included Chloroflexi, Proteobacteria, Actinobacteriota, Acidobacteriota, Bacteroidota, Desulfobacterota, Myxococcota, Nitrospirota, Firmicutes, Gemmatimonadota, Patescibacteria, Latescibacterota, and "others" (bacteria with an abundance of < 1%; Figure 1A). Straw retention altered the compositions of the microbial communities (Supplementary Table S6); retention for 1 year significantly increased the abundance of Actinobacteria ($p < 0.05$), and retention for 5 years significantly increased the abundances of Proteobacteria, Bacteroidetes, Myxococcus, and Firmicutes ($p < 0.05$) and significantly decreased that of Latescibacterota ($p < 0.05$). At the genus level, straw retention for 5 years significantly increased the abundance of *Trichococcus* and *Bradyrhizobium* (Supplementary Table S7).

The predominant fungal phyla (>1%) in the soil were Ascomycota, Basidiomycota, Mortierellomycota, Chytridiomycota, Monoblepharomycota, Blastocladiomycota, Rozellomycota, and "others" (fungi with an abundance of <1%; Figure 1B). Straw retention for 5 years significantly increased the abundance of Ascomycota and significantly decreased that of Monoblepharomycota ($p < 0.05$; Supplementary Table S6). At the genus level, straw retention for 1 year significantly increased the abundances of *Mortierella*, *Mrakia*, and *Glaciozymade* and significantly decreased the abundance of *Tausonia*. All abundances returned to CK levels after 3 and 5 years (Supplementary Table S7). Straw retention for 3 and 5 years also stimulated the growth of *Pseudeurotium*, *Pseudogymnoascus*, *Sordariales*, *Trichosporiella*, *Achroiostachys*, *Clavidisculum*, and *Schizothecium* but hindered the growth of *Stellatospora* and *Linnemannia* ($p < 0.05$). Furthermore, straw retention for 5 years significantly increased the absolute abundances of *M. oryza* and *U. virens* by 348.65 and 524.73%, respectively, compared with the CK (Supplementary Table S4). Correlation network analysis of fungal communities and pathogenic fungi (Supplementary Figure S3)

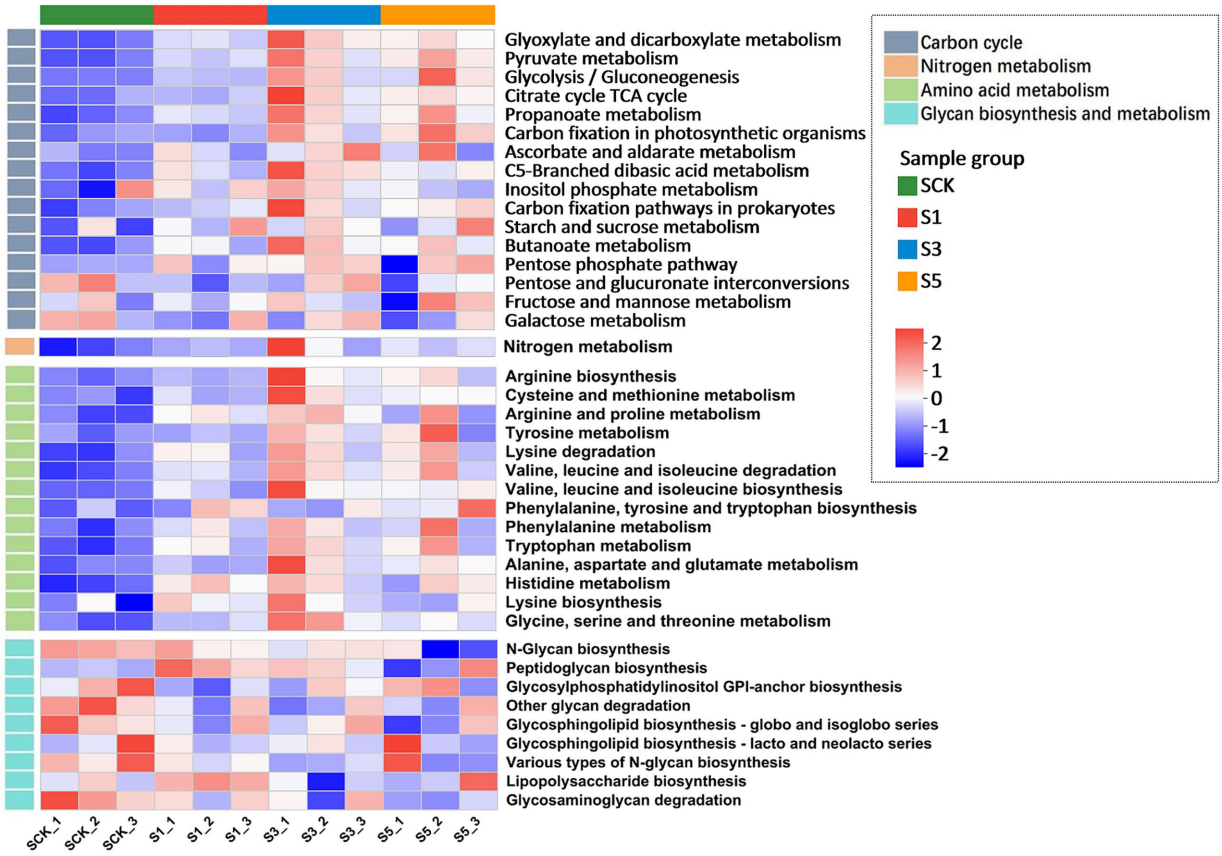


FIGURE 2
Heatmaps indicating differences in the relative abundances of functional genes related to the C and N cycles based on the Kyoto Encyclopedia of Genes and Genomes (KEGG) database. The relative abundances of the functional genes are indicated by the color intensity within the legend. The correlation coefficients ranging from negative to positive are indicated by color intensity changing from blue to red. SCK, the straw was not returned to the field; S1, S3, and S5, the straw was returned to the field consecutively for 1, 3, and 5 years, respectively.

revealed that the abundance of *U. virens* was significantly positively correlated with *Ustilaginoidea*, *Tausonia*, *Mortierellaceae*, and *Spizellomycetales* ($|r| > 0.5$, $p < 0.05$), while being significantly negatively correlated with *Sordariales* and *Mortierella* ($|r| > 0.5$, $p < 0.05$). The abundance of *M. oryzae* was significantly positively associated with *Bisifusarium* ($|r| > 0.5$, $p < 0.05$), but significantly negatively correlated with *Pseudeurotium* ($|r| > 0.5$, $p < 0.05$). Notably, *M. oryzae* was annotated as *Sordariomycetes*, which may be attributed to incomplete taxonomic coverage of the strain in the SILVA reference database, particularly for certain specialized strains or newly sequenced variants, resulting in classification resolution limited to the class level.

PICRUSt2 analysis predicted the functional abundance of soil microbiota involved in C- and N-cycling enzymes (Supplementary Figure S4). In S3 and S5, the urease abundance followed a trend consistent with measured enzyme activity and was significantly higher than in SCK ($p < 0.05$). Compared to SCK, S3 and S5 exhibited an increasing trend in β-xylosidase and NAG abundance, though the differences were not statistically significant ($p > 0.05$).

3.3 Straw retention enriches C cycling and N metabolic pathway genes

Metagenomic sequencing generated 553,203,650 raw reads across all treatments. Following normalization, we identified 2,996,412 reads matching 525 carbohydrate-active enzymes (CAZymes). The CAZy annotation identified six primary CAZy functional gene families: glycoside hydrolases (GHs), glycosyl transferases (GTs), polysaccharide lyases (PLs), carbohydrate esterases (CEs), carbohydrate-binding modules (CBMs), and auxiliary activities (AAs; Supplementary Figure S2). In S3 and S5, the abundance of GHs in the soil increased significantly ($p < 0.05$), whereas the abundance of GTs and PLs decreased significantly ($p < 0.05$).

Straw retention for 3 and 5 years significantly increased the absolute abundance of *sdimo* ($p < 0.05$; Supplementary Table S4). The S3 and S5 treatments significantly increased the absolute abundance of some soil functional genes associated with N cycling, such as nitrification-related genes (*amoA* and *amoB*) and N fixation-related genes (*nifH*), but significantly decreased the abundance of denitrification-related genes (*nirS*; $p < 0.05$).

Metabolic pathway heat map analysis showed that straw retention stimulated the enrichment of genes involved in the C cycle, N metabolism, and amino acid metabolism (Figure 2). The results of the C cycling functional enrichment analysis showed that straw retention for 1 year (Figure 3A) increased the abundances of genes related to the metabolism of glyoxylate, dicarboxylate, C5-branched dibasic acid, pyruvate, propionate, and butanoate and decreased genes related to the metabolism of inositol phosphate, fructose, mannose, galactose, pentose, and glucuronate interconversions. Furthermore, straw retention for 3 years increased the abundance of genes related to C fixation pathways in prokaryotes (Figure 3B). Straw retention for 5 years increased the abundance of genes related to citrate (TCA) cycling and C fixation in photosynthetic organisms (Figure 3C).

Functional enrichment analysis showed that straw retention enriched genes related to N metabolism (Figure 3D). Differentially enriched KEGG pathway analysis for N metabolism (Figure 4) showed that compared with the CK, dissimilatory nitrate reduction-related genes (*nirD*, *nirB* (1.7.1.15)) and assimilatory nitrate reduction-related genes (*narB* (1.7.7.2)) were significantly increased ($p < 0.05$) with straw retention. Conversely, straw retention decreased the abundance of denitrification-related pathway genes (*norB*, *norC* (1.7.2.5)). Furthermore, straw retention for 5 years enriched the abundance of L-asparaginase genes (*gltB*, *gltD* (1.4.1.13)), increasing the conversion between glutamine and glutamate with $NH4^+$.

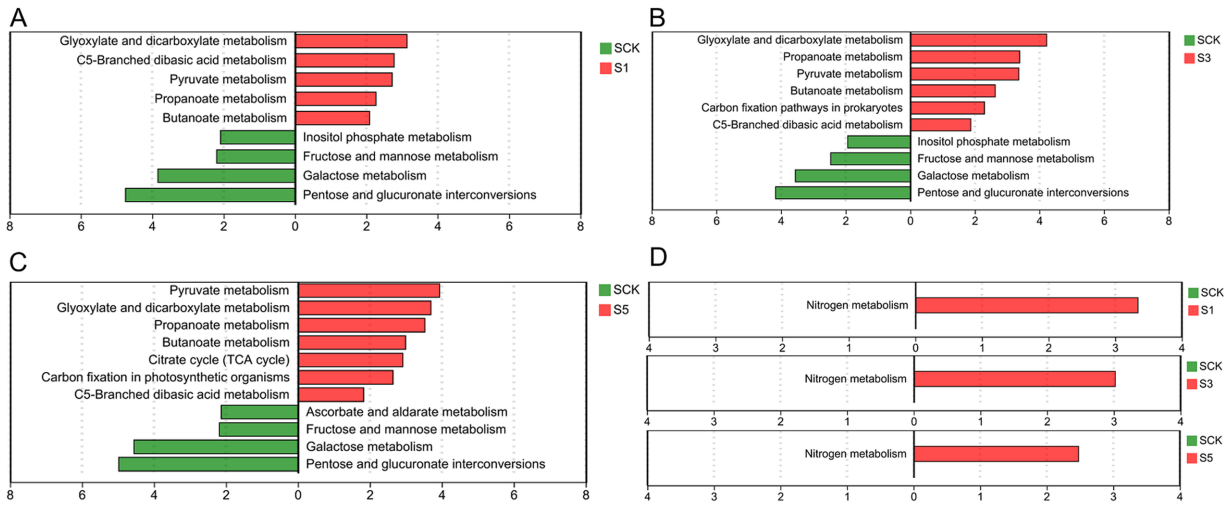


FIGURE 3
KEGG functional enrichment analysis. **(A–C)** Carbon cycling functional genes and **(D)** nitrogen metabolism genes. Green indicates genes enriched in the control group; red indicates genes enriched in the treatment group. The Student's *t*-test was used to compare statistical differences between groups. The *p* value was corrected using a multiple test with false discovery rate (FDR). SCK, the straw was not returned to the field; S1, S3, and S5, the straw was returned to the field consecutively for 1, 3, and 5 years, respectively.

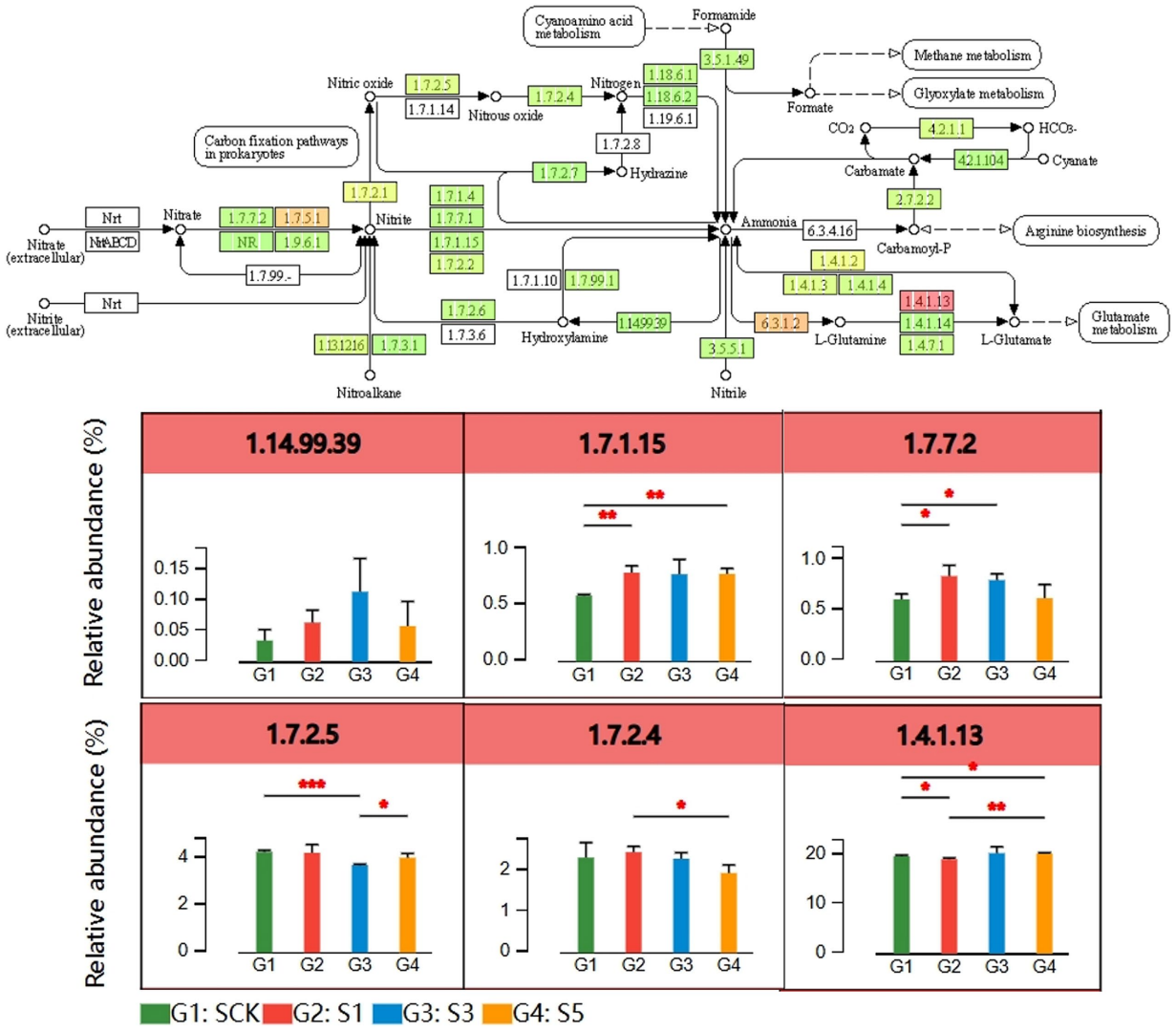


FIGURE 4
Analysis of differentially enriched KEGG pathways related to N metabolism (*$p < 0.05$; **$p < 0.01$; ***$p < 0.001$). The Student's *t*-test was used to compare statistical differences between groups. The *p* value was corrected using a multiple test with false discovery rate (FDR). SCK, the straw was not returned to the field; S1, S3, and S5, the straw was returned to the field consecutively for 1, 3, and 5 years, respectively.

3.4 Correlations among the soil microbial communities, microbial functions, and soil physiochemical properties

RDA was conducted to evaluate correlations among microbial communities, microbial functions, and soil physicochemical factors. AK significantly affected soil bacterial communities ($r = 0.576$; $p = 0.026$; Figure 5A), whereas soil TN ($r = 0.509$; $p = 0.042$) and AK ($r = 0.465$; $p = 0.056$) were positively correlated with the soil fungal communities (Figure 5B). SOC ($r = 0.423$; $p = 0.122$) was positively correlated with soil microbial C cycling and N metabolic pathways (Figure 5C).

Spearman's correlation coefficient analysis revealed that soil TN was significantly positively correlated with the abundance of Myxococcota, and soil TP and AP were significantly negatively correlated with the abundance of Spirospirota. The soil AK was significantly positively correlated with Acidobacteriota but significantly negatively correlated with Firmicutes (Figure 5D).

Analysis of the soil fungi community showed that the soil SOC and TP significantly correlated with the abundance of Ascomycota. Soil TK was significantly positively correlated with the abundance of Rozellomycota, whereas soil AN was negatively correlated with the abundance of Zoopagomycota. A significant negative correlation was observed between soil AP and the abundance of Blastocladiomycota (Figure 5E).

Analysis of the microbial function pathways showed that soil pH, TP, and C fixation by photosynthetic organisms were significantly positively correlated. TP and AP were significantly positively correlated with the TCA cycle. Furthermore, TK was significantly negatively correlated with galactose, starch, and sucrose metabolism, and AN was significantly positively correlated with ascorbate and aldarate metabolism. Soil AK was significantly negatively correlated with carbon fixation in photosynthetic organisms but positively correlated with galactose metabolism (Figure 5F).

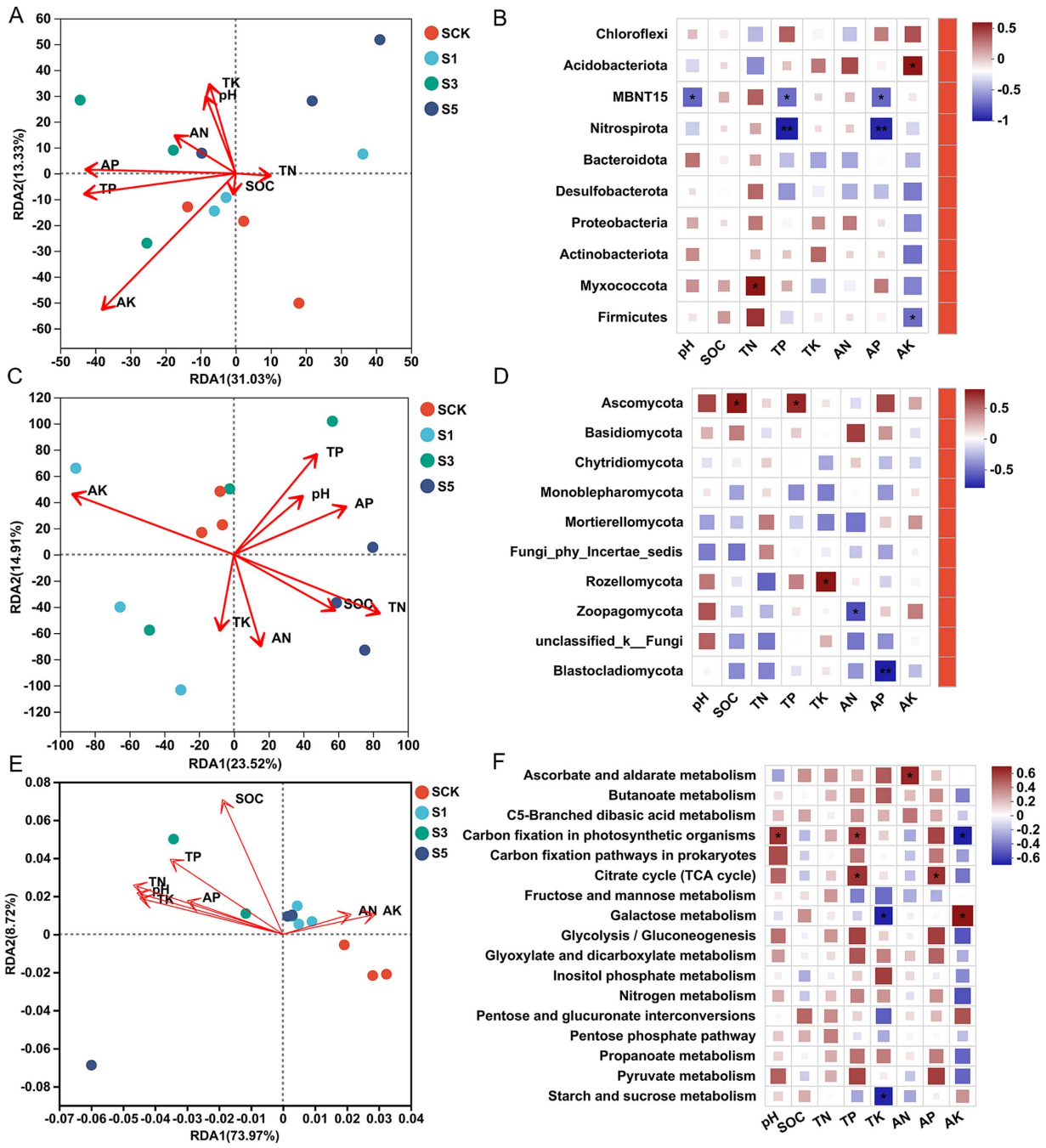


FIGURE 5
Redundancy analysis (RDA) and Spearman's correlation analysis of soil physicochemical properties with bacteria **(A,D)**, fungal microbial communities **(B,E)**, and microbial functions **(C,F)**. The *p* value was corrected using a multiple test with false discovery rate (FDR). *$p < 0.05$ and **$p < 0.01$.

3.5 C cycle- and N metabolism-related taxa and function contribution analysis

The correlations between the top 100 genera in terms of microbial abundance, C cycle, and N metabolism in the soil were evaluated using a correlation network diagram ($|r| > 0.8$; $p < 0.001$; Figure 6A). Thirty-three genera showed significant positive correlations with the C cycling pathway. Furthermore, *Planctomycetota*, *Deltaproteobacteria*, *Terriglobia*, *Armatimonadota*, *Thermoanaerobaculia*, *Acidobacteriota*, and *Nitrospirota* were significantly positively correlated with 10 or more C cycling pathways and N metabolic pathways, indicating that these bacteria form core functional microbiomes in the soil. In addition, g__*Sphingomonas* was significantly negatively correlated with seven C cycling and N metabolic pathways.

Species and functional contribution analysis revealed (Figure 6B) that the abundance of *Actinomycetes*, *Nocardioides*, *Actinomycetota*, *Bradyrhizobium*, *Hyphomicrobiales*, *Alphaproteobacteria*, and *Thermoflexales* increased in eight enhanced C cycling pathways. The abundance of *Nocardioides*, *Bradyrhizobium*, *Actinomycetota*,

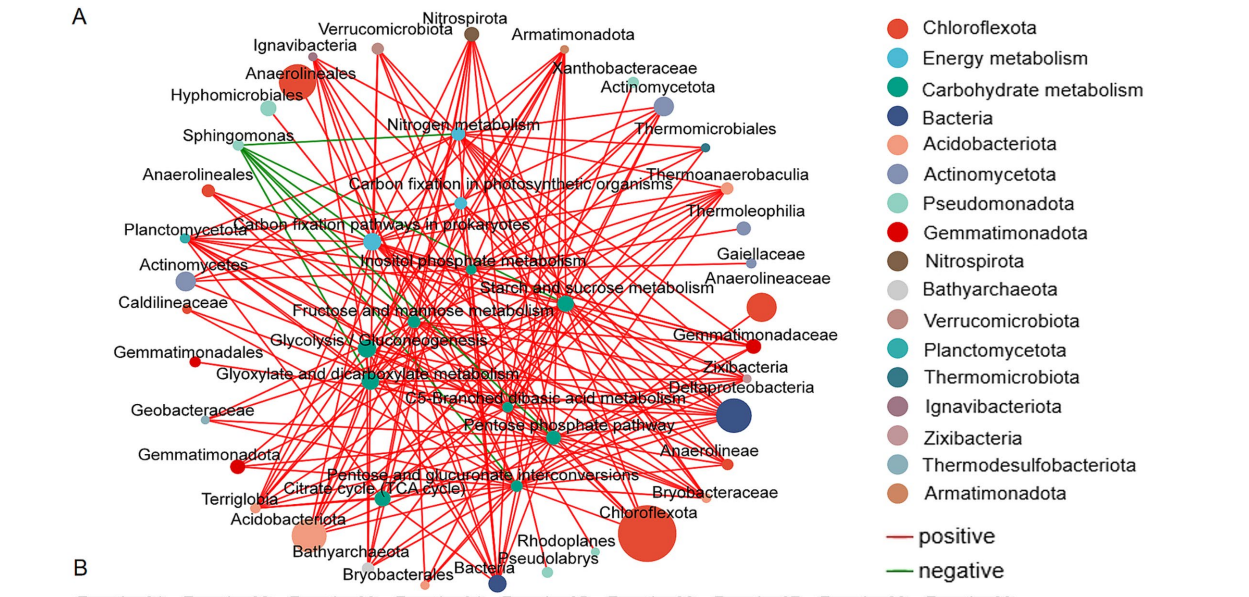


FIGURE 6
Correlation network analysis between species and the C-cycle, N-metabolism **(A)**, and functional contribution analysis **(B)**. Statistical correlations were examined through Spearman's rank-order correlation analysis, with strong significant associations defined by $|r| > 0.8$ and $p < 0.001$. The r value is indicated by the color intensity within the legend. The correlation coefficients ranging from negative to positive are indicated by color intensity changing from blue to red. Function01: pyruvate metabolism; Function02: carbon fixation pathways in prokaryotes; Function03: glyoxylate and dicarboxylate metabolism; Function04: butanoate metabolism; Function05: citrate cycle (TCA cycle); Function06: propanoate metabolism; Function07: nitrogen metabolism; Function08: carbon fixation in photosynthetic organisms; Function09: C5-branched dibasic acid metabolism.

Burkholderiales, *Hyphomicrobiales*, and *Thermoleophilia* increased in the N metabolic pathways.

4 Discussion

4.1 Effects of straw retention on soil nutrient content

Straw decomposition releases nutrients such as C, N, P, and K, which enhance the availability of nutrients in the soil and increase soil fertility and organic matter content. Long-term, straw return with appropriate fertilizer can significantly enhance SOC, TN, AP, and AK (Su et al., 2020; Huang W. et al., 2021). In a previous study, short-term (5 years) straw return significantly enhanced soil SOC and AP levels (Xu et al., 2021). Similarly, SOC content was significantly increased when corn straw was returned to the field for two consecutive years (Fan and Wu, 2020), which is consistent with our findings. In this study, straw retention for 3 and 5 years significantly increased SOC and AP contents in the soil. These results indicate that continuous straw return rapidly increases SOC and AP. In contrast, increases in TK, TP, TN, AN, and AK levels were gradual and nonsignificant, even after 5 years of continuous straw return. SOC is recognized as a crucial indicator of soil fertility and significantly contributes to the sustainability of agroecosystems because of its effects on soil nutrient cycling,

microbial properties, and physical structures (Liu et al., 2020; Peng et al., 2025).

4.2 Effects of straw retention on soil microbial communities

The soil microbial community, the most dynamic component of the soil microecosystem, is the vital biological indicator of soil quality and the most responsive factor to straw return (Liu et al., 2020). Straw retention increases microbial biomass by providing energy and nutrients for the growth of microbial communities (Sarker et al., 2019). Previous studies have found that short-term (3 years) crop residue return increases soil bacterial and fungal biomass (Chen et al., 2017). Long-term (14 and 30 years) straw return increases the soil fungal biomass but not bacterial biomass (Liu et al., 2022; Zhao et al., 2016). In this study, the bacterial biomass increased significantly, whereas the fungal biomass did not change significantly during the first year of straw retention. After 3 and 5 years of straw retention, the bacterial biomass reverted to the control levels, whereas the fungal biomass increased significantly. In the early stages of straw return, the presence of fresh, loosely structured plant residues with high water content attracts a large number of soil bacteria that facilitate the decomposition of straw. Initially, easily degradable components such as starch, hemicellulose, and cellulose are decomposed. In later stages, more recalcitrant compounds such as lignin are gradually broken down by soil fungi (Yu et al., 2020). With continuous straw return, the accumulation of lignin stimulates the growth of fungal biomass responsible for its decomposition.

Although 1 year of straw incorporation increased the absolute abundance of bacterial, it significantly decreased bacterial species richness. This reduction may be attributed to straw addition promoting the growth of cellulose-degrading bacteria, which occupied ecological niches and suppressed non-cellulose-degrading bacteria. With continuous straw incorporation, soil fungal diversity showed a significant decline by the fifth year. This phenomenon primarily resulted from the progressive accumulation of recalcitrant lignin in the soil under long-term straw application. This process selectively enriched lignin-degrading fungi, which gradually became the dominant decomposers, while the abundance of non-lignin-degrading fungi remained stable or decreased. Consequently, these changes led to a less even distribution of fungal species, ultimately reducing overall diversity.

The bacterial community composition underwent significant alterations. Straw retention for 5 years stimulated significant eutrophic bacterial growth, including Proteobacteria, Bacteroidota, and Firmicutes, which use labile forms of C for growth and metabolism and grow faster in nutrient-rich environments. The observed increase in bacterial growth can be attributed to enhanced soil fertility resulting from continuous straw retention. Bacteroidota and Firmicutes are fast-growing bacteria that exploit recalcitrant C sources (Huang et al., 2023). The continuous straw retention provided an abundant metabolic substrate for the growth of both Bacteroidota and Firmicutes. Moreover, compared with CK levels, straw retention tended to reduce the abundance of Nitrospirota, which could be due to their preference for lower C and N concentrations (Jin et al., 2020). Although straw return decreased the abundance of *Nitrospirae*, it significantly increased that of the N-fixing bacterium *Bradyrhizobium* and tended to decrease that of the denitrifying bacterium *Gemmatimonadetes*. This indicates that returning straw to the soil annually enhances N fixation and reduces soil denitrification, ultimately increasing TN content and reducing N loss from the soil.

For the fungal community, successive straw retention for 5 years significantly stimulated the growth of Ascomycota phylum and *Pseudeurotium*, *Pseudogymnoascus*, *Sordariales*, *Trichosporiella*, *Clavidisculum*, and *Schizothecium* genera. Ascomycota effectively degrades cellulose and lignocellulose, playing a crucial role in decomposing recalcitrant substrates (Ma et al., 2013). Compared to decomposed straw return, the abundance of Ascomycota increased with fresh straw return (Su et al., 2020). *Schizothecium* is a cellulose-degrading fungus that promotes the conversion of lignin and cellulose into humus (Liu et al., 2022). The combined application of straw and fertilizer enriched the *Schizothecium,* accelerating straw degradation (Zhang et al., 2021). Overall, continuous straw return promoted the growth and proliferation of cellulose-decomposing microbial groups.

Studies have used multitrophic ecological networks to confirm that keystone species, rather than overall microbial communities, dominate microbial stability, soil nutrient cycling function, and crop production (Fan et al., 2021; Xun et al., 2021). In this study, we identified key microbial communities related to soil C and N nutrient cycling in paddy ecosystems using correlation network, species, and functional contribution analyses. Thirty-three genera were positively correlated with C cycling and N metabolic pathways. These genera belong to Chloroflexota, Actinomycetota, Acidobacteriota, and Pseudomonadota. Moreover, *Sphingomonas* was negatively correlated with the C and N cycles. The increase in C cycling and N metabolic functions was attributed to the functional contributions of *Nocardioides*, *Actinomycetota*, *Bradyrhizobium*, *Hyphomicrobiales*, and *Thermoflexales*. These microorganisms are key to nutrient cycling in paddy soils.

4.3 Effects of straw retention on the nutrient cycling functions of soil microorganisms

Soil microorganisms play a crucial role in the mineralization and decomposition of organic matter by releasing extracellular enzymes and engaging in nutrient cycling and metabolic processes (Cui et al., 2018). An imbalance between the microbial growth environment and their stoichiometry is the primary driver of soil extracellular enzyme C decomposition (Zhou J. S. et al., 2024). Straw retention provides large amounts of C and N as substrate sources for soil enzymes, promoting enzyme activity and providing a shield against C and N loss via a buffering effect (Ning et al., 2020). In a recent study, the addition of maize straw was found to enhance the activities of BG, CBH, and dehydrogenase, as well as the abundances of the *GH48*, *cbhI*, and *cbbL* genes, indicating enhanced native SOC mineralization (Zhou G. P. et al., 2024). Another study found that maize straw return effectively improved the activities of urease, BG, and NAG (Ning et al., 2021), which is consistent with our findings. In this study, the continuous input of rice straw provided organic substrates for C cycling and N metabolic enzymes and significantly increased the activities of β-xylosidase, NAG, and urease; however, it had no significant effect on the activities of CBH and BG. This may be because CBH and BG are

active during the initial stage of straw decomposition, whereas β-xylosidase is activated during the later stages (Huang et al., 2023).

Straw retention for 3 and 5 years promoted soil C decomposition and mineralization by enhancing the abundance of GH family genes involved in C fixation and carbohydrate metabolism. GHs are primary carbohydrate enzymes that facilitate the hydrolysis of glycoside bonds of complex sugars into carbohydrates (Wardman et al., 2022). A recent study showed that adding exogenous C can affect the abundance of microbial genes involved in C cycling, which typically play critical roles in SOC decomposition and CO_2 fixation (Tang et al., 2021). A high C:N ratio increases the bacterial C fixation potential (Li et al., 2021; Wang et al., 2024). The input of maize straw into the soil stimulates the enrichment of soil microbial C-sequestration genes (Duan et al., 2021). Similarly, rice straw was a substrate with a high C:N ratio that enriched the genes involved in the CO_2 fixation pathway.

Biological N fixation is a crucial ecological process. Approximately 24% of the total crop biomass in farmland ecosystems originates from N fixation by nonsymbiotic microorganisms. However, long-term fertilization management has significantly weakened the N-fixing capabilities of soil microorganisms in agricultural lands. Consequently, the soil environment can no longer actively select essential N-fixing bacteria, leading to an irreversible decline in the N-fixation capacity of the soil (Fan et al., 2019). In this study, the absolute abundance of N fixation genes was increased in the fertilizer-treated straw return. This approach may help mitigate the decline in the soil microbial N fixation function typically associated with fertilizer use alone. Moreover, genes related to nitrate reduction (dissimilation and assimilation) significantly increased with the high C:N ratio established after returning rice straw to the field, reducing the rate of nitrate N to ammonia N and its accumulation in the soil ecosystem. In addition, compared with the CK, straw retention for 5 years significantly increased the abundance of functional genes associated with nitrification and significantly decreased the abundance of functional genes associated with the denitrification pathway. This shows that the addition of straw significantly improves N availability and N fertilizer usage and reduces the risk of N loss in gaseous form from soil.

4.4 Limitations and future prospects

Straw return is an effective method for improving soil fertility and functional diversity; however, it has some disadvantages. In this study, straw retention for 3 and 5 years significantly enriched the abundances of *M. oryza* and *U. virens*, which may increase the risk of pathogen infection in the following seasons. These results are consistent with those of previous studies. For example, long-term (10 years) crop residue retention significantly increased the abundances of *Fusarium graminearum* and *Fusarium moniliforme*, increasing the risk of maize root rot (Wang H. H. et al., 2020). This phenomenon was attributed to the straw used being infected by pathogenic fungi. This hypothesis is supported by another study that showed that incorporating diseased straw led to significant increases in disease severity; conversely, adding healthy rice straw (no disease) resulted in no significant increase in disease severity (Zhu et al., 2014). In addition, crop straw can create a favorable environment and supply substantial amounts of organic C and nutrient substrates, promoting the proliferation of certain phytopathogenic fungi (Kerdraon et al., 2019). The return of decomposed straw reduced pathogenic fungal populations (Su et al., 2020), and straw combined with a microbial inoculant reduced the pathogen content (Liu H. L. et al., 2021). To avoid pathogen accumulation, diseased straws should be removed from the field, pretreated, or combined with a microbial inoculant before incorporation.

5 Conclusion

The findings suggest that rice straw return for a year has negligible effects on soil nutrient content, enzyme activity, microbial composition, and microbial function. However, continuous rice straw return for 3 and 5 years significantly increased SOC, AP, and fungal biomass contents and promoted the growth and proliferation of microbial communities involved in cellulose decomposition. Moreover, rice straw retention improved soil fertility and nutrient availability by enhancing soil enzyme activity, improving microbial structure, and enriching genes associated with C and N cycling. However, rice straw return for 3 and 5 consecutive years also significantly accumulated rice pathogenic fungi. The results indicate that continuous rice straw return is an effective strategy for improving the microecological environment and ecological function of soil. Further research will be required to devise an effective strategy to limit or avoid the accumulation of pathogenic fungi, thus ensuring safe and efficient straw return to the field.

Data availability statement

The datasets presented in this study can be found in online repositories. The names of the repository/repositories and accession number(s) can be found at: https://www.ncbi.nlm.nih.gov/, PRJNA1209629; https://www.ncbi.nlm.nih.gov/, PRJNA1209633; https://www.ncbi.nlm.nih.gov/, PRJNA121128.

Author contributions

SJ: Conceptualization, Data curation, Formal analysis, Writing – original draft. Y-DL: Formal analysis, Investigation, Methodology, Validation, Writing – review & editing. HQ: Data curation, Software, Supervision, Validation, Writing – review & editing. BL: Funding acquisition, Resources, Software, Visualization, Writing – review & editing. Y-hJ: Resources, Supervision, Visualization, Writing – review & editing. Y-hX: Software, Supervision, Funding acquisition, Investigation, Writing – review & editing. YL: Formal analysis, Writing – review & editing. H-jB: Investigation, Writing – review & editing. W-tS: Conceptualization, Formal analysis, Funding acquisition, Investigation, Project administration, Writing – review & editing.

Funding

The author(s) declare that financial support was received for the research and/or publication of this article. This research was funded by the Shenyang Science and Technology Plan Project Black Land Special (grant no.: 23-409-2-05 and 22-317-2-09) and National Key

Research and Development Program of China (grant no.: 2024YFD1500703).

Conflict of interest

The authors declare that the research was conducted in the absence of any commercial or financial relationships that could be construed as a potential conflict of interest.

Generative AI statement

The authors declare that no Gen AI was used in the creation of this manuscript.

Publisher's note

All claims expressed in this article are solely those of the authors and do not necessarily represent those of their affiliated organizations, or those of the publisher, the editors and the reviewers. Any product that may be evaluated in this article, or claim that may be made by its manufacturer, is not guaranteed or endorsed by the publisher.

Supplementary material

The Supplementary material for this article can be found online at: https://www.frontiersin.org/articles/10.3389/fmicb.2025.1590788/full#supplementary-material

References

Bai, X., Hu, X. J., Liu, J. J., Wei, D., Zhu, P., Cui, X., et al. (2022). Ammonia oxidizing bacteria dominate soil nitrification under different fertilization regimes in black soils of Northeast China. *Eur. J. Soil Biol.* 111:103410. doi: 10.1016/j.ejsobi.2022.103410

Chen, Z. M., Wang, H. Y., Liu, X. W., Zhao, X. L., Lu, D. J., Zhou, J. M., et al. (2017). Changes in soil microbial community and organic carbon fractions under short-term straw return in a rice-wheat cropping system. *Soil Tillage Res.* 165, 121–127. doi: 10.1016/j.still.2016.07.018

Chen, S. F., Zhou, Y. Q., Chen, Y. R., and Gu, J. (2018). fastp: an ultra-fast all-in-one FASTQ preprocessor. *Bioinformatics* 34, i884–i890. doi: 10.1093/bioinformatics/bty560

Coban, O., Deyn, G. B. D., and Ploeg, M. J. (2022). Soil microbiota as game-changers in restoration of degraded lands. *Science* 375:abe0725. doi: 10.1126/science.abe0725

Cui, Y. X., Fang, L. C., Guo, X. B., Wang, X., Zhang, Y. J., Li, P., et al. (2018). Ecoenzymatic stoichiometry and microbial nutrientlimitation in rhizosphere soil in the arid area of the northern loess plateau, China. *Soil Biol. Biochem.* 116, 11–21. doi: 10.1016/j.soilbio.2017.09.025

Cui, H., Shutes, B., Hou, S. N., Wang, X. Y., and Zhu, H. (2024). Long-term organic fertilization increases phosphorus content but reduces its release in soil aggregates. *Appl. Soil Ecol.* 203:105684. doi: 10.1016/j.apsoil.2024.105684

Cui, H., Zhu, H., Shutes, B., Rousseau, A. N., Feng, W. D., Hou, S. N., et al. (2023). Soil aggregate-driven changes in nutrient redistribution and microbial communities after 10-year organic fertilization. *J. Environ. Manag.* 348:119306. doi: 10.1016/j.jenvman.2023.119306

Duan, Y., Chen, L., Li, Y. M., Wang, Q. Y., Zhang, C. Z., Ma, D. H., et al. (2021). N, P and straw return influence the accrual of organic carbon fractions and microbial traits in a Mollisol. *Geoderma* 403:115373. doi: 10.1016/j.geoderma.2021.115373

Fan, K. K., Delgado-Baquerizo, M., Guo, X. S., Wang, D. Z., Wu, Y. Y., Zhu, M., et al. (2019). Suppressed N fixation and diazotrophs after four decades of fertilization. *Microbiome* 7:143. doi: 10.1186/s40168-019-0757-8

Fan, K. K., Delgado-Baquerizo, M., Guo, X. S., Wang, D. Z., Zhu, Y. G., and Chu, H. Y. (2021). Biodiversity of key-stone phylotypes determines crop production in a 4-decade fertilization experiment. *ISME J.* 15, 550–561. doi: 10.1038/s41396-020-00796-8

Fan, W., and Wu, J. G. (2020). Short-term effects of returning granulated straw on soil microbial community and organic carbon fractions in dryland farming. *J. Microbiol.* 58, 657–667. doi: 10.1007/s12275-020-9266-5

Huang, J. J., Gao, K. L., Yang, L., and Lu, Y. H. (2023). Successional action of Bacteroidota and Firmicutes in decomposing straw polymers in a paddy soil. *Environ. Microbiome* 18:76. doi: 10.1186/s40793-023-00533-6

Huang, Y. P., Wang, Q. Q., Zhang, W. J., Zhu, P., Xiao, Q., Wang, C. J., et al. (2021). Stoichiometric imbalance of soil carbon and nutrients drives microbial community structure under long-term fertilization. *Appl. Soil Ecol.* 168:104119. doi: 10.1016/j.apsoil.2021.104119

Huang, W., Wu, J. F., Pan, X. H., Tan, X. M., Zeng, Y. J., Shi, Q. H., et al. (2021). Effects of long-term straw return on soil organic carbon fractions and enzyme activities in a double-cropped rice paddy in South China. *J. Agricult. Sci.* 20, 236–247. doi: 10.1016/S2095-3119(20)63347-0

Jin, S. L., Jin, W., Dong, C. X., Bai, Y. J., Jin, D. C., Hu, Z. J., et al. (2020). Effects of rice straw and rice straw ash on rice growth and α-diversity of bacterial community in rare-earth mining soils. *Sci. Rep.* 10:10331. doi: 10.1038/s41598-020-67160-w

Kerdraon, L., Laval, V., and Suffert, F. (2019). Microbiomes and pathogen survival in crop residues, an ecotone between plant and soil. *Phytobiomes J.* 3, 246–255. doi: 10.1094/PBIOMES-02-19-0010-RVW

Klimasmith, I. M., and Kent, A. D. (2022). Micromanaging the nitrogen cycle in agroecosystems. *Trends Microbiol.* 30, 1045–1055. doi: 10.1016/j.tim.2022.04.006

Li, Q., Kong, B. H., Fan, J. H., Cai, H., Fu, Y., and Chen, H. R. (2011). Early detection of rice blast by TaqMan real-time flourescence quantitative polymerase chain reaction. *Acta Phytopathol. Sin.* 41, 118–123. doi: 10.13926/j.cnki.apps.2011.02.002

Li, Z. W., Tong, D., Nie, X. D., Xiao, H. B., Jiao, P. P., Jiang, J. Y., et al. (2021). New insight into soil carbon fixation rate: the intensive co-occurrence network of autotrophic bacteria increases the carbon fixation rate in depositional sites. *Agric. Ecosyst. Environ.* 320:107579. doi: 10.1016/j.agee.2021.107579

Li, Y. L., Tremblay, J. L., Bainard, L. D., Cade-Menun, B., and Hamel, C. (2020). Long-term effects of nitrogen and phosphorus fertilization on soil microbial community structure and function under continuous wheat production. *Environ. Microbiol.* 22, 1066–1088. doi: 10.1111/1462-2920.14824

Lin, J., Cheng, Q., Kumar, A., Zhang, W., Yu, Z., Hui, D., et al. (2025). Effect of degradable microplastics, biochar and their coexistence on soil organic matter decomposition: a critical review. *TrAC Trends Anal. Chem.* 183:118082. doi: 10.1016/j.trac.2024.118082

Liu, W. J., Graham, E. B., Zhong, L. H., Zhang, J. W., Li, W. T., Li, Z. P., et al. (2020). Dynamic microbial assembly processes correspond to soil fertility in sustainable paddy agroecosystems. *Funct. Ecol.* 34, 1244–1256. doi: 10.1111/1365-2435.13550

Liu, H. L., Qi, Y. Q., Wang, J. H., Jiang, Y., and Geng, M. X. (2021). Synergistic effects of crop residue and microbial inoculant on soil properties and soil disease resistance in a Chinese Mollisol. *Sci. Rep.* 11:24225. doi: 10.1038/s41598-021-03799-3

Liu, J. A., Shu, A. P., Song, W. F., Shi, W. C., Li, M. C., Zhang, W. X., et al. (2021). Long-term organic fertilizer substitution increases rice yield by improving soil properties and regulating soil bacteria. *Geoderma* 404, 115287–115296. doi: 10.1016/j.geoderma.2021.115287

Liu, B., Xia, H., Jiang, C. C., Riaz, M., Yang, L., Chen, Y. F., et al. (2022). 14 year applications of chemical fertilizers and crop straw effects on soil labile organic carbon fractions, enzyme activities and microbial community in rice-wheat rotation of middle China. *Sci. Total Environ.* 841:156608. doi: 10.1016/j.scitotenv.2022.156608

Ma, A. Z., Zhuang, X. L., Wu, J. M., Cui, M. M., Lv, D., Liu, C. Z., et al. (2013). Ascomycota members dominate fungal communities during straw residue decomposition in arable soil. *PLoS One* 8, 1475–1478. doi: 10.1371/journal.pone.0066146

Ning, X. L., Wang, X. H., Guan, Z. Y., Gu, Y., Wu, C. S., and Hu, W. H. (2021). Effects of different patterns of maize-straw application on soil microorganisms, enzyme activities, and grain yield. *Bioengineered* 12, 3684–3698. doi: 10.1080/21655979.2021.1931639

Ning, Y. F., Wei, L., Wei, X. M., Zhu, Z. K., and Wu, J. S. (2020). Response of extracellular enzyme activities to substrate availability in paddy soil with long-term fertilizer management. *Huan Jing Ke Xue* 41, 2852–2860. doi: 10.13227/j.hjkx.201909140

Pang, Q., Zhao, G., Wang, D., Zhu, X., Xie, L., Zuo, D., et al. (2024). Water periods impact the structure and metabolic potential of the nitrogen-cycling microbial communities in rivers of arid and semi-arid regions. *Water Res.* 267:122472. doi: 10.1016/j.watres.2024.122472

Peng, C., Xu, W., Wang, X., Meng, F., Zhao, Y., Wang, Q., et al. (2025). Alginate oligosaccharides trigger multiple defence responses in tobacco and induce resistance to *Phytophthora infestans*. *Front. Plant Sci.* 16:1506873. doi: 10.3389/fpls.2025.1506873

Sarker, J. R., Singh, B. P., Fang, Y. Y., Cowie, A. L., Dougherty, W. J., Collins, D., et al. (2019). Tillage history and crop residue input enhanced native carbon mineralisation

and nutrient supply in contrasting soils under long-term farming systems. *Soil Tillage Res.* 193, 71–84. doi: 10.1016/j.still.2019.05.027

Su, Y., Lv, J., Yu, M., Ma, Z. H., Xi, H., Kou, C., et al. (2020). Long-term of decomposed straw return positively affects the soil microbial community. *J. Appl. Microbiol.* 128, 138–150. doi: 10.1111/jam.14435

Sun, X. Y., Kang, S., Zhang, Y. J., Tan, X. Q., Yu, Y. F., He, H. Y., et al. (2013). Genetic diversity and population structure of rice pathogen Ustilaginoidea virens in China. *PLoS One* 8:e76879. doi: 10.1371/journal.pone.0076879

Tang, H. M., Li, C., Xu, Y. L., Cheng, K. K., Shi, L. H., Wen, L., et al. (2021). Effects of fertilizer practice on fungal and actinobacterial cellulolytic community with different humified particle-size fractions in double-cropping field. *Sci. Rep.* 11:18441. doi: 10.1038/s41598-021-97975-0

Tang, Q., Xia, Y. Q., Ti, C. P., Shan, J., Zhou, W., Li, C. L., et al. (2023). Partial organic fertilizer substitution promotes soil multifunctionality by increasing microbial community diversity and complexity. *Pedosphere* 33, 407–420. doi: 10.1016/j.pedsph.2022.06.044

Wang, Y. F., Chen, P., Wang, F. H., Han, W. X., Qiao, M., Dong, W. X., et al. (2022). The ecological clusters of soil organisms drive the ecosystem multifunctionality under long-term fertilization. *Environ. Int.* 161:107133. doi: 10.1016/j.envint.2022.107133

Wang, H. H., Li, X., Li, X., Wang, J., Li, X. Y., Guo, Q. C., et al. (2020). Long-term no-tillage and different residue amounts alter soil microbial community composition and increase the risk of maize root rot in Northeast China. *Soil Tillage Res.* 196:104452. doi: 10.1016/j.still.2019.104452

Wang, C., Liu, D. W., and Bai, E. (2018). Decreasing soil microbial diversity is associated with decreasing microbial biomass under nitrogen addition. *Soil Biol. Biochem.* 120, 126–133. doi: 10.1016/j.soilbio.2018.02.003

Wang, Y. J., Liu, L., Yang, J. F., Duan, Y. M., Luo, Y., Taherzadeh, M. J., et al. (2020). The diversity of microbial community and function varied in response to different agricultural residues composting. *Sci. Total Environ.* 715:136983. doi: 10.1016/j.scitotenv.2020.136983

Wang, Y., Lyu, H., Du, Y., Cheng, Q., Liu, Y., Ma, J., et al. (2024). Unraveling how Fe-Mn modified biochar mitigates sulfamonomethoxine in soil water: the activated biodegradation and hydroxyl radicals formation. *J. Hazard. Mater.* 465:133490. doi: 10.1016/j.jhazmat.2024.133490

Wardman, J. F., Bains, R. K., Rahfeld, P., and Withers, S. G. (2022). Carbohydrate-active enzymes (CAZymes) in the gut microbiome. *Nat. Rev. Microbiol.* 20, 542–556. doi: 10.1038/s41579-022-00712-1

Xu, G. H., Chen, X. M., Mao, W., Li, W. X., Yu, J., and Xia, W. (2021). Effect of continuous Total amount straw returning to field on soil properties and Rice yield. *Mod. Agricult. Sci. Technol.* 23, 1–3+7. doi: 10.3969/j.issn.1007-5739.2021.23.001

Xu, Z. Y., Sun, R. H., He, T. Y., Sun, Y. Z., Wu, M. C., Xue, Y. H., et al. (2023). Disentangling the impact of straw incorporation on soil microbial communities: enhanced network complexity and ecological stochasticity. *Sci. Tot. Environ.* 863:160918. doi: 10.1016/j.scitotenv.2022.160918

Xun, W. B., Liu, Y. P., Li, W., Ren, Y., Xiong, W., Xu, Z. H., et al. (2021). Specialized metabolic functions of keystone taxa sustain soil microbiome stability. *Microbiome* 9:35. doi: 10.1186/s40168-020-00985-9

Yang, Y., Chen, X. L., Liu, L. X., Li, T., Dou, Y. X., Qiao, J. B., et al. (2022). Nitrogen fertilization weakens the linkage between soil carbon and microbial diversity: a global meta-analysis. *Glob. Chang. Biol.* 28, 6446–6461. doi: 10.1111/gcb.16361

Yang, J. Q., Diao, H. J., Hu, S. Y., and Wang, C. H. (2021). Effects of nitrogen addition at different levels on soil microorganisms in saline-alkaline grassland of northern China. *Chinese J. Plant Ecol.* 45, 780–789. doi: 10.17521/cjpe.2021.0072

Yang, Y., Gunina, A., Cheng, H., Liu, L., Wang, B., Dou, Y., et al. (2025). Unlocking mechanisms for soil organic matter accumulation: carbon use efficiency and microbial Necromass as the keys. *Glob. Chang. Biol.* 31:e70033. doi: 10.1111/gcb.70033

Yang, X., Xia, X., Zhang, Z., Nong, B., Zeng, Y., Wu, Y., et al. (2019). Identification of anthocyanin biosynthesis genes in rice pericarp using PCAMP. *Plant Biotechnol. J.* 17, 1700–1702. doi: 10.1111/pbi.13133

Yin, Y., Gong, H., Chen, Z., Tian, X., Wang, Y., Wang, Z., et al. (2025). Underestimated sequestration of soil organic carbon in China. *Environ. Chem. Lett.* 23, 373–379. doi: 10.1007/s10311-024-01813-4

Yu, C., Li, Y., Mo, R. L., Deng, W., Zhu, Z. X., Liu, D. B., et al. (2020). Effects of long-term straw retention on soil microorganisms under a rice-wheat cropping system. *Arch. Microbiol.* 202, 1915–1927. doi: 10.1007/s00203-020-01899-8

Yuan, L. H., Gao, Y., Mei, Y., Liu, J. R., Kalkhajeh, Y. K., Hu, H. X., et al. (2023). Effects of continuous straw returning on bacterial community structure and enzyme activities in rape-rice soil aggregates. *Sci. Rep.* 13:2357. doi: 10.1038/s41598-023-28747-1

Yuan, A., Kumar, S. D., Wang, H., Wang, S., Impa, S., Wang, H., et al. (2024). Dynamic interplay among soil nutrients, rhizosphere metabolites, and microbes shape drought and heat stress responses in summer maize. *Soil Biol. Biochem.* 191:109357. doi: 10.1016/j.soilbio.2024.109357

Zhang, C. F., Lin, Z. L., Que, Y. X., Fallah, F., Tayyab, M., Li, S. Y., et al. (2021). Straw retention efficiently improves fungal communities and functions in the fallow ecosystem. *BMC Microbiol.* 21:52. doi: 10.1186/s12866-021-02115-3

Zhang, T., Song, B., Han, G., Zhao, H., Hu, Q., Zhao, Y., et al. (2023). Effects of coastal wetland reclamation on soil organic carbon, total nitrogen, and total phosphorus in China: a meta-analysis. *Land Degrad. Dev.* 34, 3340–3349. doi: 10.1002/ldr.4687

Zhao, S. C., Li, K. J., Zhou, W., Qiu, S. J., Huang, S. W., and He, P. (2016). Changes in soil microbial community, enzyme activities and organic matter fractions under long-term straw return in north Central China. *Agric. Ecosyst. Environ.* 216, 82–88. doi: 10.1016/j.agee.2015.09.028

Zhou, G. P., Fan, K. K., Gao, S. J., Chang, D., Li, G. L., Liang, T., et al. (2024). Green manuring relocates microbiomes in driving the soil functionality of nitrogen cycling to obtain preferable grain yields in thirty years. *Sci. China Life Sci.* 67, 596–610. doi: 10.1007/s11427-023-2432-9

Zhou, J. S., Zhang, S. B., Lv, J. Y., Tang, C. X., Zhang, H. B., Fang, Y. Y., et al. (2024). Maize straw increases while its biochar decreases native organic carbon mineralization in a subtropical forest soil. *Sci. Total Environ.* 939:173606. doi: 10.1016/j.scitotenv.2024.173606

Zhu, H., Wang, Z., Luo, X., Song, J. X., and Huang, B. (2014). Effects of straw incorporation on Rhizoctonia solani inoculum in paddy soil and rice sheath blight severity. *J. Agric. Sci.* 152, 741–748. doi: 10.1017/S002185961300035X

frontiers | Frontiers in Microbiology

TYPE Original Research
PUBLISHED 26 May 2025
DOI 10.3389/fmicb.2025.1588030

Check for updates

OPEN ACCESS

EDITED BY
Muhammad Zahid Mumtaz,
Gansu Agricultural University, China

REVIEWED BY
Mohd Musheer Altaf,
Institute of Information Management and Technology, Aligarh, India
Abubakar Dar,
The Islamia University of Bahawalpur, Pakistan

*CORRESPONDENCE
Shaohui Huang
✉ shaohui1988@sina.com
Haoan Luan
✉ luanhaoan@163.com

†These authors have contributed equally to this work

RECEIVED 10 March 2025
ACCEPTED 12 May 2025
PUBLISHED 26 May 2025

CITATION
Yang M, He X, Liang J, Liu Q, Fu L, Cui X, Huang S and Luan H (2025) Linkage of living microbial biomass, function, and necromass to soil organic carbon storage along a chronosequence of *Larix principis-rupprechtii* plantation in North China. *Front. Microbiol.* 16:1588030. doi: 10.3389/fmicb.2025.1588030

COPYRIGHT
© 2025 Yang, He, Liang, Liu, Fu, Cui, Huang and Luan. This is an open-access article distributed under the terms of the Creative Commons Attribution License (CC BY). The use, distribution or reproduction in other forums is permitted, provided the original author(s) and the copyright owner(s) are credited and that the original publication in this journal is cited, in accordance with accepted academic practice. No use, distribution or reproduction is permitted which does not comply with these terms.

Linkage of living microbial biomass, function, and necromass to soil organic carbon storage along a chronosequence of *Larix principis-rupprechtii* plantation in North China

Mengyun Yang[1†], Xiaomeng He[1†], Jingfei Liang[1], Qiang Liu[1], Lihua Fu[2], Xiaodong Cui[1], Shaohui Huang[3]* and Haoan Luan[1]*

[1]College of Forestry, Hebei Agricultural University, Baoding, China, [2]Saihanba Mechanical Forest Farm, Chengde, China, [3]Hebei Fertilizer Technology Innovation Centre, Institute of Agricultural Resources and Environment, Hebei Academy of Agriculture and Forestry Sciences, Shijiazhuang, China

Introduction: Clarifying the temporal dynamics of soil organic carbon (SOC) characteristics within aggregates and its underlying microbially mediated mechanisms is essential for long-term SOC sequestration in forest ecosystems; nevertheless, this information remains largely unknown during stand development.

Methods: Five *Larix principis-rupprechtii* plantations of different ages (7a, 18a, 25a, 34a, and 44a) at the Saihanba Mechanical Forest Farm were chosen to elucidate the temporal variations in SOC characteristics and microbial attributes within aggregates (>2 mm, 2–0.25 mm, and <0.25 mm) following reforestation, based on ^{13}C NMR, phospholipid fatty acid (PLFAs) analysis, micro-plate enzyme technique, and amino sugar analysis, etc.

Results: Results demonstrated that as stand ages increased, aggregate stability as well as aggregate-associated SOC, microbial residue C (MRC), hydrolytic exo-enzymatic activities, and microbial biomass (as indicated by total PLFAs) initially increased and subsequently decreased, with most parameters peaking in the 18a stand, which indicated that long-term *Larix principis-rupprechtii* plantations (>25a) were not favorable for promoting microbial growth, hydrolytic functions, and microbial metabolism. Besides, regardless of the stand age, the above-mentioned indices were generally higher in larger aggregates (>2 mm and 2–0.25 mm) compared to smaller aggregates (<0.25 mm). Notably, the increased stand ages (i.e., 34a and 44a) or decreased aggregate sizes (<0.25 mm) enhanced SOC stability (as indicated by the recalcitrance index) and oxidative exo-enzymatic activities, as well as enlarged MRC (especially fungal residue C) contribution to SOC. The partial least squares path model highlighted that SOC stocks were primarily regulated by MRC, while the microbial community altered SOC stability by modulating exo-enzyme activities.

Discussion: These results offered novel insights into elucidating the coupling connections between microbial attributes and SOC sequestration during forest development in northern China.

KEYWORDS

stand age, *Larix principis-rupprechtii*, soil aggregates, microbial characteristics, soil organic C dynamics

1 Introduction

Soil organic C (SOC), the biggest terrestrial C reservoirs (ca. 2,344 Gt) (Sakschewski et al., 2016), is receiving increasing attention due to its potential role in alleviating global warming and maintaining terrestrial ecological stability (Stockmann et al., 2013; Liu Q. et al., 2024). Nevertheless, since the Industrial Revolution, a series of human activities, such as extensive deforestation, urbanization, and overgrazing, have resulted in large amounts of CO_2 emissions and SOC loss (Wiesmeier et al., 2019). Afforestation (i.e., planted forests), an effective approach to mitigate global CO_2 emission and promote SOC stocks, has been developed rapidly in recent decades (Liang et al., 2022). By 2023, the global area of planted forests had reached 360.22 million ha, accounting for ca. 7.35% of the world's total forest area (Xu et al., 2024). Consequently, it is imperative to assess soil C sequestration capability of these newly established planted forests and to elucidate the underlying mechanisms influencing this capacity, in order to deeply evaluate the role of afforestation in mitigating global climate change (Wang et al., 2024).

Recent research revealed that the forest's capability for SOC sequestration is associated with stand age, as the variations in forest structure and understory vegetation with stand age can affect soil microenvironment and litter input conditions (Mujuru et al., 2014; Dong et al., 2020). Nevertheless, studies examining changes in SOC stocks across stands of varying ages had yielded conflicting results, reporting positive (Abaker et al., 2016), negative (Liu et al., 2023), and no effects (Jing et al., 2022) on SOC storage. These inconsistent results are likely attributed to the variations in forest species, climate, and edaphic characteristics (Chen et al., 2020; Wang et al., 2024). To better elucidate SOC dynamics, it is essential to address this knowledge gap regarding the underlying mechanisms for SOC sequestration along stand development.

Researchers revealed that the processes involved SOC cycling, such as degradation and polymerization, etc., are primarily regulated by microbes and their secreted exo-enzymes (Shao et al., 2018; Sokol et al., 2022). Recently, the response of stand ages to microbial attributes has been widely attracting scholarly attention (Wang et al., 2021; Zhang et al., 2023). Studies have demonstrated that stand age, a crucial parameter for assessing the rewilding level of plantations post-afforestation, can strongly influence the dynamics of microbial communities and exo-enzymatic activities through the modulation of understory vegetation composition and the exogenous resources (e.g., litter debris and root depositions) inputs (Zhang et al., 2023; Liu X. et al., 2024). Notably, traditional perspectives emphasize that SOC is mainly derived from plant-originated C, with microbes accounting for <4% of SOC and playing a crucial role in SOC decomposition and mineralization (Wang et al., 2017). Nevertheless, increasing evidence suggests that microbial anabolic functions are important in mediating persistent soil C storage (Shao et al., 2018; Hu H. et al., 2024). Based on the "microbial C pump" theory, Liang et al. (2017) indicated that microbial residues (i.e., microbial-derived C), producted through microbial anabolism, are considered to be the important constituents of stable SOC pools and contribute approximately 50–80% to SOC storage. Taken together, the study of combining microbial communities, exo-enzymes, and microbial residues, can comprehensively provide several valuable insights for elucidating microbial-driven SOC dynamics with plantation development (Ma et al., 2023). Yet, to date, the integrated study of the above-mentioned microbial attributes during the development of plantations is lacking.

To further elucidate the temporal variations in the aforementioned microbial attributes during stand development, they should be investigated at different spatial scales (e.g., the aggregate scale) (Chen et al., 2014; Mao et al., 2023). Soil aggregates, which serve as the basic units of soil structure, are the primary "sites" for SOC storage and act as "hotspots" for microbial activity (Gupta and Germida, 2015; Kuzyakov and Blagodatskaya, 2015). Recent studies have identified distinct distribution patterns of microbial attributes within different aggregates, attributed to their spatial heterogeneity and diverse physicochemical characteristics (e.g., pore properties and nutritional conditions) (Yao Y. et al., 2019; Wang and Hu, 2023). However, the impacts of aggregate size on microbial attributes along stand development remains inconsistent, with studies reporting increases, decreases, or no changes (Liao et al., 2023; Mao et al., 2023). To address this knowledge gap, an integrated study of microbial attributes, i.e., microbial communities, exo-enzymes, and microbial residue dynamics, within aggregates, to some extent, will enhance our understanding of microbial-driven soil C dynamics during forest development.

To fulfill our research objectives, five distinct age classes of *Larix principis-rupprechtii* plantations, i.e., 7a, 18a, 25a, 34a, and 44a, were selected from the Saihanba Mechanized Forest Farm, which represents the biggest plantation base in China (Wang Z. et al., 2018). It is noteworthy that since 1962, afforestation efforts, primarily involving *Larix principis-rupprechtii*, have been systematically and continuously implemented in Saihanba to address the issue of land desertification resulting from previous indiscriminate logging practices (Zhang et al., 2022). Consequently, *Larix principis-rupprechtii* of various ages are prevalent throughout this region. In this study, based on a series of technologies (e.g., ^{13}C NMR, phospholipid fatty acids, exo-enzyme, and microbial residue analysis, etc.), we attempt to clarify the temporal changes in SOC dynamics within aggregates and the underlying microbial-driven mechanisms resulting in these variations after afforestation. Specifically, we hypothesized that (i) the growth and metabolism of microbes would be progressively strengthen during the development of plantations due to increased nutrient availability from annual continuous litter inputs; (ii) the variations in aggregate-related nutrient and pore properties induced by stand ages would alter the contents of microbial biomass and residues within soil aggregates; and (iii) the storage and composition of SOC would change along stand development, which were closely linked to the temporal changes in microbial attributes (i.e., microbial community, exo-enzymes, and microbial residues). These results can offer several valuable information for the sustainable development of planted forests in northern China.

2 Materials and methods

2.1 Study sites description and experimental design

The study was conducted at the Saihanba Mechanical Forest Farm, located in Hebei Province, North China (42°10′–42°50′N, 117°12′–117°30′E) with an elevation between 1,100 and 1940 m (Figure 1). This region belongs to a typical forest-steppe eco-tone with a

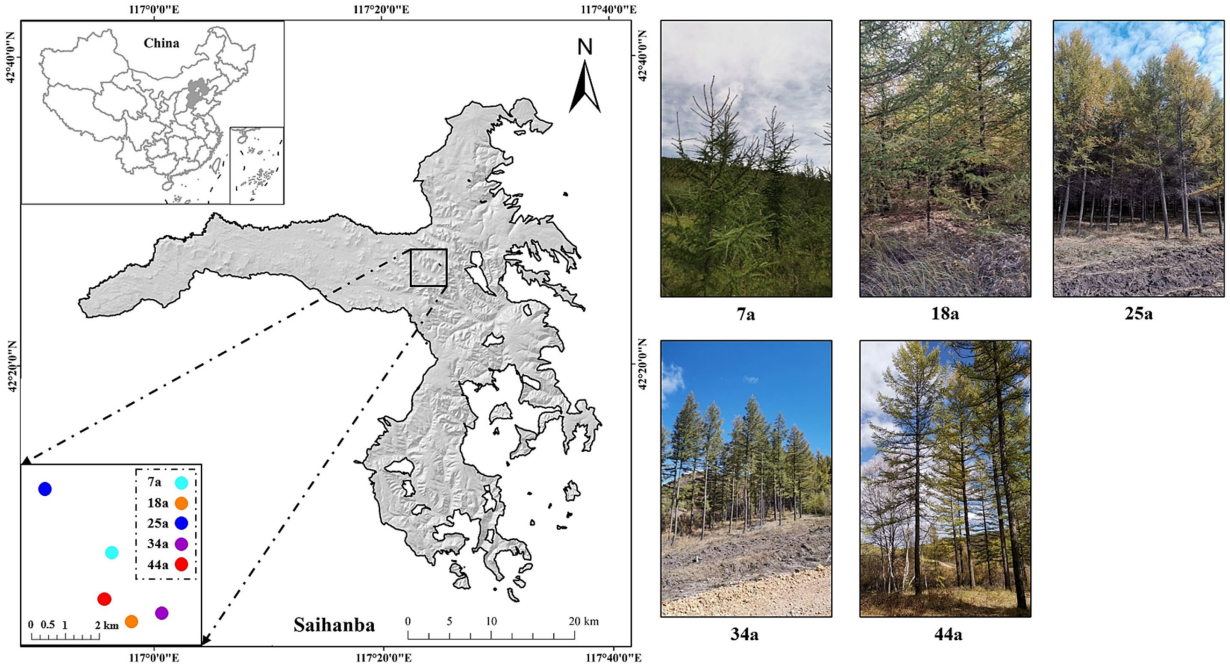


FIGURE 1
The study area and layout of plots for the five different-aged *Larix principis-rupprechtii* plantations.

temperate continental monsoon climate. The mean annual temperature and precipitation are −1.4°C and 450.1 mm, respectively. The average annual frost-free period is 68 days. The soils in the study site belong to brown soil (FAO, 2014). Besides, The cold-temperate coniferous forests, e.g., *Larix principis-rupprechtii* (shorted as larch), are the major forest types in this region due to their extreme cold tolerance and strong adaptability to soil.

The means of space-for-time substitution, a valuable method to survey soil temporal changes, was suitable for evaluating the temporal dynamics of forest's soil evolution (Sparling et al., 2003). In the present study, five different-aged larch plantations, i.e., young (7a), middle-aged (18a and 25a), near mature (34a), and mature (41a) forests (see Figure 1), were selected to elucidate the temporal changes of soil characteristics that occur during the growth and development process of larch plantation. Three plots (20 m × 30 m) were randomly selected for investigation and sampling from each age of larch plantation. Besides, to be regarded as independent replications, each plot of the same stand age is separated by at least 0.2 km; meanwhile, all plots are within 10 km to ensure similar climatic and edaphic conditions. Other detailed information was shown in Table 1.

2.2 Soil sampling and aggregate fractionation

In late August 2023, five undisturbed soil samples were randomly collected from the surface soil (0–20 cm depth) under the canopy of the larch stand in each plot and placed in a hard plastic box (20 cm × 12 cm × 6 cm) to ensure that they could sustain their original structure during transport to the laboratory. In total, 15 soil samples (3 replicates × 5 stand age) were stored in 4°C conditions and immediately transferred to the laboratory for further analysis. Then, after the removal of impurities (e.g., leaf debris and stone, etc.), these soil samples were gently broken along natural fracture planes and passed through an 8 mm sieve for determination of aggregate fractionation.

Based on the optimal-moisture sieving method, the above soil samples were manually fractionated through a nest of 2 sieves (2 mm and 0.25 mm) into three aggregate-size classes: >2 mm, 2–0.25 mm, and <0.25 mm aggregates. The specific procedure was described in Mao et al. (2021). Then, the aggregate samples were separated into two parts. One part was air-dried and passed through 0.15 mm sieve to determine aggregate-associated physicochemical properties and microbial residues; the other part was stored at −80°C for the determination of aggregate-associated microbial characteristics.

2.3 Determination of soil physicochemical properties

Soil pH was measured with a glass electrode at a water-to-soil ratio of 2.5:1 (v/w). Soil organic C (SOC, i.e., total C, due to soils being acidic) and total nitrogen (TN) were measured by the dry combustion method using an elemental analyzer (VELP EMA 502, Italy) (Vitti et al., 2016).

2.4 Soil microbial community (PLFAs) analysis

The aggregate-associated microbial community was classified and quantified by the phospholipid fatty acids (PLFAs) analysis, as described by Kramer et al. (2013). Briefly, the frozen-dried soil samples were treated with mild alkaline methanolysis to form fatty

TABLE 1 The basic information, as well as the distribution characteristics of soil aggregates in the selected five aged stands of *Larix principis-rupprechtii* in the study sites.

Characteristics	Stand age	7a	18a	25a	34a	44a
Basic information	Elevation (m)	1,665	1,668	1,617	1,675	1,661
	Slope aspect	Northeast	East	North	East	Northeast
	Slope gradient (°)	8	4	10	11	6
	Mean tree height (m)	4.9	8.8	11.9	15.9	19.5
	Mean DBH (cm)	5.4	9.7	13.7	18.6	22.5
	Stand density (trees ha^{-1})	3,143	2,449	2,539	1,447	1,278
Aggregate distribution (%)	>2 mm	41.2 ± 2.5b	50.5 ± 0.7a	47.8 ± 4.2a	35.2 ± 0.5c	30.8 ± 1.4d
	0.25–2 mm	42.5 ± 1.4a	34.3 ± 3.2b	35.0 ± 3.3b	42.0 ± 3.4a	41.0 ± 2.4a
	<0.25 mm	16.3 ± 3.8c	15.1 ± 2.7c	17.1 ± 1.4c	22.8 ± 3.4b	28.2 ± 1.0a
Aggregate stability	MWD (mm)	2.56 ± 0.13b	2.93 ± 0.02a	2.81 ± 0.17a	2.26 ± 0.04c	2.04 ± 0.05d
	GMD (mm)	1.46 ± 0.18b	1.72 ± 0.09a	1.58 ± 0.13ab	1.15 ± 0.09c	0.96 ± 0.01c

The aggregate-associated data was shown as means values ± S.E. (n = 3). Different lower-case letters indicate significant differences ($p < 0.05$) among differently-aged *Larix principis-rupprechtii* stands. DBH, diameter at breast height. MWD, mean weight diameter; GMD, geometric mean diameter.

acid methyl esters (FAMEs), and then dissolved in hexane and estimated by gas chromatography (Agilent 6,890 GC, Santa Clara, CA, USA) with the MIDI peak identification 4.5 software (MIDI Inc., Newark, DE). Subsequently, 24 individual PLFAs were chosen and quantified based on the internal standard (C19:0), and classified into fungi, bacteria, and actinomycetes, etc. (Supplementary Table S1). The contents of PLFAs were expressed in units of nmol g^{-1}.

2.5 Soil exo-enzyme activity analysis

Seven exo-enzyme activities (five hydrolytic exo-enzymes and two oxidative exo-enzymes; Supplementary Table S2) were determined to evaluate microbial functional attributes using the micro-plate enzyme method (Zhang et al., 2015). Five labeled fluorogenic substrates and *L*-DOPA substrate (Supplementary Table S2) were applied for the determination of hydrolytic and oxidative exo-enzymatic activities, respectively. The detailed procedure was referred to Luan et al. (2020). Then, the hydrolytic or oxidative exo-enzymatic activities were measured through a microplate reader (Synergy 2, Biotek, USA) with 365 nm excitation and 450 nm emission filters or 450 nm absorbance, respectively. The seven exo-enzyme activities were calculated as nmol g^{-1} soil h^{-1}.

2.6 Soil microbial residue (amino sugar) analysis

The amino sugars (AS), valuable indicators widely used to describe microbial necromass, were quantified by the procedure described by Ding et al. (2010). The AS generally contains three constitutes [i.e., glucosamine (GluN), galactosamine (GalN), and muramic acid (MurA)], which were extracted (i.e., hydrolysis, filtration, nitrogen-evaporation) and derivatized into aldononitrile derivatives. Finally, they were determined by the internal standard myo-inositol, which was added before hydrolyzation. The sum of GluN, GalN, and MurA was used to evaluate the total microbial necromass pool.

2.7 Solid-state ^{13}C NMR analysis

The SOC chemical composition was assessed by solid-state ^{13}C NMR spectroscopy. Before NMR measurements, aggregate samples were repeatedly pre-treated using hydrofluoric acid (5%) to eliminate paramagnetic compounds (i.e., Fe^{3+} and Mn^{2+}, etc.) following Zhuang et al. (2011). The ^{13}C NMR spectra were obtained on a Bruker AVANCE 400 NMR spectrometer (Germany) equipped with a 4-mm probe. Besides, the spectra were divided into four major regions, i.e., alkyl C (0–45 ppm), O-alkyl C (45–110 ppm), aromatic C (110–160 ppm), and carbonyl C (160–190 ppm) (Simpson and Simpson, 2012), and calculated by integration with the MestReNova 8.0 software (Mestrelab Research, Santiago de Compostela, Spain).

2.8 Calculations

2.8.1 The indices of soil aggregate stability

By using the mass proportions of >2 mm, 2–0.25 mm, and <0.25 mm aggregates, mean weight diameter (MWD; mm) and geometric mean diameter (GMD; mm) were calculated to evaluate the stability of soil aggregates (Wang S. et al., 2018):

$$MWD = \sum_{i=1}^{3}(Xi \times Wi)$$

$$GMD = EXP\sum_{i=1}^{3}(Wi \times \ln(Xi))$$

Where Xi is the average diameter of aggregates (mm); and Wi is the mass proportions of aggregates (%).

2.8.2 The geometric mean of the exo-enzyme activities

The geometric mean of the assayed hydrolytic and oxidative eco-enzymatic activities (GH and GOR) were calculated as follows:

$$GH = \sqrt[5]{\alpha G \times \beta G \times CBH \times XYL \times NAG}$$

$$GOR = \sqrt[2]{PHOs \times Perx}$$

Where the full names of αG, βG, CBH, XYL, NAG, PHOs, and PerX are shown in Supplementary Table S2.

2.8.3 Microbial residue C

Fungal and bacterial residue C (FRC and BRC, g kg^{-1}) were calculated as follows (Cheng et al., 2024):

$$FRC = \frac{\left(GluN/179.2 - 2 \times MurA/251\right) \times 179.2 \times 9}{1000}$$

$$BRC = \frac{MurA \times 45}{1000}$$

Where 179.2 and 251 are the molecular masses of GluN and MurA, respectively, and 9 is the conversion factor of fungal GluN to fungal C.

2.8.4 The indices of SOC stability

Three indices of SOC stability were calculated based on the relative abundance of SOC functional groups (Guo et al., 2019):

$$AI = \frac{\text{aromatic C}}{\text{alkyl C} + \text{O} - \text{alkyl C} + \text{aromatic C}} \times 100$$

$$RI = \frac{\text{aromatic C} + \text{alkyl C}}{\text{O} - \text{alkyl C} + \text{carbonyl C}}$$

$$A/OA = \frac{\text{alkyl C}}{\text{O} - \text{alkyl C}}$$

Where AI and RI are aromaticity index and recalcitrance index, respectively.

2.9 Statistical analysis

One-way analysis of variance (ANOVA) with Duncan tests was conducted to assess the effect of different stand ages (or soil aggregates) on the physicochemical and microbial variables. Two-way ANOVA based on 45 soil samples (5 stand ages × 3 soil aggregates × 3 replicates) was applied to compare the differences in these above-mentioned variables with the five stand ages and three soil aggregates as the main factors. These statistical analyses were conducted with SPSS 16.0 software (SPSS Inc. Chicago, IL, USA). By using CANOCO 4.5 software, principal component analysis (PCA) was applied to identify the differences of microbial community across five different-aged larch plantations within soil aggregates. Besides, the effects of microbial characteristics (i.e., microbial communities, exo-enzyme activities, and microbial residues) on SOC dynamics were explored by the partial least squares path model (PLS-PM; 1,000 bootstraps) with the packages "plspm" through the R software (version 3.6.1).

3 Results

3.1 Soil aggregates distribution and stability

The aggregates in the surface soils (0–20 cm) across five different-aged larch plantations were found to be dominated by >2 mm and 2–0.25 mm aggregates (30.8–50.5 and 34.3–42.5%, respectively), followed by the <0.25 mm aggregates (15.1–28.2%) (Table 1). The proportion of >2 mm aggregates were significantly ($p < 0.05$) higher by 16.0–64.0% in the 18a and 25a stands than those in other stands (7a, 34, and 44a). In contrast, the 18a and 25a stands contained lower proportions of 2–0.25 mm and <0.25 mm aggregates than other stands. Additionally, the values of MWD and GMD first increased and then decreased with increasing stand age, reaching the highest value at 18a stand (2.93 mm and 1.72 mm) (Table 1).

3.2 The physicochemical properties within aggregates

The physicochemical properties, e.g., soil organic C (SOC), total N (TN), SOC/TN, and pH within soil aggregates, are shown in Table 2. Overall, these physicochemical indices were significantly ($p < 0.05$) affected by stand ages (except for pH) and soil aggregates. The contents of SOC and TN as well as their ratios (SOC/TN) were observed highest in the 18a and 25a stands, followed by the 7a stand, and lowest in the 34a and 44a stands within aggregates; meanwhile, 0.25–2 mm aggregates contained higher values of SOC, TN, and SOC/TN by 15.2–26.8, 7.1–11.3, and 7.3–13.6%, respectively, than other aggregates (>2 mm and <0.25 mm). The soil pH was significantly ($p < 0.05$) higher in the 7a, 18a, and 25a stands than those in the 34 and 44a stands within aggregates; meanwhile, there were no significant differences in the values of pH across all aggregates (5.91–5.96) irrespective of the stand ages.

3.3 The microbial community composition within aggregates

Table 3 revealed that the contents of total microbes (i.e., total PLFAs) showed a unimodal trend with increasing stand ages within aggregates. Specifically, the values of total PLFAs were found higher by 21.5–53.4, 23.0–72.2, and 25.0–72.2%, respectively, in the 18a and 25a stands than other stands within >2 mm, 2–0.25 mm and <0.25 mm aggregates; meanwhile, >2 mm and 2–0.25 mm aggregates owned higher contents of total microbes by 27.4% on average than <0.25 mm aggregates. The relative abundance of fungi was found significantly ($p < 0.05$) lower in the 7a stand than that in the 18a, 25a, 34a, and 44a stands within aggregates. Besides, the relative abundance of bacteria showed ranked in the order: 18a and 25a > 7a, 34a, and 44a within aggregates. Notably, regardless of the stand age, the

10.3389/fmicb.2025.1588030

TABLE 2 The physicochemical properties within soil aggregates in differently-aged *Larix principis-rupprechtii* stands.

Indices	Stand age (S)	Soil aggregate size (A)			Effects		
		>2 mm	0.25–2 mm	<0.25 mm	A	S	A × S
SOC (g kg^{-1})	7a	26.9 ± 2.7b	30.7 ± 3b	24.1 ± 2.8ab	**	**	ns
	18a	33.2 ± 1.4a	40.0 ± 3.1a	30.7 ± 3.8a			
	25a	31.1 ± 2.2a	34.4 ± 2.3ab	26.8 ± 3.8a			
	34a	20.1 ± 1.8c	22.9 ± 4.4c	19.2 ± 3.5b			
	44a	20.1 ± 2.1c	23.4 ± 2.6c	18.6 ± 3.9b			
	Average	26.3B	30.3A	23.9B			
TN (g kg^{-1})	7a	2.45 ± 0.24a	2.56 ± 0.36ab	2.31 ± 0.3a	*	**	ns
	18a	2.58 ± 0.26a	2.88 ± 0.26a	2.50 ± 0.23a			
	25a	2.59 ± 0.28a	2.69 ± 0.34ab	2.35 ± 0.15a			
	34a	2.3 ± 0.12ab	2.42 ± 0.25ab	2.27 ± 0.43a			
	44a	2.06 ± 0.16b	2.27 ± 0.12b	2.09 ± 0.3a			
	Average	2.39AB	2.56A	2.30B			
SOC/TN	7a	11.0 ± 0.3bc	12.0 ± 0.6bc	10.4 ± 0.1b	**	**	ns
	18a	13.0 ± 1.3a	13.9 ± 0.8a	12.3 ± 1.1a			
	25a	12.1 ± 1.1ab	12.9 ± 1.1ab	11.3 ± 1.1ab			
	34a	8.8 ± 0.6d	9.4 ± 1.3d	8.5 ± 0.1c			
	44a	9.8 ± 0.4 cd	10.3 ± 0.6 cd	8.8 ± 0.5c			
	Average	10.9B	11.7A	10.3C			
pH	7a	6.27 ± 0.12a	6.24 ± 0.03a	6.23 ± 0.11a	ns	**	ns
	18a	6.16 ± 0.09a	6.13 ± 0.08a	6.12 ± 0.03ab			
	25a	6.14 ± 0.04a	6.09 ± 0.12a	6.10 ± 0.05b			
	34a	5.61 ± 0.08b	5.54 ± 0.10b	5.49 ± 0.08c			
	44a	5.61 ± 0.15b	5.53 ± 0.04b	5.63 ± 0.02c			
	Average	5.96A	5.91A	5.91A			

Data were shown as means values ± S.E. (n = 3 or 15). Different uppercase and lowercase letters indicate significant differences among different soil aggregates and differently-aged *Larix principis-rupprechtii* stands within the same soil aggregates at the $P < 0.05$ level, respectively. Two-way ANOVA are applied for identifying the effects of stand age (S), aggregate size (A), and their interaction (S × A) on the above-mentioned indices (The results are shown in the right side of the table). **, * and "ns" represent significant at $P < 0.01$, $p < 0.05$, and no significant differences ($P > 0.05$), respectively. SOC, soil organic C; TN, total N.

2–0.25 mm aggregates contained lower relative abundance of fungi and higher relative abundance of bacteria than the >2 mm and <0.25 mm aggregates. These results induced the higher F/B ratios to be found in the 34a and 44a stands (or the <0.25 mm aggregates) than the 7a, 18a, and 25a stands (or the >2 mm and 2–0.25 mm aggregates) (Table 3). The PCA results (Figure 2) further identified stand age could alter the microbial community structure within aggregates. Specifically, the microbial profiles within >2 mm, 2–0.25 mm, and <0.25 mm aggregates among different-aged stands owned similar and obvious boundaries, which were categorized into four groups, i.e., 7a vs. 18a and 25a vs. 34a vs. 44a.

3.4 The exo-enzyme activities within aggregates

Table 4 and Figure 3 revealed that the activities of hydrolytic and oxidative exo-enzymes were significantly ($p < 0.01$) influenced by stand age and soil aggregates. For hydrolytic eco-enzymatic activities, these indices (e.g., GH, αG, βG, CBH, XYL, and NAG) within aggregates initially increased and subsequently decreased, with most parameters peaking in 18a or 25a stands. For oxidative exo-enzymatic activities, these indices (e.g., GOR, PHOs, and PerX) basically exhibited increasing trends as the stand age increased. Besides, regardless of the stand age, the >2 mm and 2–0.25 mm aggregates owned higher hydrolytic eco-enzymatic activities by 25.8–41.7% and lower oxidative exo-enzymatic activities by 21.8–26.7% than the <0.25 mm aggregates. Notably, the values of GH/GOR were consistently greater in the 18a stand (or >2 mm and 2–0.25 mm aggregates) than in the 7a, 25a, 34a, and 44a stands (or <0.25 mm aggregates) (Figure 3c).

3.5 The microbial residue C within aggregates

The contents of amino sugars (total AS, GluN, GalN, and MurA; Table 5) and microbial residue C (FRC and BRC; Figure 4) basically

10.3389/fmicb.2025.1588030

TABLE 3 The contents of total PLFAs, the relative abundance of microbial subgroups as well as associated ratios (F/B) within soil aggregates in differently-aged *Larix principis-rupprechtii* stands.

Indices	Stand age (S)	Soil aggregate size (A)			Effects		
		>2 mm	0.25–2 mm	<0.25 mm	A	S	A × S
Total PLFAs (nmol g^{-1})	7a	27.1 ± 3.3b	32.6 ± 4.0b	22.9 ± 2.8b	**	**	ns
	18a	35.1 ± 1.5a	45.7 ± 2.8a	30.3 ± 1.4a			
	25a	37.3 ± 2.9a	41.2 ± 0.5a	31.0 ± 1.9a			
	34a	28.9 ± 2.7b	33.5 ± 3.4b	24.2 ± 2.3b			
	44a	24.3 ± 1.6b	26.5 ± 1.7c	20.4 ± 1.8b			
	Average	30.6B	35.9A	25.8C			
Fungi (%)	7a	8.5 ± 0.8b	7.6 ± 0.4b	9.5 ± 0.8b	**	**	ns
	18a	9.8 ± 0.4a	10.0 ± 0.2a	11.2 ± 0.3a			
	25a	10.7 ± 0.4a	9.6 ± 0.7a	11.9 ± 0.2a			
	34a	10.4 ± 0.1a	9.2 ± 0.1a	11.5 ± 0.1a			
	44a	10.2 ± 0.7a	9.6 ± 0.6a	12.0 ± 0.4a			
	Average	10.0B	9.2C	11.2A			
Bacteria (%)	7a	53.0 ± 1.1b	57.3 ± 2.3b	53.3 ± 1.3c	**	**	ns
	18a	58.0 ± 2.7a	62.0 ± 2.4a	58.1 ± 1.5a			
	25a	57.6 ± 3.8ab	61.1 ± 0.5a	57.4 ± 2.8ab			
	34a	53.3 ± 1.8b	57.3 ± 1.7b	53.3 ± 1.7c			
	44a	54.4 ± 1.7ab	58.6 ± 1.7ab	54.6 ± 1.4bc			
	Average	55.2B	59.3A	55.4B			
Actinomycetes (%)	7a	4.52 ± 0.71ab	3.78 ± 0.52b	4.29 ± 0.65ab	ns	*	ns
	18a	4.56 ± 0.07ab	4.04 ± 0.12ab	4.36 ± 0.07ab			
	25a	3.88 ± 0.99b	4.17 ± 0.22ab	3.88 ± 0.73b			
	34a	5.50 ± 1.23a	5.02 ± 0.98a	5.31 ± 1.15a			
	44a	4.99 ± 0.47ab	4.53 ± 0.41ab	4.76 ± 0.53ab			
	Average	4.69A	4.31A	4.52A			
F/B	7a	0.160 ± 0.012c	0.133 ± 0.002b	0.178 ± 0.01c	**	**	ns
	18a	0.169 ± 0.002bc	0.162 ± 0.006a	0.193 ± 0.002b			
	25a	0.185 ± 0.007ab	0.157 ± 0.012a	0.207 ± 0.006ab			
	34a	0.195 ± 0.004a	0.161 ± 0.004a	0.216 ± 0.005a			
	44a	0.194 ± 0.012a	0.163 ± 0.01a	0.220 ± 0.011a			
	Average	0.181B	0.155C	0.203A			

Data were shown as means values ± S.E. (n = 3 or 15). Different uppercase and lowercase letters indicate significant differences among different soil aggregates and differently-aged *Larix principis-rupprechtii* stands within the same soil aggregates at the $P < 0.05$ level, respectively. Two-way ANOVA are applied for identifying the effects of stand age (S), aggregate size (A), and their interaction (S × A) on the above-mentioned indices (The results are shown in the right side of the table). **, *, and "ns" represent significant at $P < 0.01$, $P < 0.05$, and no significant differences ($P > 0.05$), respectively. F, fungi; B, bacteria.

and gradually increased from 7a to 14a stands but then declined in the 25a, 34a and 44a stands within aggregates; meanwhile, regardless of the stand age, the contents of FRC and BRC were higher by 5.3–15.6% and 20.6–40.9%, respectively, in the 2–0.25 mm aggregates than the >2 mm and <0.25 mm aggregates. Notably, the ratios of FRC/BRC and MRC/SOC were observed significantly ($p < 0.05$) higher in the 34a and 44a stands (3.50–5.18 and 29.2–33.5%) compared to the 7a, 14a, and 25a stands (2.61–4.06 and 24.6–31.1%) within aggregates; meanwhile, these indices were ranked as: [<0.25 mm aggregates (4.27 and 31.0%)] > [>2 mm and 2–0.25 mm aggregates (3.22–3.36 and 27.0–275%)].

3.6 The SOC chemical composition within aggregates

The results of ^{13}C NMR analysis (Table 6) demonstrated that the effects of stand ages and aggregate sizes on SOC functional groups were primarily focused on aromatic C ($p < 0.01$) and O-alkyl C ($p < 0.01$), rather than carbonyl C and alkyl C ($p > 0.05$). Specifically, the relative abundance of aromatic C within aggregates increased with stand ages (except for 34a in 0.25–2 mm aggregates), whereas the relative abundance of O-alkyl C showed an opposite trend (7a, 18a, and 25a > 34a and 44a). Regardless of the stand ages, the SOC in

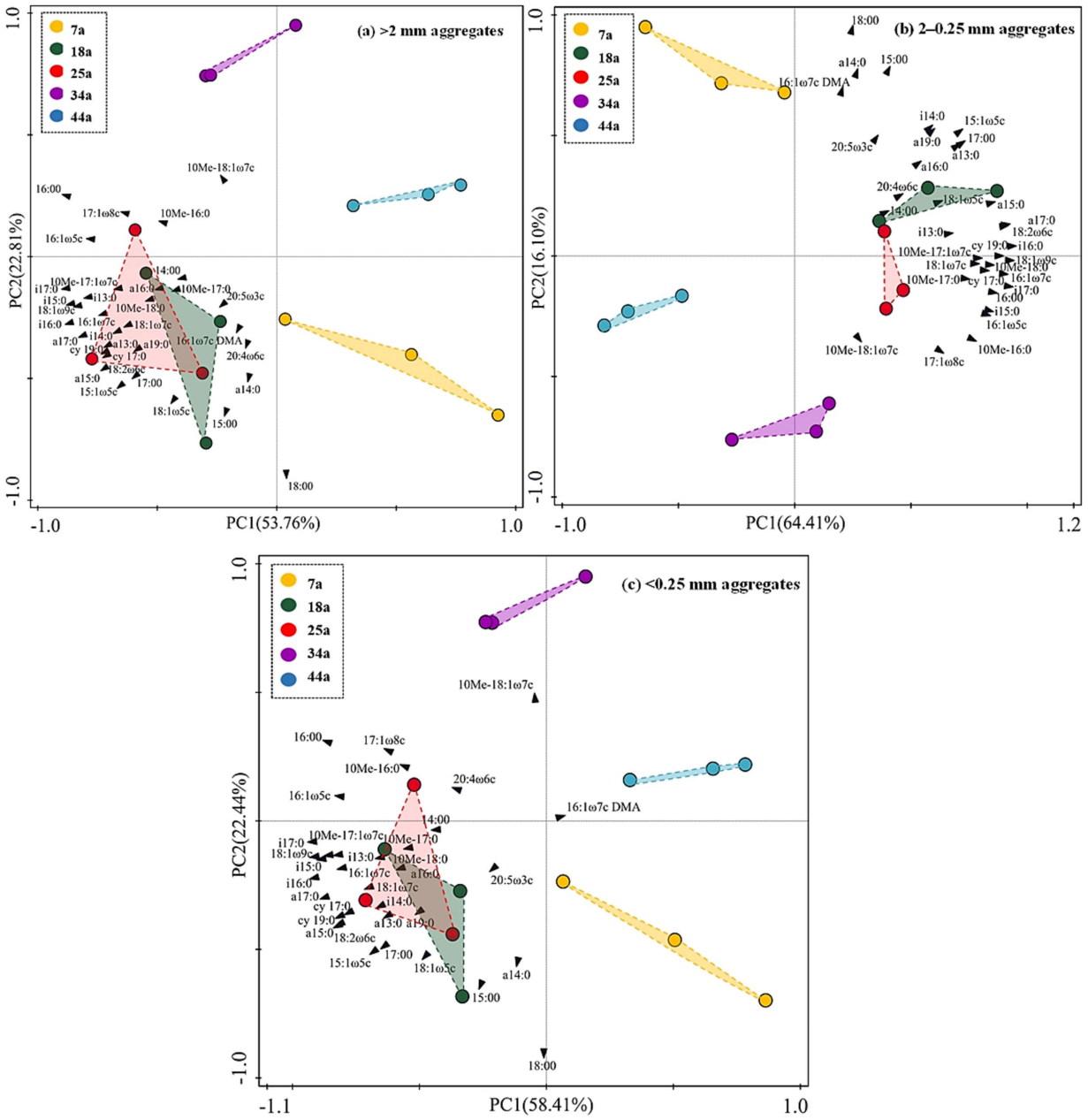


FIGURE 2
The principal component analysis (PCA) based on 24 individual PLFAs in the present study across differently-aged *Larix principis-rupprechtii* stands within different soil aggregates. The "10Me" in 10Me-18:1ω7c, 10Me-17:1ω7c, 10Me-16:0, 10Me-17:0, and 10Me-18:0 means "10-methyl"; the "i" in i13:0, i14:0, i15:0, i16:0, i17:0 means "iso"; the "a" in a14:0 a15:0, a16:0, a17:0 means "anteiso"; the "DMA" in 16:1ω7c DMA means "dimethyl acetal"; the "cy" in cy17:0 and cy19:0 means "cyclo".

the >2 mm and 0.25–2 mm aggregates exhibited greater relative abundance of O-alkyl C and lower relative abundance of aromatic C than those in the <0.25 mm aggregates; meanwhile, no significant differences ($p > 0.05$) were observed in the relative abundance of carbonyl C and alkyl C across different aggregates (Table 6). Notably, the values of RI, AI, and A/OA within aggregates were all ranked as 44a > 18a, 25a, and 34a > 7a (except for the RI and A/OA within >2 mm aggregates); meanwhile, the SOC in <0.25 mm aggregates owned significantly higher values of RI, AI, and A/OA than those in >2 mm and 0.25–2 mm aggregates irrespective of the stand ages (Table 6).

3.7 Interaction mechanisms between microbial attributes and SOC characteristics

The partial least squares path modeling (PLS-PM, GOF = 0.690; Figure 5) was conducted to investigate the correlation between microbial attributes (i.e., microbial community, exo-enzyme activities, and microbial residues) and SOC characteristics within soil aggregates of different-aged larch plantations and their potential mechanisms. The PLS-PM analysis validated the hypothesis (iii) and demonstrated that stand ages have significant and negative impacts on microbial

TABLE 4 The exo-enzyme activities (nmol g^{-1} soil h^{-1}) within soil aggregates in differently-aged *Larix principis-rupprechtii* stands.

Indices	Stand age (S)	Soil aggregate size (A)			Effects		
		>2 mm	0.25–2 mm	<0.25 mm	A	S	A × S
αG	7a	8.0 ± 0.3d	13.7 ± 2.2a	9.6 ± 1.7ab	**	**	ns
	18a	13.8 ± 0.4a	16.2 ± 0.5a	11.0 ± 2.0a			
	25a	12.7 ± 1.2ab	15.6 ± 1.4a	9.9 ± 0.6a			
	34a	10.8 ± 1.9bc	13.8 ± 1.3a	7.2 ± 1.1b			
	44a	10.1 ± 1.3 cd	13.5 ± 1.8a	8.5 ± 0.9ab			
	Average	11.0B	14.6A	9.3C			
βG	7a	74.8 ± 3.3b	87.9 ± 7.5b	67.8 ± 10.7b	**	**	ns
	18a	98.4 ± 7.3a	128.2 ± 19.2a	101.8 ± 14.5a			
	25a	103.5 ± 10.8a	115.9 ± 15.0a	69.8 ± 16.8b			
	34a	76.3 ± 10.1b	78.7 ± 10.4bc	62.6 ± 15.0b			
	44a	56.2 ± 4.8c	57.7 ± 6.1c	49.3 ± 8.3b			
	Average	81.8AB	93.7A	70.3B			
XYL	7a	42.7 ± 3.6b	40.0 ± 3.2c	25.6 ± 4.5b	**	**	*
	18a	63.1 ± 5.4a	66.3 ± 6.6a	34.5 ± 6.1ab			
	25a	68.0 ± 7.1a	54.6 ± 6.6b	42.6 ± 4.5a			
	34a	43.5 ± 6.7b	40.9 ± 4.6c	31.4 ± 2.3b			
	44a	46.9 ± 6.0b	42.2 ± 5.1c	29.4 ± 4.8b			
	Average	52.8A	48.8A	32.7B			
CBH	7a	47.2 ± 1.8bc	54.6 ± 9.6c	39.4 ± 8.5b	**	**	ns
	18a	71.0 ± 9.2a	90.0 ± 8.6a	66.6 ± 7.2a			
	25a	68.8 ± 1.9a	74.2 ± 10.5b	63.3 ± 10.1a			
	34a	53.5 ± 3.7b	54.7 ± 5.0c	44.7 ± 7.2b			
	44a	42.4 ± 3.1c	55.6 ± 3.4c	34.4 ± 7.2b			
	Average	56.6AB	65.8A	49.7B			
NAG	7a	27.0 ± 1.8b	26.5 ± 4.9bc	20.2 ± 0.8bc	**	**	ns
	18a	30.2 ± 2.2b	34.8 ± 4.4ab	25.9 ± 4.1a			
	25a	35.6 ± 4.2a	42.5 ± 5.2a	25.5 ± 4.1ab			
	34a	20.5 ± 2.8c	23.6 ± 3.4c	19.9 ± 2.7bc			
	44a	20.7 ± 2.1c	24.2 ± 4.5c	19.6 ± 1.3c			
	Average	26.8AB	30.3A	22.2B			
PHOs	7a	4.95 ± 0.31c	4.60 ± 0.47c	6.21 ± 0.55b	**	**	ns
	18a	4.72 ± 0.39c	4.68 ± 0.33c	5.88 ± 0.32b			
	25a	6.18 ± 0.20b	6.29 ± 0.29b	7.94 ± 0.91a			
	34a	7.07 ± 0.32a	7.19 ± 0.56a	8.15 ± 0.28a			
	44a	7.10 ± 0.09a	7.74 ± 0.66a	7.88 ± 0.50a			
	Average	6.00B	6.10B	7.21A			
PerX	7a	3.45 ± 0.36c	4.10 ± 0.25c	4.91 ± 0.72d	**	**	ns
	18a	5.29 ± 0.77b	5.79 ± 0.55b	6.87 ± 0.86c			
	25a	5.18 ± 0.51b	5.70 ± 0.74b	7.21 ± 0.14bc			
	34a	6.52 ± 0.30a	6.44 ± 0.32ab	8.78 ± 0.90a			
	44a	6.47 ± 0.62a	6.75 ± 0.40a	8.38 ± 0.55ab			
	Average	5.38B	5.76B	7.23A			

Data were shown as means values ± S.E. (n = 3 or 15). Different uppercase and lowercase letters indicate significant differences among different soil aggregates and differently-aged *Larix principis-rupprechtii* stands within the same soil aggregates at the $P < 0.05$ level, respectively. Two-way ANOVA are applied for identifying the effects of stand age (S), aggregate size (A), and their interaction (S × A) on the above-mentioned indices (The results are shown in the right side of the table). **, *, and "ns" represent significant at $P < 0.01$, $P < 0.05$, and no significant differences ($P > 0.05$), respectively. αG, α-Glucosidase; βG, β-Glucosidase; CBH, β-Cellobiosidase; XYL, β-Xylosidase; NAG, N-acetyl-glucosaminidase; PHOs, phenol oxidase; PerX, peroxidase.

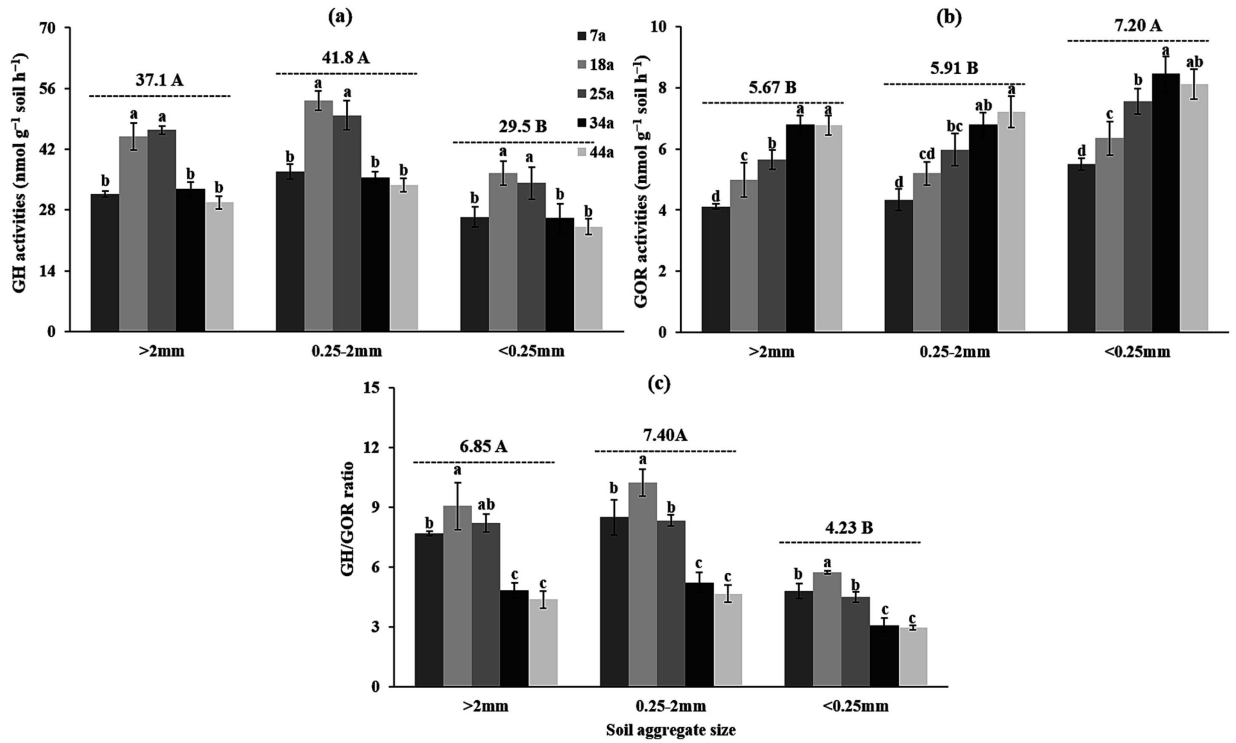


FIGURE 3
The geometric mean of the assayed exo-enzyme activities [**(a)** GH, **(b)** GOR and **(c)** GH/GOR] within soil aggregates across differently-aged *Larix principis-rupprechtii* stands. Different uppercase and lowercase letters indicate significant differences among different soil aggregates and differently-aged *Larix principis-rupprechtii* stands within the same soil aggregates at the $p < 0.05$ level, respectively. GH, the geometric mean of the hydrolytic exo-enzyme activities; GOR, the geometric mean of the oxidative exo-enzyme activities.

communities (path coefficient = −0.354**) and exo-enzyme activities (−0.053**); concurrently, the aggregate sizes exhibited significantly positive and negative effects on microbial residue C (0.333**) and exo-enzyme activities (−0.284**), respectively. Besides, microbial community (0.348*) and exo-enzyme activities (0.670**) together positively regulated microbial residue C. Furthermore, microbial residue C (0.822**) and exo-enzyme activities (0.276**), rather than microbial community, were considered to be critical factors that positively affected SOC contents. Simultaneously, exo-enzyme activities (−0.960**) exhibited a significantly negative effect on SOC stability.

4 Discussion

4.1 Changes in soil aggregate distribution and nutrient characteristics along stand development

Soil aggregate's characteristics (i.e., aggregate distribution, MWD, and GMD), essential indicators for evaluating soil structure and quality, are governed by a series of factors, e.g., organic matter, Fe/Al oxides, and other biological attributes (Cheng et al., 2024). In this study, the proportion of > 2 mm aggregates and aggregate stability (as indicated by the values of MWD and GMD) increased along the stand ages, reaching the highest in the 18a stand (Table 1). This finding was consistent with previous study at the Beijiang River Forest Farm in Guangxi Zhuang Autonomous Region, China (He et al., 2021), which suggested with increasing stand ages, the proportions of > 2 mm aggregates and MWD initially increase and then decrease, and peak in the 17a stand. These findings could be ascribed to the temporal changes in organic C contents in soils during forest development (Ayoubi et al., 2012). Sun et al. (2024) also revealed that organic C in soils served as key "binding agents" for aggregate formation and enhancing aggregate stability. The similar temporal variation patterns between organic C and MWD in the present study also confirmed the above-mentioned opinions.

The stocks of SOC and nutrients (e.g., nitrogen) depends on the dynamic balance of exo-resources inputs (e.g., litters) vs. outputs (e.g., mineralization) (Luan et al., 2022). Generally, it is expected that SOC and nutrients would increase with stand age due to the annual input and accumulation of forest litters and root exudates in the subtropical regions in China (Chen et al., 2020; Hu J. et al., 2024). Nevertheless, our findings indicated that the contents of SOC and TN within aggregates initially increase, then decrease, peaking in the 18a stand (Table 2), which were contradicted the hypothesis (i). These inconsistent findings may be explained by the differences in climatic conditions across different study regions (i.e., subtropical region vs. temperate region in this study). Ma et al. (2022) highlighted that temperature, as one vital part of soil microclimates, may alter microbial growth and functional characteristics, thereby indirectly affecting litter degradation and SOC cycling processes. Donhauser and Frey (2018) also demonstrated that several adverse soil microenvironment, e.g., severely low temperature and desiccation, can impose significant stress on microbial communities, potentially inhibiting their activity and growth. Consequently, the climatic conditions characterized by low temperature (annual average

10.3389/fmicb.2025.1588030

TABLE 5 The amino sugars (mg kg^{-1}) within soil aggregates in differently-aged *Larix principis-rupprechtii* stands.

Indices	Stand age (S)	Soil aggregate size (A)			Effects		
		>2 mm	0.25–2 mm	<0.25 mm	A	S	A × S
GluN	7a	610.1 ± 56.4b	697.7 ± 51.7b	668.6 ± 84.5ab	**	**	ns
	18a	753.6 ± 53.0a	873.6 ± 12.6a	804.8 ± 57.4a			
	25a	730.4 ± 35.3a	859.3 ± 59.7a	794.5 ± 114.2a			
	34a	574.5 ± 35.0b	634.6 ± 58.8b	608.6 ± 33.5b			
	44a	562.2 ± 40.7b	682.3 ± 78.1b	606.8 ± 87.4b			
	Average	646.1B	749.5A	696.6AB			
GalN	7a	372.8 ± 42.3 cd	432.7 ± 53.2b	386.4 ± 57.9bc	**	**	ns
	18a	482.8 ± 23.3a	589.3 ± 17.9a	488.9 ± 16.3a			
	25a	454.7 ± 49.8ab	511.0 ± 45.8ab	434.9 ± 50.2ab			
	34a	400.8 ± 30.9bc	462.6 ± 78.5ab	408.1 ± 67.9abc			
	44a	324.3 ± 26.4d	393.2 ± 104.9b	337.4 ± 6.5c			
	Average	407.1B	477.7A	411.1B			
MurA	7a	37.4 ± 4.1b	44.1 ± 3.5c	31.2 ± 3.6bc	**	**	ns
	18a	48.6 ± 1.1a	60.4 ± 3.0a	42.0 ± 3.7a			
	25a	43.6 ± 4.4a	51.8 ± 5.2b	36.5 ± 3.9ab			
	34a	28.7 ± 1.8c	33.8 ± 5.3d	25.3 ± 3.9 cd			
	44a	25.3 ± 3.6c	31.4 ± 3.6d	22.2 ± 3.1d			
	Average	36.7B	44.3A	31.5C			
Total AS	7a	1020.3 ± 51.9b	1174.5 ± 62.3b	1086.2 ± 138.1bc	**	**	ns
	18a	1285.0 ± 52.0a	1523.3 ± 6.8a	1335.7 ± 75.4a			
	25a	1228.7 ± 86.5a	1422.1 ± 103.8a	1265.8 ± 167.9ab			
	34a	1004.0 ± 64.7b	1131.0 ± 139.1b	1042.1 ± 103.9bc			
	44a	911.8 ± 30.3b	1106.9 ± 180.1b	966.4 ± 94.6c			
	Average	1090.0B	1271.6A	1139.3B			

Data were shown as means values ± S.E. (n = 3 or 15). Different uppercase and lowercase letters indicate significant differences among different soil aggregates and differently-aged *Larix principis-rupprechtii* stands within the same soil aggregates at the $P < 0.05$ level, respectively. Two-way ANOVA are applied for identifying the effects of stand age (S), aggregate size (A), and their interaction (S × A) on the above-mentioned indices (the results are shown in the right side of the table). ** and "ns" represent significant at $P < 0.01$ and no significant differences ($P > 0.05$), respectively. AS, amino sugar.

temperature of −1.4°C) at the study sites impede microbial activity and litter decomposition (Tian et al., 2025). Meanwhile, the annual storage of litter detritus led to the development of thicker litter layers in the elder stands, which diminished soil aeration, thereby further inhibiting litter decomposition (Keiluweit et al., 2016). In other words, the continuous cold temperature and progressively worsening aeration conditions in soils were not beneficial for the conversion of litter into SOC, resulting in a reduction of SOC in the 25a, 34a and 44a stands in this study.

Yao Y. et al. (2019) demonstrated that SOC and nutrients were unevenly distributed across aggregates. In the present study, the contents of SOC and TN showed a similar distribution pattern within different aggregates, i.e., higher contents of SOC and TN were basically observed in the larger aggregates than those in the smaller aggregates irrespective of the stand ages (Table 2), which were verified the hypothesis (ii) and indicated that larger aggregates owned a higher capacity to retain these nutrients. This phenomenon could be explained by the "aggregate hierarchy model," which posits that larger aggregates are constituted by smaller aggregates in conjunction with several "binding agents" (e.g., organic C constitutes); meanwhile, this process facilitated the storage of C within the larger aggregates (Ji et al., 2024). Wang et al. (2017) also reported that exogenous C and nutrient (e.g., forest litters) resources are difficult to reach the smaller aggregates due to the preferential "localization" of these resources within the larger aggregates, which further confirmed that the larger aggregates contained higher SOC and TN than the smaller aggregates in the present study.

4.2 Changes in microbial attributes within aggregates along stand development

Given the important role of microbes in the process of SOC cycling, clarifying the temporal–spatial changes in microbial attributes (e.g., microbial community, function, and metabolism) can provide valuable information for better understanding the mechanisms of SOC stabilization during forest development (Zhang et al., 2021). In the present study, it was observed that as stand age increased, microbial biomass (as indicated by the contents of total PLFAs; Table 3), hydrolytic exo-enzyme activities (Figure 3), and microbial residue C (Figure 4) within aggregates, initially increased and then

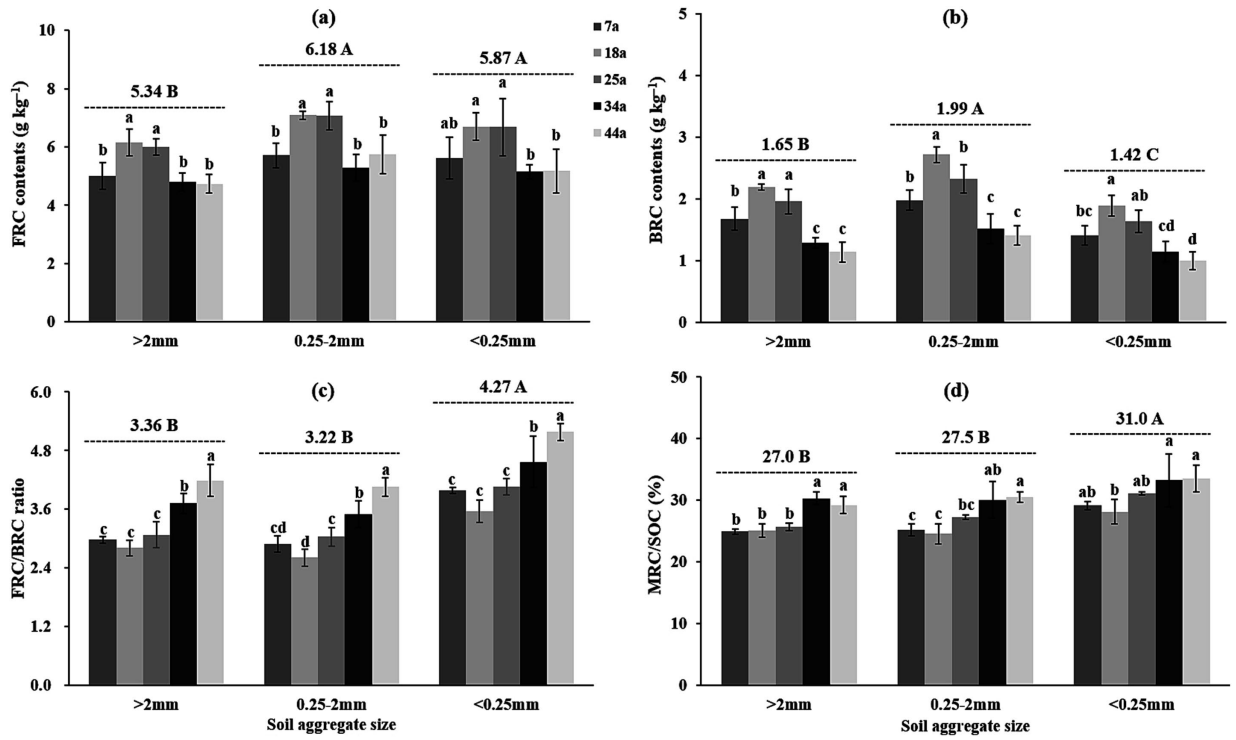


FIGURE 4
The contents of microbial residue C [**(a)** MRC, **(b)** FRC, and **(c)** BRC] as well as the associated ratio [**(d)** MRC/SOC] within soil aggregates across differently-aged *Larix principis-rupprechtii* stands. Different uppercase and lowercase letters indicate significant differences among different soil aggregates and differently-aged *Larix principis-rupprechtii* stands within the same soil aggregates at the $p < 0.05$ level, respectively. FRC, fungal residue C; BRC, bacterial residue C; MRC, microbial residue C; SOC, soil organic C.

decreased, and the highest values for these indices were observed in the 18a or 25a stands. This was partially aligned with the findings of Zhao et al. (2019), who reported microbial biomass showed a unimodal pattern with the progression of afforestation through meta-analysis. The likely reasons for these findings are as follows. Francini et al. (2018) revealed that appropriate soil microenvironment (e.g., adequate nutrients and O_2) is the prerequisites for facilitating microbial growth and metabolism. In the present study, the better soil nutrient status (i.e., higher TN level) in the 18a and 25a stands, as presented in Table 2, created favorable soil conditions for microbial growth and metabolism, which caused higher contents of microbial biomass and microbial residue C in these stands. Sokol et al. (2022) indicated that the exo-enzymes, i.e., hydrolytic and oxidative exo-enzymes, are mainly secreted and produced by bacteria and fungi, respectively, with their activities being mainly regulated by soil properties (e.g., pH) and microbial community structure, etc. Therefore, the higher microbial biomass (Table 3) in the 18a and 25a stands were conducive to enhance hydrolytic exo-enzyme activities. Interestingly, we found that the variations in oxidative exo-enzymes, i.e., the gradually increasing oxidative exo-enzyme activities (as indicated by the values of GOR) during forest development (Figure 3b), were positively correlated with the values of F/B (Figure 6b), rather than with the contents of fungi (Figure 6a). Wang and Kuzyakov (2024) demonstrated that fungi can enhance their competitive ability for nutrients against bacteria by secreting more oxidative exo-enzymes under the premise of limited soil nutrient resources. Namely, although the restricted soil nutrient resources in the elder stands was not favorable for microbial growth (Table 3), they can stimulate fungi to secrete more oxidases to cope with this situation, which partially corroborates the results of Figure 6 and accounts for the observed variations in GOR across differently-aged stands in the present study.

Nowadays, the distribution patterns of microbial attributes within aggregates have been widely reported, but these results remain controversial (Wang S. et al., 2018; Murugan et al., 2019). Our findings indicated that larger aggregates owned higher microbial biomass (Table 3) and hydrolytic exo-enzyme activities, alongside reduced oxidative exo-enzyme activities (Figure 3), compared to smaller aggregates, regardless of the stand ages. This could be explained by exo-enzyme function and aggregate's characteristics (Yao S. et al., 2019; Sokol et al., 2022). The higher nutrient level (see Table 2) as well as more pore structure in the larger aggregates (Wang and Hu, 2023), rather than smaller aggregates, could create a better microenvironment for microbial growth. Furthermore, the nutrient deficiency in the smaller aggregates (see Table 2) may exacerbate bacterial–fungal competition for soil resources, thereby causing fungi to secrete more oxidative exo-enzymes to meet this competition (Wang and Kuzyakov, 2024). Notably, the increased FRC/BRC ratios observed in the smaller aggregates (Figure 4) suggested that FRC played a more dominant role than BRC in forming SOC in these aggregates. The possible explanation for these findings could be associated with differences in microbial necromass properties (Ding et al., 2010) and microbial community structure among different aggregates (Wang S. et al., 2018). He et al. (2022) indicated that fungal and bacterial biomass are the prerequisites for the formation of FRC and BRC, respectively. Hu J. et al. (2024) demonstrated BRC is relatively unstable and more

10.3389/fmicb.2025.1588030

TABLE 6 The relative abundance (%) of different SOC functional groups and their spectroscopic indices within soil aggregates in differently-aged *Larix principis-rupprechtii* stands.

Indices	Stand age (S)	Soil aggregate size (A)			Effects		
		>2 mm	0.25–2 mm	<0.25 mm	A	S	A × S
Carbonyl C	7a	5.22 ± 0.59b	5.94 ± 0.37a	6.93 ± 1.09a	ns	ns	*
	18a	6.38 ± 1.39ab	5.25 ± 1.24a	6.95 ± 0.74a			
	25a	6.21 ± 0.47ab	6.39 ± 0.92a	7.05 ± 0.36a			
	34a	6.89 ± 0.61a	6.54 ± 0.64a	5.09 ± 0.66b			
	44a	6.71 ± 0.39ab	6.33 ± 0.42a	6.18 ± 0.9ab			
	Average	6.28A	6.09A	6.44A			
Aromatic C	7a	12.2 ± 0.8c	12.9 ± 0.9b	14.0 ± 0.7c	**	**	ns
	18a	13.5 ± 0.5b	14.4 ± 1.2ab	14.7 ± 0.8bc			
	25a	15.4 ± 0.1a	15.2 ± 0.1a	16.3 ± 0.1ab			
	34a	15.4 ± 0.8a	14.3 ± 1.2ab	16.3 ± 1.4ab			
	44a	15.7 ± 0.2a	16.0 ± 0.9a	16.7 ± 1.4a			
	Average	14.5B	14.6B	15.6A			
O-alkyl C	7a	52.1 ± 0.8a	52.8 ± 0.4a	49.8 ± 1.3a	**	**	ns
	18a	52.4 ± 0.6a	50.9 ± 0.7ab	48.9 ± 1.9ab			
	25a	51.1 ± 1.7ab	50.1 ± 0.5bc	49.0 ± 0.2ab			
	34a	49.0 ± 2.6b	50.1 ± 2.5bc	48.6 ± 1.3ab			
	44a	49.0 ± 0.4b	48.0 ± 0.8c	47.3 ± 0.6b			
	Average	50.7A	50.4A	48.72B			
Alkyl C	7a	30.5 ± 1.2a	28.3 ± 0.2a	29.3 ± 0.9ab	ns	ns	ns
	18a	27.7 ± 2.0a	29.5 ± 2.2a	29.5 ± 1.0a			
	25a	27.3 ± 1.7a	28.3 ± 0.5a	27.7 ± 0.3b			
	34a	28.7 ± 2.2a	29.1 ± 1.9a	30.0 ± 0.7a			
	44a	28.5 ± 0.9a	29.6 ± 0.6a	29.8 ± 1.2a			
	Average	28.5A	29.0A	29.2A			
RI	7a	0.746 ± 0.040a	0.703 ± 0.021c	0.764 ± 0.010b	**	**	ns
	18a	0.702 ± 0.059a	0.781 ± 0.033ab	0.791 ± 0.043b			
	25a	0.746 ± 0.054a	0.770 ± 0.015bc	0.784 ± 0.005b			
	34a	0.793 ± 0.097a	0.768 ± 0.068bc	0.861 ± 0.024a			
	44a	0.794 ± 0.023a	0.842 ± 0.023a	0.870 ± 0.014a			
	Average	0.756B	0.773B	0.814A			
AI	7a	0.129 ± 0.009c	0.138 ± 0.009b	0.151 ± 0.006b	**	**	ns
	18a	0.144 ± 0.006b	0.152 ± 0.015ab	0.158 ± 0.010ab			
	25a	0.164 ± 0.001a	0.163 ± 0.002a	0.175 ± 0.002a			
	34a	0.166 ± 0.008a	0.153 ± 0.014ab	0.172 ± 0.016ab			
	44a	0.168 ± 0.003a	0.171 ± 0.010a	0.178 ± 0.015a			
	Average	0.154B	0.155B	0.167A			
A/OA	7a	0.585 ± 0.030a	0.537 ± 0.003b	0.589 ± 0.034ab	*	*	ns
	18a	0.529 ± 0.045a	0.579 ± 0.043ab	0.603 ± 0.038ab			
	25a	0.535 ± 0.050a	0.564 ± 0.007ab	0.564 ± 0.003b			
	34a	0.588 ± 0.078a	0.583 ± 0.061ab	0.616 ± 0.001a			
	44a	0.582 ± 0.023a	0.618 ± 0.012a	0.630 ± 0.022a			
	Average	0.564B	0.576AB	0.600A			

Data were shown as means values ± S.E. (n = 3 or 15). Different uppercase and lowercase letters indicate significant differences among different soil aggregates and differently-aged *Larix principis-rupprechtii* stands within the same soil aggregates at the $P < 0.05$ level, respectively. Two-way ANOVA are applied for identifying the effects of stand age (S), aggregate size (A), and their interaction (S × A) on the above-mentioned indices (The results are shown in the right side of the table). **, *, and "ns" represent significant at $P < 0.01$, $P < 0.05$, and no significant differences ($P > 0.05$), respectively. RI, recalcitrance index; AI, aromaticity index; A/OA, alkyl C/O-alkyl C.

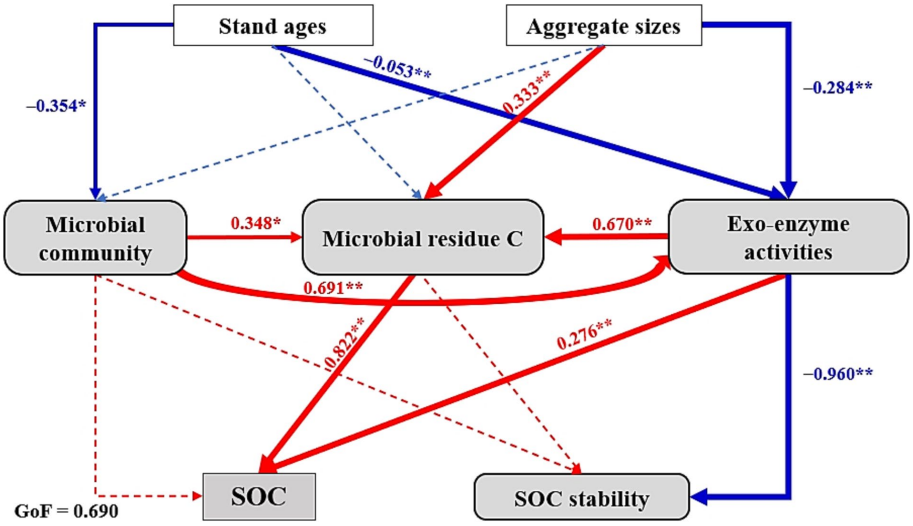


FIGURE 5
Partial least squares path model (PLS-PM) disentangling major pathways of microbial characteristics (i.e., microbial community, exo-enzyme activities, and microbial residue C) influences on SOC contents and their stability within aggregates across differently-aged *Larix principis-rupprechtii* stands. The arrows indicate the hypothesized direction of causation. The solid red and blue arrows indicate significant ($p < 0.05$) positive and negative relationships, respectively. Besides, the dashed arrows indicate non-significant effect ($p > 0.05$). The following variables were included: microbial community (total PLFAs, fungi, bacteria, and actinomycetes), exo-enzyme activities (α-Glucosidase, β-Glucosidase, β-Cellobiosidase, β-Xylosidase, N-acetyl-glucosaminidase, phenol oxidase, and peroxidase) and SOC stability (recalcitrance index, aromaticity index, and alkyl C/O-alkyl C). Asterisks indicate the statistical significance (**$p < 0.01$ and *$p < 0.05$).

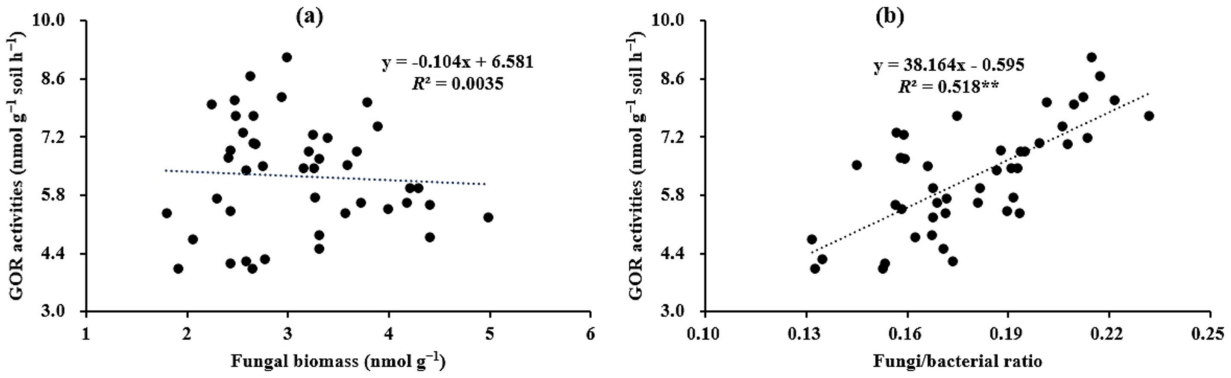


FIGURE 6
Relationships between the GOR activities and the fungal biomass **(a)** or the fungi/bacteria ratio **(b)** within soil aggregates across differently-aged *Larix principis-rupprechtii* stands ($n = 45$). GOR, the geometric mean of the oxidative exo-enzyme activities; F, fungi; B, bacteria. **Indicates significant at $p < 0.01$.

susceptible to decomposition compared to FRC in soils characterized by "poor" nutrient levels. Based on the above-mentioned findings, the lower SOC and TN, along with higher F/B values observed in the smaller aggregates (Tables 5, 6), led to increased consumption of BRC and enhanced production of FRC, which explained the higher FRC/BRC in the smaller aggregates.

4.3 Changes in SOC characteristics within aggregates along stand development

Understanding the temporal dynamics in SOC chemical composition within aggregates can provide several new insights for better clarifying the mechanisms of SOC stabilization process during forest development (Wu et al., 2021). In the present study, the lower O-alkyl C abundance and higher aromatic C abundance were observed in the older stands (34a and 44a) compared to the younger stands (Table 6). This result was consistent with observations from Yang et al. (2021), in which the 64a stands contained higher aromatic C abundance and lower O-alkyl C abundance than the 19a and 37a stands in the Moso bamboo plantations. This could be mostly ascribed to the imbalance between soil resource vs. microbial nutrient demand (Gurmessa et al., 2024). The O-alkyl C (i.e., the labile C constitutes), rather than aromatic C (i.e., the stable C fractions), were preferentially consumed by microbes for their growth and metabolism under the "poor" soil nutrient status in the older stands (Table 2) (Yao S. et al., 2019). Notably, in accordance

with previous studies (Luan et al., 2021; Wang et al., 2022), we observed that the SOC in the larger aggregates owned lower O-alkyl C abundance and higher aromatic C abundance than those in the smaller aggregates. The reduced nutrient levels observed in the smaller aggregates (see Table 2) could enhance the consumption of labile C (e.g., O-alkyl C) by microbes (Gurmessa et al., 2024), which could partially elucidate the above-mentioned findings. Besides, fungi are recognized as the key decomposers of stable C constitutes (e.g., aromatic C) and preferentially thrive in soils with high O_2 levels (Liu et al., 2021). Consequently, the diminished fungal biomass and poor gas (e.g., O_2) status in the smaller aggregates are not favorable for the decomposition of recalcitrant C (e.g., aromatic C). Taken together, the above-mentioned findings offer an explanation for the variations in SOC functional group composition across different aggregates.

The RI, AI, and A/OA were calculated by the four C functional groups, which could be applied to evaluate SOC stability, aromaticity, and degradation degree, respectively (Guo et al., 2019). In this study, as aggregate sizes decreased, these indices (i.e., RI, AI, and A/OA) showed increasing trends (Table 6), indicating that SOC in the smaller aggregates exhibited higher stability, greater aromaticity, and a higher degree of degradation. These rising patterns with decreasing aggregate sizes are likely attributed to enhanced consumption of O-alkyl C and diminished decomposition of aromatic C in the smaller aggregates (Table 6; Guo et al., 2019). The above-mentioned findings, in conjunction with our results (i.e., elevated RI, AI, and A/OA values in the 44a stand), also suggested an enhancement in SOC stability and aromaticity in the older stands.

5 Conclusion

The elucidation of the temporal dynamics of SOC characteristics and microbial attributes at the aggregate scale, employing a series of technologies (i.e., ^{13}C NMR, PLFAs, exo-enzymatic activity, and microbial residue analysis, etc.), can offer novel insights into SOC stocks in relation to stand ages in *Larix principis-rupprechtii* plantations in Northern China. Firstly, with increasing stand age, the levels of SOC, microbial biomass, hydrolytic exo-enzymatic activities, and microbial residues, initially increase and then decrease, and generally peak in the 18a stand; meanwhile, these indices were generally higher in larger aggregates compared to smaller aggregates irrespective of the stand ages. Secondly, we observed that the increased stand ages and reduced aggregate size altered SOC chemical composition (more "labile" O-alkyl C and less "stable" aromatic C), enhanced SOC stability and oxidative exo-enzymatic activities, as well as enlarged the microbial contribution to SOC stocks. Finally, the PLS-PM model confirmed that SOC stocks were closely linked to microbial residues; meanwhile, the microbial community altered SOC stability by modulating exo-enzyme activities. These findings enhance our understanding of the microbial-driven mechanisms underlying SOC stabilization during forest development in Northern China.

Data availability statement

The data analyzed in this study is subject to the following licenses/restrictions: requests to access these datasets should be directed to luanhaoan@163.com.

Author contributions

MY: Data curation, Formal analysis, Investigation, Methodology, Writing – original draft. XH: Conceptualization, Investigation, Software, Writing – original draft. JL: Data curation, Investigation, Resources, Software, Writing – original draft. QL: Data curation, Investigation, Methodology, Software, Writing – review & editing. LF: Investigation, Methodology, Software, Writing – review & editing. XC: Data curation, Investigation, Methodology, Software, Writing – review & editing. SH: Conceptualization, Data curation, Methodology, Resources, Supervision, Validation, Writing – review & editing. HL: Conceptualization, Funding acquisition, Resources, Writing – original draft, Writing – review & editing.

Funding

The author(s) declare that financial support was received for the research and/or publication of this article. This work was financially supported by the National Key Research and Development Program of China (2021YFD1901001), the Natural Science Foundation of Hebei Province (C2024204108), the Scientific Research Projects for Talents Introduce in Hebei Agricultural University (YJ2020054 and YJ2020058), Hebei Province Forest and Grass Key Technology Innovation and Demonstration Project (2303087), Hebei Province Forest and Grass Technology Promotion Demonstration Project (JITG[2022]012), and College Student Innovation and Entrepreneurship Training Program Project (2025231).

Conflict of interest

The authors declare that the research was conducted in the absence of any commercial or financial relationships that could be construed as a potential conflict of interest.

Generative AI statement

The authors declare that no Gen AI was used in the creation of this manuscript.

Publisher's note

All claims expressed in this article are solely those of the authors and do not necessarily represent those of their affiliated organizations, or those of the publisher, the editors and the reviewers. Any product that may be evaluated in this article, or claim that may be made by its manufacturer, is not guaranteed or endorsed by the publisher.

Supplementary material

The Supplementary material for this article can be found online at: https://www.frontiersin.org/articles/10.3389/fmicb.2025.1588030/full#supplementary-material

References

Abaker, W. E., Berninger, F., Saiz, G., Braojos, V., and Starr, M. (2016). Contribution of *Acacia senegal* to biomass and soil carbon in plantations of varying age in Sudan. *For. Ecol. Manag.* 368, 71–80. doi: 10.1016/j.foreco.2016.03.003

Ayoubi, S., Karchegani, P. M., Mosaddeghi, M. R., and Honarjoo, N. (2012). Soil aggregation and organic carbon as affected by topography and land use change in western Iran. *Soil Till. Res.* 121, 18–26. doi: 10.1016/j.still.2012.01.011

Chen, Y., Day, S. D., Wick, A. F., and McGuire, K. J. (2014). Influence of urban land development and subsequent soil rehabilitation on soil aggregates, carbon, and hydraulic conductivity. *Sci. Total Environ.* 495, 329–336. doi: 10.1016/j.scitotenv.2014.06.099

Chen, A., Wang, Z., Lin, Y., Wang, X., Li, Y., Zhang, Y., et al. (2020). Temporal variation of soil organic carbon pools along a chronosequence of reforested land in Southwest China. *Catena* 194:104650. doi: 10.1016/j.catena.2020.104650

Cheng, Z., Guo, J., Jin, W., Liu, Z., Wang, Q., Zha, L., et al. (2024). Responses of SOC, labile SOC fractions, and amino sugars to different organic amendments in a coastal saline-alkali soil. *Soil Till. Res.* 239:106051. doi: 10.1016/j.still.2024.106051

Ding, X., Zhang, X., He, H., and Xie, H. (2010). Dynamics of soil amino sugar pools during decomposition processes of corn residues as affected by inorganic N addition. *J. Soils Sediments* 10, 758–766. doi: 10.1007/s11368-009-0132-7

Dong, L., Lu, W., and Liu, Z. (2020). Determining the optimal rotations of larch plantations when multiple carbon pools and wood products are valued. *For. Ecol. Manag.* 474:118356. doi: 10.1016/j.foreco.2020.118356

Donhauser, J., and Frey, B. (2018). Alpine soil microbial ecology in a changing world. *FEMS Microbiol. Ecol.* 94:fiy099. doi: 10.1093/femsec/fiy099

FAO (2014). World Reference Base for soil resources. World soil resources reports no.106. Rome: FAO.

Francini, G., Hui, N., Jumpponen, A., Kotze, D. J., Romantschuk, M., Allen, J. A., et al. (2018). Soil biota in boreal urban greenspace: responses to plant type and age. *Soil Biol. Biochem.* 118, 145–155. doi: 10.1016/j.soilbio.2017.11.019

Guo, Z., Zhang, Z., Zhou, H., Wang, D., and Peng, X. (2019). The effect of 34-year continuous fertilization on the SOC physical fractions and its chemical composition in a vertisol. *Sci. Rep.* 9:2505. doi: 10.1038/s41598-019-38952-6

Gupta, V. V. S. R., and Germida, J. J. (2015). Soil aggregation: influence on microbial biomass and implications for biological processes. *Soil Biol. Biochem.* 80, A3–A9. doi: 10.1016/j.soilbio.2014.09.002

Gurmessa, B., Cocco, S., Ashworth, A. J., Udawatta, R. P., Cardelli, V., Serrani, D., et al. (2024). Enzyme activities and microbial nutrient limitations in response to digestate and compost additions in organic matter poor soils in the marches, Italy. *Soil Till. Res.* 242:106136. doi: 10.1016/j.still.2024.106136

He, M., Fang, K., Chen, L., Feng, X., Qin, S., Kou, D., et al. (2022). Depth-dependent drivers of soil microbial necromass carbon across Tibetan alpine grasslands. *Glob. Chang. Biol.* 28, 936–949. doi: 10.1111/gcb.15969

He, X., Huang, Y., Zhang, Q., Ye, S., and Wang, S. (2021). Distribution of organic carbon fractions in soil aggregates in *Chinese fir* plantations with different stand ages. *Ecol. Process.* 10:49. doi: 10.1186/s13717-021-00321-5

Hu, J., Liu, C., Gou, M., Lei, L., Chen, H., and Zhang, J. (2024). Contrasting change patterns of lignin and microbial necromass carbon and the determinants in a chronosequence of subtropical *Pinus massoniana* plantations. *Appl. Soil Ecol.* 198:105385. doi: 10.1016/j.apsoil.2024.105385

Hu, H., Qian, C., Xue, K., Jörgensen, R. G., Keiluweit, M., Liang, C., et al. (2024). Reducing the uncertainty in estimating soil microbial-derived carbon storage. *P. Natl. Acad. Sci. USA.* 121:e2401916121. doi: 10.1073/pnas.2401916121

Ji, L., Chen, X., Huang, C., and Tan, W. (2024). Arbuscular mycorrhizal hyphal networks and glomalin-related soil protein jointly promote soil aggregation and alter aggregate hierarchy in Calcaric Regosol. *Geoderma* 452:117096. doi: 10.1016/j.geoderma.2024.117096

Jing, Y., Zhao, X., Liu, S., Tian, P., Sun, Z., Chen, L., et al. (2022). Microbial residue distribution in microaggregates decreases with stand age in subtropical plantations. *Forests* 13:1145. doi: 10.3390/f13071145

Keiluweit, M., Nico, P. S., Kleber, M., and Fendorf, S. (2016). Are oxygen limitations under recognized regulators of organic carbon turnover in upland soils? *Biogeochemistry* 127, 157–171. doi: 10.1007/s10533-015-0180-6

Kramer, S., Marhan, S., Haslwimmer, H., Ruess, L., and Kandeler, E. (2013). Temporal variation in surface and subsoil abundance and function of the soil microbial community in an arable soil. *Soil Biol. Biochem.* 61, 76–85. doi: 10.1016/j.soilbio.2013.02.006

Kuzyakov, Y., and Blagodatskaya, E. (2015). Microbial hotspots and hot moments in soil: concept & review. *Soil Biol. Biochem.* 83, 184–199. doi: 10.1016/j.soilbio.2015.01.025

Liang, C., Schimel, J. P., and Jastrow, J. D. (2017). The importance of anabolism in microbial control over soil carbon storage. *Nat. Microbiol.* 2:17105. doi: 10.1038/nmicrobiol.2017.105

Liang, B., Wang, J., Zhang, Z., Zhang, J., Zhang, J., Cressey, E. L., et al. (2022). Planted forest is catching up with natural forest in China in terms of carbon density and carbon storage. *Fundamental Res.* 2, 688–696. doi: 10.1016/j.fmre.2022.04.008

Liao, Z., Ye, S., and Wang, S. (2023). Soil bacterial community structure as affected by stand age in *Chinese fir* plantations: insights at the aggregate scale. *Land Degrad. Dev.* 34, 389–402. doi: 10.1002/ldr.4467

Liu, G., Deng, D., Yang, M., and Sun, Y. (2023). Root traits and soil bacterial composition explain the rhizosphere effects along a Chronosequence of *rubber* plantations. *Forests* 14:2209. doi: 10.3390/f14112209

Liu, X., Hou, L., Ding, C., Su, X., Zhang, W., and Peng, Z. (2024). Effects of stand age and soil microbial communities on soil respiration throughout the growth cycle of poplar plantations in northeastern China. *Front. Microbiol.* 15:1477571. doi: 10.3389/fmicb.2024.1477571

Liu, Z., Hou, L., Zhu, Y., and Xu, X. (2021). Vertical distribution and regulation of Olsen-phosphorus in 6-m soil profiles after farmland-to-apple orchard conversion on the Chinese loess plateau. *Catena* 202:105254. doi: 10.1016/j.catena.2021.105254

Liu, Q., Wang, S., Ma, R., Huang, F., Li, J., Ye, S., et al. (2024). Comparative analysis of forest soil carbon sink and source based on bibliometrics: development, hotspots, and trends. *J. Clean. Prod.* 480:144106. doi: 10.1016/j.jclepro.2024.144106

Luan, H., Gao, W., Tang, J., Li, R., Li, M., and Zhang, H. (2020). Aggregate-associated changes in nutrient properties, microbial community and functions in a greenhouse vegetable field based on an eight-year fertilization experiment of China. *J. Integr. Agr.* 19, 2530–2548. doi: 10.1016/S2095-3119(20)63269-5

Luan, H., Liu, Y., Huang, S., Qiao, W., Chen, J., and Guo, T. (2022). Successive walnut plantations alter soil carbon quantity and quality by modifying microbial communities and enzyme activities. *Front. in Microbiol.* 13:953552. doi: 10.3389/fmicb.2022.953552

Luan, H., Yuan, S., Gao, W., Tang, J., Li, R., and Zhang, H. (2021). Changes in organic C stability within soil aggregates under different fertilization patterns in a greenhouse vegetable field. *J. Integr. Agr.* 20, 2758–2771. doi: 10.1016/S2095-3119(21)63646-8

Ma, L., Liu, L., Lu, Y., Chen, L., Zhang, Z., Zhang, H., et al. (2022). When microclimates meet soil microbes: temperature controls soil microbial diversity along an elevational gradient in subtropical forests. *Soil Biol. Biochem.* 166:108566. doi: 10.1016/j.soilbio.2022.108566

Ma, T., Yang, Z., Shi, B., Gao, W., Li, Y., Zhu, J., et al. (2023). Phosphorus supply suppressed microbial necromass but stimulated plant lignin phenols accumulation in soils of alpine grassland on the Tibetan plateau. *Geoderma* 431:116376. doi: 10.1016/j.geoderma.2023.116376

Mao, L., He, X., Ye, S., and Wang, S. (2023). Soil aggregate-associated carbon-cycle and nitrogen-cycle enzyme activities as affected by stand age in *Chinese fir* plantations. *J. Soil Sci. Plant Nut.* 23, 4361–4372. doi: 10.1007/s42729-023-01355-8

Mao, L., Tang, L., Ye, S., and Wang, S. (2021). Soil organic C and total N as well as microbial biomass C and N affect aggregate stability in a chronosequence of *Chinese fir* plantations. *Eur. J. Soil Biol.* 106:103347. doi: 10.1016/j.ejsobi.2021.103347

Mujuru, L., Gotora, T., Velthorst, E. J., Nyamangara, J., and Hoosbeek, M. R. (2014). Soil carbon and nitrogen sequestration over an age sequence of *Pinus patula* plantations in Zimbabwean eastern highlands. *For. Ecol. Manag.* 313, 254–265. doi: 10.1016/j.foreco.2013.11.024

Murugan, R., Djukic, I., Keiblinger, K., Zehetner, F., Bierbaumer, M., Zechmeister-Bolternstern, S., et al. (2019). Spatial distribution of microbial biomass and residues across soil aggregate fractions at different elevations in the central Austrian Alps. *Geoderma* 339, 1–8. doi: 10.1016/j.geoderma.2018.12.018

Sakschewski, B., Bloh, W. V., Boit, A., Poorter, L., and Thonicke, K. (2016). Resilience of Amazon forests emerges from plant trait diversity. *Nat. Clim. Chang.* 6, 1032–1036. doi: 10.1038/nclimate3109

Shao, P., He, H., Zhang, X., Xie, H., Bao, X., and Liang, C. (2018). Responses of microbial residues to simulated climate change in a semiarid grassland. *Sci. Total Environ.* 644, 1286–1291. doi: 10.1016/j.scitotenv.2018.07.055

Simpson, M. J., and Simpson, A. J. (2012). The chemical ecology of soil organic matter molecular constituents. *J. Chem. Ecol.* 38, 768–784. doi: 10.1007/s10886-012-0122-x

Sokol, N. W., Slessarev, E., Marschmann, G. L., Nicolas, A., Blazewicz, S. J., Brodie, E. L., et al. (2022). Life and death in the soil microbiome: how ecological processes influence biogeochemistry. *Nat. Rev. Microbiol.* 20, 415–430. doi: 10.1038/s41579-022-00695-z

Sparling, G., Ross, D., Trustrum, N., Arnold, G., West, A., Speir, T., et al. (2003). Recovery of topsoil characteristics after landslip erosion in dry hill country of New Zealand, and a test of the space-for-time hypothesis. *Soil Biol. Biochem.* 35, 1575–1586. doi: 10.1016/j.soilbio.2003.08.002

Stockmann, U., Adams, M. A., Crawford, J. W., Field, D. J., Henakaarchchi, N., Jenkins, M., et al. (2013). The knowns, known unknowns and unknowns of sequestration of soil organic carbon. *Agric. Ecosyst. Environ.* 164, 80–99. doi: 10.1016/j.agee.2012.10.001

Sun, X., Xing, Y., Yan, G., Liu, G., Wang, X., and Wang, Q. (2024). Dynamics of glomalin-related soil protein and soil aggregates during secondary succession in the temperate forest. *Catena* 234:107602. doi: 10.1016/j.catena.2023.107602

Tian, C., Cui, D., Cao, Y., Luo, S., Song, H., Yang, P., et al. (2025). Temperature-dependent soil storage: changes in microbial viability and respiration in semiarid grasslands. *Soil Biol. Biochem.* 202:109673. doi: 10.1016/j.soilbio.2024.109673

Vitti, C., Stellacci, A. M., Leogrande, R., Mastrangelo, M., Cazzato, E., and Ventrella, D. (2016). Assessment of organic carbon in soils: a comparison between the springer–Klee wet digestion and the dry combustion methods in Mediterranean soils (southern Italy). *Catena* 137, 113–119. doi: 10.1016/j.catena.2015.09.001

Wang, T., Dong, L., and Liu, Z. (2024). Factors driving carbon accumulation in forest biomass and soil organic carbon across natural forests and planted forests in China. *Front. For. Glob. Change* 6:1333868. doi: 10.3389/ffgc.2023.1333868

Wang, R., and Hu, X. (2023). Pore structure characteristics and organic carbon distribution of soil aggregates in alpine ecosystems in the Qinghai Lake basin on the Qinghai-Tibet plateau. *Catena* 231:107359. doi: 10.1016/j.catena.2023.107359

Wang, C., and Kuzyakov, Y. (2024). Rhizosphere engineering for soil carbon sequestration. *Trends Plant Sci.* 29, 447–468. doi: 10.1016/j.tplants.2023.09.015

Wang, S., Li, T., and Zheng, Z. (2017). Distribution of microbial biomass and activity within soil aggregates as affected by tea plantation age. *Catena* 153, 1–8. doi: 10.1016/j.catena.2017.01.029

Wang, S., Li, T., and Zheng, Z. (2018). Response of soil aggregate-associated microbial and nematode communities to tea plantation age. *Catena* 171, 475–484. doi: 10.1016/j.catena.2018.07.041

Wang, C., Xue, L., and Jiao, R. (2021). Soil organic carbon fractions, C-cycling associated hydrolytic enzymes, and microbial carbon metabolism vary with stand age in Cunninghamia lanceolate (lamb.) hook plantations. *For. Ecol. Manag.* 482:118887. doi: 10.1016/j.foreco.2020.118887

Wang, Z., Yao, X., and Wang, W. (2018). Variation of soil carbon pools in *Pinus sylvestris* plantations of different ages in North China. *Acta Ecol. Sin.* 38, 248–254. doi: 10.1016/j.chnaes.2017.08.004

Wang, X., Zhao, L., Comeau, L., Bian, Q., Jiang, Y., and Mao, J. (2022). Divergent carbon stabilization pathways in aggregates in Ultisols with and without organic amendments: implications from ^{13}C natural abundance and NMR analysis. *Geoderma* 426:116088. doi: 10.1016/j.geoderma.2022.116088

Wiesmeier, M., Urbanski, L., Hobley, E., Lang, B., von Lützow, M., Marin-Spiotta, E., et al. (2019). Soil organic carbon storage as a key function of soils - a review of drivers and indicators at various scales. *Geoderma* 333, 149–162. doi: 10.1016/j.geoderma.2018.07.026

Wu, M., Pang, D., Chen, L., Li, X., Liu, L., Liu, B., et al. (2021). Chemical composition of soil organic carbon and aggregate stability along an elevation gradient in Helan Mountains, Northwest China. *Ecol. Indic.* 131:108228. doi: 10.1016/j.ecolind.2021.108228

Xu, H., He, B., Guo, L., Yan, X., Zeng, Y., Yuan, W., et al. (2024). Global forest plantations mapping and biomass carbon estimation. *J. Geophys. Res-Biogeo.* 129:e2023JG007441. doi: 10.1029/2023JG007441

Yang, C., Zhang, X., Ni, H., Gai, X., Huang, Z., du, X., et al. (2021). Soil carbon and associated bacterial community shifts driven by fine root traits along a chronosequence of Moso bamboo (*Phyllostachys edulis*) plantations in subtropical China. *Sci. Total Environ.* 752:142333. doi: 10.1016/j.scitotenv.2020.142333

Yao, Y., Ge, N., Yu, S., Wei, X., Wang, X., Jin, J., et al. (2019). Response of aggregate associated organic carbon, nitrogen and phosphorous to re-vegetation in agro-pastoral ecotone of northern China. *Geoderma* 341, 172–180. doi: 10.1016/j.geoderma.2019.01.036

Yao, S., Zhang, Y., Han, Y., Han, X., Mao, J., and Zhang, B. (2019). Labile and recalcitrant components of organic matter of a Mollisol changed with land use and plant litter management: an advanced ^{13}C NMR study. *Sci. Total Environ.* 660, 1–10. doi: 10.1016/j.scitotenv.2018.12.403

Zhang, M., Bai, X., Wang, Y., Li, Y., Cui, Y., Hu, S., et al. (2023). Soil microbial trait-based strategies drive the storage and stability of the soil carbon pool in *Robinia pseudoacacia* plantations. *Catena* 222:106894. doi: 10.1016/j.catena.2022.106894

Zhang, K., Maltais-Landry, G., and Liao, H. (2021). How soil biota regulate C cycling and soil C pools in diversified crop rotations. *Soil Biol. Biochem.* 156:108219. doi: 10.1016/j.soilbio.2021.108219

Zhang, X., Yu, P., Wang, D., and Xu, Z. (2022). Density- and age- dependent influences of droughts and intrinsic water use efficiency on growth in temperate plantations. *Agric. For. Meteorol.* 325:109134. doi: 10.1016/j.agrformet.2022.109134

Zhang, Q., Zhou, W., Liang, G., Sun, J., Wang, X., and He, P. (2015). Distribution of soil nutrients, extracellular enzyme activities and microbial communities across particle size fractions in a long-term fertilizer experiment. *Appl. Soil Ecol.* 94, 59–71. doi: 10.1016/j.apsoil.2015.05.005

Zhao, F., Ren, C., Han, X., Yang, G., Wang, J., and Doughty, R. (2019). Trends in soil microbial communities in afforestation ecosystem modulated by aggradation phase. *Forest. Ecol. Manag.* 441, 167–175. doi: 10.1016/j.foreco.2019.03.036

Zhuang, S., Sun, X., Liu, G., Wong, M., and Cao, Z. (2011). Carbon sequestration in bamboo plantation soil with heavy winter organic mulching management. *Bot. Rev.* 77, 252–261. doi: 10.1007/s12229-011-9081-0

frontiers | Frontiers in Microbiology

TYPE Original Research
PUBLISHED 02 June 2025
DOI 10.3389/fmicb.2025.1588169

Check for updates

OPEN ACCESS

EDITED BY
Brahim Bouizgarne,
Ibn Zohr University, Morocco

REVIEWED BY
Xiaomeng Chen,
Northeast Agricultural University, China
Azim Khalid,
National Institute for Agricultural Research, Morocco

*CORRESPONDENCE
Xiaojun Zhang
xjzhang68@sjtu.edu.cn

†PRESENT ADDRESS
Qiaoyu Wu,
State Key Laboratory of Pollution Control and Resources Reuse, Shanghai Institute of Pollution Control and Ecological Security, College of Environmental Science and Engineering, Tongji University, Shanghai, China

RECEIVED 06 March 2025
ACCEPTED 13 May 2025
PUBLISHED 02 June 2025

CITATION
Ma Y, Wu Q, Wang X, Sui W and Zhang X (2025) Carbon components in organic amendments drive nitrogen metabolism in one-year-long anaerobic soil microcosms.
Front. Microbiol. 16:1588169.
doi: 10.3389/fmicb.2025.1588169

COPYRIGHT
© 2025 Ma, Wu, Wang, Sui and Zhang. This is an open-access article distributed under the terms of the Creative Commons Attribution License (CC BY). The use, distribution or reproduction in other forums is permitted, provided the original author(s) and the copyright owner(s) are credited and that the original publication in this journal is cited, in accordance with accepted academic practice. No use, distribution or reproduction is permitted which does not comply with these terms.

Carbon components in organic amendments drive nitrogen metabolism in one-year-long anaerobic soil microcosms

Yiming Ma, Qiaoyu Wu†, Xinhui Wang, Weikang Sui and Xiaojun Zhang*

State Key Laboratory of Microbial Metabolism, Joint International Research Laboratory of Metabolic and Developmental Sciences, School of Life Sciences and Biotechnology, Shanghai Jiao Tong University, Shanghai, China

Introduction: Long-term studies on the dynamic changes in nitrogen metabolism and functional microbial communities under anaerobic conditions, particularly those driven by organic amendments, remain scarce.

Methods: We conducted a year-long anaerobic microcosm experiment using three organic amendments—aerobically fermented pig-manure digestate (ACM), compost (ACP) and straw powder (ACS)—alongside an inorganic fertilizer-only control (ACN).

Results: Temporal shifts revealed that organic amendments drove distinct nitrogen metabolism pathways. Amendments of digestate and compost promoted the proliferation of nitrogen-mineralizing bacteria such as *Ramlibacter* and *Lysobacter*, leading to significant ammonium accumulation. After 12-month incubation, the ACM treatment caused a 75.6-fold increase in ammonium, a 43.4% rise in total nitrogen (TN), and a 27.0% increase in total organic carbon (TOC). In contrast, the ACS treatment exhibited superior nitrogen fixation, with an average of 1.69-fold higher rate than ACM and 5.30 fold higher than ACP The ACS treatment enriched cellulolytic nitrogen-fixing bacteria, including *Clostridium*, and nitrogen-fixing archaea.

Discussion: This study provides profound insights in to the unique nitrogen metabolism pathways influenced by organic amendments under anoxic conditions, ultimately offering valuable insights into improved soil fertility and sustainable nitrogen management practices in agricultural systems.

KEYWORDS

metagenome, functional genes, microcosm experiment, nitrogen cycling, organic amendments

1 Introduction

Nitrogen fertilizers have been widely applied in recent decades to support high agricultural crop yields (Ladha et al., 2016; Guo et al., 2022). However, excess fertilization and low utilization lead to several environmental problems, such as nitrous oxide (N_2O) emissions (Li et al., 2024), ammonia volatilization (Ju and Zhang, 2017), and nitrate leaching (Zhao et al., 2022). Various management strategies to overcome the above issues have been evaluated (Young et al., 2021; Hassan et al., 2022; Gao and Cabrera Serrenho, 2023). Deeper application of fertilizers reduces ammonia volatilization by minimizing nitrogen exposure to the atmosphere (Ju and Zhang, 2017; Li et al., 2022), and simultaneously promote the formation of anaerobic micro-zones within the soil (Li et al., 2016; Schlüter et al., 2025). Additionally, combining organic amendments, such as manure (Wang et al., 2022), manure compost

(Oyetunji et al., 2022), crop residue (Fu et al., 2021), and digestate (Samoraj et al., 2022; Chozhavendhan et al., 2023), with nitrogen fertilizers can improve soil fertility, enhance nitrogen use efficiency, and contribute to stable crop yields and environmental benefits (Selim, 2020; Liu et al., 2021a; Zhai et al., 2022; Liu et al., 2023).

Long-term field trials have revealed that organic amendment inputs contribute to soil organic carbon (SOC) stabilization by increasing the abundance of stable aliphatic and aromatic carbon compounds, as evidenced by solid-state nuclear magnetic resonance (solid-state NMR) spectroscopy (Guo et al., 2019; Yuan et al., 2025). Importantly, such carbon-fraction diversity is increasingly recognized as a key factor influencing soil microbial community composition, with potential consequences for biogeochemical cycling processes (Fierer, 2017). Material-driven heterogeneity, particularly variations in carbon fraction composition, has also been increasingly recognized as a critical driver of microbial community assembly and biogeochemical processes (Kallenbach et al., 2016; Liang et al., 2017). Changes in the soil carbon-to-nitrogen ratios (C/N) may regulate nitrogen immobilization and mineralization by influencing soil microbial community composition and the activities of microorganisms in decomposing organic matter fractions (Lin et al., 2019; Cui et al., 2022). In addition, exogenous organic matter can stimulate soil organic matter (SOM) mineralization through positive priming effects, enhancing nutrient availability in soil (Hicks et al., 2019). Several long-term field experiments have demonstrated that manure application promotes organic nitrogen accumulation and mineralization (Abubaker et al., 2012; Wu et al., 2017; Xia et al., 2021).

Deeper placement of fertilizers helps to create anaerobic zones, which consequently enhance denitrification and increase N_2O emissions (Meng et al., 2022). However, inconsistent findings regarding the impacts of combined inorganic and organic fertilization on N_2O emissions have been reported in literature (Reddy and Crohn, 2014; Akhtar et al., 2020; Zhang et al., 2023; Zuo et al., 2023; Wu et al., 2024). These discrepancies are likely due to variations in the types of organic amendments and differences in nitrogen-cycling microbial communities (He et al., 2019; Zhou et al., 2022). Thus, it is critical to investigate how organic amendments with distinct carbon compositions modulate the structure and function of nitrogen-transforming microbiomes under oxygen-limited conditions. Such insights are essential for unraveling the microbial mechanisms underlying nitrogen cycling and for informing fertilization strategies that improve nitrogen use efficiency while reducing environmental risks.

Previous studies have investigated the effects of organic amendments on soil microbial community compositions and nitrogen cycling functions (Liu et al., 2021b; Cui et al., 2022; Chen et al., 2023). However, most investigations have relied on short-term incubations or endpoint sampling, which provide limited insights into the long-term succession dynamics of nitrogen-transforming microbiomes (Ouyang et al., 2020; Bossolani et al., 2023; Pastorelli et al., 2024). While a few efforts have introduced a dynamic perspective, such as a 16-week anaerobic incubation tracking microbial community shifts under straw-amended soils (Yang et al., 2023). In that study, 16S rRNA gene-based taxonomic profiling was employed, but without any functional analysis.

Yet nitrogen transformation processes, such as denitrification, nitrogen fixation, and organic matter decomposition, typically involve slow and progressive shifts in microbial community composition and functional activity. Localized anaerobic conditions frequently arise in agricultural soils following deep fertilizer placement or intense microbial respiration, and the biogeochemical processes occurring within these zones unfold over extended periods. Consequently, short-term studies may fail to capture the cumulative functional succession of nitrogen-transforming microbiomes under oxygen-limited conditions, underscoring the need for long-term incubation experiments that better simulate these ecological dynamics. Nevertheless, the mechanisms by which amendment-derived carbon fraction differences drive the functional succession of nitrogen-transforming microbiomes under prolonged oxygen limitation remain poorly understood. To address these gaps, we designed a one-year-long anaerobic incubation experiment using γ-ray irradiated, carbon-normalized organic amendments with standardized nitrate additions, coupled with multi-time-point shotgun metagenomics and nitrogenous gas flux monitoring, aiming to elucidate the microbial mechanisms by which the discrepancy of amendment-derived carbon fractions drives nitrogen cycling under sustained oxygen limitation.

2 Materials and methods

2.1 Experimental materials

Soil samples were collected from the Shangzhuang Experimental Station (39°48′N, 116°28′E) of China Agricultural University, which was initiated in October 2006. The experimental site followed a winter wheat–summer maize rotation, with fertilizers applied based on basal and follow-up applications. The original soil used in this study was topsoil (0–20 cm) collected from the conventional fertilizer straw-no-return treatment group (Abbreviated C for original soil), passed through a 2 mm sieve, and stored at 4°C before subsequent experiments. The main properties of the soil were displayed in Supplementary Table S1.

Three types of organic amendments were used in this study: digestate remaining after anaerobic fermentation of swine manure for methane production (abbreviated as M), compost from aerobic fermentation of pig manure (abbreviated as P), and a 1:1 (w:w) mixture of wheat straw and corn straw powder (abbreviated as S). These amendments were selected for their relevance to agricultural practices and their distinct impacts on nitrogen cycling and microbial dynamics. Straw was chosen to simulate in-situ straw return, representing crop residues from the experimental field. Compost and digestate, both derived from pig manure, were selected due to their widespread use in agricultural practices. The differences in fermentation methods influence nitrogen release patterns and microbial community impacts.

The organic amendments were sterilized to exclude the introduction of exogenous bacteria before being added to the soil. Sterilization was conducted with cobalt 60 irradiation using a sterilization dose of 50 kGy by the Shanghai Radiant Technology Company, following established laboratory protocols and methods validated in previous studies (Wu et al., 2019). The main properties of the organic amendments were displayed in Supplementary Table S1.

2.2 Experimental design

To investigate the effects of adding organic matter with different carbon and nitrogen fractions on soil nitrogen metabolism, four experimental groups were established. The experimental groups

consisted of anaerobically fermented pig manure digestate (ACM), aerobically fermented pig manure compost (ACP), straw powder (ACS), and a control group without organic matter amendment (ACN). In these group designations, 'A' represents anaerobic conditions, and 'C' refers to conventional nitrogen-fertilized soil.

Organic matters were added to the soil based on equivalent total carbon input to ensure that any observed effects were caused by differences in the composition of the amendments rather than differences of carbon content. The total amount of aerobically fermented pig manure compost, which had the highest nitrate content, was set to be added to 10% (w:w) of the soil (with an initial total carbon content of 8.992 g per kg of dry soil). The amounts of anaerobically fermented pig manure digestate and straw powder were calculated to match the total carbon content applied in the ACP treatment, ensuring consistency in carbon input across all treatments.

To control the unexpected effects of variations in carbon and nitrate content, we ensured consistency in the total carbon content and nitrate levels before the start of the incubation. This would ensure that observed differences in nitrogen metabolism and microbial community composition were solely due to variations in the carbon components of the amendments.

Organic amendment was introduced in two batches: the first at the start of the incubation and the second after six months of incubation. The total amount of organic matters addition was evenly divided between these two batches, maintaining equivalent carbon input across all treatments, as described above. This two-batch application was designed to simulate a basal and follow-up fertilization pattern commonly used in agricultural management. Potassium nitrate solution was added to maintain consistent nitrate levels across all treatments, accounting for the nitrate already present in the organic amendments.

The organic matters and potassium nitrate solution were added to 25 g of soil in serum bottles, and the headspace was replaced with pure helium (99.99%) to maintain anaerobic conditions. Anaerobic conditions were achieved by performing multiple rounds of gas replacement with helium, and the anaerobic level was confirmed through monitoring, which showed oxygen concentrations remained below detection limits throughout the experiment. Incubation was carried out at 25°C in the dark, with soil moisture maintained at 75% water holding capacity (WHC). Additional nitrate and water were injected every three months to sustain the experimental conditions. Periodic supplementation every 3 months mimicked the fertilization pulses typical in agricultural settings, allowing for a more realistic assessment of the impact of organic amendments on nitrogen metabolism.

The experiment followed a parallel replicated design with 18 replicates per group. Triplicate samples were destructively collected from each group at time point of 7 days (D7), 3 months (M3), 6 months (M6), 9 months (M9), and 1 year (M12), for high-throughput sequencing of the 16S rRNA gene (V3-V4 regions) and for physicochemical analysis, including total carbon (TC), total nitrogen (TN), total organic carbon (TOC), pH, nitrate, nitrite, and ammonium. Before each sampling, headspace gas in the system was measured using the ROBOT (Supplementary Figure S2), an instrument capable of continuously monitoring the gas concentrations in the headspace of the bottles (Molstad et al., 2007). Bacterial community composition and functional gene profiles were analyzed through metagenomic shotgun sequencing at 7 days, 6 months, and 1 year.

The detailed information of experimental design is provided in Supplementary Figures S1, S2 and Supplementary Table S2.

2.3 Physical and chemical analysis of soils and organic amendment

TC, TOC, and TN were analyzed with an elemental analyzer (Vario EL III/Isoprime). TOC was determined after removing inorganic carbon by hydrochloric acid fumigation (Ramnarine et al., 2011). Inorganic nitrogen contents were determined with the cadmium reduction column method for nitrate and nitrite (Huffman and Barbarick, 1981) and with the indophenol blue method for ammonium (Dorich and Nelson, 1983). Total organic nitrogen (TON) was calculated as the total nitrogen minus the inorganic nitrogen (nitrate, nitrite, and ammonium). pH was determined in a solution with a distilled water–soil ratio of 2.5:1 using a pH meter (Mettler Toledo, Switzerland).

The organic carbon fractions of the four experimental groups were determined at Day 0 following the addition of the corresponding organic matter using the 13C cross-polarization/total sideband suppression (CP/TOSS) method of solid-state NMR (Bruker Avance Neo 600 MHz). The NMR integrals of each functional group in the organic carbon fractions were calculated using the Topspin 4.13 program (Chen et al., 2018).

To compare the denitrifying potential of soil before and after 1-year incubation, the denitrification gas kinetics with addition of 150 mg N/kg of nitrate were assessed using the ROBOT system (Supplementary Figure S2) for multiple sampling during 3 day period (Molstad et al., 2007).

2.4 Calculation of nitrogen fixation rates

To quantify nitrogen fixation, we developed a calculation approach based on the difference between the total amount of added nitrate and the remaining nitrogen gas (N_2) concentration in each closed system. The calculation of nitrogen fixation was conducted separately for two stages, as the seal of the vials was opened in between. They are stages of the first 6 months (1) and the second 6 months (2), as indicated below.

$$F1 = A1 - NG1 \quad (1)$$

$$F2 = A2 - NG2 + F1 \quad (2)$$

where (1) F1 represents the amount of nitrogen fixation of each group in the first stage, A1 represents the total amount of nitrate nitrogen added to each sample during the D0–M6 period (210 mg/kg), and NG1 represents the nitrogen content measured in each closed system at M6. (2) F2 represents the amount of nitrogen fixation of each group during the second stage, and A2 represents the total amount of nitrate nitrogen added to each sample during the M6–M12 period (120 mg/kg), while NG2 represents the nitrogen content measured in each closed system at M12.

2.5 16S rRNA gene amplicon sequencing and bioinformatics analysis

DNA was extracted from 0.5 g of soil samples as described previously (Griffiths et al., 2000; Paulin et al., 2013). Two rounds of polymerase chain reaction (PCR) were used to amplify the V3-V4 hypervariable regions of 16S rRNA genes from the soil

DNA to construct high-throughput sequencing libraries (Zhang et al., 2016; Wu et al., 2019). The first round of PCR was performed using the universal primers B341F/B785R and the PCR products were purified by magnetic bead adsorption. The second round of PCR was performed using purified products as the template and primers with sequencing index tags added to the DNA amplicons obtained by the second round of PCR. The constructed sequencing libraries were then mixed in equal concentrations and subjected to high-throughput sequencing on the Illumina Miseq sequencing platform.

The obtained sequences were processed using the QIIME2 platform (Bolyen et al., 2019), and the "cutadapt" plug-in was used to excise junctions and primers, followed by the use of the DADA2 program to perform quality control of sequences (trimming, filtering, denoising, and chimera removal) and to merge amplicon sequence variants (ASVs) to obtain the original abundance matrix and ASV sequence information. A total of 1,949,178 high-quality sequences were obtained from 63 samples after quality control and filtration, and 9,561 ASVs were obtained after clustering (Supplementary Table S3). The sequence numbers of all samples were normalized to 17,000 (the number of sequences in the sample with the fewest sequences) to enable direct comparisons among samples. The subsequent analyses conducted in this study were based on normalized data. The ASV classifications were then taxonomically annotated using the SILVA138.2 database (Bolyen et al., 2019). The rarefaction curves (Supplementary Figure S7A) eventually flattened, indicating that the sequencing depth was sufficient to meet the requirements of the subsequent data analysis.

2.6 Metagenome shotgun sequencing and bioinformatics analysis

Soil metagenomic DNA was used for library construction and sequenced on an Illumina NovaSeq high-throughput sequencing platform (Personal Co. Ltd., Shanghai). A total of 39 samples were collected in triplicates from initial samples, and from four incubation groups in D7, M6 and M12 for metagenomic sequencing. Clean metagenomic sequencing reads were obtained after quality control using FastQC (Andrews, 2010), followed by assembly with the MEGAHIT (Li et al., 2015) to obtain contigs that were assembled into scaffolds using IDBA (Peng et al., 2010). Basic sequencing and quality control metrics for all samples, including raw data, GC content, Q30, and assembly statistics, are summarized in Supplementary Table S4. Gene prediction was then performed using the MetaGeneMark (Hyatt et al., 2012), followed by clustering of proteins using CD-HIT (Fu et al., 2012) into groups with >90% sequence similarity to enable removal of redundancy. The longest sequence was then used as the representative sequence to obtain non-redundant protein sets. The htseq-count was used to count the number of reads mapped to the non-redundant genes and assess gene abundances using transcripts per million (TPM) values. Nitrogen-related functional proteins were then annotated using the NcycDB based on the non-redundant protein datasets (Tu et al., 2019). Furthermore, carbohydrate degradation-related functional proteins (referred to as CAZymes) were annotated using the CAZy database (Drula et al., 2022), while taxonomic annotation was conducted using the NCBI non-redundant (NR) protein database.

Each sample was subjected to generate metagenome-assembled genome (MAG) using MetaBAT2 (Kang et al., 2019). The obtained MAGs were then quality-filtered using the CheckM (Parks et al., 2015). "High-quality draft genomes" with estimates of completeness >90% and contamination <5%, in addition to "medium-quality draft genomes" with estimates of completeness ≥50% and contamination <10%, were retained, for a total of 651 MAGs (Bowers et al., 2017). The genome datasets were subjected to de-redundancy using the dRep (Olm et al., 2017) based on 99% average nucleotide identity (ANI), leading to a total of 470 non-redundant MAGs. The relative abundances of non-redundant MAGs were calculated using CoverM (https://github.com/wwood/CoverM/releases/tag/v0.6.1). Taxonomic annotations of the non-redundant MAGs were then assigned using the GTDB-Tk (release 207) (Chaumeil et al., 2022). Phylophlan v.3.0 was subsequently used for phylogenetic tree construction (Asnicar et al., 2020), followed by visualization of trees using iTOL (Letunic and Bork, 2019). Nitrogen cycling gene annotations within MAGs were assigned using NcycDB, while annotations of lignin, cellulose, and hemicellulose degrading enzymes were assigned with the CAZy database. Kyoto Encyclopedia of Genes and Genomes (KEGG) Orthology (KO) annotation of MAGs for the KEGG database was conducted using kofam_scan v.1.3.0 (ver. 2023-03-02 KEGG release 105.0) (Aramaki et al., 2020). The KEGGDecoder was then used to parse the kofam_scan module outputs to determine the completeness of various metabolic pathways (Graham et al., 2018). Detailed sequencing and analysis parameters were provided in Supplementary Table S12.

2.7 Statistical analysis

Repeated measures Two-way analysis of variance (ANOVA) was applied to analyze the denitrification gas data (e.g., N_2O and N_2 dynamics) to assess the effects of organic amendment type and incubation duration across multiple time points. For other physicochemical indicators (e.g., ammonium concentration, nitrogen fixation rate), standard Two-way ANOVA was used. To meet ANOVA assumptions, logarithmic transformation was applied to the data where necessary, based on assessments of normality (Shapiro–Wilk test) and homogeneity of variances (Brown-Forsythe test). *Post hoc* comparisons were conducted using Tukey's honestly significant difference (HSD) test to identify significant differences between group means (Ratsiatosika et al., 2024). All analyses were performed using GraphPad Prism 10 (Swift, 1997), with the significance level set at $\alpha = 0.05$ for all tests. Full details of the statistical analysis are provided in Supplementary Tables S8–S11.

Principal coordinates analysis (PCoA) was calculated using R vegan package for Bray-Curtis distances and plotted using ggplot2 (Wickham, 2011) package. The overall statistical significance of group separation was assessed using permutational multivariate analysis of variance (PERMANOVA).

We constructed six random forest regression models using the R package 'randomForest' (Breiman, 2001) to identify MAGs associated with changes in ammonium content (Figure 1G), nitrogen fixation (Figure 1I), N_2O accumulation (Figures 1A,D), and total denitrification ($N_2O + N_2$, Figures 1B,E) across incubation stages. The significance of selected MAGs was assessed using the percentage increase in mean square error (MSE%), with higher values indicating

greater importance (Jiao et al., 2018). Model performance was evaluated using the 'A3' package for cross-validation R^2 and permutation significance tests, while predictor variable significance was assessed via 'rfPermute' (Jiao et al., 2018). Full model details and the importance and significance of selected MAGs are provided in Supplementary Tables S6, S7, respectively.

3 Results

3.1 Effects of different organic amendments on nitrogen metabolic processes

The three types of organic amendments differentially affected soil physicochemical parameters in Fluvo-aquic soils (Supplementary Figures S3–S5). Solid-state NMR measurement of composition of carbon fractions in the four experimental groups at day 0 of incubation indicated that all three organic matter additions increased the percentage of labile carbon fractions (Supplementary Figure S3B), as the TOC content of the ACM, ACP, and ACS groups were equally and significantly higher than that of ACN ($p < 0.05$, Supplementary Figure S4B). The N-alkyl functional group with a chemical shift of 45–65 ppm (Supplementary Figure S3C) was higher in the ACM than ACP.

The three organic amendments differentially affected nitrogen metabolism, specially, all of them enhanced soil denitrification capacity (Figures 1A–C). Furthermore, organic amendment significantly increased the production and accumulation of N_2O and N_2 at the beginning of incubation ($p < 0.05$, Figures 1A,B). After one year of incubation, N_2 concentrations were high in all of the organic matter addition groups (Figure 1E), while only minimal N_2O accumulation was detected in the ACM group (Figures 1D,F). At the beginning of the incubations, the ACP and ACS group treatments

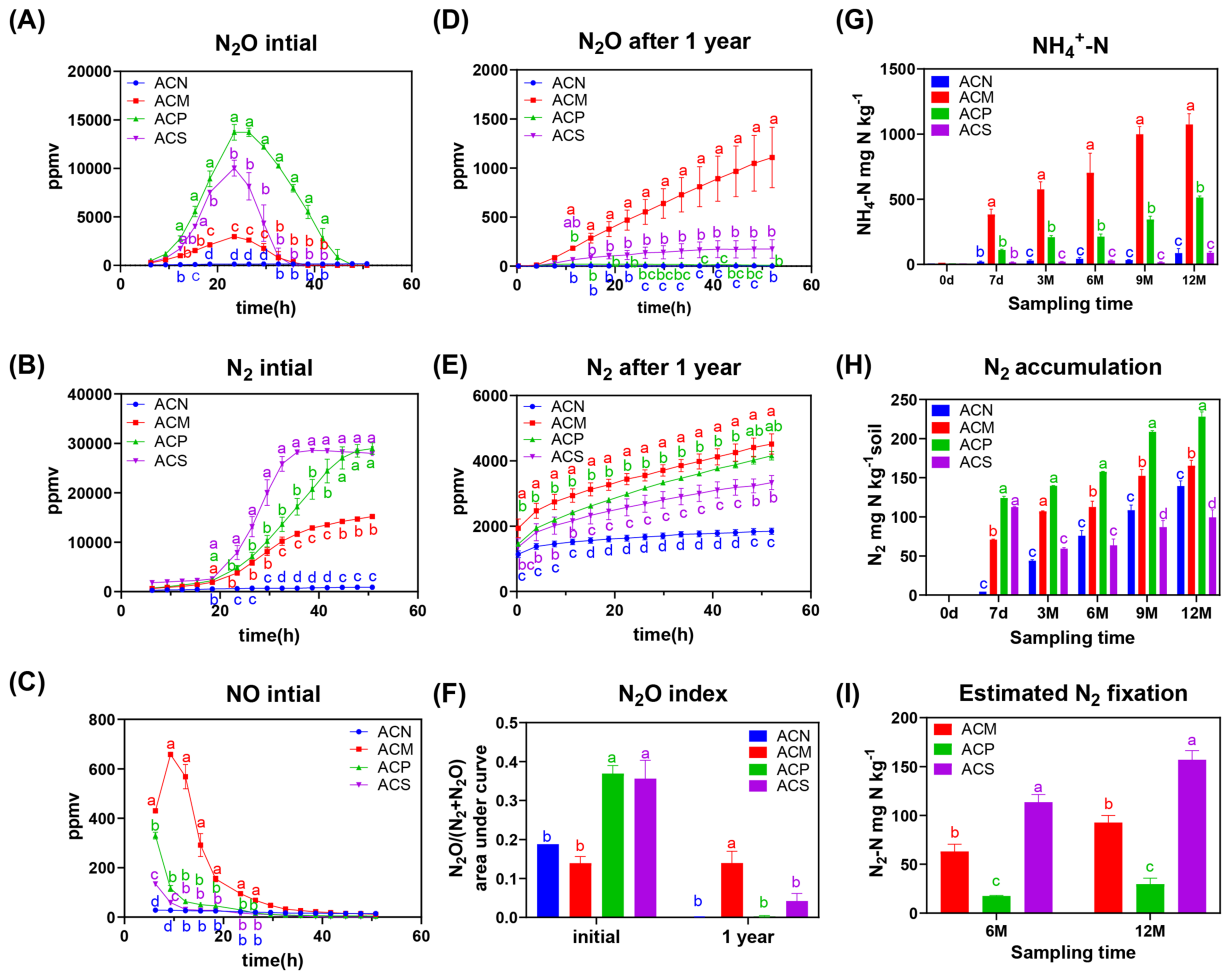


FIGURE 1
Dynamic variations in N_2O, NH_4^+-N, N_2, NO and nitrogen fixation activity during the one - year incubation. N_2O **(A)**, N_2 **(B)**, and NO **(C)** dynamics measured in soil sample before the1-year incubation. N_2O **(D)** and N_2 **(E)** dynamics measured in soil after the 1-year incubation. **(F)** N_2O index before and after 1-year incubation. **(G)** Accumulation of ammonium during the incubation. **(H)** Accumulation of nitrogen gas during the incubation. **(I)** Amount of fixed nitrogen after 6 and 12 months of incubation. Error bars indicate the standard error of the means ($n = 3$). Significance was determined using repeated measures Two-way ANOVA for **(A–E)** and standard Two-way ANOVA for **(F–I)**, followed by Tukey's HSD *post hoc* test. Different letters indicate significant differences between groups at each time period ($p < 0.05$). Global and inter-time point significance results are provided in Supplementary Tables S8, S10, and Supplementary Figure S6.

accumulated greater N_2O, while the ACS group consumed nitrate more rapidly through denitrification (Figures 1A,B). Among the three organic treatments, ACM addition accumulated the least amount of N_2O and consumed nitrate through denitrification most slowly (Figures 1A,B).

During the incubation period, ammonium significantly accumulated in the ACM and ACP groups with incubation time ($p < 0.05$, Figure 1G). Moreover, nitrogen balance calculations revealed that the amount of accumulated ammonium significantly exceeded the initial nitrate input (Supplementary Figure S5B), suggesting that the primary source of ammonium was the mineralization of organic nitrogen from the added organic amendments. In contrast, the ACS group exhibited an initial increase followed by a decrease in nitrogen levels, implying the presence of nitrogen fixation within the incubation systems (Figure 1H). The calculated nitrogen fixation suggested the highest levels in the ACS compared with the ACM and ACP groups, with a increasing trend observed within all treatments over time (Figure 1I).

3.2 Effects of different organic amendments on microbial communities

After one year of incubation, the Shannon diversity index was consistently lower in all experimental groups with organic amendments (ACM, ACP and ACS) than in the control group (ACN) ($p < 0.05$, Supplementary Figure S7B). Furthermore, PCoA analysis based on Bray–Curtis distances (Figure 2A) indicated that the type of organic amendment and incubation time significantly affected microbial community composition ($p < 0.001$, Supplementary Table S11). Consistently, differences in phylum-level compositions were observed among groups (Figure 2B and Supplementary Table S13). For example, the organic amendments notably increased Firmicutes abundance ($p < 0.05$, Supplementary Table S13). Microbial community compositions in different groups also showed observable changes with incubation time, with the exception of the ACN group in which the majority of phyla remained relatively stable. Overall, ACS communities exhibited different variation tendency compared to the communities of two manure-based groups, ACM and ACP.

3.3 Temporal effects of organic amendments on nitrogen metabolism genes

From samples of this study, all sixty-eight nitrogen cycling genes annotated in NcycDB and associated with eight nitrogen cycling pathways were successfully identified in the metagenomic data (Supplementary Table S5). Among these pathways, Organic

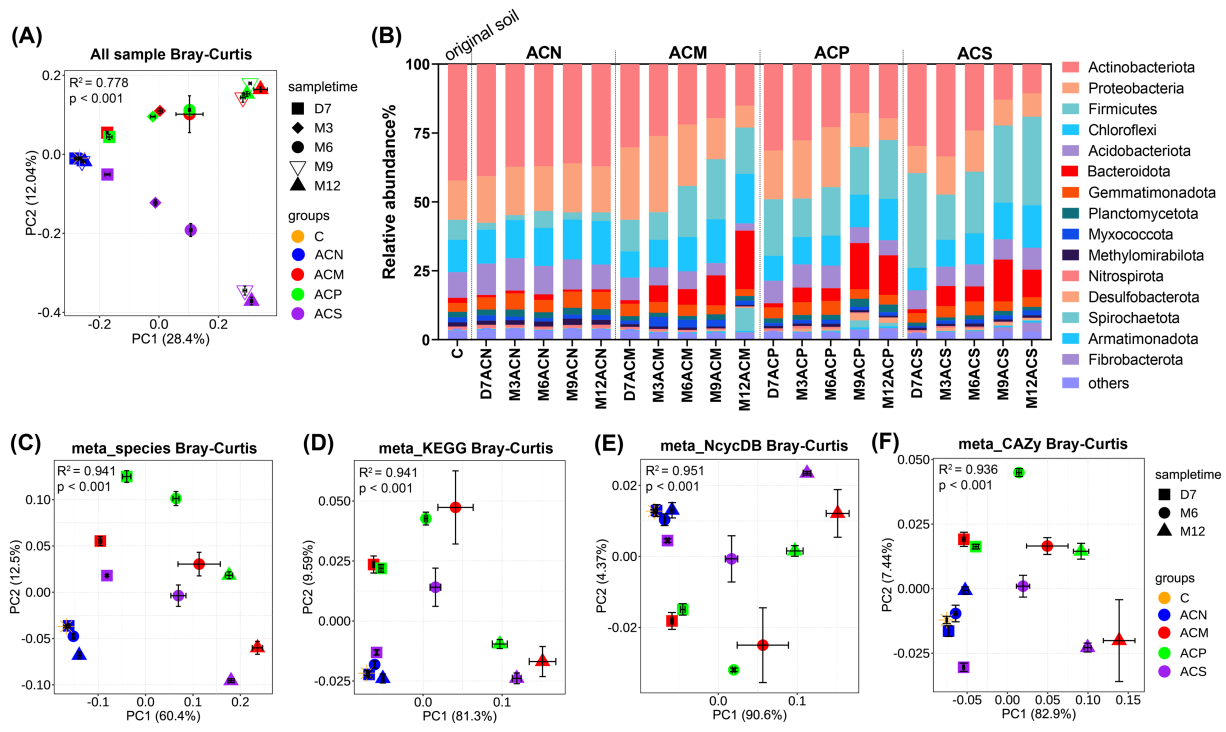


FIGURE 2
Microbial community compositional variation among treatments. **(A)** PCoA analysis of all samples based on Bray–Curtis distances of 16S rRNA gene sequence data. **(B)** Bacterial composition at the phylum level of samples. **(C)** PCoA analysis of microbial community composition based on species-level Bray–Curtis distances of metagenomic sequence data. **(D)** PCoA analysis of all KOs annotated based on kegg database. **(E)** PCoA analysis of functional genes related to the nitrogen cycle annotated based on NcycDB. **(F)** PCoA analysis of functional genes related to carbohydrate metabolism annotated based on CAZY database. All PCoA analyses were based on Bray–Curtis distances. The coordinates of each point in each PCoA plot were the mean of each group of samples, and the error bars indicate the standard error of the means ($n = 3$). Differences among groups were calculated via PERMANOVA **(A,C–F)**.

degradation and synthesis (ODAS), denitrification, Dissimilatory nitrate reduction (DNRA), and Assimilatory nitrate reduction (ANRA) showed consistently higher relative abundances across all samples (Supplementary Figure S8). Among these, two nitrogen mineralization functional genes (*gdh_K00262* and *gdh_K15371*) were identified in the ODAS pathway, which is associated with organic nitrogen degradation and ammonium production. Specifically, *gdh_K00262* was enriched over whole peroid in the experimental group with organic amendment, while *gdh_K15371* was enriched only in the early stage of incubation in ACM and ACP groups. In contrast, DNRA-related functional genes (*nirB*, *nirD*, *nrfA*, *nrfC*) and ANRA-related genes (*nirA*), which are associated with ammonium production, were consistently less abundant in the ACM and ACP groups compared to the ACN group (Figure 3). Furthermore, the total abundances of DNRA and ANRA pathway genes showed declining trends over time compared to the original soil (Supplementary Figures S8D,E). The nitrogen fixation genes *nifD*, *nifK*, and *nifH* were significantly enriched with incubation time in the ACS group ($p < 0.05$, Figure 3). In the organic amendment groups, enrichment of the denitrification functional genes *napA*, *nirK*, and *nosZ* decreased with incubation time (Supplementary Figure S9), while the relative abundances of *norB* genes significantly increased in these three groups ($p < 0.05$, Figure 3).

3.4 Effects of organic amendments on the functional microbiome of nitrogen mineralization and denitrification

Considering the microorganisms that encoded nitrogen mineralization functional genes (Figures 4A–C), organic amendment enriched some specific taxa in all communities including *Lysobacter* and *Luteimonas*, in addition to the enrichment of *Anaeromyxobacter* and *Lentimicrobium* harboring the *gdh_K00262* genes at the later stage of cultivation. Organic matter addition also enriched *Anaeromyxobacter* that contains the denitrifying genes of *narG*, *napA*, and *norB* (Figures 4D,E,H). *Lysobacter* and *Luteimonas* harbor genes of *nirK*, *norB*, and *nosZ* (Figures 4F,H,I). In the microbial communities carrying the functional genes *gdh_K00262*, *gdh_K15371*, *ureC*, *nirK* and *nosZ*, compared with the ACN group, the abundances of *Luteitalea* and *Solirubrobacter* decreased across the incubation in the ACM, ACP, and ACS groups. Among the microorganisms carrying *nifH*, *nifD* and *nifK*, *Anaeromyxobacter* was enriched in organic amendment groups,

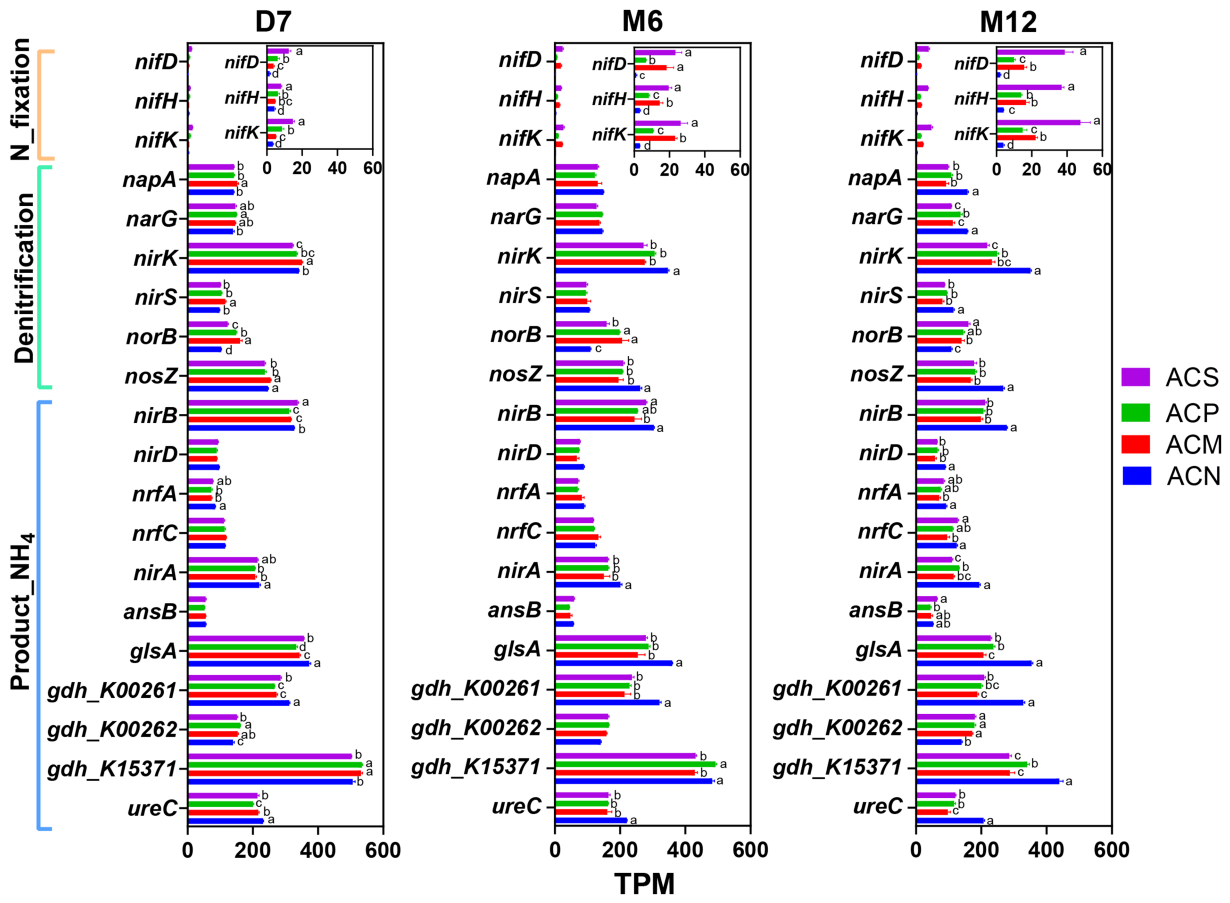


FIGURE 3
The abundances of functional genes for nitrogen fixation, denitrification and catalytic ammonium production function at different time points (D7: 7 days; M6: 6 months; M12: 12 months). Gene abundance in the metagenomic data was normalized and expressed as transcripts per million (TPM). Error bars indicate the standard error of the means (n = 3). Differences in the values were calculated based on analysis of variance (ANOVA) and Tukey's HSD post hoc test. Different letters denote significant differences among groups at a significance level of $p < 0.05$.

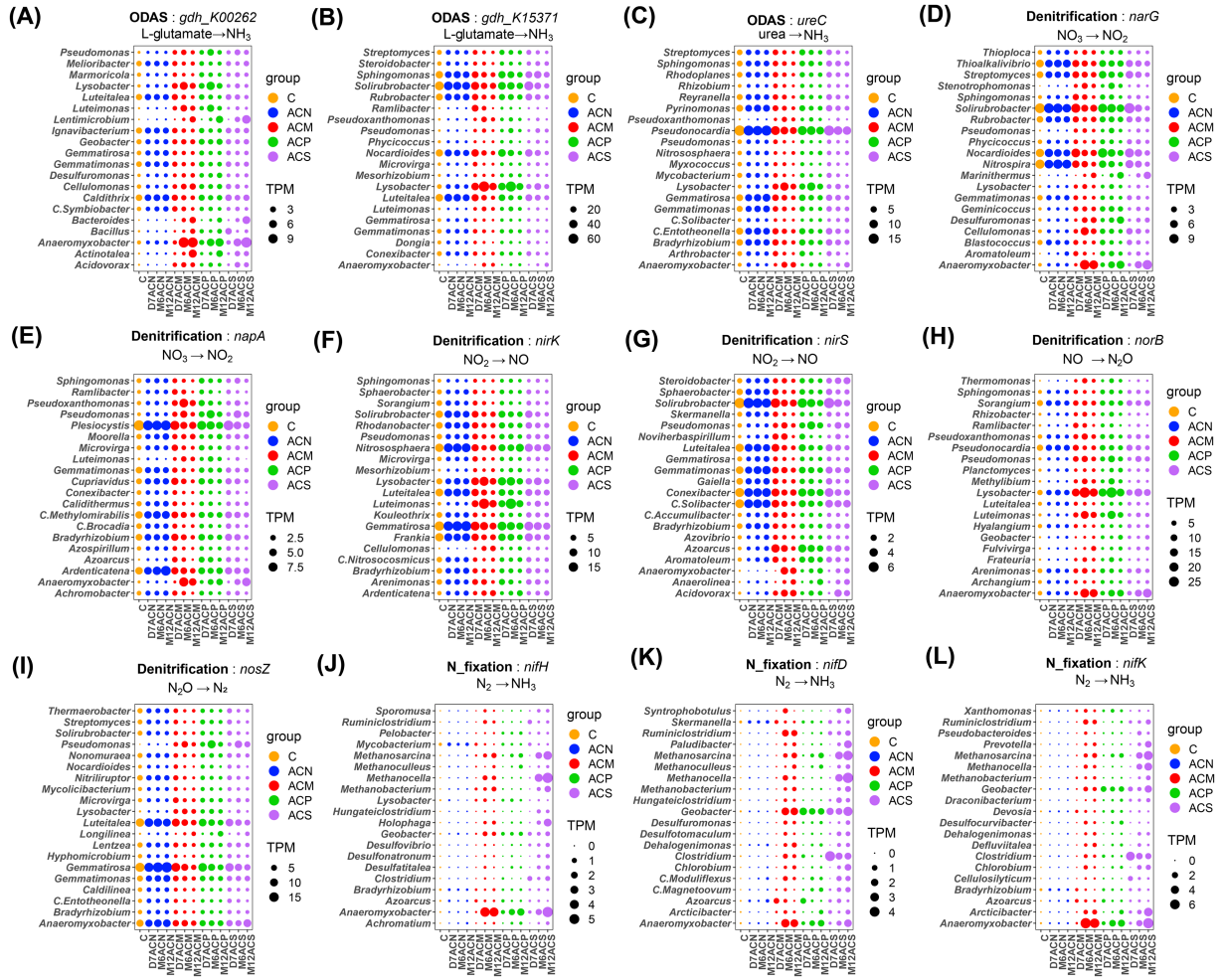


FIGURE 4
Top 20 dominant bacterial genera involved in nitrogen mineralization, denitrification and nitrogen fixation pathways. Dominant bacteria contain *gdh_K00262* **(A)**, *gdh_K15371* **(B)**, *ureC* **(C)**, *narG* **(D)**, *napA* **(E)**, *nirK* **(F)**, *nirS* **(G)**, *norB* **(H)**, *nosZ* **(I)**, *nifH* **(J)**, *nifD* **(K)**, *nifK* **(L)**, respectively. Circle size is the TPM value. Different colors represent different groups.

while *Clostridium*, *Methanocella*, and *Methanosarcina* were only enriched in the ACS group (Figures 4J–L).

3.5 Diversity and nitrogen functional annotations of MAGs

To better understand the links between microbial species and nitrogen cycling processes, we conducted metagenome binning to reconstruct MAGs. A total of 651 MAGs were reconstructed, of which 208 were high-quality draft genomes and 443 were medium-quality draft genomes (Bowers et al., 2017). 470 MAGs were retained after de-redundancy based on 99% ANI. The MAGs were assigned to 29 phyla, 47 classes, 84 orders (464 MAGs), 107 families (453 MAGs), and 105 genera (369 MAGs) based on annotation by the GTDB database (Figure 5). NcycDB-based functional annotation of nitrogen cycling genes indicated that 373 MAGs contained one or more functional genes for denitrification, while 443 MAGs contained genes related to ammonium production from organic nitrogen mineralization and 79 MAGs encoded functional genes for nitrogen fixation (Figure 5). Among all the 79 MAGs predicted for nitrogen fixation, 33 MAGs contained multiple cellulolytic and hemicellulolytic enzyme-encoding genes (Supplementary Figure S12), which were primarily derived from Bacteroidota, Fibrobacterota, and Firmicutes.

Twenty-six MAGs associated with changes in ammonium content were enriched in the ACM and ACP groups (Figure 6). In particular, MAGs primarily annotated as Burkholderiaceae, Xanthomonadaceae, and Anaeromyxobacteraceae were identified by the random forest regression model as important predictors contributing to ammonium accumulation. Among these, *Ramlibacter* exhibited higher relative abundance in the early cultivation stages, while *Luteimonas_B* had a higher relative abundance in the middle cultivation stage, and *Anaeromyxobacter* was more abundant in both the middle and late culture stages ($p < 0.05$, Supplementary Figure S13). Twelve MAGs that were important for changes in nitrogen fixation exhibited higher relative abundance in the late culture stage of the ACS group, with some also showing higher relative abundance at the late culture stage of the ACM group (Figure 6). Furthermore, MAGs with higher relative abundance at the late culture stage were primarily affiliated with the *JAAUTT01*, *Methanocella_A*, *Methanosarcina*, and *Methanoculleus*

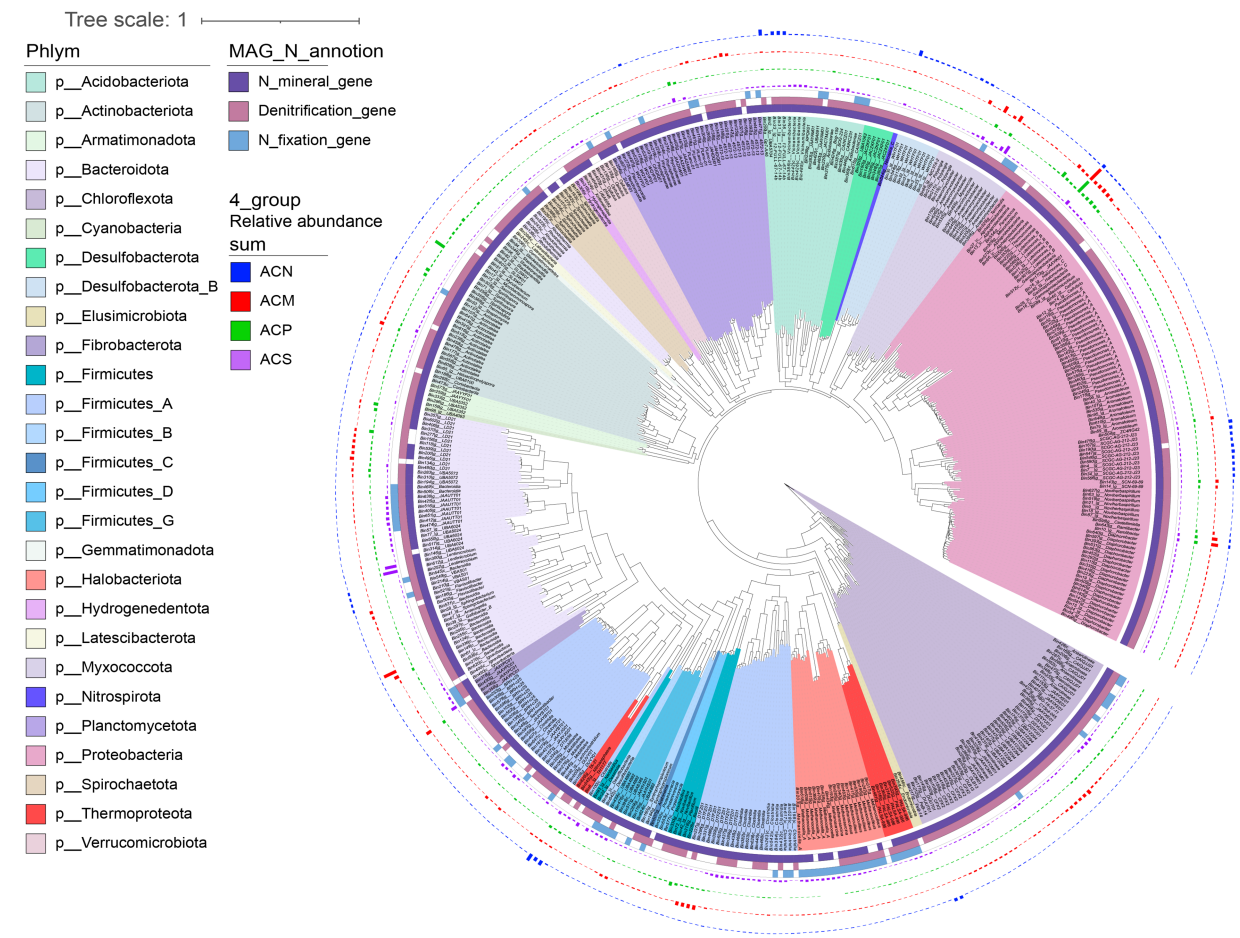


FIGURE 5
Phylogenetic tree showing the diversity, total abundances, and annotated nitrogen-related function of 470 reconstructed metagenome-assembled genomes (MAGs). Different colors on the phylogenetic tree branches represent different bacterial or archaeal phyla. The four outer circles of different colored bars represent the relative abundance of MAGs in the four experimental groups, with ACN in blue, ACM in red, ACP in green, and ACS in purple. The 3 inner circles indicate the types of nitrogen functional genes annotated in the MAG. The dark purple color indicates that a nitrogen mineralization gene is annotated, the light purple color indicates that a denitrification gene is annotated, and the light blue color indicates that a nitrogen fixation gene is annotated.

genera ($p < 0.05$, Supplementary Figure S13). Among the 25 MAGs associated with the denitrification process, 10 MAGs contained only N_2O production genes and lacked *nosZ* for N_2O reduction; these MAGs were primarily found in the ACM group (Figure 6). Additionally, *Neobacillus* MAG93 was identified as a complete denitrifier capable of converting nitrate to N_2 and had high abundance in the ACS group at day 7 ($p < 0.05$, Supplementary Figure S13).

4 Discussion

4.1 Organic amendment and organic matter mineralization

During the incubation period, the ACM and ACP treatments resulted in significant ammonium accumulation, far exceeding the initial nitrate input (Supplementary Figure S5B). This results suggests that the primary source of ammonium derived from organic matter mineralization. The low abundances of DNRA and ANRA pathway-related genes (e.g., *nirB*, *nirD*, *nrfA*, *nirA*; Figure 3) and the overall declining trends of these pathways (Supplementary Figures S8D,E) further support their minimal contributions to ammonium accumulation. The increased gross nitrogen mineralization rates in these treatments were primarily attributed to one or more of several mechanisms, which are explored in the following sections.

First, the differences in the added organic matter fractions drove distinct nitrogen transformation pathways and fluxes. Solid-state NMR analysis indicated that the digestate and compost addition groups contained higher N-alkyl C fractions compared with the straw group, and this fraction primarily originated from proteins and amino acids (Chen et al., 2018). The rapid turnover of amino acids in soil (Jones and Kielland, 2012) may be one of the reasons for quick accumulation of mineralization-derived ammonium nitrogen in the ACM and ACP samples. By contrast, the higher percentage of the N-alkyl C component of ACM compared with the ACP group resulted in greater accumulation of ammonium in the ACM group. The stability index (Chen et al., 2018) relating to the ratio of alkyl-C to O-alkyl-C (A/O-A ratio) of the ACM group was lower than within the ACP group (Supplementary Figure S3D), indicating that its components were more easily degraded.

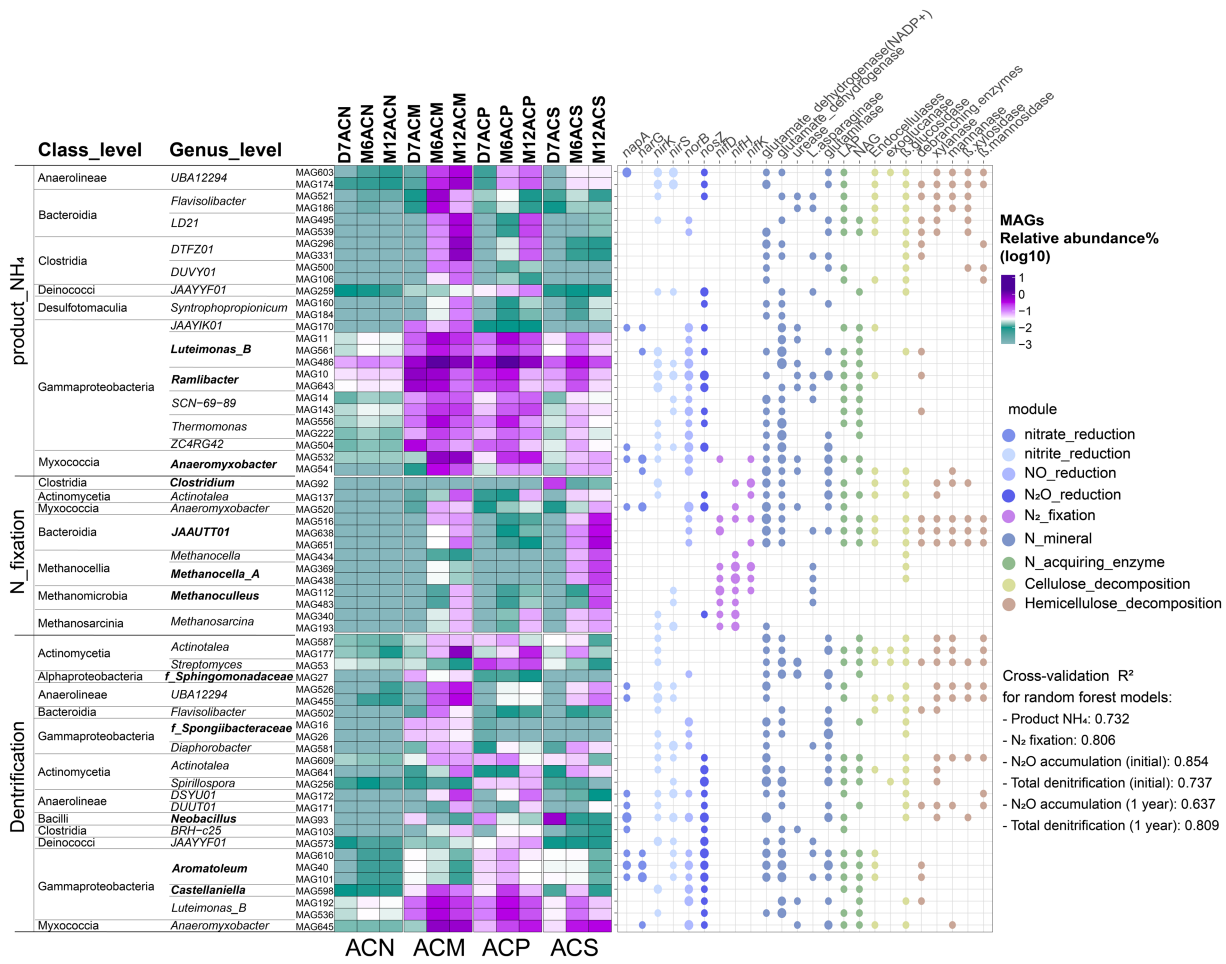


FIGURE 6
Random forest-selected metagenome-assembled genomes (MAGs) associated with the function of ammonium accumulation, nitrogen fixation, and denitrification. Heatmap indicates the relative abundance of the selected important MAGs. The bubble map represents the carbon and nitrogen-related functional genes annotated in the selected MAGs, different colors represent different modules. The cross-validation R^2 values for the random forest regression models are as follows: ammonium accumulation (R^2 = 0.73), nitrogen fixation (R^2 = 0.81), and denitrification (R^2 = 0.64 to 0.85 across different models). The details of the random forest regression model are displayed in Supplementary Table S6.

Second, manure additions greatly increased the abundance of the glutamate dehydrogenase encoding gene *gdh_k15371*, in addition to the abundances of the nitrogen-acquiring enzyme-encoding genes *K01255* (leucine aminopeptidase, LAP) and *K01207* (*β*-1,4-n-acetylglucosaminidase, NAG) during the early incubation stage (Supplementary Figure S10). The higher abundance of these functional genes during the initial stage suggests that the ACM and ACP groups had higher potential activities of organic nitrogen mineralizing enzymes and extracellular nitrogen-acquiring enzymes (Hu et al., 2020; Chen and Sinsabaugh, 2021). Nitrogen-acquiring enzyme activities have been shown to be positively correlated with nitrogen mineralization rates (Wang et al., 2023). These changes would increase the supply of dissolved organic nitrogen (DON) required for microbial nitrogen uptake and mineralization, as well as improve the ability to utilize organic nitrogen (Jian et al., 2016). Consistently with Wang et al. (2024), field applications of manure and digestate increased nitrogen-acquiring enzyme activities. This also aligns with the microbial nitrogen mining hypothesis (Craine et al., 2007), which suggests that excess exogenous carbon promotes microbial secretion of extracellular enzymes to acquire the nitrogen needed for growth.

Third, compost and digestate pig manure additions led to the enrichment of key bacterial taxa involved in nitrogen mineralization. MAGs associated with ammonium nitrogen production were enriched in the ACM and ACP groups. Among these, MAG10 and MAG643 of the genus *Ramlibacter*, which annotated contain the nitrogen-acquiring enzyme LAP encoding gene *K01255*, were most abundant in the early stage of incubation when ammonium accumulation rate was at its peak. Random forest regression analysis identified these MAGs as important predictors of ammonium levels. The abundance of genus *Ramlibacter* was also significantly and positively correlated with ammonium accumulation in another study (Hu et al., 2023).

4.2 Nitrogen fixation triggered by straw addition

The significant amount of nitrogen fixed in the ACS group could be due to the combined involvement of cellulolytic nitrogen-fixing bacteria (CNFB) and methanogenic archaea.

Straw addition enriched CNFB (Harindintwali et al., 2020), which produce cellulases and nitrogen-fixing enzymes, facilitating the degradation of cellulose into simple sugars and promoting nitrogen fixation. CNFB have been widely studied in agricultural composting due to their cellulose-degrading and nitrogen-enriching functions (Harindintwali et al., 2020; Harindintwali et al., 2022). Lignocellulose is a carbon-rich component of crop residues such as straw that primarily comprises cellulose, hemicellulose, and lignin (Harindintwali et al., 2020). Bacteria encoding *nifH*, *nifD*, and *nifK* were enriched in the ACS group, as represented by the anaerobic cellulose-degrading *Clostridium* (Figures 4J–L), with species having cellulolytic and nitrogen-fixing functions (McDonald et al., 2012; Poehlein et al., 2017). These bacteria may play a key role in both straw degradation and nitrogen fixation in the ACS group during early incubation. The D7ACS group was enriched in CAZymes involved in cellulose and hemicellulose catabolism (Bredon et al., 2018) (Supplementary Figure S11). Consequently, straw addition was hypothesized to rapidly promote the abundance of bacteria encoding cellulose and hemicellulose catabolic enzyme, such as MAG92 (Figure 6).

Nitrogen-fixing taxa enriched in the ACS group in mid-to late-culture periods comprised several methanogenic archaea, including *Methanocella* and *Methanosarcina*. The end products of the anaerobic degradation of lignocellulose are primarily carbon dioxide and methane (Nguyen and Khanal, 2018; Song et al., 2023). Methanogenic archaea in confined anaerobic systems use the products from the final step of lignocellulose fermentation, such as acetic acid, hydrogen, and carbon dioxide, to produce methane (Evans et al., 2019). These organisms were enriched over time in this study. Nitrogen fixation abilities had been documented in some methanogenic archaea (Belay et al., 1984; Murray and Zinder, 1984; Bomar et al., 1985; Scherer, 1988), although it is not a common trait among all methanogenic archaea. It is consistent with the result that the methanogen MAGs from the ACS group encoded genes for nitrogen fixation. The enrichment of these organisms should promote nitrogen fixation and methanogenesis by using fermentation products such as short fatty acids.

However, although this study provides insights into the regulation of soil N-functional communities by exogenous organic matter additions, we recognize that there are some limitations in the study. Our study did not adequately consider all factors that may affect the soil microbial community and N cycling. The factors, such as aeration in soil and plant cultivation and so on, deserve to be further explored in future studies for a more comprehensive understanding of the complexity of soil ecosystems. Despite these limitations, our findings offer promising insights for practical applications. The rapid accumulation of ammonium from anaerobically fermented pig manure digestate highlights its potential as a readily available nitrogen source to meet the early-stage nutrient demands of plants in agricultural cropping systems. Conversely, the enrichment of nitrogen-fixing CNFB and methanogenic archaea in straw-amended soils promoted long-term nitrogen fixation under anaerobic conditions. These results highlight the opportunity to optimize organic amendment strategies, balancing immediate nutrient availability with sustained nitrogen-fixing capacity in soils.

5 Conclusion

Adding compost, digestate, or straw to soil differentially shapes nitrogen (N) cycling via microbial mechanisms. Compost/digestate boosted microbial enzymes for nitrogen acquisition and ammonium accumulation via mineralization, while straw enriched methanogenic nitrogen-fixing archaea. These organic inputs create distinct nitrogen metabolism pathways by altering microbial communities and functional genes, ultimately affecting soil N availability and greenhouse gases. Strategically selecting organic amendments could synchronize nutrient release with crop demands while suppressing nitrous oxide emissions. This microbial-driven nitrogen partitioning offers a framework to optimize organic input timing/location, balancing soil fertility and environmental sustainability in intensive agriculture. Digestate provides a readily available nitrogen source for early-stage plant growth, while straw promotes long-term nitrogen fixation under anaerobic conditions. By selecting appropriate organic amendments based on the actual soil conditions, farmers may benefit from optimizing nitrogen cycling and improve soil sustainability.

Data availability statement

The data presented in the study are deposited in the NCBI Sequence Read Archive repository, accession number PRJNA1013701.

Author contributions

YM: Conceptualization, Investigation, Methodology, Writing – original draft, Writing – review & editing. QW: Investigation, Writing – review & editing. XW: Formal analysis, Software, Writing – review & editing. WS: Investigation, Writing – review & editing. XZ: Conceptualization, Funding acquisition, Supervision, Writing – review & editing, Writing – original draft.

Funding

The author(s) declare that financial support was received for the research and/or publication of this article. This work was supported by the National Natural Science Foundation of China (NSFC project 31971526) and the National Key Research and Development Program of China (2017YFD0200102).

Acknowledgments

The authors would like to express their gratitude to Shanshan Zhang and Bona Dai (Instrumental Analysis Center of Shanghai Jiao Tong University, IAC-SJTU) for their help in the pretreatment method of soil total organic carbon determination and in the detection method of soil solid-state NMR, respectively.

Conflict of interest

The authors declare that the research was conducted in the absence of any commercial or financial relationships that could be construed as a potential conflict of interest.

Generative AI statement

The authors declare that no Gen AI was used in the creation of this manuscript.

Publisher's note

All claims expressed in this article are solely those of the authors and do not necessarily represent those of their affiliated organizations, or those of the publisher, the editors and the reviewers. Any product that may be evaluated in this article, or claim that may be made by its manufacturer, is not guaranteed or endorsed by the publisher.

Supplementary material

The Supplementary material for this article can be found online at: https://www.frontiersin.org/articles/10.3389/fmicb.2025.1588169/full#supplementary-material

References

Abubaker, J., Risberg, K., and Pell, M. (2012). Biogas residues as fertilisers – effects on wheat growth and soil microbial activities. *Appl. Energy* 99, 126–134. doi: 10.1016/j.apenergy.2012.04.050

Akhtar, K., Wang, W., Ren, G., Khan, A., Enguang, N., Khan, A., et al. (2020). Straw mulching with inorganic nitrogen fertilizer reduces soil CO(2) and N(2)O emissions and improves wheat yield. *Sci. Total Environ.* 741:140488. doi: 10.1016/j.scitotenv.2020.140488

Andrews, S. (2010). FastQC: A quality control tool for high throughput sequence data. Cambridge, United Kingdom: Babraham Bioinformatics, Babraham Institute.

Aramaki, T., Blanc-Mathieu, R., Endo, H., Ohkubo, K., Kanehisa, M., Goto, S., et al. (2020). KofamKOALA: KEGG Ortholog assignment based on profile HMM and adaptive score threshold. *Bioinformatics* 36, 2251–2252. doi: 10.1093/bioinformatics/btz859

Asnicar, F., Thomas, A. M., Beghini, F., Mengoni, C., Manara, S., Manghi, P., et al. (2020). Precise phylogenetic analysis of microbial isolates and genomes from metagenomes using PhyloPhlAn 3.0. *Nature. Communications* 11:2500. doi: 10.1038/s41467-020-16366-7

Belay, N., Sparling, R., and Daniels, L. (1984). Dinitrogen fixation by a thermophilic methanogenic bacterium. *Nature* 312, 286–288. doi: 10.1038/312286a0

Bolyen, E., Rideout, J. R., Dillon, M. R., Bokulich, N. A., Abnet, C. C., Al-Ghalith, G. A., et al. (2019). Reproducible, interactive, scalable and extensible microbiome data science using QIIME 2. *Nat. Biotechnol.* 37, 852–857. doi: 10.1038/s41587-019-0209-9

Bomar, M., Knoll, K., and Widdel, F. (1985). Fixation of molecular nitrogen by *Methanosarcina barkeri*. *FEMS Microbiol. Ecol.* 31, 47–55. doi: 10.1016/0378-1097(85)90046-1

Bossolani, J. W., Leite, M. F. A., Momesso, L., ten Berge, H., Bloem, J., and Kuramae, E. E. (2023). Nitrogen input on organic amendments alters the pattern of soil–microbe-plant co-dependence. *Sci. Total Environ.* 890:164347. doi: 10.1016/j.scitotenv.2023.164347

Bowers, R. M., Kyrpides, N. C., Stepanauskas, R., Harmon-Smith, M., Doud, D., Reddy, T. B. K., et al. (2017). Minimum information about a single amplified genome (MISAG) and a metagenome-assembled genome (MIMAG) of bacteria and archaea. *Nat. Biotechnol.* 35, 725–731. doi: 10.1038/nbt.3893

Bredon, M., Dittmer, J., Noël, C., Moumen, B., and Bouchon, D. (2018). Lignocellulose degradation at the holobiont level: teamwork in a keystone soil invertebrate. *Microbiome* 6:162. doi: 10.1186/s40168-018-0536-y

Breiman, L. (2001). Random forests. *Mach. Learn.* 45, 5–32. doi: 10.1023/A:1010933404324

Chaumeil, P. A., Mussig, A. J., Hugenholtz, P., and Parks, D. H. (2022). GTDB-Tk v2: memory friendly classification with the genome taxonomy database. *Bioinformatics* 38, 5315–5316. doi: 10.1093/bioinformatics/btac672

Chen, J., and Sinsabaugh, R. L. (2021). Linking microbial functional gene abundance and soil extracellular enzyme activity: implications for soil carbon dynamics. *Glob. Chang. Biol.* 27, 1322–1325. doi: 10.1111/gcb.15506

Chen, M., Xu, J., Li, Z., Li, D., Wang, Q., Zhou, Y., et al. (2023). Long-term nitrogen fertilization-induced enhancements of acid hydrolyzable nitrogen are mainly regulated by the most vital microbial taxa of keystone species and enzyme activities. *Sci. Total Environ.* 874:162463. doi: 10.1016/j.scitotenv.2023.162463

Chen, X., Xu, Y., Gao, H. J., Mao, J., Chu, W., and Thompson, M. L. (2018). Biochemical stabilization of soil organic matter in straw-amended, anaerobic and aerobic soils. *Sci. Total Environ.* 625, 1065–1073. doi: 10.1016/j.scitotenv.2017.12.293

Chozhavendhan, S., Karthigadevi, G., Bharathiraja, B., Praveen Kumar, R., Abo, L. D., Venkatesa Prabhu, S., et al. (2023). Current and prognostic overview on the strategic exploitation of anaerobic digestion and digestate: a review. *Environ. Res.* 216:114526. doi: 10.1016/j.envres.2022.114526

Craine, J. M., Morrow, C., and Fierer, N. (2007). Microbial nitrogen limitation increases decomposition. *Ecology* 88, 2105–2113. doi: 10.1890/06-1847.1

Cui, J., Zhu, R., Wang, X., Xu, X., Ai, C., He, P., et al. (2022). Effect of high soil C/N ratio and nitrogen limitation caused by the long-term combined organic-inorganic fertilization on the soil microbial community structure and its dominated SOC decomposition. *J. Environ. Manag.* 303:114155. doi: 10.1016/j.jenvman.2021.114155

Dorich, R. A., and Nelson, D. W. (1983). Direct colorimetric measurement of ammonium in potassium chloride extracts of soils. *Soil Sci. Soc. Am. J.* 47, 833–836. doi: 10.2136/sssaj1983.03615995004700040042x

Drula, E., Garron, M.-L., Dogan, S., Lombard, V., Henrissat, B., and Terrapon, N. (2022). The carbohydrate-active enzyme database: functions and literature. *Nucleic Acids Res.* 50, D571–D577. doi: 10.1093/nar/gkab1045

Evans, P. N., Boyd, J. A., Leu, A. O., Woodcroft, B. J., Parks, D. H., Hugenholtz, P., et al. (2019). An evolving view of methane metabolism in the Archaea. *Nat. Rev. Microbiol.* 17, 219–232. doi: 10.1038/s41579-018-0136-7

Fierer, N. (2017). Embracing the unknown: disentangling the complexities of the soil microbiome. *Nat. Rev. Microbiol.* 15, 579–590. doi: 10.1038/nrmicro.2017.87

Fu, B., Chen, L., Huang, H., Qu, P., and Wei, Z. (2021). Impacts of crop residues on soil health: a review. *Environmental Pollutants Bioavailability* 33, 164–173. doi: 10.1080/26395940.2021.1948354

Fu, L., Niu, B., Zhu, Z., Wu, S., and Li, W. (2012). CD-HIT: accelerated for clustering the next-generation sequencing data. *Bioinformatics* 28, 3150–3152. doi: 10.1093/bioinformatics/bts565

Gao, Y., and Cabrera Serrenho, A. (2023). Greenhouse gas emissions from nitrogen fertilizers could be reduced by up to one-fifth of current levels by 2050 with combined interventions. *Nature Food* 4, 170–178. doi: 10.1038/s43016-023-00698-w

Graham, E. D., Heidelberg, J. F., and Tully, B. J. (2018). Potential for primary productivity in a globally-distributed bacterial phototroph. *ISME J.* 12, 1861–1866. doi: 10.1038/s41396-018-0091-3

Griffiths, R. I., Whiteley, A. S., O'Donnell, A. G., and Bailey, M. J. (2000). Rapid method for Coextraction of DNA and RNA from natural environments for analysis of ribosomal DNA-and rRNA-based microbial community composition. *Appl. Environ. Microbiol.* 66, 5488–5491. doi: 10.1128/AEM.66.12.5488-5491.2000

Guo, C., Liu, X., and He, X. (2022). A global meta-analysis of crop yield and agricultural greenhouse gas emissions under nitrogen fertilizer application. *Sci. Total Environ.* 831:154982. doi: 10.1016/j.scitotenv.2022.154982

Guo, Z., Zhang, Z., Zhou, H., Wang, D., and Peng, X. (2019). The effect of 34-year continuous fertilization on the SOC physical fractions and its chemical composition in a vertisol. *Sci. Rep.* 9:2505. doi: 10.1038/s41598-019-38952-6

Harindintwali, J. D., Wang, F., Yang, W., Zhou, J., Muhoza, B., Mugabowindekwe, M., et al. (2022). Harnessing the power of cellulolytic nitrogen-fixing bacteria for biovalorization of lignocellulosic biomass. *Ind. Crop. Prod.* 186:115235. doi: 10.1016/j.indcrop.2022.115235

Harindintwali, J. D., Zhou, J., and Yu, X. (2020). Lignocellulosic crop residue composting by cellulolytic nitrogen-fixing bacteria: a novel tool for environmental sustainability. *Sci. Total Environ.* 715:136912. doi: 10.1016/j.scitotenv.2020.136912

Hassan, M. U., Aamer, M., Mahmood, A., Awan, M. I., Barbanti, L., Seleiman, M. F., et al. (2022). Management strategies to mitigate N2O emissions in agriculture. *Life* 12:439. doi: 10.3390/life12030439

He, T., Yuan, J., Luo, J., Wang, W., Fan, J., Liu, D., et al. (2019). Organic fertilizers have divergent effects on soil N2O emissions. *Biol. Fertil. Soils* 55, 685–699. doi: 10.1007/s00374-019-01385-4

Hicks, L. C., Meir, P., Nottingham, A. T., Reay, D. S., Stott, A. W., Salinas, N., et al. (2019). Carbon and nitrogen inputs differentially affect priming of soil organic matter in tropical lowland and montane soils. *Soil Biol. Biochem.* 129, 212–222. doi: 10.1016/j.soilbio.2018.10.015

Hu, X., Gu, H., Sun, X., Wang, Y., Liu, J., Yu, Z., et al. (2023). Distinct influence of conventional and biodegradable microplastics on microbe-driving nitrogen cycling

processes in soils and plastispheres as evaluated by metagenomic analysis. *J. Hazard. Mater.* 451:131097. doi: 10.1016/j.jhazmat.2023.131097

Hu, R., Wang, X. P., Xu, J. S., Zhang, Y. F., Pan, Y. X., and Su, X. (2020). The mechanism of soil nitrogen transformation under different biocrusts to warming and reduced precipitation: from microbial functional genes to enzyme activity. *Sci. Total Environ.* 722:137849. doi: 10.1016/j.scitotenv.2020.137849

Huffman, S., and Barbarick, K. (1981). Soil nitrate analysis by cadmium reduction. *Commun. Soil Sci. Plant Anal.* 12, 79–89. doi: 10.1080/00103628109367129

Hyatt, D., LoCascio, P. F., Hauser, L. J., and Uberbacher, E. C. (2012). Gene and translation initiation site prediction in metagenomic sequences. *Bioinformatics* 28, 2223–2230. doi: 10.1093/bioinformatics/bts429

Jian, S., Li, J., Chen, J., Wang, G., Mayes, M. A., Dzantor, K. E., et al. (2016). Soil extracellular enzyme activities, soil carbon and nitrogen storage under nitrogen fertilization: a meta-analysis. *Soil Biol. Biochem.* 101, 32–43. doi: 10.1016/j.soilbio.2016.07.003

Jiao, S., Chen, W., Wang, J., Du, N., Li, Q., and Wei, G. (2018). Soil microbiomes with distinct assemblies through vertical soil profiles drive the cycling of multiple nutrients in reforested ecosystems. *Microbiome* 6:146. doi: 10.1186/s40168-018-0526-0

Jones, D. L., and Kielland, K. (2012). Amino acid, peptide and protein mineralization dynamics in a taiga forest soil. *Soil Biol. Biochem.* 55, 60–69. doi: 10.1016/j.soilbio.2012.06.005

Ju, Xt., and Zhang, C. (2017). Nitrogen cycling and environmental impacts in upland agricultural soils in North China: a review. *J. Integr. Agric.* 16, 2848–2862. doi: 10.1016/S2095-3119(17)61743-X

Kang, D. D., Li, F., Kirton, E., Thomas, A., Egan, R., An, H., et al. (2019). MetaBAT 2: an adaptive binning algorithm for robust and efficient genome reconstruction from metagenome assemblies. *PeerJ* 7:e7359. doi: 10.7717/peerj.7359

Kallenbach, C. M., Frey, S. D., and Grandy, A. S. (2016). Direct evidence for microbial-derived soil organic matter formation and its ecophysiological controls. *Nature Communications* 7:13630. doi: 10.1038/ncomms13630

Ladha, J. K., Tirol-Padre, A., Reddy, C. K., Cassman, K. G., Verma, S., Powlson, D. S., et al. (2016). Global nitrogen budgets in cereals: a 50-year assessment for maize, rice and wheat production systems. *Sci. Rep.* 6:19355. doi: 10.1038/srep19355

Letunic, I., and Bork, P. (2019). Interactive tree of life (iTOL) v4: recent updates and new developments. *Nucleic Acids Res.* 47, W256–W259. doi: 10.1093/nar/gkz239

Li, L., Hong, M., Zhang, Y., and Paustian, K. (2024). Soil N2O emissions from specialty crop systems: a global estimation and meta-analysis. *Glob. Chang. Biol.* 30:e17233. doi: 10.1111/gcb.17233

Li, Y., Kronzucker, H. J., and Shi, W. (2016). Microprofiling of nitrogen patches in paddy soil: analysis of spatiotemporal nutrient heterogeneity at the microscale. *Sci. Rep.* 6:27064. doi: 10.1038/srep27064

Li, D., Liu, C. M., Luo, R., Sadakane, K., and Lam, T. W. (2015). MEGAHIT: an ultra-fast single-node solution for large and complex metagenomics assembly via succinct de Bruijn graph. *Bioinformatics* 31, 1674–1676. doi: 10.1093/bioinformatics/btv033

Li, L., Wu, T., Li, Y., Hu, X., Wang, Z., Liu, J., et al. (2022). Deep fertilization improves rice productivity and reduces ammonia emissions from rice fields in China; a meta-analysis. *Field Crop Res.* 289:108704. doi: 10.1016/j.fcr.2022.108704

Liang, C., Schimel, J. P., and Jastrow, J. D. (2017). The importance of anabolism in microbial control over soil carbon storage. *Nature Microbiol.* 2:17105. doi: 10.1038/nmicrobiol.2017.105

Lin, Y., Ye, G., Kuzyakov, Y., Liu, D., Fan, J., and Ding, W. (2019). Long-term manure application increases soil organic matter and aggregation, and alters microbial community structure and keystone taxa. *Soil Biol. Biochem.* 134, 187–196. doi: 10.1016/j.soilbio.2019.03.030

Liu, P., Guo, X., Zhou, D., Zhang, Q., Ren, X., Wang, R., et al. (2023). Quantify the effect of manure fertilizer addition and optimal nitrogen input on rainfed wheat yield and nitrogen requirement using nitrogen nutrition index. *Agric. Ecosyst. Environ.* 345:108319. doi: 10.1016/j.agee.2022.108319

Liu, J., Shu, A., Song, W., Shi, W., Li, M., Zhang, W., et al. (2021b). Long-term organic fertilizer substitution increases rice yield by improving soil properties and regulating soil bacteria. *Geoderma* 404:115287. doi: 10.1016/j.geoderma.2021.115287

Liu, B., Wang, X., Ma, L., Chadwick, D., and Chen, X. (2021a). Combined applications of organic and synthetic nitrogen fertilizers for improving crop yield and reducing reactive nitrogen losses from China's vegetable systems: a meta-analysis. *Environ. Pollut.* 269:116143. doi: 10.1016/j.envpol.2020.116143

McDonald, J. E., Rooks, D. J., and McCarthy, A. J. (2012). Methods for the isolation of cellulose-degrading microorganisms. *Methods Enzymol.*510, 349–74. doi: 10.1016/B978-0-12-415931-0.00019-7

Meng, X., Ma, C., and Petersen, S. O. (2022). Sensitive control of N2O emissions and microbial community dynamics by organic fertilizer and soil interactions. *Biol. Fertil. Soils* 58, 771–788. doi: 10.1007/s00374-022-01662-9

Molstad, L., Dorsch, P., and Bakken, L. R. (2007). Robotized incubation system for monitoring gases (O2, NO, N2O N2) in denitrifying cultures. *J. Microbiol. Methods* 71, 202–211. doi: 10.1016/j.mimet.2007.08.011

Murray, P. A., and Zinder, S. H. (1984). Nitrogen fixation by a methanogenic archaebacterium. *Nature* 312, 284–286. doi: 10.1038/312284a0

Nguyen, D., and Khanal, S. K. (2018). A little breath of fresh air into an anaerobic system: how microaeration facilitates anaerobic digestion process. *Biotechnol. Adv.* 36, 1971–1983. doi: 10.1016/j.biotechadv.2018.08.007

Olm, M. R., Brown, C. T., Brooks, B., and Banfield, J. F. (2017). dRep: a tool for fast and accurate genomic comparisons that enables improved genome recovery from metagenomes through de-replication. *ISME J.* 11, 2864–2868. doi: 10.1038/ismej.2017.126

Ouyang, Y., Norton, J. M., and Parales, R. E. (2020). Short-term nitrogen fertilization affects microbial community composition and nitrogen mineralization functions in an agricultural soil. *Appl. Environ. Microbiol.* 86:e02278-19. doi: 10.1128/aem.02278-19

Oyetunji, O., Bolan, N., and Hancock, G. (2022). A comprehensive review on enhancing nutrient use efficiency and productivity of broadacre (arable) crops with the combined utilization of compost and fertilizers. *J. Environ. Manag.* 317:115395. doi: 10.1016/j.jenvman.2022.115395

Parks, D. H., Imelfort, M., Skennerton, C. T., Hugenholtz, P., and Tyson, G. W. (2015). CheckM: assessing the quality of microbial genomes recovered from isolates, single cells, and metagenomes. *Genome Res.* 25, 1043–1055. doi: 10.1101/gr.186072.114

Pastorelli, R., Casagli, A., Rocchi, F., Tampio, E., Laaksonen, I., Becagli, C., et al. (2024). Effects of anaerobic Digestates and biochar amendments on soil health, greenhouse gas emissions, and microbial communities: a Mesocosm study. *Appl. Sci.* 14:1917. doi: 10.3390/app14051917

Paulin, M. M., Nicolaisen, M. H., Jacobsen, C. S., Gimsing, A. L., Sørensen, J., and Bælum, J. (2013). Improving Griffith's protocol for co-extraction of microbial DNA and RNA in adsorptive soils. *Soil Biol. Biochem.* 63, 37–49. doi: 10.1016/j.soilbio.2013.02.007

Peng, Y., Leung, H. C. M., Yiu, S. M., and Chin, F. Y. L. (2010). IDBA - a practical iterative de bruijn graph de novo assembler. *Lecture Notes Comput. Sci.* 426–440. doi: 10.1007/978-3-642-12683-3-28

Poehlein, A., Funkner, K., Schüler, M. A., and Daniel, R. (2017). First insights into the genome sequence of the cellulolytic bacterium *Clostridium hungatei* DSM 14427. *Genome Announc.* 5:e00363-17. doi: 10.1128/genomea.00363-17

Ramnarine, R., Voroney, R. P., Wagner-Riddle, C., and Dunfield, K. E. (2011). Carbonate removal by acid fumigation for measuring the δ13C of soil organic carbon. *Can. J. Soil Sci.* 91, 247–250. doi: 10.4141/cjss10066

Ratsiatosika, O., Trap, J., Herinasandratra, V., Razafimbelo, T., Bernard, L., and Blanchart, E. (2024). Earthworms enhance the performance of organic amendments in improving rice growth and nutrition in poor ferralsols. *Soil Biol. Biochem.* 195:109477. doi: 10.1016/j.soilbio.2024.109477

Reddy, N., and Crohn, D. M. (2014). Effects of soil salinity and carbon availability from organic amendments on nitrous oxide emissions. *Geoderma* 235-236, 363–371. doi: 10.1016/j.geoderma.2014.07.022

Samoraj, M., Mironiuk, M., Izydorczyk, G., Witek-Krowiak, A., Szopa, D., Moustakas, K., et al. (2022). The challenges and perspectives for anaerobic digestion of animal waste and fertilizer application of the digestate. *Chemosphere* 295:133799. doi: 10.1016/j.chemosphere.2022.133799

Scherer, P. (1988). Vanadium and molybdenum requirement for the fixation of molecular nitrogen by two Methanosarcina strains. *Arch. Microbiol.* 151, 44–48. doi: 10.1007/BF00444667

Schlüter, S., Lucas, M., Grosz, B., Ippisch, O., Zawallich, J., He, H., et al. (2025). The anaerobic soil volume as a controlling factor of denitrification: a review. *Biol. Fertil. Soils* 61, 343–365. doi: 10.1007/s00374-024-01819-8

Selim, M. M. (2020). Introduction to the integrated nutrient management strategies and their contribution to yield and soil properties. *Int. J. Agronomy* 2020, 1–14. doi: 10.1155/2020/2821678

Song, Y., Pei, L., Chen, G., Mu, L., Yan, B., Li, H., et al. (2023). Recent advancements in strategies to improve anaerobic digestion of perennial energy grasses for enhanced methane production. *Sci. Total Environ.* 861:160552. doi: 10.1016/j.scitotenv.2022.160552

Swift, M. L. (1997). GraphPad prism, data analysis, and scientific graphing. *J. Chem. Inf. Comput. Sci.* 37, 411–412. doi: 10.1021/ci960402j

Tu, Q., Lin, L., Cheng, L., Deng, Y., and He, Z. (2019). NCycDB: a curated integrative database for fast and accurate metagenomic profiling of nitrogen cycling genes. *Bioinformatics* 35, 1040–1048. doi: 10.1093/bioinformatics/bty741

Wang, C., Ma, Y., He, W., Kuzyakov, Y., Bol, R., Chen, H., et al. (2024). Soil quality and ecosystem multifunctionality after 13-year of organic and nitrogen fertilization. *Sci. Total Environ.* 931:172789. doi: 10.1016/j.scitotenv.2024.172789

Wang, C., Ma, X., Shen, J., Chen, D., Zheng, L., Ge, T., et al. (2022). Reduction in net greenhouse gas emissions through a combination of pig manure and reduced inorganic fertilizer application in a double-rice cropping system: three-year results. *Agric. Ecosyst. Environ.* 326:107799. doi: 10.1016/j.agee.2021.107799

Wang, J., Wu, L., Xiao, Q., Huang, Y., Liu, K., Wu, Y., et al. (2023). Long-term manuring enhances soil gross nitrogen mineralization and ammonium immobilization in subtropical area. *Agric. Ecosyst. Environ.* 348:108439. doi: 10.1016/j.agee.2023.108439

Wickham, H. (2011). ggplot2. *Wiley Interdiscip. Rev.* 3, 180–185. doi: 10.1002/wics.147

Wu, G., Liang, F., Wu, Q., Feng, X.-G., Shang, W. D., Li, H. W., et al. (2024). Soil pH differently affects N2O emissions from soils amended with chemical fertilizer and manure by modifying nitrification and denitrification in wheat-maize rotation system. *Biol. Fertil. Soils* 60, 101–113. doi: 10.1007/s00374-023-01775-9

Wu, Y., Shaaban, M., Deng, C., Peng, Q., and Hu, R. (2017). Changes in the soil N potential mineralization and nitrification in a rice paddy after 20 years application of chemical fertilizers and organic matter. *Can. J. Soil Sci.* 97, 290–299. doi: 10.1139/cjss-2016-0065

Wu, X., Wang, Y., Zhu, Y., Tian, H., Qin, X., Cui, C., et al. (2019). Variability in the response of bacterial community assembly to environmental selection and biotic factors depends on the immigrated Bacteria, as Revealed by a Soil Microcosm Experiment. *mSystems* 4:e00496-19. doi: 10.1128/msystems.00496-19

Xia, Y., Chen, X., Zheng, S., Gunina, A., Ning, Z., Hu, Y., et al. (2021). Manure application accumulates more nitrogen in paddy soils than rice straw but less from fungal necromass. *Agric. Ecosyst. Environ.* 319:107575. doi: 10.1016/j.agee.2021.107575

Yang, Y., Shen, L., Zhao, X., Agathokleous, E., Wang, S., Ren, B., et al. (2023). Long-term fertilization enhances the activity of anaerobic oxidation of methane coupled to nitrate reduction and associated microbial abundance in paddy soils. *Soil Biol. Biochem.* 185:109130. doi: 10.1016/j.soilbio.2023.109130

Young, M. D., Ros, G. H., and de Vries, W. (2021). Impacts of agronomic measures on crop, soil, and environmental indicators: a review and synthesis of meta-analysis. *Agric. Ecosyst. Environ.* 319:107551. doi: 10.1016/j.agee.2021.107551

Yuan, Y., Liang, Y., Cai, H., Yuan, J., Li, C., Liu, H., et al. (2025). Soil organic carbon accumulation mechanisms in soil amended with straw and biochar: entombing effect or biochemical protection? *Biochar* 7:33. doi: 10.1007/s42773-025-00431-9

Zhai, L., Wang, Z., Zhai, Y., Zhang, L., Zheng, M., Yao, H., et al. (2022). Partial substitution of chemical fertilizer by organic fertilizer benefits grain yield, water use efficiency, and economic return of summer maize. *Soil Tillage Res.* 217:105287. doi: 10.1016/j.still.2021.105287

Zhang, C., Ju, X., Zhang, J., Rees, R. M., and Müller, C. (2023). Soil pH and long-term fertilization affect gross N transformation and N2O production pathways in Chinese and UK croplands. *Biol. Fertil. Soils* 59, 527–539. doi: 10.1007/s00374-022-01695-0

Zhang, Q., Wu, Y., Wang, J., Wu, G., Long, W., Xue, Z., et al. (2016). Accelerated dysbiosis of gut microbiota during aggravation of DSS-induced colitis by a butyrate-producing bacterium. *Sci. Rep.* 6:27572. doi: 10.1038/srep27572

Zhao, J., Pullens, J. W. M., Sørensen, P., Blicher-Mathiesen, G., Olesen, J. E., and Børgesen, C. D. (2022). Agronomic and environmental factors influencing the marginal increase in nitrate leaching by adding extra mineral nitrogen fertilizer. *Agric. Ecosyst. Environ.* 327:107808. doi: 10.1016/j.agee.2021.107808

Zhou, W., Ma, Q., Wu, L., Hu, R., Jones, D. L., Chadwick, D. R., et al. (2022). The effect of organic manure or green manure incorporation with reductions in chemical fertilizer on yield-scaled N2O emissions in a citrus orchard. *Agric. Ecosyst. Environ.* 326:107806. doi: 10.1016/j.agee.2021.107806

Zuo, S., Wu, D., Du, Z., Xu, C., Tan, Y., Bol, R., et al. (2023). Mitigation of soil N2O emissions by decomposed straw based on changes in dissolved organic matter and denitrifying bacteria. *Sci. Total Environ.* 905:167148. doi: 10.1016/j.scitotenv.2023.167148

frontiers | Frontiers in Microbiology

TYPE Original Research
PUBLISHED 05 June 2025
DOI 10.3389/fmicb.2025.1592834

Check for updates

OPEN ACCESS

EDITED BY
Muhammad Zahid Mumtaz,
Gansu Agricultural University, China

REVIEWED BY
Salvador Mirete,
Spanish National Research Council (CSIC), Spain
Maria Elena Antinori,
Catholic University of the Sacred Heart, Italy

*CORRESPONDENCE
Yuhua Li
✉ lyhshen@126.com
Shurong Ma
✉ msryz@nefu.edu.cn

†These authors have contributed equally to this work

RECEIVED 13 March 2025
ACCEPTED 07 May 2025
PUBLISHED 05 June 2025

CITATION
Song J, Guan X, Cui H, Liu L, Li Y, Li Y and Ma S (2025) The impact of salt-tolerant plants on soil nutrients and microbial communities in soda saline-alkali lands of the Songnen plain. *Front. Microbiol.* 16:1592834. doi: 10.3389/fmicb.2025.1592834

COPYRIGHT
© 2025 Song, Guan, Cui, Liu, Li, Li and Ma. This is an open-access article distributed under the terms of the Creative Commons Attribution License (CC BY). The use, distribution or reproduction in other forums is permitted, provided the original author(s) and the copyright owner(s) are credited and that the original publication in this journal is cited, in accordance with accepted academic practice. No use, distribution or reproduction is permitted which does not comply with these terms.

The impact of salt-tolerant plants on soil nutrients and microbial communities in soda saline-alkali lands of the Songnen plain

Junjie Song†, Xueting Guan†, Haojun Cui, Lin Liu, Yan Li, Yuhua Li* and Shurong Ma*

Key Laboratory of Saline-Alkali Vegetation Ecology Restoration, Ministry of Education, College of Life Science, Northeast Forestry University, Harbin, China

Introduction: Soil salinization poses a significant threat to agricultural development and ecosystem health. While phytoremediation is an effective approach, the mechanisms by which salt-tolerant plants mediate saline-alkali soil amelioration in the Songnen Plain remain unclear.

Methods: We selected seven common salt-tolerant plants from the Songnen Plain to compare soil nutrients and microbial communities between vegetated areas and bare alkali patches. Soil salinity, pH, nutrient content (TN, TP, TK), enzyme activities (Catalase, Cellulase, Saccharase, Urease), and microbial structure were analyzed.

Results: Plant presence significantly reduced soil salinity and pH while increasing nutrient levels and enzyme activities, with SL (*Salix linearistipularis*) showing the most comprehensive improvement. Vegetation enhanced microbial abundance/diversity (bacteria and fungi), with EC ($R^2 = 0.7308$, $P = 0.0001$) and TN ($R^2 = 0.5706$, $P = 0.0001$) as key drivers of diversity changes. Microbial composition shifted markedly: beneficial phyla (e.g., Mortierellomycota, Acidobacteriota) increased, while pathogenic Chytridiomycota decreased. Community variations were primarily influenced by EC ($R^2 = 0.8778$, $P = 0.001$) and pH ($R^2 = 0.8661$, $P = 0.001$). Plants also promoted functional groups involved in carbon/nitrogen cycling.

Discussion: These findings demonstrate that salt-tolerant plants enhance soil fertility and restructure microbial communities in saline-alkali soils, with EC/pH and TN as critical regulatory factors. This study provides a scientific basis for sustainable saline land rehabilitation via targeted vegetation restoration.

KEYWORDS

salt tolerant plants, soda saline-alkali soil, soil physical and chemical properties, rhizosphere microorganisms, driving factors

1 Introduction

Soil salinization has become one of the most significant global environmental and economic issues, severely threatening food security and ecosystem health. It adversely affects plant growth, crop yield, soil structure, and fertility (Hassani et al., 2021; Tarolli et al., 2024; Zhang et al., 2024a). In China, the area of saline-alkali land reaches 99 million

hectares (Chen et al., 2024). The Songnen Plain in Northeast China, with over 3 million hectares affected by salinization, is one of the world's three major concentrated distribution areas of soda saline-alkali land (Yang et al., 2016). The salts in soda saline-alkali land are primarily composed of NaHCO3 and Na_2CO3, characterized by high pH and rich soil colloid content. This results in simultaneous salinization and alkalization, making the soil in this region more barren and unsuitable for cultivation, severely restricting agricultural development (Chi et al., 2011; Li et al., 2016). Against the backdrop of the global food crisis, how to effectively utilize saline-alkali land and transform it into fertile farmland has become a hot research topic. Current methods for improving saline-alkali land mainly include physical approaches (irrigation and drainage, soil replacement), chemical methods (application of gypsum, humic acid), and biological methods (phytoremediation, microbial remediation) (Elmeknassi et al., 2024; Heng et al., 2022; Hu et al., 2024). Physical methods require significant labor, while chemical methods may cause secondary pollution (Wang et al., 2024a; Zhang et al., 2024b). In contrast, biological remediation not only offers a low-cost solution for soil improvement but also reduces the risk of soil pollution, making it a key direction in current research on saline-alkali soil remediation (Hu et al., 2024; Jiang et al., 2015).

Halophytes are naturally salt-tolerant plants that can endure salinity levels intolerable to most plants, thriving and surviving in saline soils. Halophytes and salt-tolerant plants have evolved various adaptive mechanisms to cope with salt-alkali stress, including salt gland secretion, regulation of cellular ion homeostasis and osmotic pressure, detoxification of reactive oxygen species, and alterations in membrane composition (Flowers and Colmer, 2008; Meng et al., 2018). With the continuous expansion of saline-alkali land, the sustainable development of traditional agriculture faces significant challenges. Phytoremediation is a sustainable and cost-effective approach. Cotton/halophytes can reduce soil salinity through intercropping, improving soil physicochemical properties and crop yield, thereby generating higher economic benefits (Liang and Shi, 2021). Salt-tolerant legumes such as *Glycine soja* and *Sesbania cannabina* have successfully rehabilitated saline soils by reducing soil electrical conductivity (EC) and accumulating carbon and nitrogen, enriching microbial communities at different soil depths (Zheng et al., 2023). Furthermore, plant cultivation not only ameliorates saline-alkali soils but also enhances ecosystem multifunctionality (EMF), increasing microbial community richness and network complexity (Hu et al., 2024; Qiu et al., 2022).

Soil microorganisms are crucial for the sustainable development of ecosystems (Zhang et al., 2024a). They facilitate the decomposition of plant litter, the formation of humus, and play a significant role in biogeochemical cycles (Djukic et al., 2010). In natural environments, soil microorganisms are highly sensitive to environmental changes and are easily influenced by factors such as soil salinity, nutrients, and pH. Therefore, the structure and diversity of soil microbial communities serve as important indicators of soil health and ecosystem stability (Fierer et al., 2021; Liu et al., 2020; Yang et al., 2024). Soil electrical conductivity (EC) and salt ion content are considered primary factors affecting soil microorganisms. Increases in soil EC and salinity significantly reduce microbial diversity and richness, altering microbial community structure (Guan et al., 2021; Guo et al., 2023; Zhang et al., 2024a, 2021). Compared to bulk soil, the plant rhizosphere actively shapes a distinct microenvironment through continuous secretion of organic compounds (e.g., sugars, organic acids) (Kumar et al., 2023), characterized by: enhanced nutrient availability; and generally reduced pH and EC values (Balyan and Pandey, 2024; Ström et al., 2002). This plant-mediated niche construction drives significant microbial community shifts, manifesting as: increased abundance of exudate-utilizing taxa (Vives-Peris et al., 2020); and elevated overall microbial diversity (Qiu et al., 2022), though with potential reduction of halophilic specialists (Wang et al., 2020). Concurrently, rhizosphere microbes engage in bidirectional interactions with plants through signal exchange, ultimately enhancing plant stress tolerance (Gupta et al., 2021; Peng et al., 2023).

The root system of plants serves as the primary source of nutrient acquisition and represents the most dynamic microenvironment in the soil. In this region, plant-microbe-environment interactions collectively maintain ecosystem stability. However, the mechanisms underlying the interactions between microbial communities and plants remain unclear, hindering our understanding of how salt-tolerant plants influence microbial community assembly. The Songnen Plain, one of the world's three major soda saline-alkali regions, exhibits severe salinization but supports a variety of salt-tolerant plants. Nevertheless, the impact of these plants on the microbial communities in saline-alkali soils is not well understood. Therefore, in this study, we evaluated the remediation effects of these plants on saline-alkali soils by measuring the physicochemical properties and enzyme activities of rhizosphere soils and alkali patches under different salt-tolerant plants. Using high-throughput sequencing, we investigated the effects of salt-tolerant plants on the richness and diversity of microbial communities. Finally, we identified key environmental factors influencing microbial community diversity and composition, as well as the functional group dynamics of microbial communities.

2 Materials and methods

2.1 Study site and soil sampling

The study area is located in Anda City, Heilongjiang Province (46°4′-47°1′N, 124°53′-125°55′E). Sampling was conducted within the experimental station of Northeast Forestry University in Anda (Figure 1). Established in 2002, the station initiated large-scale phytoremediation of saline-alkali soils in 2005, with continuous restoration efforts until the sampling year (2020), totaling 15 years of intervention. The sampling area covered approximately 6 hectares, characterized by flat terrain (slope <2°) and uniform sandy loam saline-alkali soil, with consistent historical management practices (no fertilization or irrigation). The region experiences a northern temperate continental semi-arid monsoon climate, with a mean annual temperature of 4.2°C, a frost-free period of 129 days, and an average annual precipitation of 432.5 mm, of which approximately half occurs during summer.

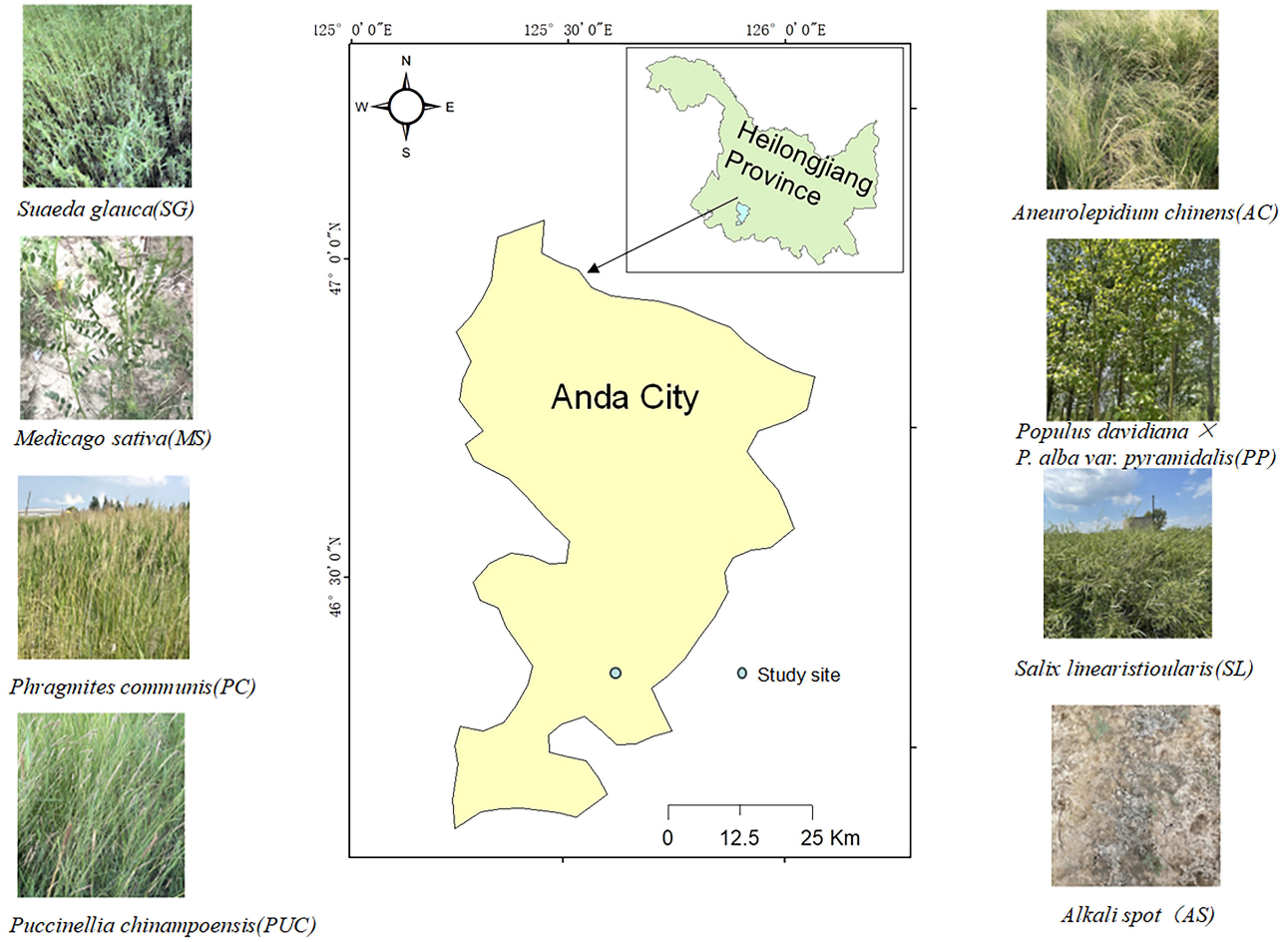


FIGURE 1
Schematic diagram of sampling area and vegetation at sampling sites.

Prior to restoration, the area exhibited severe saline-alkalization with relatively simple vegetation community structure.

For sampling design, quadrats (1 m × 1 m) were randomly established for seven plant species—*Phragmites communis* (PC), *Puccinellia chinampoensis* (PUC), *Medicago sativa* (MS), *Aneurolepidium chinense* (AC), *Suaeda glauca* (SG), *Salix linearistipularis* (SL), and *Populus davidiana* × *P. alba var. Pyramidalis* (PP), with Alkaline spot (AS, bare soil patches with pH >10 and EC >5.3 dS/m) as the control. To minimize interspecific interference and local soil heterogeneity, a minimum spacing of ≥15 meters was maintained between quadrats. For each plant species, three replicate quadrats were established, with rhizosphere soil samples (0–20 cm depth) collected using a soil auger at five points (four corners and center) per quadrat. After removing roots and debris, samples from each quadrat were homogenized to form a composite sample, from which 1 kg subsamples were obtained by quartering and stored in sterile ziplock bags. During sampling, microtopographic consistency (no significant elevation differences) was ensured across all plant quadrats and control spots, with surrounding vegetation cover (absence of tree interference) documented. All soil samples were immediately stored in iceboxes and transported to the laboratory within 24 h. Each sample was divided into two aliquots: one preserved at −80°C for high-throughput sequencing, and the other air-dried in a ventilated area, then ground and sieved through a 2-mm mesh (with roots and stones removed) for physicochemical property and enzyme activity analyses.

2.2 Determination of soil physicochemical properties and enzyme activities

Soil pH was measured using a pH meter (FE28, METTLER-TOLEDO, USA) at a soil-to-water ratio of 1:2.5 (m/v). Soil electrical conductivity (EC) was determined using a conductivity meter (Bante902P, Bante, CN) at a soil-to-water ratio of 1:5 (m/v). Soil total nitrogen (TN) was assayed using the Kjeldahl method. Soil total potassium (TK) was quantified via an ammonium acetate extraction flame photometric method (JHR-2, Ye Tuo, Shanghai). Total phosphorus (TP) was determined by the colorimetric method (JHR-2, Ye Tuo, Shanghai). Soil organic matter (SOM) was measured using the spectrophotometric method. Soil NO_3^--N and NH_4^+-N were determined by the micro method. Soil bulk density

(BD) and soil water content (SWC) were measured using the ring knife method and the drying-weighing method, respectively (Chen et al., 2021b; Kang et al., 2002). The activities of soil urease, alkaline phosphatase, catalase, and sucrase were measured using kits provided by Nanjing Convinced Testing Technology Corporation (Nanjing, China). All tests were conducted in triplicate, and the final results were averaged.

2.3 DNA extraction, amplicon sequencing and data processing

Bacterial 16S rRNA sequences were amplified using forward primer 338F (5′-ACTCCTACGGAGGCAGCAG-3′) and reverse primer 806R (5′-GGACTACHVGGGTWTCTAAT-3′; Caporaso et al., 2011). Fungal ITS sequences were amplified with forward primer ITS1F (5′-CTTGTCATTTAGAGGAAGTAAGTAA-3′) and reverse primer ITS2R (5′-GCTGCGTTCTTCATCGATGC-3′; Chen et al., 2021a). PCR was performed in 20 μl reactions containing 10 μl 2×Pro Taq mix, 0.8 μl of each primer (5 μM), and 10 ng template DNA, with ddH_2O added to a final volume of 20 μl. The amplification protocol consisted of initial denaturation at 95°C for 5 min, followed by 30 cycles of denaturation at 95°C for 30 s, annealing at 55°C for 30 s, and extension at 72°C for 45 s, with a final extension at 72°C for 5 min. PCR products were verified by 1.5% agarose gel electrophoresis, and samples showing distinct bands between 400–450 bp were selected for subsequent analysis.

After high-throughput sequencing, the resulting paired-end (PE) reads were spliced using FLASH 1.2.11 software and simultaneously subjected to quality control and filtering. For the optimized sequences, non-repetitive sequences were extracted, and single sequences without repetition were removed. High-quality sequences obtained by the Uparse algorithm were clustered into operational taxonomic units (OTUs) at a 97% similarity level, and representative sequences of OTUs were obtained by removing chimeras during the clustering process. The representative sequences of OTUs were analyzed using the RDP classifier Bayesian algorithm. Bacterial 16S rRNA sequences were compared against the SILVA database (http://www.arb-silva.de), and fungal ITS sequences were compared against the UNITE fungal database (http://unite.ut.ee/index.php).

2.4 Statistical analysis

Soil microbial α-diversity was calculated using Mothur (http://www.mothur.org/wiki), and rarefaction curves were generated based on the Shannon index using the R language (version 3.3.1). Principal Coordinate Analysis (PCoA) based on Bray-Curtis distance was performed using QIIME (version 2020.2.0) to assess structural differences in microbial communities. Redundancy Analysis (RDA) and Monte Carlo tests were employed to evaluate the influence of environmental factors on microbial community structure. The impact of environmental factors on microbial community diversity was tested using ordination regression analysis. Bar plots of soil microbial communities, intergroup difference tests, and FAPROTAX functional prediction analysis were conducted and visualized using R software. All data analyses were performed on the free Majorbio I-Sanger Cloud Platform (https://www.majorbio.com). The differences in soil physicochemical properties (pH, EC, SOM, TK, TP, NH_4^+-N, NO_3^--N, BD, and SWC) and soil enzyme activities (catalase, cellulase, saccharase, and urease) among different vegetation types were assessed using one-way analysis of variance (ANOVA) followed by least significant difference (LSD) multiple comparison test ($P < 0.05$). Unless otherwise specified, all between-group differences reported in Results were statistically significant at $P < 0.05$ based on LSD *post-hoc* tests. Data analysis was completed using SPSS software (version 26.0).

3 Results

3.1 Physicochemical properties and enzyme activities of rhizosphere soil in halophytes

The physicochemical properties of rhizosphere soil varied significantly among different vegetation types (Figures 2a–j). All vegetation types significantly increased the contents of SOM, TN, and NH_4^+-N, while reducing NO_3^--N content and EC. However, the effects of different vegetation types on soil physicochemical properties varied considerably. The SOM levels across vegetation types followed the order: SL > AC > PP > PC > PUC > MS > SG > AS, while TN levels followed: SL > AC > PP > PC > PUC > MS > SG > AS. The pH of all soil samples exceeded 7.8, indicating alkaline soil. Among them, *Populus davidiana* × *P. alba var. Pyramidalis* (PP) had the most significant effect on soil pH, with a pH of 7.82. *Salix linearistipularis* (SL) showed the best improvement in Physical and chemical properties of saline-alkali soils, with high levels of SOM, TN, TP, and TK, and lower EC and pH. Among all vegetation types, SWC and BD showed no significant differences.

Soil enzyme activity is an important indicator of soil health. Compared to Alkaline spot (AS), different vegetation types significantly enhanced soil enzyme activities to varying degrees (Figures 2k–n). For example, sucrase and cellulase activities were significantly increased in all vegetation types. The catalase activities of *Aneurolepidium chinense* (AC) and SL were 1.16 U/g and 1.23 U/g, respectively, significantly higher than AS. Except for *Suaeda glauca* (SG), the urease activities of other vegetation types were significantly increased.

3.2 Composition and differences of rhizosphere microbial communities in salt-tolerant plants

A total of 1,115,143 optimized bacterial sequences and 1,488,479 optimized fungal sequences were obtained from the soil samples. The coverage indices for both fungi and bacteria exceeded 97% (Supplementary Figure 1), indicating that the

10.3389/fmicb.2025.1592834

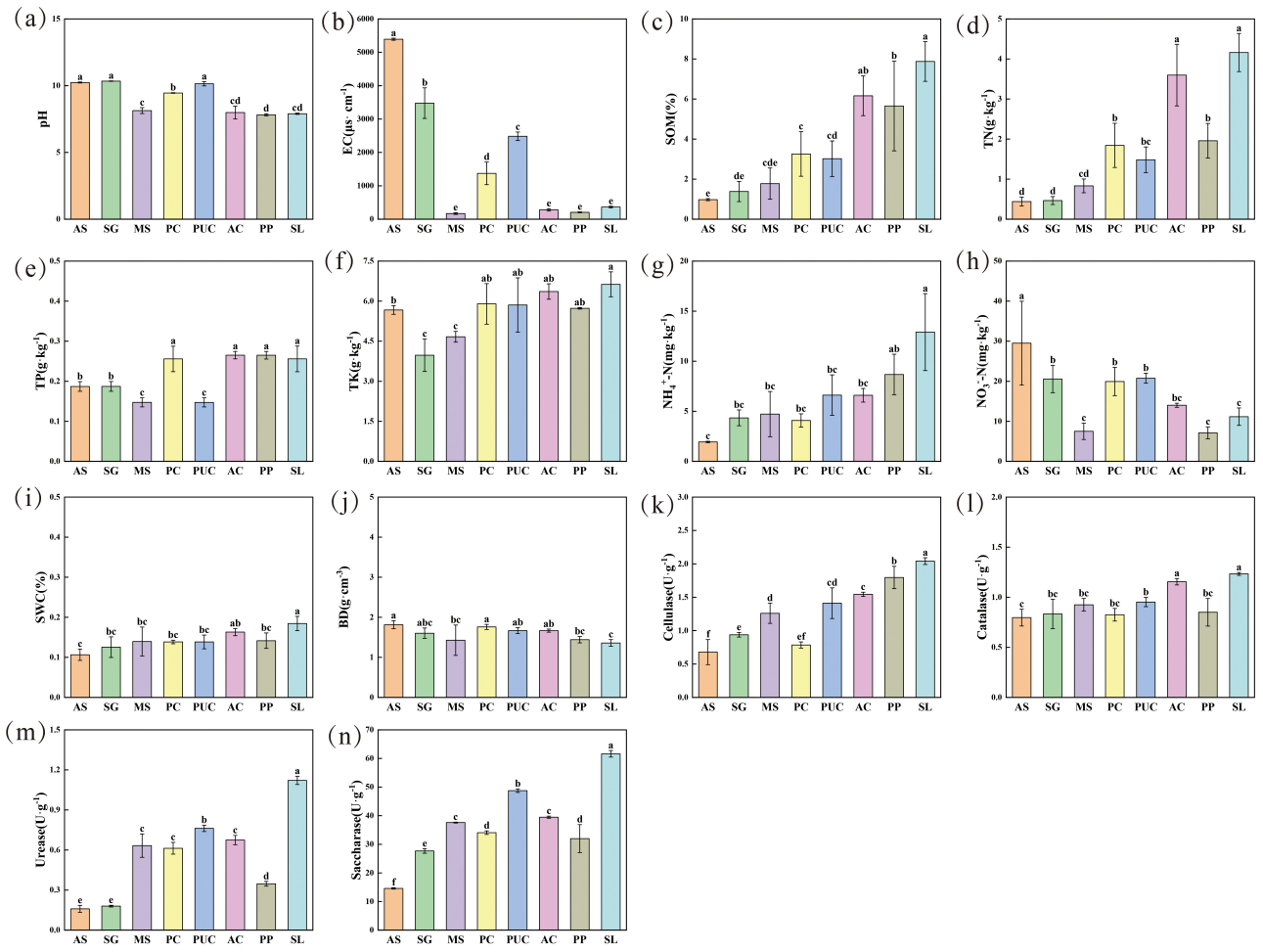


FIGURE 2
Soil characteristics under different vegetation types. **(a)** pH. **(b)** EC. **(c)** SOM. **(d)** TN. **(e)** TP. **(f)** TK. **(g)** NH_4^+-N. **(h)** NO_3^--N. **(i)** SWC. **(j)** BD. **(k)** Cellulase. **(l)** Catalase. **(m)** Urease. **(n)** Saccharase. Different letters at the top of each figure indicate significant differences among various halophyte rhizospheres and bulk soil ($P < 0.05$, Duncan test).

microbial community sequences obtained were of high quality. The rarefaction curves (Supplementary Figure 2) showed that all samples reached a plateau, suggesting that the sequencing depth was sufficient for subsequent analysis. The diversity and richness of rhizosphere microbial communities in different salt-tolerant plants were evaluated based on the S_{obs} and Shannon index from α-diversity analysis (Figure 3a). The results demonstrated that: for bacterial communities, both S_{obs} and Shannon index were significantly higher in the vegetated rhizosphere compared to AS; for fungal communities, while the Shannon index showed significant differences between vegetated and AS areas, no significant variation was observed in S_{obs}. These findings reveal distinct vegetation-type effects on rhizosphere bacterial vs. fungal communities. Principal Coordinates Analysis (PCoA) revealed significant differences in microbial community structure among samples ($p = 0.001$). As shown in Figure 3b, distinct separation was observed between bacterial and fungal communities across different samples. The AS samples exhibited pronounced differentiation from other vegetation types in the PCoA ordination space.

By analyzing the unique and shared soil microbial OTUs among different samples at the OTU level using Venn diagrams (Supplementary Figure 3), the results showed that AS accounted for 19.37% (436/2251) of the total bacterial OTUs analyzed, while the shared OTUs among salt-tolerant plants represented 9.60% (216/2251). Among these, *Phragmites communis* (PC) had the highest number of unique OTUs. For fungi, 35 OTUs were shared across all samples, and the number of unique OTUs in salt-tolerant plants was consistently higher than that in AS. AS had the fewest unique OTUs, with only 90. The analysis of microbial community structure at the phylum level (Figures 4a, c) revealed the presence of 15 dominant bacterial phyla (relative abundance > 1%) and 8 dominant fungal phyla (relative abundance > 1%) in the rhizosphere soil. Among the 15 dominant bacterial phyla, Actinobacteriota and Proteobacteria emerged as the predominant lineages, collectively comprising 49.50% to 66.01% of the total bacterial community. Compared to AS (Supplementary Figure 4), the relative abundances of Acidobacteriota, and Myxococcota were higher in the rhizosphere of plants, while Firmicutes and

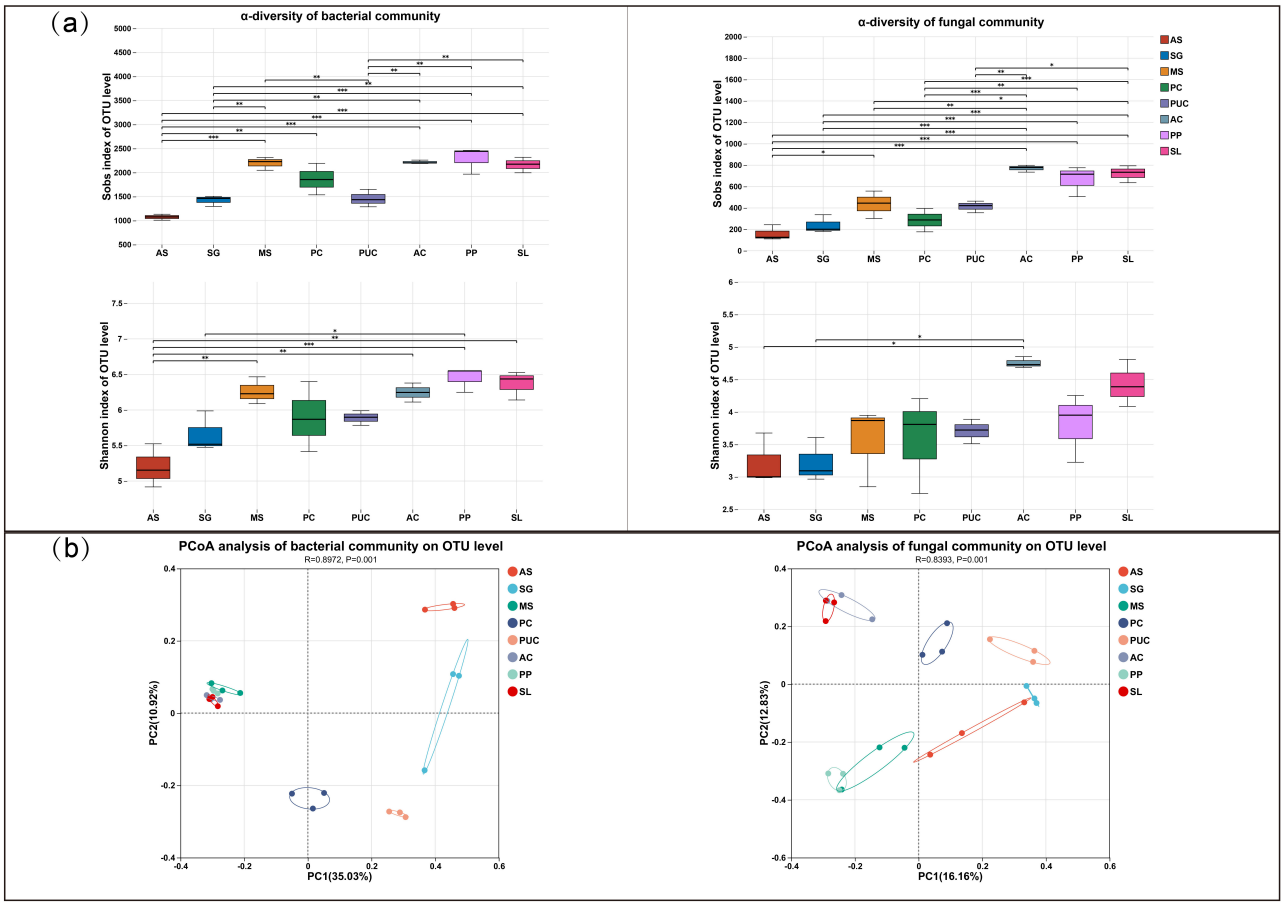


FIGURE 3
Diversity and differential analysis of rhizosphere microbial communities under different vegetation types. **(a)** S_{obs} and Shannon index. **(b)** Principal coordinate analysis (PCoA). Significant differences: $*p < 0.05$, $**p < 0.01$, $***p < 0.001$.

RCP2-54 were lower. Among the eight dominant fungal phyla, Ascomycota exhibited the highest relative abundance. The relative abundance of Mortierellomycota increased significantly, whereas that of Chytridiomycota decreased.

Furthermore, the microbial community structure was analyzed at the genus level, with the top 20 genera in relative abundance classified as dominant genera. These top 20 genera accounted for 28.02% to 45.67% of the total bacterial abundance and 25.28% to 53.12% of the total fungal abundance (Figures 4b, d). Among them, the dominant bacterial genera in AS were *Actinomarinales* (10.04%), *Geminicoccaceae* (5.12%), and *Longimicrobiaceae* (4.66%). Notably, *Longimicrobiaceae* was the most dominant bacterial genus in SG and *Puccinellia chinampoensis* (PUC). *Vicinamibacteraceae* exhibited high abundance in *Medicago sativa* (MS), PP, and SL, accounting for 4.38, 3.47, and 6.4%, respectively, while *Geminicoccaceae* (9.27%) *and 67–14* (7.44%) were the most abundant bacterial genera in SG and AC, respectively. For fungi, *Ramophialophora* (11.69%) was the dominant genus in AS, whereas *Articulospora* (10.35%) and *Acremonium* (10.21%) predominated in the rhizosphere of SG. Additionally, *Mortierella* held a significant presence in the rhizosphere fungal communities of MS, PC, AC, PP, and SL.

3.3 Interrelationships between soil physicochemical properties and microbial communities

Correlation analysis revealed the relationships among soil physicochemical properties, soil enzyme activities, and the richness and diversity of soil microbial communities (Figure 5a). Soil enzyme activities showed a significant negative correlation with soil EC, pH and, NO_3^--N while exhibiting a positive correlation with fundamental soil physicochemical indicators (TN, TP, TK, and NH_4^+-N). Additionally, the richness and diversity of fungi and bacteria (Shannon index and S_{obs}) were significantly negatively correlated with pH and EC ($p < 0.05$). This indicates that high pH and EC can influence fundamental soil physicochemical properties to some extent and significantly affect the richness and diversity of soil microbial communities.

Redundancy Analysis (RDA) models and Monte Carlo tests (Figures 5b, c, and Supplementary Table 2) were employed to examine the relationships between soil physicochemical properties and soil microbial community composition. For bacterial communities, EC ($R^2 = 0.8778$; $P = 0.001$) was the most significant factor influencing community structure, followed by pH,

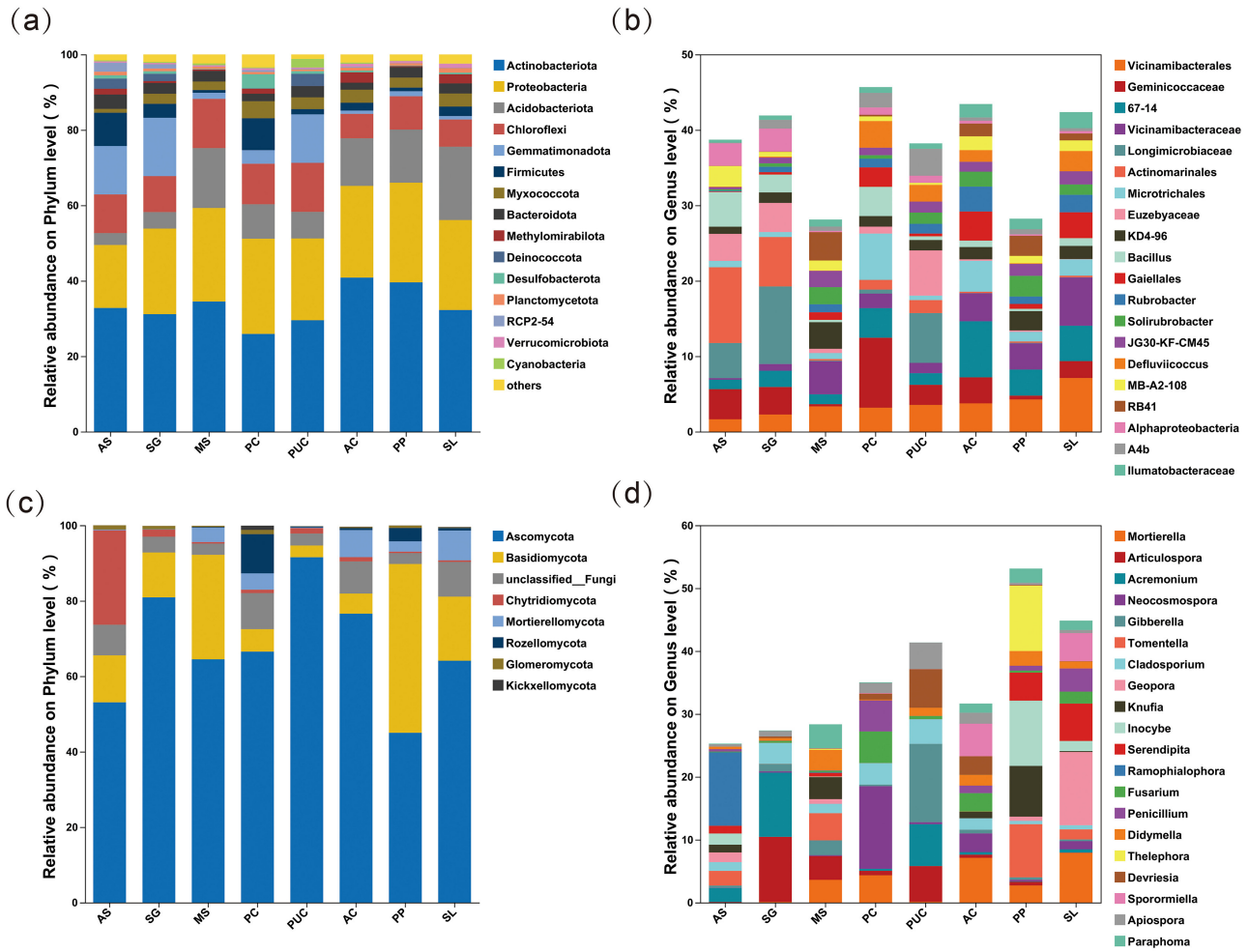


FIGURE 4
Composition of rhizosphere microbial communities across different vegetation types **(a)** Bacterial community composition at the phylum level. **(b)** Fungal community composition at the phylum level. **(c)** Relative abundance of the top 20 bacterial genera. **(d)** Relative abundance of the top 20 fungal genera.

NO_3^--N, and TP. For fungal communities, pH (R^2 = 0.8661; P = 0.001) was the primary factor, followed by cellulase activity, TN, and EC. Additionally, pH and EC were positively correlated with salt-tolerant or oligotrophic microorganisms (Figures 5d, e), such as the bacterial phyla Firmicutes, Nitrospirota, RCP2-54, Gemmatimonadota, Deinococcota, Bacteroidota, and Chloroflexi, as well as the fungal phyla Chytridiomycota, Glomeromycota, Ascomycota, and Aphelidiomycota. When soil pH and EC decreased and nutrient levels increased, the abundance of these microorganisms declined. Our results indicate that different microbial communities in saline-alkali soils are sensitive to soil physicochemical properties.

Microbial diversity is crucial for ecosystem stability. Using the Shannon index as an indicator, we identified the primary factors influencing soil fungal and bacterial diversity through ordination regression analysis of environmental factors (Figure 6). A decrease in EC was the driving factor affecting bacterial community diversity (R^2 = 0.7308, P = 0.0001), while an increase in SOM was a significant factor enhancing bacterial diversity (R^2 = 0.374, P = 0.0015). In contrast, TN was the main factor increasing fungal diversity (R^2 = 0.5706, P = 0.0001).

3.4 Changes in rhizosphere microbial community functions

To further understand the potential functions of rhizosphere microbial communities, we conducted FAPROTAX analysis based on existing databases (Figure 7). A total of 2 fungal functional groups were identified, primarily involved in cellulolysis and chemoheterotrophy processes, with no significant changes observed. Among the 65 bacterial functional groups, the most abundant were those primarily involved in carbon (C) cycling, such as chemoheterotrophy and aerobic chemoheterotrophy, followed by nitrate reduction and aromatic compound degradation. Significant changes were observed in certain functional groups involved in material cycling across different treatments. Functional

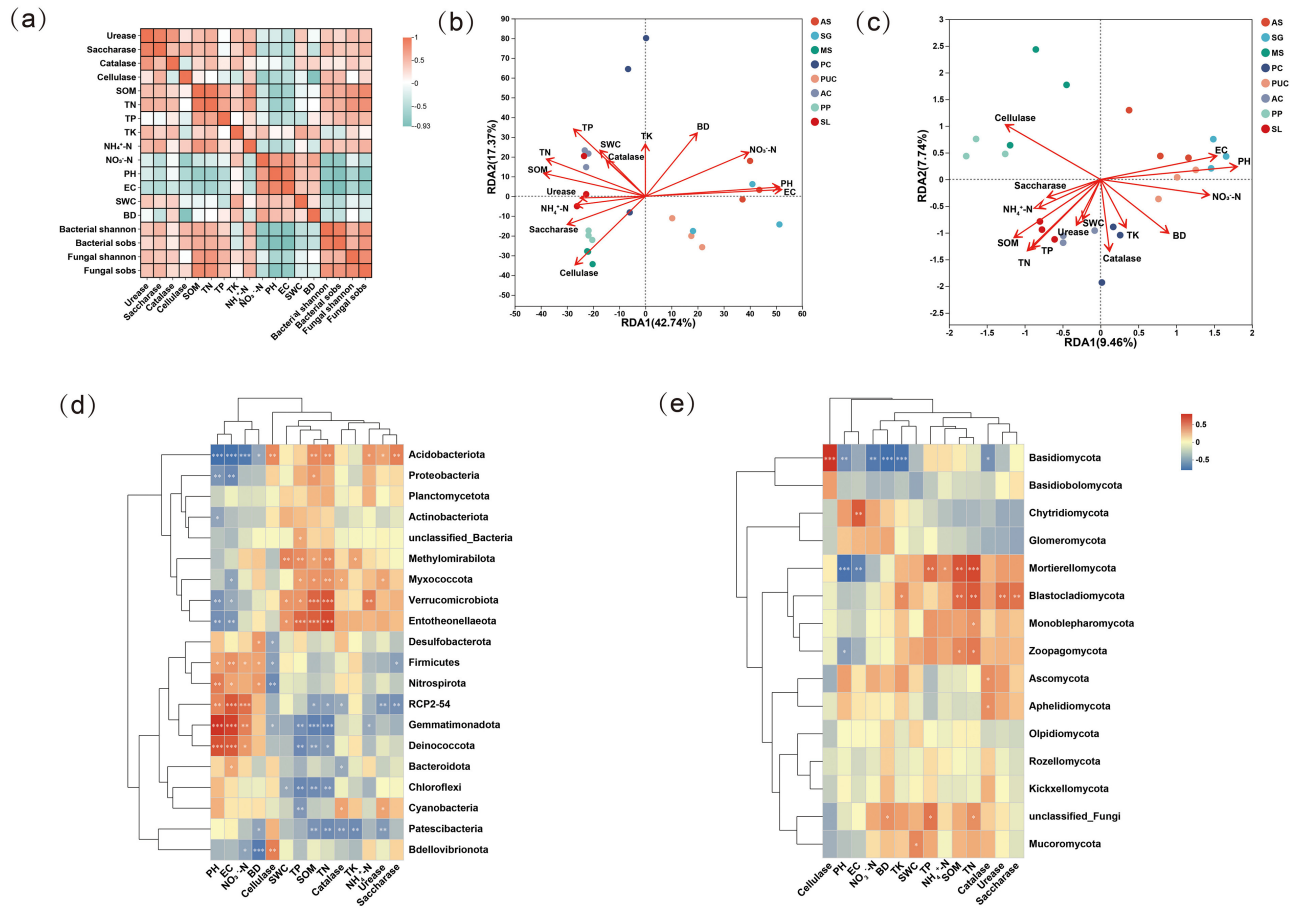


FIGURE 5
Interaction between environmental factors and microbial communities. **(a)** Pairwise interactions between environmental factors and microbial diversity. **(b)** Redundancy analysis (RDA) for bacteria. **(c)** Redundancy analysis (RDA) for fungi. **(d)** Interaction between the top 20 bacterial phyla and environmental factors. **(e)** Interaction between the top 20 fungal phyla and environmental factors.Significance levels: $*p < 0.05$, $**p < 0.01$, $***p < 0.001$. The range from red to blue represents the relative abundance from high to low.

groups associated with C cycling (cellulolysis and chitinolysis), nitrogen fixation, denitrification (denitrification, nitrous oxide denitrification, and nitrite denitrification), and reduction (nitrite reduction) were significantly enhanced compared to AS. Therefore, we conclude that plants alter the composition of their rhizosphere microbial communities, recruiting relevant functional groups that contribute to improving soil properties.

4 Discussion

4.1 Effects of salt-tolerant plants on soil physicochemical properties and enzyme activities

Soil salinization severely affects plant growth and leads to reduced crop yields. Phytoremediation is an effective strategy for rehabilitating saline-alkali soils (Jesus et al., 2015; Wang et al., 2020). Plant root exudates can not only improve soil structure and promote the dissolution and leaching of salts (Balyan and Pandey, 2024), but also recruit specific rhizosphere microbial communities to enhance plant tolerance to saline-alkali stress (Lei et al., 2025). Additionally, plant root growth increases soil porosity and promotes downward salt leaching (Gong-Neng et al., 2016), while rhizosphere microorganisms (e.g., PGPR and AMF) enhance salt leaching efficiency by secreting extracellular polymeric substances to stabilize soil aggregates (Peng et al., 2025). Plant-microbe interactions also facilitate biological desalination. Plants can absorb dissolved salts (e.g., Na^+ and Cl^- ions) from soil and translocate these ions to specific tissues or cells (such as old leaves and salt glands), thereby preventing salt accumulation around roots and reducing soil salinity (Flowers and Colmer, 2008; Munns and Tester, 2008; Zhao et al., 2020). Concurrently, rhizosphere microbiota mitigate salt accumulation in the root zone through ion immobilization, volatilization, and by facilitating selective K^+ uptake in plants (Qin et al., 2016). However, the remediation effects and mechanisms of common salt-tolerant plants in the Songnen Plain remain unclear. This study evaluated the soil quality under seven common salt-tolerant plants and a control (AS) in the same region of the Songnen Plain. We found that plants can alter soil pH and EC. As a key indicator of soil salinity, EC significantly decreased across different treatment groups, indicating reduced

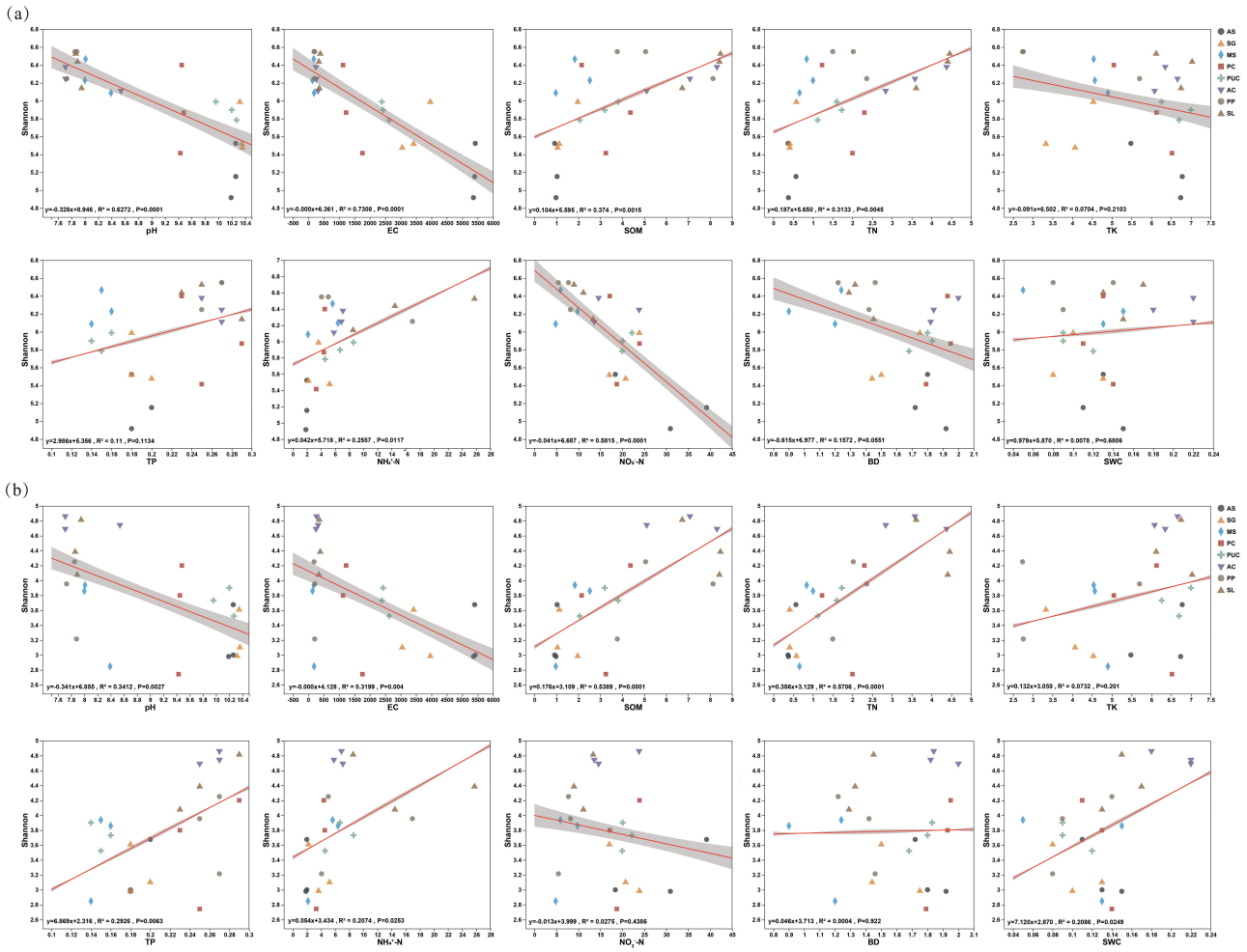


FIGURE 6
Correlation analysis between shannon index of bacterial and fungal communities and environmental factors. **(a)** Bacterial communities. **(b)** Fungal communities.

soil salinity and improved saline-alkali conditions (Figure 2b). MS, PP, and SL showed the most pronounced reduction in salinity, along with the greatest decrease in soil BD. We hypothesize that this may be due to increased soil porosity resulting from root expansion, further reducing salt levels. These plants may promote salt leaching through developed root expansion (reducing BD) and synergistic effects with rhizosphere microorganisms (e.g., organic acid secretion and Na^+ immobilization).

Salt-tolerant plants not only directly reduce soil salinity but also indirectly improve soil quality by regulating rhizosphere microbial functions. Plant residues (e.g., litter) and root exudates (including organic acids, sugars, and amino acids) provide microorganisms with abundant carbon sources and energy substrates, significantly enhancing the decomposition and mineralization of soil organic matter (Cheng et al., 2014; Liu et al., 2025). Previous studies have demonstrated that salt-tolerant plants (*Medicago sativa*, *Agropyron elongatum*, *Sesbania cannabina*) can significantly increase soil nutrient contents, SOM, TN, and TP (Wang et al., 2024b; Zheng et al., 2023), which is closely associated with the metabolic activities of rhizosphere microorganisms (e.g., nitrogen-fixing and phosphate-solubilizing bacteria; Yue et al., 2023). Functional prediction analysis in this study further confirmed this mechanism, revealing a significant increase in the abundance of functional genes related to carbon and nitrogen cycling in the rhizosphere microbial communities (Figure 7). Moreover, soil enzyme activities (e.g., urease, sucrase, cellulase, and catalase) serve as important indicators for evaluating microbial-mediated carbon and nitrogen cycling (Zuccarini et al., 2023). Our results showed that salt-tolerant plants significantly enhanced soil enzyme activities, with the SL treatment exhibiting the most pronounced effects (Figure 2). This improvement may be attributed to the enrichment of highly efficient degrading microbial communities in the rhizosphere. These microorganisms accelerate organic matter transformation through the secretion of extracellular enzymes, thereby further improving soil fertility (Hu et al., 2024; Zuccarini et al., 2023).

4.2 Effects of salt-tolerant plants on soil microbial abundance and diversity

The richness and diversity of soil microorganisms are important indicators of soil health (Wagg et al., 2019). Soil physicochemical properties are considered key factors influencing

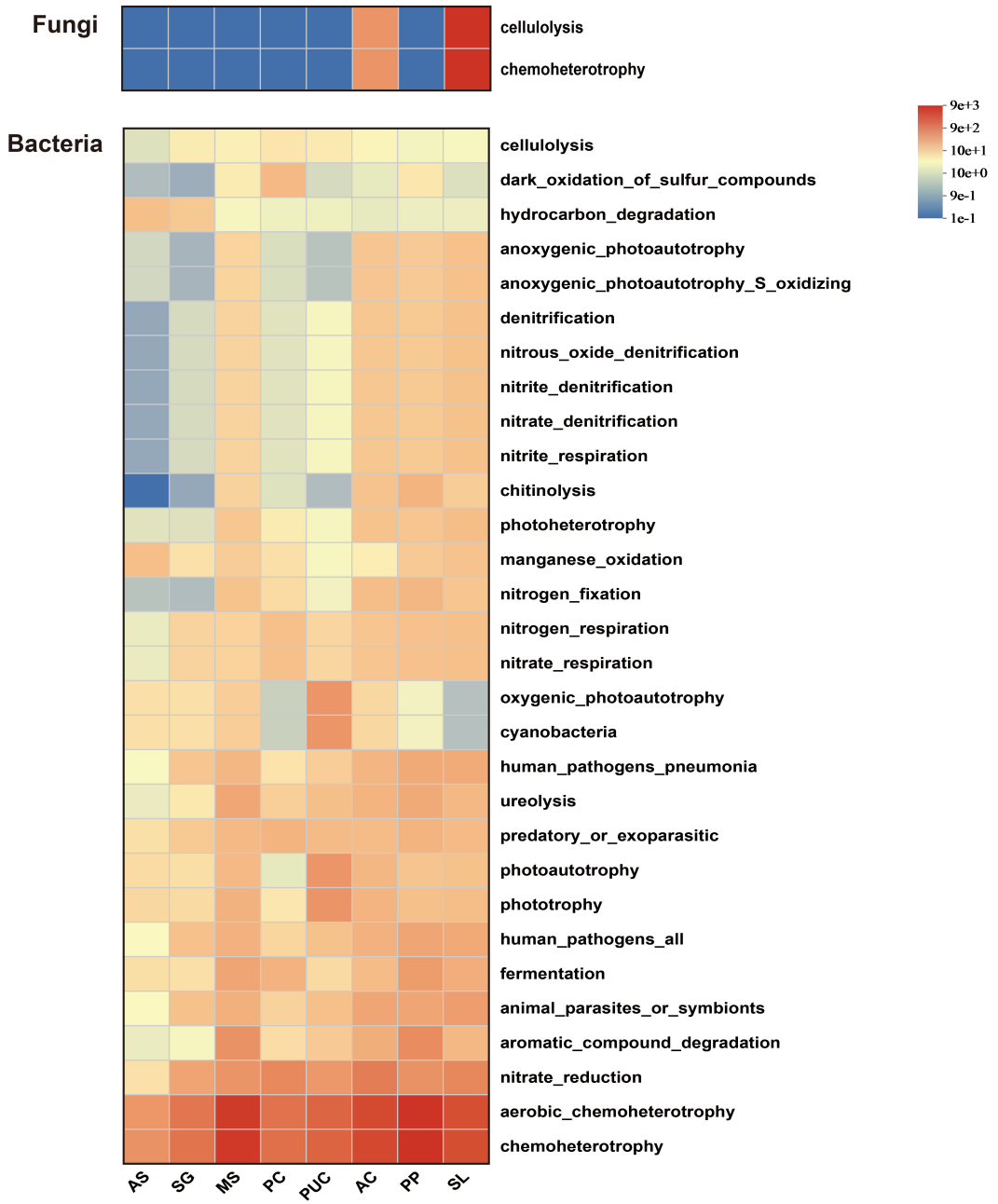


FIGURE 7
Prediction of the top 30 functional groups in bacterial and fungal communities using FAPROTAX. The range from red to blue represents the relative abundance from high to low.

microbial communities, with microbial diversity and richness showing a significant negative correlation with soil salinity and decreasing as salinity increases (Ma et al., 2016; Qadir et al., 2007). This outcome may be attributed to the elevated osmotic pressure caused by high salt levels, which inhibits the activity of many microorganisms due to water deficiency and can even lead to their death (Wang et al., 2010). Only extremophiles (halophiles and alkaliphiles) can adapt to high-salt conditions through osmotic regulation, thereby surviving and growing. Consequently, high salinity and pH significantly reduce microbial richness and diversity. As demonstrated in this study, AS exhibited the highest pH and total salt content, corresponding to the lowest microbial abundance (Supplementary Figure 3).

Numerous studies have shown that plant cultivation reduces soil salinity, increases soil nutrients, and improves the soil environment, thereby enhancing soil microbial diversity and richness (Cuevas et al., 2019; Wang et al., 2021; Xing et al., 2024; Xu et al., 2023). The decomposition of plant litter inputs a significant amount of organic matter into the soil, serving as a vital energy

source for soil microorganisms (Gessner et al., 2010). Additionally, plant root activities promote the formation of soil aggregates, optimize soil pore structure, and significantly enhance soil aeration as roots penetrate deeper soil layers, creating a more favorable microenvironment for microbial growth and metabolic activities (Rabot et al., 2018). Meanwhile, root exudates directly influence the composition of rhizosphere microorganisms. For example, *Suaeda salsa* secretes more compounds under high salt stress, thereby increasing the richness of rhizosphere microorganisms (Liu et al., 2020). These favorable conditions provide an excellent environment for microbial growth and reproduction, promoting increases in microbial richness and diversity. The study found that SL exhibited high diversity indices for both fungi and bacteria (Figure 3), likely due to significant differences in root exudates compared to other vegetation, which influenced fungal growth and reproduction. The results of this study indicate that increases in SOM and TN content are key factors driving significant improvements in soil bacterial and fungal diversity (Supplementary Table 1), further confirming the central role of carbon and nitrogen sources as primary energy and nutrient sources for microbial growth and metabolism (Liang et al., 2017). Based on this finding, in saline-alkali soil vegetation restoration practices, optimizing soil carbon and nitrogen input strategies (e.g., straw return, organic fertilizer application, and biochar amendment; Luo et al., 2011; Zhang et al., 2018) can effectively enhance microbial community richness and diversity, thereby improving ecosystem stability.

4.3 Effects of salt-tolerant plants on soil microbial structure

The results demonstrate distinct responses of soil microbial communities to different vegetation types in the Songnen Plain. Multiple factors, including rhizosphere exudates, plant litter, and soil physicochemical properties, collectively influence microbial composition (Buyer et al., 2010). Variations in both quality and quantity of litter and root exudates were observed among different vegetation types. Consequently, although the phylum-level composition of soil microbial communities remained generally consistent across vegetation types, significant differences were observed in the relative abundance of constituent taxa.

In this study, bacterial communities were predominantly composed of Actinobacteriota, Acidobacteriota, Proteobacteriota, Chloroflexi, and Gemmatimonadetes, consistent with previous findings (Buyer et al., 2010; Campbell and Kirchman, 2013). Actinobacteriota emerged as the dominant phylum under stress conditions due to their capacity to degrade recalcitrant organic compounds (Yaradoddi and Kontro, 2021). Notably, *Streptomyces* and *Frankia* within Actinobacteriota contributed to soil health through organic matter decomposition, pathogen antagonism, and nitrogen cycling (Dhanasekaran, 2016; Mitra et al., 2022). Our results indicate that vegetation establishment significantly increased the relative abundance of Actinobacteriota, concomitantly enhancing soil nutrient accumulation. *Proteobacteriota*, comprising predominantly facultative or obligate aerobes, exhibited broad environmental adaptability and consequently maintained high abundance across all soil types (Yang et al., 2014). Several taxa within this phylum (e.g., *Rhizobium*, *Bradyrhizobium*, *Azospirillum*) demonstrated nitrogen-fixing capabilities (Kim et al., 2021; Timofeeva et al., 2023). Acidobacteriota played a crucial role in organic matter cycling among plants, fungi, and insects, with their relative abundance showing strong positive correlation with soil organic matter content, aligning with previous reports (Ward Naomi et al., 2009). In our study, pH emerged as a primary determinant of bacterial composition, with Acidobacteriota representing only 3.19% in CK and displaying significant negative correlation with pH values. This observation may reflect the capacity of certain Acidobacteriota members to degrade cellulose with concomitant acetate production (Pankratov et al., 2012). Gemmatimonadetes reached maximal abundance in CK samples with highest salinity, with progressive decline following vegetation establishment, suggesting osmoregulatory adaptation to extreme environments, as reported elsewhere (Gao et al., 2021).

Fungal communities were predominantly composed of Basidiomycota and Ascomycota, which exhibited high relative abundance across all vegetation types. As the dominant functional groups in soil microbial communities, these two phyla play crucial roles in organic matter decomposition and significantly influence global biogeochemical cycles (Zeng et al., 2020). Within Basidiomycota, *Phanerochaete* and *Pleurotus* demonstrated efficient lignin degradation through the secretion of laccase and manganese peroxidase, converting lignin into water and carbon dioxide (Hormiga et al., 2008; Martinez et al., 2001). This enzymatic activity likely contributes to the observed positive correlation between Basidiomycota abundance and cellulase activity (Figure 5). In Ascomycota, *Penicillium* species not only enhanced plant tolerance to abiotic stress (Chaudhary et al., 2018) but also exhibited cellulose-degrading capacity (Rastegari, 2018). Our study revealed significantly higher abundance of *Penicillium* in PC and SL treatments. *Cladosporium*, another prevalent Ascomycete genus, promoted plant growth through indole-3-acetic acid (IAA) production and phosphate solubilization (Rut et al., 2021). Notably, *Mortierella* (representing Mortierellomycota) displayed unique ecological adaptations to saline-alkali stress. Through organic acid secretion and symbiotic associations, *Mortierella* significantly improved host plant phosphorus uptake efficiency (Ozimek and Hanaka, 2021). In contrast, Chytridiomycota, a plant-pathogenic fungal group, showed marked reduction in relative abundance following vegetation establishment (van de Vossenberg et al., 2019).

5 Conclusion

The seven salt-tolerant plants studied all demonstrated varying degrees of improvement in soil physicochemical properties, with *Salix linearistipularis* (SL) showing the most significant reduction in soil salinity and enhancement in soil nutrients compared to other vegetation types. Plant cover altered the α-diversity of soil microorganisms in saline-alkali soils, with SL exhibiting high levels of both the Shannon and S_{obs} indices. EC and TN content were identified as key factors driving differences in bacterial and fungal diversity. The remediation effects of the seven plants led to varying

changes in microbial community structure, with EC being the primary factor influencing bacterial community structure. Under different vegetation restoration models, soil pH also decreased to varying degrees, with pH serving as a driving factor for changes in fungal community structure.

In summary, the findings highlight the significant potential of plants in the remediation of saline-alkali soils. Comparative analysis revealed that SL outperformed the other six tested plants in terms of soil improvement and ecosystem stability, making it particularly suitable for the remediation of soda saline-alkali soils.

Data availability statement

The original contributions presented in the study are publicly available. This data can be found at: https://www.ncbi.nlm.nih.gov/, accession numbers PRJNA1267771 and PRJNA1267766.

Author contributions

JS: Software, Visualization, Formal analysis, Project administration, Data curation, Writing – original draft, Conceptualization, Validation, Writing – review & editing, Methodology. XG: Formal analysis, Visualization, Data curation, Validation, Software, Methodology, Conceptualization, Writing – original draft, Investigation. HC: Investigation, Validation, Resources, Methodology, Writing – original draft, Formal analysis, Data curation. LL: Conceptualization, Methodology, Supervision, Writing – original draft, Data curation, Formal analysis, Validation. YaL: Visualization, Writing – original draft, Formal analysis, Supervision, Validation, Methodology. YuL: Writing – original draft, Resources, Funding acquisition, Project administration, Supervision, Writing – review & editing, Methodology. SM: Project administration, Conceptualization, Supervision, Data curation, Writing – original draft, Writing – review & editing, Funding acquisition, Resources.

Funding

The author(s) declare that financial support was received for the research and/or publication of this article. This work was financially supported by the Special Fund for Basic Scientific Research of the Central Universities (2572023CT08) and the National Natural Science Foundation of China (U23A20151).

Acknowledgments

We thank the financial support of the Fundamental Research Funds for the Central Universities for our study. The sampling work was carried out in Anda Saline-Alkali land test base of Northeast Forestry University. We are especially grateful to Dr. Tan Wenbo and Dr. Pang Qiuying for illuminating discussions on the manuscript.

Conflict of interest

The authors declare that the research was conducted in the absence of any commercial or financial relationships that could be construed as a potential conflict of interest.

Generative AI statement

The author(s) declare that no Gen AI was used in the creation of this manuscript.

Publisher's note

All claims expressed in this article are solely those of the authors and do not necessarily represent those of their affiliated organizations, or those of the publisher, the editors and the reviewers. Any product that may be evaluated in this article, or claim that may be made by its manufacturer, is not guaranteed or endorsed by the publisher.

Supplementary material

The Supplementary Material for this article can be found online at: https://www.frontiersin.org/articles/10.3389/fmicb.2025.1592834/full#supplementary-material

References

Balyan, G., and Pandey, A. K. (2024). Root exudates, the warrior of plant life: revolution below the ground. *South Afr. J. Bot.* 164, 280–287. doi: 10.1016/j.sajb.2023.11.049

Buyer, J. S., Teasdale, J. R., Roberts, D. P., Zasada, I. A., and Maul, J. E. (2010). Factors affecting soil microbial community structure in tomato cropping systems. *Soil Biol. Biochem.* 42, 831–841. doi: 10.1016/j.soilbio.2010.01.020

Campbell, B. J., and Kirchman, D. L. (2013). Bacterial diversity, community structure and potential growth rates along an estuarine salinity gradient. *ISME J.* 7, 210–220. doi: 10.1038/ismej.2012.93

Caporaso, J. G., Lauber, C. L., Walters, W. A., Berg-Lyons, D., Lozupone, C. A., Turnbaugh, P. J., et al. (2011). Global patterns of 16S rRNA diversity at a depth of millions of sequences per sample. *Proc. Natl. Acad. Sci. USA* 108 Suppl 1, 4516–4522. doi: 10.1073/pnas.1000080107

Chaudhary, S., Shankar, A., Singh, A., and Prasad, V. (2018). "Usefulness of penicillium in enhancing plants resistance to abiotic stresses: an overview," in *New and Future Developments in Microbial Biotechnology and Bioengineering*, 277–284. doi: 10.1016/B978-0-444-63501-3.00017-X

Chen, J., Huang, X., Tong, B., Wang, D., Liu, J., Liao, X., et al. (2021a). Effects of rhizosphere fungi on the chemical composition of fruits of the medicinal plant Cinnamomum migao endemic to southwestern China. *BMC Microbiol.* 21:206. doi: 10.1186/s12866-021-02216-z

Chen, L., Zhou, G., Feng, B., Wang, C., Luo, Y., Li, F., et al. (2024). Saline-alkali land reclamation boosts topsoil carbon storage by preferentially accumulating plant-derived carbon. *Sci. Bull.* 69, 2948–2958. doi: 10.1016/j.scib.2024.03.063

Chen, Y., Liu, D., Ma, J., Jin, B., Peng, J., He, X., et al. (2021b). Assessing the influence of immobilization remediation of heavy metal contaminated farmland on the physical properties of soil. *Sci. Total Environ.* 781:146773. doi: 10.1016/j.scitotenv.2021.146773

Cheng, W., Parton, W. J., Gonzalez-Meler, M. A., Phillips, R., Asao, S., McNickle, G. G., et al. (2014). Synthesis and modeling perspectives of rhizosphere priming. *New Phytol.* 201, 31–44. doi: 10.1111/nph.12440

Chi, C-. M., Zhao, C-. W., Sun, X-. J., and Wang, Z-. C. (2011). Estimating exchangeable sodium percentage from sodium adsorption ratio of salt-affected soil in the songnen plain of Northeast China. *Pedosphere* 21, 271–276. doi: 10.1016/S1002-0160(11)60127-6

Cuevas, J., and Daliakopoulos, I. N. del Moral, F., Hueso, J. J., Tsanis, I. K. (2019). A review of soil-improving cropping systems for soil salinization. *Agronomy* 9:295. doi: 10.3390/agronomy9060295

Dhanasekaran, D. (2016). "An introduction to Actinobacteria," in *Actinobacteria-Basics and Biotechnological Applications*. doi: 10.5772/60457

Djukic, I., Zehetner, F., Mentler, A., and Gerzabek, M. H. (2010). Microbial community composition and activity in different Alpine vegetation zones. *Soil Biol. Biochem.* 42, 155–161. doi: 10.1016/j.soilbio.2009.10.006

Elmeknassi, M., Elghali, A., Carvalho, d. e., Laamrani, H. W. P., and Benzaazoua, A. M. (2024). A review of organic and inorganic amendments to treat saline-sodic soils: emphasis on waste valorization for a circular economy approach. *Sci. Total Environ.* 921:171087. doi: 10.1016/j.scitotenv.2024.171087

Fierer, N., Wood, S. A., and Bueno de Mesquita, C. P. (2021). How microbes can, and cannot, be used to assess soil health. *Soil Biol. Biochem.* 153:108111. doi: 10.1016/j.soilbio.2020.108111

Flowers, T. J., and Colmer, T. D. (2008). Salinity tolerance in halophytes. *New Phytol.* 179, 945–963. doi: 10.1111/j.1469-8137.2008.02531.x

Gao, Y., Liu, L., Zhu, P., Yang, S., Guo, W., Yu, X., et al. (2021). Patterns and dynamics of the soil microbial community with gradual vegetation succession in the yellow river delta, China. *Wetlands* 41:9. doi: 10.1007/s13157-021-01414-9

Gessner, M. O., Swan, C. M., Dang, C. K., McKie, B. G., Bardgett, R. D., Wall, D. H., et al. (2010). Diversity meets decomposition. *Trends Ecol. Evol.* 25, 372–380. doi: 10.1016/j.tree.2010.01.010

Gong-Neng, F., Bin, P., Rong, S., Wen-Yan, S., and Wei, X. (2016). Growth of *Suaeda salsa* tin response to salt stress in different habitats. *Acta Prataculturae Sinica*, 25, 81–90. doi: 10.11686/cyxb2015312

Guan, Y., Jiang, N., Wu, Y., Yang, Z., Bello, A., Yang, W., et al. (2021). Disentangling the role of salinity-sodicity in shaping soil microbiome along a natural saline-sodic gradient. *Sci. Total Environ.* 765:142738. doi: 10.1016/j.scitotenv.2020.142738

Guo, L., Tóth, T., Yang, F., and Wang, Z. (2023). Effects of different types of vegetation cover on soil microorganisms and humus characteristics of soda-saline land in the Songnen plain. *Front. Microbiol.* 14:1163444. doi: 10.3389/fmicb.2023.1163444

Gupta, S., Schillaci, M., Walker, R., Smith, P. M. C., Watt, M., Roessner, U., et al. (2021). Alleviation of salinity stress in plants by endophytic plant-fungal symbiosis: current knowledge, perspectives and future directions. *Plant Soil* 461, 219–244. doi: 10.1007/s11104-020-04618-w

Hassani, A., Azapagic, A., and Shokri, N. (2021). Global predictions of primary soil salinization under changing climate in the 21st century. *Nat. Commun.* 12:6663. doi: 10.1038/s41467-021-26907-3

Heng, T., He, X-. L., Yang, L-. L., Xu, X., and Feng, Y. (2022). Mechanism of Saline-Alkali land improvement using subsurface pipe and vertical well drainage measures and its response to agricultural soil ecosystem. *Environm. Pollut.* 293:118583. doi: 10.1016/j.envpol.2021.118583

Hormiga, J. A., Vera, J., Frías, I., and Torres Darias, N. V. (2008). Growth and ligninolytic system production dynamics of the *Phanerochaete chrysosporium* fungus: a modelling and optimization approach. *J. Biotechnol.* 137, 50–58. doi: 10.1016/j.jbiotec.2008.07.1814

Hu, J-. P., He, Y-. Y., Li, J-. H., Lü, Z-. L., Zhang, Y-. W., Li, Y-. H., et al. (2024). Planting halophytes increases the rhizosphere ecosystem multifunctionality via reducing soil salinity. *Environ. Res.* 261:119707. doi: 10.1016/j.envres.2024.119707

Jesus, J. M., Danko, A. S., Fiúza, A., and Borges, M-. T. (2015). Phytoremediation of salt-affected soils: a review of processes, applicability, and the impact of climate change. *Environ. Sci. Pollut. Res.* 22, 6511–6525. doi: 10.1007/s11356-015-4205-4

Jiang, N., Cai, D., He, L., Zhong, N., Wen, H., Zhang, X., et al. (2015). A facile approach to remediate the microenvironment of saline-alkali soil. *ACS Sustain. Chem. Eng.* 3, 374–380. doi: 10.1021/sc500785e

Kang, S., Zhang, L., Liang, Y., Hu, X., Cai, H., Gu, B., et al. (2002). Effects of limited irrigation on yield and water use efficiency of winter wheat in the Loess Plateau of China. *Agric. Water Manage.* 55, 203–216. doi: 10.1016/S0378-3774(01)00180-9

Kim, H-. S., Lee, S-. H., Jo, H. Y., Finneran, K. T., and Kwon, M. J. (2021). Diversity and composition of soil *Acidobacteria* and *Proteobacteria* communities as a bacterial indicator of past land-use change from forest to farmland. *Sci. Total Environ.* 797:148944. doi: 10.1016/j.scitotenv.2021.148944

Kumar, N., Haldar, S., and Saikia, R. (2023). Root exudation as a strategy for plants to deal with salt stress: an updated review. *Environ. Exp. Bot.* 216:105518. doi: 10.1016/j.envexpbot.2023.105518

Lei, J., Gu, H., Liu, Z., Hu, X., Yu, Z., Guan, Q., et al. (2025). Recruitment of specific rhizosphere microorganisms in saline-alkali tolerant rice improves adaptation to saline-alkali stress. *Sci. Total Environ.* 963:178413. doi: 10.1016/j.scitotenv.2025.178413

Li, Y., Li, Q., Guo, D., Liang, S., and Wang, Y. (2016). Ecological stoichiometry homeostasis of *Leymus chinensis* in degraded grassland in western Jilin Province, NE China. *Ecol. Eng.* 90, 387–391. doi: 10.1016/j.ecoleng.2016.01.079

Liang, C., Schimel, J. P., and Jastrow, J. D. (2017). The importance of anabolism in microbial control over soil carbon storage. *Nat. Microbiol.* 2:17105. doi: 10.1038/nmicrobiol.2017.105

Liang, J., and Shi, W. (2021). Cotton/halophytes intercropping decreases salt accumulation and improves soil physicochemical properties and crop productivity in saline-alkali soils under mulched drip irrigation: a three-year field experiment. *Field Crops Res.* 262:108027. doi: 10.1016/j.fcr.2020.108027

Liu, F., Mo, X., Kong, W., and Song, Y. (2020). Soil bacterial diversity, structure, and function of Suaeda salsa in rhizosphere and non-rhizosphere soils in various habitats in the yellow river Delta, China. *Sci. Total Environ.* 740:140144. doi: 10.1016/j.scitotenv.2020.140144

Liu, X., Tou, C., Zhou, J., Chen, J., Wanek, W., Chadwick, D. R., et al. (2025). Plant litter decomposition is regulated by its phosphorus content in the short term and soil enzymes in the long term. *Geoderma* 457:117283. doi: 10.1016/j.geoderma.2025.117283

Luo, Y., Durenkamp, M., de Nobili, M., Lin, M., and Brookes, P. C. (2011). Short term soil priming effects and the mineralisation of biochar following its incorporation to soils of different pH. *Soil Biol. Biochem.* 43, 2304–2314. doi: 10.1016/j.soilbio.2011.07.020

Ma, J., Ibekwe, A. M., Yang, C-. H., and Crowley, D. E. (2016). Bacterial diversity and composition in major fresh produce growing soils affected by physiochemical properties and geographic locations. *Sci. Total Environ.* 563–564, 199–209. doi: 10.1016/j.scitotenv.2016.04.122

Martinez, A. T., Camarero, S., Gutiérrez, A., Bocchini, P., Galletti, G. C. (2001). Studies on wheat lignin degradation by Pleurotus species using analytical pyrolysis. *J. Anal. Appl. Pyrol.* 58–59, 401–411. doi: 10.1016/S0165-2370(00)00116-9

Meng, X., Zhou, J., and Sui, N. (2018). Mechanisms of salt tolerance in halophytes: current understanding and recent advances. *Open Life Sci.* 13, 149–154. doi: 10.1515/biol-2018-0020

Mitra, D., Mondal, R., Khoshru, B., Senapati, A., Radha, T. K., Mahakur, B., et al. (2022). Actinobacteria-enhanced plant growth, nutrient acquisition, and crop protection: advances in soil, plant, and microbial multifactorial interactions. *Pedosphere* 32, 149–170. doi: 10.1016/S1002-0160(21)60042-5

Munns, R., and Tester, M. (2008). Mechanisms of salinity tolerance. *Annu. Rev. Plant. Biol.* 59, 651–681. doi: 10.1146/annurev.arplant.59.032607.092911

Ozimek, E., and Hanaka, A. (2021). Mortierella species as the plant growth-promoting fungi present in the agricultural soils. *Agriculture* 11:7. doi: 10.3390/agriculture11010007

Pankratov, T. A., Kirsanova, L. A., Kaparullina, E. N., Kevbrin, V. V., and Dedysh, S. N. (2012). Telmatobacter bradus gen. nov., sp. nov., a cellulolytic facultative anaerobe from subdivision 1 of the Acidobacteria, and emended description of *Acidobacterium capsulatum*. *Int. J. Syst. Evol. Microbiol.* 62, 430–437. doi: 10.1099/ijs.0.029629-0

Peng, M., Jiang, Z., Zhou, F., and Wang, Z. (2023). From salty to thriving: plant growth promoting bacteria as nature's allies in overcoming salinity stress in plants [review]. *Front. Microbiol.* 14:1169809. doi: 10.3389/fmicb.2023.1169809

Peng, Y., Zhang, H., Li, G., and Zhang, J. (2025). Microbial inoculum improved soil aggregate formation and increased cucumber yield in a greenhouse under secondary salinization conditions. *J. Environ. Manage.* 376:124576. doi: 10.1016/j.jenvman.2025.124576

Qadir, M., Oster, J. D., Schubert, S., Noble, A. D., and Sahrawat, K. L. (2007). "Phytoremediation of sodic and saline-sodic soils," in *Advances in Agronomy* (Vol. 96, Academic Press), 197–247. doi: 10.1016/S0065-2113(07)96006-X

Qin, Y., Druzhinina, I. S., Pan, X., and Yuan, Z. (2016). Microbially mediated plant salt tolerance and microbiome-based solutions for saline agriculture. *Biotechnol. Adv.* 34, 1245–1259. doi: 10.1016/j.biotechadv.2016.08.005

Qiu, L., Kong, W., Zhu, H., Zhang, Q., Banerjee, S., Ishii, S., et al. (2022). Halophytes increase rhizosphere microbial diversity, network complexity and function in inland saline ecosystem. *Sci. Total Environ.* 831:154944. doi: 10.1016/j.scitotenv.2022.154944

Răut, I., Călin, M., Capră, L., Gurban, A-. M., Doni, M., Radu, N., et al. (2021). *Cladosporium* sp. isolate as fungal plant growth promoting agent. *Agronomy* 11:392. doi: 10.3390/agronomy11020392

Rabot, E., Wiesmeier, M., Schlüter, S., and Vogel, H. J. (2018). Soil structure as an indicator of soil functions: a review. *Geoderma* 314, 122–137. doi: 10.1016/j.geoderma.2017.11.009

Rastegari, A. A. (2018). "Molecular mechanism of cellulase production systems in penicillium," in *New and Future Developments in Microbial Biotechnology and Bioengineering*, 153–166. doi: 10.1016/B978-0-444-63501-3.00008-9

Ström, L., Owen, A. G., Godbold, D. L., and Jones, D. L. (2002). Organic acid mediated P mobilization in the rhizosphere and uptake by maize roots. *Soil Biol. Biochem.* 34, 703–710. doi: 10.1016/S0038-0717(01)00235-8

Tarolli, P., Luo, J., Park, E., Barcaccia, G., and Masin, R. (2024). Soil salinization in agriculture: mitigation and adaptation strategies combining nature-based solutions and bioengineering. *iScience* 27:108830. doi: 10.1016/j.isci.2024.108830

Timofeeva, A. M., Galyamova, M. R., and Sedykh, S. E. (2023). Plant growth-promoting soil bacteria: nitrogen fixation, phosphate solubilization, siderophore production, and other biological activities. *Plants* 12:4074. doi: 10.3390/plants12244074

van de Vossenberg, B. T. L. H., Warris, S., Nguyen, H. D. T., van Gent-Pelzer, M. P. E., Joly, D. L., van de Geest, H. C., et al. (2019). Comparative genomics of chytrid fungi reveal insights into the obligate biotrophic and pathogenic lifestyle of Synchytrium endobioticum. *Sci. Rep.* 9:8672. doi: 10.1038/s41598-019-45128-9

Vives-Peris, V., de Ollas, C., Gómez-Cadenas, A., and Pérez-Clemente, R. M. (2020). Root exudates: from plant to rhizosphere and beyond. *Plant Cell Rep.* 39, 3–17. doi: 10.1007/s00299-019-02447-5

Wagg, C., Schlaeppi, K., Banerjee, S., Kuramae, E. E., and van der Heijden, M. G. A. (2019). Fungal-bacterial diversity and microbiome complexity predict ecosystem functioning. *Nat. Commun.* 10:4841. doi: 10.1038/s41467-019-12798-y

Wang, F., Peng, W., Zhang, B., Cao, Y., Zhao, J., Cao, H., et al. (2021). Succession of bacterial community composition in coastal agricultural soils along a 1000-year reclamation chronosequence in Hangzhou Bay, China. *Ecol. Indic.* 121:106972. doi: 10.1016/j.ecolind.2020.106972

Wang, X., Ding, J., Wang, J., Han, L., Tan, J., Ge, X., et al. (2024a). Ameliorating saline-sodic soils: a global meta-analysis of field studies on the influence of exogenous amendments on crop yield. *Land Degrad. Dev.* 35, 3330–3343. doi: 10.1002/ldr.5133

Wang, X., Sun, R., Tian, Y., Guo, K., Sun, H., Liu, X., et al. (2020). Long-Term Phytoremediation of coastal saline soil reveals plant species-specific patterns of microbial community recruitment. *mSystems* 5, e00741–19. doi: 10.1128/mSystems.00741-19

Wang, Y., Gong, H., Zhang, Z., Sun, Z., Liu, S., Ma, C., et al. (2024b). Effects of microbial communities during the cultivation of three salt-tolerant plants in saline-alkali land improvement [Original Research]. *Front. Microbiol.* 15:1470081. doi: 10.3389/fmicb.2024.1470081

Wang, Z-. Y., Xin, Y-. Z., Gao, D-. M., Li, F-. M., Morgan, J., Xing, B-. S., et al. (2010). Microbial community characteristics in a degraded wetland of the yellow river delta. *Pedosphere* 20, 466–478. doi: 10.1016/S1002-0160(10)60036-7

Ward Naomi, L., Challacombe Jean, F., Janssen Peter, H., Henrissat, B., Coutinho Pedro, M., Wu, M., et al. (2009). Three genomes from the phylum acidobacteria provide insight into the lifestyles of these microorganisms in soils. *Appl. Environ. Microbiol.* 75, 2046–2056. doi: 10.1128/AEM.02294-08

Xing, J., Li, X., Li, Z., Wang, X., Hou, N., Li, D., et al. (2024). Remediation of soda-saline-alkali soil through soil amendments: microbially mediated carbon and nitrogen cycles and remediation mechanisms. *Sci. Total Environ.* 924:171641. doi: 10.1016/j.scitotenv.2024.171641

Xu, X., Guo, L., Wang, S., Wang, X., Ren, M., Zhao, P., et al. (2023). Effective strategies for reclamation of saline-alkali soil and response mechanisms of the soil-plant system. *Sci. Total Environ.* 905:167179. doi: 10.1016/j.scitotenv.2023.167179

Yang, F., An, F., Ma, H., Wang, Z., Zhou, X., Liu, Z., et al. (2016). Variations on soil salinity and sodicity and its driving factors analysis under microtopography in different hydrological conditions. *Water* 8:227. doi: 10.3390/w8060227

Yang, J-. K., Zhang, J-. J., Yu, H-. Y., Cheng, J-. W., and Miao, L-. H. (2014). Community composition and cellulase activity of cellulolytic bacteria from forest soils planted with broad-leaved deciduous and evergreen trees. *Appl. Microbiol. Biotechnol.* 98, 1449–1458. doi: 10.1007/s00253-013-5130-4

Yang, Y., Li, Y., Hao, K., Zhao, Y., Li, M., Fan, Y., et al. (2024). Microbial community composition and co-occurrence network analysis of the rhizosphere soil of the main constructive tree species in Helan Mountain of Northwest China. *Sci. Rep.* 14:24557. doi: 10.1038/s41598-024-76195-2

Yaradoddi, J. S., and Kontro, M. H. (2021). "Actinobacteria: basic adaptation to harsh environments," in *Actinobacteria: Ecology, Diversity, Classification and Extensive Applications*, eds. J. S. Yaradoddi, M. H. Kontro, and S. V. Ganachari (Singapore: Springer Nature), 69–88. doi: 10.1007/978-981-16-3353-9

Yue, H., Yue, W., Jiao, S., Kim, H., Lee, Y-. H., Wei, G., et al. (2023). Plant domestication shapes rhizosphere microbiome assembly and metabolic functions. *Microbiome* 11:70. doi: 10.1186/s40168-023-01513-1

Zeng, Q., Liu, Y., Xiao, L., and An, S. (2020). Climate and soil properties regulate soil fungal communities on the Loess Plateau. *Pedobiologia* 81–82, 150668. doi: 10.1016/j.pedobi.2020.150668

Zhang, G., Bai, J., Zhai, Y., Jia, J., Zhao, Q., Wang, W., et al. (2024a). Microbial diversity and functions in saline soils: a review from a biogeochemical perspective. *J. Adv. Res.* 59, 129–140. doi: 10.1016/j.jare.2023.06.015

Zhang, X., Xin, X., Zhu, A., Yang, W., Zhang, J., Ding, S., et al. (2018). Linking macroaggregation to soil microbial community and organic carbon accumulation under different tillage and residue managements. *Soil Tillage Res.* 178, 99–107. doi: 10.1016/j.still.2017.12.020

Zhang, Y., Cai, L., Chen, L., Zhang, H., Li, G., Wang, G., et al. (2024b). Effect of micro-nano bubbles on the remediation of saline-alkali soil with microbial agent. *Sci. Total Environ.* 912:168940. doi: 10.1016/j.scitotenv.2023.168940

Zhang, Z., Feng, S., Luo, J., Hao, B., Diao, F., Li, X., et al. (2021). Evaluation of microbial assemblages in various saline-alkaline soils driven by soluble salt ion components. *J. Agric. Food Chem.* 69, 3390–3400. doi: 10.1021/acs.jafc.1c00210

Zhao, C., Zhang, H., Song, C., Zhu, J-. K., and Shabala, S. (2020). Mechanisms of plant responses and adaptation to soil salinity. *Innovation* 1:100017. doi: 10.1016/j.xinn.2020.100017

Zheng, Y., Cao, X., Zhou, Y., Li, Z., Yang, Y., Zhao, D., et al. (2023). Effect of planting salt-tolerant legumes on coastal saline soil nutrient availability and microbial communities. *J. Environ. Manage.* 345:118574. doi: 10.1016/j.jenvman.2023.118574

Zuccarini, P., Sardans, J., Asensio, L., and Peñuelas, J. (2023). Altered activities of extracellular soil enzymes by the interacting global environmental changes. *Glob. Change Biol.* 29, 2067–2091. doi: 10.1111/gcb.16604

frontiers | Frontiers in Microbiology

TYPE Review
PUBLISHED 31 July 2025
DOI 10.3389/fmicb.2025.1549022

Check for updates

OPEN ACCESS

EDITED BY
Ayansina Segun Ayangbenro,
North-West University, South Africa

REVIEWED BY
Marika Pellegrini,
University of L'Aquila, Italy
Ahmed M. El-Sawah,
Mansoura University, Egypt

*CORRESPONDENCE
Amit C. Kharkwal
✉ ackharkwal@amity.edu

RECEIVED 20 December 2024
ACCEPTED 16 June 2025
PUBLISHED 31 July 2025

CITATION
Pradhan N, Singh S, Saxena G, Pradhan N, Koul M, Kharkwal AC and Sayyed R (2025) A review on microbe–mineral transformations and their impact on plant growth. *Front. Microbiol.* 16:1549022. doi: 10.3389/fmicb.2025.1549022

COPYRIGHT
© 2025 Pradhan, Singh, Saxena, Pradhan, Koul, Kharkwal and Sayyed. This is an open-access article distributed under the terms of the Creative Commons Attribution License (CC BY). The use, distribution or reproduction in other forums is permitted, provided the original author(s) and the copyright owner(s) are credited and that the original publication in this journal is cited, in accordance with accepted academic practice. No use, distribution or reproduction is permitted which does not comply with these terms.

A review on microbe–mineral transformations and their impact on plant growth

Nikita Pradhan[1], Shikha Singh[1], Garima Saxena[1,2], Nischal Pradhan[3], Monika Koul[4], Amit C. Kharkwal[1]* and Riyaz Sayyed[5]

[1]Amity Institute of Microbial Technology, Amity University, Noida, India, [2]Division of Microbiology, Indian Council of Agricultural Research (ICAR)-Indian Agricultural Research Institute (PUSA), New Delhi, India, [3]Amity Institute of Biotechnology, Amity University, Noida, India, [4]Department of Botany, Hansraj College, University of Delhi, New Delhi, India, [5]Department of Biological Sciences and Chemistry, College of Arts and Sciences, University of Nizwa, Nizwa, Oman

Mineral–microbe interaction is a driving environmental changes, regulating the biogeochemical cycling of elements, and contributing to the formation of ore deposits. Microorganisms are fundamental to mineral transformation processes, exerting a profound influence on biogeochemical cycles and the bioavailability of critical nutrients required for plant growth. In this review, we delve into the various mechanisms by which microbes facilitate mineral dissolution, precipitation, and transformation, with a particular focus on how these processes regulate the availability of both macronutrients and micronutrients in soils. Essential microbial activities such as phosphate solubilization, iron chelation, and sulfur oxidation play a pivotal role in enhancing nutrient uptake in plants, thereby supporting sustainable agricultural practices and reducing dependence on chemical fertilizers. Furthermore, microbial-driven mineral transformations are vital for environmental remediation efforts, as they contribute to the immobilization of toxic metals and the detoxification of contaminated soils. By examining key microbial–mineral interactions—including nitrogen fixation, siderophore production, and metal precipitation—this review underscores the indispensable role of microorganisms in improving soil fertility, fostering plant growth, and bolstering ecosystem resilience. The exploration of these microbial processes reveals significant potential for advancing bioremediation strategies and the development of biofertilizers, offering promising solutions to enhance agricultural productivity and address environmental challenges.

KEYWORDS

arbuscular mycorrhizal fungi (AMF), biofertilizers, biogeochemical, bioremediation, heavy metal detoxification, microbial nutrient mobilization, microbial–mineral interactions, mineral transformation

1 Introduction

Minerals serve as the fundamental constituents of Earth's materials, with their physical and chemical properties preserving critical information about the environmental conditions prevailing at the time of their formation. Microorganisms, representing the majority of phylogenetic diversity, have been integral agents in shaping Earth's

biogeochemical processes throughout its geological history. Minerals are important for the plant growth and productivity where microbes act as providers for the various minerals that are essential for plant growth (Vessey, 2003; Dong et al., 2022). Plants rely on a diverse array of nutrients, predominantly taken up as mineral ions from the soil, to support critical physiological functions, including photosynthesis, cellular respiration, and enzymatic activity. In addition to the well-recognized roles of macronutrients such as nitrogen (N), phosphorus (P), and potassium (K) in plant nutrition, a suite of micronutrients—such as zinc (Zn), copper (Cu), iron (Fe), and manganese (Mn)—is essential in trace amounts for various enzymatic and metabolic processes (Jabborova et al., 2021a). However, in most soils, these nutrients are often sequestered within insoluble mineral complexes, rendering them largely unavailable for direct plant uptake (Bhat et al., 2024). Therefore, microbes play an important role in the Earth's Critical Zone (CZ), as they possess a variety of properties that affects dissolution, transformation and formation of minerals through metabolic activities (Lepot, 2020). The process of mineral solubilization in soils is primarily mediated by microorganisms, which are essential in converting insoluble mineral forms into bioavailable nutrients for plant uptake (Kapadia et al., 2022). This microbially driven mineral transformation occurs through diverse biochemical mechanisms, including the secretion of organic acids, enzymes, and siderophores that chelate or solubilize mineral compounds, facilitating their assimilation by plants (Jabborova et al., 2021b; Kusale et al., 2021; Ribeiro et al., 2020). For example, phosphates are an important macronutrient for energy metabolism, root growth and DNA synthesis, but majorly it is present in insoluble forms bound in soil particles like in alkaline and calcareous soil (hydroxyapatite [$Ca_{10}(PO_4)_6(OH)_2$ and tricalcium phosphate [$Ca_3(PO_4)_2$]) (Elhaissoufi et al., 2021). Phosphate solubilizing bacteria including species of *Pseudomonas, Bacillus,* and *Aspergillus*, secrete organic acids like gluconic, citric, and oxalic acids. Microorganisms, particularly those that produce siderophores—small, high-affinity iron-chelating molecules—play a pivotal role in the mobilization of these essential micronutrients (Nithyapriya et al., 2024). *Pseudomonas, Burkholderia*, and *Streptomyces*, along with the fungi *Trichoderma pseudokoningii* and *Trichoderma longibrachiatum*, produce siderophores that bind to iron ions, sequestering them from insoluble oxide forms. This process increases the solubility of iron, thereby enhancing its availability for plant uptake (Pecoraro et al., 2021). This microbial capability to transform not only macronutrients but also trace elements is fundamental to their role in improving soil fertility and promoting plant growth (Pecoraro et al., 2021).

The widespread use of fertilizers and pesticides has been shown to adversely affect global food production by disrupting the natural composition, structure, and diversity of soil microflora, ultimately compromising soil quality and nutrient availability (Prashar and Shah, 2016; Mandal et al., 2020). For instance, excessive application of nitrogen-based fertilizers leads to soil acidification, while chemical fungicides and insecticides have detrimental effects on soil health (Bitew and Alemayehu, 2017). Enhancing the population of microorganisms that facilitate nutrient transformation in soils can help preserve soil (Wei et al., 2024; Basu et al., 2021). Agricultural practices that promote the proliferation of beneficial microorganisms offer a sustainable, environmentally friendly, and cost-effective alternative to the reliance on agrochemicals and fertilizers, thereby improving soil quality (Eswaran et al., 2024; Wei et al., 2024).

The importance of microbe–mineral interactions in enhancing soil fertility, nutrient availability, and sustainable agriculture has been highlighted in recent research. However, most current literature concentrates broadly on the general contribution microbes play in plant growth, with limited research review to the specific biochemical strategies employed to mobilize or transform mineral-bound nutrients (Alzate Zuluaga et al., 2024). Additionally, little is studied about how these mechanisms function in various soil types and environmental conditions, making a huge research area to be studied and investigated.

In this review, we aim to understand how microbe–mineral interaction plays a pivotal role in environment and agricultural area. The review emphasis on different mechanisms involved in microbe mediated mineral transformation and impact on plant growth and development, underlying the different environmental changes and the soil type. We also have highlighted and summarized the applications and challenges for microbe–mineral interactions in sustainable agriculture and environmental remediation.

2 Microbial-mediated mineral transformation processes

Microbial-mediated mineral transformation involves the dynamic interaction between microorganisms and minerals, playing a crucial role in element cycling and driving biogeochemical processes (Ortiz-Castillo et al., 2021). This interaction allows for various applications in geological, environmental, and biotechnological domains. Through various mechanisms such as dissolution, precipitation, and transformation, which in turn impact metal mobility and alter oxidation states (Dong and Lu, 2012). It involves diverse microorganisms which includes prokaryotes and eukaryotes, and their symbiotic associations with each other and higher organisms (Ortiz-Castillo et al., 2021), playing a key role in various applications such as in mine waste management, where microbial communities affect both the formation of secondary minerals and the release of contaminants (Ortiz-Castillo et al., 2021). For example, remediation of chromium and uranium contamination, with microbes transforming aqueous metal ions into amorphous or crystalline precipitates (Cheng et al., 2012). Herein, we elucidate the various types of microbe-mediated processes that occur in nature, along with their underlying mechanisms. These processes include key phenomena such as calcification, silicification, and iron mineralization, which are carried out by a wide array of microorganisms like bacteria, fungi, algae, and viruses.

2.1 Mineral dissolution

Mineral dissolution is a key process in which minerals undergo chemical breakdown, typically involving the interaction between a mineral's solid phase and an aqueous solution. This process plays a significant role in geochemical cycles, environmental remediation, and the availability of essential nutrients (Dong and Lu, 2012). This

process can be significantly influenced through the use of microbes that utilize minerals for nutrients or energy, often accelerating the breakdown through biochemical reactions.

In microbial-mediated dissolution, microbes release organic acids or chelating compounds that facilitate the dissolution of minerals by weakening their chemical bonds. For example, *Pseudomonas* strains are capable of extracting zinc, manganese, and aluminum from low-grade ores and secondary minerals through bioleaching processes. Likewise, *Burkholderia* sp. SX9 can mobilize copper, zinc, and cadmium from insoluble oxides or carbonate forms. Siderophores are low-molecular-weight organic compounds produced by microorganisms and plants under iron-limited conditions (Ahmed and Holmström, 2014). These chelators have high affinity for iron and can enhance its solubility from minerals, making it bioavailable (Williamson et al., 2021). Furthermore, it can promote the biodegradation of organic contaminants through reactive oxygen species (ROS) production (Roskova et al., 2022), which is further supported with a study on chrysotile asbestos, where both fungal and bacterial siderophores were shown to remove structural iron from fibers, potentially reducing their toxicity and health risks (Mohanty et al., 2018). Additionally, redox reactions driven by microbial respiration can alter the oxidation states of metals, influencing the solubility of minerals containing those metals. For instance, iron-reducing bacteria can reduce ferric iron (Fe^{3+}) to its more soluble ferrous form (Fe^{2+}) thus promoting the dissolution of iron-containing minerals. The transformation of elements between different valence states provides a critical energy source for the metabolic systems of many microorganisms. These redox reactions involve the transfer of electrons, releasing varying amounts of energy based on the specific reactants, products, and the metabolic pathways utilized by the microorganisms (Dong and Lu, 2012).

These processes are essential in natural biogeochemical cycles and have both beneficial and detrimental consequences in human contexts, such as bioremediation of metallic and radionuclide pollutants and the development of novel biomaterials.

2.2 Mineral precipitation

Mineral precipitation is a critical process in the transformation and formation of minerals, which plays a vital role in bioremediation. This process is driven by the activities of microbes that create local chemical conditions conducive to mineral precipitation. Specifically, microbes can influence the precipitation of metal-bearing minerals by altering redox states, producing reactive metabolites, or creating local environments that favor nucleation and precipitation of minerals (Dong et al., 2022). Mineral precipitation by microorganisms can occur through biologically induced mineralization (BIM), where microbes indirectly modify their local microenvironment leading to extracellular mineral deposition. This happens without direct control over the crystallization process by the microorganisms. BIM typically results from microbial metabolic activities such as metal reduction, oxidation, or the production of metabolic byproducts such as sulfides, oxalates, and carbonates (Han et al., 2020). Biologically Controlled Mineralization (BCM) refers to the process where organisms regulate and direct the formation of minerals. This differs from BIM where external environmental factors trigger mineral precipitation. In BCM, organisms exert precise control over mineral formation, both in terms of location and composition. This process is crucial for the development of specific structures in certain microorganisms, such as the formation of magnetosomes in magnetotactic bacteria, which produce magnetic minerals like magnetite (Fe_3O_4) (Hoffmann et al., 2021).

One prominent example is sulfate-reducing bacteria (SRB) that generate sulfide ions as a metabolic byproduct. These ions can react with metal ions such as iron or cadmium, leading to the formation of metal sulfide minerals, which are typically insoluble. This process is essential in environments like contaminated sediments, where SRB can immobilize toxic metals, reducing their bioavailability and mobility, with studies having shown that SRB can remove over 98% of various metal ions from solution, primarily through precipitation and biosorption mechanisms (Neria-González and Aguilar-López, 2021).

Microbial-mediated mineral precipitation is especially relevant in the context of bioremediation. In polluted environments, microbes can transform soluble toxic metals into insoluble mineral forms, effectively removing them from water and soil. For instance, the microbial reduction of soluble uranium U^{6+} to insoluble U^{4+} results in the precipitation of uraninite, a process utilized in the bioremediation of uranium-contaminated groundwater (You et al., 2021). Additionally, microorganisms can promote the precipitation of other environmentally relevant metals like chromium, selenium, and iron, further contributing to bioremediation efforts by immobilizing these elements (Ojuederie et al., 2017).

2.3 Microbial transformations

2.3.1 Nitrogen fixation

Nitrogen a crucial nutrient for ecosystems, exists in various forms such as ammonium (NH_4^+), nitrate (NO_3^-), and nitrogen gas (N_2). The availability of nitrogen in soils is largely controlled by microbial activity, with bacteria and fungi playing central roles in its transformation, immobilization, and release (Grzyb et al., 2021). These microbial processes are vital for maintaining soil fertility and ensuring that plants receive the mineral nitrogen they need for growth. One of the most important microbial processes affecting nitrogen is nitrogen fixation. Certain bacteria, such as Rhizobium, form symbiotic relationships with legume plants, converting atmospheric nitrogen (N_2) into ammonia (NH_3), which plants can readily use (Abd-Alla et al., 2023). This process supplies a significant portion of the nitrogen in many ecosystems. Additionally, free-living nitrogen fixers, such as *Azotobacter* and *cyanobacteria*, contribute to nitrogen fixation in environments without legumes, including in aquatic systems (Lawal, 2021; Rana et al., 2023; Khumairah et al., 2022).

Nitrification is another key microbial process in which bacteria like *Nitrosomonas* and *Nitrobacter* oxidize ammonia into nitrite (NO_2^-), and subsequently into nitrate (NO_3^-), a form of nitrogen that plants can easily absorb. This process occurs in aerobic soil conditions and is critical for converting ammonia, derived from organic matter or fertilizers, into plant-available nitrates (Lu et al., 2021). However, in anaerobic conditions, a different set of microbes performs denitrification. Bacteria such as *Pseudomonas*

and *Clostridium* reduce nitrate back into nitrogen gas (N_2) or nitrous oxide (N_2O), thereby removing nitrogen from the soil and releasing it into the atmosphere (Torres et al., 2016). While this process prevents the buildup of nitrates in the environment, it also results in nitrogen loss, impacting soil fertility.

Microbial activity also drives ammonification, the process by which organic nitrogen compounds, like proteins and nucleic acids, are broken down into ammonium (NH_4^+) (Lu et al., 2021). Fungi and bacteria decompose complex organic matter, releasing ammonium that can either be taken up directly by plants or further transformed by nitrifying bacteria. Through these interconnected processes—nitrogen fixation, nitrification, denitrification, and ammonification—microbial activity plays a fundamental role in regulating the availability of nitrogen in mineral forms, which is essential for plant growth and the maintenance of healthy ecosystems (Giordano et al., 2021).

2.3.2 Sulfur oxidation

Sulfur, a key mineral nutrient, undergoes various transformations in the soil primarily through microbial activity, which significantly influences its availability to plants and its role in ecosystems. Sulfur exists in different oxidation states, from sulfide (S^{2-}) to sulfate (SO_4^{2-}), with microbial processes driving the cycling of sulfur between these forms, impacting its mineralization and bioavailability (Jørgensen et al., 2019).

One of the most critical processes is sulfate reduction, carried out by SRB in anaerobic environments. These microorganisms use sulfate as a terminal electron acceptor, reducing it to hydrogen sulfide (H_2S). This biogenic sulfide can then react with metal ions to form metal sulfides like pyrite (FeS_2), contributing to mineral transformations in sediments (Neria-González and Aguilar-López, 2021).

This process is crucial in environments such as wetlands and marine sediments, where oxygen is limited.

Conversely, sulfur oxidation is carried out by sulfur-oxidizing bacteria, such as *Acidithiobacillus ferrooxidans* and *Thiobacillus neapolitanus*. These bacteria oxidize sulfide minerals or elemental sulfur to sulfate, which is a more plant-available form of sulfur (Wang et al., 2019). This microbial oxidation is particularly important in soils with high sulfide concentrations, such as those exposed to mining activities, where it can lead to the formation of acid mine drainage—a detrimental environmental issue.

Microorganisms also facilitate sulfur mineralization through the decomposition of sulfur-containing organic matter. In this process, fungi and bacteria break down organic sulfur compounds, releasing inorganic sulfate that can be assimilated by plants. This microbial activity plays a pivotal role in nutrient cycling, as it ensures the continuous supply of sulfur in its mineral form to support plant growth (Narayan et al., 2023).

2.3.3 Phosphorus solubilization

Phosphorus is a vital macronutrient essential for several biological processes in plants, such as photosynthesis, energy transfer (through ATP), nucleic acid synthesis, and membrane production (Wang et al., 2025). However, most phosphorus in the soil is not readily available to plants, as it is often present in insoluble forms. Soil microorganisms, including bacteria, fungi, and mycorrhizal fungi, play a significant role in the solubilization and mobilization of phosphorus, enhancing its availability to plants (Chen et al., 2023; Pan and Cai, 2023).

Microorganisms contribute to phosphorus solubilization through several biochemical mechanisms. Phosphate-solubilizing bacteria (PSB) like, *Pseudomonas* sp., *Rhizobium* sp., and *Escherichia* sp. and fungi *Talaromyces albobiverticillius* HNB9, release organic acids such as acetic acid, citric acid, and gluconic acid, which lower the pH and dissolve insoluble phosphate complexes in the soil. This process converts phosphorus into a form that can be absorbed by plant roots as orthophosphate (Lee et al., 2012; Kharkwal et al., 2024). Additionally, enzymes like phosphatases, phytases, and C-P lyases produced by these microorganisms mineralize organic phosphorus compounds, making them accessible to plants (Ipsilantis et al., 2018).

For instance, arbuscular mycorrhizal fungi (AMF) form symbiotic relationships with plant roots and significantly aid in phosphorus uptake. The extraradical hyphae of AMF extend beyond the depletion zones around plant roots, exploring larger soil volumes for phosphorus acquisition. These hyphae secrete phosphatases that hydrolyze organic phosphorus and release orthophosphate. In exchange, plants provide carbohydrates to the fungi (Das et al., 2022).

Another example of microbial phosphorus solubilization can be observed in leguminous plants like mung beans (*Vigna radiata*). When coupled with PSB, such as those from the genera *Serratia* and *Enterobacter*, along with inorganic phosphorus fertilizers, these bacteria enhance phosphorus acquisition and promote nitrogen fixation in the plant's root nodules. This dual action increases phosphorus and nitrogen availability, boosting overall plant growth and yield (Das et al., 2022).

2.3.4 Iron sequestration

Microbial roles in iron transformation play a crucial role in the microbial-mediated mineral transformation of iron, essential for many metabolic activities within cells, including electron transfer during respiration and photosynthesis. Iron is abundant in the environment, but it often exists in forms like hydroxides and oxides, which are not easily accessible to plants due to low solubility (Kermeur et al., 2023; Sayyed et al., 2012).

Microorganisms aid in iron solubilization by producing siderophores, which are small, high-affinity iron-chelating compounds. These siderophores bind to ferric iron (Fe^{3+}), transforming it into a soluble form that can be taken up by both plants and microbes (Bridge and Johnson, 2000). For example, the fluorescent *Pseudomonas* species produces siderophores that enhance the iron-acquisition capacity of plants. The iron-siderophore complex is then transported into microbial or plant cells through specific membrane receptors (Gomes et al., 2024). These bacteria can also synthesize other siderophores like pyochelin, pseudopaline, and thioquinolobactin, which may have additional functions such as antimicrobial activity (Timofeeva et al., 2022).

Moreover, the microbial transformation of iron can result in the formation of specific iron minerals. For instance, the bacterium *Geobacter sulfurreducens* reduces Fe^{3+} to Fe^{2+}, which can then react with carbonate to form minerals like siderite ($FeCO_3$).

Additionally, the reduction of Fe^{3+} by bacteria often leads to the formation of magnetite (Fe_3SO_4), a mixed-valence iron oxide, which is important in both environmental and geological contexts (Han et al., 2020).

3 Effects of mineral solubilization on plant growth and development

3.1 Nutrient uptake and assimilation

Plant–microbe interactions significantly influence plant growth, development, and resilience to environmental challenges. These interactions span nutrient acquisition, stress alleviation, and their broader applications in agriculture (Etesami and Adl, 2020). This section discusses the direct mechanisms of microbial-mediated nutrient uptake, the indirect strategies for stress mitigation, and specific applications for enhancing agricultural productivity.

3.1.1 Direct mechanisms of nutrient uptake

Microbial communities associated with plant roots play critical roles in facilitating the uptake of essential nutrients (Table 1). These mechanisms are crucial in nutrient-deficient environments, contributing to the sustainability of agricultural systems by reducing dependency on chemical fertilizers.

3.1.1.1 Nitrogen fixation

Nitrogen is a vital macronutrient for plants, serving as a building block for proteins, nucleic acids, and chlorophyll. However, plants cannot directly utilize atmospheric nitrogen (N_2). Nitrogen-fixing microbes, such as *Rhizobium*, *Frankia*, *Azotobacter*, and *cyanobacteria* (Nostoc), convert N_2 into ammonium (NH_4^+) through the enzymatic activity of nitrogenase, a complex enzyme requiring ATP and low oxygen conditions for functionality (Talaat and Shawky, 2014; Ramesh et al., 2023).

Symbiotic bacteria like *Rhizobium* establish nodules on leguminous roots, forming mutualistic associations where plants provide carbon while bacteria fix nitrogen. Non-symbiotic nitrogen fixers, such as *Azospirillum*, colonize the rhizosphere and enhance nitrogen availability for cereals and non-leguminous crops (Glick, 2012). These interactions contribute to significant reductions in nitrogen fertilizer application, promoting sustainable agriculture (Normand et al., 2007). Studies have shown that inoculating soybeans with *Bradyrhizobium japonicum* raised grain protein content by 28% and improved yield by 15% through enhanced nitrogen absorption and biomass growth. In a multi-location field study in Northern Ghana, using commercial strains like Biofix dramatically increased nodule numbers (up to 118%), dry weight (more than twofold), and grain yield (12%–19%) compared to uninoculated controls, showcasing substantial symbiotic efficiency and economic viability (Ulzen et al., 2016).

3.1.1.2 Phosphate solubilization

Phosphorus is essential for energy transfer, photosynthesis, and genetic material synthesis in plants. Despite its abundance in soil, phosphorus is often locked in insoluble forms, such as calcium phosphate or aluminum phosphate complexes. Phosphate-solubilizing microbes (PSM), including *Bacillus*, *Pseudomonas*, and *Penicillium*, produce organic acids like citric, oxalic, and gluconic acids, which dissolve these complexes into plant-available forms (monobasic and dibasic phosphate ions) (Miliute et al., 2015). These microbes also release phosphatases that hydrolyze organic phosphorus compounds, further enhancing soil fertility. For example, inoculating wheat and maize with PSB has demonstrated increased phosphorus uptake, root biomass, and grain yield (Mitter et al., 2013; Rawat et al., 2021). A recent study indicated that *Pseudomonas putida* enhanced phosphorus acquisition efficiency in maize by 33% and increased dry biomass by 19%, underscoring the significance of PSM in nutrient uptake and growth (Singh et al., 2024).

3.1.1.3 Potassium mobilization

Potassium is critical for enzymatic activation, photosynthesis, and osmoregulation in plants. However, most soil potassium is bound in feldspar, mica, and other silicate minerals, making it unavailable for plant uptake (Baba et al., 2021). Potassium-solubilizing bacteria (KSB), such as *Acinetobacter* and fungi like *Aspergillus aculeatus*, employ acidolysis, chelation, and other biochemical processes to release potassium ions from these minerals (Sardans and Peñuelas, 2021; Peng et al., 2021). Field trials have shown that inoculating potassium-deficient soils with KSB enhances potassium availability, resulting in improved crop performance, particularly under stress conditions. For instance, perennial ryegrass inoculated with *Aspergillus* exhibited better potassium uptake, photosynthesis, and biomass production (Sardans and Peñuelas, 2021). Additionally, *Bacillus mucilaginosus* enhanced potassium uptake and grain yield by 25% in wheat, emphasizing its importance in plant growth and nutrient uptake under potassium stress. Similarly, under salt-affected soil conditions, the combination of *Bacillus circulans* inoculation with 1. Notably, 5% K-leaf foliar application significantly improved the physiological and biochemical traits of wheat, resulting in a 16. 41% increase in grain yield and enhanced potassium uptake, while decreasing the harmful Na^+/K^+ ratio (El-Egami et al., 2024).

3.1.1.4 Iron chelation

Iron, though abundant in the earth's crust, is often inaccessible to plants due to its tendency to oxidize into insoluble ferric form (Fe^{3+}). Plant growth-promoting rhizobacteria (PGPR), such as *Pseudomonas fluorescens* and *Rhizobium*, produce siderophores—iron-chelating molecules that bind Fe^{3+} and reduce it to bioavailable ferrous form (Fe^{2+}) (Ahemad and Kibret, 2014; Sayyed et al., 2012). This process not only enhances iron uptake but also reduces pathogen proliferation by depriving them of iron. Siderophore-producing microbes have been particularly effective in managing iron deficiencies in crops like wheat and rice while promoting plant vigor under iron-limited conditions. For instance, siderophore-producing Rhizobium increased chlorophyll content by 35% and shoot dry weight by 20% in rice grown in iron-deficient soils, revealing the relationship between microbial iron chelation and improved growth performance (Ahemad and Kibret, 2014).

3.1.1.5 Micronutrient solubilization (Zn and Mn)

Micronutrients such as zinc (Zn), and manganese (Mn) play vital roles in enzymatic activity, photosynthesis, and stress tolerance. Zinc-deficient soils are common globally, necessitating external supplementation. Zn-mobilizing bacteria like *Bacillus* and *Pseudomonas* solubilize zinc compounds through organic acid

TABLE 1 Microbial mechanisms enhancing plant macro and micronutrient uptake (Bhat et al., 2024).

Nutrient	Microbial mechanism	Key microorganisms	Effect on plant growth
Nitrogen (N)	Nitrogen fixation	*Rhizobium, Azotobacter, Nostoc*	Convert atmospheric nitrogen into ammonium for plant use
Phosphorus (P)	Phosphate solubilization	*Bacillus, Rhizobium, Enterobacter*	Converts insoluble phosphorus into soluble forms, enhancing growth
Potassium (K)	Potassium solubilization	*Clitopilus hobsonii, Aspergillus aculeatus*	Releases K from minerals, promoting growth under K-limited conditions
Iron (Fe)	Siderophore production	*Rhizobium, Pseudomonas*	Chelates Fe^{3+} into bioavailable Fe^{2+} for plant uptake
Zinc (Zn)	Zinc mobilization	*Pseudomonas, Bacillus*	Enhances Zn uptake, boosts photosynthesis, and gene expression for Zn tolerance
Manganese (Mn)	Mn solubilization	*Aspergillus terreus, Acinetobacter*	Improves Mn availability, critical for stress tolerance in low-Mn soils

production, siderophore secretion, and rhizosphere acidification (Kamran et al., 2017). Recent findings by Kamran et al. (2017) showed that various rhizobacterial strains, including *Pseudomonas fragi*, *Pantoea dispersa*, and *Enterobacter cloacae*, significantly enhanced both shoot and root dry weights, as well as zinc content in wheat tissues. Notably, *P. fragi* improved zinc translocation to grains, indicating that zinc-solubilizing rhizobacteria not only promote biomass growth but also enhance zinc bioavailability and uptake efficiency in wheat under zinc-deficient conditions.

In a related study at the National Agriculture Research Center (NARC), Islamabad, during 2020–2021, several promising indigenous bacterial strains, such as *Pantoea* sp., *Klebsiella* sp., and *Acinetobacter* sp. were identified for their ability to significantly boost wheat growth and zinc biofortification. Inoculating with these zinc-solubilizing bacteria led to a 14% increase in shoot length and up to 14% enhancement in root dry weight, alongside an impressive 1177% rise in zinc content in wheat shoots compared to the control, highlighting the potential of native bioinoculants for sustainable zinc management (Ali et al., 2023).

Manganese availability is often limited in well-aerated, calcareous soils. Acidophilic bacteria (*Acinetobacter* and *Lysinibacillus*) and fungi (*Aspergillus terreus*) release Mn^{2+} ions, making manganese accessible to plants. These interactions enhance the photosynthetic efficiency and stress tolerance of crops such as soybeans and rice (Nagaraju et al., 2024; Sanket et al., 2017).

3.1.2 Indirect mechanisms: stress alleviation

Microbial communities mitigate abiotic stresses by improving water retention, regulating stress-responsive hormones, and detoxifying harmful substances. These mechanisms are critical for enhancing crop resilience under adverse environmental conditions (Table 2).

3.1.2.1 Drought stress

Drought stress is caused by limited water availability, which severely affects plant growth, development, and productivity, particularly in arid and semi-arid regions. It reduces turgor pressure, stunted growth, wilting, and impaired photosynthesis, which lowers crop yields (Ilyas et al., 2020). Additionally, drought induces oxidative stress and increases ethylene levels, accelerating leaf senescence (Khan et al., 2019). Recent studies have shed light on the vital role that certain drought-tolerant microbes, such as PGPR (like *Bacillus subtilis*) and AMF (such as *Glomus intraradices*), play in helping plants cope with drought conditions. These microorganisms enhance the resilience of plants through various interconnected mechanisms, making a significant difference when water is scarce (Ilyas et al., 2020).

For instance, PGPR like *B. subtilis* and *P. fluorescens* produce substances called exopolysaccharides (EPS), which improve soil structure and increase its ability to hold water. This creates a safer environment for plants, helping them survive during dry spells (Sheteiwy et al., 2021; Ilyas et al., 2020). Additionally, some PGPR have a unique capability to reduce ethylene levels in stressed plants by breaking down the precursor to this gas [1-aminocyclopropane-1-carboxylate (ACC)]. Lower ethylene levels mean that plants can slow down aging and keep their photosynthesis running smoothly even under drought stress (Khan et al., 2021a). These helpful microorganisms also contribute to the production of osmolytes, like proline, glycine betaine, and soluble sugars, within host plants, which assist in maintaining the right balance of water in cells. At the same time, they enhance the activity of vital antioxidant enzymes, such as superoxide dismutase (SOD), catalase (CAT), and peroxidases (POD), which protect plants by detoxifying harmful ROS and ensuring cellular balance during drought conditions (Nader et al., 2024; Wu and Zou, 2017).

Another important aspect is how these microbes help regulate plant hormones. Drought-resistant microbes can elevate levels of abscisic acid (ABA), a crucial hormone that helps plants close their stomata and conserve water. They also boost auxins like indole-3-acetic acid (IAA), which encourage roots to grow longer and branch out, allowing plants to absorb more water (Ahmad et al., 2020; Cohen et al., 2015). Moreover, AMF, such as *G. intraradices*, form beneficial partnerships with plant roots, significantly improving how well roots can take up water and nutrients, particularly phosphorus. When these fungi colonize plant roots, they prompt the expression of proteins called aquaporins and increase compatible solutes in plant tissues, further enhancing water retention and tolerance to drought (Sheteiwy et al., 2021) (Figure 1).

3.1.2.2 Salinity stress

Salinity stress, mainly caused by high levels of sodium chloride (NaCl), can be quite detrimental to plants. It leads to osmotic stress, hinders their ability to absorb water, and often results in dehydration and stunted growth (Tiwari et al., 2016). Beyond this, it can cause ion toxicity, disrupt how nutrients are taken up, diminish chlorophyll content, and negatively impact photosynthesis (Al-Turki et al., 2023). Much like drought, salinity stress initiates oxidative stress by producing ROS, which can harm cells and upset

TABLE 2 Microbial mechanisms for abiotic stress alleviation.

Abiotic stress	Microbial mechanism	Key microorganisms	Impact on plant	Citations
Drought	EPS production, ABA regulation, osmolytes	*Bacillus*, *Azospirillum*	Enhances water retention and drought tolerance	Ahmad et al., 2022; Cohen et al., 2015
Salinity	ACC deaminase, ionic balance, antioxidants	*Pseudomonas*, *Azospirillum*	Reduces ion toxicity and oxidative stress	Ayuso-Calles et al., 2021; Navarro et al., 2014
Heavy metals	Siderophores, biosorption, metal transformation	*Saccharomyces cerevisiae*, *Pseudomonas*	Decreases metal toxicity, improves phytoremediation	Saha et al., 2016; Ullah et al., 2015

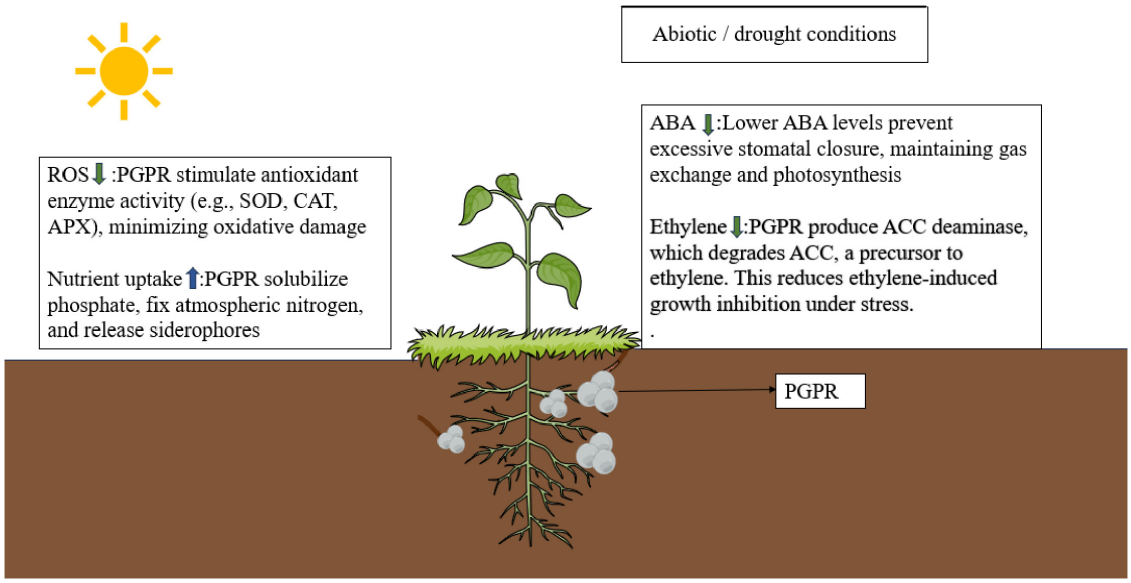


FIGURE 1
The figure highlights function of plant growth-promoting rhizobacteria (PGPR) in relieving abiotic stress and increasing plant growth in conditions of drought. PGPR improve drought resistance in plants by minimizing oxidative stress through the induction of antioxidant enzymes (SOD, CAT, and APX) and enhancing nutrient acquisition through phosphate solubilization, nitrogen fixation, and siderophore production. PGPR regulate hormone response by inhibiting ABA levels to preserve stomatal function and photosynthesis. PGPR also produce ACC deaminase, which breaks down ACC and decreases ethylene synthesis and ethylene-induced growth inhibition during stress. Figure created using BioRender. Root structure was illustrated in a style inspired by published figures from Dr. Guillaume Lobet (ORCID: 0000-0002-5883-4572).

nutrient balance, ultimately degrading membrane integrity and cellular function (Tiwari et al., 2016).

A study conducted by Ahmed et al. (2023) found that inoculating maize with *Funneliformis constrictum* can help these plants cope with salinity by enhancing their antioxidant defenses and polyamine metabolism. In light of increasing seawater stress, AMF were found to alleviate oxidative damage by reducing levels of hydrogen peroxide (H_2O_2) and malondialdehyde (MDA). They also boosted the activity of key antioxidant enzymes such as CAT, SOD, and ascorbate peroxidase (APX). Additionally, AMF increased amino acid levels, which promoted the production of important polyamines like putrescine, spermidine, and spermine. This was achieved by activating certain biosynthetic genes while suppressing those responsible for breaking down these compounds. These changes significantly improved the plants' ability to endure stress and support growth under high-salinity conditions.

Moreover, PGPR, which have the ability to break down ACC deaminase, can help stressed plants by lowering ethylene levels. This process aids in preventing premature aging and encourages root growth (Damodaran et al., 2013). These beneficial microorganisms also enhance the activity of antioxidant enzymes like SOD, CAT, and APX, which aid in neutralizing ROS and restoring redox balance. In summary, these microbial partnerships can significantly enhance plant resilience against drought and salinity stresses by improving water retention, modulating hormonal levels, and reducing oxidative damage.

3.1.2.3 Phytoremediation and heavy metal detoxification

Phytoremediation is a green and sustainable approach to cleaning up soil that's been contaminated with heavy metals such as cadmium (Cd), lead (Pb), arsenic (As), and beryllium (Be). This method becomes even more effective with the help of plant growth-promoting microorganisms (PGPM), which assist in extracting these harmful metals through various processes, including their accumulation inside and outside plant cells, their sequestration, and transforming them into less toxic forms (Ullah et al., 2015; Ma et al., 2016).

Specifically, beneficial strains like *Pseudomonas*, *Bacillus*, and *Azospirillum* play a key role in reducing metal stress on plants. They do this by producing siderophores, which are small molecules that can bind to iron and heavy metals such as Cd, Ni, and Zn, thereby affecting how these metals move and are absorbed by plants

(Złoch et al., 2016; Saha et al., 2016). In addition to metal binding, PGPM also releases organic acids, like citric, oxalic, and malic acids, which help to lower the pH of the soil around plant roots, making metal ions more soluble and accessible for uptake (Ullah et al., 2015). They also produce various enzymes, including nitrogenase and phosphatase, which facilitate nutrient cycling and bolster plant health, especially in contaminated environments. Moreover, PGPM helps plants grow by providing essential nutrients, managing pathogens, and improving metal accumulation capacity. When combined with AMF, this partnership significantly enhances the effectiveness of phytoremediation by boosting nutrient absorption and resistance against heavy metals (Vigliotta et al., 2016).

Recent studies have shown that inoculating plants with AMF such as *Rhizophagus irregularis* can help reduce beryllium (Be) toxicity in ryegrass and chickpeas. This leads to decreased Be absorption and improved physiological resilience. When AMF are present, plants display better photosynthetic performance, less oxidative stress (as indicated by lower levels of hydrogen peroxide and lipid damage), and an increase in protective substances like proline and sucrose. These beneficial changes are associated with better nitrogen metabolism and increased activity of an enzyme called nitrate reductase, with ryegrass showing an even stronger response than chickpeas (Sheteiwy et al., 2022).

3.1.3 Specific case studies and applications

3.1.3.1 PGPR in improving crop yield

Inoculation with PGPR like *Azospirillum brasilense* and *B. subtilis* has consistently shown improvements in root architecture, nutrient uptake, and resistance to abiotic stresses. Field applications in crops such as wheat, maize, and rice demonstrate increased yields and reduced fertilizer dependency (Etesami and Glick, 2024).

3.1.3.2 Mycorrhizal fungi in enhancing resource use efficiency

Arbuscular mycorrhizal fungi (*Glomus mosseae*) extend their hyphal networks beyond the root zone, enhancing phosphorus and water uptake in resource-limited environments (Vafa et al., 2021). Their application in crops like barley and maize has shown improved nutrient efficiency and drought tolerance (Ferrol et al., 2016).

3.2 Root growth and architecture

Plant–microbe interactions profoundly influence root architecture and rhizosphere dynamics, which significantly impact plant performance and soil ecosystem functions. Root architecture traits, such as branching, elongation, and exudation, are essential for nutrient acquisition and stress adaptation and are heavily influenced by microbes like AMF and PGPR. These microbes enhance root development, modulate exudates, and improve nutrient uptake, particularly under stress conditions. Additionally, rhizodeposition, the release of organic compounds from roots, plays a crucial role in shaping rhizosphere microbial communities by attracting beneficial microbes and supporting nutrient cycling. This section discusses microbial effects on root traits, rhizodeposition processes, and their role in shaping rhizosphere microbial communities (Vafa et al., 2024).

Root phenotypic traits, such as branching, elongation, and surface area, are crucial for nutrient acquisition, stress tolerance, and plant–microbe interactions. Microbes significantly influence these traits, promoting root development and enhancing functionality. Mycorrhizal fungi, especially AMF, extend root systems through fungal hyphae, leading to increased root branching, lateral root formation, and enhanced root length, thereby improving nutrient uptake (Rawat et al., 2021). Similarly, PGPR produce phytohormones like IAA, which stimulate root elongation and branching, increasing the root surface area for nutrient acquisition. For example, inoculation with *P. fluorescens* significantly improved lateral root density in wheat, thereby enhancing phosphate uptake (Etesami and Adl, 2020). Under stress conditions, root plasticity plays a key role in adaptation, such as increased root length and surface area in response to low phosphorus availability. PGPR further augment these adaptive traits by influencing root exudate composition, thereby enhancing microbial colonization and nutrient availability in the rhizosphere (Bouremani et al., 2023). Rhizodeposition, involving the release of organic compounds such as sugars, amino acids, and secondary metabolites from roots, is pivotal in shaping the rhizosphere microbiome. These exudates not only provide carbon sources for soil microbes but also act as chemical signals that attract beneficial microbes, including AMF and PGPR, while repelling pathogens. For instance, maize roots release flavonoids that promote AMF colonization, improving phosphorus uptake and drought tolerance (Zhang et al., 2015). Rhizodeposition is most concentrated at root tips, where microbial colonization is typically highest. Root traits, such as growth angle, rooting depth, and lateral root density, influence the spatial distribution and persistence of exudates, thereby shaping the rhizosphere microbial community. Root system architecture, including root growth angle and depth, also determines microbial community composition. Shallow roots are associated with processes like nitrification and organic matter degradation, whereas deeper roots facilitate reductive processes such as denitrification (Galindo-Castañeda et al., 2022). Moreover, axial and lateral root traits significantly affect microbial interactions; plants with more axial roots enhance microbial colonization through increased carbon deposition via exudates, while higher lateral root branching density provides additional attachment points for microbes, fostering diverse microbial communities and improving nutrient uptake under phosphorus-limited conditions (Chen and Liu, 2024). Collectively, these microbe-mediated interactions influence root architecture and exudation patterns, enhancing nutrient cycling, stress resilience, and soil health. Such interactions underscore the potential for sustainable agricultural practices and reveal strategies for improving crop productivity, particularly in resource-limited environments (Shah et al., 2021) (Table 3).

3.3 Plant stress tolerance

Abiotic stresses such as drought, salinity, and heavy metal toxicity limit crop yield by disrupting metabolic and physiological processes including water uptake, ion homeostasis, photosynthesis, and oxidative balance. Beneficial microbes such as PGPR, AMF mitigate these effects through multiple synergistic mechanisms (Table 2).

Microorganisms play a vital role in enhancing plant resilience under challenging environmental conditions. During drought stress, for instance, many soil microbes secrete exopolysaccharides (EPS), which help bind soil particles together, improving both soil structure and its capacity to retain water. This not only facilitates better root access to moisture but also leads to the formation of a protective biofilm around the rhizosphere (Ahmad et al., 2020). PGPR equipped with the enzyme ACC deaminase further assist in managing drought stress by breaking down ACC, a precursor to ethylene, a hormone that tends to accumulate during stress and accelerates plant senescence. By lowering ethylene levels, these microbes support prolonged root growth and delayed aging of plant tissues (Sagar et al., 2020; Ayuso-Calles et al., 2021). In parallel, beneficial microbes stimulate the accumulation of osmoprotective compounds such as proline, glycine betaine, and soluble sugars. These molecules help maintain cellular integrity and enzyme function during osmotic stress by balancing the internal water potential (Eswaran et al., 2024). Microbial activity also influences plant hormone levels, particularly increasing ABA, which regulates stomatal closure to conserve water, and auxins, which promote root elongation and branching, traits critical for improved water uptake under limited moisture conditions (Cohen et al., 2015; Tanveer et al., 2023). AMF, like *G. intraradices*, add another layer of drought defense by enhancing root hydraulic conductivity and upregulating aquaporin genes, thus boosting water transport efficiency in plants (Sheteiwy et al., 2021).

Under salinity stress, microbes help mitigate ionic imbalance and toxicity. One key strategy is enhancing the selective absorption of potassium (K^+) over sodium (Na^+), preserving ionic homeostasis. At the same time, microbial partners activate the plant's antioxidant machinery, elevating enzymes such as SOD, catalase (CAT), and APX, which detoxify ROS and protect plant cells from oxidative damage (Hamidian et al., 2023; Kapadia et al., 2022; Gupta et al., 2013). For example, *P. putida* has been shown to improve salinity tolerance in rice by enhancing both antioxidant activity and ion regulation mechanisms. Interestingly, ACC deaminase activity again plays a dual role here, limiting ethylene accumulation under salinity stress, thereby supporting continued root development (Sagar et al., 2020; Ayuso-Calles et al., 2021). Certain AMF species, like *F. constrictum,* contribute by modulating polyamine pathways, increasing compounds such as putrescine and spermidine. These not only stabilize cell membranes but also help maintain ionic balance within plant tissues (Ahmed et al., 2023).

When it comes to heavy metal stress, microbes aid plants in multiple ways. Some bacteria, notably those that produce siderophores like *Pseudomonas* and *Bacillus*, bind toxic metals such as cadmium (Cd) and nickel (Ni), thereby reducing their availability and toxicity. Others secrete organic acids that chelate metals, improving their uptake by roots for eventual detoxification (Złoch et al., 2016; Saha et al., 2016; Sagar et al., 2022). AMF like *R. irregularis* limit the movement of heavy metals into the shoots, thereby protecting photosynthetic tissues. They also boost the plant's antioxidant system and support better photosynthetic efficiency under stress (Sheteiwy et al., 2022; Ullah et al., 2015). Altogether, the collaboration between PGPR and AMF forms a multi-tiered defense mechanism, biochemical, physiological, and molecular that significantly enhances plant adaptation and tolerance to a variety of abiotic stressors.

3.3.1 Biotic stress tolerance

Soil and plant roots host a variety of pathogens and beneficial microbes. Biotic stress caused by pathogens can lead to imbalanced hormonal regulation, nutrient deficiencies, and physiological disorders (Ramegowda and Senthil-Kumar, 2015). Using PGPM as a biological control agent offers a sustainable alternative to chemical pesticides. PGPM promotes plant growth and development by enhancing nutrient uptake, activating defense mechanisms, and suppressing pathogens. Co-inoculation with PGPR and mycorrhizae can improve plant resistance to biotic stress (Alkilayh et al., 2024).

3.3.1.1 Mechanism of biotic stress tolerance

Plant–microbe interactions are crucial for managing biotic stress. PGPM can induce systemic resistance (ISR) and systemic acquired resistance (SAR) in plants. Non-pathogenic root-associated microbes activate ISR, while SAR involves changes in gene expression and the production of defense-related proteins. PGPM can also produce allelopathic compounds, siderophores, and antibiotics that inhibit pathogen growth. For instance, *Bacillus* strains have effectively managed diseases like bacterial leaf blight and black rot through ISR (Ghazalibiglar et al., 2016; Vinothini et al., 2024; Anbalagan et al., 2024; Paliwal et al., 2023). Microbial solubilization of minerals (MSMs) plays a crucial role in promoting plant growth and development by improving nutrient availability and activating defense mechanisms, particularly against biotic stressors such as pathogens and pests. A prominent defense strategy supported by MSMs is ISR, a comprehensive immune response that primes plants to respond swiftly and effectively to biotic challenges. ISR operates through signaling pathways regulated by jasmonic acid (JA) and ethylene (ET), which coordinate proactive defense strategies (Ali et al., 2022). The JA pathway begins with the synthesis of jasmonic acid from linolenic acid in the chloroplast, followed by its conversion to jasmonoyl-isoleucine (JA-Ile), the bioactive form. JA-Ile binds to the COI1 receptor, triggering the degradation of JAZ repressors and activating transcription factors like MYC2. These transcription factors drive the expression of defense-related genes, enhancing the production of pathogenesis-related (PR) proteins, antimicrobial secondary metabolites, and enzymes that reinforce cell walls. Simultaneously, the ET pathway, derived from methionine through the Yang cycle, stabilizes EIN3, a key transcription factor, upon ethylene binding. This pathway complements JA signaling, enabling a robust and comprehensive defense, particularly effective against necrotrophic pathogens (Ruan et al., 2019).

Beyond triggering ISR through microbe-associated molecular patterns (MAMPs), MSMs enhance plant resilience by solubilizing essential nutrients such as phosphorus, iron, and potassium. For instance, microbial siderophores chelate iron, supporting the production of ROS, which serve as an early line of defense against pathogen invasion. Solubilized calcium and silicon further strengthen plant cell walls, providing a physical barrier against infection (Tiwari et al., 2024). Additionally, ISR stimulates the synthesis of secondary metabolites like flavonoids and phytoalexins, which act as potent antimicrobial compounds. A notable advantage of ISR is its ability to balance growth and defense by conserving resources until an actual threat is encountered. This ensures plants maintain their growth

and development even under stress conditions. Moreover, ISR offers broad-spectrum resistance, reducing disease severity and improving overall plant health (Pusztahelyi et al., 2015). The use of ISR-inducing MSMs as bioinoculants in agriculture presents an eco-friendly and sustainable strategy to enhance crop resilience and productivity while minimizing dependence on chemical pesticides. By combining nutrient solubilization with immune activation, MSMs contribute significantly to sustainable agricultural practices and stress management in crop production systems.

3.3.1.2 Hormonal modulation

Plant growth-promoting rhizobacteria can influence plant hormonal levels, promoting root and shoot development, which enhances overall plant growth and productivity:

Auxin production: IAA is a widely studied auxin involved in plant growth and development. It is primarily produced in plant buds and young leaves through various biosynthetic pathways (Kundan et al., 2015). IAA promotes key processes such as cell division, differentiation, elongation, and wall extensibility in young stems, improving the plant's ability to absorb water and nutrients. It also regulates apical dominance, bud formation, and adventitious and lateral root development (Grobelak et al., 2015). Additionally, IAA plays a role in leaf and flower abscission. Other auxin-like compounds include indole-3-acetamide, indole-3-pyruvate, and 4-chloroindole-3-acetic acid (Olanrewaju et al., 2017).

Gibberellin production: GAs regulate key growth processes, including seed germination, stem elongation, flowering, and fruit setting. They enhance photosynthesis and chlorophyll content, promote shoot growth, and inhibit root growth through GA signaling and DELLA repressors (Martínez et al., 2016).

Cytokinin production: cytokinins produced by some PGPR can delay plant aging (senescence) and promote cell division, leading to improved plant vigor and yield.

Ethylene inhibition: ACC deaminase, produced by some PGPR, promotes plant growth by lowering ethylene levels, a hormone linked to stress responses in plants. Excess ethylene, triggered by biotic and abiotic stresses, negatively affects plant shoot and root development (Gamalero and Glick, 2015). ACC deaminase reduces ethylene by converting its precursor, ACC, into α-ketobutyrate and ammonia, thereby restoring normal plant growth (Olanrewaju et al., 2017). PGPR application helps plants manage stress by reducing ethylene-induced damage.

4 Microbial–plant–mineral interactions

Plants need minerals both macronutrients and micronutrients for their growth and form a symbiotic association with microbes for their uptake from soil. This interaction between plants, microbes and minerals is a key system for the biosphere. Their interaction with microbes increases plant growth and overall health, crop productivity, mineral uptake, plant defense, soil fertility, etc. Through improved soil fertility and weathering of rocks, vital nutrients (N, P, and K) can be acquired from minerals (Ahemad and Kibret, 2014). Various plant–microbial associations such as mycorrhizal, cyanobacterial, nitrogen fixers, etc. contribute to plant nutrition by increasing the soil health and mineral cycles. Microbial activity supports the breakdown of organic matter by degradation, dissolution, transformation, and precipitation which releases crucial minerals back to the soil while minerals provide protection to microbes from harsh environments such as physical abrasion, thermal fluctuation and UV irradiation (Dong et al., 2022). Understanding these interactions and their mechanisms are very essential for sustainable agriculture and ecosystem management.

4.1 Rhizosphere processes

Rhizosphere is the key area where microbial–plant–mineral interactions occur. In rhizosphere, soil is directly influenced by plant roots and microbial activities. Plant roots exude low molecular weight organic compounds which aggressively support microbial colonization. In natural ecosystem, most mineral nutrients are in their non-available forms and their availability rely on soil pH, organic acids, microbial activity, etc (Zaidi et al., 2015). Microbes such as plant growth promoting rhizobacteria, diazotrophs, AMF, and cyanobacteria are well known for mineralization process through solubilization, absorption, oxidization, fixation, etc (Figure 2). Microorganisms maintain soil structure by improving aeration and water retention which helps in plant growth. In natural environment, these microbial mediated mineral transformations are rate-limiting and essential processes for plant growth, and ecosystem abundance (Thepbandit and Athinuwat, 2024). So, understanding the dynamics of the rhizosphere is requisite for enhanced agricultural practices in future.

4.2 Mycorrhizal associations

Arbuscular mycorrhizal fungi represent an obligate symbiotic relation with plant roots which colonize the 80% of terrestrial plants including cereals, vegetables, legumes, fruits, medicinal plants, and various commercial crops such as sunflower, sugarcane, cotton, etc. (Saboor et al., 2021; Jabborova et al., 2022; Vafa et al., 2024). AMF promote the uptake and transfer of solubilized minerals from soil toward the plant roots through extra radical mycelium (ERM) which absorbs water and nutrients beyond the depletion zones and in-turn gets the photosynthates (carbohydrates) from the plants. AMF spores infect the root cortical cells, travel by hyphae inside the root and form arbuscule which is the key component for nutrient exchange (Liu et al., 2022). AMF hyphae network can lengthen up to 25 cm around the plant root and help in establishment of other microbes as well by enhancing the root zone 10%–100% (Smith and Read, 2008). Various studies showed under drought stress where the mobility of P and N is low, AMF can effectively uptake the nutrients through ERM. By dipeptide transporters, *R. irregularis* efficiently assimilate organic N from soil likewise *G. mosseae* membrane Pi transporters (PT) govern the Pi repositioning from soil to ERH (Khoso et al., 2025).

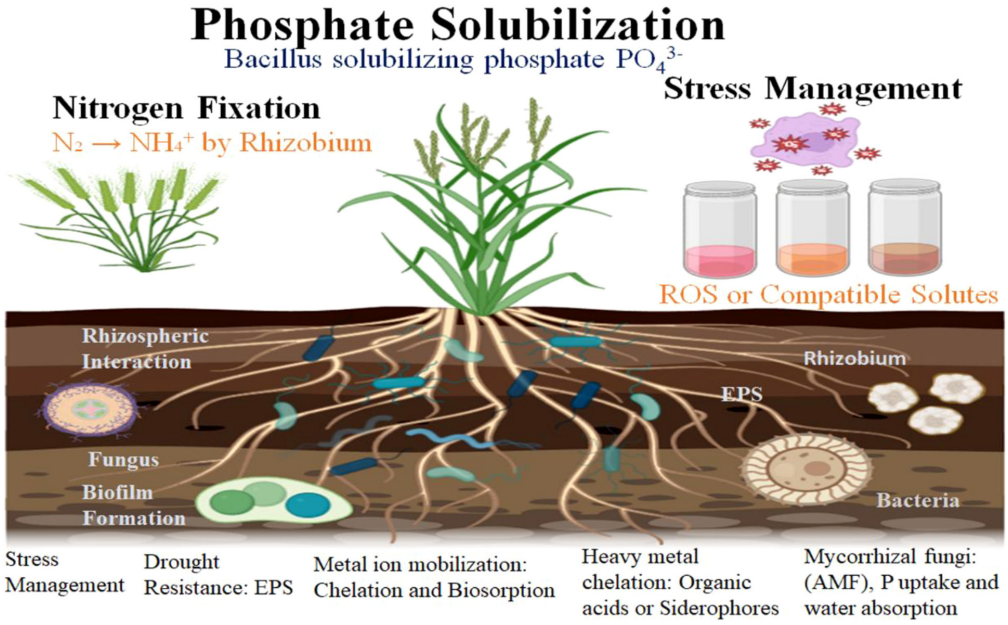


FIGURE 2
The figure highlights the interactions between plants and microbes in the rhizosphere, showcasing processes such as nitrogen fixation (Rhizobium converting N_2 to NH_4^+), phosphorus solubilization by microbes like *Bacillus* and *Pseudomonas*, and stress adaptation mechanisms like EPS production for drought tolerance and heavy metal detoxification by fungi such as *Aspergillus*. These microbial activities boost nutrient uptake, support plant growth, and enhance stress resistance. The figure has been made using Bio render.

4.3 Plant growth-promoting rhizobacteria

Plant growth-promoting rhizobacteria are useful symbiotic bacteria which make a niche in rhizosphere and strengthen the plant growth by several mechanisms such as absorption of nitrogen and phosphorus, phytohormone production, mineral solubilization, iron chelating siderophore production, etc. (Parray et al., 2023). The bacterial potential to solubilize mineral P increase the availability of phosphate and iron for plants. They solubilize insoluble P by the production of organic acids- acetic acid, butyric acid, citric acid, lactic acid, oxalic acid, maleic acid etc. *Pseudomonas, Bacillus*, and *Rhizobium* are some common bacteria which participate in P solubilization. Similarly, reduction in pH is also reported by *Staphylococcus saprophyticus* SM7 and *Staphylococcus haemolyticus* MS7 when solubilize the mineral Zn in medium (Javaid et al., 2023). By the process of biological nitrogen fixation (BNF) microbes can fix atmospheric nitrogen and make it available for plant use. Significant nitrogen-fixers such as *Rhizobium, Azospirillum, Azotobacter*, etc. are used for growing cash crops and some other cereals now a days along with leguminous crops (Basu et al., 2021). Some of the efficient mineral solubilizing bacteria (MSB) are from the genera *Bacillus licheniformis, Arthrobacter, Enterobacter, Bacillus cereus, Staphylococcus, B. subtilis, Paenibacillus polymyxa, Bacillus aryabhattai* (Javaid et al., 2023; Basu et al., 2021; Ahmad et al., 2020; Thomas et al., 2018). So, MSB provide an encouraging replacement to the usage of traditional chemical fertilizers, because they augment the bioavailability of mineral nutrients in soil which enhance plant growth, development, defense and hence crop productivity and yield. The application of such MSB strains in crops can overcome mineral deficiency in plants which can be environmentally and profitably more noteworthy in future.

5 Impact of microbial mineral transformation on plant growth

Microbial transformations play a critical role in influencing the availability of both macro and micronutrients to plants, directly impacting soil fertility and crop productivity (Figure 3). These transformations primarily occur within the rhizosphere, where the interactions between plant roots and beneficial microbes help regulate nutrient cycling, solubilization, mobilization, and translocation processes.

Microorganisms, such as PGPR, fungi, and cyanobacteria, enhance the availability of nutrients through a series of biochemical processes. These include the production of organic acids, enzymes, and other metabolites that convert unavailable forms of nutrients into ones that plants can absorb more efficiently (Singh et al., 2020).

One of the most important microbial processes for nutrient availability is solubilization. Microbes enhance the solubilization of essential elements such as phosphorus, zinc, and potassium by secreting organic acids, which lower soil pH and help dissolve minerals bound in insoluble forms (Paul and Parihar, 2021). For example, specific species of *Bacillus* and *Pseudomonas* produce citric, oxalic, and malic acids, which play a significant role in solubilizing zinc and iron, making them more accessible to plant roots (Da Silva et al., 2023; Kuhad et al., 2011). These microbial actions are especially important in soils where these nutrients tend to precipitate and become unavailable to plants under normal conditions.

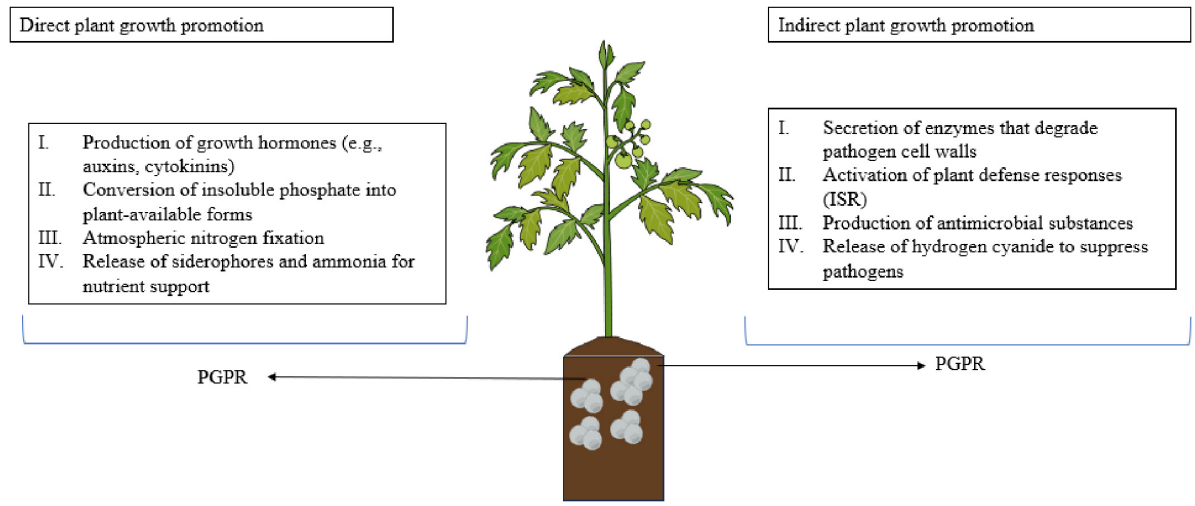


FIGURE 3
The figure highlights the mechanisms through which plant growth-promoting rhizobacteria (PGPR) increase crop yield are by both direct and indirect means. This figure demonstrates the two-way function of PGPR in sustainable agriculture. Direct mechanisms are production of phytohormones (e.g., auxins and cytokinins), solubilization of phosphate, nitrogen fixation, and siderophore and ammonia production for improving nutrient availability. Indirect mechanisms are induction of plant defense through production of cell wall-degrading enzymes, induction of induced systemic resistance (ISR), production of antimicrobial compounds, and production of hydrogen cyanide to inhibit phytopathogens. Figure created using BioRender. Root structure was illustrated in a style inspired by published figures from Dr. Guillaume Lobet (ORCID: 0000-0002-5883-4572).

Mobilization is another key microbial function that enhances nutrient availability. Certain microbes release chelating compounds, such as siderophores, that bind to metals like Fe, Mn, and Zn, aiding their transport into plant systems (Singh et al., 2020). This microbial activity is particularly beneficial in alkaline or calcareous soils, where nutrient availability is often limited due to the formation of insoluble complexes. By mobilizing these micronutrients, microbes ensure a steady supply to the plants, thus supporting their metabolic functions and overall growth (Vélez-Bermúdez and Schmidt, 2022).

Redox reactions mediated by microbes also significantly affect nutrient availability, particularly for elements like iron and manganese. In soils with low oxygen levels, microbes convert oxidized forms of these nutrients, such as Fe^{3+} and Mn^{4+}, into their reduced, more soluble states (Fe^{2+} and Mn^{2+}), which are readily absorbed by plant roots (Jones et al., 2020). These biological reduction processes are essential for maintaining nutrient supply in flooded or poorly drained soils, where the availability of such micronutrients would otherwise be limited.

In addition to these chemical transformations, microbes can alter the physical structure of plant roots to enhance nutrient uptake (Saeed et al., 2021).

For example, PGPR play a crucial role in enhancing plant growth and development through various mechanisms. They colonize the rhizosphere and modify root system architecture by producing phytohormones and other signals, leading to increased lateral root branching and root hair development (Vocciante et al., 2022). PGPR improve nutrient uptake efficiency, tolerance to abiotic stressors, and crop quality through direct and indirect mechanisms (Rouphael and Colla, 2018). Moreover, these modifications in root architecture are often accompanied by an increase in the density and efficiency of nutrient transporters in the root cells, further improving nutrient acquisition.

Through these various mechanisms, microbial transformations significantly improve the availability of essential nutrients to plants. This not only leads to enhanced plant growth and higher crop yields but also contributes to better nutritional quality in food crops, as plants more efficiently accumulate important minerals such as zinc, iron, and manganese.

Recent developments in microbe–mineral interactions have greatly expanded our understanding of their diverse roles in enhancing plant health and supporting sustainable agriculture. Over the past 10 years, research has increasingly recognized the crucial influence of PGPR especially PSB in boosting soil fertility and crop productivity. These beneficial microbes not only aid in nutrient mobilization but also contribute to a range of plant-supportive functions, including improved tolerance to environmental stresses. Field experiments consistently demonstrate that microbial interactions with soil minerals can increase the availability of essential nutrients such as phosphorus, potassium, and micronutrients, often translating into significant yield improvements. In soils that are degraded or contaminated, integrated approaches using customized biochar in combination with PSB or PGPR–plant systems have achieved over 60% immobilization of toxic metals while simultaneously restoring vital soil health indicators (Zhang et al., 2025).

Within the broader PGPR category, PSB have emerged as effective biofertilizers capable of enhancing nutrient uptake, stimulating plant growth, and raising overall crop yields. Recent studies have also shown that PSB can mitigate abiotic stresses such

as drought and salinity by modulating plant hormone pathways and activating defense mechanisms (Al-Turki et al., 2023). Long-term field studies further confirm their effectiveness, particularly in crops like maize and peanuts. For example, peanut yields have increased by up to 19.5% when PSB are applied alongside other beneficial microorganisms (Wang D. et al., 2024). These treatments have also been associated with improved nitrogen use efficiency and elevated seed protein levels, highlighting their contribution to crop quality.

Similarly, KSB have shown promise in enhancing crop performance while reducing reliance on chemical fertilizers. In wheat, KSB application has been linked to increases in root length ranging from 16% to 40% and biomass gains of two- to threefold compared to untreated controls (Gandhi et al., 2022). In multi-year trials conducted in India, cold-tolerant *Pseudomonas* strains (L3 + P2) led to a 22% rise in grain yield and a 16% increase in total biomass relative to uninoculated plots (Dasila et al., 2023). Under dryland farming conditions, co-application with phosphorus fertilizers has resulted in yield gains of up to 63% (Peng et al., 2024).

Beyond nutrient dynamics, certain microbial species such as *B. subtilis* MP1 have demonstrated the ability to accelerate silicate mineral weathering and enhance the accumulation of inorganic carbon in soils. Field data indicate sequestration rates of up to 2.02 tonnes of carbon per hectare per year, accompanied by increased levels of important soil cations like Ca^{2+}, Mg^{2+}, and Fe^{2+} (Timmermann et al., 2025). Altogether, these findings underscore the practical benefits of leveraging microbe–mineral strategies to boost soil fertility, promote carbon storage, and rehabilitate degraded ecosystems—offering a pathway toward more resilient and environmentally sustainable agricultural systems.

5.1 Soil structure and fertility: the role of microbial mineral transformation in soil aggregation

Soil structure is intricately linked to fertility, with soil aggregates playing a pivotal role in the retention of nutrients, water, and organic matter. Aggregates, composed of mineral particles and organic carbon, are held together by electrostatic interactions and encrusted organic materials, forming microaggregates (<250 μm) and macroaggregates (0.25–2 mm) (Wilpiszeski et al., 2019). These structures influence soil fertility by controlling water retention, nutrient flow, and microbial habitat availability. Microbial processes are central to the formation and stabilization of these aggregates, especially through microbial mineral transformations. Soil microorganisms, particularly bacteria and fungi, contribute to aggregate stability by producing extracellular polymeric substances (EPS), which bind soil particles together. This biotic activity not only enhances the mechanical strength of aggregates but also plays a significant role in geochemical cycling (Costa et al., 2018). Moreover, microbes also participate in the transformation of soil minerals. For example, microbial activity can lead to the destruction of rock-forming minerals and the formation of new minerals, such as calcite and iron-containing compounds (Maksimovich et al., 2021).

Microorganisms also play a crucial role in shaping porosity of soil through their interactions with organic matter and minerals. The architecture of soil aggregates, shaped by microbial activity, has a direct effect on nutrient availability and soil fertility. Pore spaces created by microbial transformations facilitate the movement of water and nutrients, while also providing protection to microbial communities within the aggregates. Microorganisms living in these confined spaces help maintain the balance between oxygen and nutrient levels, contributing to essential processes like nitrogen fixation and denitrification.

Furthermore, microbial decomposition of organic matter leads to the formation of water-stable macro-aggregates, with microbial-derived carbon acting as a cementing agent (Rabbi et al., 2019). The resulting pore networks within aggregates vary in size and connectivity, influencing the transport of soluble organic carbon, nutrients, and contaminants (Guhra et al., 2022). Pore size distribution affects microbial community composition and associations, with larger pores promoting diversity under low hydraulic connectivity (Xia et al., 2021). These microbial-driven changes in soil architecture directly impact carbon decomposition rates and bacterial diversity. The complex interplay between substrate availability, microbial activity, and pore geometry creates a dynamic system that influences soil function and carbon cycling.

Additionally, microbial by-products such as organic acids and enzymes also facilitate the weathering of minerals, contributing to soil aggregation and the formation of organ mineral complexes that further stabilize the soil matrix.

5.2 Specific example of microbe–plant interactions and their outcomes on plant growth

5.2.1 Case study: mycorrhizal fungi and rock weathering

A notable example of specific microbe–plant interactions and their outcomes on plant growth occurs with mycorrhizal fungi in forest ecosystems. Mycorrhizal fungi form symbiotic relationships with plant roots, where they provide plants with critical nutrients in exchange for carbohydrates (Drijber and McPherson, 2021). In nutrient-poor soils, particularly in boreal forests, these fungi secrete organic acids that dissolve minerals like feldspar and apatite, releasing phosphorus and calcium into the soil (Luo et al., 2024). This weathering process not only sustains forest fertility but also plays a crucial role in global nutrient cycles.

In agricultural systems, this process has been harnessed to enhance crop productivity in areas with poor soil fertility. For example, PSB are known to release phosphate from insoluble mineral sources such as apatite through the secretion of organic acids (Pang et al., 2024). This microbial action provides a natural and sustainable alternative to synthetic phosphate fertilizers, improving soil fertility while reducing the environmental impact of agriculture.

5.2.2 Case study: biofertilizers

Another practical application of microbial mineral weathering is the use of biofertilizers containing weathering microbes. In India, farmers in regions with low-phosphorus soils have used

biofertilizers enriched with PSB to improve crop yields. A meta-analysis revealed an average yield improvement of 1.59 tonnes per hectare due to biofertilizer application, with the highest effects observed in cereals (Praveen and Singh, 2019). PSB, often combined with AMF, can significantly enhance plant growth, nutrient uptake, and crop yield, as demonstrated in wheat cultivation in Rajasthan (Saxena et al., 2014). The effectiveness of PSB as biofertilizers varies based on their solubilization mechanisms and molecular composition, highlighting the need for further research to identify efficient strains for agricultural use.

5.2.3 Case study: common bean and plant growth-promoting bacteria

In a study involving common beans inoculated with *Bacillus* sp., *Pseudomonas* sp., *Serratia* sp., *Trichoderma koningiopsis*, and *Burkholderia* sp., significant improvements in plant growth and yield were observed. These microorganisms enhanced nutrient uptake, especially nitrogen, through mechanisms such as phosphate solubilization and BNF (Jalal et al., 2024). The presence of these bacteria facilitated increased root biomass, leading to more efficient water and nutrient absorption. For example, P*seudomonas* sp. is efficient PSM that produce organic acids, primarily gluconic acid, to solubilize inorganic phosphates (Blanco-Vargas et al., 2020).

5.2.4 Case study: wheat and zinc-solubilizing bacteria

Wheat has been effectively biofortified with zinc through the inoculation of zinc-solubilizing bacteria such as *B. subtilis* and *Acinetobacter* sp. These bacteria release organic acids that solubilize zinc from insoluble soil compounds, making it bioavailable to the plant (Yadav et al., 2023). Inoculation with these microbes not only improved zinc uptake but also enhanced wheat growth, productivity, and grain zinc concentration.

5.2.5 Maize and diazotrophic bacteria

Maize plants inoculated with diazotrophic bacteria such as *A. brasilense* and *Burkholderia cepacia* displayed improved growth and nitrogen content in the leaves. These bacteria fix atmospheric nitrogen and make it available to the plant, which reduces dependency on nitrogen fertilizers (Kumar et al., 2022). Furthermore, *Azospirillum* produces phytohormones like IAA, which stimulate root development, enhancing water and nutrient uptake (Jalal et al., 2024).

6 Applications in agriculture and biotechnology

Advances in plant–microbe interactions have paved the way for eco-friendly solutions to enhance crop productivity and address environmental challenges. These applications, including biofertilizers, climate change mitigation, sustainable agriculture, and bioremediation, underscore the role of beneficial microbes in modern agricultural systems (Table 3).

6.1 Biofertilizers: enhancing nutrient availability

Biofertilizers are substances containing living microorganisms that enhance plant growth by improving the availability of essential nutrients like nitrogen, phosphate, and iron when applied to seeds, plant surfaces, or soil. Nitrogen-fixing bacteria such as *Rhizobium* and *Azotobacter* play a crucial role in biofertilizers. These bacteria reside in the nodules of plant roots, particularly in legumes, and transform atmospheric nitrogen into organic forms that plants can utilize (Talaat and Shawky, 2014; Alami et al., 2024). Similarly, cyanobacteria convert environmental nitrogen into ammonia for plant uptake. Phosphate is another vital nutrient for plants, crucial for stress tolerance, maturity, and quality. *Penicillium bilaii*, a beneficial fungus, enhances phosphate availability by producing organic acids that dissolve soil phosphates, making them accessible to plant roots (Mosttafiz et al., 2012; Miliute et al., 2015; Rawat et al., 2021).

Iron, though abundant in nature, is often unavailable to plants in its ferric form (Fe^{3+}). PGPRs address this by secreting siderophores—iron-binding proteins that solubilize Fe^{3+} into a bioavailable form. These siderophores form complexes with Fe^{3+}, reducing it to Fe^{2+} for uptake by plant roots. Similarly, PSB like *Azotobacter*, *Bacillus*, and *Rhizobium* secrete enzymes and organic acids to solubilize insoluble phosphate, making it available to plants (Mitter et al., 2013).

By improving nutrient availability, biofertilizers reduce the need for chemical fertilizers, lower agricultural production costs, and contribute to environmental sustainability. Additionally, these microbes increase organic matter content in the soil, mobilize nutrients from the rhizosphere, and aid in soil fertility recovery through various direct and indirect mechanisms (Gamalero et al., 2020).

Arbuscular mycorrhizal fungi play a pivotal role in regulating plant–soil interactions, especially under elevated atmospheric CO_2 conditions. As CO_2 levels rise, plant photosynthesis and carbon assimilation typically increase, leading to a greater flow of carbohydrates into the rhizosphere. This enhanced carbon availability supports more robust AMF colonization, resulting in increased fungal biomass, denser hyphal networks, and greater production of glomalin, a glycoprotein crucial for soil structure and long-term carbon stability. The mutualistic relationship between plants and AMF becomes especially important under abiotic stresses like drought and salinity. AMF enhances plant tolerance by improving water and nutrient uptake, maintaining photosynthetic efficiency, and supporting osmotic balance. These physiological benefits, in turn, help sustain carbon transfer from plants to soil, even in stressful environments. The enhanced hyphal networks and glomalin secretion contribute to the formation of stable soil aggregates, which help protect soil organic matter and promote long-term carbon storage. Furthermore, elevated CO_2 levels combined with AMF colonization foster greater microbial diversity and increase rhizodeposition, exudation of organic compounds from roots, thereby accelerating carbon cycling and nutrient turnover in the soil ecosystem. However, the effectiveness of these interactions is not uniform; it varies with plant genotype, AMF species,

TABLE 3 Microbial applications in agriculture.

Application	Microbial group	Mechanism	Example crops	Citations
Biofertilizers	*Rhizobium*, AMF, *Bacillus*	Nitrogen fixation, phosphate solubilization	Legumes, maize, wheat	Mitter et al., 2013; Etesami and Glick, 2024
Climate change mitigation	Cyanobacteria, *Sporosarcina*	Carbon fixation, biomineralization	All agricultural crops	Mitchell et al., 2010; Khan et al., 2021b
Bioremediation	*Pseudomonas*, *Saccharomyces*	Hydrocarbon degradation, heavy metal sequestration	Contaminated agricultural soils	Ullah et al., 2015; Saha et al., 2016

and the nature of the environmental stress. Still, AMF serve as key ecological buffers and facilitators, supporting both plant productivity and ecosystem-level carbon sequestration under changing climatic conditions.

Beyond AMF, a broader community of soil microorganisms, including bacteria, fungi, and archaea, plays a vital role in the biogeochemical cycling of carbon. With rising atmospheric CO_2, traditional carbon mitigation strategies such as emission reduction and energy efficiency face scaling challenges. This has led to growing interest in biologically mediated carbon sequestration approaches, particularly those that convert CO_2 into stable mineral forms. One promising approach is the microbial-induced precipitation of carbonate minerals, such as calcite, magnesite, and dolomite. Microorganisms like *Sporosarcina pasteurii* facilitate this process through microbial-induced calcium carbonate precipitation (MICCP), which involves the enzymatic activity of carbonic anhydrase (CA) to accelerate the conversion of CO_2 into stable carbonates (Mukhtar et al., 2019; Dupraz et al., 2009). This not only locks carbon into mineral form but also helps reinforce geological formations by sealing fractures, improving the security of subsurface carbon storage. Cyanobacteria, such as *Microcoleus chthonoplastes*, further contribute to carbon capture by converting CO_2 into durable calcium carbonate structures using sunlight as an energy source (Jansson and Northen, 2010; Kamennaya et al., 2012). These biomineralization processes offer innovative, nature-based solutions for long-term CO_2 sequestration.

Altogether, integrating microbial mechanisms, especially AMF symbiosis under high CO_2 with mineral-based carbon fixation strategies presents a promising frontier in climate mitigation. Advancing our understanding of these microbial–plant–soil interactions is essential for developing scalable, sustainable carbon management systems that align with ecological principles and global carbon reduction goals (Khan et al., 2021b; Mukhtar et al., 2019).

6.2 Climate change mitigation

Climate change, marked by increasing CO_2 levels and rising temperatures, has significantly impacted ecological processes, including the interactions between plants and microbial communities (Fahad et al., 2020). The rise in CO_2 alters root exudates by increasing carbon concentration in the root zone, which affects the composition and activity of soil microbes. This change disrupts the ratio of plant chemo attractants and the carbon-to-nitrogen (C/N) ratio, potentially altering the mutualistic relationships between plants and beneficial microbes.

6.2.1 The potential of microbe-mediated mineral transformations in carbon sequestration and mitigating climate change

Microorganisms, including bacteria, fungi, and archaea, are essential for the biogeochemical cycling of elements, particularly carbon, and play a key role in long-term carbon sequestration in stable mineral forms (Khan et al., 2021b). As CO_2 levels rise, traditional methods of reducing emissions and increasing energy efficiency have been challenging on a large scale, leading to interest in carbon sequestration through the conversion of CO_2 into stable carbonate minerals like calcite, magnesite, and dolomite. This biomimetic approach utilizes biological catalysts, such as CA, to accelerate CO_2 fixation into carbonate minerals (Mukhtar et al., 2019). AMF respond to high CO_2 (eCO_2) with enhanced root colonization, spore density, and biomass due to increased plant carbon input. Enhanced fungal activity increases nutrient acquisition (e.g., phosphorus and zinc), stimulates microbially mediated mineral weathering, and enables soil carbon sequestration via glomalin production and organic matter stabilization (Laza et al., 2023). Under stressful environments (e.g., drought and nutrient stress), AMF increase plant tolerance by enhancing water use efficiency and mobilizing bound minerals, often in combination with PSB. Benefits are, however, modulated by soil fertility, with heavy carbon investment in AMF potentially limiting plant growth when returns are low in nutrients. Understanding these processes is essential to the optimization of the potential of AMF in sustainable crop systems under a changing climate (AbdElgawad et al., 2022).

Field experiments have shown that eCO_2 can cause extreme changes in AMF community structure. For example, long-term eCO_2 exposure in submerged paddy soils led to the reduction of frequently occurring AMF species such as *Claroideoglomus* and *Glomus*, whereas *Scutellospora* species were dominant, reflecting their tolerance at high CO_2 levels (Panneerselvam et al., 2020). This change is caused by variations in physiological and ecological factors affecting carbon utilization efficiency, tolerance to stress, and symbiotic compatibility with host plants. *Scutellospora* species have been reported to exhibit greater adaptation to carbon-rich environments, sustaining consistent symbiotic performance and nutrient exchange under these changed conditions. These changes in composition can impact the mobilization of mineral nutrients and the general functionality of the soil–plant system, especially in scenarios of nutrient deficiency or enhanced susceptibility to stress.

The AMF mineral interaction is controlled by abiotic factors (e.g., redox potential, soil water, and pH) and by the co-occurrence

of microbial species. During low-phosphate conditions, AMF may interact with PSB to solubilize inorganic phosphate from mineral complexes, augmenting microbe–mineral synergy. Elevated CO_2 may stimulate synergistic effects by increasing rhizospheric carbon input, and consequently, increasing associated microbial activity, driving mineral transformation. These interactions control the formation of secondary minerals and biogenic phases, contributing to soil weathering and long-term mineral cycling. MICCP by organisms like *S. pasteurii* enhances CO_2 storage by increasing dissolved CO_2 in subsurface water or precipitating it as carbonate minerals. This process not only stabilizes CO_2 but also helps seal fractures in geological formations, improving long-term CO_2 storage security (Dupraz et al., 2009). Cyanobacteria, such as *M. chthonoplastes*, also contribute to carbon capture and sequestration by converting CO_2 into recalcitrant calcium carbonate biominerals using solar energy (Jansson and Northen, 2010; Kamennaya et al., 2012). These microbial processes offer promising solutions for mitigating climate change by securely transforming CO_2 into stable mineral forms.

6.3 Sustainable agriculture

Microbial biotechnology offers tools to enhance resource use efficiency, reduce dependency on agrochemicals, and address biotic and abiotic stresses. Beneficial microbes, including PGPR and AMF, improve nutrient availability, pathogen resistance, and stress tolerance ((Kumar et al., 2025; De Bruijn, 2015). PGPR improves nutrient uptake and reduce chemical input dependency (Etesami and Adl, 2020; Olivares et al., 2013). Microbes activate systemic resistance pathways, reducing the incidence of soil-borne diseases in crops such as rice and maize. Advances in microbial biotechnology, such as genetically engineered microbial strains, offer new avenues for addressing the challenges of modern agriculture.

6.4 Bioremediation of contaminated soils

Microorganisms are integral to bioremediation efforts, contributing significantly to pollutant detoxification and soil health restoration (Ayangbenro and Babalola, 2017). They play a crucial role in heavy metal remediation through biosorption, facilitated by exopolysaccharides and siderophores, which immobilize toxic metals such as cadmium and lead (Saha et al., 2016; Beiyuan et al., 2017). Furthermore, hydrocarbon-degrading bacteria like *Pseudomonas* spp. degrade petroleum hydrocarbons enzymatically, aiding in soil recovery and fertility enhancement (Mustapha and Halimoon, 2015; Ullah et al., 2015). Combining PGPR with AMF has proven to amplify the effectiveness of phytoremediation strategies, offering a sustainable and eco-friendly approach to addressing soil contamination. Collectively, these microbial-driven processes are vital for detoxifying pollutants and fostering the rehabilitation of degraded ecosystems (Gupta and Diwan, 2017).

7 Challenges and future perspective

The intricacy of the soil ecosystem brings a significant challenge in understanding and manipulating microbial mediated mineral transformation. It is well understood that microbes and microbe associates play a vital role in mineral transport and availability, however, the mechanisms associated with how different microbes enhance the mineral uptake and how the mineral acquisition by the microbes takes place is still not understood properly. The microbial diversity is highly variable in soil and soil associated parameters such as pH, water availability, aeration and cation exchange capability are affected by the available microbes (Chen et al., 2024). Also, some microbes work synergistically with each other and can enhance mineral uptake while there are reports that some microbes are antagonists (Das et al., 2022). This might create a state of disequilibrium in the soil ecosystem, indirectly or directly affecting the growth of plants. Also, the interactions occurring at soil microbial level are not bipartite, these are multipartite interactions, studying the multipartite interactions may be conducted in controlled experiments, but is difficult to be monitored at the field levels (Chauhan et al., 2023). Ascertaining the taxonomy of microbes and assigning the functional role to a microbial community for nutrient uptake is another challenge that needs to be addressed (Castellano-Hinojosa and Strauss, 2021). Furthermore, it is now well understood that the structural complexity of xylem also has a role in nutrient uptake as mineral transport works in cognizance with the conducting tissue.

A major challenge lies in translating laboratory findings into the real-world application. With change and shifts in the environment in a geological and microbial stage, the controlled laboratory experiments which provide mechanistic insights into the microbial processes often fails to capture the full complexity of the natural environment (Chen et al., 2024). Bridging this gap requires iterative and integrative strategies: field-derived hypotheses should inform laboratory studies, while lab-based findings must be tested under realistic soil and climatic conditions (Wang D. et al., 2024). Numerical modeling and geochemical simulations can further aid in scaling these processes by reflecting the evolving nature of geological systems. Databases such as the Deep-Time Digital Earth (DDE) archive offer valuable insights into the temporal evolution of mineral compositions and can help identify biogenic signatures preserved over geological timescales (Wang D. et al., 2024).

With emerging tools and new techniques in synthetic biology and multi omics platforms, it has escalated in redefining a different approach to mineral–microbe–plant interactions. The study offers the ability to reprogram microbial strains with customized functional gene, where a specific targeted gene is modulated with respect with the stress, which helps in the enhancement of plant growth. For instance, *Bacillus megaterium* and *Serratia liquefaciens* are being applicated to improve the pH value of the soil and the mass concentration of NH_4^+, in soil with excessive lead and cadmium content contain urease synthesis (Fu et al., 2024). Engineered biosynthetic pathways can also produce novel chelators or exopolysaccharides that increase solubilization and immobilization of trace metals, improving their availability to plants or reducing their toxicity (Ghosh et al., 2024). Microbes

have been known to form iron oxides or sulfides biogenically that alter the adsorption or absorption of other minerals. Many microbes are known to release acids, synthesize siderophores and enhance oxidation-reduction processes in the soil. This is going to have important consequences on the soil-mineral continuum. It is, therefore, important to identify the genes involved in the said processes (Chaudhary et al., 2023). Besides, identifying the genes, studying the gene expression in altered mineral regimes is also important. Assessing microbial communities in the presence of minerals to identify the active pathways involved in mineral transformation and nutrient acquisition is also important (Wang S. et al., 2024). Furthermore, it will be rewarding to use novel analytical techniques and interdisciplinary approach using various omics techniques to clearly pin-point how microbes in the soil alter nutrient uptake in plants and subsequently affect the plant growth and health (Diwan et al., 2022).

The application of advanced omics technologies like genomics, transcriptomics, proteomics, and metabolomics have given researchers the potential to understand and manipulate the field of microbe–mineral interactions, where they gain a system level perspective on the functional role and adaptive mechanisms of different microbial communities in various environmental stress. Genomic and transcriptomic technology has been applied to analyze the identification of genes and regulatory pathways for critical mineral transformation processes such as metal reduction, mineral weathering, and nutrient mobilization (Raza et al., 2024). Proteomics and metabolomics technologies are also parallelly applicated for understanding of the altercation in microbial responses by revealing in what ways the respective pathways are altered when the cellular activities behind minerals' transformations, or when cells are impacted by abiotic stressors (limiting nutrients or toxicity due to metals) (Sandrini et al., 2022). For example, metagenomic and metatranscriptomics research on microbial assemblages in mine tailings have identified genes that confer the functional capacity for sulfate reduction, iron oxidation, and arsenic detoxification to microbial communities – which ultimately informs the design of successful bioaugmentation approaches (Li et al., 2022). Furthermore, the integration of multi-omics has led to the construction of genome-scale metabolic models (GEMs), which allow for the simulation and prediction of microbial behavior in complex mineral environments. These models not only deepen our mechanistic understanding of microbe–mineral systems but also enable the development of predictive tools to optimize biogeochemical processes for applications such as bioremediation, sustainable resource extraction, and the synthesis of novel biomaterials (Kong et al., 2025). Therefore, multi-omics-driven insights with genome-based modeling frameworks holds a significant promise for advancing mineral biotechnologies and promoting environmentally sound and efficient industrial practices.

One of the most promising research directions is the combination of genome-edited crops with synthetic microbes. With the development of CRISPR/Cas9 and associated biotechnologies, genetically engineered plants with enhanced root architecture, metal uptake efficacy, or detoxification can now be designed. Co-engineering plant and microbial systems provides a synergistic solution to increased abiotic stress tolerance, phytoremediation, and nutrient cycling (Chen et al., 2024). For example, the combination of microbes specifically designed for iron chelation or phosphate solubilization with crops designed for increased nutrient acquisition can significantly boost agricultural productivity from marginal or contaminated soils (Pattnaik et al., 2021; Mishra et al., 2023).

In summary, overcoming microbial-mediated mineral transformation challenges involves a multidisciplinary approach involving microbial ecology, soil science, systems biology, and plant physiology. Future work should focus on the development of stable synthetic consortia, dynamic simulation models, and plant–microbe co-engineering strategies to engineer sustainable and resilient agroecosystems that can withstand environmental stressors and foster long-term soil health.

8 Conclusion

Microbially mediated mineral transformation is essential for nutrient cycling, soil fertility, and plant growth. Microorganisms have a very strong impact on the bioavailability of vital macro- and micronutrients through dissolution, precipitation, redox conversions, and chelation, thus plant growth and stability directly. Microbe–mineral conversions also contribute a vital role in bioremediation, thus providing eco-friendly alternatives to remediate soil pollution and heavy metal toxicity. Despite substantial advances, the functional dynamics of such conversions in the complex soil ecosystem are a challenge, especially under dynamic environmental conditions.

Future research needs to focus on integration of novel approaches, such as multi-omics and synthetic biology, to define microbial functionalities on a systems level, and microbial strain development, which is specifically tailored for mineral transformation based on specific environmental or agronomic conditions. In addition, integration of laboratory-sourced research with field-sourced applications will be needed. An interdisciplinary platform focusing on geochemistry, microbial ecology, and plant physiology will be needed for optimization of novel biofertilizers and precision microbial consortia, which can contribute toward sustainable agriculture production and ecological restoration processes as we all must work together for green earth and knowledge could mechanistically guide the highly promising approaches to use microbes for more sustainable plant nutrition.

Author contributions

NkP: Writing – original draft, Writing – review and editing. SS: Writing – original draft, Writing – review and editing. GS: Writing – original draft, Writing – review and editing. NsP: Writing – original draft, Writing – review and editing. MK: Supervision, Writing – review and editing. AK: Conceptualization, Supervision, Visualization, Writing – original draft, Writing – review and editing. RS: Writing – review and editing, Supervision.

Funding

The author(s) declare that no financial support was received for the research and/or publication of this article.

Acknowledgments

We would like to thank Anil Chandra for editing the diagram.

Conflict of interest

The authors declare that the research was conducted in the absence of any commercial or financial relationships that could be construed as a potential conflict of interest.

Generative AI statement

The author(s) declare that no Generative AI was used in the creation of this manuscript.

Publisher's note

All claims expressed in this article are solely those of the authors and do not necessarily represent those of their affiliated organizations, or those of the publisher, the editors and the reviewers. Any product that may be evaluated in this article, or claim that may be made by its manufacturer, is not guaranteed or endorsed by the publisher.

References

Abd-Alla, M. H., Al-Amri, S. M., and El-Enany, A.-W. E. (2023). Enhancing Rhizobium–Legume symbiosis and reducing nitrogen fertilizer use are potential options for mitigating climate change. *Agriculture* 13:2092. doi: 10.3390/agriculture13112092

AbdElgawad, H., El-Sawah, A. M., Mohammed, A. E., Alotaibi, M. O., Yehia, R. S., Selim, S., et al. (2022). Increasing atmospheric CO2 differentially supports arsenite stress mitigating impact of arbuscular mycorrhizal fungi in wheat and soybean plants. *Chemosphere* 296:134044. doi: 10.1016/j.chemosphere.2022.134044

Ahemad, M., and Kibret, M. (2014). Mechanisms and applications of plant growth promoting rhizobacteria: Current perspective. *J. King Saud University-Sci.* 26, 1–20. doi: 10.1016/j.jksus.2013.05.001

Ahmad, H. M., Fiaz, S., Hafeez, S., Zahra, S., Shah, A. N., Gul, B., et al. (2022). Plant growth-promoting rhizobacteria eliminate the effect of drought stress in plants: A review. *Front. Plant Sci.* 13:875774. doi: 10.3389/fpls.2022.875774

Ahmad, I., Ahmad, M., Hussain, A., and Jamil, M. (2020). Integrated use of phosphate-solubilizing *Bacillus subtilis* strain IA6 and zinc-solubilizing *Bacillus sp.* strain IA16: A promising approach for improving cotton growth. *Folia Microbiol.* 66, 115–125. doi: 10.1007/s12223-020-00831-3

Ahmed, E., and Holmström, S. J. (2014). Siderophores in environmental research: Roles and applications. *Microb. Biotechnol.* 7, 196–208. doi: 10.1111/1751-7915.12117

Ahmed, M., Abdel-Fattah, G. G., Holford, P., Korany, S. M., Alsherif, E. A., AbdElgawad, H., et al. (2023). Funneliformis constrictum modulates polyamine metabolism to enhance tolerance of *Zea mays* L. to salinity. *Microbiol. Res.* 266:127254. doi: 10.1016/j.micres.2022.127254

Alami, S., Kaddouri, K., Lamrabet, M., Chaddad, Z., Bouhnik, O., Bennis, M., et al. (2024). "Selection and application of soil bacterial elite strains as biofertilizers for the reclamation of deteriorated soil health," in *Soil bacteria: Biofertilization and soil health*, eds S. Dheeman, M. T. Islam, D. Egamberdieva, and M. N. Siddiqui (Singapore: Springer Nature Singapore).

Ali, M., Ahmed, I., Tariq, H., Abbas, S., Zia, M. H., Mumtaz, A., et al. (2023). Growth improvement of wheat (*Triticum aestivum*) and zinc biofortification using potent zinc-solubilizing bacteria. *Front. Plant Sci.* 14:1140454. doi: 10.3389/fpls.2023.1140454

Ali, S. A. M., Sayyed, R. Z., Mir, M. I., Khan, M. Y., Hameeda, B., Alkhanani, M. F., et al. (2022). Induction of systemic resistance in maize and antibiofilm activity of surfactin from *Bacillus velezensis* MS20. *Front. Microbiol.* 13:879739. doi: 10.3389/fmicb.2022.879739

Alkilayh, O. A., Hamed, K. E., Sayyed, R. Z., Abdelaal, K., and Omar, A. F. (2024). Characterization of *Botrytis cinerea*, the causal agent of tomato grey mould, and its biocontrol using *Bacillus subtilis*. *Physiol. Mol. Plant Pathol.* 133:102376. doi: 10.1016/j.pmpp.2024.102376

Al-Turki, A., Murali, M., Omar, A. F., Rehan, M., and Sayyed, R. Z. (2023). Recent advances in PGPR-mediated resilience toward interactive effects of drought and salt stress in plants. *Front. Microbiol.* 14:1214845. doi: 10.3389/fmicb.2023.1214845

Alzate Zuluaga, M. Y., Fattorini, R., Cesco, S., and Pii, Y. (2024). Plant-microbe interactions in the rhizosphere for smarter and more sustainable crop fertilization: The case of PGPR-based biofertilizers. *Front. Microbiol.* 15:1440978. doi: 10.3389/fmicb.2024.1440978

Anbalagan, S. A., Appusamy, S., Kumaresan, P. V., Chellappan, G., Narayanan, S., Rangasamy, A., et al. (2024). Deciphering the biocontrol potential of *Trichoderma asperellum* (Tv1) against fusarium-nematode wilt complex in tomato. *J. Basic Microbiol.* 65:e2400595. doi: 10.1002/jobm.202400595

Ayangbenro, A. S., and Babalola, O. O. (2017). A new strategy for heavy metal polluted environments: A review of microbial biosorbents. *Int. J. Environ. Res. Public Health* 14:94. doi: 10.3390/ijerph14010094

Ayuso-Calles, M., García-Estévez, I., Jiménez-Gómez, A., Flores-Félix, J. D., Escribano-Bailón, M. T., and Rivas, R. (2021). *Rhizobium laguerreae* improves productivity and phenolic compound content of lettuce (*Lactuca sativa* L.) under saline stress conditions. *Foods* 9:1166. doi: 10.3390/foods9091166

Baba, Z. A., Hamid, B., Sheikh, T. A., Alotaibi, S. H., El Enshasy, H. A., Ansari, M. J., et al. (2021). Psychrotolerant *Mesorhizobium sp.* isolated from temperate and cold desert regions solubilizes potassium and produces multiple plant growth promoting metabolites. *Molecules* 26:5758. doi: 10.3390/molecules26195758

Basu, A., Prasad, P., Das, S. N., Kalam, S., Sayyed, R. Z., Reddy, M. S., et al. (2021). Plant growth promoting rhizobacteria (PGPR) as green bioinoculants: Recent developments, constraints, and prospects. *Sustainability* 13:1140. doi: 10.3390/su13031140

Bhat, M. A., Mishra, A. K., Shah, S. N., Bhat, M. A., Jan, S., Rahman, S., et al. (2024). Soil and mineral nutrients in plant health: A prospective study of iron and phosphorus in the growth and development of plants. *Curr. Issues Mol. Biol.* 46, 5194–5222. doi: 10.3390/cimb46060312

Beiyuan, J., Awad, Y. M., Beckers, F., Tsang, D. C., Ok, Y. S., and Rinklebe, J. (2017). Mobility and phytoavailability of As and Pb in a contaminated soil using pine sawdust biochar under systematic change of redox conditions. *Chemosphere* 178, 110–118. doi: 10.1016/j.chemosphere.2017.03.022

Bhat, M. A., Mishra, A. K., Shah, S. N., Bhat, M. A., Jan, S., Rahman, S., et al. (2024). Soil and mineral nutrients in plant health: A prospective study of iron and phosphorus in the growth and development of plants. *Curr. Issues Mol. Biol.* 46, 5194–5222. doi: 10.3390/cimb46060312

Bitew, Y., and Alemayehu, M. (2017). Impact of crop production inputs on soil health: A review. *Asian J. Plant Sci.* 16, 109–131. doi: 10.3923/ajps.2017.109.131

Blanco-Vargas, A., Rodríguez-Gacha, L. M., Sánchez-Castro, N., Garzón-Jaramillo, R., Pedroza-Camacho, L. D., Poutou-Piñales, R. A., et al. (2020). Phosphate-solubilizing *Pseudomonas sp.*, and *Serratia sp.*, co-culture for *Allium cepa* L. growth promotion. *Heliyon* 6:e05218. doi: 10.1016/j.heliyon.2020.e05218

Bouremani, N., Cherif-Silini, H., Silini, A., Bouket, A. C., Luptakova, L., Alenezi, F. N., et al. (2023). Plant growth-promoting rhizobacteria (PGPR): A rampart against the adverse effects of drought stress. *Water* 15:418. doi: 10.3390/w15030418

Bridge, T. A. M., and Johnson, D. B. (2000). 'Reductive dissolution of ferric iron minerals byAcidiphilium SJH,'. *Geomicrobiol. J.* 17, 193–206. doi: 10.1080/01490450050121161

Castellano-Hinojosa, A., and Strauss, S. L. (2021). Insights into the taxonomic and functional characterization of agricultural crop core rhizobiomes and their potential microbial drivers. *Sci. Rep.* 11:10068. doi: 10.1038/s41598-021-89569-7

Chaudhary, S., Sindhu, S. S., Dhanker, R., and Kumari, A. (2023). Microbes-mediated sulphur cycling in soil: Impact on soil fertility, crop production and environmental sustainability. *Microbiol. Res.* 271:127340. doi: 10.1016/j.micres.2023.127340

Chauhan, P., Sharma, N., Tapwal, A., Kumar, A., Verma, G. S., Meena, M., et al., (2023). Soil microbiome: Diversity, benefits and interactions with plants. *Sustainability* 15:14643. doi: 10.3390/su151914643

Chen, J., Zhang, Y., Kuzyakov, Y., Wang, D., and Olesen, J. E. (2023). Challenges in upscaling laboratory studies to ecosystems in soil microbiology research. *Glob. Chang Biol.* 29, 569–574. doi: 10.1111/gcb.16537

Chen, L., and Liu, Y. (2024). The function of root exudates in the root colonization by beneficial soil rhizobacteria. *Biology (Basel)* 13:95. doi: 10.3390/biology13020095

Chen, Q., Song, Y., An, Y., Lu, Y., and Zhong, G. (2024). Soil microorganisms: Their role in enhancing crop nutrition and health. *Diversity* 16:734. doi: 10.3390/d16120734

Cheng, Y., Holman, H.-Y., and Lin, Z. (2012). Remediation of chromium and uranium contamination by microbial activity. *Elements* 8, 107–112. doi: 10.2113/gselements.8.2.107

Cohen, A. C., Bottini, R., Pontin, M., Berli, F. J., Moreno, D., Boccanlandro, H., et al. (2015). *Azospirillum brasilense* ameliorates the response of Arabidopsis thaliana to drought mainly via enhancement of ABA levels. *Physiol. Plant* 153, 79–90. doi: 10.1111/ppl.12221

Costa, O. Y. A., Raaijmakers, J. M., and Kuramae, E. E. (2018). Microbial extracellular polymeric substances: Ecological function and impact on soil aggregation. *Front. Microbiol.* 9:1636. doi: 10.3389/fmicb.2018.01636

Da Silva, L. I., Pereira, M. C., Carvalho, A. M. X. d., Buttrós, V.H., Pasqual, M., and Dória, J. (2023). Phosphorus-Solubilizing microorganisms: A key to sustainable agriculture. *Agriculture* 13:462. doi: 10.3390/agriculture13020462

Damodaran, T., Sah, V., Rai, R. B., Sharma, D. K., Mishra, V. K., Jha, S. K., et al. (2013). Isolation of salt tolerant endophytic and rhizospheric bacteria by natural selection and screening for promising plant growth-promoting rhizobacteria (PGPR) and growth vigour in tomato under sodic environment. *Afr. J. Microbiol. Res.* 7, 5082–5089. doi: 10.5897/AJMR2013.6003

Das, P. P., Singh, K. R., Nagpure, G., Mansoori, A., Singh, R. P., Ghazi, I. A., et al. (2022). Plant-soil-microbes: A tripartite interaction for nutrient acquisition and better plant growth for sustainable agricultural practices. *Environ. Res.* 214(Pt 1):113821. doi: 10.1016/j.envres.2022.113821

Dasila, H., Sah, V. K., Jaggi, V., Kumar, A., Tewari, L., Taj, G., et al. (2023). Cold-tolerant phosphate-solubilizing *Pseudomonas* strains promote wheat growth and yield by improving soil phosphorous (P) nutrition status. *Front. Microbiol.* 14:1135693. doi: 10.3389/fmicb.2023.1135693

De Bruijn, F. J. (2015). "The quest for biological nitrogen fixation in cereals: A perspective and prospective," in *Biological nitrogen fixation*, ed. F. J. de Bruijn (Hoboken, NJ: Wiley-Blackwell Publishers).

Diwan, D., Rashid, M. M., and Vaishnav, A. (2022). Current understanding of plant-microbe interaction through the lenses of multi-omics approaches and their benefits in sustainable agriculture. *Microbiol. Res.* 265:127180. doi: 10.1016/j.micres.2022.127180

Dong, H., Huang, L., Zhao, L., Zeng, Q., Liu, X., Sheng, Y., et al. (2022). A critical review of mineral-microbe interaction and co-evolution: Mechanisms and applications. *Natl. Sci. Rev.* 9:nwac128. doi: 10.1093/nsr/nwac128

Dong, H., and Lu, A. (2012). Mineral-microbe interactions and implications for remediation. *Elements* 8, 95–100. doi: 10.2113/gselements.8.2.95

Drijber, R. A., and McPherson, M. R. (2021). Mycorrhizal symbioses. *Principles Appl. Soil Microbiol.* 2021, 303–325. doi: 10.1016/b978-0-12-820202-9.00012-5

Dupraz, S., Ménez, B., Gouze, P., Leprovost, R., Bénézeth, P., Pokrovsky, O. S., et al. (2009). Experimental approach of CO2 biomineralization in deep saline aquifers. *Chem. Geol.* 265, 54–62. doi: 10.1016/j.chemgeo.2008.12.012

El-Egami, H. M., Hegab, R. H., Montaser, H., El-Hawary, M. M., and Hasanuzzaman, M. (2024). Impact of potassium-solubilizing microorganisms with potassium sources on the growth, physiology, and productivity of wheat crop under salt-affected soil conditions. *Agronomy* 14:423. doi: 10.3390/agronomy14030423

Elhaissoufi, W., Ghoulam, C., Barakat, A., Zeroual, Y., and Bargaz, A. (2021). Phosphate bacterial solubilization: A key rhizosphere driving force enabling higher P use efficiency and crop productivity. *J. Adv. Res.* 38, 13–28. doi: 10.1016/j.jare.2021.08.014

Eswaran, S. U. D., Sundaram, L., Perveen, K., Bukhari, N. A., and Sayyed, R. Z. (2024). Osmolyte-producing microbial biostimulants regulate the growth of *Arachis hypogaea* L. under drought stress. *BMC Microbiol.* 24:165. doi: 10.1186/s12866-024-03320-6

Etesami, H., and Adl, S. M. (2020). "Plant growth-promoting rhizobacteria (PGPR) and their action mechanisms in availability of nutrients to plants," in *Phyto-Microbiome in stress regulation. environmental and microbial biotechnology*, eds M. Kumar, V. Kumar, and R. Prasad (Singapore: Springer).

Etesami, H. and Glick, B. R. (2024). Bacterial indole-3-acetic acid: A key regulator for plant growth, plant-microbe interactions, and agricultural adaptive resilience. *Microbiol. Res.* 281:127602. doi: 10.1016/j.micres.2024.127602

Fahad, S., Hasanuzzaman, M., Alam, M., Ullah, H., Saeed, M., Khan, I. A., et al. (eds) (2020). *Environment, climate, plant and vegetation growth*. Berlin: Springer International Publishing.

Ferrol, N., Tamayo, E., and Vargas, P. (2016). The heavy metal paradox in arbuscular mycorrhizas: From mechanisms to biotechnological applications. *J. Exp. Bot.* 67, 6253–6265. doi: 10.1093/jxb/erw403

Fu, S., Iqbal, B., Li, G., Alabbosh, K. F., Khan, K. A., Zhao, X., et al. (2024). The role of microbial partners in heavy metal metabolism in plants: A review. *Plant Cell Rep.* 43:111. doi: 10.1007/s00299-024-03194-y

Galindo-Castañeda, T., Lynch, J. P., Six, J., and Hartmann, M. (2022). Improving soil resource uptake by plants through capitalizing on synergies between root architecture and anatomy and root-associated microorganisms. *Front. Plant Sci.* 13:827369. doi: 10.3389/fpls.2022.827369

Gamalero, E., and Glick, B. R. (2015). Bacterial modulation of plant ethylene levels. *Plant Physiol.* 169, 13–22. doi: 10.1104/pp.15.00284

Gamalero, E., Bona, E., Todeschini, V., and Lingua, G. (2020). Saline and arid soils: Impact on bacteria. plants, and their interaction. *Biology (Basel)* 9:116. doi: 10.3390/biology9060116

Gandhi, R., Prittesh, P., Jinal, H. N., Chavan, S. M., Paul, D., and Amaresan, N. (2022). Evaluation of the effect of potassium solubilizing bacterial strains on the growth of wheat (*Triticum aestivum* L.). *J. Plant Nutrit.* 46, 1479–1490. doi: 10.1080/01904167.2022.2074859

Ghazalibiglar, H., Hampton, J. G., de Jong, E. V. Z., and Holyoake, A. (2016). Is induced systemic resistance the mechanism for control of black rot in *Brassica oleracea* by a *Paenibacillus sp*. *Biol. Control* 92, 195–201. doi: 10.1016/j.biocontrol.2015.10.014

Ghosh, A., Sah, D., Chakraborty, M., and Rai, J. P. N. (2024). Mechanism and application of bacterial exopolysaccharides: An advanced approach for sustainable heavy metal abolition from soil. *Carbohydr. Res.* 544:109247. doi: 10.1016/j.carres.2024.109247

Giordano, M., Petropoulos, S. A., and Rouphael, Y. (2021). The fate of nitrogen from soil to plants: Influence of agricultural practices in modern agriculture. *Agriculture* 11:944. doi: 10.3390/agriculture11100944

Glick, B. R. (2012). Plant growth-promoting bacteria: Mechanisms and applications. *Scientifica (Cairo)* 2012:963401. doi: 10.6064/2012/963401

Gomes, A. F. R., Almeida, M. C., Sousa, E., and Resende, D. I. S. P. (2024). Siderophores and metallophores: Metal complexation weapons to fight environmental pollution. *Sci. Total Environ.* 932:173044. doi: 10.1016/j.scitotenv.2024.173044

Grobelak, A., Napora, A., and Kacprzak, M. J. E. E. (2015). Using plant growth-promoting rhizobacteria (PGPR) to improve plant growth. *Ecol. Eng.* 84, 22–28. doi: 10.1016/j.ecoleng.2015.07.019

Grzyb, A., Wolna-Maruwka, A., and Niewiadomska, A. (2021). The significance of microbial transformation of nitrogen compounds in the light of integrated crop management. *Agronomy* 11:1415. doi: 10.3390/agronomy11071415

Guhra, T., Stolze, K., and Totsche, K. U. (2022). Pathways of biogenically excreted organic matter into soil aggregates. *Soil Biol. Biochem.* 164:108483. doi: 10.1016/j.soilbio.2021.108483

Gupta, G., Panwar, J., and Jha, P. N. (2013). Natural occurrence of *Pseudomonas aeruginosa*, a dominant cultivable diazotrophic endophytic bacterium colonizing *Pennisetum glaucum* (L.) R. *Br. Appl. Soil Ecol.* 64, 252–261. doi: 10.1016/j.apsoil.2012.12.016

Gupta, P., and Diwan, B. (2017). Bacterial exopolysaccharide mediated heavy metal removal: A review on biosynthesis, mechanism and remediation strategies. *Biotechnol. Rep.* 13, 58–71. doi: 10.1016/j.btre.2016.12.006

Hamidian, M., Movahhedi-Dehnavi, M., Sayyed, R. Z., Almalki, W. H., Gafur, A., and Fazeli-Nasab, B. (2023). Co-application of mycorrhiza and methyl jasmonate regulates morpho-physiological and antioxidant responses of *Crocus sativus* (Saffron) under salinity stress conditions. *Sci. Rep.* 13:7378. doi: 10.1038/s41598-023-34359-6

Han, L., Li, J., Xue, Q., Chen, Z., Zhou, Y., and Poon, C. S. (2020). Bacterial-induced mineralization (BIM) for soil solidification and heavy metal stabilization: A critical review. *Sci. Total Environ.* 746:140967. doi: 10.1016/j.scitotenv.2020.140967

Hoffmann, T. D., Reeksting, B. J., and Gebhard, S. (2021). Bacteria-induced mineral precipitation: A mechanistic review. *Microbiology (Reading)* 167:001049. doi: 10.1099/mic.0.001049

Ilyas, N., Mumtaz, K., Akhtar, N., Yasmin, H., Sayyed, R. Z., Khan, W., et al. (2020). Exopolysaccharides producing bacteria for the amelioration of drought stress in wheat. *Sustainability* 12:8876. doi: 10.3390/su12218876

Ipsilantis, I., Karamesouti, M., and Gasparatos, D. (2018). *Beneficial microorganisms for the management of soil phosphorus. in sustainable agriculture reviews*. Berlin: Springer.

Jabborova, D., Annapurna, K., Azimov, A., Tyagi, S., Pengani, K. R., Sharma, P., et al. (2022). Co-inoculation of biochar and arbuscular mycorrhizae for growth promotion and nutrient fortification in soybean under drought conditions. *Front. Plant Sci.* 13:947547. doi: 10.3389/fpls.2022.947547

Jabborova, D., Sayyed, R. Z., Azimov, A., Jabbarov, Z., Matchanov, A., Enakiev, Y., et al. (2021a). Impact of mineral fertilizers on mineral nutrients in the ginger rhizome and on soil enzymes activities and soil properties. *Saudi J. Biol. Sci.* 28, 5268–5274. doi: 10.1016/j.sjbs.2021.05.037

Jabborova, D., Sulaymanov, K., Sayyed, R. Z., Alotaibi, S. H., Enakiev, Y., Azimov, A., et al. (2021b). Mineral fertilizers improves the quality of turmeric and soil. *Sustainability* 13:9437. doi: 10.3390/su13169437

Jalal, A., Oliveira, C. E. D. S., Gato, I. M. B., Moreira, V. D. A., de Lima, B. H., Bastos, A. D. C., et al. (2024). Interaction of mineral nutrients and plant growth-promoting microbes for biofortification of different cropping systems. *J. Plant Growth Regul.* doi: 10.1007/s00344-024-11380-1

Jansson, C., and Northen, T. (2010). Calcifying cyanobacteria–the potential of biomineralization for carbon capture and storage. *Curr. Opin. Biotechnol.* 21, 365–371. doi: 10.1016/j.copbio.2010.03.017

Javaid, S., Mushtaq, S., Mumtaz, M. Z., Rasool, G., Naqqash, T., Afzal, M., et al. (2023). Mineral solubilizing rhizobacterial strains mediated biostimulation of rhodes grass seedlings. *Microorganisms* 11:2543. doi: 10.3390/microorganisms11102543

Jones, M. E., LaCroix, R. E., Zeigler, J., Ying, S. C., Nico, P. S., and Keiluweit, M. (2020). Enzymes, manganese, or iron? drivers of oxidative organic matter decomposition in soils. *Environ. Sci. Technol.* 54, 14114–14123. doi: 10.1021/acs.est.0c04212

Jørgensen, B. B., Findlay, A. J., and Pellerin, A. (2019). The biogeochemical sulfur cycle of marine sediments. *Front. Microbiol.* 10:849. doi: 10.3389/fmicb.2019.00849

Kamennaya, N. A., Ajo-Franklin, C. M., Northen, T., and Jansson, C. (2012). Cyanobacteria as biocatalysts for carbonate mineralization. *Minerals* 2, 338–364. doi: 10.3390/min2040338

Kamran, S., Shahid, I., Baig, D. N., Rizwan, M., Malik, K. A., and Mehnaz, S. (2017). Contribution of zinc solubilizing bacteria in growth promotion and zinc content of wheat. *Front. Microbiol.* 8:2593. doi: 10.3389/fmicb.2017.02593

Kapadia, C., Patel, N., Rana, A., Vaidya, H., Alfarraj, S., Ansari, M. J., et al. (2022). Evaluation of plant growth-promoting and salinity ameliorating potential of halophilic bacteria isolated from saline soil. *Front. Plant Sci.* 13:946217. doi: 10.3389/fpls.2022.946217

Kermeur, N., Pédrot, M., and Cabello-Hurtado, F. (2023). Iron availability and homeostasis in plants: A review of responses, adaptive mechanisms, and signaling. *Methods Mol. Biol.* 2642, 49–81. doi: 10.1007/978-1-0716-3044-0_3

Khan, A., Sayyed, R. Z., and Seifi, S. (2019). "Rhizobacteria: Legendary soil guards in abiotic stress management," in *Plant growth promoting rhizobacteria for sustainable stress management. microorganisms for sustainability*, eds R. Sayyed, N. Arora, and M. Reddy (Singapore: Springer).

Khan, I., Awan, S. A., Ikram, R., Rizwan, M., Akhtar, N., Yasmin, H., et al. (2021a). Effects of 24-epibrassinolide on plant growth, antioxidants defense system, and endogenous hormones in two wheat varieties under drought stress. *Physiol. Plant* 172, 696–706. doi: 10.1111/ppl.13237

Khan, I., Khan, F., Ahmad, S., Pandey, P., and Khan, M. M. (2021b). "Microbes and climate: A tangled relation," in *Microbiomes and the global climate change*, eds S. A. Lone and A. Malik (Singapore: Springer).

Kharkwal, A. C., Joshi, H., Shandilya, C., Dabral, S., Kumar, N., and Varma, A. (2024). Isolation and characterization of a newly discovered plant growth-promoting endophytic fungal strain from the genus *Talaromyces*. *Sci. Rep.* 14:6022. doi: 10.1038/s41598-024-54687-5

Khumairah, F. H., Setiawati, M. R., Fitriatin, B. N., Simarmata, T., Alfaraj, S., Ansari, M. J., et al. (2022). Halotolerant plant growth-promoting rhizobacteria isolated from saline soil improve nitrogen fixation and alleviate salt stress in rice plants. *Front. Microbiol.* 13:905210. doi: 10.3389/fmicb.2022.905210

Khoso, A. G., Li, Y., and Liu, D. (2025). The arbuscular mycorrhizal fungus *Claroideoglomus etunicatum* (Glomerales: Claroideoglomeraceae) inoculated wheat plants mediated responses of *Sitobion avenae* (Fabricius) (Hemiptera: Aphididae) to water deficit. *J. Econ. Entomol.* 118, 203–218. doi: 10.1093/jee/toae293

Kong, Y., Chen, H., Huang, X., Chang, L., Yang, B., and Chen, W. (2025). Precise metabolic modeling in post-omics era: Accomplishments and perspectives. *Crit. Rev. Biotechnol.* 45, 683–701. doi: 10.1080/07388551.2024.2390089

Kuhad, R. C., Singh, S., Lata, and Singh, A. (2011). Phosphate-solubilizing microorganisms," in *Bioaugmentation, biostimulation and biocontrol*, eds A. S. Nagina Parmar, R. C. Kuhad, and O. P. Ward (New York, NY: Springer Verlag).

Kumar, R., Farda, B., Mignini, A., Djebaili, R., Koolman, L., Paul, A., et al. (2025). Microbial solutions in agriculture: Enhancing soil health and resilience through bio-inoculants and bioremediation. *Bacteria* 4:28. doi: 10.3390/bacteria4030028

Kumar, S., Choudhary, A. K., Suyal, D. C., Makarana, G., and Goel, R. (2022). Leveraging arsenic-resistant plant growth-promoting rhizobacteria for arsenic abatement in crops. *J. Hazard. Mater.* 425:127965. doi: 10.1016/j.jhazmat.2021.127965

Kundan, R., Pant, G., Jadon, N., and Agrawal, P. K. (2015). Plant growth promoting rhizobacteria: Mechanism and current prospective. *J. Fertil. Pestic.* 6:155. doi: 10.4172/2471-2728.1000155

Kusale, S. P., Attar, Y. C., Sayyed, R. Z., Malek, R. A., Ilyas, N., Suriani, N. L., et al. (2021). Production of plant beneficial and antioxidants metabolites by klebsiellavariicola under salinity stress. *Molecules* 26:1894. doi: 10.3390/molecules26071894

Lawal, I. (2021). Nitrogen fixing bacteria and their application for heavy metal removal: A mini review. *J. Biochem. Microbiol. Biotechnol.* 9, 43–47. doi: 10.54987/jobimb.v9i2.617

Laza, H. E., Acosta-Martinez, V., Cano, A., Baker, J., Mahan, J., Gitz, D., et al. (2023). Elevated [CO2] enhances soil respiration and AMF abundance in a semiarid peanut agroecosystem. *Agricult. Ecosyst. Environ.* 355:108592. doi: 10.1016/j.agee.2023.108592

Lee, K., Mok, I., Yoon, M., Kim, H., and Chung, D. (2012). Mechanisms of phosphate solubilization by PSB (Phosphate-solubilizing bacteria) in soil. *Kor. J. Soil Sci. Fertil.* 45, 169–176. doi: 10.7745/kjssf.2012.45.2.169

Lepot, K. (2020). Signatures of early microbial life from the Archean (4 to 2.5 Ga) eon. *Earth-Sci. Rev.* 209:103296. doi: 10.1016/j.earscirev.2020.103296

Li, J. T., Jia, P., Wang, X. J., Ou, S. N., Yang, T. T., Feng, S. W., et al. (2022). Metagenomic and metatranscriptomic insights into sulfate-reducing bacteria in a revegetated acidic mine wasteland. *NPJ Biofilms Microb.* 8:71. doi: 10.1038/s41522-022-00333-9

Liu, Z., Li, M., Liu, J., Wang, J., Lin, X., and Hu, J. (2022). Higher diversity and contribution of soil arbuscular mycorrhizal fungi at an optimal P-input level. *Agric. Ecosyst. Environ.* 337:108053. doi: 10.1016/j.agee.2022.108053

Lu, J., Hong, Y., Wei, Y., Gu, J. D., Wu, J., Wang, Y., et al. (2021). Nitrification mainly driven by ammonia-oxidizing bacteria and nitrite-oxidizing bacteria in an anammox-inoculated wastewater treatment system. *AMB Exp.* 11:158. doi: 10.1186/s13568-021-01321-6

Luo, Y., Ma, L., Feng, Q., Luo, H., Chen, C., Wang, S., et al. (2024). Influence and role of fungi, bacteria, and mixed microbial populations on phosphorus acquisition in plants. *Agriculture* 14:358. doi: 10.3390/agriculture14030358

Ma, Y., Rajkumar, M., Zhang, C., and Freitas, H. (2016). Inoculation of Brassica oxyrrhina with plant growth promoting bacteria for the improvement of heavy metal phytoremediation under drought conditions. *J. Hazard. Mater.* 320, 36–44. doi: 10.1016/j.jhazmat.2016.08.009

Maksimovich, N. G., Demenev, A. D., and Khmurchik, V. T. (2021). Transformation of the mineral composition of dispersed soil under microbiological impact. *Bull. Perm Univ. Geol.* 20, 24–32.

Mandal, A., Sarkar, B., Mandal, S., Vithanage, M., Patra, A. K., and Manna, M. C. (2020). *Impact of agrochemicals on soil health. in agrochemicals detection, treatment and remediation*. Oxford: Butterworth-Heinemann.

Martínez, C., Espinosa-Ruiz, A., and Prat, S. (2016). Gibberellins and plant vegetative growth. *Ann. Plant Rev.* 49, 285–322. doi: 10.1002/9781119210436.ch10

Miliute, I., Buzaite, O., Baniulis, D., and Stanys, V. (2015). Bacterial endophytes in agricultural crops and their role in stress tolerance: A review. *Zemdirbyste-Agriculture* 102, 465–478. doi: 10.13080/z-a.2015.102.060

Mishra, P., Mishra, J., and Arora, N. K. (2023). Biofortification revisited: Addressing the role of beneficial soil microbes for enhancing trace elements concentration in staple crops. *Microbiol. Res.* 275:127442. doi: 10.1016/j.micres.2023.127442

Mitchell, A. C., Dideriksen, K., Spangler, L. H., Cunningham, A. B., and Gerlach, R. (2010). Microbially enhanced carbon capture and storage by mineral-trapping and solubility-trapping. *Environ. Sci. Technol.* 44, 5270–5276. doi: 10.1021/es903270w

Mitter, B., Petric, A., Shin, M. W., Chain, P. S., Hauberg-Lotte, L., Reinhold-Hurek, B., et al. (2013). Comparative genome analysis of *Burkholderia phytofirmans* PsJN reveals a wide spectrum of endophytic lifestyles based on interaction strategies with host plants. *Front. Plant Sci.* 4:120. doi: 10.3389/fpls.2013.00120

Mohanty, S. K., Gonneau, C., Salamatipour, A., Pietrofesa, R. A., Casper, B., Christofidou-Solomidou, M., et al. (2018). Siderophore-mediated iron removal from chrysotile: Implications for asbestos toxicity reduction and bioremediation. *J. Hazard Mater.* 341, 290–296. doi: 10.1016/j.jhazmat.2017.07.033

Mosttafiz, S., Rahman, M., and Rahman, M. (2012). Biotechnology: Role of microbes in sustainable agriculture and environmental health. *Int. J. Microbiol.* 10, 1937–8289. doi: 10.5580/2b91

Mukhtar, S., Mehnaz, S., Mirza, M. S., and Malik, K. A. (2019). Isolation and characterization of bacteria associated with the rhizosphere of halophytes (*Salsola stocksii* and *Atriplex amnicola*) for production of hydrolytic enzymes. *Braz. J. Microbiol.* 50, 85–97. doi: 10.1007/s42770-019-00044-y

Mustapha, M. U., and Halimoon, N. (2015). Microorganisms and biosorption of heavy metals in the environment: A review paper. *J. Microb. Biochem. Technol.* 7, 253–256. doi: 10.4172/1948-5948.1000219

Nader, A. A., Hauka, F. I. A., Afify, A. H., and El-Sawah, A. M. (2024). Drought-tolerant bacteria and arbuscular mycorrhizal fungi mitigate the detrimental effects of drought stress induced by withholding irrigation at critical growth stages of soybean (*Glycine max*, L.). *Microorganisms* 12:1123. doi: 10.3390/microorganisms12061123

Nagaraju, Y., Kumar, D. M., Patted, P. S., Sahu, P. K., and Kumar, S. A. (2024). "Supplementing micronutrients to plants through microbes," in *Metabolomics, proteomics and gene editing approaches in biofertilizer industry*, eds. S. Kaur, V. Dwibedi, and P. K. Sahu (Singapore: Springer Nature Singapore), 247–260.

Narayan, O. P., Kumar, P., Yadav, B., Dua, M., and Johri, A. K. (2023). Sulfur nutrition and its role in plant growth and development. *Plant Signal Behav.* 18:2030082. doi: 10.1080/15592324.2022.2030082

Navarro, J. M., Pérez-Tornero, O., and Morte, A. (2014). Alleviation of salt stress in citrus seedlings inoculated with arbuscular mycorrhizal fungi depends on the rootstock salt tolerance. *J. Plant Physiol.* 171, 76–85. doi: 10.1016/j.jplph.2013.06.006

Neria-González, M. I., and Aguilar-López, R. (2021). "Heavy metal removal processes by sulfate-reducing bacteria," in *Environmental and microbial biotechnology*, ed. R. Prasad (Singapore: Springer).

Nithyapriya, S., Sundaram, L., Eswaran, S. U. D., Perveen, K., Alshaikh, N. A., Sayyed, R. Z., et al. (2024). Purification and characterization of desferrioxamine B of *Pseudomonas fluorescens* and its application to improve oil content, nutrient uptake, and plant growth in peanuts. *Microb. Ecol.* 87:60. doi: 10.1007/s00248-024-02377-0

Normand, P., Queiroux, C., Tisa, L. S., Benson, D. R., Rouy, Z., Cruveiller, S., et al. (2007). Exploring the genomes of Frankia. *Physiol. Plant.* 130, 331–343. doi: 10.1111/j.1399-3054.2007.00918.x

Olanrewaju, O. S., Glick, B. R., and Babalola, O. O. (2017). Mechanisms of action of plant growth promoting bacteria. *World J. Microbiol. Biotechnol.* 33:197. doi: 10.1007/s11274-017-2364-9

Olivares, J., Bedmar, E. J., and Sanjuán, J. (2013). Biological nitrogen fixation in the context of global change. *Mol. Plant Microbe Interact.* 26, 486–494. doi: 10.1094/MPMI-12-12-0293-CR

Ortiz-Castillo, J. E., Mirazimi, M., Mohammadi, M., Dy, E., and Liu, W. (2021). The role of microorganisms in the formation, dissolution, and transformation of secondary minerals in mine rock and drainage: A review. *Minerals* 11:1349. doi: 10.3390/min11121349

Paliwal, K., Jajoo, A., Tomar, R. S., Prakash, A., Syed, A., Bright, J. P., et al. (2023). Enhancing biotic stress tolerance in soybean affected by rhizoctonia solani root rot through an integrated approach of biocontrol agent and fungicide. *Curr. Microbiol.* 80:304. doi: 10.1007/s00284-023-03404-y

Pan, L., and Cai, B. (2023). Phosphate-Solubilizing bacteria: Advances in their physiology. *Mol. Mechan. Microb. Commun. Effects Microorgan.* 11:2904. doi: 10.3390/microorganisms11122904

Pang, F., Li, Q., Solanki, M. K., Wang, Z., Xing, Y.-X., and Dong, D.-F. (2024). Soil phosphorus transformation and plant uptake driven by phosphate? Solubilizing microorganisms. *Front. Microbiol.* 15:1383813. doi: 10.3389/fmicb.2024.1383813

Panneerselvam, P., Kumar, U., Senapati, A., Parameswaran, C., Anandan, A., Kumar, A., et al. (2020). Influence of elevated CO2 on arbuscular mycorrhizal fungal community elucidated using Illumina MiSeq platform in sub-humid tropical paddy soil. *Appl. Soil Ecol.* 145:103344. doi: 10.1016/j.apsoil.2019.08.006

Paul, S., and Parihar, M. (2021). "Role of soil microbes in micronutrient solubilization," in *New and future developments in microbial biotechnology and bioengineering*, (Amsterdam: Elsevier eBooks).

Parray, J. A., Egamberdieva, D., Abd_Allah, E. F., and Sayyed, R. Z. (2023). Soil microbiome metabolomics: A way forward to sustainable intensification. *Front. Sustainable Food Syst.* 7:1251054. doi: 10.3389/fsufs.2023.1251054

Pattnaik, S., Mohapatra, B., and Gupta, A. (2021). Plant growth-promoting microbe mediated uptake of essential nutrients (Fe, P, K) for crop stress management: Microbe–soil–plant continuum. *Front. Agronomy* 3:689972. doi: 10.3389/fagro.2021.689972

Pecoraro, L., Wang, X., Shah, D., Song, X., Kumar, V., Shakoor, A., et al. (2021). Biosynthesis pathways, transport mechanisms and biotechnological applications of fungal siderophores. *J. Fungi (Basel)* 8:21. doi: 10.3390/jof8010021

Peng, L., Shan, X., Yang, Y., Wang, Y., Druzhinina, I. S., Pan, X., et al. (2021). Facultative symbiosis with a saprotrophic soil fungus promotes potassium uptake in American sweetgum trees. *Plant Cell Environ.* 44, 2793–2809. doi: 10.1111/pce.14053

Peng, Y., Huo, W., and Feng, G. (2024). Maximising cotton phosphorus utilisation for zero surplus and high yields: A review of innovative P management strategies. *Field Crops Res.* 313:109429. doi: 10.1016/j.fcr.2024.109429

Prashar, P., and Shah, S. (2016). "Impact of fertilizers and pesticides on soil microflora in agriculture," in *Sustainable agriculture reviews*, vol. 19, ed. E. Lichtfouse (Cham: Springer), 331–361. doi: 10.1007/978-3-319-26777-7_8

Praveen, K. V., and Singh, A. (2019). Realizing the potential of a low-cost technology to enhance crop yields: Evidence from a meta-analysis of biofertilizers in India. *Agricult. Econ. Res. Rev.* 32, 77–91. doi: 10.22004/ag.econ.303653

Pusztahelyi, T., Holb, I. J., and Pócsi, I. (2015). Secondary metabolites in fungus-plant interactions. *Front. Plant Sci.* 6:573. doi: 10.3389/fpls.2015.00573

Rabbi, S. M. F., Minasny, B., McBratney, A. B., and Young, I. M. (2019). Microbial processing of organic matter drives stability and pore geometry of soil aggregates. *Geoderma* 360:114033. doi: 10.1016/j.geoderma.2019.114033

Ramegowda, V., and Senthil-Kumar, M. (2015). The interactive effects of simultaneous biotic and abiotic stresses on plants: Mechanistic understanding from drought and pathogen combination. *J. Plant Physiol.* 176, 47–54. doi: 10.1016/j.jplph.2014.11.008

Ramesh, R. D., Selvaraj, K., Muthusamy, K., Lakshmanan, L., Francis, S. P., Tharumasivam, S. V., et al. (2023). "Endurance of microbes against nitrogen starvation by altering the biochemical and physiological activities of plants," in P*lant-Microbe interaction-recent advances in mole*, eds. P. Swapnil, M. Meena, Harish, A. Marwal, S. Vijayalakshmi, and A. Zehra (Cambridge, MA: Academic Press). doi: 10.1016/B978-0-323-91876-3.00014-2

Rana, K. L., Kour, D., Kaur, T., Negi, R., Devi, R., Yadav, N., et al. (2023). Endophytic nitrogen-fixing bacteria: Untapped treasurer for agricultural sustainability. *J. Appl. Biol. Biotechnol.* 11, 75–93. doi: 10.7324/JABB.2023.110207

Rawat, P., Das, S., Shankhdhar, D., and Shankhdhar, S. C. (2021). Phosphate-solubilizing microorganisms: Mechanism and their role in phosphate solubilization and uptake. *J. Soil Sci. Plant Nutrit.* 21, 49–68. doi: 10.1007/s42729-020-00342-7

Raza, A., Salehi, H., Bashir, S., Tabassum, J., Jamla, M., Charagh, S., et al. (2024). Transcriptomics, proteomics, and metabolomics interventions prompt crop improvement against metal(loid) toxicity. *Plant Cell Rep.* 43:80. doi: 10.1007/s00299-024-03153-7

Ribeiro, I. D. A., Volpiano, C. G., Vargas, L. K., Granada, C. E., Lisboa, B. B., and Passaglia, L. M. P. (2020). Use of mineral weathering bacteria to enhance nutrient availability in crops: A review. *Front. Plant Sci.* 11:590774. doi: 10.3389/fpls.2020.590774

Roskova, Z., Skarohlid, R., and McGachy, L. (2022). Siderophores: An alternative bioremediation strategy? *Sci. Total Environ.* 819:153144. doi: 10.1016/j.scitotenv.2022.153144

Rouphael, Y., and Colla, G. (2018). Synergistic biostimulatory action: Designing the next generation of plant biostimulants for sustainable agriculture. *Front. Plant Sci.* 9:1655. doi: 10.3389/fpls.2018.01655

Ruan, J., Zhou, Y., Zhou, M., Yan, J., Khurshid, M., Weng, W., et al. (2019). Jasmonic acid signaling pathway in plants. *Int. J. Mol. Sci.* 20:2479. doi: 10.3390/ijms20102479

Saboor, A., Ali, M. A., Hussain, S., El Enshasy, H. A., Hussain, S., Ahmed, N., et al. (2021). Zinc nutrition and arbuscular mycorrhizal symbiosis effects on maize (*Zea mays* L.) growth and productivity. *Saudi J. Biol. Sci.* 28, 6339–6351. doi: 10.1016/j.sjbs.2021.06.096

Saeed, Q., Xiukang, W., Haider, F. U., Kuèerik, J., Mumtaz, M. Z., Holatko, J., et al. (2021). Rhizosphere bacteria in plant growth promotion, biocontrol, and bioremediation of contaminated sites: A comprehensive review of effects and mechanisms. *Int. J. Mol. Sci.* 22:10529. doi: 10.3390/ijms221910529

Sagar, A., Rai, S., Ilyas, N., Sayyed, R. Z., Al-Turki, A. I., El Enshasy, H. A., et al. (2022). Halotolerant rhizobacteria for salinity-stress mitigation: Diversity, mechanisms and molecular approaches. *Sustainability* 14:490. doi: 10.3390/su14010490

Sagar, A., Sayyed, R. Z., Ramteke, P. W., Sharma, S., Marraiki, N., Elgorban, A. M., et al. (2020). ACC deaminase and antioxidant enzymes producing halophilic *Enterobacter sp*. PR14 promotes the growth of rice and millets under salinity stress. *Physiol. Mol. Biol. Plants* 26, 1847–1854. doi: 10.1007/s12298-020-00852-9

Saha, M., Sarkar, S., Sarkar, B., Sharma, B. K., Bhattacharjee, S., and Tribedi, P. (2016). Microbial siderophores and their potential applications: A review. *Environ. Sci. Pollut. Res. Int.* 23, 3984–3999. doi: 10.1007/s11356-015-4294-0

Sandrini, M., Nerva, L., Sillo, F., Balestrini, R., Chitarra, W., and Zampieri, E. (2022). Abiotic stress and belowground microbiome: The potential of omics approaches. *Int. J. Mol. Sci.* 23:1091. doi: 10.3390/ijms23031091

Sanket, A. S., Ghosh, S., Sahoo, R., Nayak, S., and Das, A. P. (2017). Molecular identification of acidophilic manganese (Mn)-solubilizing bacteria from mining effluents and their application in mineral beneficiation. *Geomicrobiol. J.* 34, 71–80. doi: 10.1080/01490451.2016.1141340

Sardans, J., and Peñuelas, J. (2021). Potassium control of plant functions: Ecological and agricultural implications. *Plants (Basel)* 10:419. doi: 10.3390/plants10020419

Saxena, J., Minaxi, and Jha, A. (2014). Impact of a phosphate solubilizing bacterium and an arbuscular mycorrhizal fungus (*Glomus etunicatum*) on growth, yield and P concentration in wheat plants. *CLEAN–Soil Air Water* 42, 1248–1252. doi: 10.1002/clen.201300492

Sayyed, R. Z., Chincholkar, S. B., Reddy, M. S., Gangurde, N. S., and Patel, P. R. (2012). "Siderophore producing PGPR for crop nutrition and phytopathogen suppression," in *Bacteria in agrobiology: Disease management*, ed. D. K. Maheshwari (Berlin: Springer).

Shah, A., Nazari, M., Antar, M., Msimbira, L. A., Naamala, J., Lyu, D., et al. (2021). in agriculture: A sustainable approach to increasing climate change resilience. *Front. Sustainable Food Syst.* 5:667546. doi: 10.3389/fsufs.2021.667546

Sheteiwy, M. S., Ali, D. F. I., Xiong, Y. C., Brestic, M., Skalicky, M., Hamoud, Y. A., et al. (2021). Physiological and biochemical responses of soybean plants inoculated with *Arbuscular mycorrhizal* fungi and *Bradyrhizobium* under drought stress. *BMC Plant Biol.* 21:195. doi: 10.1186/s12870-021-02949-z

Sheteiwy, M. S., El-Sawah, A. M., Korany, S. M., Alsherif, E. A., Mowafy, A. M., Chen, J., et al. (2022). Arbuscular mycorrhizal fungus "*Rhizophagus irregularis*" impacts on physiological and biochemical responses of ryegrass and chickpea plants under beryllium stress. *Environ. Pollut.* 315:120356. doi: 10.1016/j.envpol.2022.120356

Singh, D., Prasanna, R., Sharma, V., Rajawat, M. V. S., Nishanth, S., and Saxena, A. K. (2020). "Prospecting plant–microbe interactions for enhancing nutrient availability and grain biofortification," in *Wheat and barley grain biofortification*, eds. O. P. Gupta, V. Pandey, S. Narwal, P. Sharma, S. Ram, and G. P. Singh (Amsterdam: Elsevier eBooks), 203–228.

Singh, T., Bisht, N., Ansari, M. M., and Chauhan, P. S. (2024). *Pseudomonas putida* triggers phosphorus bioavailability and P-transporters under different phosphate regimes to enhance maize growth. *Plant Physiol. Biochem.* 217:109279. doi: 10.1016/j.plaphy.2024.109279

Smith, S. E., and Read, D. J. (2008). *Mycorrhizal symbiosis*. London: Academic Press.

Talaat, N. B., and Shawky, B. T. (2014). Protective effects of arbuscular mycorrhizal fungi on wheat (*Triticum aestivum* L.) plants exposed to salinity. *Environ. Exp. Botany* 98, 20–31. doi: 10.1016/j.envexpbot.2013.10.005

Tanveer, S., Akhtar, N., Ilyas, N., Sayyed, R. Z., Fitriatin, B. N., Perveen, K., et al. (2023). Interactive effects of *Pseudomonas putida* and salicylic acid for mitigating drought tolerance in canola (*Brassica napus* L.). *Heliyon* 9:e14193. doi: 10.1016/j.heliyon.2023.e14193

Thepbandit, W., and Athinuwat, D. (2024). Rhizosphere microorganisms supply availability of soil nutrients and induce plant defense. *Microorganisms* 12:558. doi: 10.3390/microorganisms12030558

Timmermann, T., Yip, C., Yang, Y. Y., Wemmer, K. A., Chowdhury, A., Dores, D., et al., (2025). Harnessing microbes to weather native silicates in agricultural soils for scalable carbon dioxide removal. *Glob. Change Biol.* 31:e70216. doi: 10.1111/gcb.70216

Thomas, S., Mathew, L., and Rishad, K. (2018). Isolation and molecular identification of phosphate solubilizing bacteria, *Bacillus licheniformis* UBPSB-07 capable of enhancing seed germination in *Vigna radiata* L. *Phytomorphology* 68, 13–18.

Timofeeva, A. M., Galyamova, M. R., and Sedykh, S. E. (2022). Bacterial siderophores: Classification, biosynthesis, perspectives of use in agriculture. *Plants (Basel)* 11:3065. doi: 10.3390/plants11223065

Tiwari, P., Bose, S. K., Park, K. I., Dufossé, L., and Fouillaud, M. (2024). Plant-Microbe interactions under the extreme habitats and their potential applications. *Microorganisms* 12:448. doi: 10.3390/microorganisms12030448

Tiwari, S., Lata, C., Chauhan, P. S., and Nautiyal, C. S. (2016). *Pseudomonas putida* attunes morphophysiological, biochemical and molecular responses in *Cicer arietinum* L. during drought stress and recovery. *Plant Physiol. Biochem.* 99, 108–117. doi: 10.1016/j.plaphy.2015.11.001

Torres, M. J., Simon, J., Rowley, G., Bedmar, E. J., Richardson, D. J., Gates, A. J., et al. (2016). Nitrous oxide metabolism in nitrate-reducing bacteria: Physiology and regulatory mechanisms. *Adv. Microb. Physiol.* 68, 353–432. doi: 10.1016/bs.ampbs.2016.02.007

Ullah, A., Heng, S., Munis, M. F. H., Fahad, S., and Yang, X. (2015). Phytoremediation of heavy metals assisted by plant growth promoting (PGP) bacteria: A review. *Environ. Exp. Botany* 117, 28–40. doi: 10.1016/j.envexpbot.2015.05.001

Ulzen, J., Abaidoo, R. C., Mensah, N. E., Masso, C., and AbdelGadir, A. H. (2016). Bradyrhizobium inoculants enhance grain yields of soybean and cowpea in Northern Ghana. *Front. Plant Sci.* 7:1770. doi: 10.3389/fpls.2016.01770

Vafa, Z. N., Sohrabi, Y., Mirzaghaderi, G., Heidari, G., Rizwan, M., and Sayyed, R. Z. (2024). Effect of bio-fertilizers and seaweed extract on growth and yield of wheat (*Triticum aestivum* L.) under different irrigation regimes: Two-year field study. *Chemosphere* 364:143068. doi: 10.1016/j.chemosphere.2024.143068

Vafa, Z. N., Sohrabi, Y., Sayyed, R. Z., Suriani, N. L., and Datta, R. (2021). Effects of the combinations of rhizobacteria, mycorrhizae, and seaweed, and supplementary irrigation on growth and yield in wheat cultivars. *Plants* 10:811. doi: 10.3390/plants10040811

Vélez-Bermúdez, I. C., and Schmidt, W. (2022). Plant strategies to mine iron from alkaline substrates. *Plant Soil* 483, 1–25. doi: 10.1007/s11104-022-05746-1

Vessey, J. K. (2003). Plant growth promoting rhizobacteria as biofertilizers. *Plant Soil* 255, 571–586. doi: 10.1023/A:1026037216893

Vigliotta, G., Matrella, S., Cicatelli, A., Guarino, F., and Castiglione, S. (2016). Effects of heavy metals and chelants on phytoremediation capacity and on rhizobacterial communities of maize. *J. Environ. Manage* 179, 93–102. doi: 10.1016/j.jenvman.2016.04.055

Vinothini, K., Nakkeeran, S., Saranya, N., Jothi, P., Richard, J. I., Perveen, K., et al. (2024). Rhizosphere engineering of biocontrol agents enriches soil microbial diversity and effectively controls root-knot nematodes. *Microb. Ecol.* 87:120. doi: 10.1007/s00248-024-02435-7

Vocciante, M., Grifoni, M., Fusini, D., Petruzzelli, G., and Franchi, E. (2022). The role of plant growth-promoting rhizobacteria (PGPR) in mitigating plant's environmental stresses. *Appl. Sci.* 12:1231. doi: 10.3390/app12031231

Wang, R., Lin, J., Liu, X., Pang, X., Zhang, C., Yang, C., et al. (2019). Sulfur oxidation in the acidophilic autotrophic *Acidithiobacillus spp*. *Front. Microbiol.* 9:3290. doi: 10.3389/fmicb.2018.03290

Wang, D., Xu, P. Y., An, B. W., and Guo, Q. P. (2024). Urban green infrastructure: Bridging biodiversity conservation and sustainable urban development through adaptive management approach. *Front. Ecol. Evol.* 12:1440477. doi: 10.3389/fevo.2024.1440477

Wang, S., Yuan, X., Li, T., Yang, J., Zhao, L., Yuan, D., et al. (2024). Changes in soil microbe-mediated carbon, nitrogen and phosphorus cycling during spontaneous succession in abandoned PbZn mining areas. *Sci. Total Environ.* 920:171018. doi: 10.1016/j.scitotenv.2024.171018

Wang, X., Li, Z., Li, Q., and Hu, Z. (2025). Alleviation of plant abiotic stress: Mechanistic insights into emerging applications of phosphate-solubilizing microorganisms in agriculture. *Plants (Basel)* 14:1558. doi: 10.3390/plants14101558

Wei, X., Xie, B., Wan, C., Song, R., Zhong, W., Xin, S., et al. (2024). Enhancing soil health and plant growth through microbial fertilizers: Mechanisms, benefits, and sustainable agricultural practices. *Agronomy* 14:609. doi: 10.3390/agronomy14030609

Wilpiszeski, R. L., Aufrecht, J. A., Retterer, S. T., Sullivan, M. B., Graham, D. E., Pierce, E. M., et al. (2019). Soil aggregate microbial communities: Towards understanding microbiome interactions at biologically relevant scales. *Appl. Environ. Microbiol.* 85:e00324-19. doi: 10.1128/AEM.00324-19

Williamson, A. J., Morris, C., Duhme-Klair, A.-K., Johnson, D. B., and Hallberg, K. B. (2021). Selective metal extraction by biologically produced siderophores during bioleaching from low-grade primary and secondary mineral resources. *Minerals Eng.* 163:106774. doi: 10.1016/j.mineng.2021.106774

Wu, Q. S., and Zou, Y. N. (2017). "Arbuscular mycorrhizal fungi and tolerance of drought stress in plants," in *Arbuscular mycorrhizas and stress tolerance of plants*, ed. Q. S. Wu (Berlin: Springer).

Xia, Q., Zheng, N., Heitman, J. L., and Shi, W. (2021). Soil pore size distribution shaped not only compositions but also networks of the soil microbial community. *Appl. Soil Ecol.* 170:104273. doi: 10.1016/j.apsoil.2021.104273

Yadav, R. C., Sharma, S. K., Varma, A., Singh, U. B., Kumar, A., Bhupenchandra, I., et al. (2023). Zinc-solubilizing *Bacillus spp*. in conjunction with chemical fertilizers enhance growth, yield, nutrient content, and zinc biofortification in wheat crop. *Front. Microbiol.* 14:1210938. doi: 10.3389/fmicb.2023.1210938

You, W., Peng, W., Tian, Z., and Zheng, M. (2021). Uranium bioremediation with U(VI)-reducing bacteria. *Sci. Total Environ.* 798:149107. doi: 10.1016/j.scitotenv.2021.149107

Zaidi, A., Ahmad, E., Khan, M. S., Saif, S., and Rizvi, A. (2015). Role of plant growth promoting rhizobacteria in sustainable production of vegetables: Current perspective. *Sci. Horticult.* 193, 231–239. doi: 10.1016/j.scienta.2015.07.020

Zhang, Y., Yao, Q., Li, J., Wang, Y., Liu, X., Hu, Y., and Chen, J. (2015). Contributions of an arbuscular mycorrhizal fungus to growth and physiology of loquat (*Eriobotrya japonica*) plants subjected to drought stress. *Sci. Hortic.* 186, 1–7. doi: 10.1016/j.scienta.2015.01.014

Zhang, Y., Peng, J., Wang, Z., Zhou, F., Yu, J., Chi, R., et al. (2025). Metagenomic analysis revealed the bioremediation mechanism of lead and cadmium contamination by modified biochar synergized with Bacillus cereus PSB-2 in phosphate mining wasteland. *Front. Microbiol.* 16:1529784. doi: 10.3389/fmicb.2025.1529784

Złoch, M., Thiem, D., Gadzała-Kopciuch, R., and Hrynkiewicz, K. (2016). Synthesis of siderophores by plant-associated metallotolerant bacteria under exposure to Cd(2.). *Chemosphere* 156, 312–325. doi: 10.1016/j.chemosphere.2016.04.130

Frontiers in Microbiology

Explores the habitable world and the potential of microbial life

The largest and most cited microbiology journal which advances our understanding of the role microbes play in addressing global challenges such as healthcare, food security, and climate change.

Discover the latest Research Topics

See more →



Frontiers

Avenue du Tribunal-Fédéral 34
1005 Lausanne, Switzerland
frontiersin.org

Contact us

+41 (0)21 510 17 00
frontiersin.org/about/contact